

Copy No. \_\_\_\_\_

# **Guide for Mechanistic-Empirical Design OF NEW AND REHABILITATED PAVEMENT STRUCTURES**

**FINAL DOCUMENT**

## **APPENDIX DD-1: RESILIENT MODULUS AS FUNCTION OF SOIL MOISTURE-SUMMARY OF PREDICTIVE MODELS**

**NCHRP**

**Prepared for  
National Cooperative Highway Research Program  
Transportation Research Board  
National Research Council**

**Submitted by  
ARA, Inc., ERES Division  
505 West University Avenue  
Champaign, Illinois 61820**

**June 2000**

## **Acknowledgment of Sponsorship**

This work was sponsored by the American Association of State Highway and Transportation Officials (AASHTO) in cooperation with the Federal Highway Administration and was conducted in the National Cooperative Highway Research Program which is administered by the Transportation Research Board of the National Research Council.

## **Disclaimer**

This is the final draft as submitted by the research agency. The opinions and conclusions expressed or implied in this report are those of the research agency. They are not necessarily those of the Transportation Research Board, the National Research Council, the Federal Highway Administration, AASHTO, or the individual States participating in the National Cooperative Highway Research program.

## **Acknowledgements**

The research team for NCHRP Project 1-37A: Development of the 2002 Guide for the Design of New and Rehabilitated Pavement Structures consisted of Applied Research Associates, Inc., ERES Consultants Division (ARA-ERES) as the prime contractor with Arizona State University (ASU) as the primary subcontractor. Fugro-BRE, Inc., the University of Maryland, and Advanced Asphalt Technologies, LLC served as subcontractors to either ARA-ERES or ASU along with several independent consultants.

Research into the subject area covered in this Appendix was conducted at ASU. The authors of this Appendix are Dr. M.W. Witczak, Mr. Dragos Andrei, and Dr. W.N. Houston. Specifically, Dr. Witczak coordinated the overall research effort, outlined the problems, monitored progress, set schedules and deadlines and provided periodic technical review of research results as they became available. Mr. Andrei performed the literature review, summarized the models from the literature and developed the new normalized model. Dr. Houston provided periodic supervision, review of the results as they became available, and offered numerous suggestions.

## **Foreword**

This report first summarizes existing models from the literature that incorporate the variation of resilient modulus with moisture. Subsequently, it discusses the selection of specific models to predict changes in modulus due to changes in moisture that were eventually considered for implementation in the 2002 Guide for the Design of New and Rehabilitated Pavement Structures.

The information contained in this section serves as a supporting reference to the resilient modulus discussions presented and PART 2, Chapter 3, and PART 3, Chapters 3, 4, 6, and 7 of the Design Guide.

## Table of Contents

	<u>Page</u>
Introduction.....	1
Objective .....	6
Analysis and Assumptions .....	6
Summary of Models.....	10
Li and Selig Model for Fine-grained Subgrade Soils .....	10
Drumm et al. Model for Fine-grained Subgrade Soils.....	11
Jin et al. Model for Coarse-grained Subgrade Soils .....	17
Jones and Witczak Model for Fine-grained Subgrade Soils .....	19
Rada and Witczak Model for Base Materials .....	21
Santha's Models for Coarse-grained and Fine-grained Subgrade Soils .....	21
CRREL Model for Frozen Coarse-grained and Fine-grained Materials.....	27
Muhanna et al. Model for Fine-grained Subgrade Soils .....	31
Summary .....	33
Proposed Model .....	35
Revised Model .....	56
Implementation .....	63
Recommendations for Further Study .....	65
Bibliography .....	67

## List of Tables

	<u>Page</u>
Table1. Gradient of $M_R$ with Respect to Saturation Degree .....	15
Table 2. Regression Coefficients (Rada and Witczak) .....	24
Table 3. Regression Coefficients and Symbols (CRREL/Frozen).....	30
Table 4. Coefficients for the Revised Model .....	62
Table 5. Complexity of the Model.....	64

## List of Figures

	<u>Page</u>
Figure 1. Influence of Resilient Modulus on Dry Density.....	2
Figure 2. Post-compaction Variation in Moisture Content.....	8
Figure 3. Data Points at Constant Compactive Effort.....	9
Figure 4. Data Points at Constant Dry Density.....	9
Figure 5. Variation of Modulus with Moisture/Saturation (Li and Selig) .....	12
Figure 6. Effects of Post-Compaction Saturation on $M_R$ .....	13
Figure 7. Variation of Modulus with Moisture/Saturation (Drumm et al.) .....	16
Figure 8. Normalized Modulus Vs. Measured Variation in Moisture Content .....	18
Figure 9. Variation of Modulus with Moisture/Saturation (Jin et al.) .....	20
Figure 10. Relationship between Modulus, Moisture Content and Degree of Saturation (Jones and Witczak).....	22
Figure 11. Variation of Modulus with Moisture/Saturation (Jones and Witczak).....	23
Figure 12. Variation of Modulus with Moisture/Saturation (Rada and Witczak) .....	25
Figure 13. Variation of Modulus with Moisture/Saturation (Santha/Fine-grained) .....	28
Figure 14. Variation of Modulus with Moisture/Saturation (Santha/Coarse-grained) .....	29
Figure 15. Variation of Modulus with Temperature (CRREL/Frozen) .....	32
Figure 16. Variation of Modulus with Moisture/Saturation (Muhanna et al.).....	34
Figure 17. Variation of Modulus with Moisture/Saturation for All Fine-grained Materials .....	36, 37
Figure 18. Variation of Modulus with Moisture/Saturation for All Coarse-grained Materials .....	38, 39

Figure 19. Semilog Plot (Li and Selig) .....	40
Figure 20. Semilog Plot (Drumm et al.) .....	41
Figure 21. Semilog Plot (Jin et al.) .....	42
Figure 22. Semilog Plot (Jones and Witzak).....	43
Figure 23. Semilog Plot (Rada and Witzak) .....	44
Figure 24. Semilog Plot (Santha/Fine-grained) .....	45
Figure 25. Semilog Plot (Santha/Coarse-grained) .....	46
Figure 26. Semilog Plot (Muhann et al.).....	47
Figure 27. Variation of Modulus with Moisture by AASHTO Class .....	49
Figure 28. Linear Regression in the Semi-log Space for Fine-grained Materials .....	50, 51
Figure 29. Linear Regression in the Semi-log Space for Coarse-grained Materials ...	52, 53
Figure 30. Values of $k_s$ by Model, for Fine-grained Materials .....	54
Figure 31. Values of $k_s$ by Model for Coarse-grained Materials .....	55
Figure 32. Revised Model for Fine Grained Materials .....	58, 59
Figure 33. Revised Model for Coarse Grained Materials .....	60, 61

## Introduction

It is well known that in a pavement structure, with time, the moisture content of the unbound layers may change, due to variation in environmental conditions, producing a change in modulus as well. For purposes of design of a new pavement or evaluation of an existing one; it is necessary to predict the change in modulus corresponding to an expected or measured change in moisture content. Moisture, along with other factors, affects the resilient modulus ( $M_R$ ) of unbound materials. These factors are discussed in the following paragraphs.

### Factors Related to Soil Physical State:

- *moisture content*: all other conditions being equal, the higher the moisture content the lower the modulus; however, moisture has two separate effects:
  - First, it can affect the state of stress: through suction or pore water pressure; Because suction and water content are correlated through the “soil-water characteristic curve”, it is important to investigate if both variables are needed in a predictive model;
  - Second, it can affect the structure of the soil, through destruction of the cementation between soil particles.
- *dry density*: at low moisture contents, a lower density will give a lower  $M_R$ . The relationship is reversed for high moisture contents, as shown in Figure 1 (Seed et al. 1962). Any change in volume is reflected in a change in dry density; therefore, void ratio ( $e$ ) may be used instead of dry density.
- *degree of saturation*: a third parameter, uniquely defined by moisture content, dry density (or void ratio) and specific gravity of solids ( $G_s$ ) is the degree of saturation

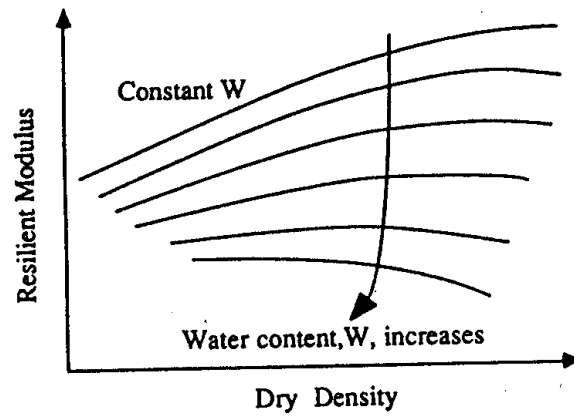


Figure 1. Influence of Dry Density on Resilient Modulus (After Seed et al. 1962)



( $S$ ). The relationship between the three physical state parameters is presented in Equations 1 and 2, depending on which parameter is used as a measure of volume changes (i.e dry density or void ratio):

$$S = \frac{w}{\left( \frac{G_s \cdot \gamma_w}{\gamma_{dry}} - 1 \right)} \quad (1)$$

$$S = G_s \cdot \frac{w}{e} \quad (2)$$

Where:

$S$  = degree of saturation (variable)

$G_s$  = specific gravity (constant)

$w$  = moisture content (variable)

$\gamma_w$  = unit weight of water (constant)

$\gamma_{dry}$  = dry unit weight (variable)

$e$  = void ratio (variable)

Equations 1 and 2 show that knowing any two of the three parameters:  $w$ ,  $S$  and  $\gamma_{dry}$ , the third may be found, provided  $G_s$  is known or can be estimated well. The use of all three parameters as predictors in a model is therefore incorrect, due to redundancy. On the other hand, the use of only one of these parameters is sufficient only if no volume change during wetting or drying (i.e. a constant dry density or void ratio) is assumed. For all cases where variations in moisture content are accompanied by volume changes, any two of the three parameters need to be used to properly predict the change in modulus, together with known  $G_s$ .

- *temperature*: becomes the most important factor in predicting the resilient modulus of frozen materials while for thawed materials it has little to no significant influence.

Factors Related to the State of Stress:

- *bulk stress*: total volumetric component – for lab test conditions such as triaxial, this stress is determined from:

$$\theta = \sigma_1 + \sigma_2 + \sigma_3$$

- *octahedral shear stress*: total deviatoric component – for triaxial test conditions this stress is determined from:

$$\tau_{oct} = \frac{1}{3} \cdot \sqrt{(\sigma_1 - \sigma_2)^2 + (\sigma_1 - \sigma_3)^2 + (\sigma_2 - \sigma_3)^2}$$

- *pore pressures/suction*: unbound materials used in pavement design are generally in a partly saturated state, especially if they fall above the phreatic surface (GWT). The state of stress in unsaturated materials can be characterized by the following parameters (Fredlund et al. (12)):

- $(\sigma_3 - u_a)$  = net confining pressure (also called net normal stress)
- $(\sigma_1 - \sigma_3)$  = deviator stress
- $(u_a - u_w)$  = matric suction

Where:

$\sigma_3$  = total confining pressure;

$\sigma_1$  = total major principal stress;

$u_a$  = pore air pressure;

$u_w$  = pore water pressure.

Matric suction greatly affects the state of stress and consequently the modulus (Gehling et al. (10), Fredlund et al. (12), Lekarp et al. 2000 (13), Drumm et al. (14), Edil and Motan (15)). For saturated elements of soil it is therefore desirable to use effective stresses (total stress minus pore water pressure) in predicting the modulus. For nearly saturated soils ( $S > 95\%$ ) where  $u_a - u_w = 0$ , using total stress minus  $u_w$  as an effective stress is normally satisfactory and this effective stress can be related to modulus. However, if the value of  $S$  is well below 95% and  $u_a - u_w$  is greater than zero, it is typically necessary to use two stress state variables,  $\sigma - u_a$  and  $u_a - u_w$ , to define the stress state which is then related to modulus. An acceptable definition of the stress state can sometimes be achieved by using total stresses, provided a parameter related to suction (e.g. water content or degree of saturation) is used in addition to the total stress. Also, both components of loading (i.e. volumetric and deviatoric) should be used (Santha (6), Andrei (16)).

Factors Related to the Structure/Type of Material:

- *compaction method;*
- *particle sizes (grain size distribution);*
- *particle shape (related to friction);*
- *nature of the bonds between particles and their sensitivity to water (moisture).*

In the field, unbound materials used in pavements are typically first compacted to moisture and density near the optimum, and then, with time, the moisture content will reach an equilibrium condition which varies depending on drainage properties and environmental conditions. In order to simulate this variation in the lab, it is recommended to first compact the specimens at optimum moisture content and maximum dry density

and then vary the moisture content (by soaking or drying) until the desired moisture content is achieved. Then, the resilient modulus test should be performed. Especially in the case of fine-grained (cohesive) soils, compacting directly at the desired moisture content and density can result in specimens with a different structure, that do not model the structure of the material in actual field conditions, because of path dependency for wetting or drying.

### **Objective**

The objective of this study was to select and then summarize existing models from the literature that incorporate the variation of resilient modulus with moisture. Using these published literature models, it was then desirable to select a model or models that would analytically predict changes in modulus due to changes in moisture. This model (models) will then be considered for implementation in the 2002 Guide for the Design of New and Rehabilitated Pavement Structures.

### **Analysis and Assumptions**

When plotting resilient modulus versus moisture for a given material, distinct curves are obtained depending on the variation of density. Therefore, constant dry density, decreasing density (swell), increasing dry density (collapse) or variable dry density (e.g. along the compaction curve) will plot, for the same material, as four different curves. Ideally, to avoid confusion and to obtain comparable plots, the best curve to use is the one that simulates the volume changes expected to occur in field for that material. However, data describing variation in dry density which is realistic for the field was

available for only one of the models. For this model, test specimens were compacted at optimum conditions and then the moisture content was varied (by soaking/drying).

Typical moisture/density combinations specific to each specimen before testing are presented in Figure 2.

For all other models, specimens were prepared directly at the desired moisture/density combinations and tested, rather than wetted or dried at a fixed stress conditions. This method has the advantage of allowing one to get data points at constant compactive effort (along the compaction curve) or at constant dry density, as shown in Figures 3 and 4.

Having a model that predicts how the modulus varies with moisture/density combinations along the compaction curve may be useful in predicting the modulus at 90% or 95% percent compaction or other intermediate values but does not simulate field conditions.

The variation of the modulus at constant dry density is reasonably close to the actual behavior of materials that do not suffer significant changes in volume with variation in moisture (only in terms of density, not structure).

Given the lack of information on the expected density variation due to changes in moisture for the great majority of the considered models/materials, and in order to obtain comparable plots of modulus versus moisture, the dry density was assumed to remain constant for all models/materials. The constant value assumed was the maximum dry density corresponding to optimum conditions for a particular material. All other parameters (moisture content, void ratio, degree of saturation) were back calculated accordingly. An immediate drawback of this assumption is that the modulus depends only on moisture content, dry density (or void ratio) is constant and saturation becomes a linear function of moisture (see Equations 1 and 2).

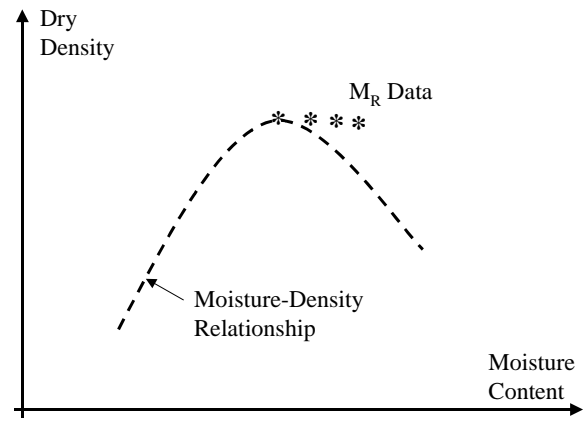


Figure 2. Post-Compaction Variation in Moisture Content

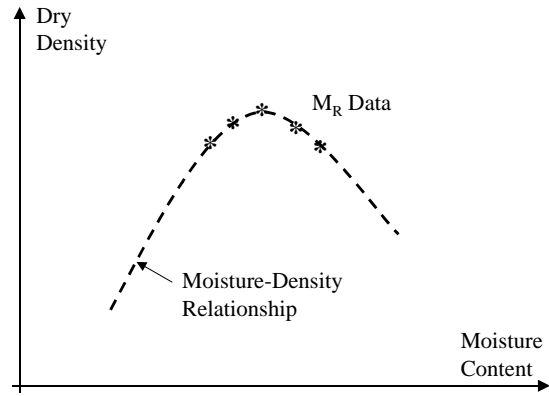


Figure 3. Data Points at Constant Compactive Effort

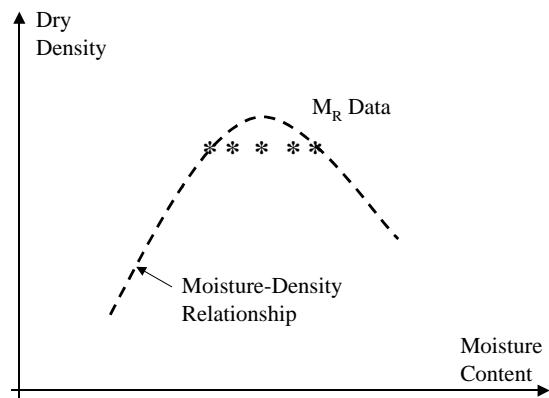


Figure 4. Data Points at Constant Dry Density

## Summary of Models

### *Li & Selig Models for Fine-grained Subgrade Soils*

In this model, the variation of the modulus ( $M_R$ ) is predicted relative to the resilient modulus of the material at optimum moisture content and maximum dry density (Li and Selig, (1)). The only predictor variable used is the moisture content and two models are developed: one for variation of the modulus at constant dry density, the other for variation of the modulus at constant compactive effort. The models were developed using test data available in literature, namely 27 resilient modulus tests on 11 fine-grained soils for the first model and 26 tests on 10 fine-grained soils for the second. The data is representative of various compactive efforts.

$$R_{m1} = \frac{M_R}{M_{R(opt)}} = 0.98 - 0.28 \cdot (w - w_{opt}) + 0.029 \cdot (w - w_{opt})^2 \quad (3-a)$$

$$(R^2 = 0.76)$$

$M_R$  = resilient modulus at moisture content  $w$  (%) and the **same dry density** as  $M_{R(opt)}$ ;

$M_{R(opt)}$  = resilient modulus at maximum dry density and optimum moisture content  $w_{opt}$  (%) for any compactive effort.

$$R_{m2} = \frac{M_R}{M_{R(opt)}} = 0.96 - 0.18 \cdot (w - w_{opt}) + 0.0067 \cdot (w - w_{opt})^2 \quad (3-b)$$

$$(R^2 = 0.83)$$

Where:

$M_R$  = resilient modulus at moisture content  $w$  (%) and the **same compactive effort** as

$M_{R(opt)}$ ;



$M_{R(opt)}$  = resilient modulus at maximum dry density and optimum moisture content  $w_{opt}$  (%) for any compactive effort.

The variation in modulus with respect to moisture content and degree of saturation as predicted by the mentioned models is presented in Figure 5.

An attempt was made by the authors to use normalized water content ( $w/w_{opt}$ ) as a predictor variable but the correlation was poorer.

Note that the models (3-a, 3-b) are irrational for  $(w-w_{opt}) = 0$ , where the value of the ratio is 0.98 and respectively 0.96 instead of 1.00. Given the nature of the data used in calibration, it was assumed that the variation of the modulus with moisture is independent of variation in compactive effort or state of stress.

The general trends noted by the authors are:

- the lower the water content , the higher the modulus (at constant dry density, or at constant compactive effort);
- at lower moisture contents, the modulus tends to increase with increasing dry density, whereas at higher moisture contents the modulus tends to decrease with increasing dry density.

The idea of plotting normalized modulus ( $M_R/MR_{(opt)}$ ) versus normalized moisture content ( $w-w_{opt}$ ) or normalized saturation degree ( $S-S_{opt}$ ) was adopted and used for all the models presented in this summary.

### ***Drumm et al. Model for Fine-grained Subgrade Soils***

Another model that uses  $M_{R(opt)}$  as a reference value (Drumm et al (2)) is based on the linear relationship observed between resilient modulus and degree of saturation, as shown in Figure 6.

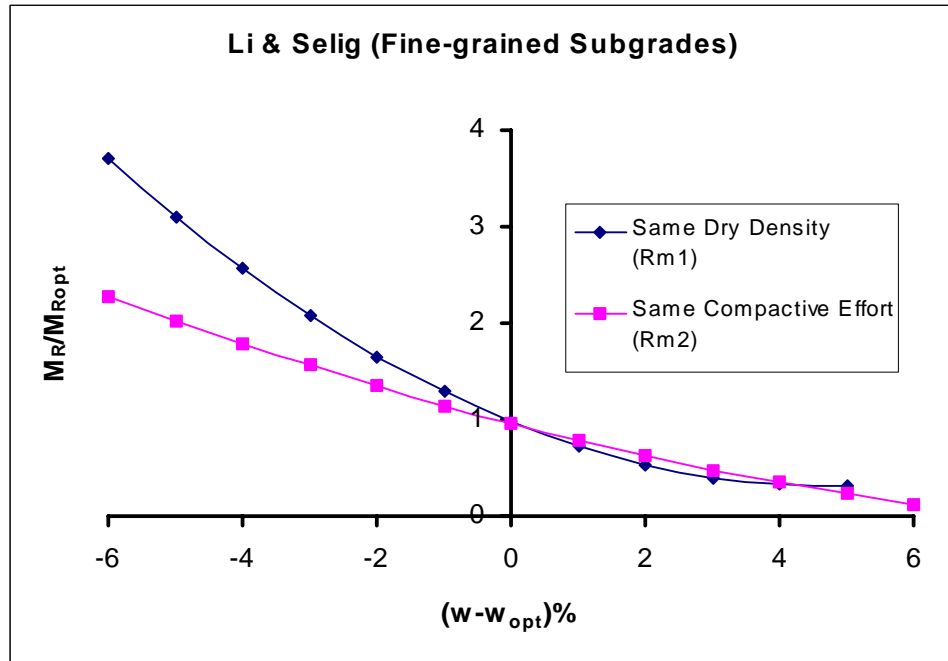


Figure 5a. Variation of the Resilient Modulus with Moisture

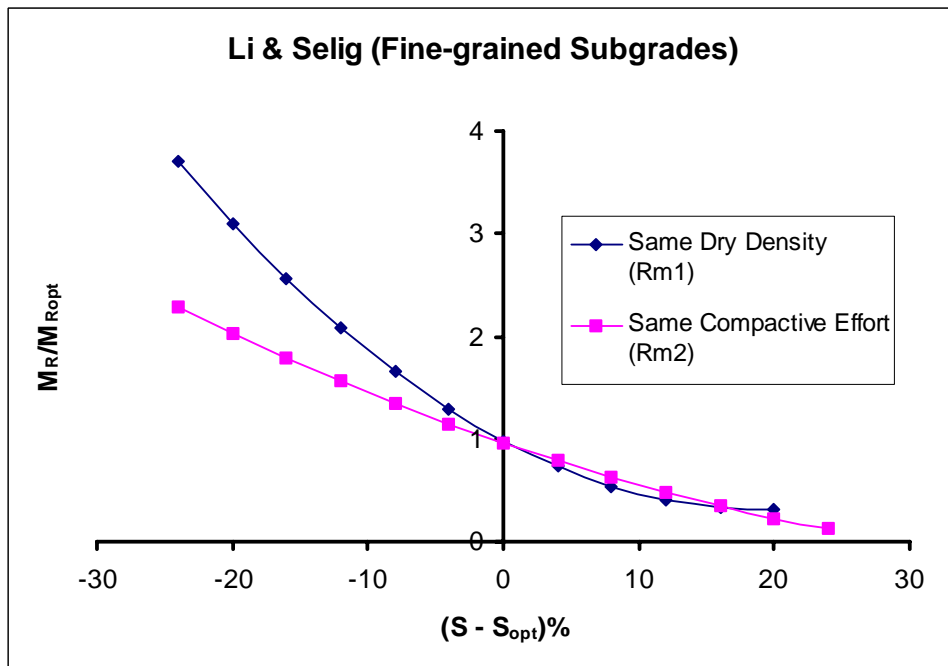


Figure 5b. Variation of the Resilient Modulus with Saturation

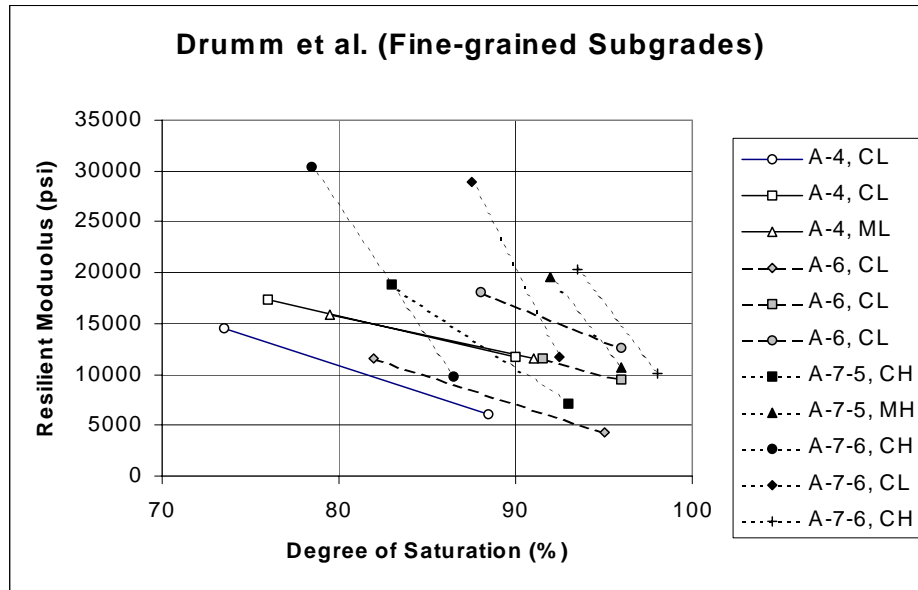


Figure 6. Effects of Post-Compaction Saturation on Resilient Modulus

$$M_{R(wet)} = M_{R(opt)} + \frac{dM_R}{dS} \cdot \Delta S \quad (4-a)$$

Where:

$M_{R(wet)}$  = resilient modulus at increased postcompaction saturation (MPa);

$M_{R(opt)}$  = resilient modulus at optimum moisture content and maximum dry density (MPa);

$\Delta S$  = change in postcompaction degree of saturation (expressed as a decimal);

$dM_R/dS$  = gradient of resilient modulus with respect to saturation, or the slope of the  $M_R$  versus degree of saturation curve (MPa) (see Table 1).

The rate of change  $dM_R/dS$  may be obtained from the given table, measured experimentally or predicted using:

$$\frac{dM_R}{dS} = 1,690 - 194 \cdot (CLASS) - 11.2 \cdot [M_{R(opt)}] \quad (4-b)$$

Where:

CLASS = AASHTO classification (e.g. for A-4, CLASS = 4.0; A-7-5, CLASS = 7.5)

$M_{R(opt)}$  = resilient modulus (MPa) at optimum moisture content and maximum dry density for  $\sigma_c = 41$  kPa (6 psi) and  $\sigma_d = 28$  kPa (4 psi).

The model can only be used for wet of optimum conditions. In all tests, the water content was increased after saturation – to simulate field variation in moisture content. It was observed that the lower the saturation, the higher the modulus (at any state of stress). The saturation degree  $S$  is considered to be a better predictor variable (than  $w$ ) since it takes into account variations in both moisture and density (another alternative is the volumetric water content). A normalized plot of the modulus with respect to variation in moisture and degree of saturation is presented in Figure 7.

Table 1. Gradient of Resilient Modulus with Respect to Saturation Degree

Soil Classification		Resilient Modulus Gradient ( $dM_R/dS$ )
AASHTO	USCS	(Measured)
A-4	CL	-390
A-4	CL	-280
A-4	ML	-260
A-6	CL	-390
A-6	CL	-330
A-6	CL	-470
A-7-5	CH	-810
A-7-5	MH	-1540
A-7-6	CH	-1780
A-7-6	CL	-2390
A-7-6	CH	-1560

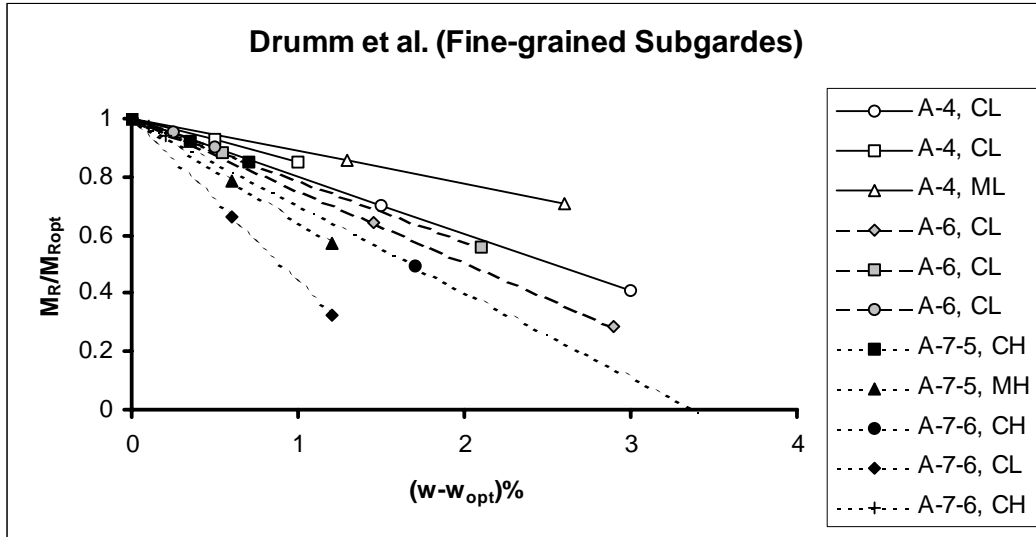


Figure 7a. Normalized Modulus Versus Back Calculated Variation in Moisture Content  
(No Volume Changes Assumed)

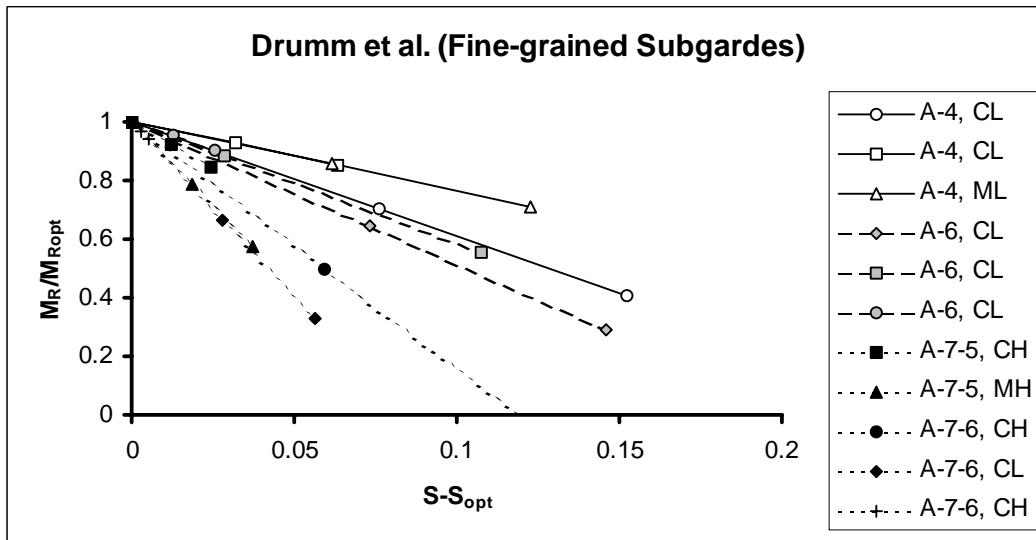


Figure 7b. Normalized Modulus Versus Back Calculated Variation in Degree of Saturation  
(No Volume Changes Assumed)

Figure 7a shows moisture content values back calculated assuming a constant dry density; in Figure 8, the actual measured moisture contents are used, in order to show the influence of volume changes upon moisture content. The need for an assumption regarding the variation of density is illustrated by soils A-4, CL, 2; A-6, CL, 3 and A-7-5, CH. For these materials, a reduction in volume makes the saturation degree increase even if the moisture content stays constant or decreases. This supports the idea that moisture content alone is not sufficient as a predictor variable. However, assuming a constant dry density, moisture content will always increase with increased saturation (see Equations 1, 2).

***Jin et al. Model for Coarse-grained Subgrade Soils***

The next model (Jin et al. (3)) has a different structure, and attempts to capture the effects of moisture, dry density, state of stress and temperature. The model was developed using data from two sites instrumented with moisture-temperature cells. Data was available for a period of two years, for two granular subgrade materials, and the following relationship was obtained:

$$\log M_R = c_1 + c_2 \cdot \log(\theta) + c_3 \cdot (w\%) + c_4 \cdot (T) + c_5 \cdot (\gamma_d) \quad (5)$$

Where:

$M_R$  = resilient modulus (MPa);

$\theta$  = bulk stress (kPa);

$w\%$  = percent water content (%);

$T$  = temperature (°C);

$\gamma_d$  = dry density (kg/m<sup>3</sup>).

$c_i$  = regression constants:

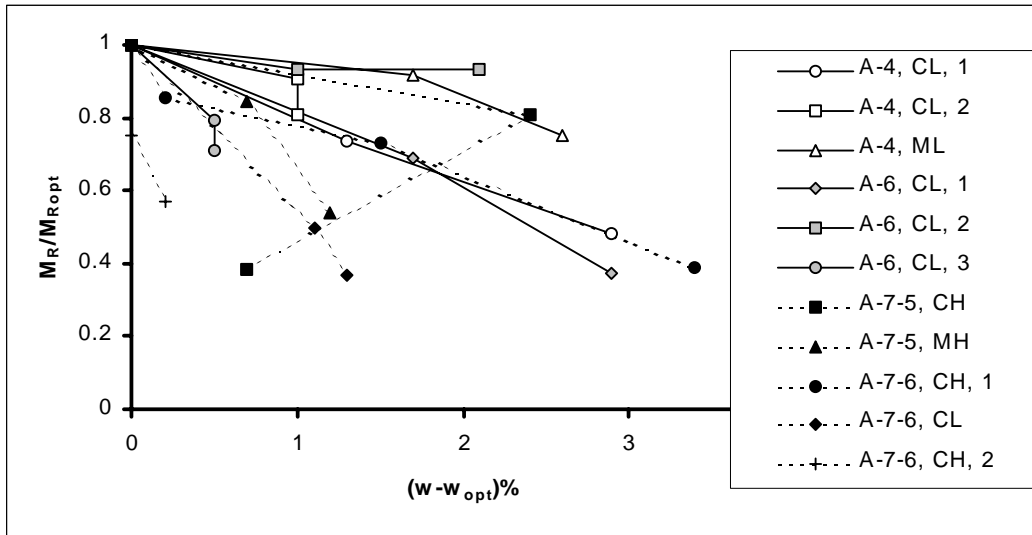


Figure 8. Normalized Modulus Versus Measured Variation in Moisture Content



	$c_1$	$c_2$	$c_3$	$c_4$	$c_5$	$R^2$
<b><i>Soil 1</i></b>	0.8956	0.278	-0.0202	-0.0091	0.0038	0.82
<b><i>Soil 2</i></b>	-3.1895	0.535	-0.00862	-0.0084	0.0021	0.72

The predicted variation of modulus with moisture/saturation is presented in Figure 9.

The model is in fact a log-log  $k_1$ - $k_2$  model in which  $k_2 = c_2$  and  $\log k_1 =$

$(c_1 + c_3(w\%) + c_4(T) + c_5(\gamma_d))$ ; it is therefore assumed that  $k_2$  is not a function of moisture, density or temperature and only  $k_1$  is influenced by these parameters. Hence, the higher the moisture content, the lower  $k_1$ , i.e. the lower the modulus.

#### ***Jones and Witczak Model for Fine-grained Subgrade Soils***

A simpler model with a similar structure (Jones, Witczak (4)) is presented here: two variables related to moisture are used for prediction: water content and saturation degree.

$$\log M_R = c_1 + c_2 \cdot (w\%) + c_3 \cdot (S) \quad (6)$$

Where:

$M_R$  = resilient modulus (ksi) at 6 psi deviatoric stress and 2 psi confining stress;

$w\%$  = percent water content (%);

$S$  = degree of saturation(%).

$c_i$  = regression constants:

	$c_1$	$c_2$	$c_3$	$R^2$
<b><i>Undisturbed Samples</i></b>	2.31909	-0.13282	0.013405	0.97
<b><i>Disturbed Samples</i></b>	1.17869	-0.111109	0.021699	0.67

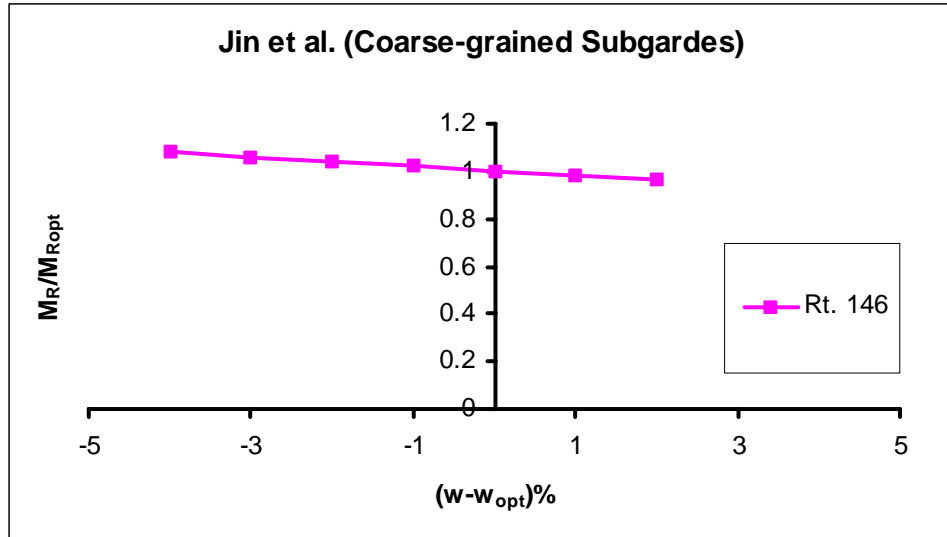


Figure 9a. Normalized Modulus Versus Variation in Moisture Content

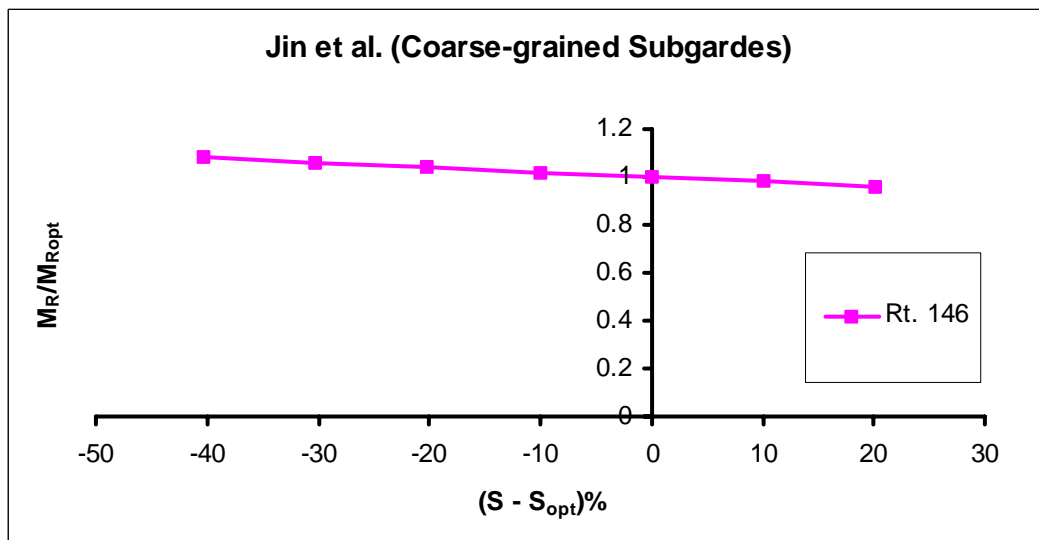


Figure 9b. Normalized Modulus Versus Variation in Degree of Saturation

The model was developed for both undisturbed (in-situ) and lab-compacted subgrade soils at the San Diego Test Road. They only predict for a given state of stress. Predicted resilient modulus values along curves of constant saturation are presented for both sets of coefficients in Figure 10. Normalized plots are presented for disturbed (lab-compacted) samples in Figure 11.

### ***Rada and Witczak Model for Base/Subbase Materials***

The next model (Rada, Witczak (5)) has a similar form but takes into account the effect of the state of stress and percent compaction of a variety of granular material used as subbase and base courses in the state of Maryland. The model form is:

$$\log M_R = c_1 + c_2 \cdot (S) + c_3 \cdot PC + c_4 \cdot \log(\theta) \quad (7)$$

Where:

$M_R$  = resilient modulus (psi);

$\theta$  = bulk stress (psi);

$S$  = degree of saturation (%);

$PC$  = percentage compaction relative to modified density (%).

$c_i$  = regression constants are given in Table 2.

This model is also a log-log  $k_1$ - $k_2$  model in which  $k_2 = c_4$  and  $\log k_1 = (c_1 + c_2(S) + c_3(PC))$ .

It is therefore assumed that  $k_2$  is not a function of moisture, density or temperature and only  $k_1$  is influenced by these parameters. The variation of the modulus with moisture/saturation is presented for all materials in Figure 12.

### ***Santha's Models for Coarse-grained and Fine-grained Subgrade Soils***

Santha used a different approach to predict how the regression constants of a predictive  $M_R$  model would vary depending on moisture, density and other parameters (Santha (6)).

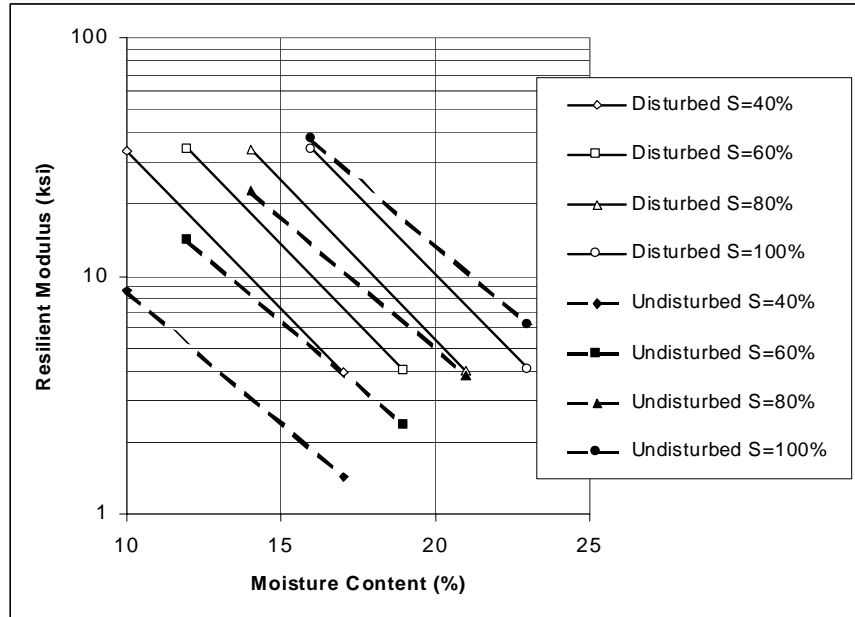


Figure 10. Relation between Modulus, Moisture Content and Degree of Saturation (Jones and Witczak)

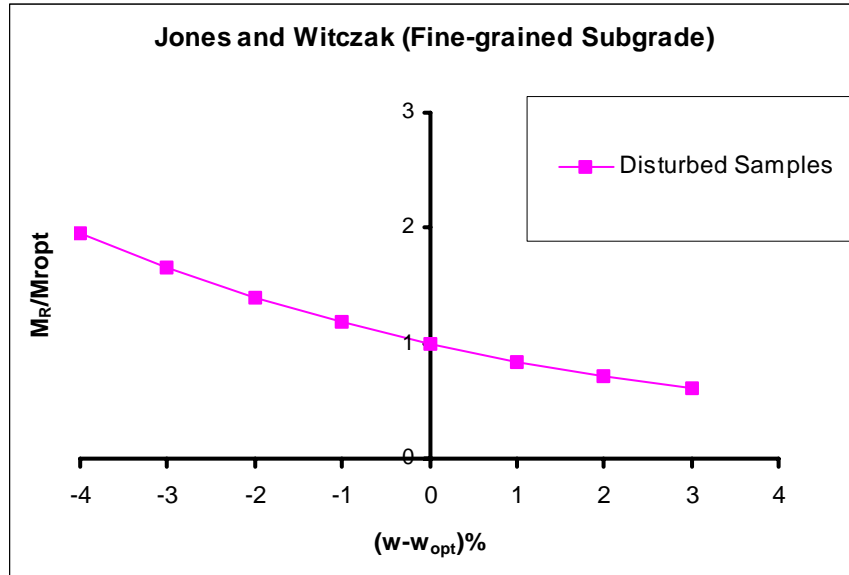


Figure 11a. Normalized Modulus Versus Variation in Moisture Content

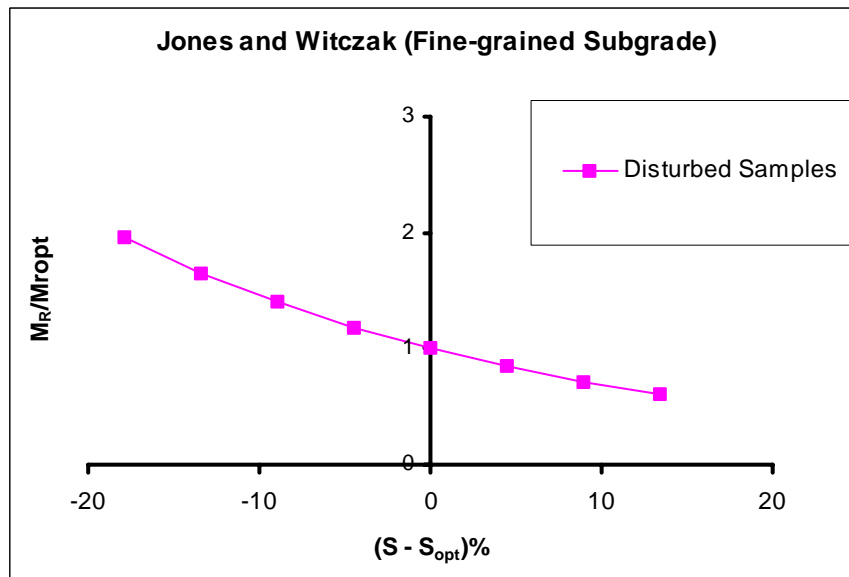


Figure 11b. Normalized Modulus Versus Variation in Degree of Saturation

Table 2. Regression Coefficients (Rada and Wiczak Model for Base/Subbase Materials)

<i>Aggregate</i>	$c_1$	$c_2$	$c_3$	$c_4$	$R^2$
DGA-limestone-1	3.4060	-0.005289	0.01194	0.4843	0.79
DGA-limestone-2	-0.3017	-0.005851	0.05054	0.4445	0.60
CR-6-crushed stone	1.0666	-0.003106	0.03556	0.6469	0.81
CR-6-slag	3.2698	-0.003999	0.01663	0.3840	0.59
Sand-aggregate blend	4.1888	-0.003312	0.02138	0.6785	0.83
Bank-run gravel	0.9529	-0.01207	0.04117	0.6035	0.84
All data	4.022	-0.006832	0.007055	0.5516	0.61

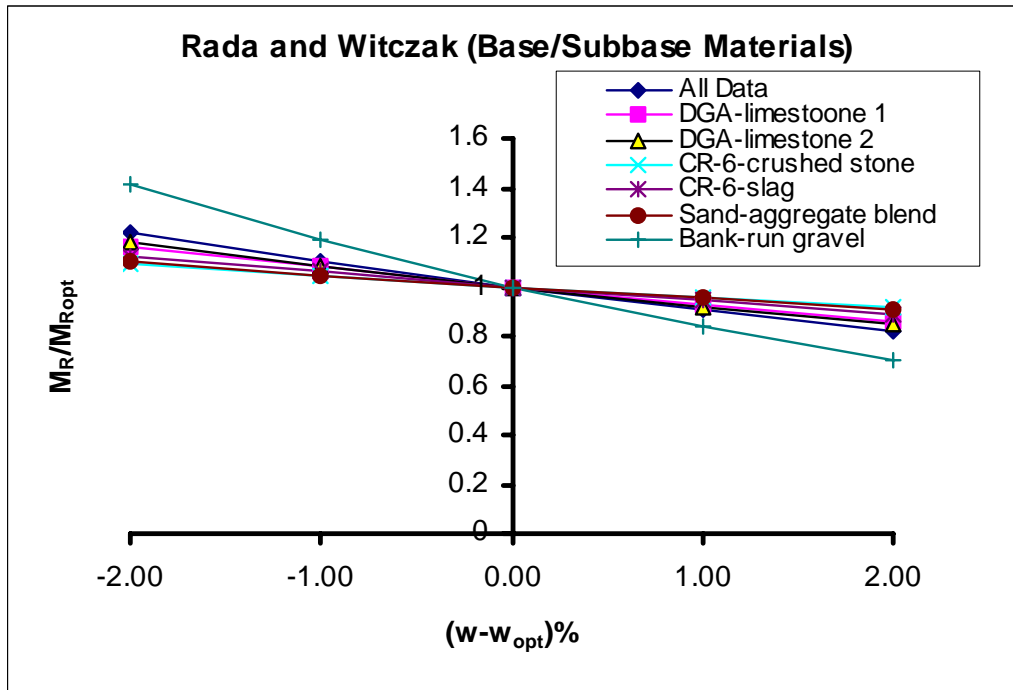


Figure 12a. Normalized Modulus Versus Variation in Moisture Content

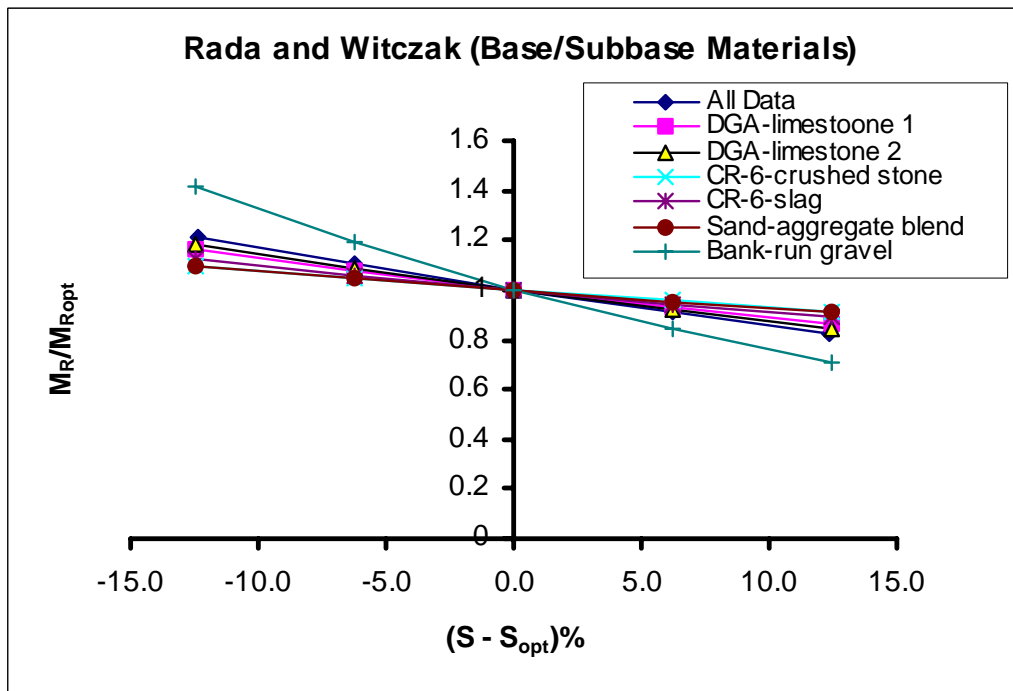


Figure 12b. Normalized Modulus Versus Variation in Degree of Saturation

Given the model:

$$M_R = k_1 \cdot p_a \cdot \left( \frac{\theta}{p_a} \right)^{k_2} \cdot \left( \frac{\tau_{oct}}{p_a} \right)^{k_3}$$

Then,

For Granular Materials: (8-a)

$$\log k_1 = 3.479 - 0.07 \cdot MC + 0.24 \cdot \frac{MC}{MOIST} + 3.681 \cdot COMP + 0.011 \cdot SLT + 0.006 \cdot CLY - \\ - 0.025 \cdot SW - 0.039 \cdot DEN + 0.004 \cdot \frac{SW^2}{CLY} + 0.003 \cdot \frac{DEN^2}{S40}$$

$$(R^2 = 0.94)$$

$$k_2 = 6.044 - 0.053 \cdot MOIST - 2.076 \cdot COMP + 0.0053 \cdot SATU - 0.0056 \cdot CLY + 0.0088 \cdot SW - \\ - 0.0069 \cdot SH - 0.027 \cdot DEN + 0.012 \cdot CBR + 0.003 \cdot \frac{SW^2}{CLY} - 0.31 \cdot \frac{SW + SH}{CLY}$$

$$(R^2 = 0.96)$$

$$k_3 = 3.752 - 0.068 \cdot MC + 0.309 \cdot MCR - 0.006 \cdot SLT + 0.0053 \cdot CLY + 0.026 \cdot SH - \\ - 0.033 \cdot DEN - 0.0009 \cdot \frac{SW^2}{CLY} + 0.00004 \cdot \frac{SATU^2}{SH} - 0.0026 \cdot (CBR \cdot SH)$$

$$(R^2 = 0.87)$$

For Cohesive Materials: (8-b)

$$\log k_1 = 19.813 - 0.045 \cdot MOIST - 0.131 \cdot MC - 9.171 \cdot COMP + 0.037 \cdot SLT + 0.015 \cdot LL - \\ - 0.016 \cdot PI - 0.021 \cdot SW - 0.052 \cdot DEN + 0.00001 \cdot (S40 \cdot SATU)$$

$$(R^2 = 0.95)$$

$$k_3 = 10.274 - 0.097 \cdot MOIST - 1.06 \cdot MCR - 3.471 \cdot COMP + 0.0088 \cdot S40 - 0.0087 \cdot PI + \\ + 0.014 \cdot SH - 0.046 \cdot DEN$$

$$(R^2 = 0.88)$$

Where:

MC = moisture content (%);



SATU = percent saturation (%);

COMP = percent compaction (%);

MOIST = optimum moisture content (%);

S40 = percent passing #40 sieve (%);

CLY = percentage of clay (%);

SLT = percentage of silt (%);

SW = percent swell (%);

SH = percent shrinkage (%);

DEN = maximum dry unit weight (pcf)

CBR = California Bearing Ratio

This is the first model that recognizes that  $k_2$  and  $k_3$  are not necessarily constant but may vary with moisture and other material properties. Repeating the stepwise regression on a larger database will probably eliminate some of the terms/predictor variables currently used. Normalized plots are presented in Figures 13 and 14, for granular materials and for cohesive materials.

### ***CRREL Model for Frozen Coarse-grained/Fine-grained Subgrade Soils***

A power model (CRREL (8)) for frozen materials is presented below:

$$M_R = k_1 \cdot f(w)^{k_2} \quad (9-a)$$

Where all symbols are explained in Table 3 and:

n = number of stress points;

$R^2$  = coefficient of determination;

$w_{u-g}$  = gravimetric unfrozen water content (%);

$w_t$  = gravimetric total water content (%);

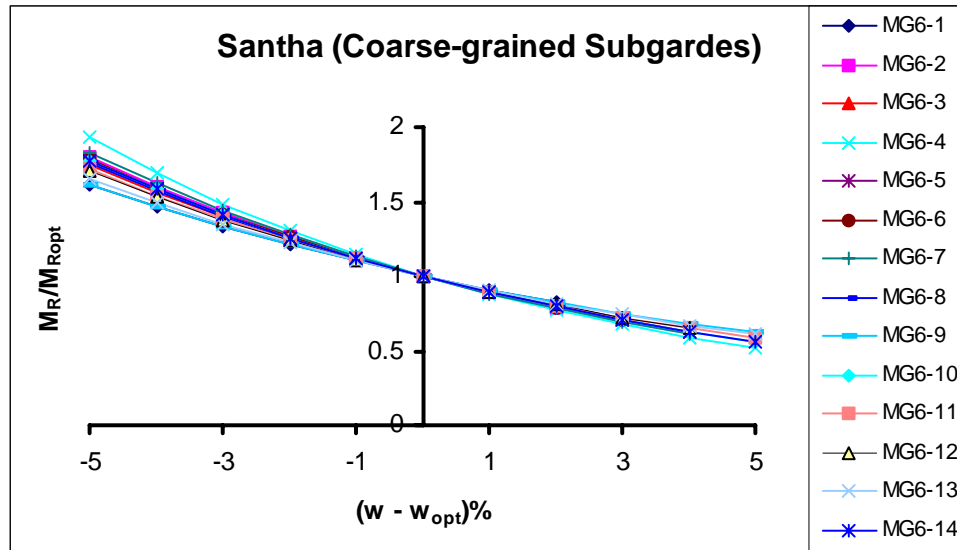


Figure 13a. Normalized Modulus Versus Variation in Moisture Content  
for Coarse-grained Soils

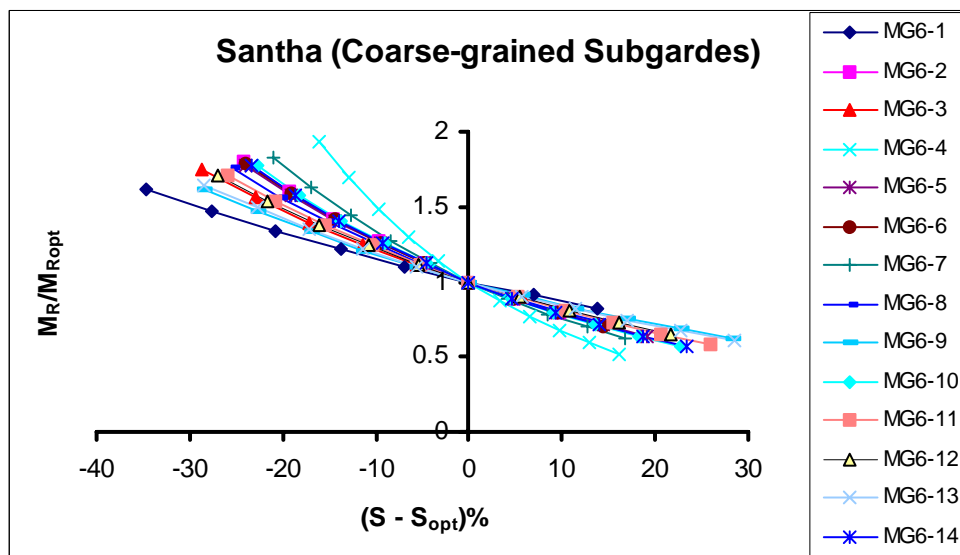


Figure 13b. Normalized Modulus Versus Degree of Saturation  
for Coarse-grained Soils

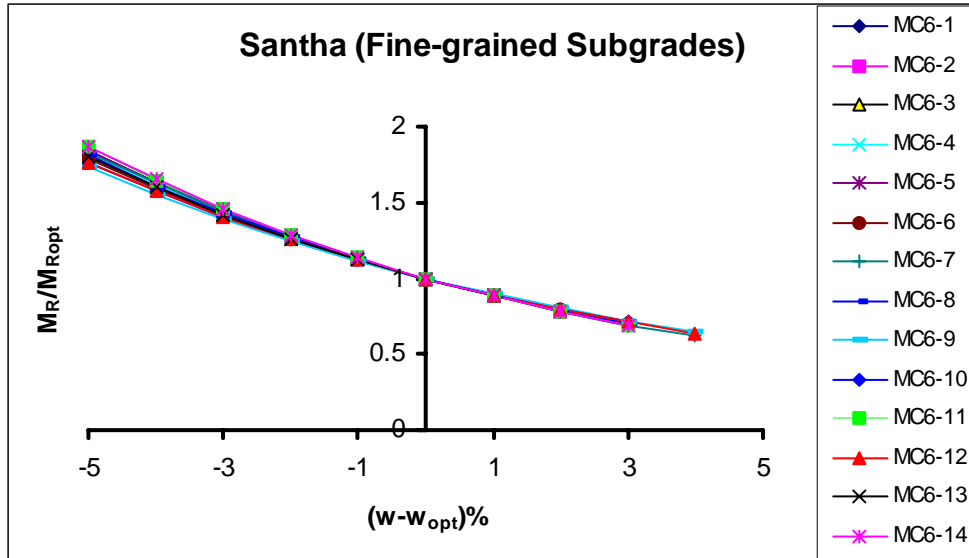


Figure 14a. Normalized Modulus Versus Variation in Moisture Content  
for Fine-grained Soils

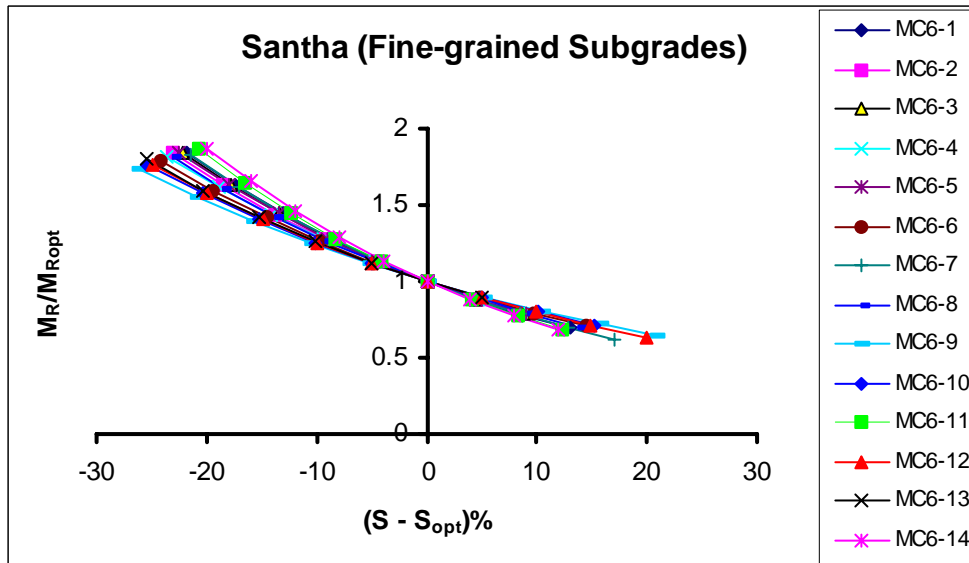


Figure 14b. Normalized Modulus Versus Degree of Saturation  
for Fine-grained Soils

Table 3. Regression Coefficients and Symbols for Equation 9-a

Material	$f(w)$	$k_1$	$k_2$	n	$R^2$
Clay/1206	$w_{u-g}/w_t$	1087	-5.259	207	0.99
	$w_{u-g}/w_0$	1049	-2.344	207	0.99
	$w_{u-v}/w_0$	1052	-2.929	207	0.99
Clay/1232	$w_{u-g}/w_t$	905	-4.821	244	0.98
	$w_{u-g}/w_0$	846	-2.161	244	0.98
	$w_{u-v}/w_0$	848	-2.633	244	0.98
Class 3	$w_{u-g}/w_t$	5824	-2.026	186	0.97
	$w_{u-g}/w_0$	5488	-1.076	210	0.97
	$w_{u-v}/w_0$	5542	-1.249	186	0.97
Class 4	$w_{u-g}/w_t$	2826	-5.220	69	0.92
	$w_{u-g}/w_0$	1813	-1.733	85	0.93
	$w_{u-v}/w_0$	1.652	-2.813	69	0.91
Class 5	$w_{u-g}/w_t$	11320	-2.036	28	0.97
	$w_{u-g}/w_0$	8695	-1.2814	28	0.95
	$w_{u-v}/w_0$	9245	-1.489	28	0.97
Class 6	$w_{u-g}/w_t$	19924	-1.243	260	0.98
	$w_{u-g}/w_0$	19427	-0.795	260	0.98
	$w_{u-v}/w_0$	19505	-0.897	260	0.98

$w_{u-v}$  = volumetric unfrozen water content (%);

$w_0$  = unit water content (1.0%)

The governing parameter for frozen materials is the unfrozen water content ( $w_u$ ) which is directly related to temperature according to equation (9-b)

$$w_{u-g} = \frac{\alpha}{100} \cdot \left( \frac{-T}{T_0} \right)^\beta ; T < 0^\circ C \quad (9-b)$$

Where:

$w_{u-g}$  = gravimetric unfrozen water content, in decimal form

T = temperature, °C

$T_0 = 1.0^\circ C$

$\alpha, \beta$  = material constants

Since the total water content (frozen + unfrozen) remains constant, the variation in unfrozen water content is in fact a measure of temperature variation, as illustrated in Figure 15.

### ***Muhanna et al. Model for Fine-grained Subgrade Soils***

The last model presented predicts plastic and resilient deformation instead of  $M_R$

(Muhanna, Rahman, Lambe (9)):

$$\log \frac{\sum \varepsilon_p^*}{SL^{\frac{7}{4}} \cdot e} = 1.3 + 2.476 \cdot \frac{w - w_o}{w_o} \quad (10-a)$$

( $R^2 = 0.915$ )

$$SL = \frac{\sigma_d}{\sigma_{df}}$$

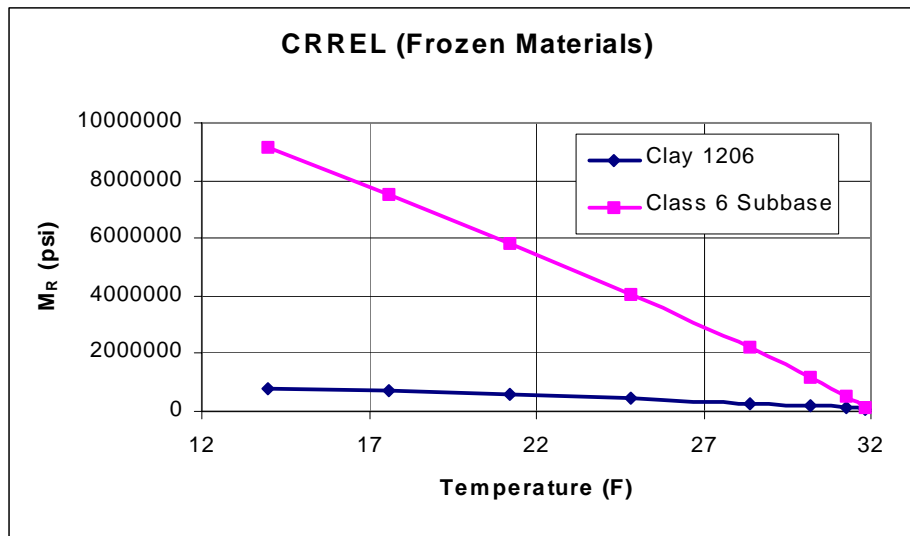


Figure 15. Variation of Modulus with Temperature for Frozen Materials

$$\frac{\varepsilon_r^*}{\left(1 - \frac{w - w_o}{w_o}\right)^4} = 0.0132 + 0.27 \cdot \sum \varepsilon_p^* \quad (10-b)$$

$$(R^2 = 0.94)$$

Where:

$\Sigma \varepsilon_p^*$  = total plastic deformation at “apparent shakedown” (%);

Apparent Shakedown State = when, after a large number of repetitions, the plastic strain is not significant (as opposed to Ratcheting State where the sample fails due to too large accumulated plastic strain).

SL = stress level;

$\sigma_d$  = deviatoric stress (kPa);

$\sigma_{df}$  = deviatoric stress at failure or at 5.0 % axial strain (kPa);

e = void ratio (decimal);

w = molding water content (%);

$w_o$  = optimum moisture content (%);

$\varepsilon_r^*$  = resilient strain at “apparent shakedown” (%).

Instead of predicting the resilient modulus, the model predicts the resilient and the total accumulated plastic deformation. Only moisture content and stress level are used as predictor variables. The variation of the modulus with moisture/saturation is presented in Figure 16.

## Summary

The variation of the modulus with moisture and density is captured by most of the models. Degree of saturation ( $S$ ), gravimetric or volumetric moisture content ( $w$ ) and

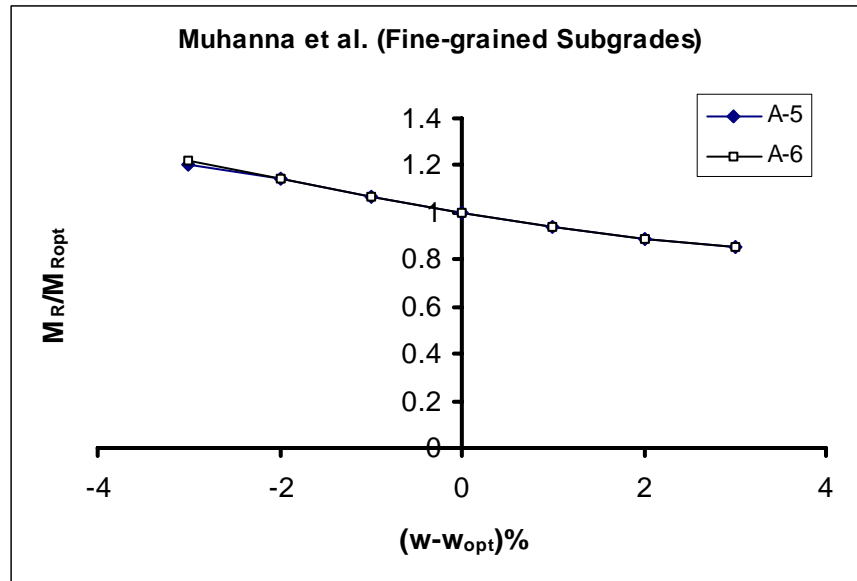


Figure 16a. Normalized Modulus Versus Variation in Moisture Content

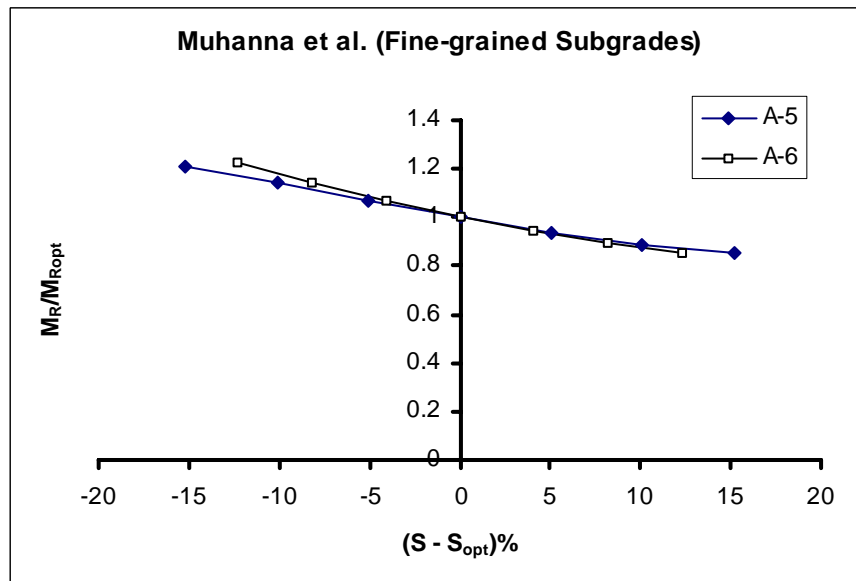


Figure 16b. Normalized Modulus Versus Variation in Degree of Saturation



suction ( $u$ ) are used to describe the effects of moisture on resilient modulus. The state of stress is described by using stress invariants ( $\theta$ ,  $\tau_{oct}$ ) or stress levels ( $\sigma_d/\sigma_{dfailure}$ ). The influence of the other parameters specific to each material is reflected by the values of the regression constants  $c_i$  or  $k_i$ . For Santha's Models, the values of the regression constants are predicted using gradation, Atterberg limits, specific gravity and other soil properties. A general trend for fine-grained materials is observed in Figure 17. A similar plot is developed for all course-grained materials (Figure 18).

### Proposed Model

An alternative way to look at the data is to plot the modulus ratio on a log scale. This would make, for example, a ratio of 3 to plot as far from 1 ( $M_R = M_{Ropt}$ ) as a ratio of 1/3, which is more rational since, in both cases, the initial modulus is three times larger than the final modulus (assume increasing moisture content). Individual plots of  $\log(M_R/M_{Ropt})$  versus moisture/saturation are presented in Figures 19 through 26 for all considered models. The plots show that using the log scale for the modulus ratio, all models approach a linear relationship, of the form:

$$\log \frac{M_R}{M_{Ropt}} = k_w \cdot (w - w_{opt}) \quad (11-1)$$

Where:

$M_R$  = resilient modulus at moisture content  $w$  (%);

$M_{R(opt)}$  = resilient modulus at maximum dry density and optimum moisture content  $w_{opt}$  (%);

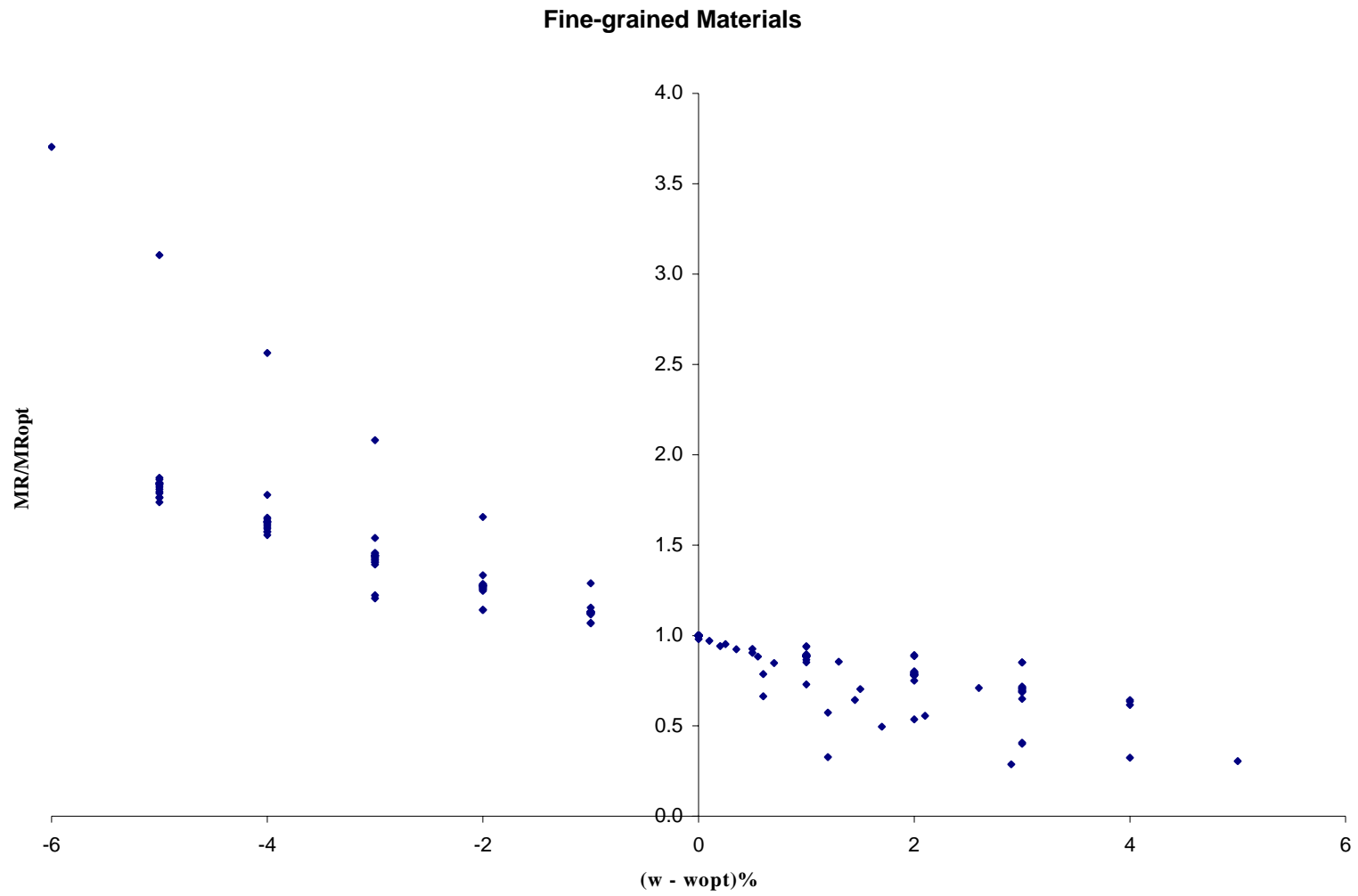


Figure 17a. Variation of Modulus with Moisture for all Fine-grained Materials

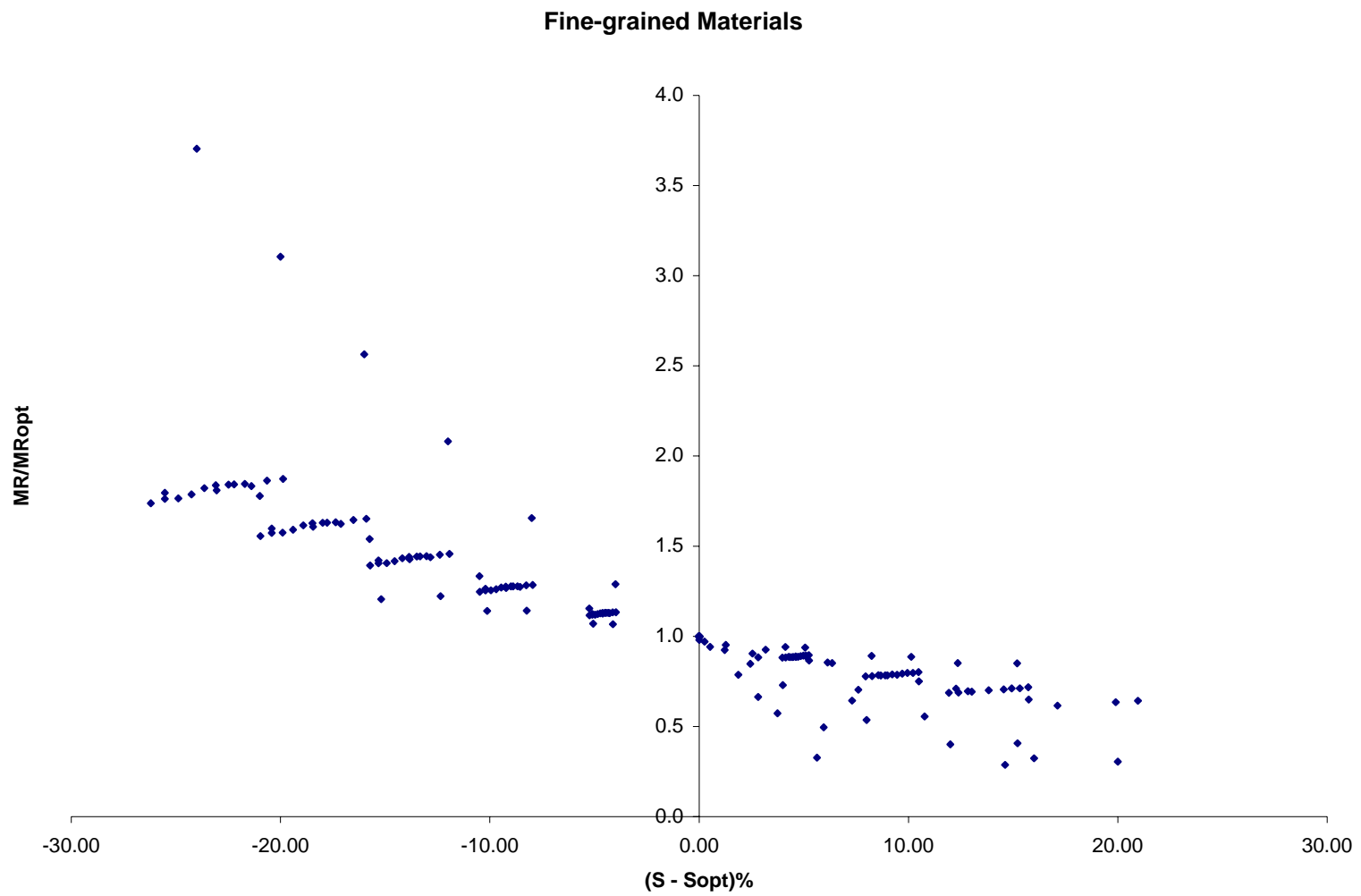


Figure 17b. Variation of Modulus with Degree of Saturation for all Fine-grained Materials

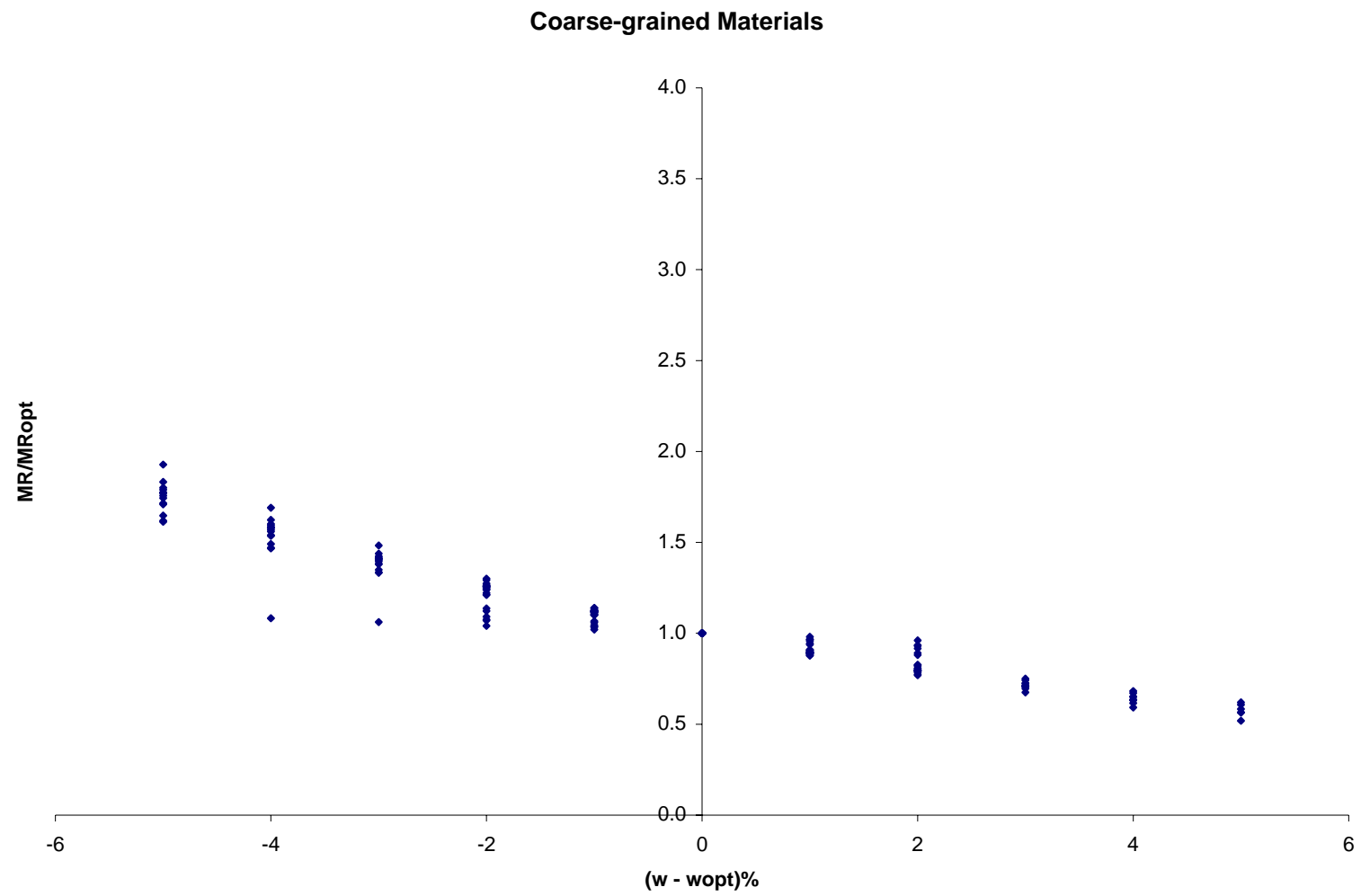


Figure 18a. Variation of Modulus with Moisture for all Coarse-grained Materials

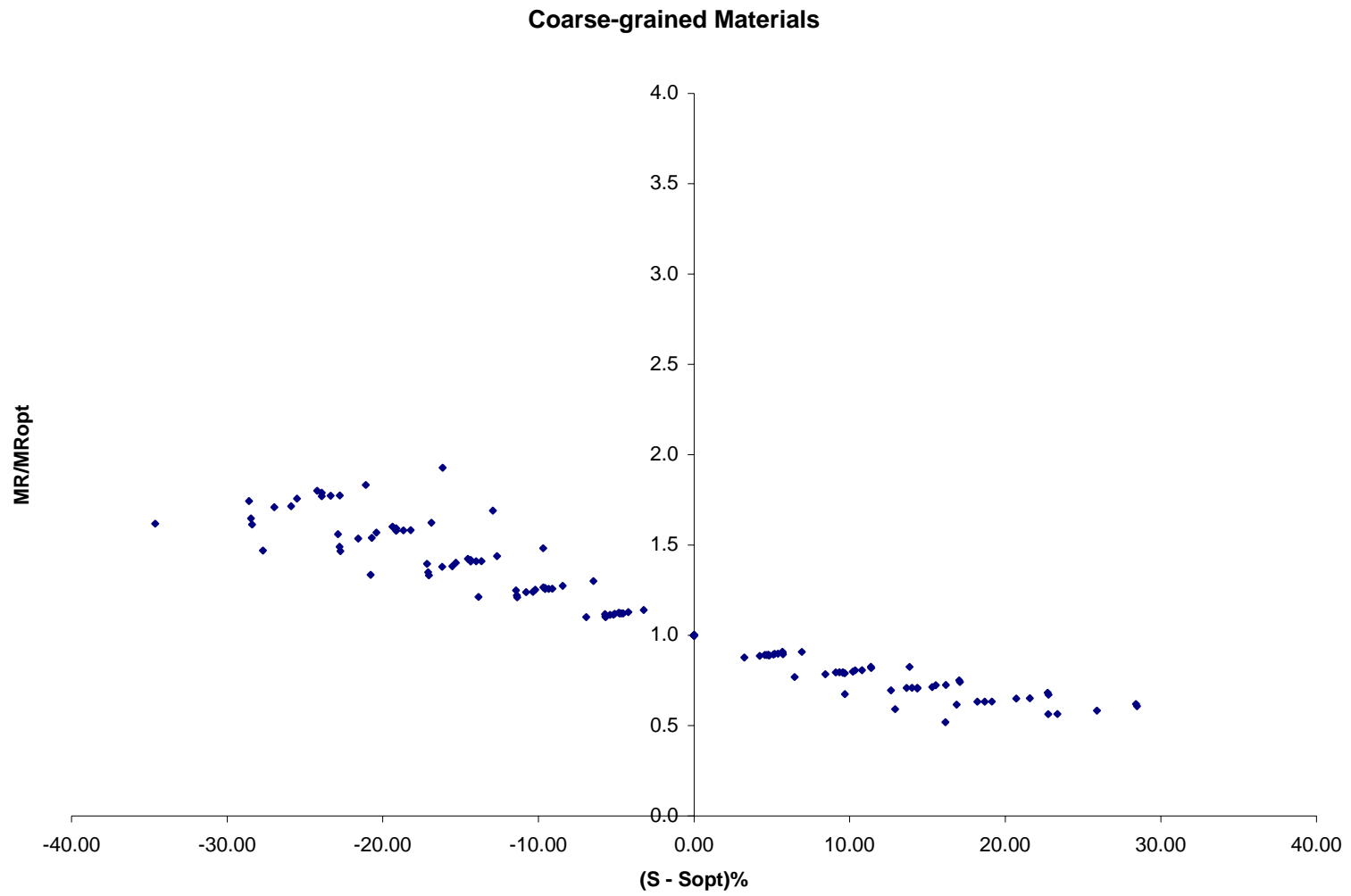


Figure 18b. Variation of Modulus with Degree of Saturation for all Coarse-grained Materials

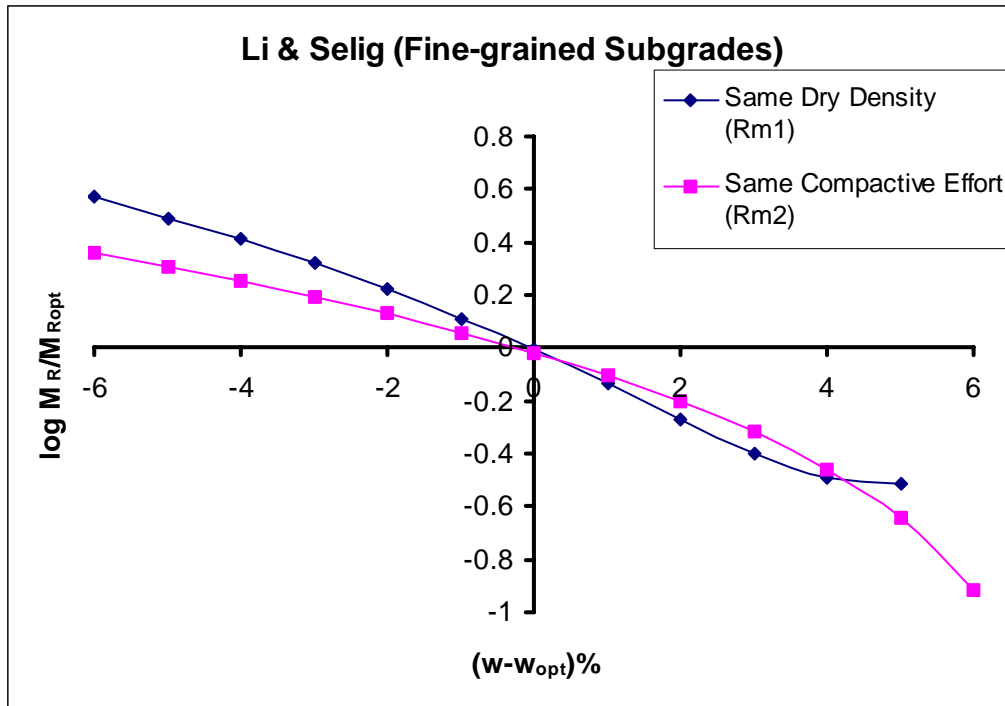


Figure 19a.

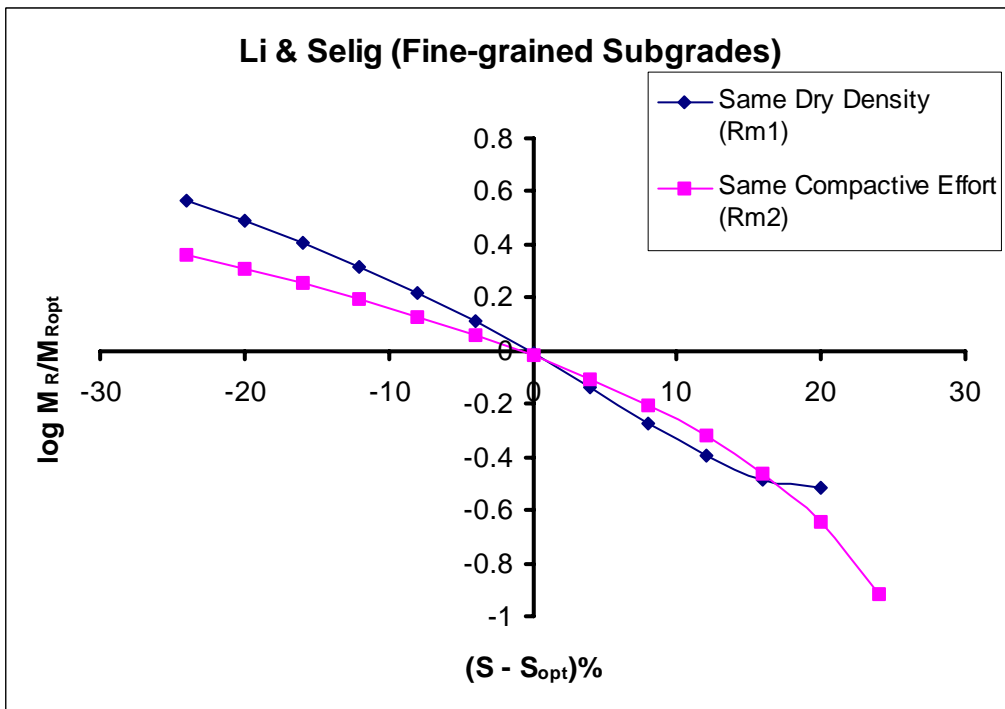


Figure 19b.

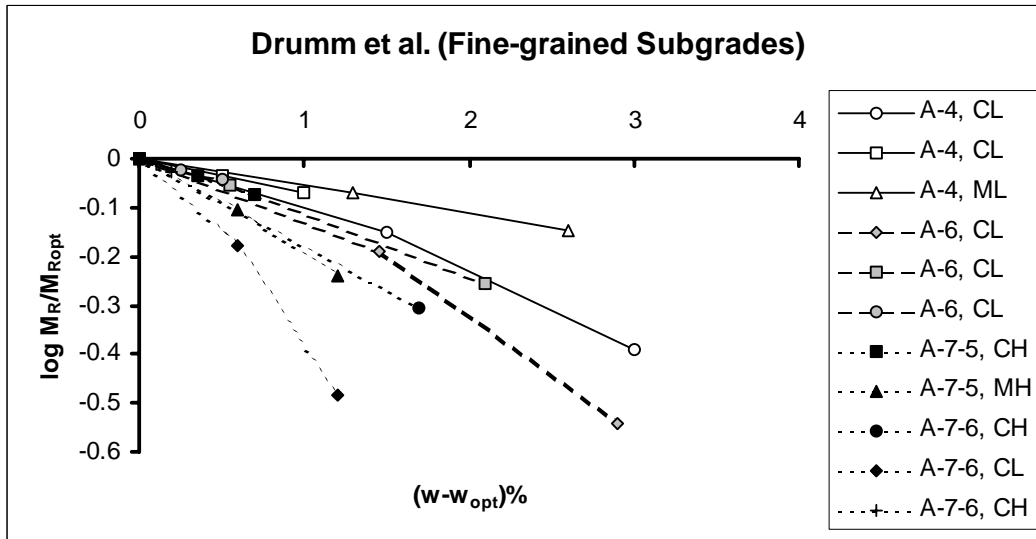


Figure 20a.

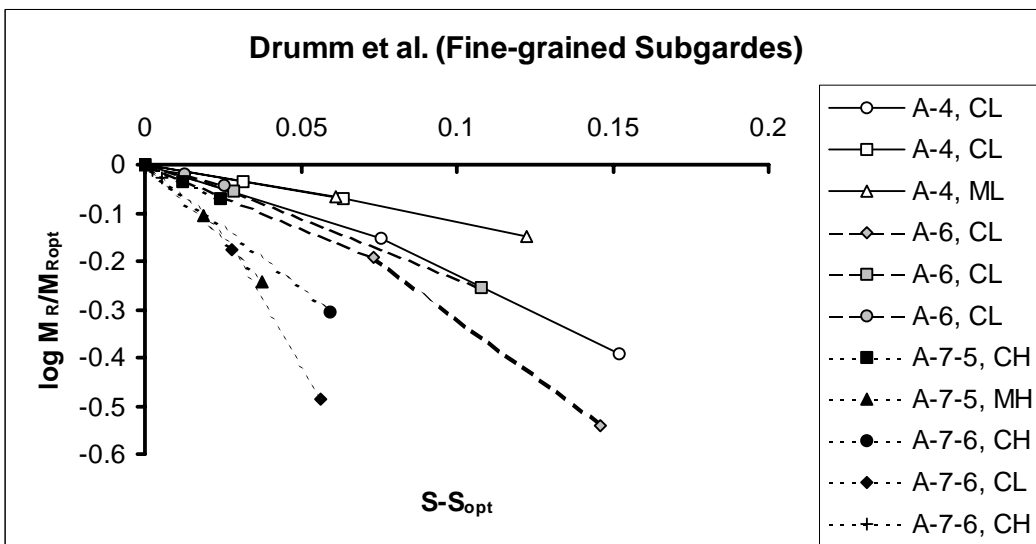


Figure 20b.

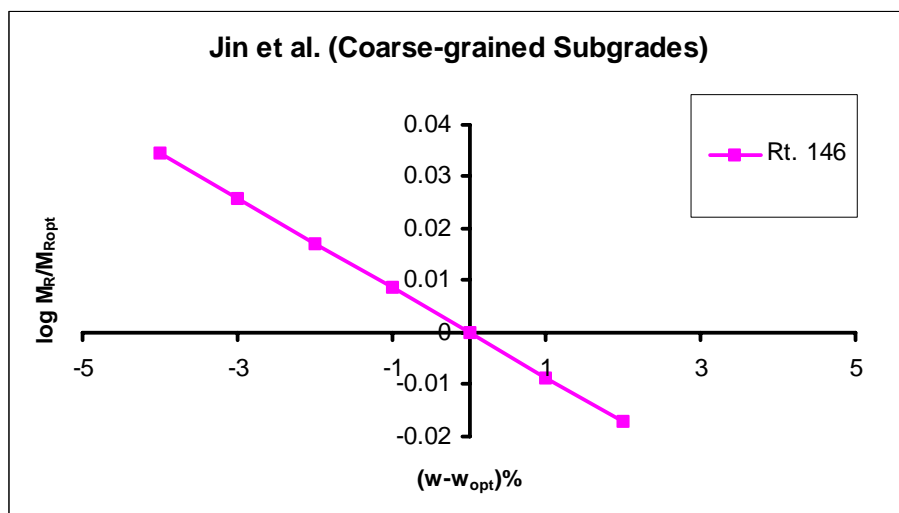


Figure 21a.

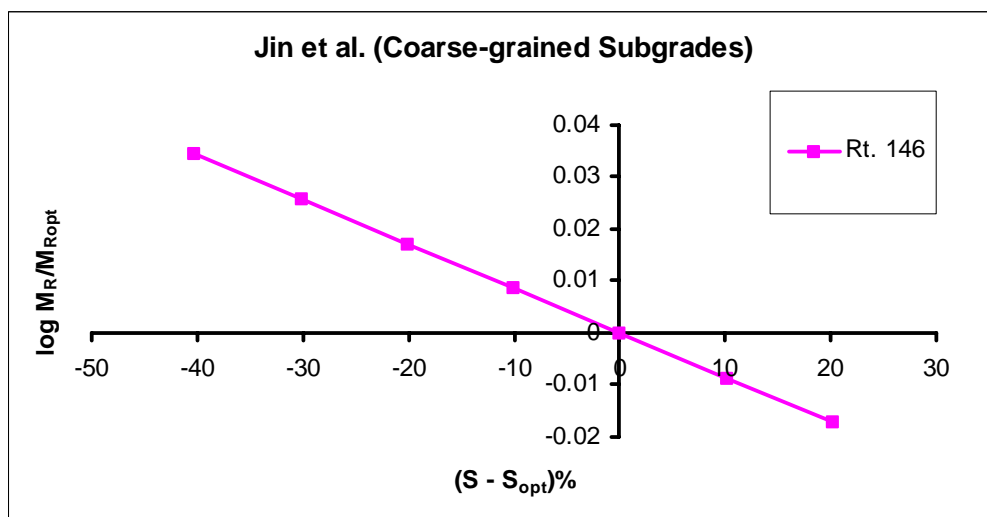


Figure 21b.



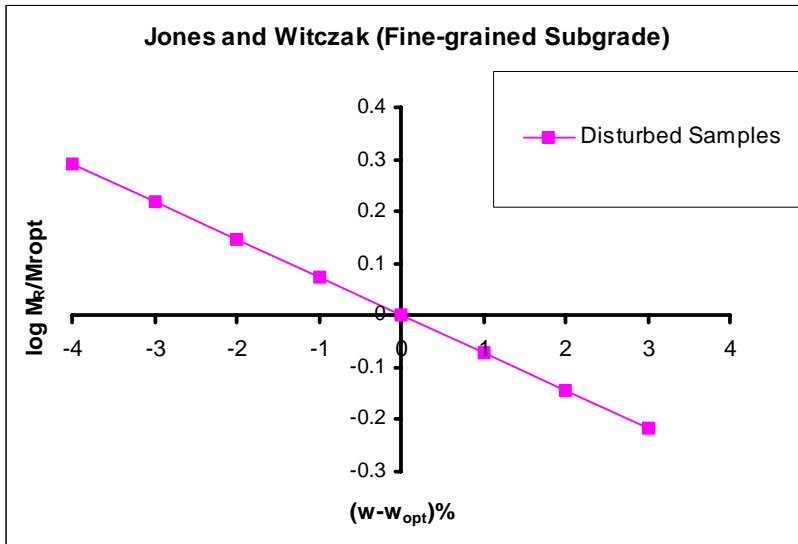


Figure 22a.

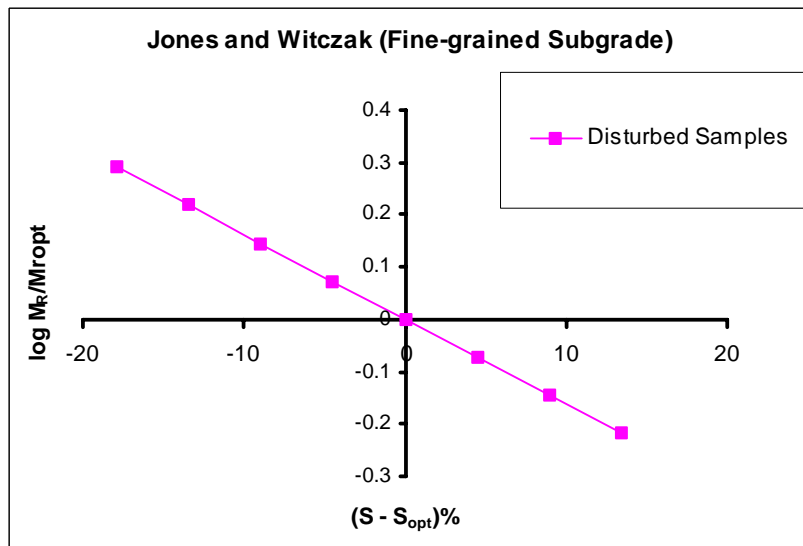


Figure 22b.

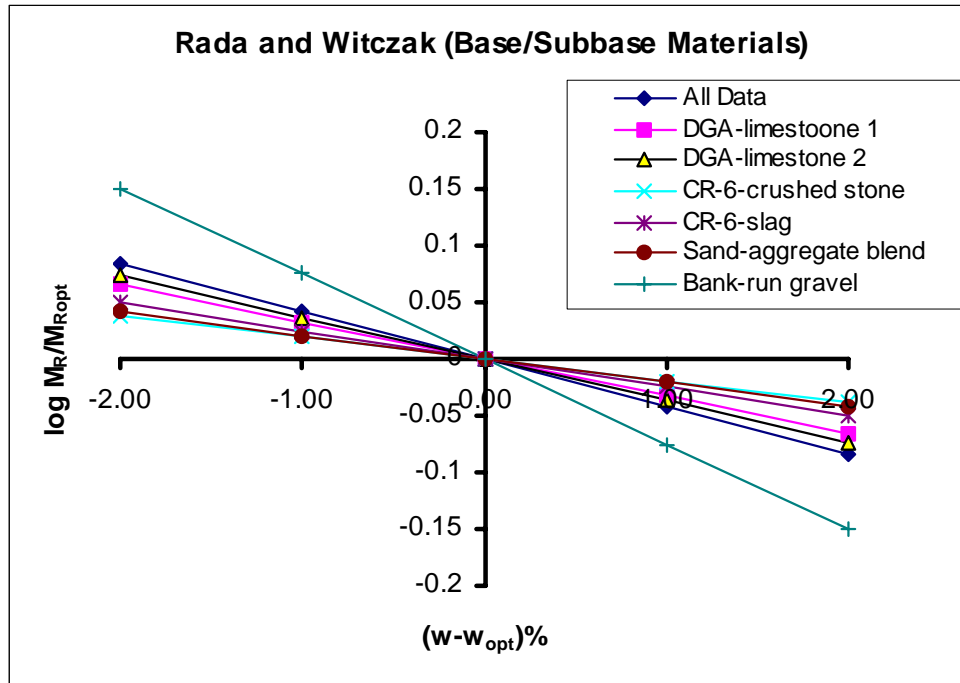


Figure 23a.

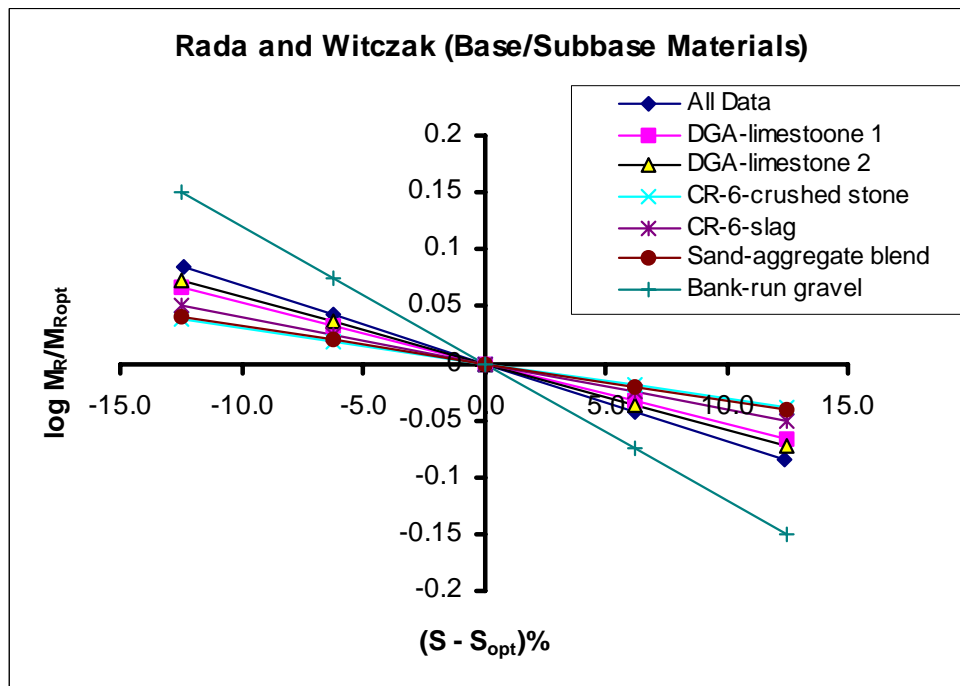


Figure 23b.

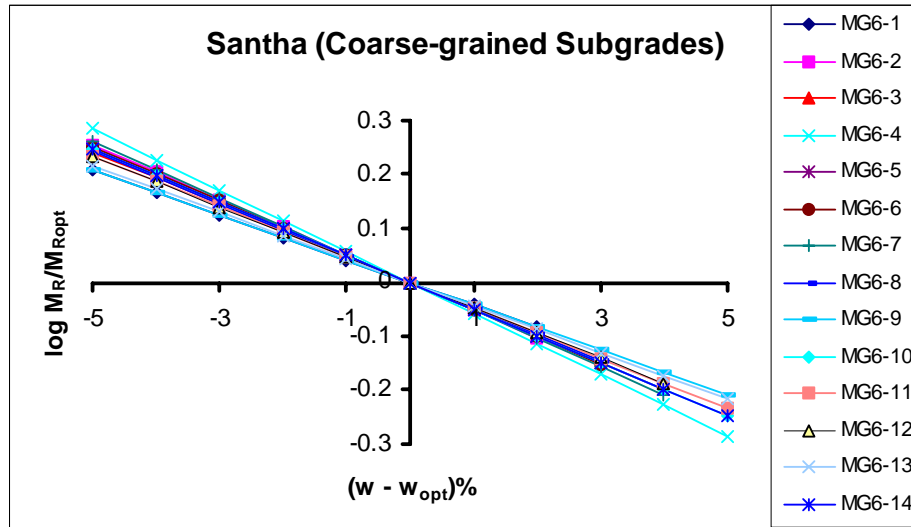


Figure 24a.

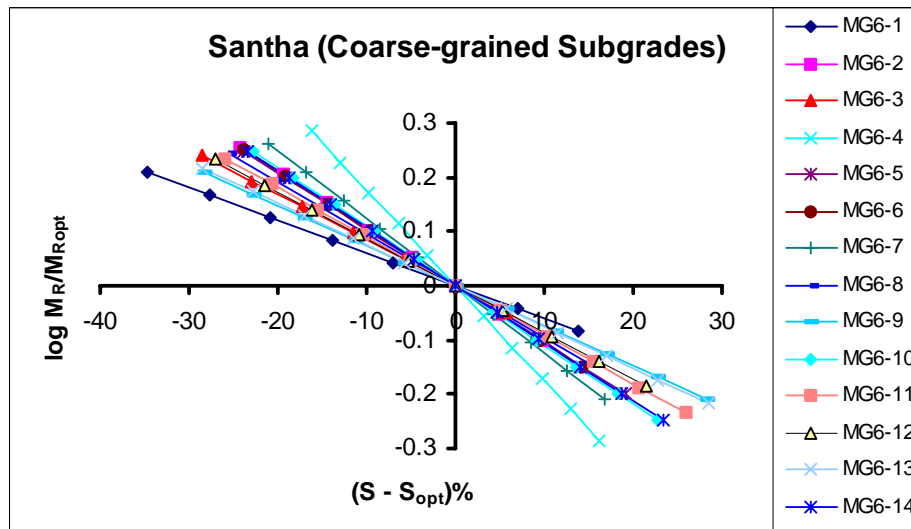


Figure 24b.

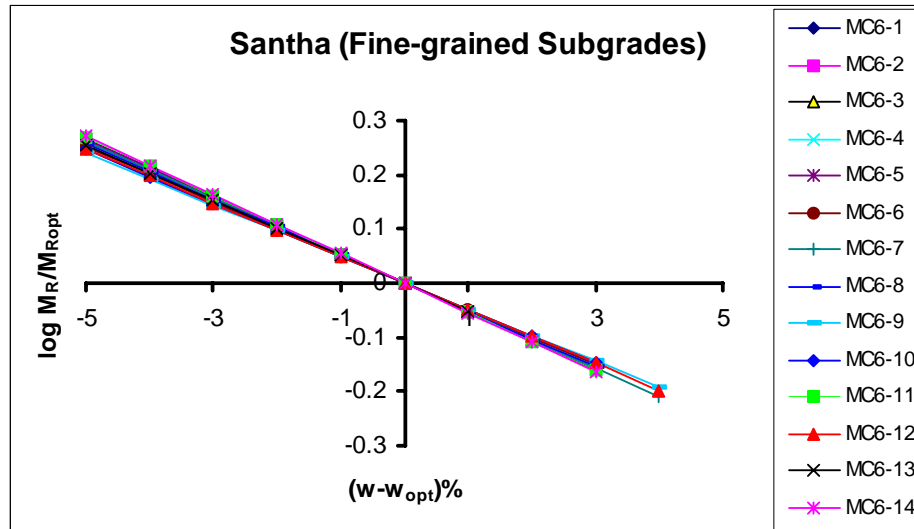


Figure 25a.

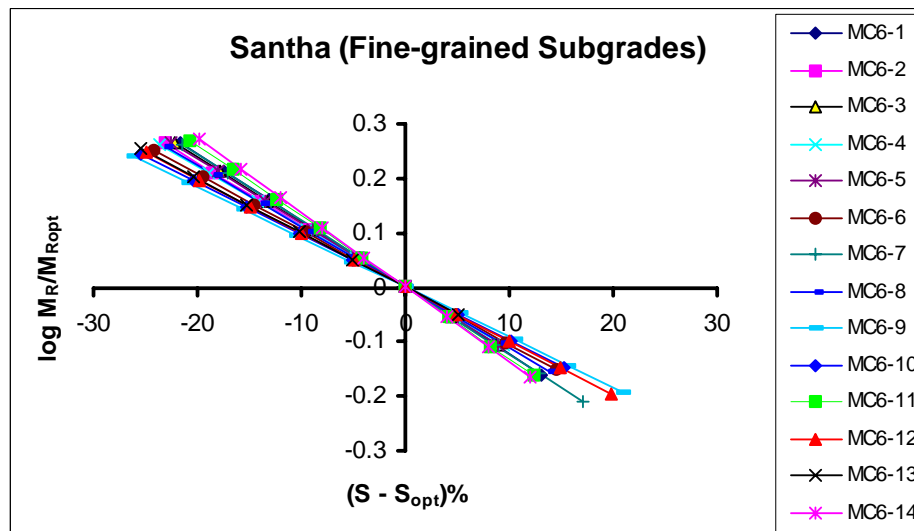


Figure 25b.

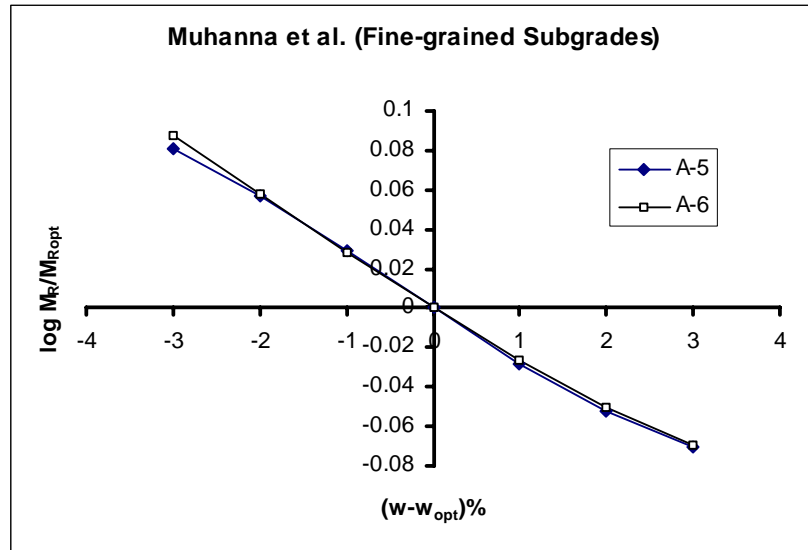


Figure 26a.

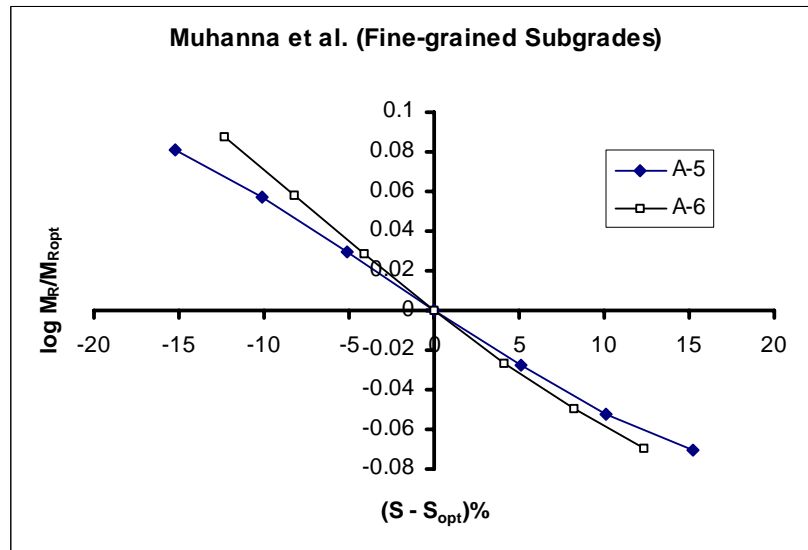


Figure 26b.

$k_w$  = gradient of log resilient modulus ratio ( $\log (M_R/M_{Ropt})$ ) with respect to variation in percent moisture content ( $w - w_{opt}$ );  $k_w$  is a material constant and can be obtained by linear regression in the semi-log space.

In terms of degree of saturation:

$$\log \frac{M_R}{M_{Ropt}} = k_S \cdot (S - S_{opt}) \quad (11-2)$$

Where:

$M_R$  = resilient modulus at degree of saturation  $S$  (%);

$M_{R(opt)}$  = resilient modulus at maximum dry density and optimum moisture content;

$S_{opt}$  = degree of saturation at maximum dry density and optimum moisture content, (%);

$k_S$  = gradient of log resilient modulus ratio ( $\log (M_R/M_{Ropt})$ ) with respect to variation in degree of saturation ( $S - S_{opt}$ ) expressed in (%);  $k_S$  is a material constant and can be obtained by regression in the semi-log space.

In Figure 27, materials are divided by AASHTO classification in an attempt to assign  $k_w$  values to each soil class. In Figures 28a and 29a, through regression in the semi-log space, typical  $k_w$  values are obtained for fine-grained materials ( $k_w = -0.0602$ ) and coarse-grained materials ( $k_w = -0.0463$ ). In other words, a 1% increase in moisture content will cause, on the average, a 13% reduction in modulus for fine-grained soils, 10% respectively for coarse-grained soils. In terms of saturation (see Figures 28b and 29b), typical  $k_S$  values are:  $k_S = -0.0128$  for fine-grained materials and  $k_S = -0.009$  for coarse-grained materials. A 1% increase in degree of saturation will cause, on the average, a 3% reduction in modulus for fine-grained soils and a 2% reduction for coarse-grained soils. In Figures 30 and 31,  $k_S$  values corresponding to each model are obtained. The database available to date includes results from 7 different investigators for 49 different soils.

# All Materials by AASHTO Classification

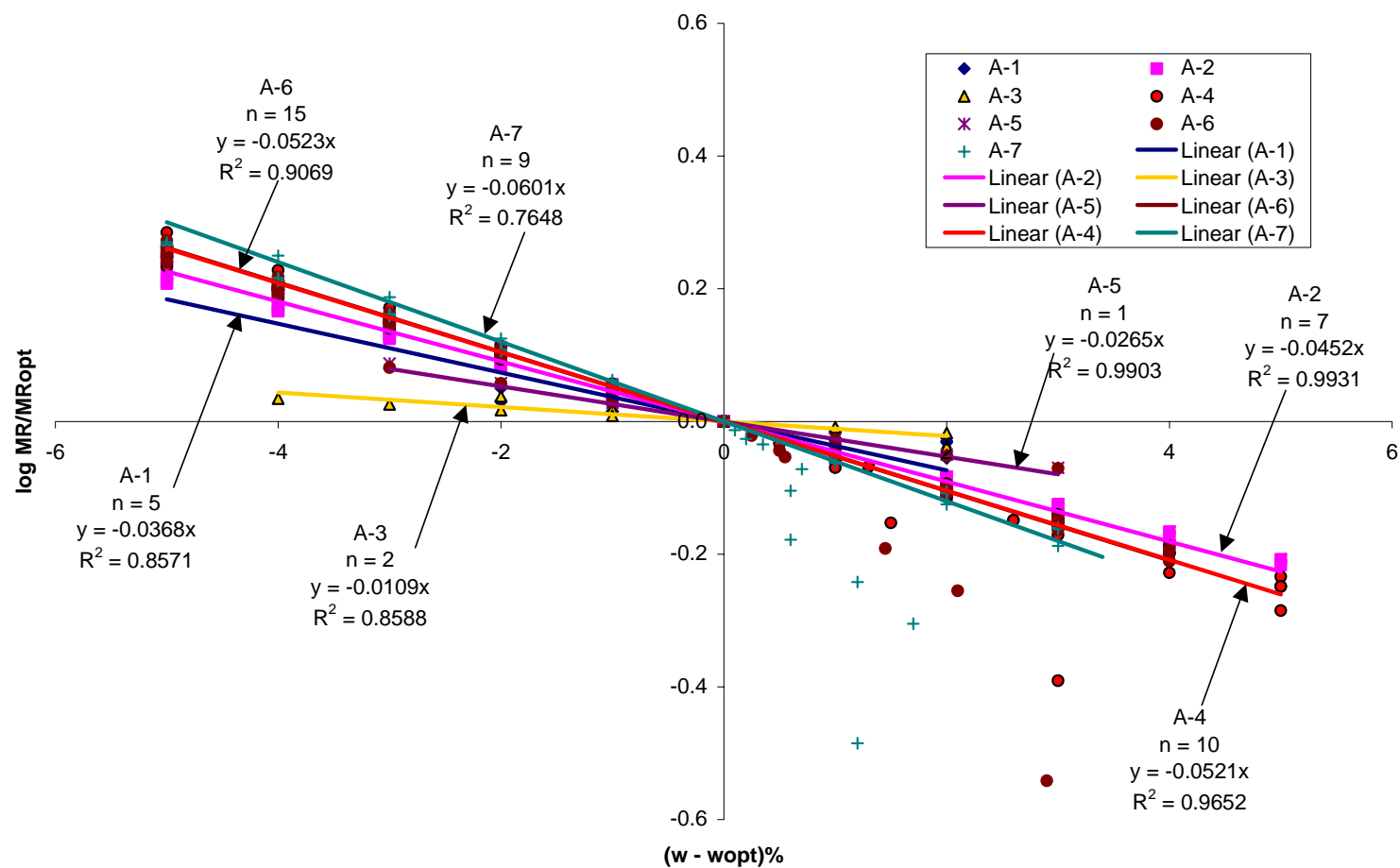


Figure 27. Variation of Modulus with Moisture by AASHTO Class

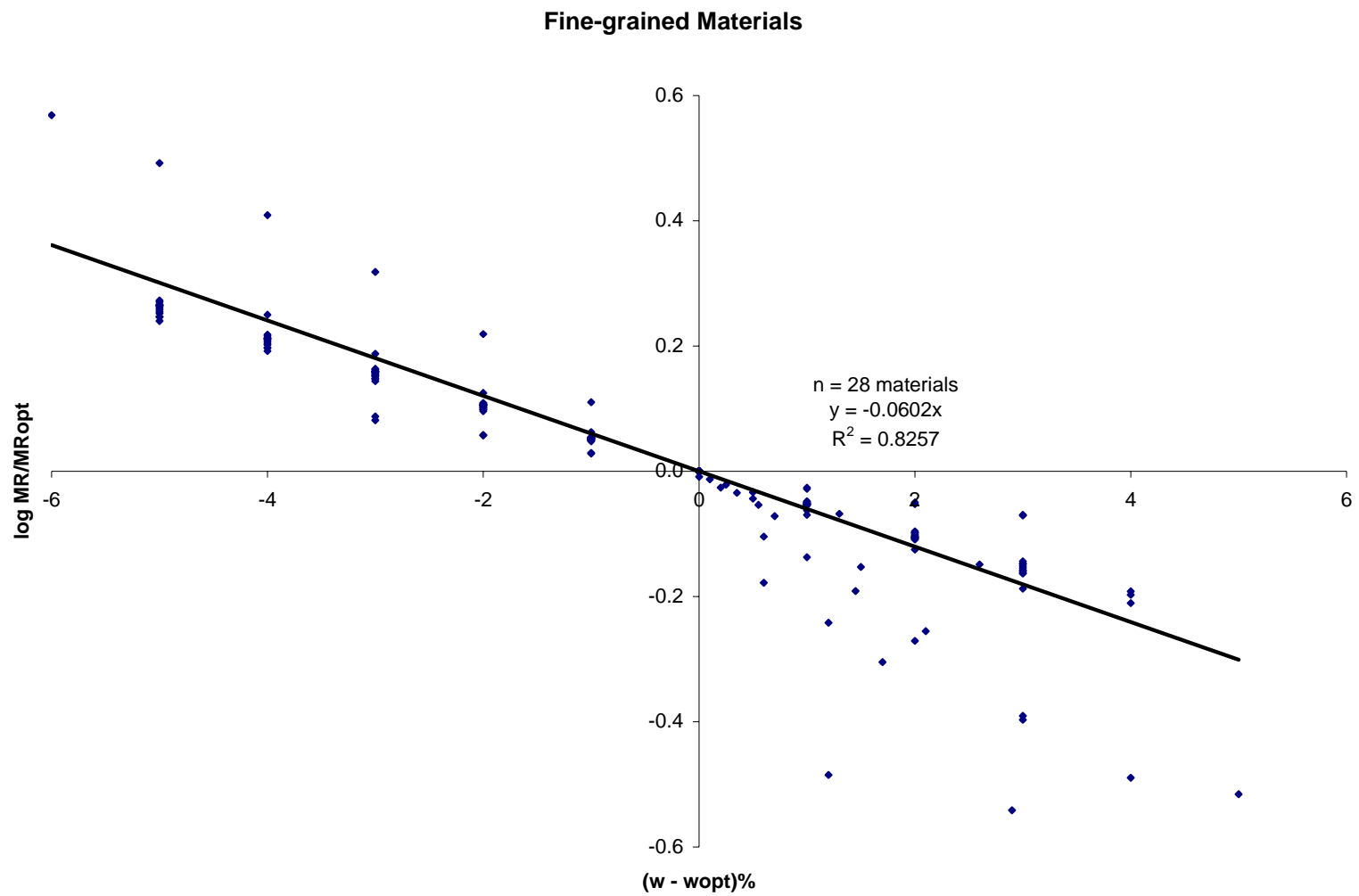


Figure 28a. Linear Regression in the Semi-log Space for Fine-grained Materials



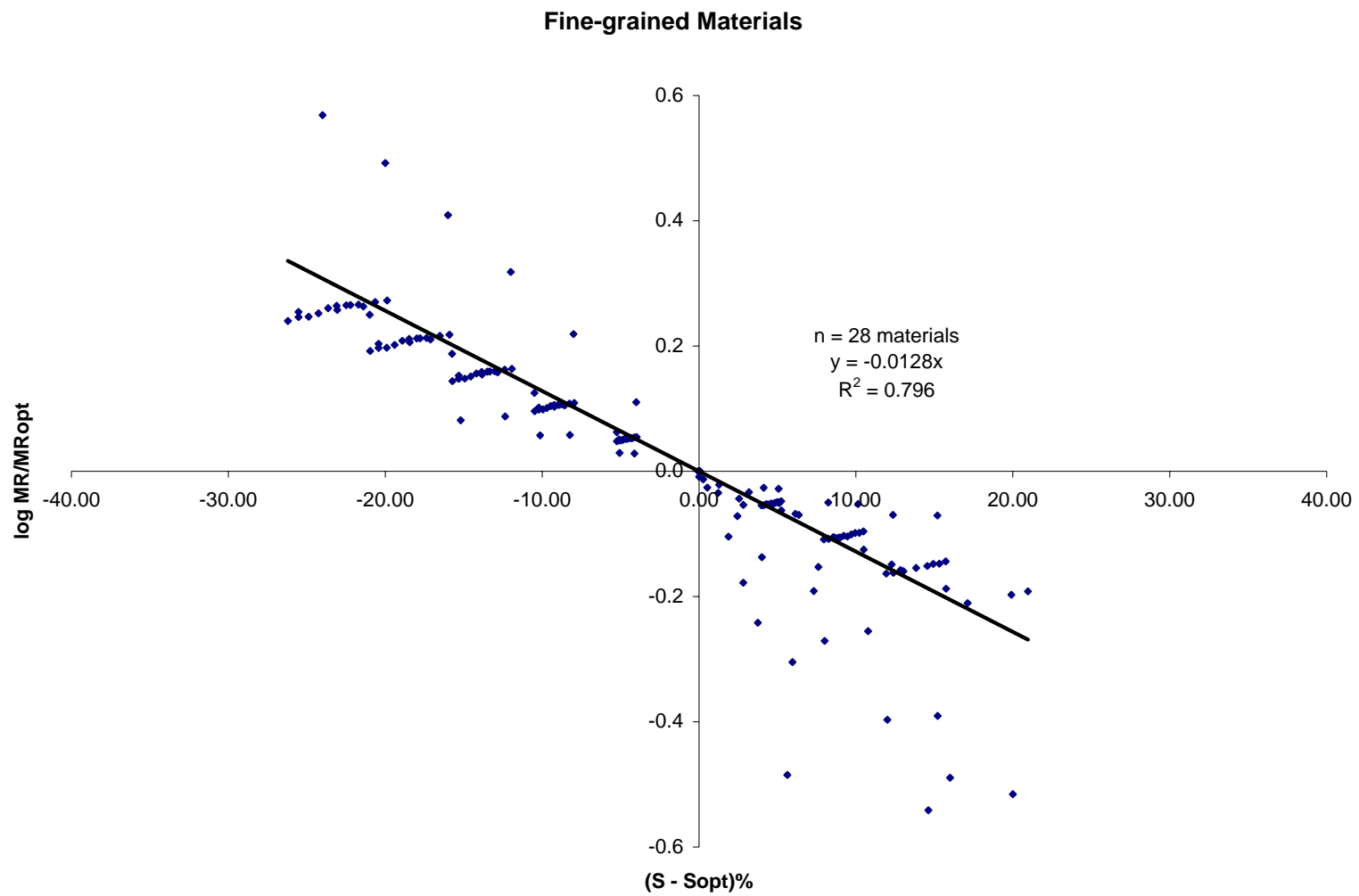


Figure 28b. Linear Regression in the Semi-log Space for Fine-grained Materials

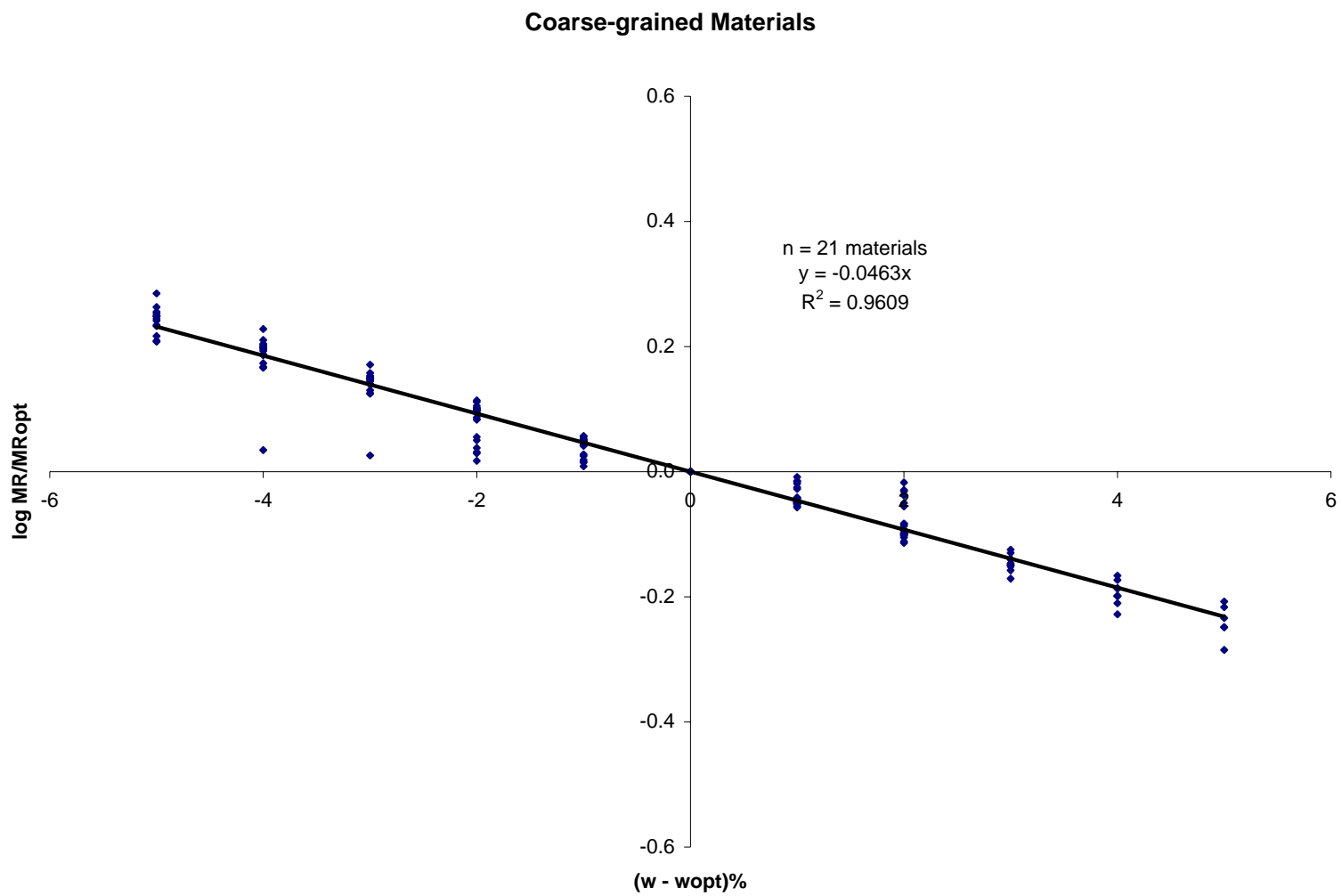


Figure 29a. Linear Regression in the Semi-log Space for Coarse-grained Materials

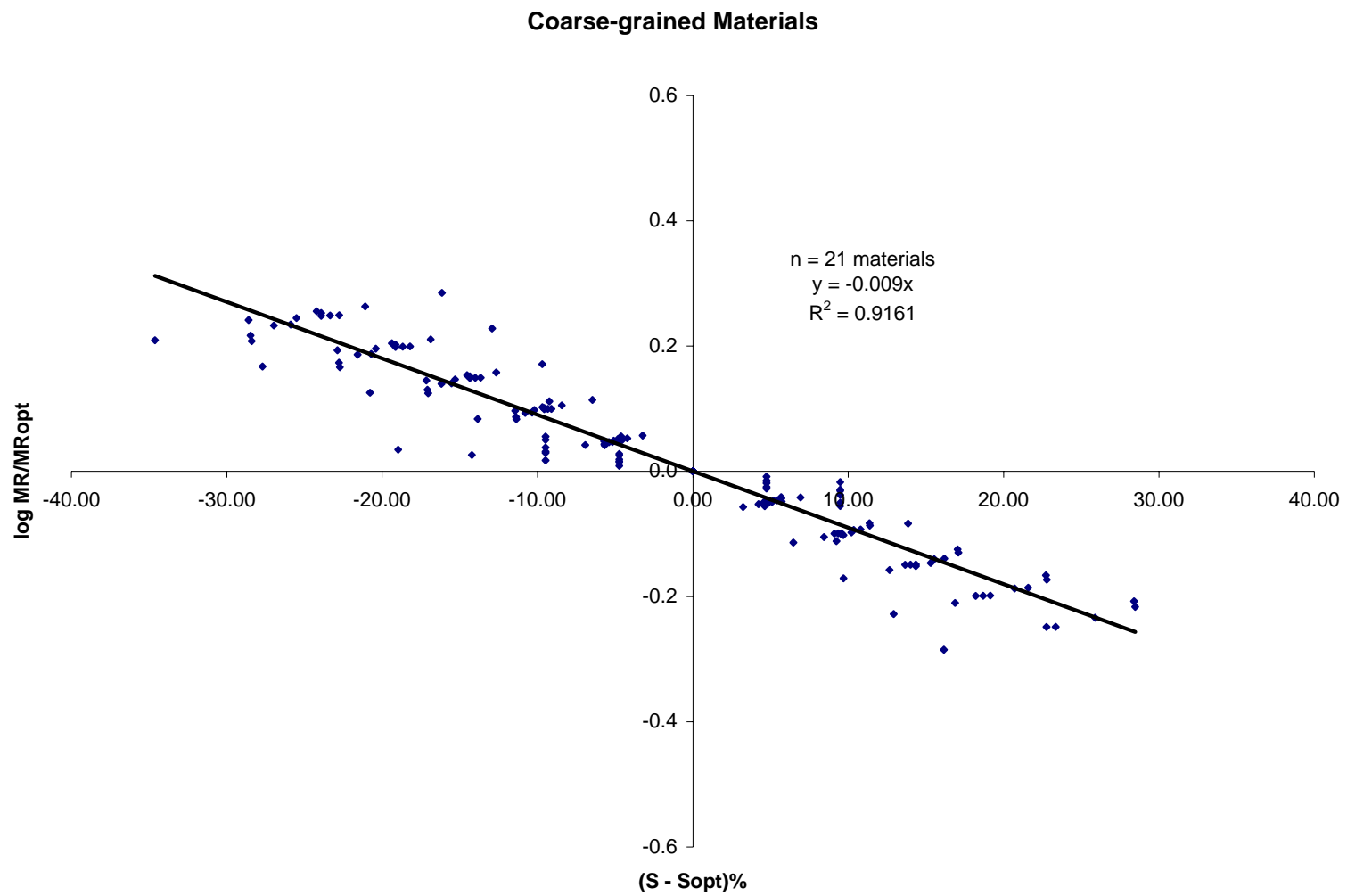


Figure 29b. Linear Regression in the Semi-log Space for Coarse-grained Materials

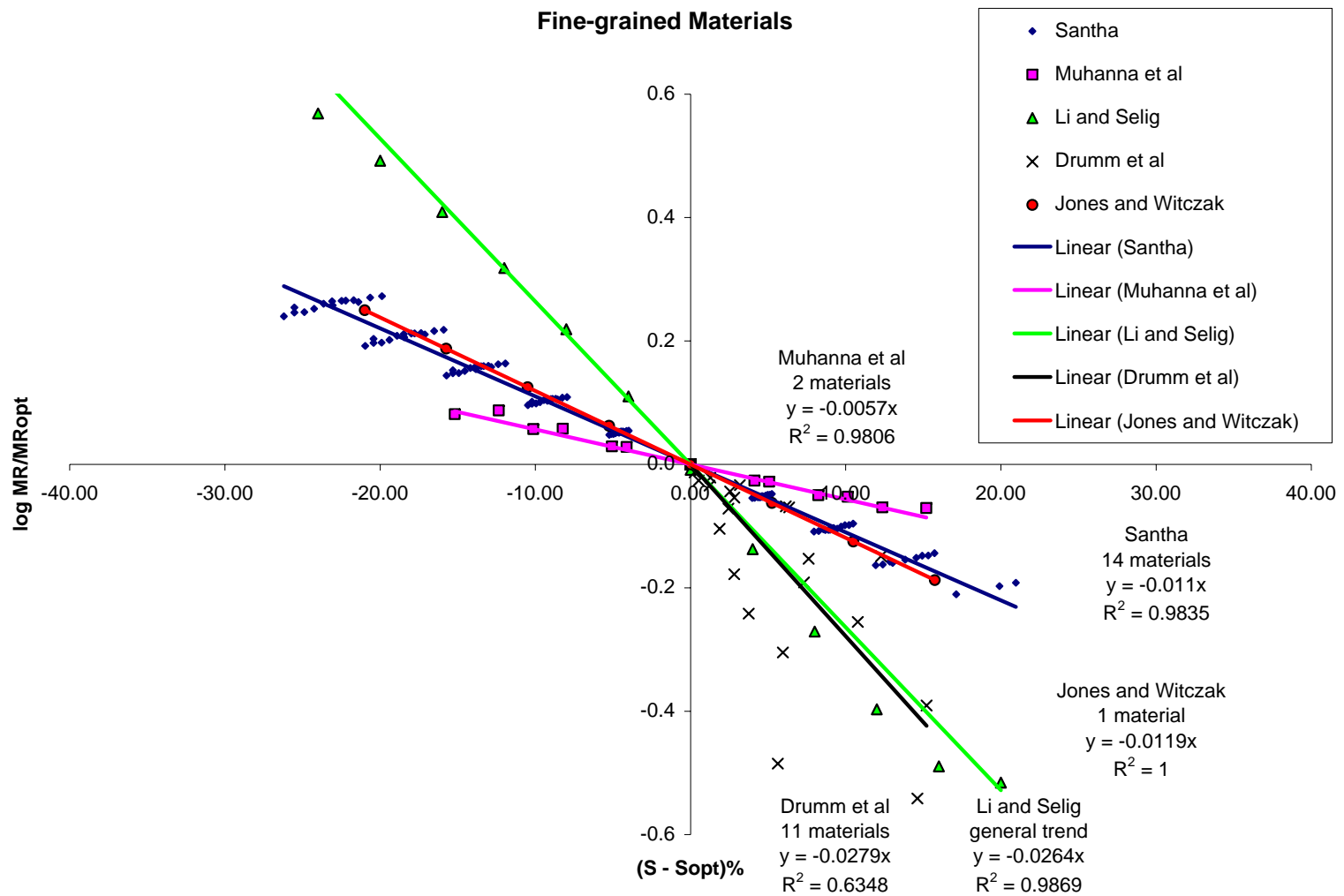


Figure 30. Values of  $k_s$  by Model, for Fine-grained Materials

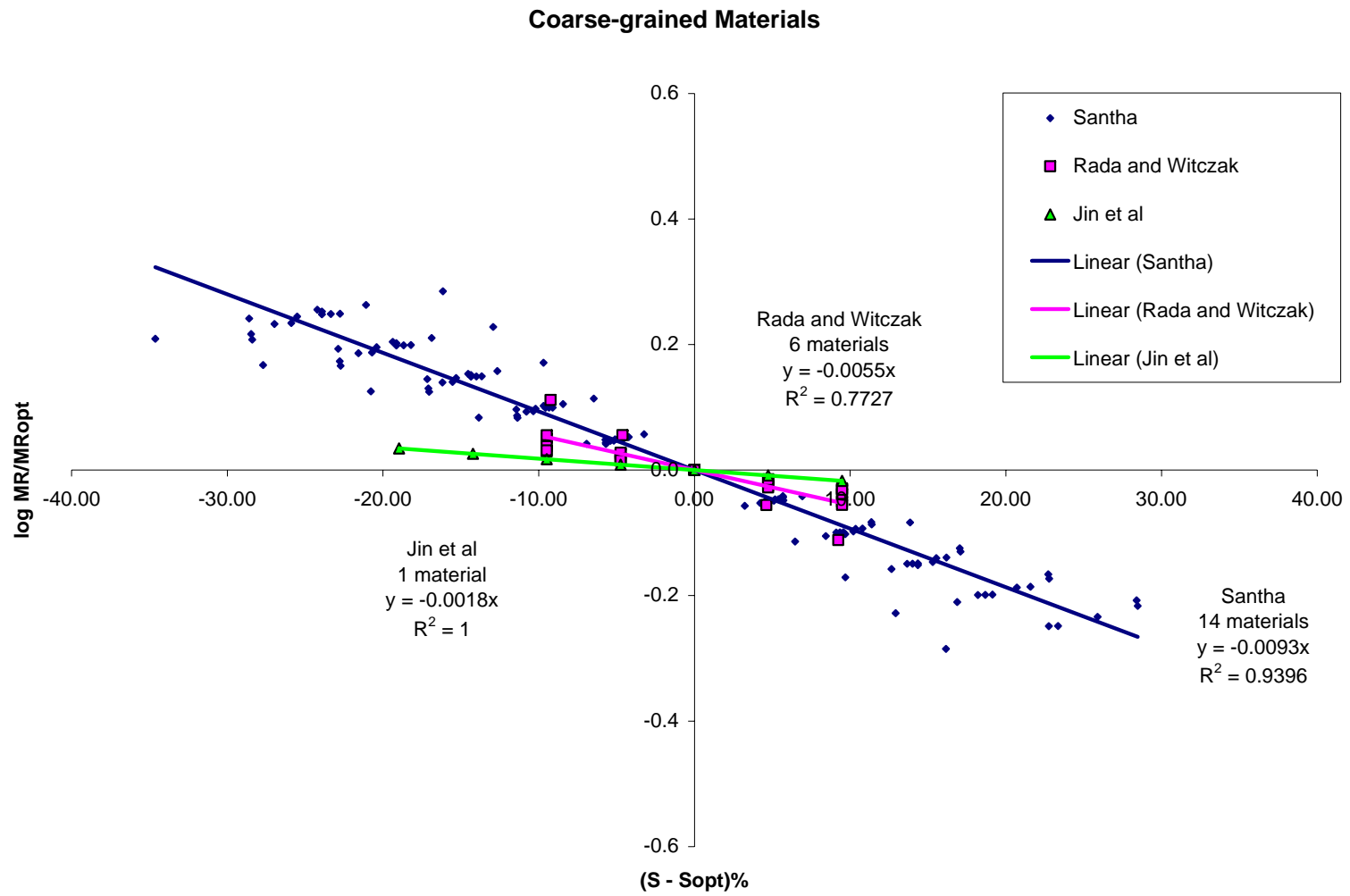


Figure 31. Values of  $k_s$  by Model, for Coarse-grained Materials

Based on this database, it appears that the difference between  $k_s$  (or  $k_w$ ) for fine and coarse-grained soil is surprisingly small. Perhaps the use of the  $M_R/M_{Ropt}$  ratio tends to normalize out the differences between fine and coarse-grained soils rather thoroughly. The difference between equations 11-1 and 11-2 is in the predictor variable used: moisture content or degree of saturation. It was observed that the choice of the predictor variable did not have a significant impact on the accuracy of prediction. However, when using moisture content, one should always check the degree of saturation in order to prevent erroneous predictions corresponding to degrees of saturation higher than 100%. Therefore, Equation 11-2 and degree of saturation are preferred rather than moisture content, because their use forces the user to be cognizant of degree of saturation and helps to detect erroneous data leading to degrees of saturation exceeding 100%. Furthermore, because  $S_{opt}$  is fairly stable in the range of 78% to 87%, erroneous data corresponding to unreasonably high or low  $S_{opt}$  values can be readily detected.

### **Revised Model**

In a parallel study on the variations in moisture for the unbound layers of 10 LTPP-SMP sites, it was found that most of the base and subbase materials are usually at very low degrees of saturation (3% - 10%), which is more than 50% below the degree of saturation corresponding to optimum conditions (Witczak et al. (16)). However, all data used in developing Equation 11-2 consisted of laboratory test results within +/- 30% of  $S_{opt}$  - the degree of saturation at maximum dry density and optimum moisture content. In order to extrapolate for values of the degree of saturation lower than 30% below the optimum (on the dry side), a conservative extrapolation was adopted. The revised predictive model

(Equation 12) uses a sigmoid that approaches the linear relationship observed within +/- 30% of  $S_{opt}$  but flattens out for the degrees of saturation lower than 30% below the optimum. This extrapolation is in general agreement with known behavior of unsaturated materials in that, when a material becomes sufficiently dry, further drying increments produce less increase in stiffness and strength (Fredlund and Rahardjo (17)). The predictions of the revised model are given in Figures 32 and 33, for coarse-grained and fine-grained materials.

$$\log \frac{M_R}{M_{Ropt}} = a + \frac{b - a}{1 + EXP(\beta + k_s \cdot (S - S_{opt}))} \quad (12)$$

Where:

$a$  = minimum of  $\log(M_R/M_{Ropt})$ ;

$b$  = maximum of  $\log(M_R/M_{Ropt})$ ;

$\beta$  = location parameter – obtained as a function of  $a$  and  $b$  by imposing the condition of a zero intercept:

$$\beta = \ln\left(-\frac{b}{a}\right) \quad (12-1)$$

$k_s$  = regression parameter;

$(S - S_{opt})$  = variation in degree of saturation expressed in decimal; (Note that the use of  $S$  in equation form was changed from percent to decimal when the revised (nonlinear) model was adopted).

Using the available literature data and assuming a maximum modulus ratio of 2.5 for fine-grained materials and 2 for coarse-grained materials, the values of  $a$ ,  $b$ ,  $\beta$  and  $k_s$  for coarse-grained and fine-grained materials are given in Table 4.

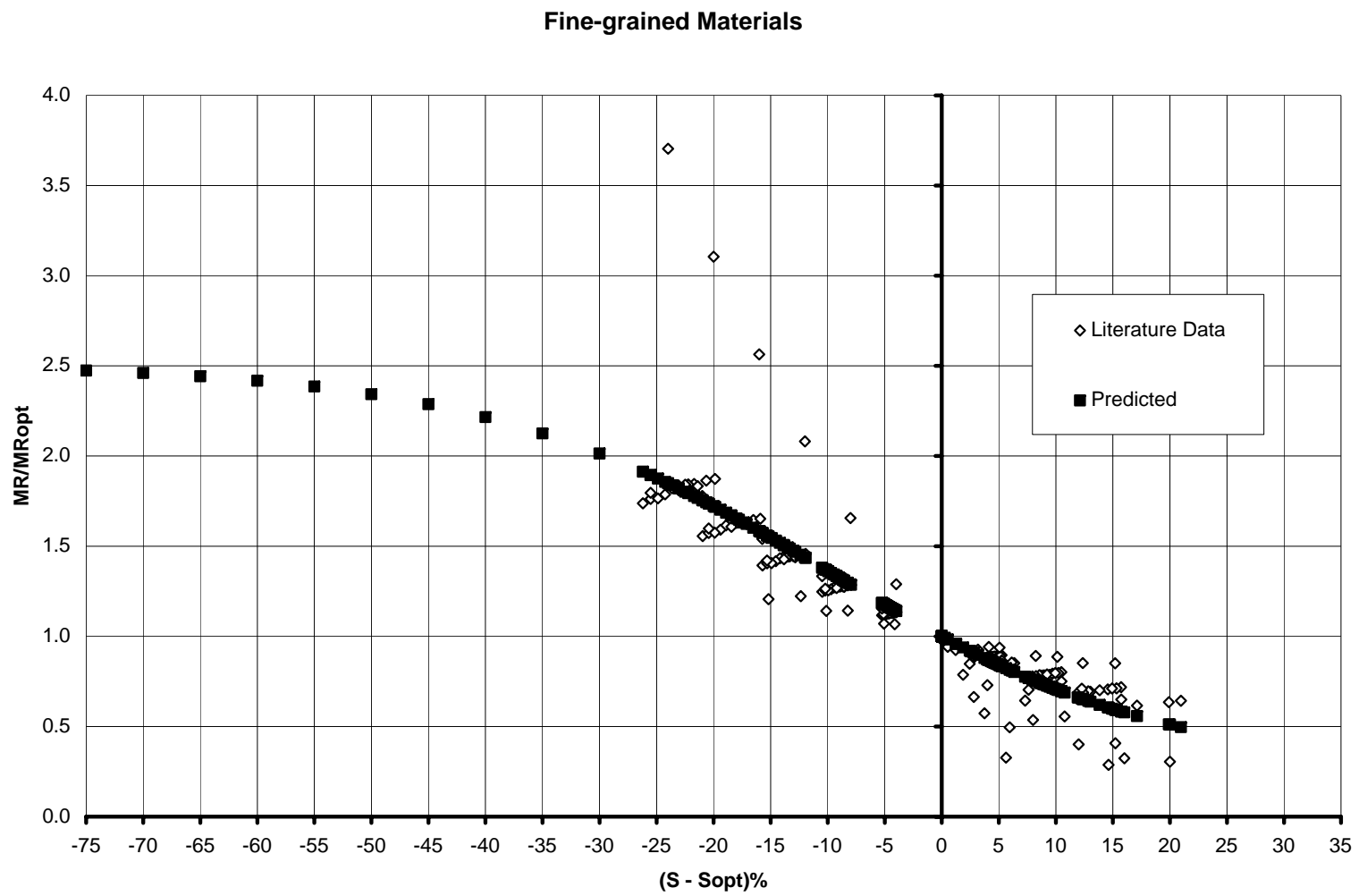


Figure 32a. Revised Model for Fine Grained Materials - Arithmetic Scale



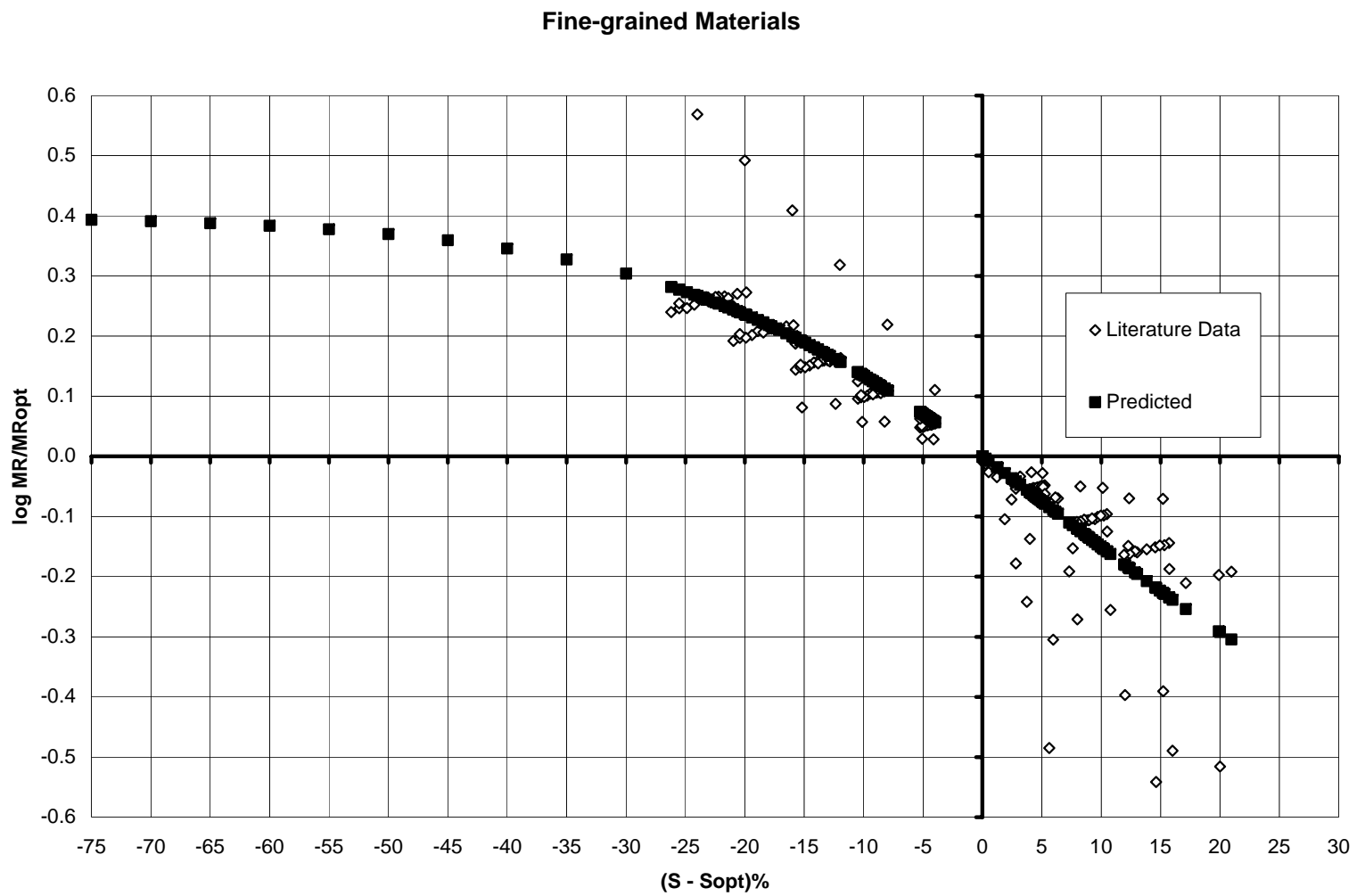


Figure 32b. Revised Model for Fine Grained Materials - Semi-Log Scale

### Coarse-grained Materials

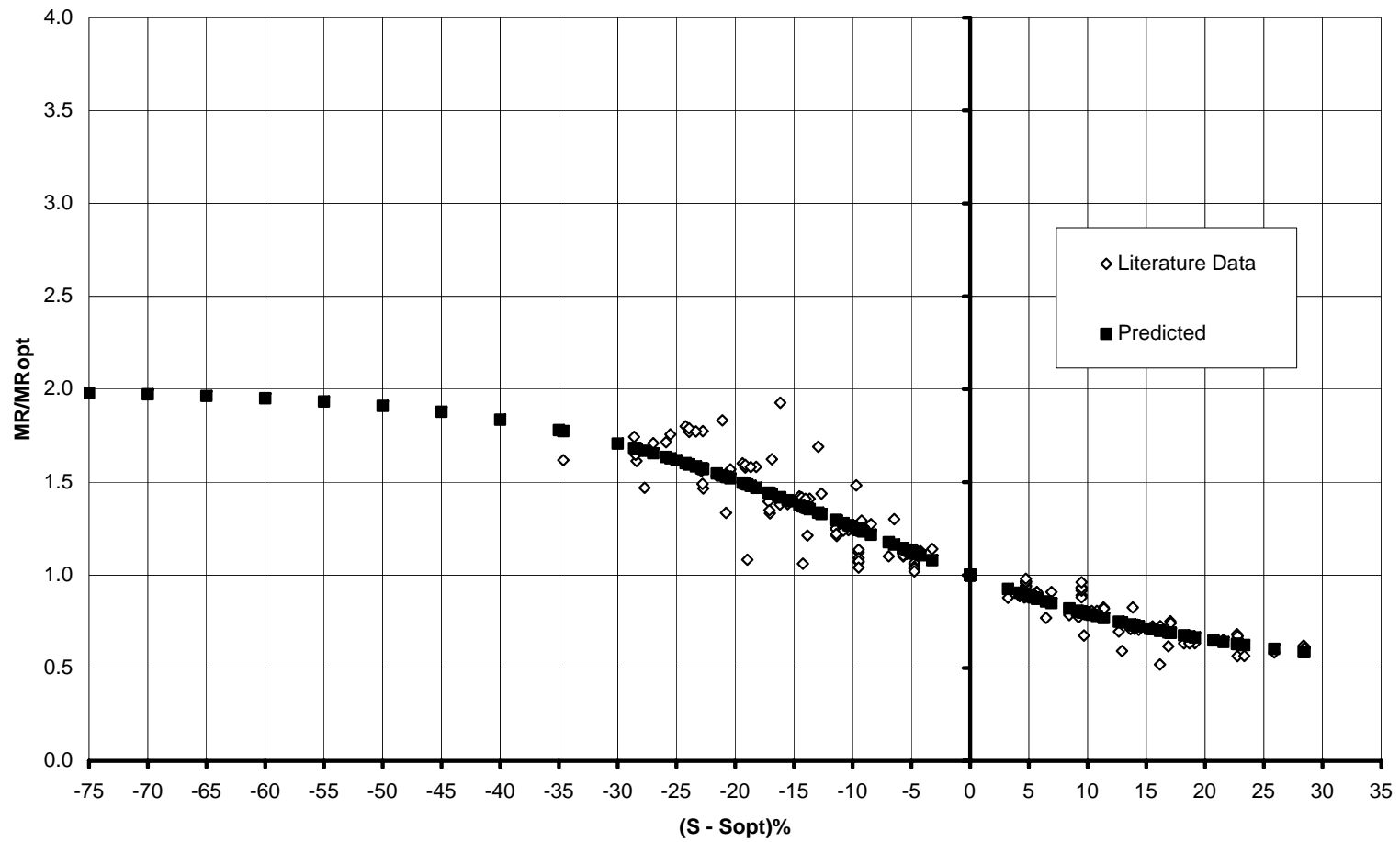


Figure 33a. Revised Model for Coarse Grained Materials - Arithmetic Scale

### Coarse-grained Materials

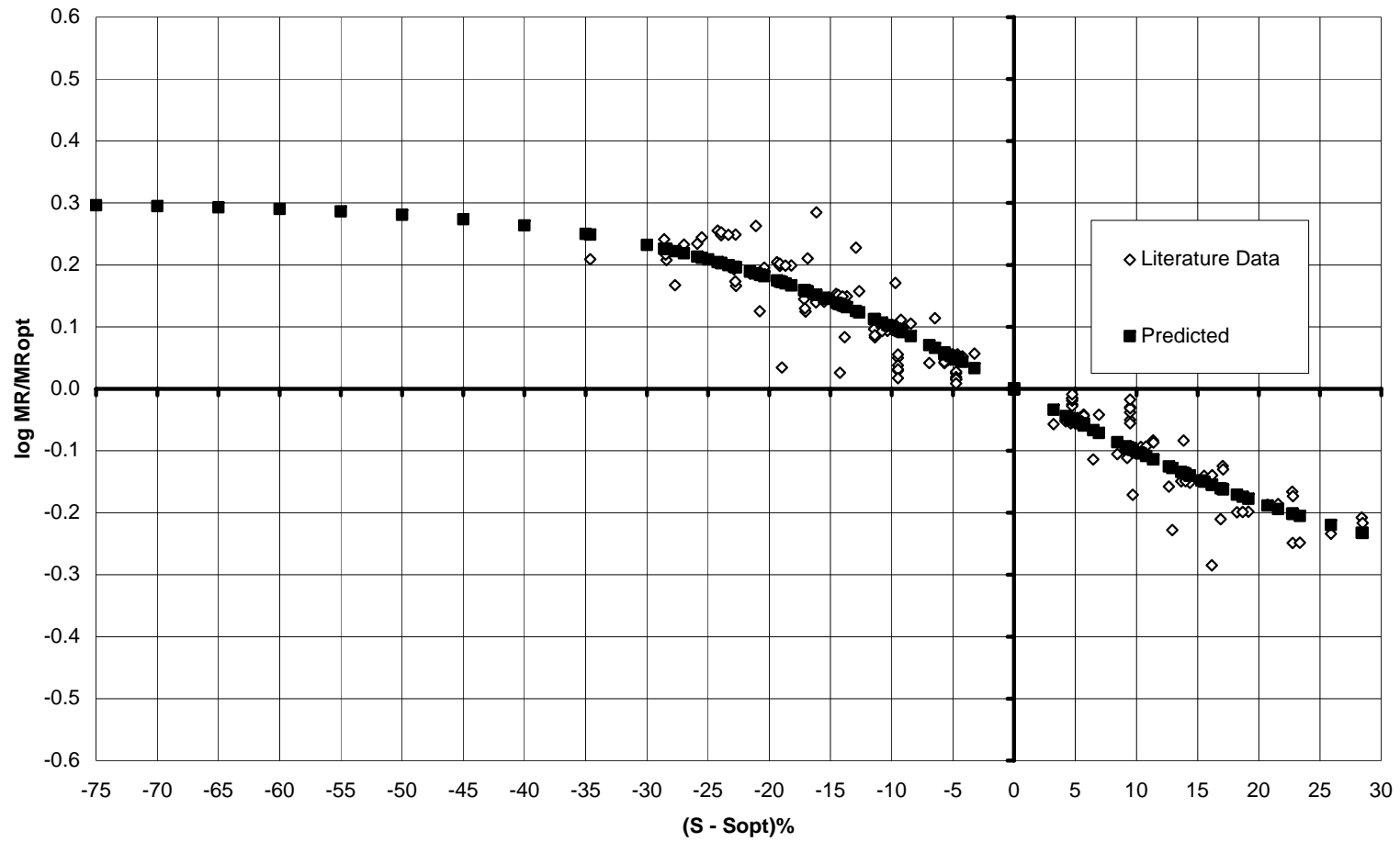


Figure 33b. Revised Model for Coarse Grained Materials - Semi-Log Scale

Table 4. Coefficients for the Revised Model

Parameter	Coarse Grained Materials	Fine Grained Materials	Comments
$a$	- 0.3123	-0.5934	Regression parameter
$b$	0.3	0.4	Conservatively assumed, until more data becomes available  (corresponding to modulus ratios of 2 and 2.5)
$\beta$	- 0.0401	- 0.3944	Obtained using Equation 12-1
$k_s$	6.8157	6.1324	Regression Parameter

The predictions of the revised model are shown in Figures 32 (a,b) and 33 (a,b), for coarse-grained and fine-grained materials, on arithmetic and semi-log scales.

## Implementation

Although Equation 12 looks much more complicated than Equation 11-2, actually, depending on the number of assumptions made, Equation 12 may degenerate to a one-parameter regression model, as illustrated in Table 5.

In the analysis presented in this report and illustrated in Figures 32 and 33, the two-parameter ( $b$  assumed) model was used. Further research will assess which of the above three alternatives is the best.

Knowing  $a$ ,  $b$  and  $k_s$  for a given material or group of materials, one can predict the resilient modulus at any degree of saturation ( $S$ ) as a function of the degree of saturation at optimum ( $S_{opt}$ ) and resilient modulus at optimum ( $M_{Ropt}$ ):

$$M_R = 10^{a + \frac{b-a}{1 + \text{EXP}(\beta + k_s \cdot (S - S_{opt}))}} \cdot M_{Ropt} \quad (12-2)$$

For  $S = S_{opt}$ ,  $M_R(S) = M_{Ropt}$  which may be predicted using Equation 13:

$$M_{Ropt} = k_1 \cdot p_a \cdot \left( \frac{\theta}{p_a} \right)^{k_2} \cdot \left( \frac{\tau_{oct}}{p_a} + 1 \right)^{k_3} \quad (13)$$

Assuming that for a given material the regression constants  $k_2$  and  $k_3$  are independent of the moisture content or the degree of saturation, combining Equations 12-2 and 13 we get:

$$M_R = 10^{a + \frac{b-a}{1 + \text{EXP}(\beta + k_s \cdot (S - S_{opt}))}} \cdot k_1 \cdot p_a \cdot \left( \frac{\theta}{p_a} \right)^{k_2} \cdot \left( \frac{\tau_{oct}}{p_a} + 1 \right)^{k_3} \quad (12-3)$$

Table 5. Complexity of the Model

Assumptions	Regression Constants to be Found	Comments
No Assumptions	$a, b, k_s$	An equivalent power or polynomial model would require the same number of regression constants (i.e. 3)
$b$	$a, k_s$	Two-parameter regression model
$a, b$	$k_s$	One-parameter regression model; the value of $a$ actually controls the shape of the predicted curve in the semi-log space, on the wet side:  a relatively high value will let the curve flatten again, as in Figure 33; a relatively low value will straighten the curve on the wet side. An extremely low value will even bend it downward.

Although better goodness of fit statistics ( $Se/Sy$ ,  $R^2$ ) could be obtained performing the regression in the arithmetic space, by regressing in the semi-log space, errors corresponding to lower  $M_R$  values are given more weight which is beneficial because we strive for higher accuracy on the “wet side” of the optimum (i.e.  $S_i - S_{opt} > 0$ ), where modulus values are lower and therefore more critical.

It should be noted that if changes in moisture content are accompanied by significant changes in soil density, the variation in  $M_R$  will not be smooth, as was shown by Figure 8. Therefore, corrections for expansion or collapse should be introduced. The effect of density changes on  $M_R$  is indicated by the coefficients appearing in models (5), (8-a,b) and (9-b). As more  $M_R$  test results become available it should be possible to better quantify the effects of density changes.

### **Recommendations for Further Study**

Very few of the studies reported in the literature on resilient modulus and moisture are based on test results obtained on specimens wetted post-compaction. Because post-compaction represents the process followed in the prototype, this shortcoming could be serious for some soils. Further, very few of these past studies have quantified the effect of density and most studies have employed only one stress level. Therefore, for a given soil it is rather difficult to assess the effect of density, stress level and moisture content. What is needed is a comprehensive test program covering a range of:

- soil types
- density

- moisture contents (wet and dry of optimum, with post-compaction moisture variation)
- stress states

If the post-compaction moisture variation were imposed under constant and realistic stress state, then any corresponding change in density would likewise be realistic.

Variations in  $M_R$  derived from a test program of this type would provide the highest possible quality of data for future estimations of  $M_R$ .



## References:

1. Li D. and Selig E.T. *Resilient Modulus for Fine Grained Subgrade Soils*. ASCE Journal of Geotechnical Engineering, Vol. 120, No. 6, June, 1994, pp. 939-957.
2. Drumm E.C., Reeves J.S., Madgett M.R. and Trolinger W.D. *Subgrade Resilient Modulus Correction for Saturation Effects*. ASCE Journal of Geotechnical and Geoenvironmental Engineering, Vol. 123, No. 7, July, 1997, pp. 663-670.
3. Jin M.S., Lee K.W. and Kovacs W.D. *Seasonal Variation of Resilient Modulus of Subgrade Soils*. ASCE Journal of Transportation Engineering, Vol. 120, No.4, July/August, 1994, pp. 603-616.
4. Jones M.P. and Witczak M.W. *Subgrade Modulus on the San Diego Test Road*. Transportation Research Record 641, TRB, National Research Council, 1977, Washington, D.C., pp. 1-6.
5. Rada G. and Witczak M.W. *Comprehensive Evaluation of Laboratory Resilient Moduli Results for Granular Material*. Transportation Research Record 810, TRB, National Research Council, 1981, Washington, D.C., pp. 23-33.
6. Santha B.L. *Resilient Modulus of Subgrade Soils: Comparison of Two Constitutive Equations*. Transportation Research Record 1462, TRB, National Research Council, Washington, D.C., pp. 79-90.
7. Berg R.L., Bigl S.R., Stark J.A. and Durell G.D. *Resilient Modulus Testing of Materials from Mn/ROAD, Phase I*. U.S. Army Corps of Engineers Cold Regions Research & Engineering Laboratory, Special Report No. 96-19, September 1996.
8. Muhanna A.S., Rahman M.S. and Lambe P.C. *A Model for Resilient Modulus and Permanent Strain of Subgrade Soils*. Preprint, Paper No. 981084, Transportation Research Board, 77<sup>th</sup> Annual Meeting, January 11-15, 1998, Washington, D.C.
9. Gehling W.Y.Y., Ceratti J.A., Nunez W.P. and Rodrigues M.R. *A Study on the Influence of Suction on the Resilient Behavior of Soils from Southern Brazil*. Proceedings of the Second Int. Conf. On Unsaturated Soils, 27-30 August, 1998, Beijing, China, Vol. 2.
10. Seed H.B., Chan C.K., and Lee C.E. *Resilience characteristics of subgrade soils and their relation to fatigue failures in asphalt pavement*. Proc. First Int. Conf. On Struct. Design of Asphalt Pavements, University of Michigan, Ann Arbor, 1962.
11. Fredlund D.G., Bergan A.T and Wong P.K. *Relation Between Resilient Modulus and Stress Conditions for Cohesive Subgrade Soils*. Transportation Research Record 642, TRB, National Research Council, 1977, Washington, D.C., pp. 73-81.

12. Lekarp F., Isacsson U., and Dawson A. *State of the Art. I: Resilient Response of Unbound Aggregates*. ASCE Journal of Transportation Engineering, Vol. 126, No. 1, Jan./Feb., 2000, pp. 76-83.
13. Drumm E.C., Rainwater R.N., Andrew J., Jackson N.M., Yoder R.E. and Wilson G.V. *Pavement Response due to Seasonal Changes in Subgrade Moisture Conditions*. Proceedings of the Second Int. Conf. On Unsaturated Soils, 27-30 August, 1998, Beijing, China, Vol. 2.
14. Edil T.B. and Motan S.E. *Soil-Water Potential and Resilient Behavior of Subgrade Soils*. Transportation Research Record 705, TRB, National Research Council, 1979, Washington, D.C., pp. 54-63.
15. Andrei D. *Development of a Harmonized Test Protocol for the Resilient Modulus of Unbound Materials Used in Pavement Design*, Master Thesis, University of Maryland at College Park, 1999.
16. Witczak M.W., Houston W.N. and Andrei D. *Resilient Modulus as Function of Soil Moisture – A Study of the Expected Changes in Resilient Modulus of the Unbound Layers with Changes in Moisture for 10 LTPP Sites*. Development of the 2002 Guide for the Development of New and Rehabilitated Pavement Structures, NCHRP 1-37 A, Inter Team Technical Report (Seasonal 2), June 2000.
17. Fredlund D.G. and Rahardjo H. *Soil Mechanics for Unsaturated Soils*. John Wiley & Sons, Inc. 1993

Copy No. \_\_\_\_\_

# **Guide for Mechanistic-Empirical Design OF NEW AND REHABILITATED PAVEMENT STRUCTURES**

**FINAL DOCUMENT**

## **APPENDIX DD-2: RESILIENT MODULUS AS FUNCTION OF SOIL MOISTURE – A STUDY OF THE EXPECTED CHANGES IN RESILIENT MODULUS OF THE UNBOUND LAYERS WITH CHANGES IN MOISTURE FOR 10 LTPP SITES**

**NCHRP**

**Prepared for  
National Cooperative Highway Research Program  
Transportation Research Board  
National Research Council**

**Submitted by  
ARA, Inc., ERES Division  
505 West University Avenue  
Champaign, Illinois 61820**

**June 2000**

## **Acknowledgment of Sponsorship**

This work was sponsored by the American Association of State Highway and Transportation Officials (AASHTO) in cooperation with the Federal Highway Administration and was conducted in the National Cooperative Highway Research Program which is administered by the Transportation Research Board of the National Research Council.

## **Disclaimer**

This is the final draft as submitted by the research agency. The opinions and conclusions expressed or implied in this report are those of the research agency. They are not necessarily those of the Transportation Research Board, the National Research Council, the Federal Highway Administration, AASHTO, or the individual States participating in the National Cooperative Highway Research program.

## **Acknowledgements**

The research team for NCHRP Project 1-37A: Development of the 2002 Guide for the Design of New and Rehabilitated Pavement Structures consisted of Applied Research Associates, Inc., ERES Consultants Division (ARA-ERES) as the prime contractor with Arizona State University (ASU) as the primary subcontractor. Fugro-BRE, Inc., the University of Maryland, and Advanced Asphalt Technologies, LLC served as subcontractors to either ARA-ERES or ASU along with several independent consultants.

Research into the subject area covered in this Appendix was conducted at ASU. The authors of this Appendix are Dr. M.W. Witczak, Dr. W.N. Houston, and Mr. Dragos Andrei. Dr. M.W. Witczak coordinated the overall research effort of the 2002 Design Guide Team, outlined problems to be addressed, and made specific assignments of tasks for this study. He was also responsible for the final review of the report. Dr. W.N. Houston provided the day-to-day supervision of the study and assisted with the analysis of the results and report preparation. Mr. Dragos Andrei conducted the literature search, gathered the data, and performed the analyses contained in this report. Moisture predictions for the 10 LTPP sites were obtained from other studies being conducted at ASU by Witczak, Houston, Zapata and Richter of the FHWA.

## **Foreword**

This appendix presents the results of applying the Design Guide model that relates changes in modular ratio to changes in degrees of saturation of unbound materials to 10 LTPP sites where moisture content variation data predicted by the EICM are available. The information contained in this appendix serves as a supporting reference to the resilient modulus discussions presented and PART 2, Chapter 3, and PART 3, Chapters 3, 4, 6, and 7 of the Design Guide.

## **Abstract**

As part of the overall effort to develop a working, practical subsystem to predict resilient moduli ( $M_R$ ) for unbound material throughout the life of a pavement system, the effect of moisture changes on  $M_R$  has been studied and evaluated. A simple model relating changes in modular ratio to changes in degree of saturation has been adopted to assess changes in the  $M_R$  values. This report presents the results of the application of this simple model to 10 LTPP sites where moisture content variation data predicted by the EICM are available.

The results show that the seasonal variations in  $M_R$  (for non frost affected zones) are typically fairly small, of the order of +/- 10 to 15%. Oscillations as high as +/- 25 to 50% occasionally occur, but are not frequent. Overall, these seasonal oscillations appear to be much smaller than the oscillations expected from freezing and thawing. Also, in most cases, particularly for the bases and subbases, the effect of change in moisture from the initial (optimum compaction) conditions to the final equilibrium condition is much larger than the seasonal oscillations.

## Table of Contents

	<u>Page</u>
Introduction.....	1
Objective .....	1
Analysis.....	2
Discussion of Results .....	11
Use of Hand Calculations as a Check on EICM output.....	32
Conclusions.....	37
Recommendations – General .....	38
Recommendations – Relative to the Implementation of the MR Model into the 2002 Guide.....	39
References.....	42

## List of Tables

	<u>Page</u>
Table 1. CBR values as a Function of Material Type.....	3
Table 2. Model Parameters .....	5
Table 3. Input Data Summary .....	10
Table 4. Check on EICM Outputs with Manual Calculations – Comparisons of $M_R$ Adjustment Factors .....	35

## List of Figures

	<u>Page</u>
Figure 1. Values of $k_s$ for Coarse Grained Materials .....	6
Figure 2. Values of $k_s$ for Fine Grained Materials .....	6
Figure 3. Arizona .....	12
Figure 4. Colorado .....	14
Figure 5. Connecticut.....	16
Figure 6. Georgia .....	18
Figure 7. Maine .....	20
Figure 8. Manitoba.....	22
Figure 9. Minnesota .....	24
Figure 10. New Hampshire .....	26
Figure 11. Texas.....	28
Figure 12. Vermont.....	30
Figure 13. Predicted SWCC based on $D_{60}$ and $PI$ .....	34



# **A Study of the Expected Changes in Resilient Modulus of Unbound Layers with Changes in Moisture for 10 LTPP Sites**

## **Introduction**

The task of quantifying the expected cumulative damage due to load associated distress of a pavement system begins with estimation of the initial resilient modulus for each layer. Next, changes in  $M_R$  with temperature are estimated for any asphalt layers and changes in moisture content are estimated for all unbound layers. Finally, in order to predict seasonal changes, these changes in moisture content must be eventually translated to changes in  $M_R$ .

A literature study was recently completed at ASU, which helped quantify the sensitivity of  $M_R$  to changes in degree of saturation (1). In general, it was found that a 1% increase in degree of saturation will cause, on the average, a 3% reduction in modulus for fine-grained soils and a 2% reduction for coarse-grained soils.

## **Objective**

The objective of this study was to investigate the magnitude of change in resilient modulus due to variation in moisture for 10 LTPP sites, as predicted by the newly developed Resilient Modulus – Moisture model developed at ASU (1). These 10 LTPP sites were the same sites that were used to examine the suitability of predictions of real time moisture content change by a revised EICM (Enhanced Integrated Climatic Model) model (2).

## Analysis

### *Resilient Modulus Model*

The resilient modulus – moisture model developed at ASU uses only degree of saturation as a predictor variable. This model that relates  $M_R$  change to moisture change is:

$$\log \frac{M_R}{M_{Ropt}} = a + \frac{b - a}{1 + EXP(\beta + k_S \cdot (S - S_{opt}))} \quad (1)$$

Where:

$M_R$  = resilient modulus at degree of saturation  $S$  (decimal); to be predicted;

$M_{R(opt)}$  = resilient modulus at maximum dry density and optimum moisture content; (Note: For the purposes of this study, CBR values were estimated from Table 1 and Equation 2 was used to estimate  $M_{Ropt}$ )

$$M_{Ropt} = 2555 \cdot CBR^{0.64} \quad (2)$$

$S_{opt}$  = degree of saturation at maximum dry density and optimum moisture content, (in decimal);

$a$  = minimum of  $\log(M_R/M_{Ropt})$ ;

$b$  = maximum of  $\log(M_R/M_{Ropt})$ ;

$\beta$  = location parameter – obtained as a function of  $a$  and  $b$  by imposing the condition of a zero intercept on semi-log scale:

$$\beta = \ln\left(-\frac{b}{a}\right) \quad (1-1)$$

$k_S$  = regression parameter.

Table 1 CBR Values as a Function of Material Type (4)

Major Division		Letter	Name	Value as Foundation When Not Subject to Frost Action	Value as Base Directly under Wearing Surface	Potential Frost Action	Compressibility and Expansion	Drainage Characteristics	Compaction Equipment	Unit Dry Weight (pcf )	Field CBR	Subgrade Modulus k (pci)
1	2	3	4	5	6	7	8	9	10	11	12	13
Coarse-grained soils	Gravel and gravelly soils	GW	Gravel or sandy gravel, well graded	Excellent	Good	None to very slight	Almost none	Excellent	Crawler-type tractor, rubber-tired equipment, steel-wheeled roller	125-140	60-80	300 or more
		GP	Gravel or sandy gravel, poorly graded	Good to excellent	Poor to fair	None to very slight	Almost none	Excellent	Crawler-type tractor, rubber-tired equipment, steel-wheeled roller	120-130	35-60	300 or more
		GU	Gravel or sandy gravel, uniformly graded	Good	Poor	None to very slight	Almost none	Excellent	Crawler-type tractor, rubber-tired equipment	115-125	25-50	300 or more
		GM	Silty gravel or silty sandy gravel	Good to excellent	Fair to good	Slight to medium	Very slight	Fair to poor	Rubber-tired equipment, sheepsfoot roller, close control of moisture	130-145	40-80	300 or more
		GC	Clayey gravel or clayey sandy gravel	Good	Poor	Slight to medium	Slight	Poor to practically impervious	Rubber-tired equipment, sheepsfoot roller	120-140	20-40	200-300
	Sand and sandy soils	SW	Sand or gravelly sand, well graded	Good	Poor	None to very slight	Almost none	Excellent	Crawler-type tractor, rubber-tired equipment	110-130	20-40	200-300
		SP	Sand or gravelly sand, poorly graded	Fair to good	Poor to not suitable	None to very slight	Almost none	Excellent	Crawler-type tractor, rubber-tired equipment	105-120	15-25	200-300
		SU	Sand or gravelly sand, uniformly graded	Fair to good	Not suitable	None to very slight	Almost none	Excellent	Crawler-type tractor, rubber-tired equipment	100-115	10-20	200-300
		SM	Silty sand or silty gravelly sand	Good	Poor	Slight to high	Very slight	Fair to poor	Rubber-tired equipment, sheepsfoot roller, close control of moisture	120-135	20-40	200-300
		SC	Clayey sand or clayey gravelly sand	Fair to good	Not suitable	Slight to high	Slight to medium	Poor to practically impervious	Rubber-tired equipment, sheepsfoot roller	105-130	10-20	200-300
Fine-grained soils	Low compressibility LL < 50	ML	Silts, sandy silts, gravelly silts, or diatomaceous soils	Fair to poor	Not suitable	Medium to very high	Slight to medium	Fair to poor	Rubber-tired equipment, sheepsfoot roller, close control of moisture	100-125	5-15	100-200
		CL	Lean clays, sandy clays, or gravelly clays	Fair to poor	Not suitable	Medium to high	Medium	Practically impervious	Rubber-tired equipment, sheepsfoot roller	100-125	5-15	100-200
		OL	Organic silts or lean organic clays	Poor	Not suitable	Medium to high	Medium to high	Poor	Rubber-tired equipment, sheepsfoot roller	90-105	4-8	100-200
	High Compressibility LL > 50	MH	Micaceous clays or diatomaceous soils	Poor	Not suitable	Medium to very high	High	Fair to poor	Rubber-tired equipment, sheepsfoot roller	80-100	4-8	100-200
		CH	Fat clays	Poor to very poor	Not suitable	Medium	High	Practically impervious	Rubber-tired equipment, sheepsfoot roller	90-110	3-5	50-100
		OH	Fat organic clays	Poor to very poor	Not suitable	Medium	High	Practically impervious	Rubber-tired equipment, sheepsfoot roller	80-105	3-5	50-100
Peat and other fibrous organic soils		P <sub>t</sub>	Peat, humus, and other	Not suitable	Not suitable	Slight	Very high	Fair to poor	Compaction not practical			

Using the available literature data and assuming a maximum modulus ratio of 2.5 for fine-grained materials and 2 for coarse-grained materials, the values of  $a$ ,  $b$ ,  $\beta$  and  $k_s$  for coarse-grained and fine-grained materials are given in Table 2. The predicted modulus ratios versus change in degree of saturation are illustrated in Figures 1 and 2.

### *Moisture*

For 10 LTPP sites documented in the LTPP database, moisture profiles were generated using EICM (Enhanced Integrated Climatic Model). Moisture was available as volumetric moisture content, at given depths, with time. For the purpose of this study, moisture contents at the middle of the structural layers of a given LTPP site were used as input. Usually, EICM predicted moisture contents were not available exactly at the middle of the layers; therefore, the EICM computation node closest to the middle of a layer was used.

Volumetric moisture content was converted to gravimetric moisture content using Equation 3.

$$w = \frac{\theta \cdot \rho_w}{\rho_{dry}} \quad (3)$$

Where:

$w$  = gravimetric water content (%);

$\rho_{dry}$  = dry density of unbound material;

$\rho_w$  = density of water;

$\theta$  = volumetric moisture content (%); available from the EICM for this study.

**Table 2. Model Parameters**

Parameter	Coarse Grained Materials	Fine Grained Materials	Comments
$a$	- 0.3123	-0.5934	Regression parameter
$b$	0.3	0.4	Conservatively assumed, until more data becomes available  (corresponding to modulus ratios of 2 and 2.5)
$\beta$	- 0.0401	- 0.3944	Obtained using Equation 1-1
$k_s$	6.8157	6.1324	Regression Parameter

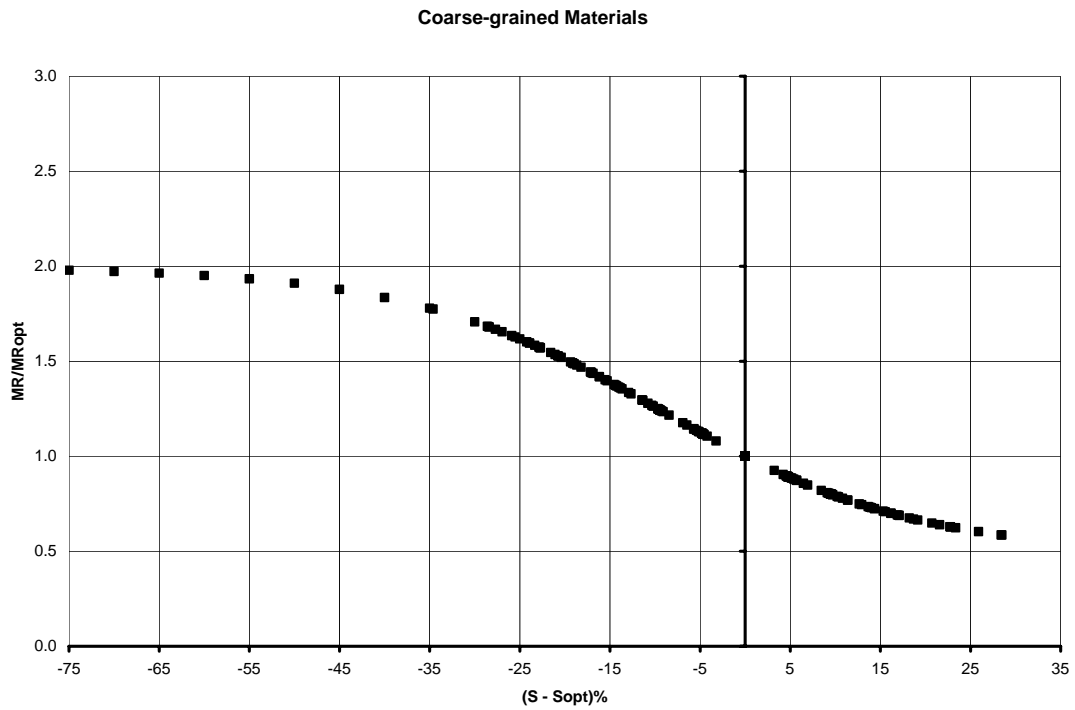


Figure 1. Modulus Ratios for Coarse Grained Materials

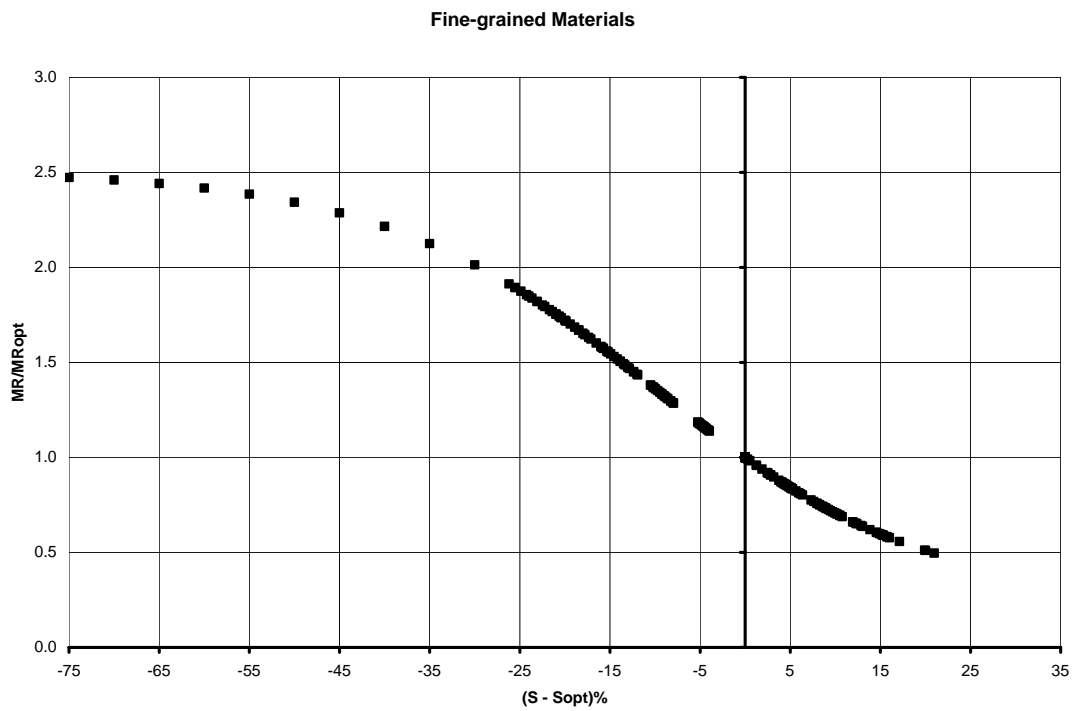


Figure 2. Modulus Ratios for Fine Grained Materials

For purposes of this study, the optimum moisture content for standard compaction was estimated using Equation 4:

$$\begin{aligned} wPI > 0 &\Rightarrow w_{opt} = 1.3 \cdot wPI^{0.73} + 11 \\ wPI = 0 &\Rightarrow w_{opt} = 8.6425 \cdot D_{60}^{-0.1038} \end{aligned} \quad (4)$$

Where:

$w_{opt}$  = optimum moisture content at maximum dry density obtained by standard compaction (AASHTO T99);

$wPI$  = plasticity index (PI) times the percent passing the No. 200 sieve (in decimal);

$D_{60}$  = particle size for which 60% of the material is finer in mm.

In order to obtain the optimum moisture content in the case of modified compactive effort (T 180), Equations 5a and 5b were used:

$$\Delta w_{opt} = 0.16 \cdot w_{opt}^2 + 0.853 \cdot w_{opt} + 0.9 \quad (5a)$$

$$w_{opt}(T180) = w_{opt}(T99) - \Delta w_{opt} \quad (5b)$$

Where  $\Delta w_{opt}$  represents the difference in the  $w_{opt}$  for T99 and T180.

The above correlations were developed as part of studies aimed at improvement of the EICM predictive capability and are described by Witczak et al. (2).

### *Degree of Saturation*

The degree of saturation was computed using Equation 6:

$$S = \frac{w}{\left( \frac{G_s \cdot \gamma_w}{\gamma_{dry}} - 1 \right)} \quad (6)$$

Where:

$S$  = degree of saturation (%);

$G_s$  = specific gravity of soil solids;

$w$  = gravimetric moisture content (%);

$\gamma_w$  = unit weight of water;

$\gamma_{dry}$  = dry unit weight of unbound material.

The degree of saturation is used in Equation 1.

The degree of saturation at optimum moisture content and maximum dry density,  $S_{opt}$ , is obtained from Equation 7:

$$S_{opt} = 6.752 \cdot wPI^{0.147} + 78 \quad (7)$$

Where:

$wPI$  = plasticity index (PI) times the percent passing the No. 200 sieve (as a decimal).

The correlation was developed from a modest database for both standard (AASHTO T99) and modified (AASHTO T180) compactive efforts. A degree of saturation at optimum of 78% (the intercept) was adopted for all non-plastic materials, as described in Witczak et al. (2).

Equations 4, 5 and 7 were developed in order to minimize errors induced by erroneous or missing values of dry density,  $w_{opt}$ , and/or specific gravity of solids.

Experience has shown that it is the rule rather than the exception that the reported value for one or more of the three variables  $w_{opt}$ ,  $G_s$  and  $\gamma_{d\ max}$  for a given soil will be erroneous, unreasonable or missing. Therefore, in order to establish an internally consistent basis for assessing the initial compaction conditions for unbound materials, the optimum state ( $\gamma_d = \gamma_{d\ max}$  and  $w = w_{opt}$ ) has been adopted as the reference condition, and  $S_{opt}$ ,  $w_{opt}$  and  $G_s$  have



been obtained from correlations with  $wPI$  or  $D_{60}$ . Equation 8 represents the correlation developed for  $G_s$ . Equation 9 is used to compute  $\gamma_{d\ max}$ , and  $\gamma_{d\ max}$  is used in Equations 3 and 6 as needed.

$$G_s = 0.041 \cdot wPI^{0.29} + 2.65 \quad (8)$$

$$\gamma_{d\ max} = \frac{G_s \cdot \gamma_w}{1 + \frac{w_{opt}}{S_{opt}} \cdot G_s} \quad (9)$$

Where:

$S_{opt}$  = degree of saturation at optimum moisture content and maximum dry density;

$G_s$  = specific gravity;

$w_{opt}$  = optimum moisture content;

$\gamma_w$  = unit weight of water;

$\gamma_{d\ max}$  = dry unit weight at optimum condition.

**For the 2002 Design Guide implementation, it will be recommended that directly-measured values of  $\gamma_{d\ max}$ ,  $w_{opt}$ , and  $G_s$  be used for Level 1. However, for Levels 2 and 3 it will be recommended that the correlations given by Equations 4, 5, 7, and 8 be used to get  $S_{opt}$ ,  $w_{opt}$  and  $G_s$  and then Equation 9 be used to get  $\gamma_{d\ max}$ .**

Using the correlations, equations, and procedures outlined in the preceding section, input data was generated for the 10 LTPP sites, as shown in Table 3.

Table 3 Input Data Summary

Layer Type	Thickness	Depth	ICM Node	Class	wPI	D60	Gs	Sopt	wopt	e	$\rho_{dry}$		1 = coarse	CBR
Units	cm	cm	cm	AASHTO		mm		%	% (std)	% (modif)	%	g/cm3	pcf	2 = fine
<b>Connecticut 9-1803</b>														
AC	18													
Gravel (uncrushed)	37	36.5	36.5	A-1-a Base	0	10	2.65	78	7	6	21.0	2.19	136.65	1 55
Well-graded sand with silt and gravel		65	67	A-2-4 Subgrade	0	0.48	2.86	78	9		34.2	2.13	133.12	1 30
<b>Minnesota 27-1018</b>														
AC	11.2													
?	10	16.2	17.9	A-1-b Base	0	2.6	2.675	78	8	7	24.4	2.15	134.16	1 25
Poorly-graded sand with silt		31.2	31.1	A-3 Subgrade	0	0.38	2.65	78	10		32.5	2.00	124.83	1 20
<b>Maine 23-1026</b>														
AC	16													
Gravel (uncrushed)	48	40	40	A-1-a Base	0	45.2	2.65	78	6	5	17.8	2.25	140.35	1 55
Silty sand with gravel		74	74	A-2-4 Subgrade	0	4.8	2.782	78	7		26.2	2.20	137.56	1 30
<b>New Hampshire 33-1001</b>														
AC	21.6													
Gravel (uncrushed)	49	46.1	46.1	A-1-a Base	0	12.3	2.65	78	7	6	20.5	2.20	137.18	1 55
Soil-aggregate mixture (coarse-grained)	37	89.1	88.6	A-1-b Subbase	0	1.3	2.678	78	8		28.9	2.08	129.67	1 50
Poorly-graded sand with silt		117.6	115.9	A-2-4 Subgrade	0	0.25	2.647	78	10		33.9	1.98	123.38	1 20
<b>Vermont 50-1002</b>														
AC	21.1													
Crushed gravel	53.8	48	50.4	A-1-a Base	0	25.6	2.65	78	6	6	19.0	2.23	138.99	1 70
Poorly graded gravel with silt and sand	34.3	92.05	94.5	A-1-a Subbase	0	7.7	2.65	78	7		23.8	2.14	133.62	1 50
?		119.2	119	A-7-5 Subgrade	12.3		2.815	88	19		61.3	1.74	108.88	2 10
<b>Manitoba 83-1801</b>														
AC	11.5													
Crushed gravel	14.2	18.6	20.67	A-1-a Base	0.545		2.684	84	12	10	33.4	2.01	125.50	1 70
Gravel (uncrushed)	33.5	42.45	42	A-2-6 Subbase	1.155		2.693	85	12		39.5	1.93	120.48	1 55
Silty sand		69.2	68.3	A-2-4 Subgrade	0	0.22	2.831	78	10		36.7	2.07	129.22	2 30
<b>Georgia 13-1005</b>														
AC	19.1													
Soil-aggregate mixture (coarse-grained)	22.4	30.3	32.5	A-1-a Base	0	8.7	2.65	78	7	6	21.3	2.18	136.30	1 50
Clayey sand	60.1	71.55	71	A-4 Subbase	0.36		2.68	84	12		37.1	1.95	121.94	2 15
?		111.6	113	A-6 Subgrade	10		2.73	87	18	56.1	35.9	1.75	109.12	2 10
<b>Colorado 8-1053</b>														
AC	11.4													
Crushed gravel	13.7	18.25	20.5	A-1-a Base	0	7.7	2.65	78	7	6	21.6	2.18	135.99	1 70
Soil-aggregate mixture (coarse-grained)	59.7	54.95	57	A-1-a Subbase	0	13.9	2.65	78	7		22.3	2.17	135.16	1 50
Lean inorganic clay		94.8	96.95	A-6 Subgrade	20.2		2.89	89	23		74.0	1.66	103.64	2 10
<b>Arizona 4-1024</b>														
AC	27.4													
Crushed gravel	22.4	38.6	40.8	A-1-a Base	0	14.4	2.65	78	7	6	20.2	2.20	137.57	1 70
Clayey sand with gravel		59.8	58	A-2-6 Subgrade	6.1		2.719	87	16		49.7	1.82	113.34	2 15
<b>Texas 48-1077</b>														
AC	13.2													
Crushed stone	27.4	26.9	26.9	A-1-a Base	0	9	2.6	78	7	6	20.8	2.15	134.26	1 70
Sandy silt		50.6	53	A-4 Subgrade	0	0.04	2.685	78	12		41.6	1.90	118.36	1 10

## Discussion of Results

Three plots have been developed for each LTPP-SMP site investigated. These plots are presented as Figure 3 through 12, with one Figure number representing each site. For each set, the variation of gravimetric moisture content, degree of saturation, and predicted resilient modulus with time is presented on three separate plots. Values corresponding to the initial (optimum) conditions are plotted as circles. For some sites freezing occurred. EICM outputs were used to identify these periods of freezing. During these frozen periods, the  $M_R$  values were set to 1 million psi, in accordance with the findings reported in Witczak et al. (3). As a result of thawing following freezing, the  $M_R$  value drops dramatically, sometimes to a value less than half the optimum condition value. As the soil suction rises after thawing, gradual recovery occurs until the pre-freezing value is approximately regained. These changes in moduli with time are described in detail in Witczak et al. (3). For this report, the moduli variations after thawing are shown schematically with dotted lines in order to present a more complete picture of the moduli variations.

Figure 3 for Arizona shows dramatic desaturation of the base and very substantial desaturation of the subgrade, even though the subgrade has significant plasticity. This substantial desaturation is no doubt due to the fact that the groundwater table was assumed to be 90 m at the site, corresponding to a suction under the pavement of around 900 kPa. As is explained when Table 3 is presented subsequently, a decrease in  $S$  of more than 50% results in a doubling of the  $M_R$ . Given that  $S_{opt}$ , the initial condition, ranges from 78% to about 88%, this means that any  $S_{equil}$  below about 30% corresponds to a doubling of  $M_R$ .

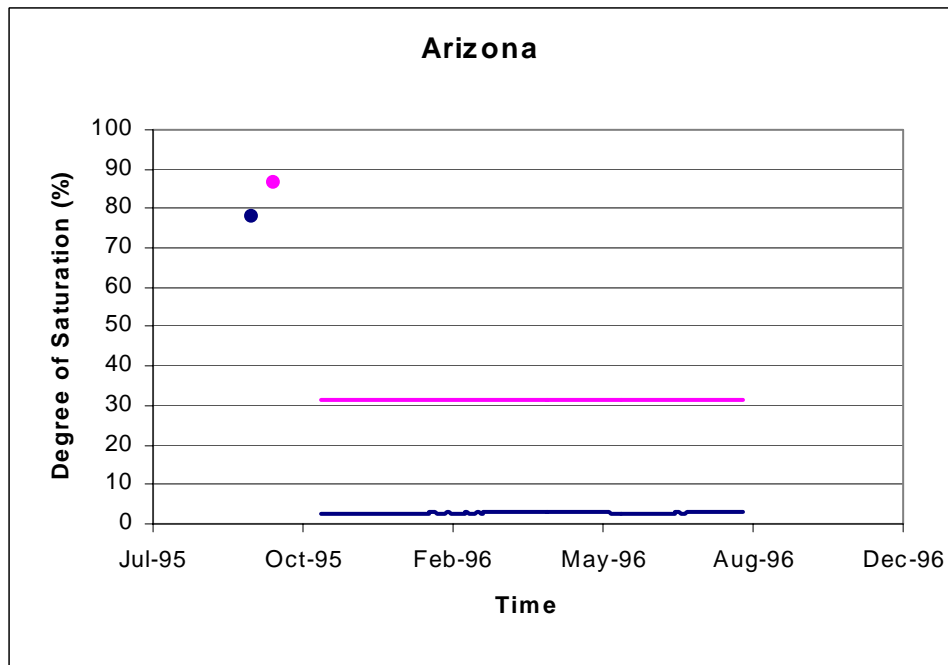
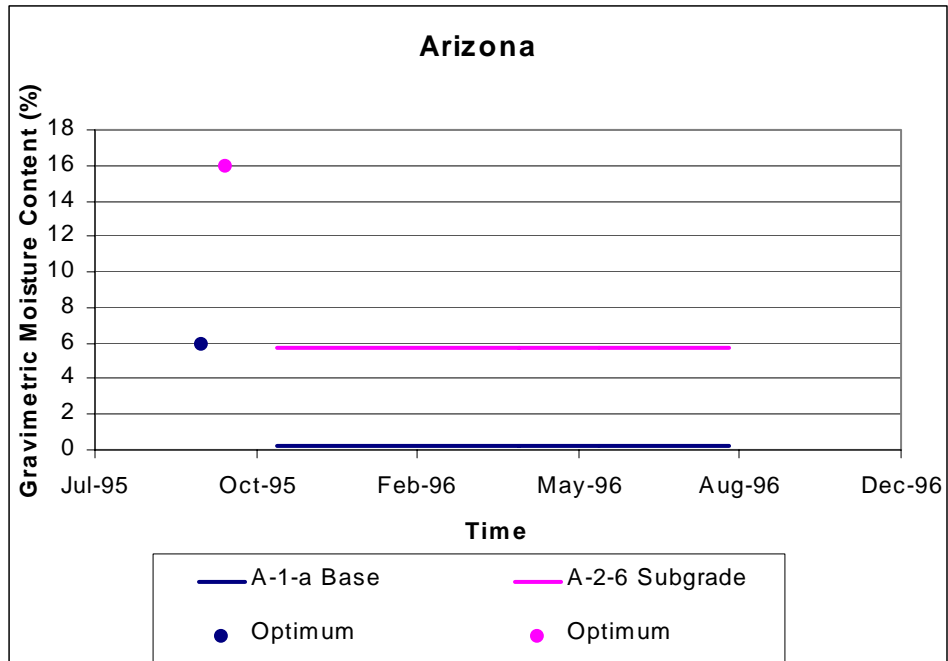


Figure 3a. Predicted Variation in Moisture Content and Degree of Saturation with Time  
for Arizona

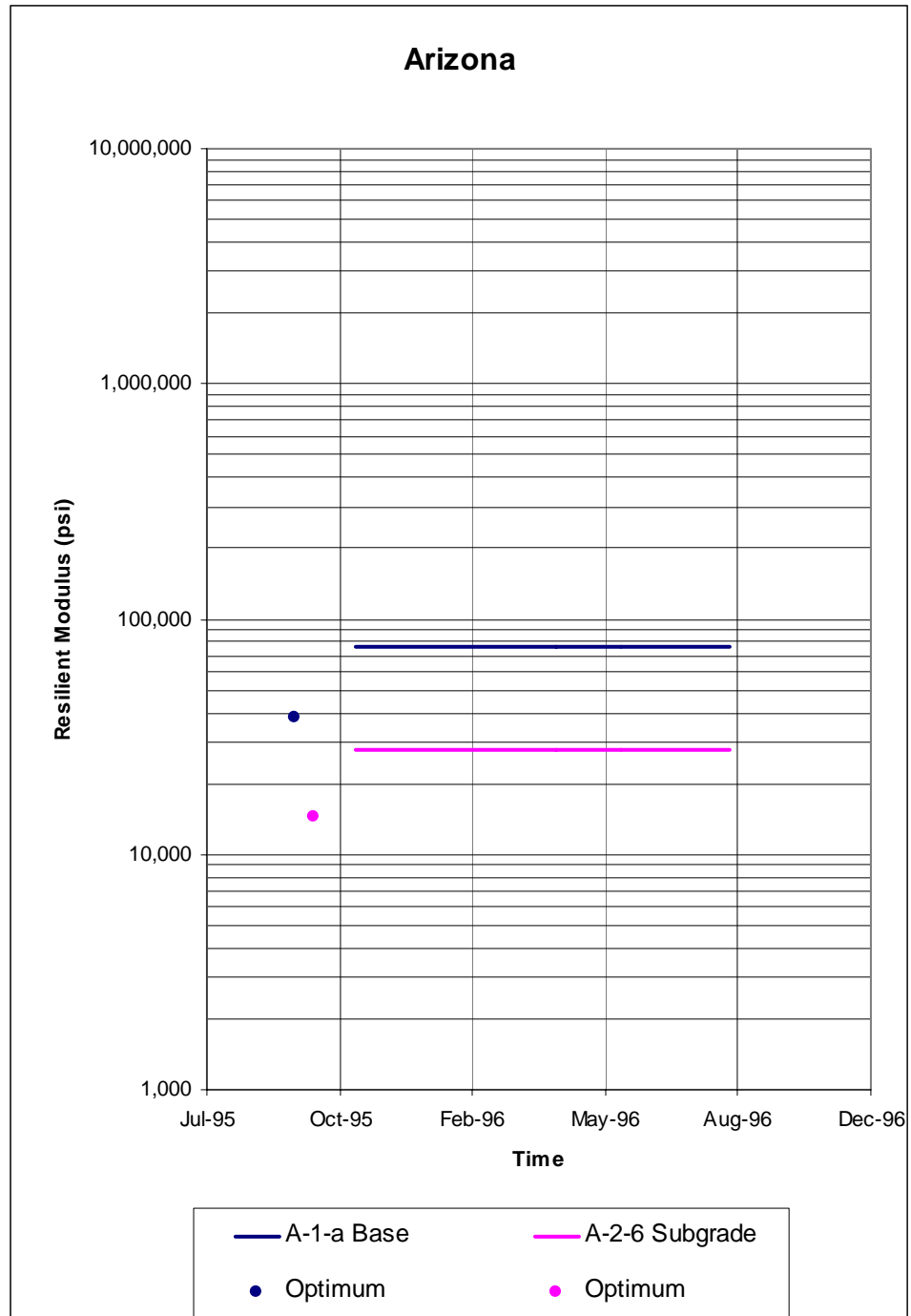


Figure 3b. Predicted Variation in Resilient Modulus with Time for Arizona

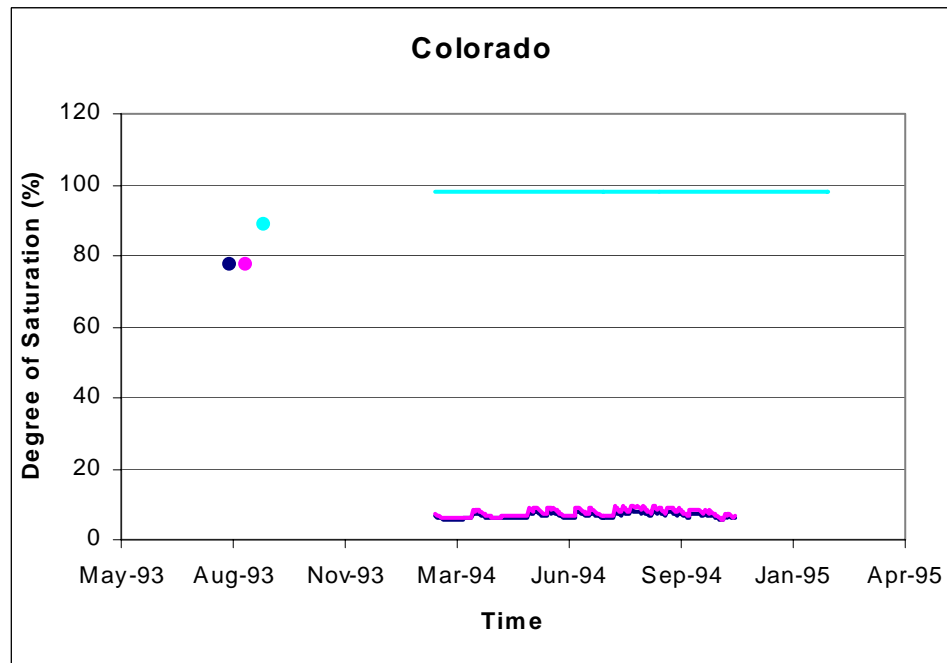
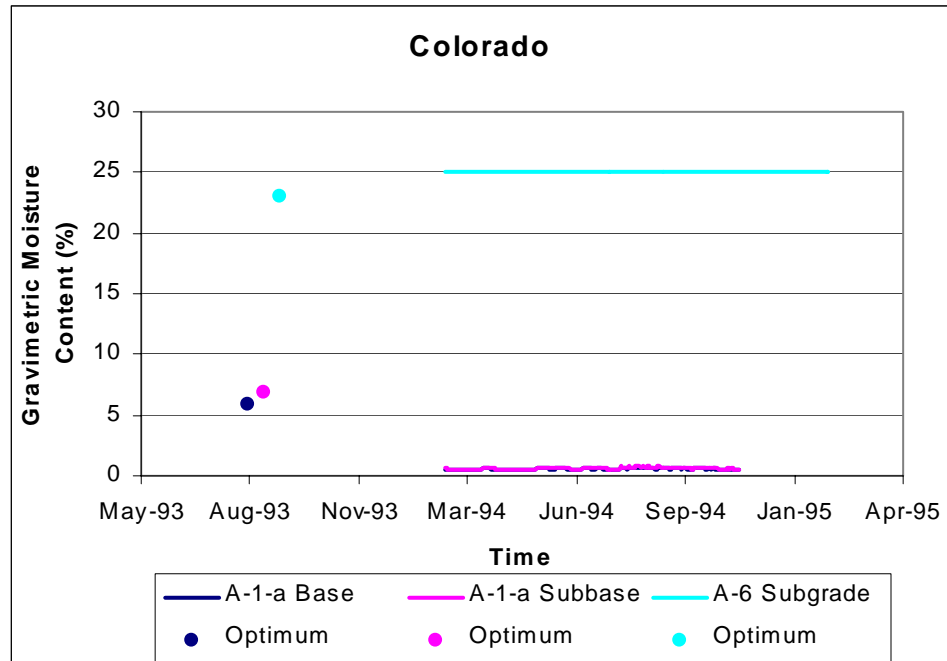


Figure 4a. Predicted Variation in Moisture Content and Degree of Saturation with Time  
for Colorado

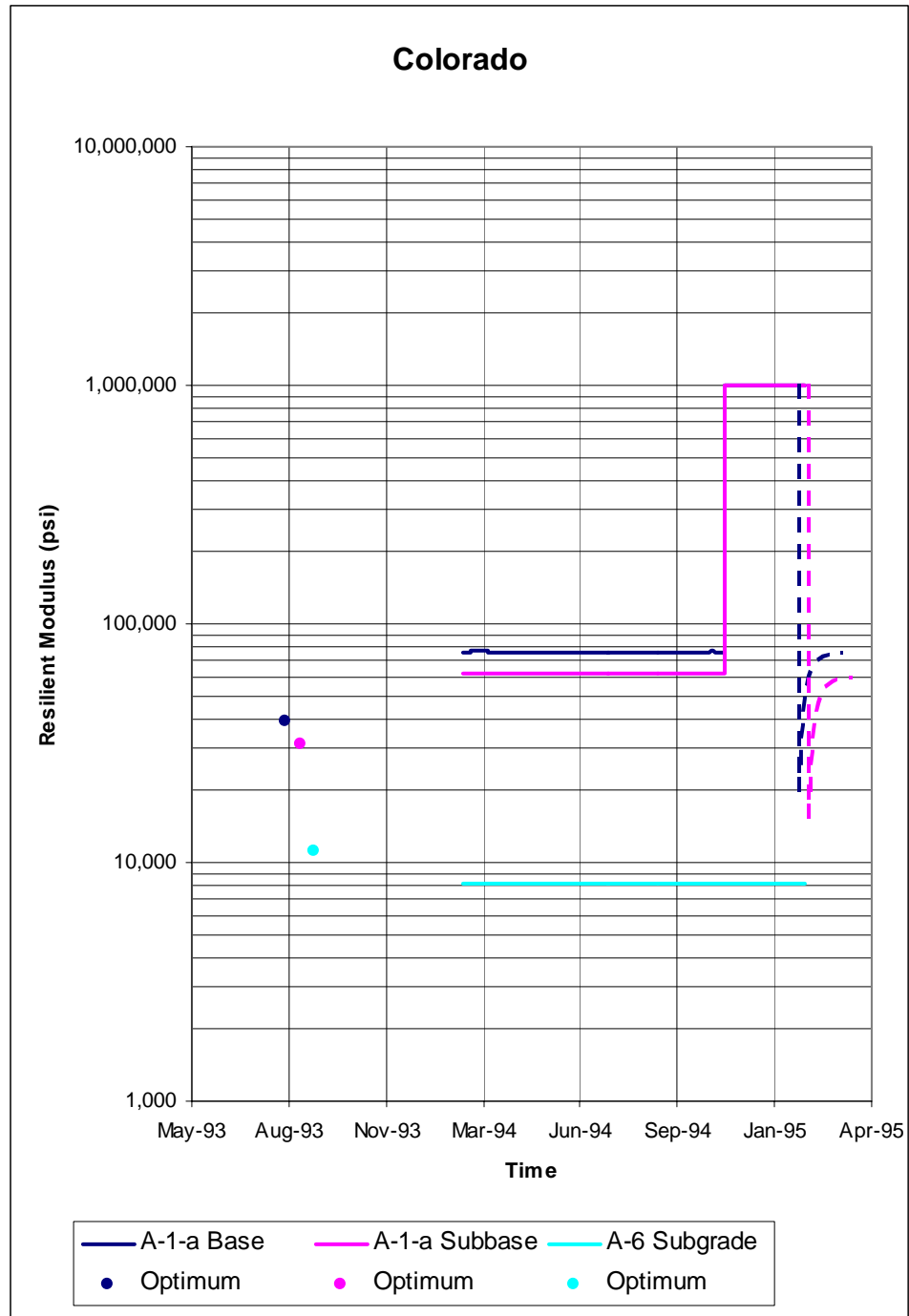


Figure 4b. Predicted Variation in Resilient Modulus with Time for Colorado

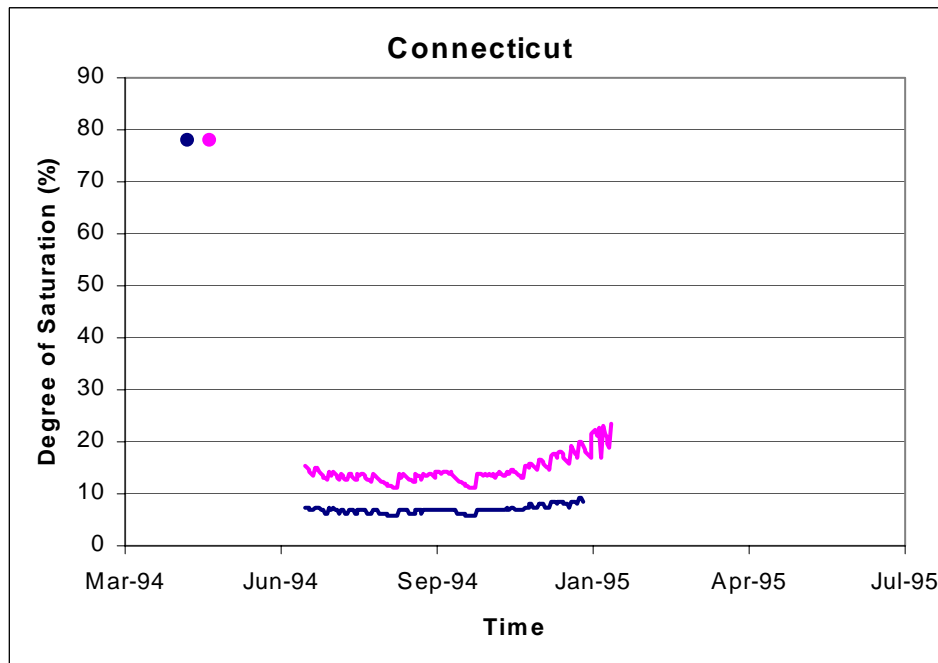
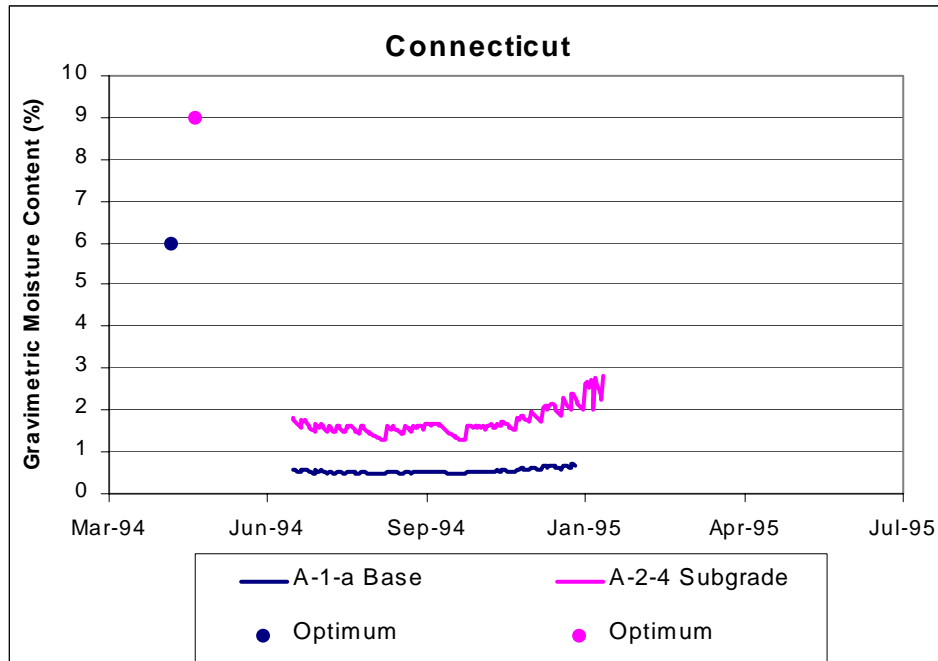


Figure 5a. Predicted Variation in Moisture Content and Degree of Saturation with Time  
for Connecticut



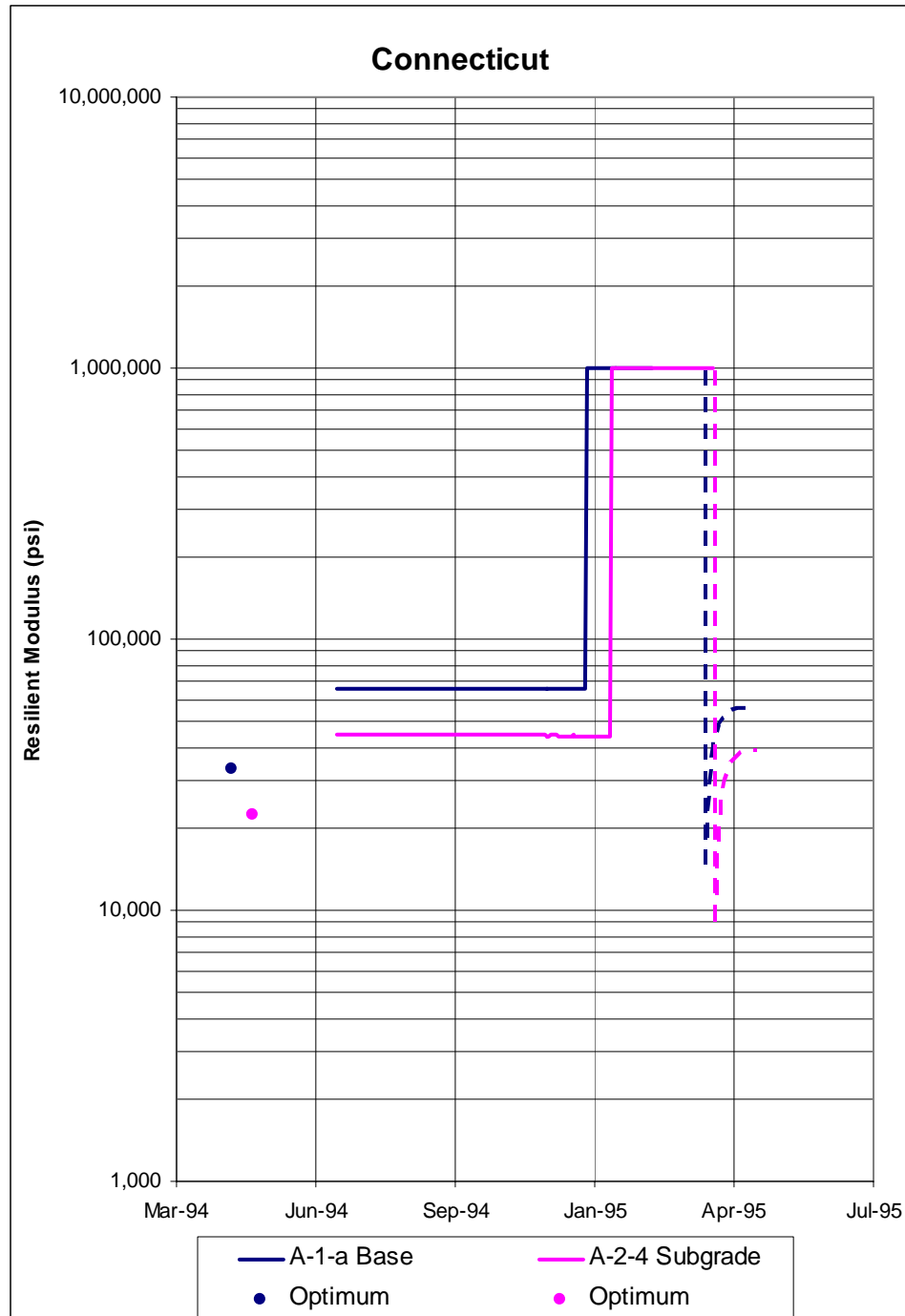


Figure 5b. Predicted Variation in Resilient Modulus with Time for Connecticut

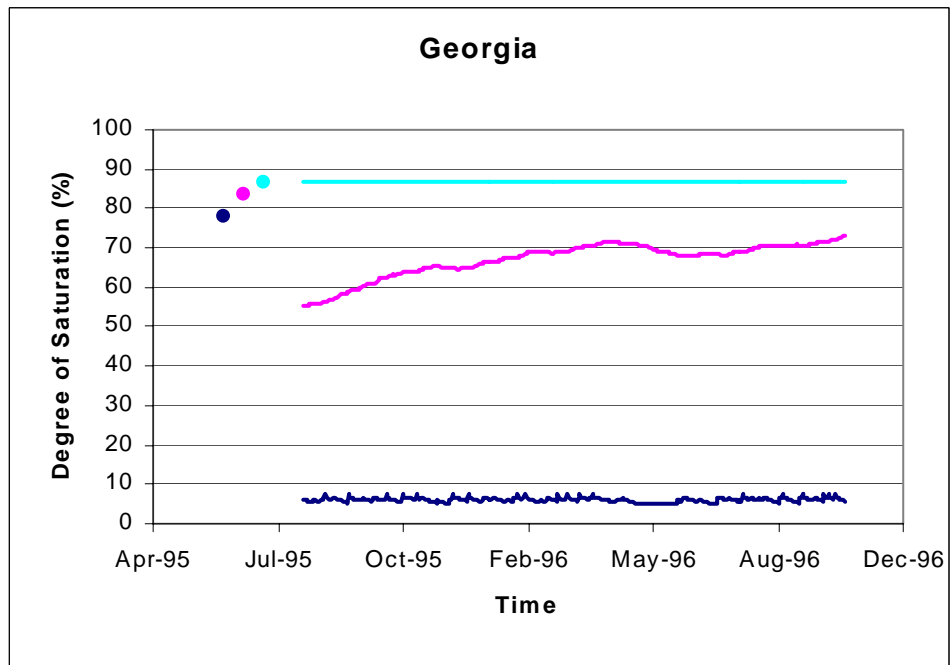
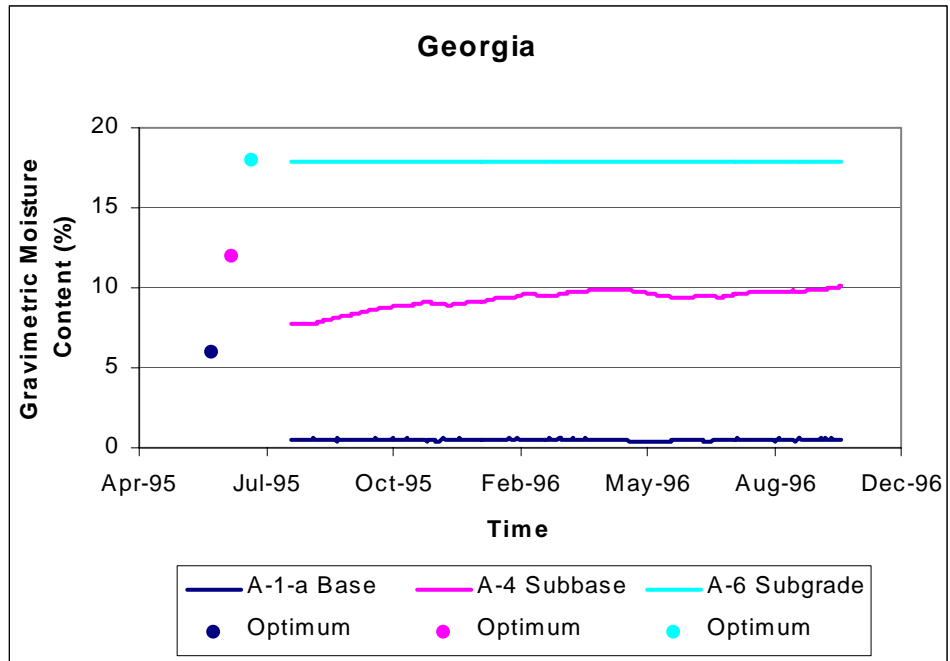


Figure 6a. Predicted Variation in Moisture Content and Degree of Saturation with Time  
for Georgia

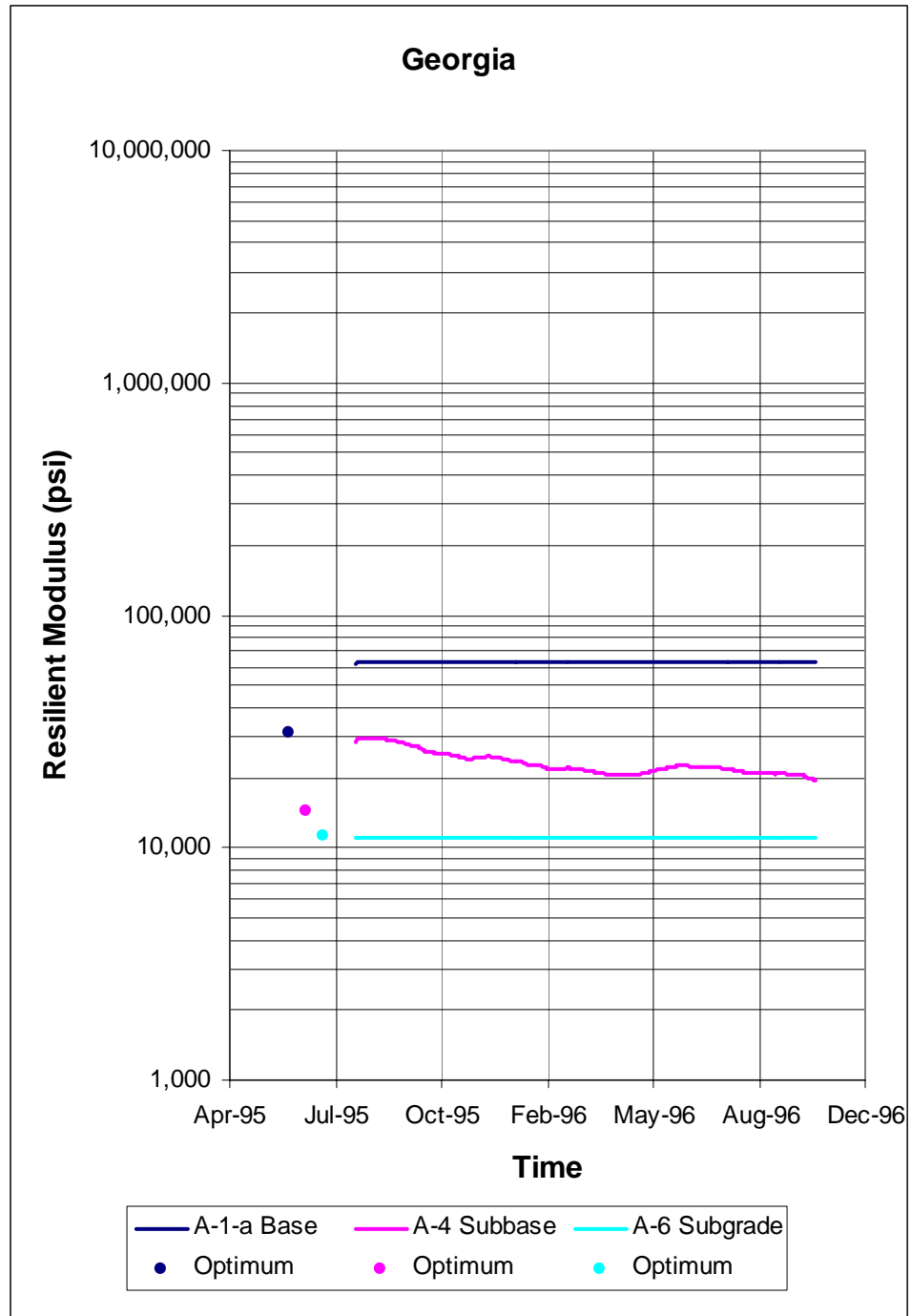


Figure 6b. Predicted Variation in Resilient Modulus with Time for Georgia

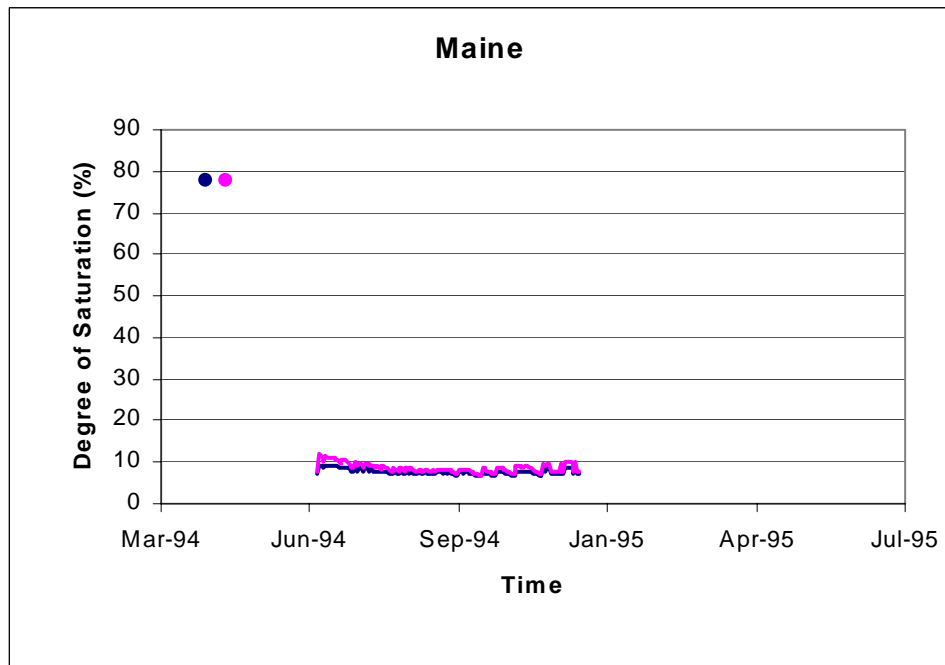
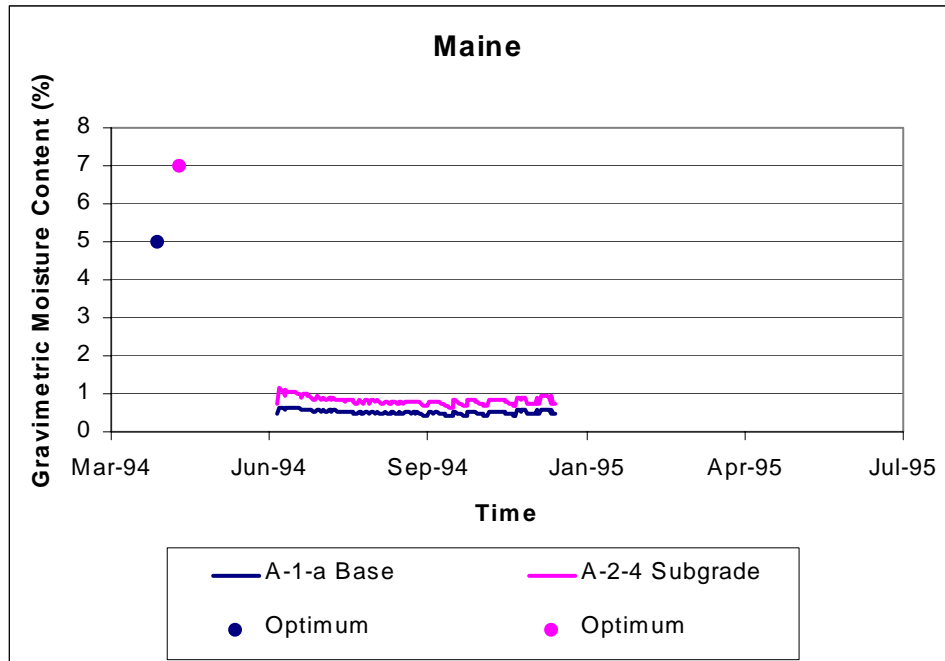


Figure 7a. Predicted Variation in Moisture Content and Degree of Saturation with Time  
for Maine

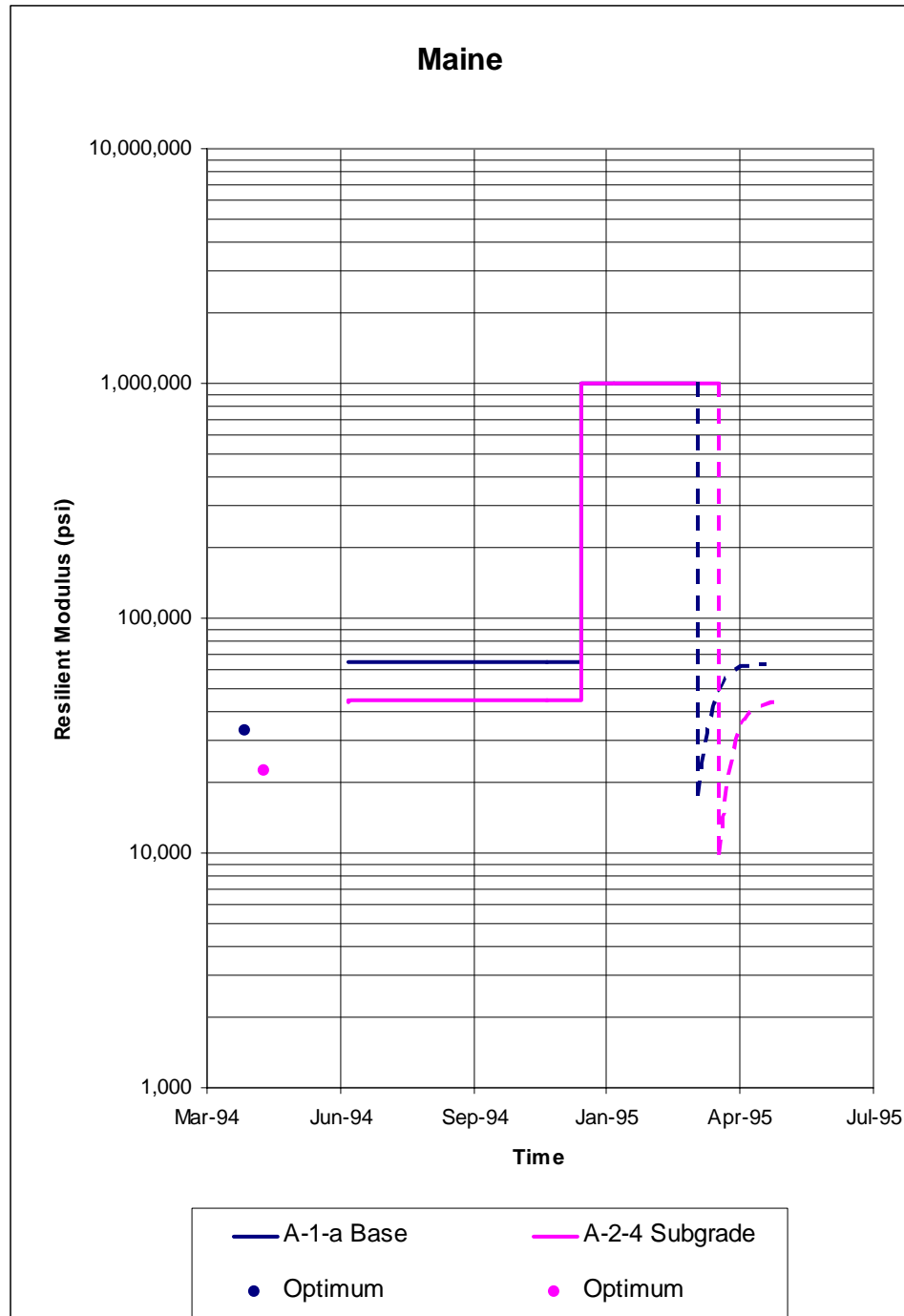


Figure 7b. Predicted Variation in Resilient Modulus with Time for Maine

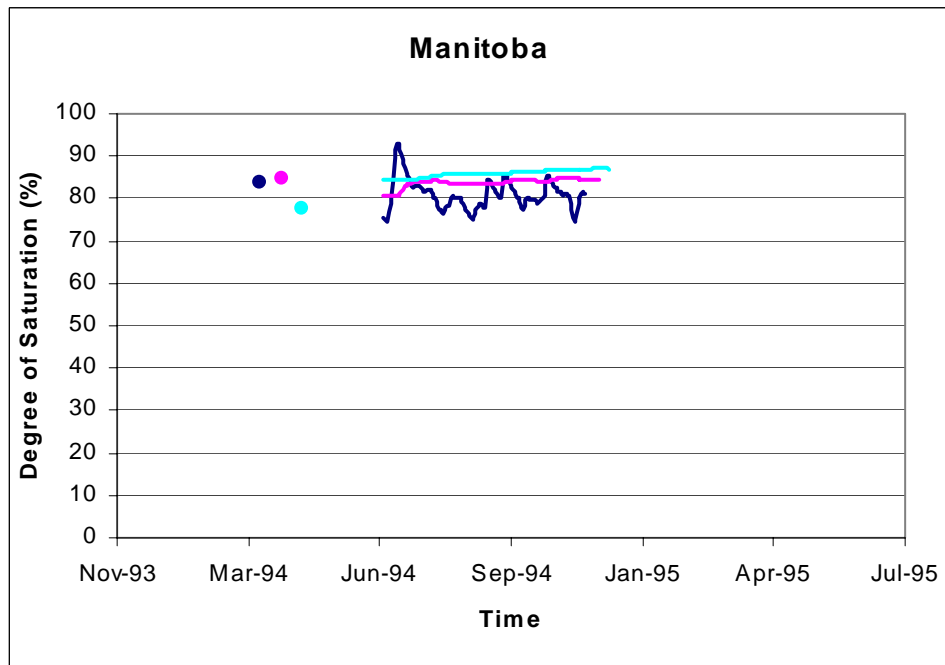
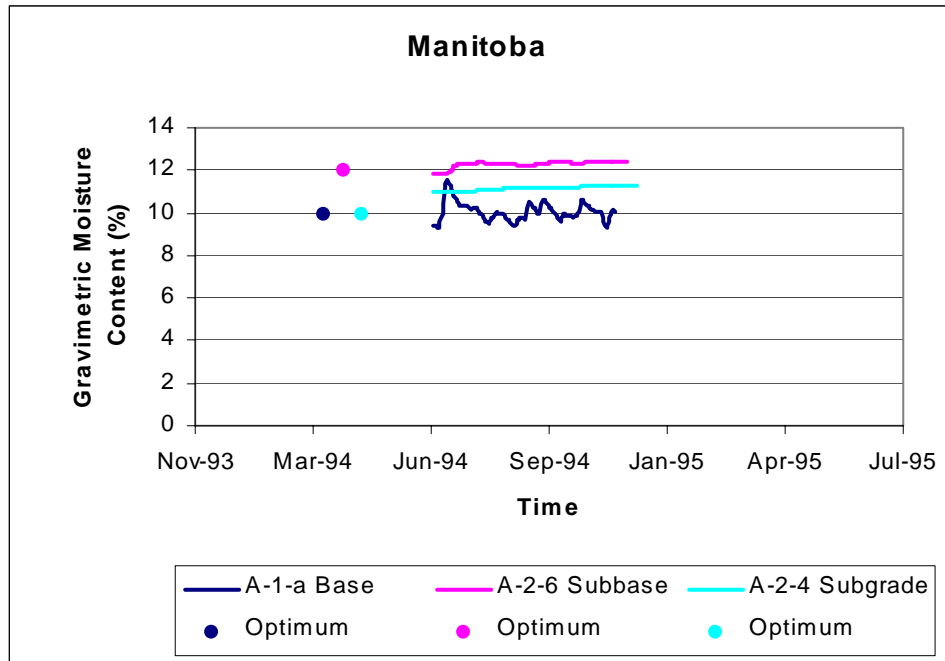


Figure 8a. Predicted Variation in Moisture Content and Degree of Saturation with Time  
for Manitoba

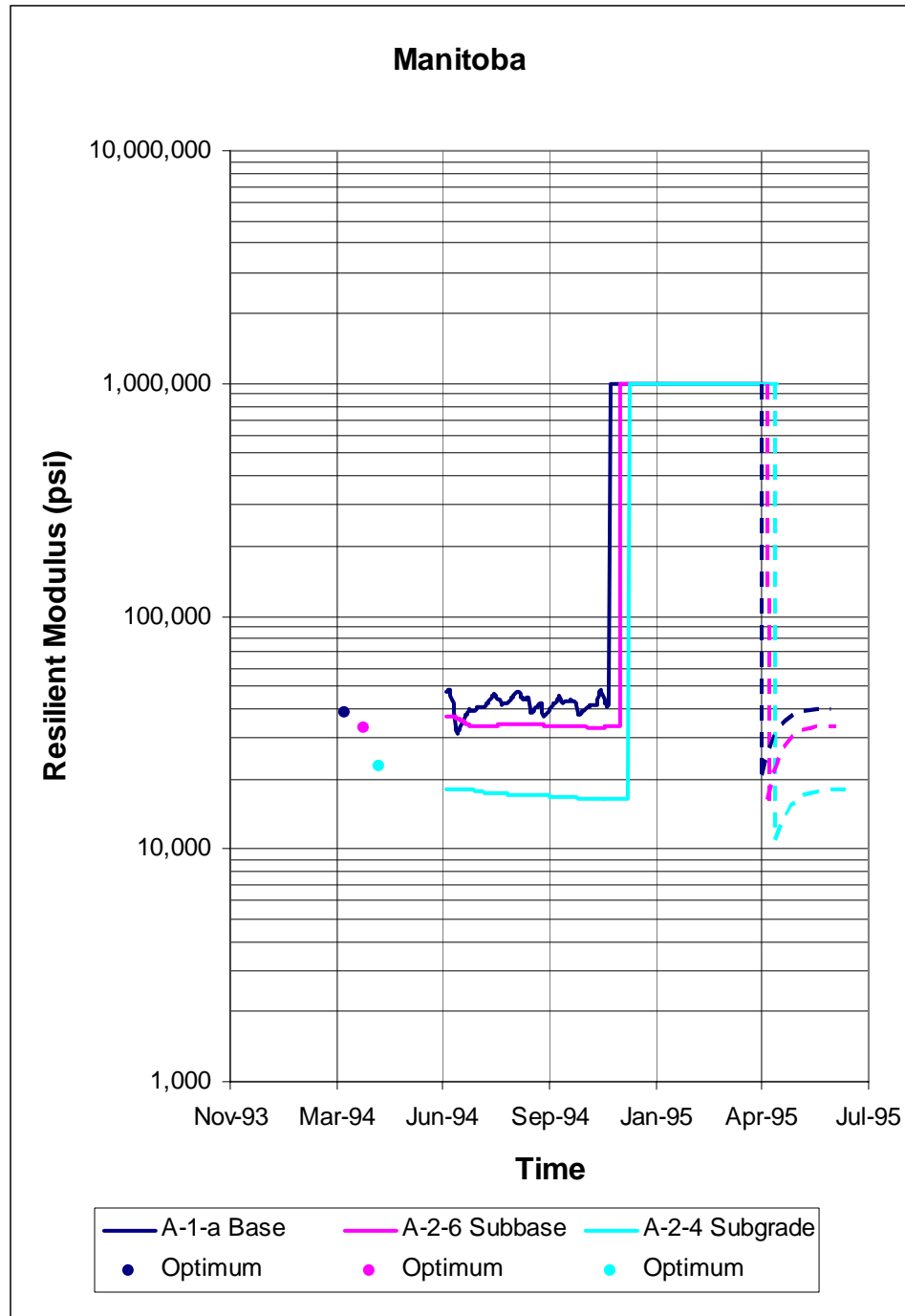


Figure 8b. Predicted Variation in Resilient Modulus with Time for Manitoba

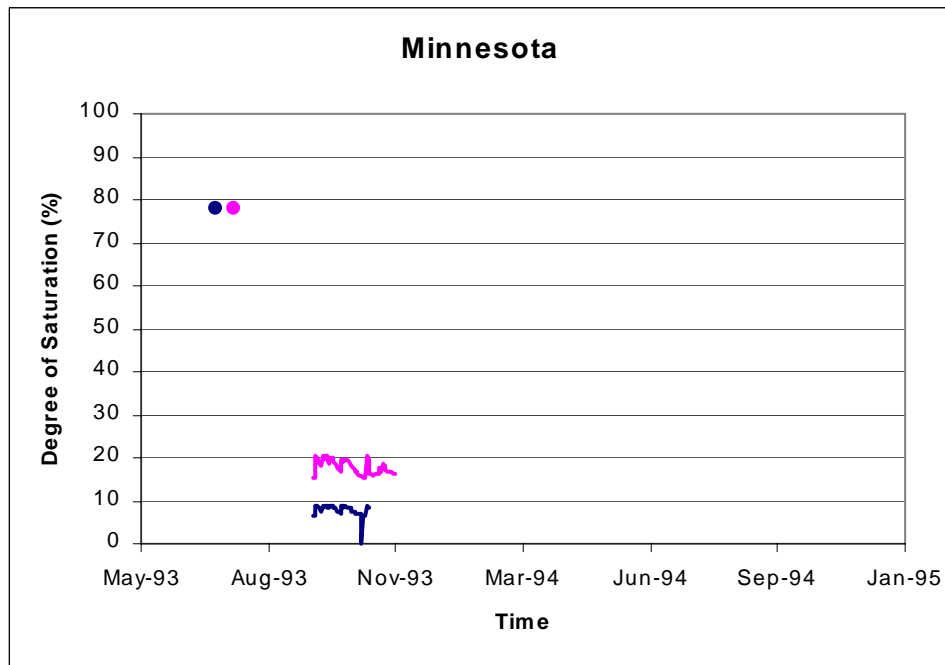
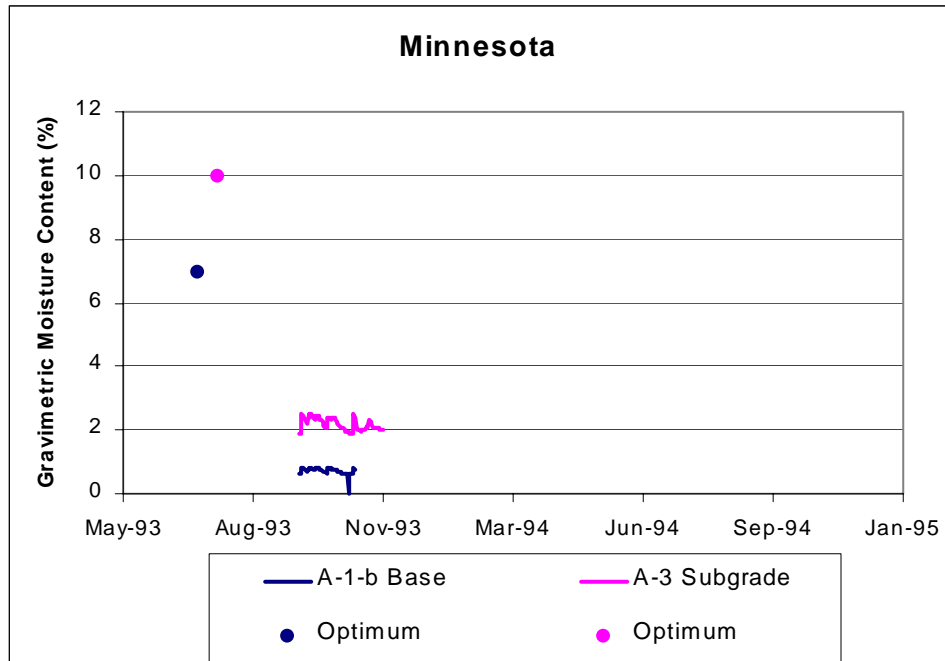


Figure 9a. Predicted Variation in Moisture Content and Degree of Saturation with Time  
for Minnesota



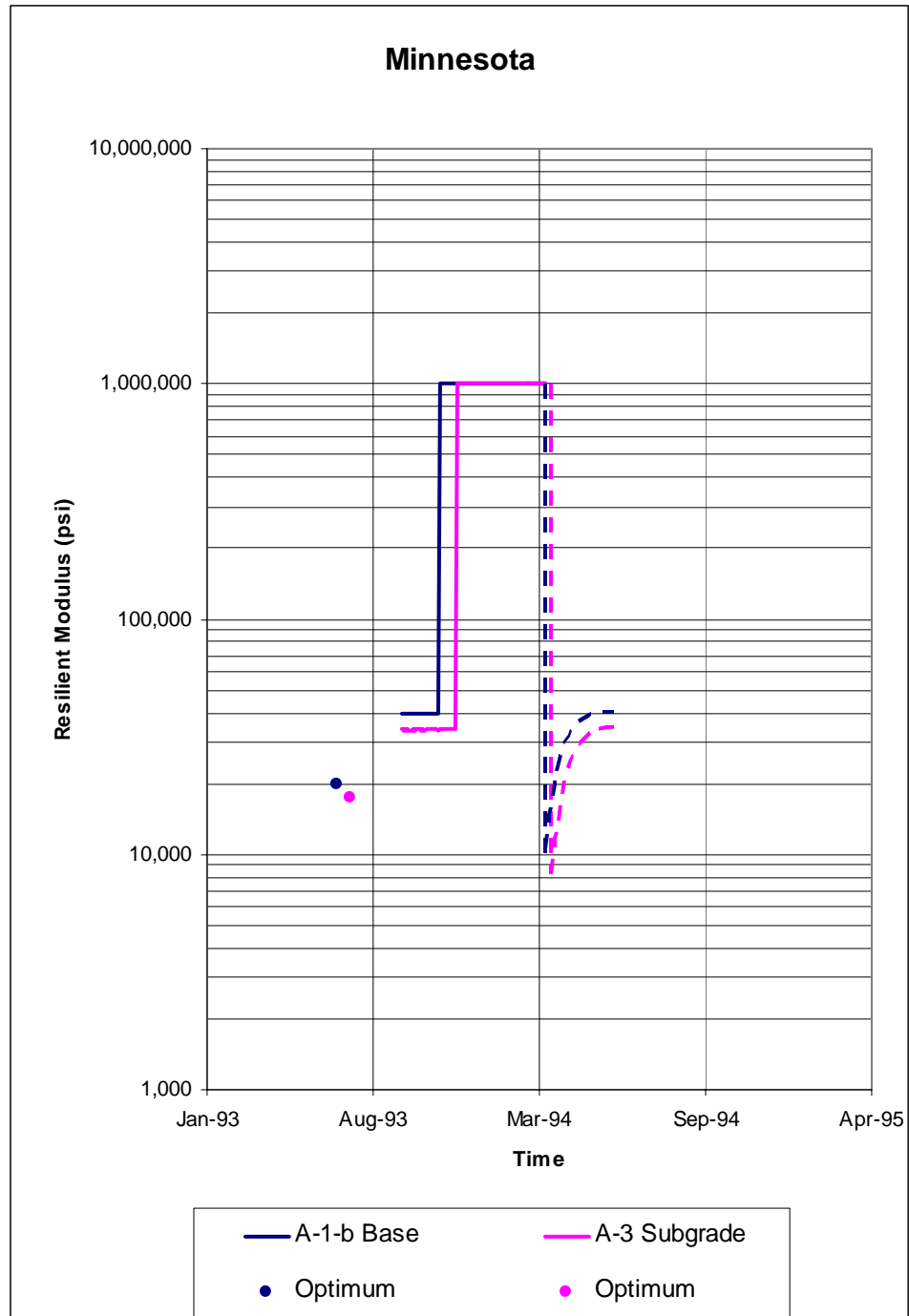


Figure 9b. Predicted Variation in Resilient Modulus with Time for Minnesota

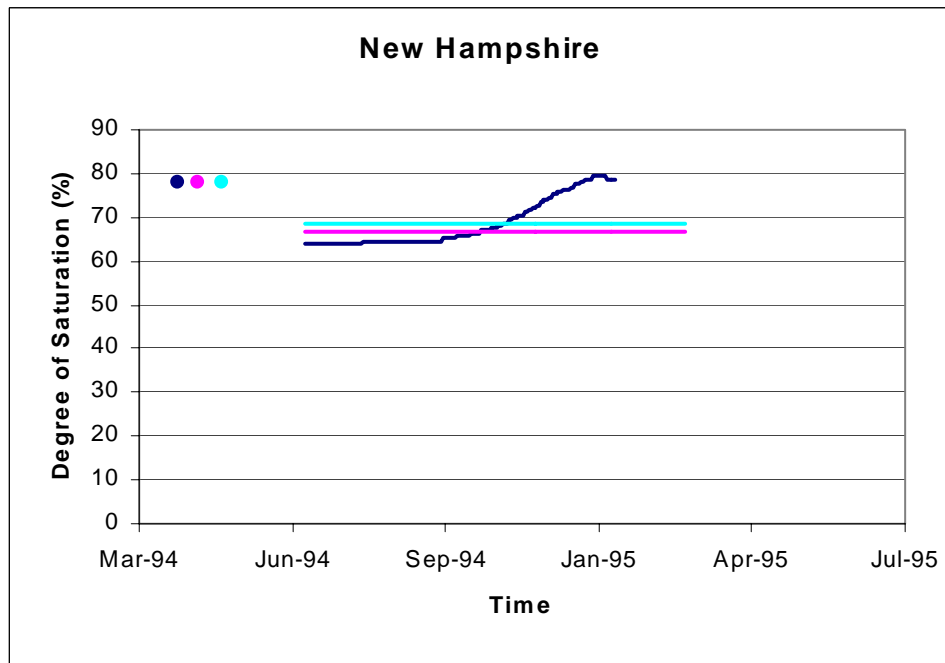
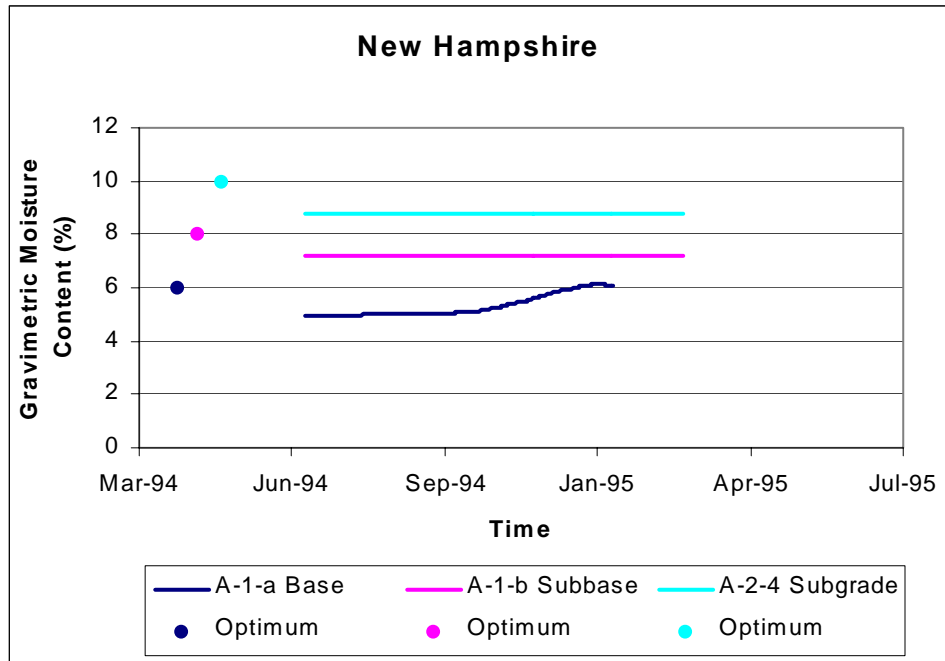


Figure 10a. Predicted Variation in Moisture Content and Degree of Saturation with Time  
for New Hampshire

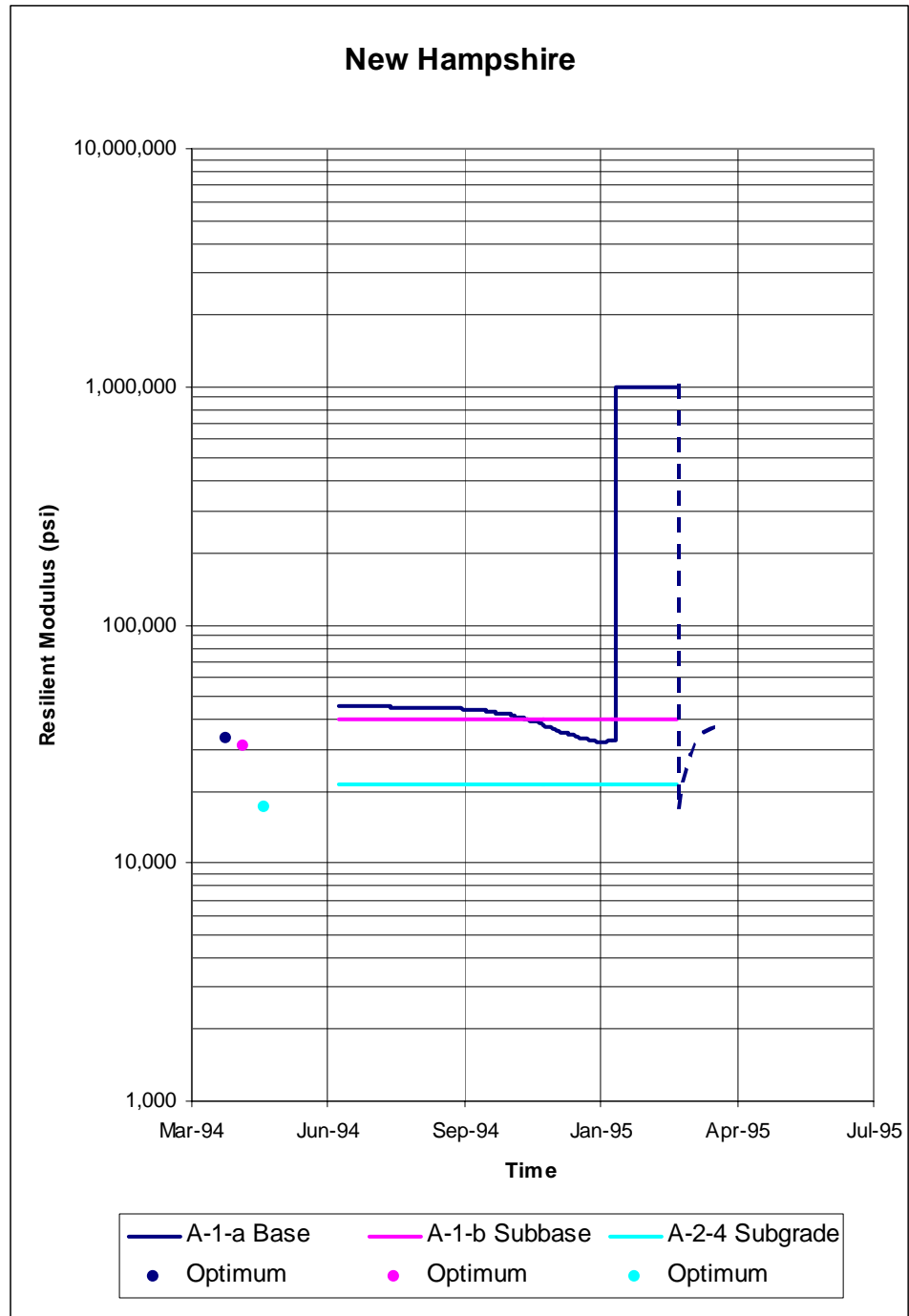


Figure 10b. Predicted Variation in Resilient Modulus with Time for New Hampshire

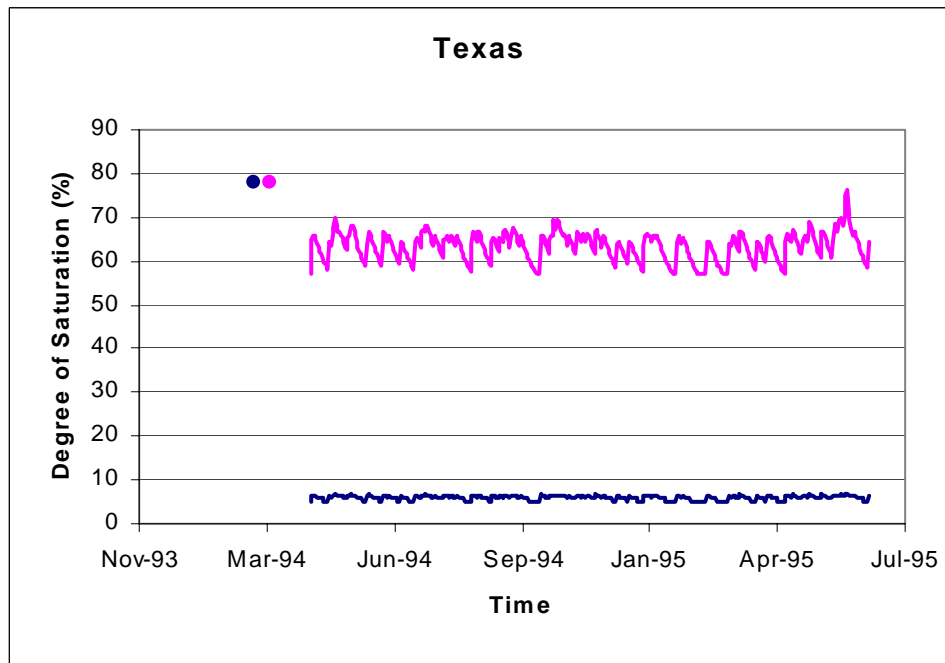
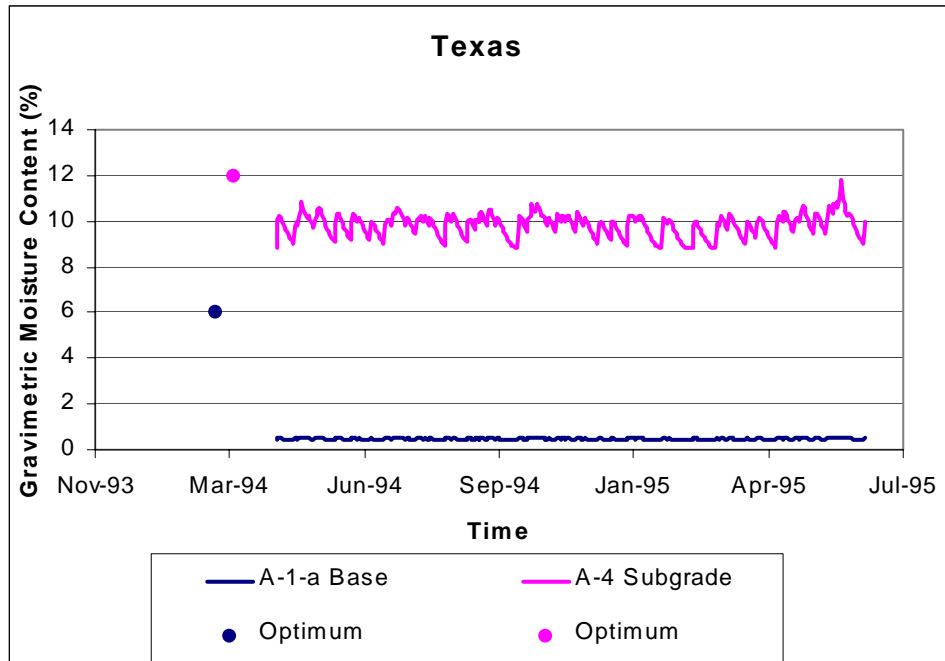


Figure 11a. Predicted Variation in Moisture Content and Degree of Saturation with Time  
for Texas

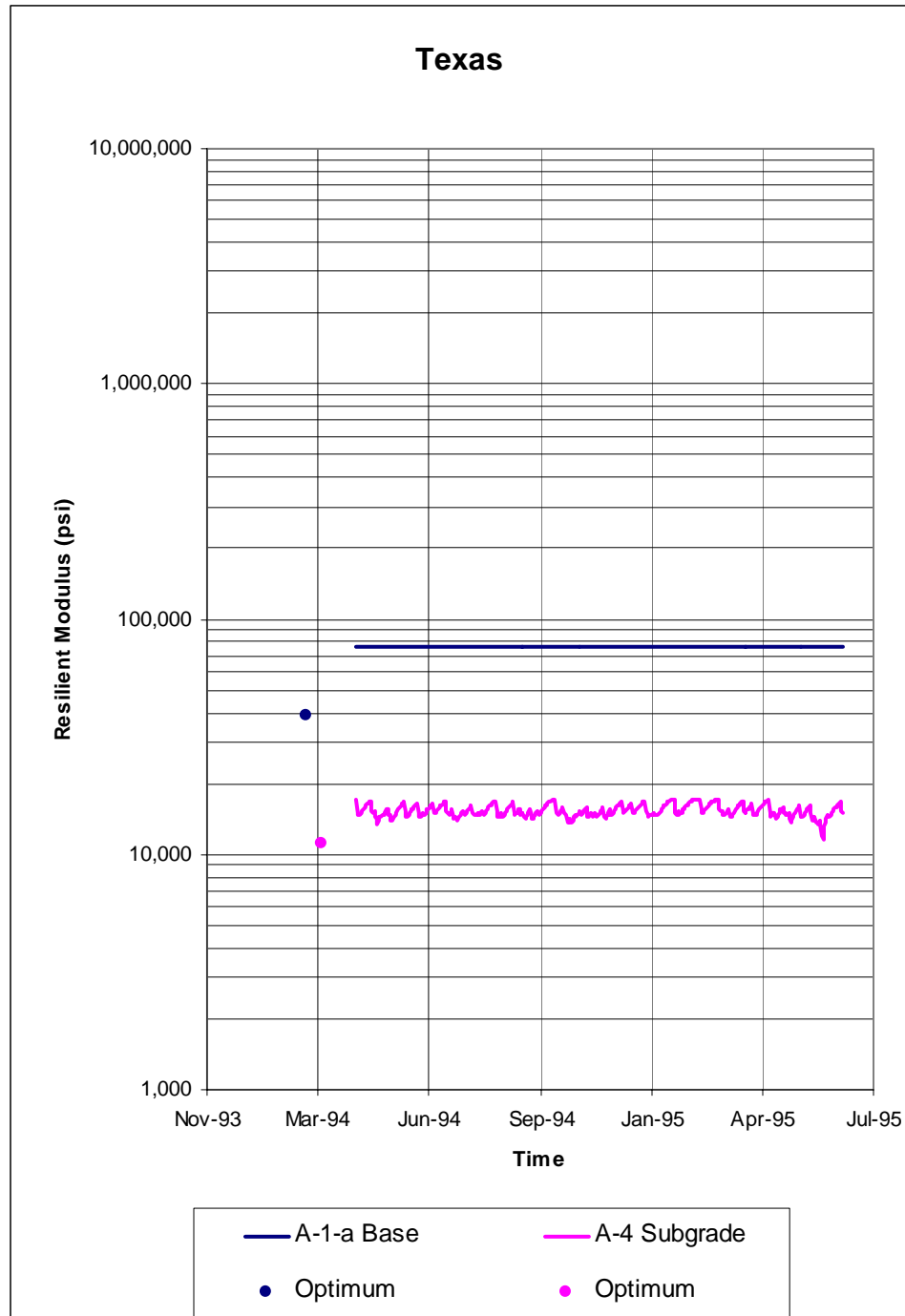


Figure 11b. Predicted Variation in Resilient Modulus with Time for Texas

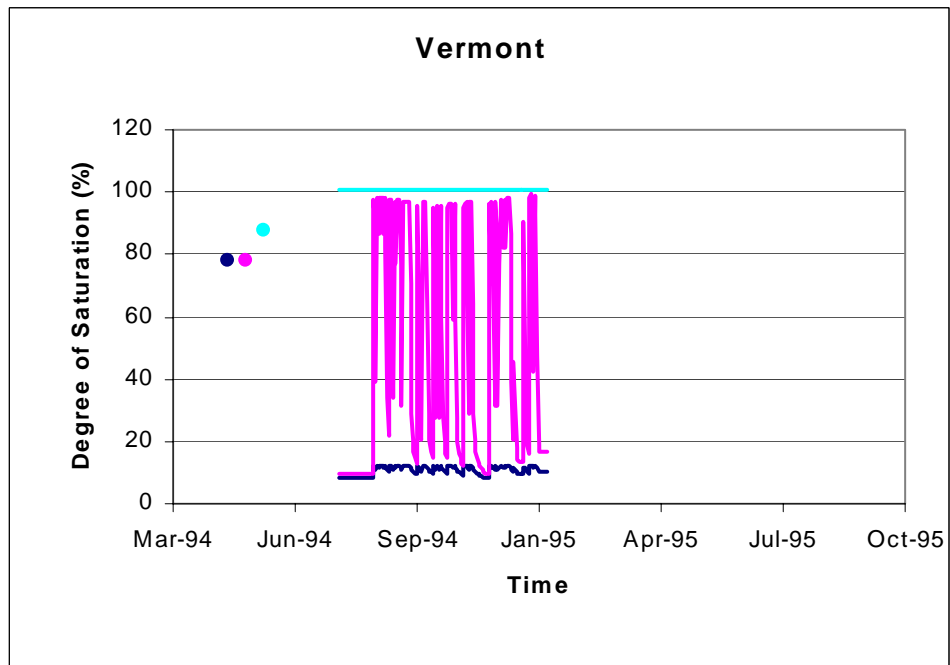
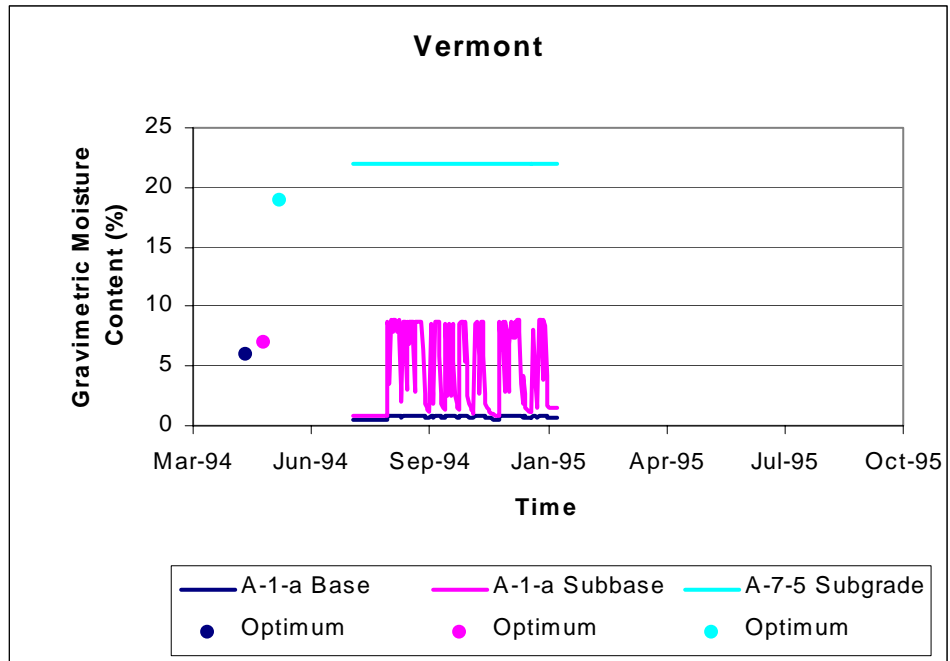


Figure 12a. Predicted Variation in Moisture Content and Degree of Saturation with Time  
for Vermont

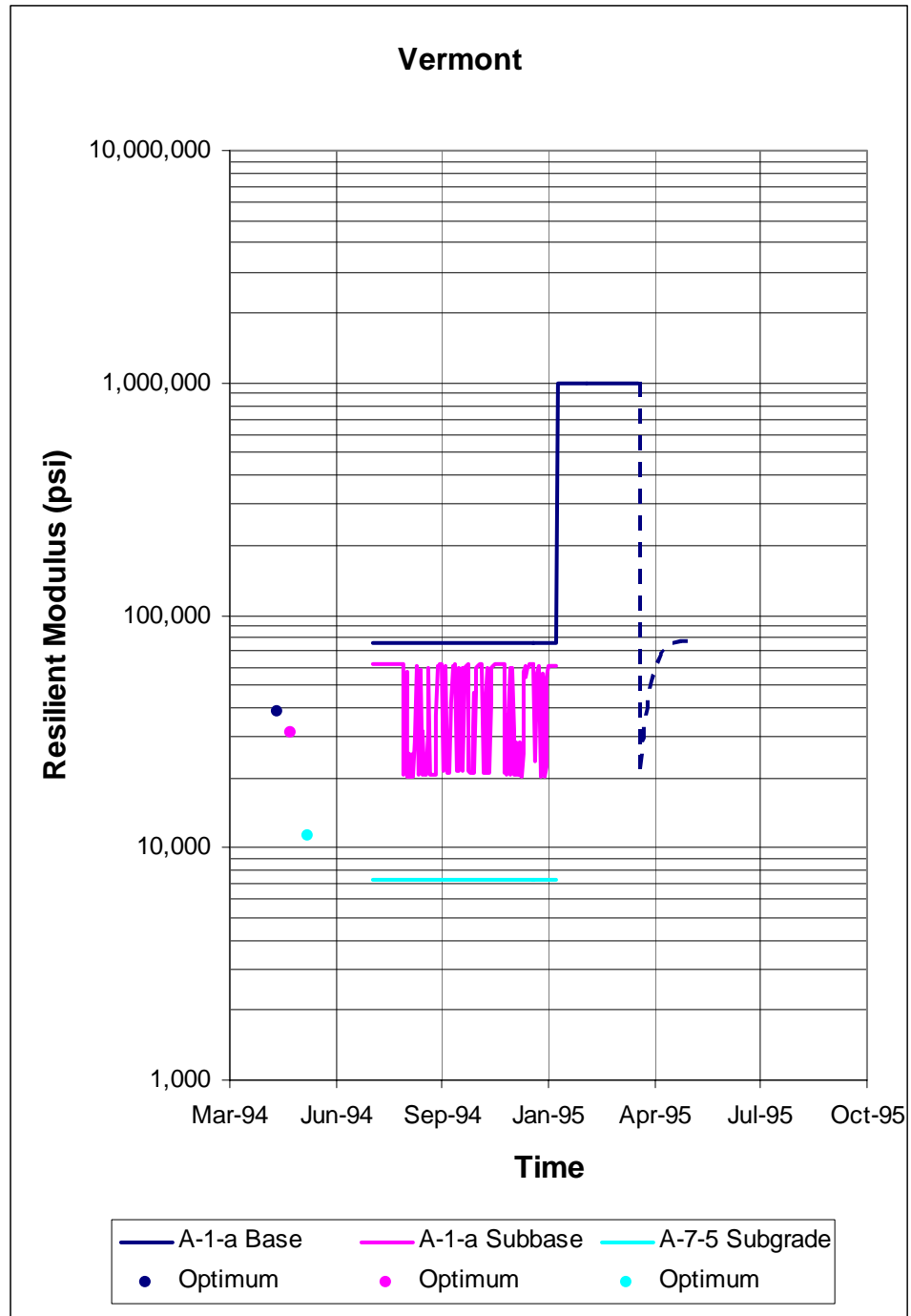


Figure 12b. Predicted Variation in Resilient Modulus with Time for Vermont

All sites except Manitoba and New Hampshire likewise exhibited marked desaturation of the base. The base for these two had a small amount of plasticity and were able to retain water under the modest suctions imposed. Sometimes the subbases, if present, and subgrades desaturated substantially and sometimes they did not, depending on plasticity. The Vermont subgrade (Figure 12) went to  $S_{equil}=100\%$ , but the point of computation chosen was only 6 cm above the GWT (in fact it was sometimes submerged due to GWT oscillations). The subgrade at the Vermont site was also fairly high plasticity and very low permeability. Therefore it was unable to accept quickly the rainfall water (through cracks in the A/C) from above. The unusually high oscillations in the subbase degree of saturation were caused by the temporary accumulation of this water. If the EICM were 2-D and able to account for lateral drainage then perhaps these oscillations would be damped to some degree.

In almost all cases the  $M_R$  values followed the expected pattern of being highest for base, lowest for subgrade and intermediate for subbase. A minor exception is New Hampshire (Figure 10), but the descriptions of the base and subbase were sufficiently similar that the initial  $M_{Ropt}$  values were almost identical.

### **Use of Hand Calculations as a Check on EICM Output**

Given the  $wPI$  product, the value of  $S_{opt}$  can readily be manually (electronically) computed from Equation 7. Once the moisture content at a particular point in the profile has stabilized to an equilibrium level; then oscillations occur about this value. In general, these oscillations are due to oscillations in the depth to groundwater (GWT) and due to rainfall, if the A/C layer has any cracks. In a great majority of cases, these oscillations



can be seen to have very minor effects on  $M_R$ , as shown by the plots of  $M_R$  versus time for the 10 LTPP sites (Figures 3 through 12). If the effects due to rainfall are more or less neglected, then the equilibrium degree of saturation,  $S_{equil}$ , can be hand-calculated by the following procedure.

1. Estimate the average depth,  $D_{equil}$ , from the point in question to the GWT in meters, for the period of interest.
2. Calculate the equilibrium soil suction,  $(u_a - u_w)_{equil}$  by  $(u_a - u_w)_{equil} = \gamma_w D_{equil}$
3. Use  $wPI$  or  $D_{60}$  to select a soil-water characteristic curve, SWCC, from Figure 13.
4. Enter the SWCC with  $(u_a - u_w)_{equil}$  and pick off  $S_{equil}$  in %.

This procedure was followed for 7 layers in 5 sites as shown in Table 3. Consider the base for the GA site as the first example.

Step 1.  $D_{equil} = 4.9$  m

Step 2.  $(u_a - u_w)_{equil} = (9.81) \times (4.9) = 48$  kPa

Step 3.  $D_{60} = 8.7$  mm, but the SWCCs are "capped" at 1 mm. Therefore, use the 1 mm SWCC curve.

Step 4. Enter with  $(u_a - u_w) = 48$  kPa to get  $S_{equil} = 5.5$  %

The computations have been carried a couple of steps further in Table 3. The value of  $S_{opt}$  has been calculated from Equation 7 to be 78%. Thus,  $(S_{equil} - S_{opt})$  is -72.5%.

Equation 1 yields the modulus adjustment factor = 2.00, meaning that  $M_R$ , after drying from optimum ( $S = 78\%$ ) to  $S_{equil} = 5.5\%$ , is 2.00 times the  $M_{Ropt}$ .

For comparison, consider the EICM output in Figure 6 for GA. The value of  $S_{equil}$  for the base is about 6.3%, which makes  $(S_{equil} - S_{opt}) = -71.7\%$ . The modulus adjustment

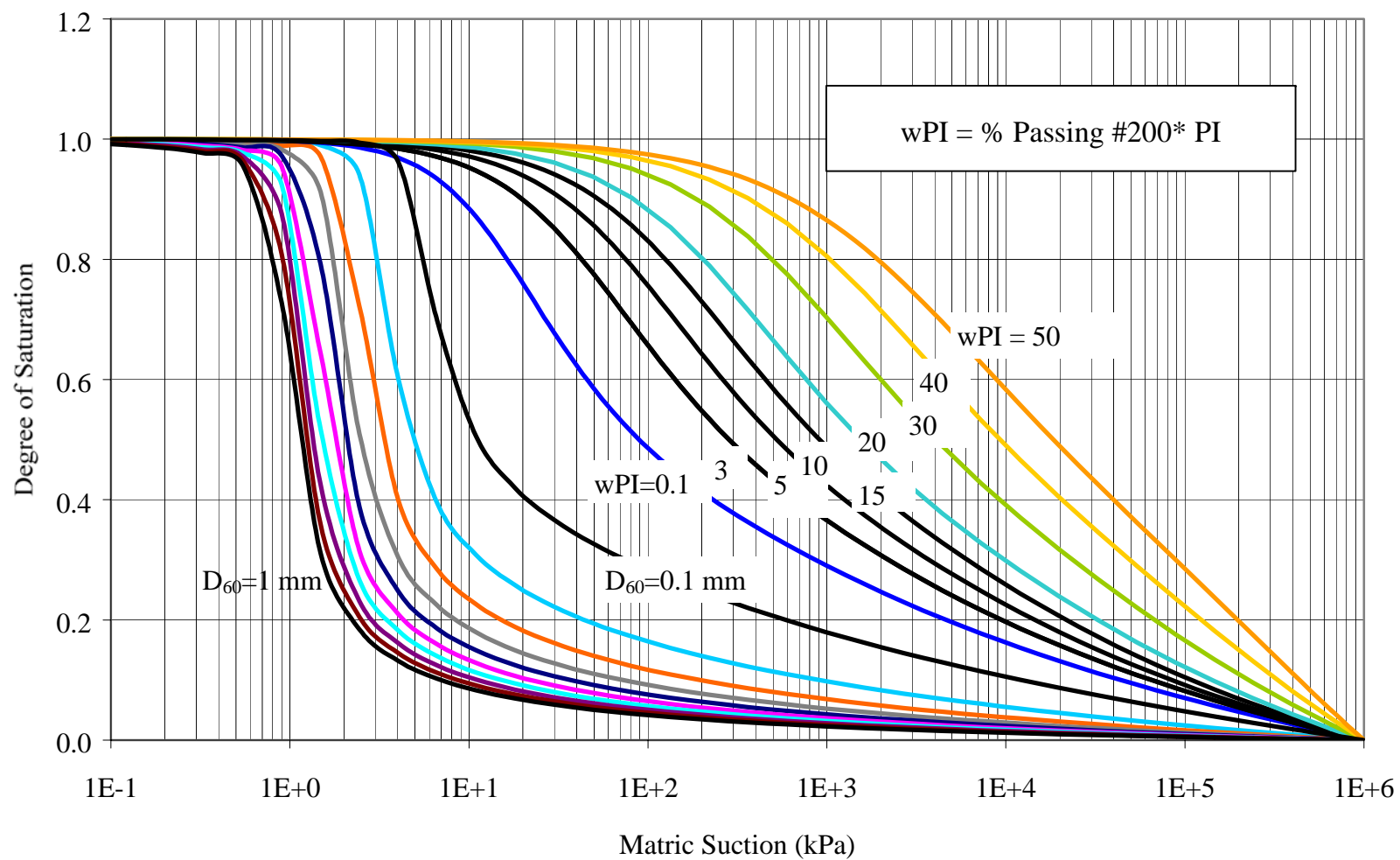


Figure 13. Predicted SWCC based on  $D_{60}$  and  $wPI$

Table 4 Check on EICM outputs with Manual Calculations –Comparison in  $M_R$  Adjustment Factors

Site	Layer	$D_{\text{equil}}$ (m) Depth to GWT	$(u_o - u_w)_{\text{equil}}$ (kPa)	$wPI$	$D_{60}$ (mm)	$S_{\text{opt}}$ %	$S_{\text{equil}}$ (hand Calcul.)	$S_{\text{equil}}$ EICM	$S_{\text{equil}} - S_{\text{opt}}$ (hand Calcul.)	$S_{\text{equil}} - S_{\text{opt}}$ EICM	$M_R$ adj Factor (hand Calculated)	$M_R$ adj Factor EICM	% Diff. In $M_R$ Values
CT	Base	1.75	17	0	10	78	7	7.5	-71	-70.5	2.00	2.00	0
GA	Base	4.9	48	0	8.7	78	5.5	6.3	-72.5	-71.7	2.00	2.00	0
GA	Subgrade	4.5	44	0.36	-	84	63	66	-21	-18	1.755	1.654	6.1
Manitoba	Base	2.37	23	0.55	-	84	77	88	-7	-4	1.156	1.086	6.4
VT	Subgrade	0.06	0.6	13	-	88	100	100	+12	+12	0.66	0.66	0
TX	Base	4.3	42	-	9	78	6.5	6.5	-72.5	-71.5	2.00	2.00	0
TX	Subgrade	4.1	40	0	0.04	78	61	57	-17	-21	1.422	1.545	8.7

factor is again 2.00, because the curve adopted in Figure 1 flattens out for  $(S - S_{opt})$  values lower than -50%.

As a second example, consider the subgrade for GA.

Step 1.  $D_{equil} = 4.5$  m

Step 2.  $(u_a - u_w)_{equil} = (9.81) \times (4.5) = 44$  kPa

Step 3.  $wPI = 0.36$ , which requires some interpolation in Figure 13 .

Step 4. Enter with  $(u_a - u_w) = 44$  kPa to get  $S_{equil} = 63$  %

Continuing with the computations indicated in Table 3,  $S_{opt} = 84\%$  from Equation 7 and  $(S_{equil} - S_{opt})$  for the hand calculations is -21% and the modulus adjustment factor is 1.755.

Figure 6 for GA shows that  $S_{equil}$  (EICM) for the same period is about  $66\% \pm 3\%$ . Using  $S_{equil}$  (EICM) = 66%,  $(S_{equil} - S_{opt}) = -18\%$  and the modulus adjustment factor is 1.654.

Given no error in the EICM input data, one would assume that the EICM values would be superior, because the EICM model accounts for climatic factors and time dependency. If one assumes the EICM answer is the right answer, then Table 3 shows that, for these examples, the error suffered by using the simplified hand calculation is typically less than 8 or 10% and sometimes as little as zero, particularly for the non-plastic bases and subbases which typically dry to  $S$  less than 30% ( $S_{equil} - S_{opt} < -50\%$ ). The last three columns of Table 3 also show that there is no reason to suspect substantial error in the EICM input (or output) for these examples.

## Conclusions

1. For compaction at optimum conditions the degree of saturation,  $S_{opt}$ , and the optimum water content,  $w_{opt}$ , have been correlated with  $wPI$  and  $D_{60}$ , as has been  $G_s$ . These correlations appear adequate for satisfactorily predicting  $e$ ,  $n$ , and  $\gamma_{dmax}$  and will be recommended for Levels 2 and 3.
2. Optimum conditions; i.e.  $\gamma_d = \gamma_{dmax}$  and  $w = w_{opt}$  and  $S = S_{opt}$  are a logical choice for:
  - a) The reference condition for evaluation of  $M_R$   
and
  - b) The initial conditions at compaction for unbound layers of the pavement section in the field.
3. The use of  $S_{opt}$  as the initial condition and the use of  $wPI$  and  $D_{60}$  correlations to obtain  $S_{opt}$ ,  $w_{opt}$ , and  $G_s$ , together with the employment of these values to generate initial input data for the EICM, guarantees that the initial  $S_o = S_{opt}$  and output values of  $S$  from the EICM will be reasonable or at least less than 100%. Thus the use of this approach avoids the dramatically spurious spikes in calculated mass – volume relationships which have been found to be very common when using reported data from the LTPP database files.
4. The model relating changes in modular ratios to changes in degree of saturation presented herein appears quite satisfactory for quantifying the effects of moisture content changes.
5. In a fairly large majority of the cases, the changes in  $M_R$  which occur due to the change from  $S_o = S_{opt}$  to  $S_{equil}$  are considerably larger than the seasonal oscillations

- which occur after the equilibrium state is reached. In fact, it appears that it is a satisfactorily good engineering approximation to simply assume the  $M_R$  values are constant and equal to an average equilibrium value, except during periods of freezing, thawing, and recovery from thawing.
6. The use of the manual calculation procedure presented for estimation of the  $S_{equil}$  value has two potentially useful applications:
    - a) It can be used to check the reasonableness of the EICM output – to check for an EICM input data error, for example.
    - b) It can be used as an independent method for estimating  $S_{equil}$  when the EICM is not used.

### **Recommendations – General**

1. The optimum condition; i.e.,  $\gamma_d = \gamma_{d\ max}$ ,  $w = w_{opt}$ , and  $S = S_{opt}$  should be adopted as:
  - a) The reference condition for evaluation of  $M_R$
  - b) The initial condition for compacted unbound pavement layers in the field.
2. If actual lab test measurement data are not available, the correlations for  $S_{opt}$ ,  $w_{opt}$ , and  $G_s$  with  $wPI$  and  $D_{60}$  should be used to estimate  $S_{opt}$ ,  $w_{opt}$  and  $G_s$  which are then used to compute  $e$ ,  $n$ , and  $\gamma_{d\ max}$  as needed for input to the EICM and other applications relating to  $M_R$  determinations.
3. The model represented by Equation 1 and illustrated in Figures 1 and 2 should be used to estimate  $M_R / M_{Ropt}$ .

4. The hand calculation procedure presented herein should be used (a) to check the reasonableness of the EICM results for  $S_{equil}$  and (b) to evaluate  $S_{equil}$  when the EICM is not used.

## **Recommendations – Relative to the Implementation of the $M_R$ Model into the 2002 Guide**

The primary objective of the  $M_R$  studies was to develop a basis and procedure for determination of  $M_R$  values for use in the 2002 Guide. Based on the studies completed and results obtained to date, the following recommendations for implementation are made.

### **Unbound Compacted Layers**

#### ***Level 1***

1. Assume initial compacted conditions are  $\gamma_d = \gamma_{dmax}$ ,  $w = w_{opt}$ . Use  $\gamma_{dmax}$  and  $w_{opt}$  for T180 for bases and use T99 for subbases and subgrades.
2. For each layer measure  $\gamma_{dmax}$ ,  $w_{opt}$  and  $G_S$ .
3. For each layer measure  $M_{Ropt}$  for a range of confining pressures and stress levels to obtain  $k_1$ ,  $k_2$  and  $k_3$ .
4. Use the output from the EICM to estimate the moisture change from the optimum condition to the equilibrium condition,  $S_{equil} - S_{opt}$ .
5. Use Equation 1 to estimate  $M_R/M_{Ropt}$  and  $M_R$  for each layer, to account for moisture change.
6. Account for change in moduli due to freezing, thawing, and recovery using the recommendations outlined in Witczak et al. (3).

#### ***Level 2***

1. Assume initial compacted conditions are  $\gamma_d = \gamma_{dmax}$ ,  $w = w_{opt}$ . Use  $\gamma_{dmax}$  and  $w_{opt}$  for T180 for bases and use T99 for subbases and subgrades.

2. Use correlations with index properties and material descriptions to estimate  $k_1$ ,  $k_2$  and  $k_3$  parameters corresponding to optimum conditions.
3. Use these  $k_i$  values to estimate  $M_{Ropt}$ .
4. Use the output from the EICM to estimate the moisture change from the optimum condition to the equilibrium condition,  $S_{equil} - S_{opt}$ .
5. Use Equation 1 to estimate  $M_R/M_{Ropt}$  and  $M_R$  for each layer, to account for moisture change.
6. Account for change in moduli due to freezing, thawing, and recovery using the recommendations outlined in Witczak et al. (3).

### ***Level 3***

1. Use soil descriptions and index properties to estimate CBR for each layer.
2. Use  $M_{Ropt} = 2555 \text{ CBR}^{0.64}$  to estimate  $M_{Ropt}$  for each layer.
3. Use the output from the EICM to estimate the moisture change from the optimum condition to the equilibrium condition,  $S_{equil} - S_{opt}$ .
4. Use Equation 1 to estimate  $M_R/M_{Ropt}$  and  $M_R$  for each layer, to account for moisture change.
5. Account for change in moduli due to freezing, thawing, and recovery using the recommendations outlined in Witczak et al. (3).

## **In-Situ Natural Material Below Compacted Layers**

### ***Level 1***

1. Use seismic profiling with 10'-15' geophone spacing to characterize the upper 15' to 20' via seismic velocity ( $v_p$  for deep GWT, and  $v_s$  for shallow GWT).
2. Use  $v_p$  and/or  $v_s$  to compute low-strain  $M_R$  values and correct these values for strain level and frequency. Adopt these values as equilibrium values for  $M_R$ , which are at equilibrium with the average moisture regime.
3. Account for change in moduli due to freezing, thawing, and recovery using the recommendations outlined in Witczak et al. (3).



As a less preferred, less accurate alternative:

1. Use index properties and soil descriptions to estimate  $k_1$ ,  $k_2$  and  $k_3$  for the in-situ layers and use the  $k_i$  to estimate  $M_{\text{Requil}} = M_{\text{Runfrz}}$ .
2. Account for change in moduli due to freezing, thawing, and recovery using the recommendations outlined in Witczak et al. (3).

### ***Level 2***

1. Use seismic profiling with 10'-15' geophone spacing to characterize the upper 15' to 20' via seismic velocity ( $v_p$  for deep GWT, and  $v_s$  for shallow GWT).
2. Use  $v_p$  and/or  $v_s$  to compute low-strain  $M_R$  values and correct these values for strain level and frequency. Adopt these values as equilibrium values for  $M_R$ , which are at equilibrium with the average moisture regime.
3. Account for change in moduli due to freezing, thawing, and recovery using the recommendations outlined in Witczak et al. (3).

As a less preferred, less accurate alternative:

1. Use index properties and soil descriptions to estimate  $k_1$ ,  $k_2$  and  $k_3$  for the in-situ layers and use the  $k_i$  to estimate  $M_{\text{Requil}}$ .
2. Account for change in moduli due to freezing, thawing, and recovery using the recommendations outlined in Witczak et al. (3).

### ***Level 3***

1. Use soil descriptions and index properties to estimate CBR for each layer.
2. Use  $M_R = 2555 \text{ CBR}^{0.64}$  to estimate  $M_R$  for each layer.
3. Neglect moisture oscillation effects.
4. Account for change in moduli due to freezing, thawing, and recovery using the recommendations outlined in Witczak et al. (3).

## References

1. Witczak M.W., Andrei D. and Houston W.N. *Resilient Modulus as Function of Soil Moisture – Summary of Predictive Models*. Development of the 2002 Guide for the Development of New and Rehabilitated Pavement Structures, NCHRP 1-37 A, Inter Team Technical Report (Seasonal 1), June 2000.
2. Witczak M.W., Houston W.N., Zapata C.E., Richter C., Larson G. and Walsh K. *Improvement of the Integrated Climatic Model for Moisture Content Predictions*. Development of the 2002 Guide for the Development of New and Rehabilitated Pavement Structures, NCHRP 1-37 A, Inter Team Technical Report (Seasonal 4), June 2000.
3. Witczak M.W., Houston W.N. and Andrei D. *Selection of Resilient Moduli for Frozen/Thawed Unbound Materials*. Development of the 2002 Guide for the Development of New and Rehabilitated Pavement Structures, NCHRP 1-37 A, Inter Team Technical Report (Seasonal 3), June 2000.
4. Yoder E.J. and Witczak M.W. *Principles of Pavement Design*. 2<sup>nd</sup> edition, New York, John Wiley and Sons Inc., 1975.

Copy No. \_\_\_\_\_

# **Guide for Mechanistic-Empirical Design OF NEW AND REHABILITATED PAVEMENT STRUCTURES**

**FINAL DOCUMENT**

## **APPENDIX DD-3: SELECTION OF RESILIENT MODULI FOR FROZEN/THAWED UNBOUND MATERIALS**

**NCHRP**

**Prepared for  
National Cooperative Highway Research Program  
Transportation Research Board  
National Research Council**

**Submitted by  
ARA, Inc., ERES Division  
505 West University Avenue  
Champaign, Illinois 61820**

**June 2000**

## **Acknowledgment of Sponsorship**

This work was sponsored by the American Association of State Highway and Transportation Officials (AASHTO) in cooperation with the Federal Highway Administration and was conducted in the National Cooperative Highway Research Program which is administered by the Transportation Research Board of the National Research Council.

## **Disclaimer**

This is the final draft as submitted by the research agency. The opinions and conclusions expressed or implied in this report are those of the research agency. They are not necessarily those of the Transportation Research Board, the National Research Council, the Federal Highway Administration, AASHTO, or the individual States participating in the National Cooperative Highway Research program.

## **Acknowledgements**

The research team for NCHRP Project 1-37A: Development of the 2002 Guide for the Design of New and Rehabilitated Pavement Structures consisted of Applied Research Associates, Inc., ERES Consultants Division (ARA-ERES) as the prime contractor with Arizona State University (ASU) as the primary subcontractor. Fugro-BRE, Inc., the University of Maryland, and Advanced Asphalt Technologies, LLC served as subcontractors to either ARA-ERES or ASU along with several independent consultants.

Research into the subject area covered in this Appendix was conducted at ASU. The authors of this Appendix are Dr. M.W. Witczak, Dr. W.N. Houston, and Mr. Dragos Andrei. Dr. M.W. Witczak provided overall guidance and coordination of the efforts of the 2002 Design Guide Team, including work plan development, scheduling, assignment of personnel and tasks and technical review of results as they became available. In connection with the current report he also identified key sources of data and performed the final review of the report. Dr. W.N. Houston provided supervision and guidance to the study Graduate Research Assistant, Mr. Dragos Andrei. Dr. W.N. Houston also reviewed publications, extracted and synthesized data, and drafted the initial report. Mr. Dragos Andrei located and secured all data sources, reviewed pertinent publications, extracted and synthesized data where available and assisted with the report (drafts and final) preparation.

## **Foreword**

This appendix presents the derivation of reasonable values of  $M_R$  for both frozen and thawed unbound materials through evaluation of published results.. The information contained in this appendix serves as a supporting reference to the resilient modulus discussions presented and PART 2, Chapter 3, and PART 3, Chapters 3, 4, 6, and 7 of the Design Guide.

This appendix is the third in a series of four volumes on environmental effects on pavements. The other volumes are:

- Appendix DD-1: Resilient Modulus As Function Of Soil Moisture-Summary Of Predictive Models
- Appendix DD-2: Resilient Modulus As Function Of Soil Moisture – A Study Of The Expected Changes In Resilient Modulus Of The Unbound Layers With Changes In Moisture For 10 LTPP Sites
- Appendix DD-4: Improvement Of The Integrated Climatic Model for Moisture

## Abstract

The purpose of this study was to derive reasonable values of  $M_R$  for both frozen and thawed unbound materials through evaluation of published results. The values of  $M_R$  for frozen materials were extracted as absolute values of  $M_{R_{fz}}$ . For thawed materials the focus was on a reduction factor, RF, which could be multiplied times the unfrozen (normal) modulus,  $M_{R_{unfz}}$ , to get the modulus after thawing,  $M_{R_{min}}$ . The following values were found to be reasonable for the material types indicated: coarse-grained materials –  $M_{R_{fz}} \sim 3 \times 10^6$  psi; Fine-grained silts and silty sands –  $M_{R_{fz}} \sim 2 \times 10^6$  psi; clays –  $M_{R_{fz}} \sim 1 \times 10^6$  psi. Average values of RF and ranges in RF were found for gravel, sand, silt and clay. In consideration of all data collected it was possible to develop recommendations for RF as function of % passing no. 200 sieve,  $P_{200}$ , and plasticity index, PI. An algorithm is proposed for using these  $M_{R_{fz}}$  and RF values in conjunction with EICM to produce time-varying values of  $M_R$  at a point, throughout the year.

## Table of Contents

	<u>Page</u>
Introduction.....	1
Objective .....	3
Background.....	3
Results of Literature Search.....	9
Summary and Conclusions .....	26
Recommendations.....	27
References.....	33

## List of Tables

	<u>Page</u>
Table 1. Values of Unfrozen, Frozen, and Thawed $M_R$ from the Literature .....	10
Table 2. Team Synthesis of $M_R$ Values for Frozen Materials .....	14
Table 3. Corps of Engineers (COE) Frost-Susceptibility Classification .....	18
Table 4. Criteria Developed by Others for Predicting Frost-Susceptibility of Soils .....	23
Table 5. Change in CBR During Thaw Weakening Period .....	24
Table 6. Recommended Values of RF for Coarse-Grained Materials ( $P_{200} < 50\%$ ).....	28
Table 7. Recommended Values of RF for Fine-Grained Materials ( $P_{200} > 50\%$ ) .....	28



## List of Figures

	<u>Page</u>
Figure 1. Schematic of Ice Lens Formation.....	4
Figure 2. Relationship Between $P_{200}$ and $P_{0.02}$ .....	20
Figure 3. Relationship Between Frost-Heave and $P_{200}$ . ....	21
Figure 4. Relationship Between Frost-Heave and PI.....	22
Figure 5. Example of Time-Varying $M_R$ .....	32

# **SELECTION OF RESILIENT MODULI FOR FROZEN/THAWED UNBOUND MATERIALS**

## **Introduction**

The overall task of evaluating the expected cumulative damage due to load associated distress of a pavement system involves numerous subtasks as follows:

- Subtask 1: Evaluation of resilient modulus,  $M_R$ , at some reference condition, such as optimum water content and maximum dry density, as a function of soil type or gradation or classification.
- Subtask 2: Evaluation of expected changes in moisture content, both from the initial or reference condition and seasonally.
- Subtask 3: Evaluation of the effect on  $M_R$  of changes in soil moisture content with respect to the reference condition as well as seasonally.
- Subtask 4: Evaluation of the effect on  $M_R$  of changes in material density with respect to the reference condition.
- Subtask 5: Evaluation of the effect of freezing on  $M_R$ .
- Subtask 6: Evaluation of the effect of thawing on  $M_R$ .
- Subtask 7: Utilization of time-varying  $M_R$  values in the computation of critical pavement response parameters at various points within the pavement system.

Various studies relevant to the above subtasks are currently in progress at ASU and some of these studies have already been completed or are near completion as of the

date of this report. The findings and recommendations from these studies are presented in a series of Inter Team Technical Reports, and are described as:

- I.     **Improvement of the Integrated Climatic Model for Moisture Content Predictions** by Dr. M.W. Witczak, Dr. W.N. Houston, Dr. C.E. Zapata, Ms. Cheryl Richter, Mr. G. Larson and Dr. K. Walsh. Development of the 2002 Guide for the Development of New and Rehabilitated Pavement Structures, NCHRP 1-37 A, Inter Team Technical Report (Seasonal 4), June 2000 (*Relates to Subtask 2*).
- II.    **Resilient Modulus as Function of Soil Moisture – Summary of Predictive Models** by Dr. M.W. Witczak, Mr. D. Andrei and Dr. W.N. Houston. Development of the 2002 Guide for the Development of New and Rehabilitated Pavement Structures, NCHRP 1-37 A, Inter Team Technical Report (Seasonal 1), June 2000 (*Relates to Subtasks 1, 3 and 4*).
- III.   **Resilient Modulus as Function of Soil Moisture – A Study of the Expected Changes in Resilient Modulus of the Unbound Layers with Changes in Moisture for 10 LTPP Sites** by Dr. M.W. Witczak, Dr. W.N. Houston and Mr. D. Andrei. Development of the 2002 Guide for the Development of New and Rehabilitated Pavement Structures, NCHRP 1-37 A, Inter Team Technical Report (Seasonal 2), June 2000 (*Relates to Subtasks 3 and 4*).
- IV.    **Selection of Resilient Modulus for Frozen/Thawed Materials** – by Dr. M.W. Witczak, Dr. W.N. Houston and Mr. D. Andrei. Development of the 2002 Guide for the Development of New and Rehabilitated Pavement Structures, NCHRP 1-

37 A, Inter Team Technical Report (Seasonal 3), (the current report) June 2000  
*(Relates to Subtasks 5 and 6).*

## **Objective**

The objective of the current report was to use existing data from the literature to evaluate the effects of freezing and thawing on  $M_R$  of unbound base, subbase and subgrade soils. The relevance of these studies to the overall task of evaluating expected load associated damage of pavement systems is indicated by the preceding list of subtasks.

## **Background**

Before presenting the results of the literature search for the  $M_R$  values for frozen and thawed materials, background information describing the conditions leading to frost action in soil is provided.

### ***Ice Lenses Formation***

When water in soil freezes, the water itself undergoes about a 9 % volume increase (2). Thus a saturated or nearly saturated soil with 35 % porosity would experience about a 3 % volume increase with a corresponding heave of the ground surface. Unsaturated soils would exhibit smaller volume changes in accordance with the degree of saturation. These volume changes are what is expected when no water is added to the water initially present in the material. However, under special circumstances freezing may be accompanied by the formation of ice lenses that can range from millimeters to several centimeters in thickness. These lenses are usually more or less pure

ice and can cause the ground surface to heave as much as several tens of centimeters (see Figure 1). When they occur under pavements the resulting damage can arise from two sources. First, the heave is likely to be differential. Secondly and more importantly, the melted lens may become a temporary water-filled void with little or no bearing strength. In any case, the excess water, unless quickly drained, may create a zone of greatly reduced strength and produce pavement distress if the pavement is loaded before recovery.

In order to anticipate the formation of ice lenses it is necessary to understand their mechanism of formation. In the field a freezing front almost always advances from the surface downward. Thus ice lenses tend to be oriented horizontally. When the water in soil freezes, adjacent water from below is pulled toward the newly formed ice. Because freezing below the ground water table (GWT) does not usually occur, the zone of interest is the capillary zone above the GWT, where the soil water is in tension. When water is pulled upward toward an ice lens, it moves in response to a fairly substantial gradient in soil moisture suction because the force of gravity must be overcome. Thus the freezing of water results in a local depression of the water pressure (or a rise in soil moisture suction). If water can be supplied to the ice lens fast enough, it will continue to grow in thickness. However, if the rate of water supply is insufficient, the freezing front will advance downward and the upward progressing water will be “frozen in its tracks”. A new ice lens may or may not be formed at greater depth.

Two factors are important to the rate of water supply to the growing ice lenses. First, the hydraulic conductivity of the soil must be high enough to sustain a substantial flow of water. Secondly, the GWT must be reasonably shallow, so that the head loss

between the GWT and the ice lenses is not too great. The saturated hydraulic conductivity of a soil is controlled by its gradation, or the size of its largest connected pores. Therefore a medium or coarser sand would appear to be capable of supplying water to the ice lenses quite adequately. However, a medium or coarser sand in the capillary zone is not likely to be initially fully saturated, and furthermore it tends to desaturate dramatically with increase in soil moisture suction (19). Its unsaturated hydraulic conductivity is typically too low to sustain ice lens growth. A clay of medium or higher plasticity has strong water retention capacity and remains at rather high degree of saturation under substantial soil moisture suction. Therefore it might initially be assumed that it could supply water at a rate sufficient to sustain ice lens growth. However, these clays have an inherent hydraulic conductivity (i.e. the saturated hydraulic conductivity) which is too low to sustain ice lens growth. The elimination of clean, medium and coarser sands and clays of medium and higher plasticity leaves us with silts, very fine silty sands and sandy silts, and silty clays of low plasticity as “frost-heave susceptible soils”. These soils have sufficient water retention capacity that they do not desaturate more or less completely when subjected to significant soil moisture tension. In addition, these soils exhibit an inherent hydraulic conductivity which is adequate to sustain ice lens growth, provided the ground water table is nearby and unobstructed. The boundaries between frost-heave susceptible and non-frost-heave susceptible soils can be shifted by altering the normal rate of freezing, by retardation of heat removal for example. However, for the environmental and boundary conditions which normally ensue in the field, the frost-heave susceptible soils are those listed above. Thus, the necessary conditions for ice lens formation can be listed:

1. A frost-heave susceptible soil, as defined above;
2. Prolonged freezing temperature;
3. A supply of water, such as a nearby, unobstructed GWT.

An example of an obstruction between the GWT and an ice lens could be a clean granular layer, which desaturates under significant soil moisture suction, or a layer of plastic clay, whose hydraulic conductivity is too low to sustain ice lens growth. However, even if the frost-heave-susceptible soil extends all the way to the GWT, ice lenses will not form unless the GWT is nearby, typically a very few meters.

### ***Traditional Remedy for Frost-Susceptible Soils***

Because the necessary conditions for ice lens formation have long been recognized, it is possible to formulate a rather simple, straightforward engineering policy for dealing with these frost-heave-susceptible soils:

*When the conditions favorable to ice lens formation exist, determine the typical, local depth of freezing empirically and remove and replace frost heave susceptible soils to this depth.*

This procedure probably has been followed fairly consistently by pavement engineers for the last few decades, but there are certainly notable exceptions to the successful execution of the general policy. In addition, it has been widely recognized that thawing after freezing, even in the absence of significant ice lens formation, results in a degradation of the resilient modulus which can be quite substantial. These effects are described generally in the next section.

### ***Degradation of Resilient Modulus due to Thawing***

When any soil freezes and then thaws, regardless of whether it is non-frost susceptible or frost susceptible, there is some degradation of the resilient modulus, even in the absence of significant ice lens formation. The most plausible explanation for this degradation is as follows. Even though ice lens formation may not be significant, or visible, it appears that some water is added to the frozen zone during freezing. This addition, together with the expansion associated with ice formation, tends to break some of the particle contacts and interlocking of soil grains. When thawing occurs, the soil-water mixture behaves as if there were excess water in the thawed zone and soil moisture suction typically falls to near zero. The reduced soil suction and broken particle contacts/bonds are in themselves sufficient to explain the observed loss in  $M_R$ , which can be as high as 50 or 60%.

The excess water and reduced soil moisture suction readjust with time, as adjacent layers absorb the excess water and cause the soil suction in the thawed zone to rise. Eventually this excess water is transmitted by unsaturated flow to the GWT, as the soil suction and moisture content return to their normal values. The return of the soil suction to its normal value is accompanied by a return of the  $M_R$  to its normal value. The duration of this recovery period is dependent on geometry and the hydraulic conductivity of the soils involved. Therefore, not surprisingly, granular soils recover much faster than clays.

The characterization of silts, silty sands, and silty clays as frost-heave-susceptible in the preceding section can be thought of as the classical characterization of frost-susceptible soils. This classical characterization speaks to the potential for a soil to form ice lenses when conditions are appropriate. In the last few decades, non-destructive field



testing, such as FWD, and laboratory resilient testing have been commonplace and it has been found that essentially all soils are frost-susceptible to some degree, when  $M_R$  degradation is used as the measuring stick. Clean granular soils are the least susceptible, clays are substantially susceptible, and silty soils are the most susceptible. Thus, a more modern definition of frost susceptibility rates soils with respect to their reduction in  $M_R$  upon thawing. Of course it is still true that if a soil actually experiences ice lens formation and then thaws, the reduction in modulus will be dramatic, typically much more than if ice lenses do not form. However, it is generally assumed that when highly frost-heave-susceptible soils combine with conditions strongly favoring ice lens formation, these soils have been removed and replaced. This assumption seems to prevail in the research studies presented in the next section, wherein researchers have measured and estimated loss in  $M_R$  due to thawing up to a maximum of about 60% loss.

### **Results of literature search**

Literature sources were consulted and salient values of moduli,  $M_R$ , and ratios of moduli were extracted. The objective of the search was to obtain absolute values of moduli for frozen material, termed  $M_{Rfrz}$ , and the ratio of  $M_R$  just after thawing, termed  $M_{Rmin}$ , to the  $M_R$  of natural, unfrozen material, termed  $M_{Runfrz}$ . The ratio is used as a reduction factor, termed RF. These definitions are repeated in equation form below.

$$M_{Rfrz} = M_{Rmax} = M_R \text{ for frozen material}$$

$$M_{Runfrz} = \text{the normal } M_R \text{ for unfrozen material}$$

$$M_{Rmin} = M_R \text{ just after thawing}$$

$$RF = \text{modulus reduction factor} = M_{Rmin}/M_{Runfrz} \quad (1)$$

All of the raw data collected is presented in Table 1 and the values for frozen materials are summarized in Table 2. Most of the data will be discussed in the paragraphs which follow.

Results from studies at the USACE-CRREL (Cold Regions Research and Engineering Laboratories) were reported by Berg et al (2). Of most relevance to the present study are the  $M_{Rfrz}$  values which range from  $0.6 \times 10^6$  psi for a CL to  $7 \times 10^6$  psi for a dense graded stone. Numerous values of  $M_{Rfrz}$  were extracted from the Vinson and the Czajkowski and Vinson papers (17, 8). Their values of  $M_{Rfrz}$  ranged from about  $0.4 \times 10^6$  psi for a silt to about  $7 \times 10^6$  psi for a gravel. These values were collected in Table 2 and averaged for coarse-grained materials ( $M_{Rfrz\_ave} \sim 3 \times 10^6$  psi), fine-grained silt and silty sands ( $M_{Rfrz\_ave} \sim 2 \times 10^6$  psi) and clays ( $M_{Rfrz\_ave} \sim 1 \times 10^6$  psi).

Of particular interest to the present report is a study reported by Janoo and Berg (11). They constructed four test sections in the CRREL Research Facility, with the following characteristics:

- 5cm < thickness of A/C < 15 cm
- 0 < thickness of base (GP) + subbase (SW) < 38cm
- all subgrades were plastic clay (CH)
- for both base and subbase,  $6\% < P_{200} < 10\%$ , where  $P_{200}$  = % passing the no. 200 sieve

They used several tools and devices to conduct the research, with heavy emphasis on FWD results. Their key findings are as follows:

- a) The FWD deflections were not much affected until the thaw depths reached well into the CH subgrade. Therefore, the sand and gravel subbase and base with 6% - 10% fines showed almost no weakening due to thawing.
- b) After substantial thawing of the CH subgrade, the ratio of the 4<sup>th</sup> sensor deflection for unfrozen material to the 4<sup>th</sup> sensor deflection for thawed material ranged from 50% to 60%. Assuming  $M_R$  of the subgrade is inversely proportional to 4<sup>th</sup> sensor deflection,  $50\% < RF \text{ for CH subgrade} < 60\%$ .
- c) The authors state, without presenting data, that commonly used RF values ranged from 50% to 85%.
- d) The measured thaw depth correlated well with total area of the FWD deflection basin.

Esch et al. also presented a very interesting study of 120 sections of highway in Alaska (9). Their study sections exhibited the following characteristics:

- sections were 0.5 to 1.0 miles long
- some sections exhibited “good” performance
- some sections exhibited “poor” performance; fatigue (alligator cracking) was the primary measure of distress
- there were very few soils in the profile with significant PI
- there were very few uniform sands or clays; most materials were gravels and silts, with a substantial range in % fines ( $P_{200}$ ).

Their most important findings are as follows:

- a) They performed a regression analysis of 175 material, dimensional, and environmental factors with performance. This analysis yielded no useful

predictions. Only after grouping sections into good performance and poor performance and looking at factors individually were they able to get some fairly good correlations.

- b) The best indicator of performance was found to be the percent passing the No. 200 sieve ( $P_{200}$ ):

If  $P_{200} < 6\%$ , good performance

If  $P_{200} > 11\%$ , poor performance

- c) The next best indicator was found to be the percent passing the 0.02 mm sieve ( $P_{0.02\text{mm}}$ ):

If  $P_{0.02\text{mm}} < 3\%$ , good performance

If  $P_{0.02\text{mm}} > 7\%$ , poor performance

Janoo et al. performed a rather extensive literature review and presented a number of useful findings and recommendations, some of which are reproduced in the current report (11). The first is the Corps of Engineers (COE) frost-susceptibility classification, shown as Table 3. Their original table provided gradation data relative to  $P_{0.02\text{mm}}$  only. Because  $P_{200}$  is somewhat easier to obtain and more frequently available, the team has chosen to focus on  $P_{200}$ . The last column showing  $P_{200}$  in Table 3 was estimated by using the Janoo et al. correlation, which is shown as Figure 2 (11). Figures 3 and 4, from Janoo et al., show the sensitivity of frost heave to  $P_{200}$  and PI respectively (11). Frost heave of greater than 18 mm is considered to be very frost-heave susceptible and 13 to 18 mm is marginal. Table 4 shows that the values of  $P_{200}$  used to separate frost-susceptible from non-frost-susceptible materials vary significantly around the country and around the world.

Table 5 from Janoo et al. shows thaw weakening data in terms of CBR (11). If Equation (2) is used to get  $M_R$  from CBR and Equation 1 defines the reduction factor RF, then Equations (1) and (2) can be used to compute RF, the last column in Table 5, which has been added to the Janoo et al. (1997)'s table.

$$M_{Ropt} = 2555 \cdot CBR^{0.64} \quad (2)$$

$$RF = M_{Rmin}/M_{Runfrz} \quad (1)$$

Where:

$M_{Rmin}$  =  $M_R$  just after thawing

Table 5 shows that RF values for these gravel bases and the subbase range from 0.54 to 0.92, with an average of about 0.70.

Janoo et al. devote considerable attention to the hydraulic conductivity of base materials (11). They conclude that the best protection against frost susceptibility of the base is the provision of rapid lateral drainage and that a  $P_{200}$  as low as 2% or 3% may be required to achieve this result.

Near the end of Table 1 values of RF are provided by Janoo for each of the COE classification categories, NFS through F3/F4 (10). These values range from 1.0 to 0.3, but they were obtained from a straight ratio of CBR values. In effect they were obtained using Equation 3:

$$M_R = 1500 \cdot CBR \quad (3)$$

Thus a ratio of CBR values is precisely equal to a ratio of  $M_R$  values, if Equation 3 is adopted. The values of RF were obtained by Janoo by measuring CBR rather than measuring  $M_R$  directly (10). If Equation 2 is embraced, rather than Equation 3, then the

RF values shown in parentheses in Table 1 are obtained. In fact, algebraic manipulation of Equations 2 and 3 shows that:

$$RF = RF_{CBR}^{0.64} \quad (4)$$

Where:

$RF_{CBR}$  = reduction factor obtained from a ratio of CBR values.

Thus the values in Table 1 under Janoo not in parentheses are values of  $RF_{CBR}$  and Equation 4 shows why the values in parentheses are a little higher (10). All other values of RF in Table 1 and the values in parentheses are as defined by Equation 1. Because Equation 2 for  $M_R$  is embraced by the authors of this report, it follows that RF is embraced by the authors rather than  $RF_{CBR}$ .

## Summary and Conclusions

Considerations of the mechanisms of frost action and the data obtained from the literature search, particularly the thorough study by Janoo et al., make it possible to reach some useful conclusions which can be summarized as follows (11):

1. The conditions necessary for ice lens formation are:
  - A frost-heave-susceptible soil such as silt, silty sand or silty clay with low PI;
  - Prolonged freezing temperatures;
  - A source of water, such as a nearby, unobstructed GWT.
2. The classical or traditional definition of frost-susceptibility focuses on the likelihood of significant ice lens formation, under the favorable conditions cited above.

3. The values of  $M_R$  for frozen materials,  $M_{R_{fz}}$ , range from about  $1 \times 10^6$  psi for clays to about  $3 \times 10^6$  psi for coarse-grained soils. If a single value were selected for all frozen soils,  $2 \times 10^6$  psi would be a reasonably unbiased estimate and  $1 \times 10^6$  psi would be a conservative estimate.
4. Classification of frost-heave-susceptibility for present day use is more likely to focus on the degree of  $M_R$  degradation upon thawing. Degradation can be quantified in terms of RF:

$$RF = M_{R_{min}}/M_{R_{unfz}} \quad (1)$$

5. Records cited in Table 1, and Janoo et al. in particular, present data and recommendations corresponding to the following ranges and average values for RF (11):

Material Type	Range in RF	Average RF
Gravel	0.35 to 1.0	0.75
Sand	0.46 to 0.79	0.63
Silt	0.30 to 0.46	0.40
Clay	0.46 to 0.70	0.52

### Recommendations

Based on all foregoing data and analyses, the authors recommend the following for adaptation in the 2002 Design Guide:

- A. The policy of replacing all highly frost-heave-susceptible soils within the frost zone, such as soils with more than 12% fines and  $PI < 12$ , should be continued

wherever practical, provided the other conditions for ice lens formation are known to be present.

- B. A resilient modulus reduction factor, RF, should be used to estimate the  $M_{Rmin}$  after thawing, by:

$$M_{Rmin} = RF \cdot M_{Runfrz} \quad (1)$$

- C. The % passing no. 200 sieve,  $P_{200}$ , and the Plasticity Index, PI, should be used to estimate RF, using Tables 6 and 7, which follow. If it is unknown whether a coarse-grained material is mostly gravel or mostly sand, assume sand.

- D. Integrate the EICM (Enhanced Integrated Climatic Model) with the  $M_R$  computational algorithms as follows:

- a) Compute  $M_R$  at some reference or initial condition (generally speaking this will coincide with the initial compaction condition during construction).
- b) Use the EICM to compute changes in moisture content from the initial condition to equilibrium, as well as seasonal oscillations. Compute the corresponding changes in  $M_R$  to obtain a profile of  $M_R$  versus time during the normal part of the season, for which the material is unfrozen. The “linkage” between changes in moisture and changes in  $M_R$  will be provided in the 2002 Design Guide. These values of  $M_R$  are considered to be the unfrozen values and are denoted by  $M_{Runfrz}$ .
- c) When the EICM signals that a point is frozen, a  $M_R = M_{Rfrz}$  will be assigned. A conservative value of  $M_{Rfrz} = 1 \times 10^6$  psi is recommended.



- d) When the EICM signals that thaw has occurred, assign  $M_R = M_{Rmin}$  and use Equation 1:

$$M_{Rmin} = RF \cdot M_{Runfrz} \quad (1)$$

[Note: The data found in the literature leads to values of RF which are sometimes related to the initial condition,  $M_{Ropt}$ , and some times to the equilibrium, after some post-compaction changes in moisture content and  $M_R$  have occurred. It is therefore recommended for the 2002 Guide that RF be made to operate on either  $M_{Ropt}$  or  $M_{Runfrz} = M_{Requil}$ , whichever is smaller. Thus the smaller of  $M_{Ropt}$  or  $M_{Runfrz}$  would be used in Equation 1]

- e) Use the EICM to compute the soil moisture suction,  $u_a - u_w$ , and compute a recovery ratio RR by:

$$RR = \frac{(u_a - u_w)}{y \cdot \gamma_w} \quad (5)$$

Where:

$u_a$  = pore air pressure;

$u_w$  = pore water pressure;

$u_a - u_w$  = matric suction;

y = distance from point of computation to the GWT.

[Note:  $y\gamma_w$  is the equilibrium value of soil moisture suction which the EICM has been programmed to seek]

If  $RR < 0$ , set  $RR = 0$

If  $RR > 1$ , set  $RR = 1$

- f) Compute  $M_{Recov}$  by:

$$\begin{aligned}
M_{R_{recov}} &= M_{R_{min}} + (M_{R_{unfrz}} - M_{R_{min}}) \cdot RR \\
&= RF \cdot M_{R_{unfrz}} + (M_{R_{unfrz}} - RF \cdot M_{R_{unfrz}}) \cdot RR \\
&= M_{R_{unfrz}} \cdot (RF + RR - RF \cdot RR)
\end{aligned} \tag{6}$$

Where:

$M_{R_{recov}} = M_R$  recovering =  $M_R$  during the recovery period

- g) When  $RR$  reaches or closely approaches a value of 1, assign  $M_R = M_{R_{unfrz}}$  and declare recovery complete. Maintain  $M_R = M_{R_{unfrz}}$ , subject to effects of moisture change, until freezing occurs again. Note that  $M_R$  returns to  $M_{R_{unfrz}} = M_{R_{equil}}$  after recovery whether or not  $M_{R_{opt}}$  is smaller than  $M_{R_{unfrz}} = M_{R_{equil}}$ .

The preceding recommended computational process is portrayed graphically in Figure 5 for an LTPP site in Manitoba. Prior to about Dec-94 the material is unfrozen, with the average  $M_{R_{unfrz}}$  ranging from about 17,000 psi for the subgrade to about 42,000 psi for the base. The small oscillations for the base indicated between July-94 and Dec-94 are due to moisture content changes. In Dec-94, freezing occurs and  $M_R$  rises to  $M_{R_{frz}} = 1 \cdot 10^6$  psi. About April 95 thawing occurs and  $M_R$  drops to  $M_{R_{min}}$ . The values of  $RF$  selected from Tables 6 and 7 as a function of  $PI$  and  $P_{200}$  are also shown in Figure 5. During recovery, the  $M_R$  rises with  $RR$  (in accordance with Equation 6) until  $RR = 1$  and  $M_R$  again equals the pre-freezing value about June-95. After June-95 the material is unfrozen until freezing occurs again.

Table 1. Values of Unfrozen, Frozen, Thawed  $M_R$  Values from the Literature

Material Type	Unfrozen, $M_{Runfrz}$	Frozen, $M_{Rfrz}$	Thawed, $M_{Rmin}$	References
1206 Subgrade CL	$2 * 10^4$ to $1 * 10^5$ psi	$0.8 * 10^6$ psi		Berg et al., 1996 (2)
1232 Subgrade CL	$1 * 10^3$ to $4 * 10^4$ psi	$0.6 * 10^6$ psi		
Class 3, Stockpile (A-1-b)	$\sim 10^4$ psi	1 to $2 * 10^6$ psi		
Class 4, Taxiway Subbase (A-1-b)	$3 * 10^3$ to $3 * 10^4$ psi	$1-3 * 10^6$ psi		
Class 5, Dense Graded Stone (A-1-a)	$1 * 10^4$ to $3 * 10^4$ psi	3 to $7 * 10^6$ psi		
Class 6, Base (A-1-a)	$3 * 10^4$ psi	2 to $6 * 10^6$ psi		
Sandy Clay (glacial till) LL = 33, PI = 17%			50% red in $M_R$ @ $w = w_{opt}$ 70% red in $M_R$ @ $w = w_0 +$ 1.5% $M_R$ (thawed) ~3100 psi	Culley, 1970 (7)
High Plasticity Glacial Clay LL = 77, PI = 30 $\gamma_d = \gamma_{d max}$			$M_R > 1500$ psi $M_R < 5700$ psi	Mickleborough, 1970 (15)

Table 1. Cont'd

Material Type	Unfrozen, $M_{Runfrz}$	Frozen, $M_{Rfrz}$	Thawed, $M_{Rmin}$	References
Sandy Clay Glacial till ( undisturbed) $75 < S < 85\%$ from Saskatchewan			$M_R = 10,000$ psi (and greater) effects on granular base and subbase were small	MacLeod, 1971 (14)
Same clay as Mickleborough, except undisturbed	8400 psi		5000 psi	Bergan, 1972 (3)
Same as Mickleborough (compacted to in-situ $\gamma_d$ and w)	15,000 psi		6500 psi	Bergan and Monismith, 1973 (4)
Silty Clay LL=32, PI=9 Lean Clay LL = 46, PI = 24			3000 to 6000 psi for both soils	Robnett and Thompson, 1976 (16)
Hanover Silt, ML 75% - #200, PI=0-10 S=88%	$3 * 10^4$ psi	$4 * 10^5$ psi @ 29 F $6 * 10^6$ psi @ 20F	$5 * 10^3$ psi to $10^4$ psi	Chamberlain et al., 1979 (5)
Morin Clay, CL 100% - #200 PI=17	$4 * 10^3$ to $10^4$ psi	$10^5$ psi @ 29 F $4 * 10^5$ to $10^6$ @ 24 F	$10^3$ to $10^4$ psi	“
Coarse Grained Soils		$1.5$ to $5 * 10^6$ psi		Vinson, 1978 (17)

Table 1. Cont'd

Material Type	Unfrozen, $M_{Runfrz}$	Frozen, $M_{Rfrz}$	Thawed, $M_{Rmin}$	References
Silts		0.8 to $3.5 * 10^6$ psi		“
Clays		0.2 to $2 * 10^6$ psi		“
Gravel		$5 * 10^6$ psi		“
Aeolian Sand		$1.3 * 10^6$ psi		“
Sand		$6 * 10^6$ psi		“
Glacial Till		$5 * 10^6$ psi		“
Glacial Till		$3 * 10^6$ psi		“
Gravel		$7 * 10^6$ psi		“
Silt	$2 * 10^5$ psi	$1.2 * 10^6$ psi		“
Silt		$2 * 10^6$ psi		“
Alluvial Clay		$1.3 * 10^6$ psi		“
Clay		$0.75 * 10^6$ psi		“
Clay		$1.5 * 10^6$ psi		“
Silt (Alaska) PI = 5		0.4 to $1 * 10^6$ psi		Czajkowski and Vinson, 1980 (8)
Silt (Hanover) PI = 0		$2 * 10^6$ psi		“
Granular Subgrade	$k_1 * \theta^{0.5}$	$300 * k_1 * \theta^{0.5}$	$0.25 * k_1 * \theta^{0.5}$	The Asphalt Institute, 1982 (1)
Subgrade			RF = 0.4	Witczak, 1972 (18)
Gravel Base			RF = 0.35	Jong et al., 1998 (13)
Clay Subgrade			RF = 0.65	“
Silty Sand (SM)		$1.5 * 10^6$	$286 * \theta^{0.456}$	Cole et al., 1981 (6)

Table 1. Cont'd

Material Type	Unfrozen, $M_{Runfrz}$	Frozen, $M_{Rfrz}$	Thawed, $M_{Rmin}$	References
GW-SW	$1151 * \theta^{0.76}$			Cole et al., 1981 (6)
NFS			RF = 1 (1.00)	Janoo, 2000 (10)
PFS			RF = 0.9 (0.93)	“
S1			RF = 0.75 (0.83)	“
S2			RF = 0.70 (0.80)	“
F1			RF = 0.60 (0.72)	“
F2			RF = 0.50 (0.64)	“
F3/F4			RF = 0.30 (0.46)	“
CH Subgrade			RF = 0.55	Janoo and Berg, 1990 (12)

Table 2. Team Synthesis of MR Values for Frozen Materials

Material Type	$M_{Rfrz}$
Coarse-Grained	1.5, 2, 5, 4, 3, 5, 4 * $10^6$ $M_{Rave} \sim 3 \pm 1 * 10^6$ psi
Fine-Grained-Silts and Silty Sands > 10% fines PI near zero	3.2, 2.2, 1.2, 2, 0.7, 2 $M_{Rave} = 2 \pm 1 * 10^6$ psi
Clay	0.8, 0.6, 1.1, 1.3, 0.75, 1.5, $M_{Rave} \sim 1.0 \pm 0.5 * 10^6$ psi

Table 3. Corps of Engineers (COE) Frost Susceptibility Classification (11)

Frost Group	Soil Description	Percentage finer than 0.02 mm by weight, $P_{0.02}$ %	Typical soil types under Unified Soil Classification System	Percentage finer than 75 $\mu$ m by weight, $P_{200}$ %
NFS <sup>(1)</sup>	(a) Gravel Crushed Stone Crushed Rock	0 – 1.5	GW, GP	0 – 3
	(b) Sands	0 - 3	SW, SP	0 – 6
PFS <sup>(2)</sup>	(a) Gravel Crushed Stone Crushed Rock	1.5 - 3	GW, GP	3 – 6
	(b) Sands	3 - 10	SW, SP	6 – 19
S1 <sup>(3)</sup>	Gravelly soils	3 - 6	GW, GP, GW-GM, GP-GM	6 – 11.5
S2 <sup>(3)</sup>	Sandy soils	3 - 6	SW, SP, SW-SM, SP-SM	6 – 11.5
F1	Gravelly soils	6 - 10	GM, GW-GM, GP-GM	11.5 – 19
F2	(a) Gravelly soils	10 - 20	GM, GW-GM, GP-GM	19– 38.5
	(b) Sands	6 - 15	SM, SW-SM, SP-SM	11.5 – 29
F3	(a) Gravelly soils	over 20	GM, GC	over 38.5
	(b) Sands, except very fine silty sands	over 15	SM, SC	over 29
	(c) Clays, $PI > 12$	-	CL, CH	-



Table 3. Cont'd.

Frost Group	Soil Description	Percentage finer than 0.02 mm by weight	Typical soil types under Unified Soil Classification System	Percentage finer than 2 $\mu$ m by weight
F4	(a) Silts	-	ML, MH	-
	(b) Very fine silty sands	over 15	SM	over 28.8
	(c) Clays, PI<12	-	CL, CL-ML	-
	(d) Varved clays and other fine-grained, banded sediments	-	CL, ML and SM, CL, CH and ML, CL, CH, ML and SM	-

<sup>(1)</sup> Non-frost-susceptible.

<sup>(2)</sup> Possibly frost-susceptible, requires lab test to determine frost potential.

<sup>(3)</sup> Usually sands used as subbases that may have some frost susceptible material.

Table 4. Criteria Developed by Others for Predicting Frost Susceptibility of Soils (11)

Agencies	Frost-susceptibility criteria (% passing no. 200 sieve)
Asphalt Institute	7
Newfoundland, Canada	6
Japan	6
Alaska	6
Colorado	5 – 10
Kansas	15
Maryland	12
Massachusetts	10
Minnesota	10
New Hampshire	8
Ohio	15
Vermont	10
Washington	10
Wisconsin	5

Table 5. Change in CBR during Thaw Weakening Period (11)

Layer	USCS	Percent passing no. 200 sieve	CBR			RF
			Normal	Thaw-weakening period	Percent reduction	
Subbase	GM	10 – 12	64	33	48	0.65
Base	GM – SM		37	27	27	0.82
Base	GC	6 – 12	37	14	62	0.54
Base	GW		58	28	52	0.63
Base	GW		24	21	13	0.92

Table 6. Recommended Values of RF for Coarse-Grained Materials (P<sub>200</sub> < 50%)

Distribution of Coarse Fraction	P <sub>200</sub> %	PI < 12%	PI = 12% - 35%	PI > 35%
Mostly Gravel	< 6	0.85	-	-
	6 – 12	0.65	0.70	0.75
	> 12	0.60	0.65	0.70
Mostly Sand	< 6	0.75	-	-
	6 – 12	0.60	0.65	0.70
	> 12	0.50	0.55	0.60

Table 7. Recommended Values of RF for Fine-Grained Materials ( $P_{200} > 50\%$ )

$P_{200}$ %	PI < 12%	PI = 12% - 35%	PI > 35%
50 - 85	0.45	0.55	0.60
> 85	0.40	0.50	0.55

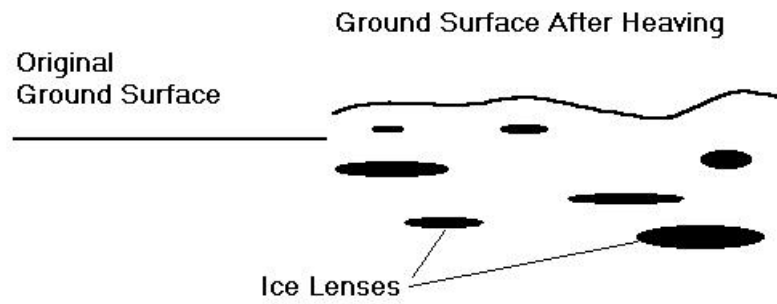


Figure 1. Schematic of Ice Lens Formation

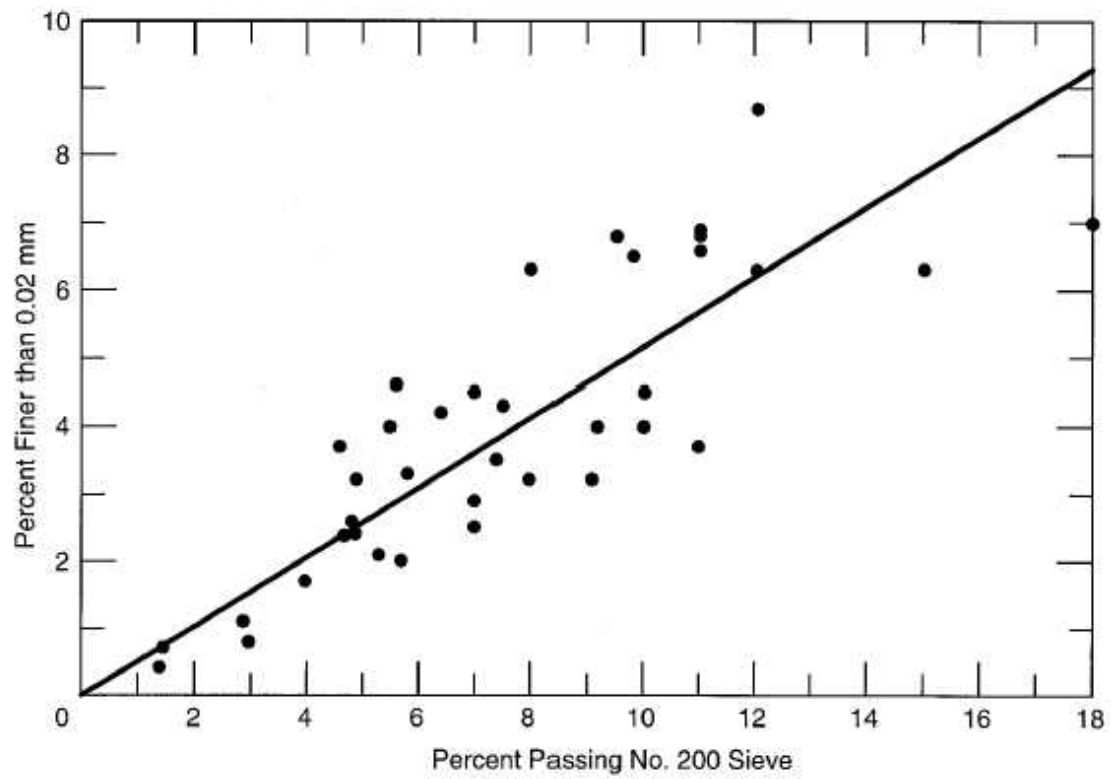


Figure 2. Relationship between Percentage Passing the No. 200 Sieve and the Percentage Finer than 0.02 mm for Coarse Grained Gravel Soils (11).

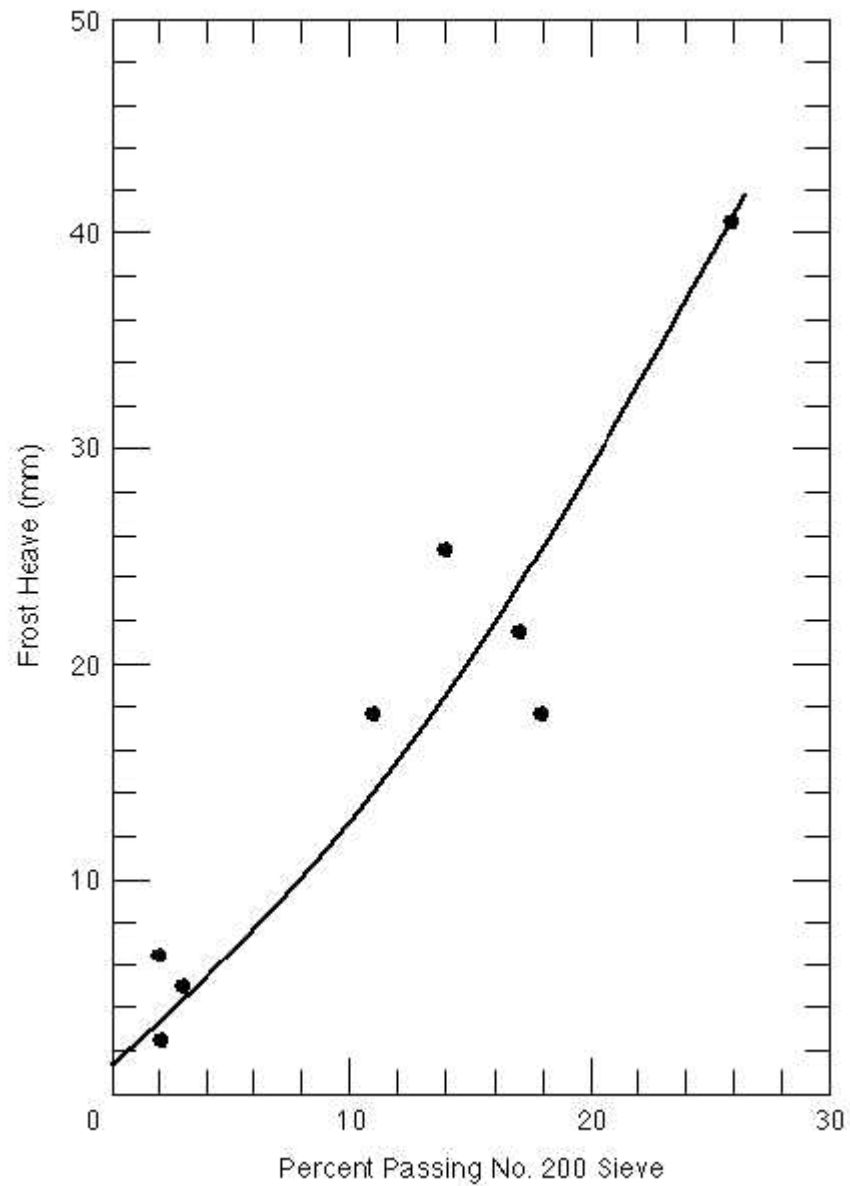


Figure 3. Relationship between Frost Heave and the Percentage Passing the No. 200 Sieve – Non Cohesive Soils Other than Limestone Gravels (11).

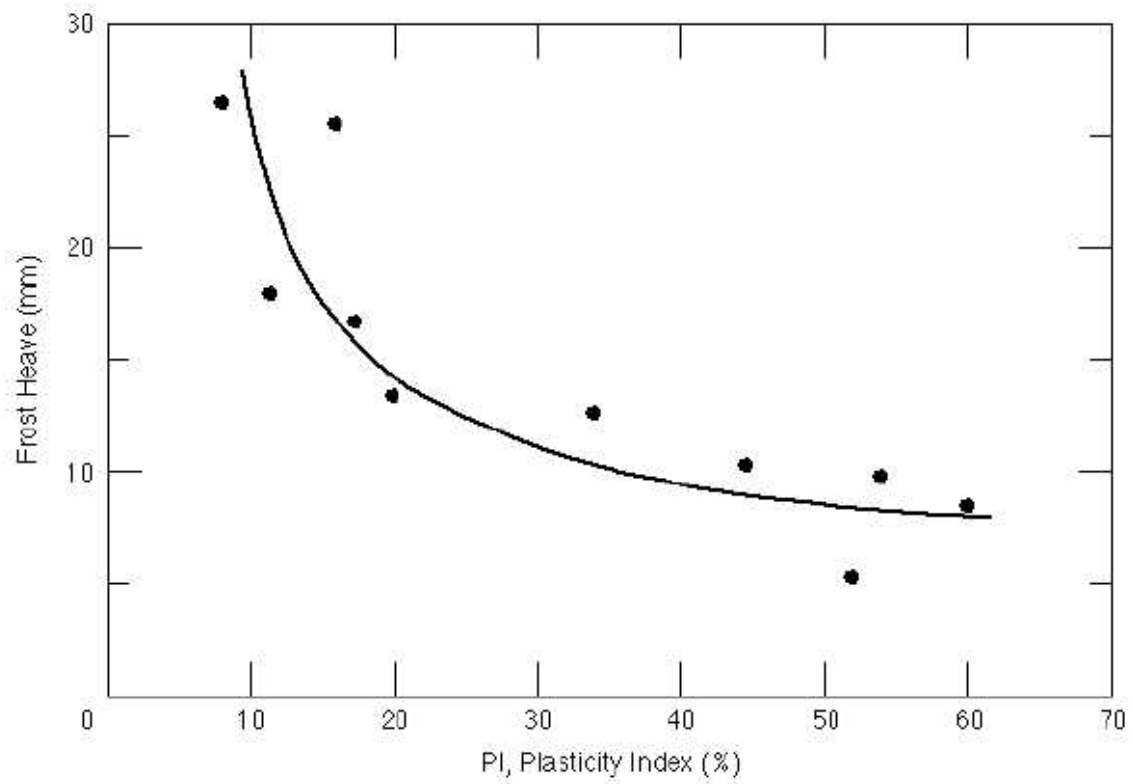
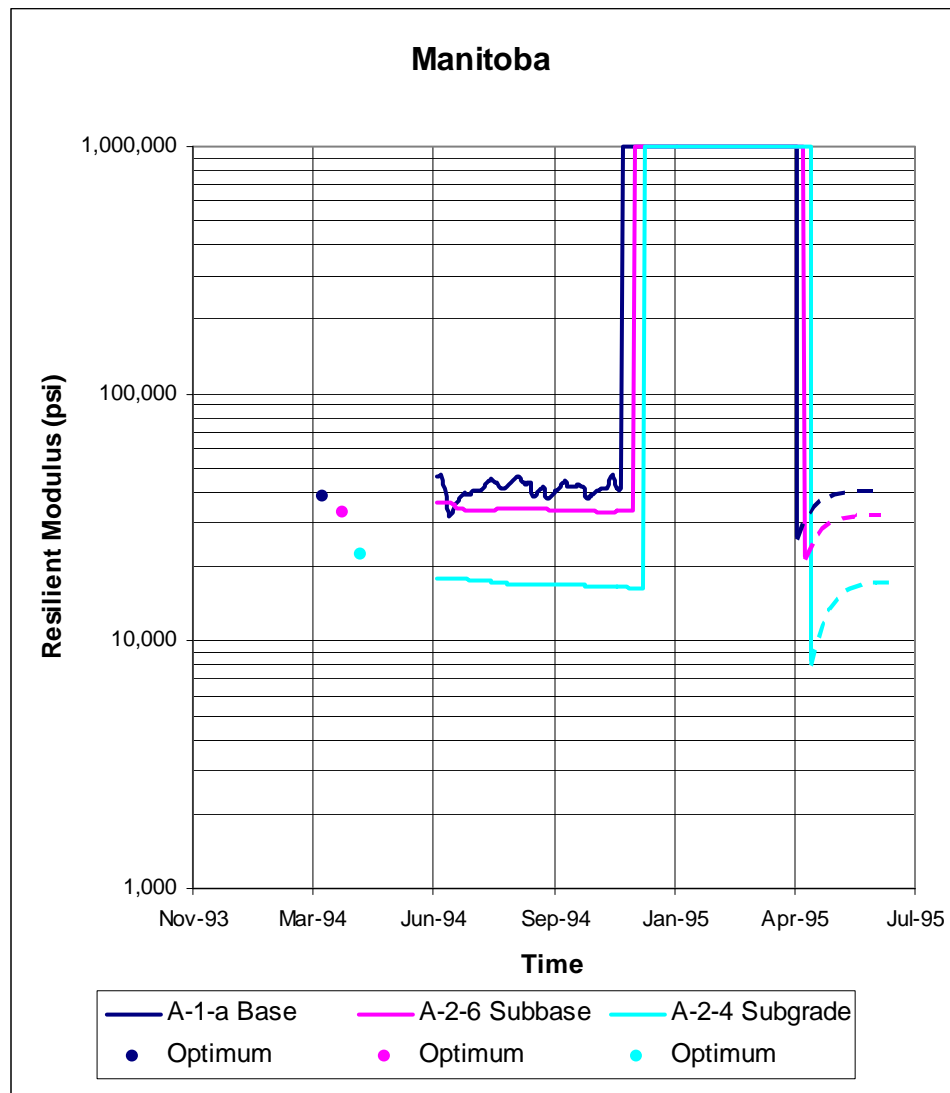


Figure 4. Relationship between Frost Heave and PI for Cohesive Soils (11).





Layer Type	Class	P <sub>200</sub>	PI	RF	M <sub>Runfrz</sub>	M <sub>Rmin</sub>
<i>Units</i>	<i>AASHTO</i>	<i>%</i>			<i>psi</i>	<i>psi</i>
Crushed gravel	A-1-a Base	10.9	5	0.65	41,000	26,650
Gravel (uncrushed)	A-2-6 Subbase	10.5	11	0.65	33,600	21,840
Silty sand	A-2-4 Subgrade	28.8	0	0.5	16,600	8,300

Figure 5. Example of time-varying  $M_R$ .

## References:

1. The Asphalt Institute. *Research and Development of the Asphalt Institute's Thickness Design Manual (MS-1) Ninth Edition*. Research Report No. 82-2, August 1982.
2. Berg R.L., Bigl S.R., Stark J.A. and Durell G.D. *Resilient Modulus Testing of Materials from Mn/ROAD, Phase I*. The U.S. Army Cold Regions Research and Engineering Laboratory, Special Report 96-19, September 1996.
3. Bergan A.T. *Some Considerations in the Design of Asphalt Concrete Pavements for Cold Regions*. Thesis presented to the University of California, at Berkeley, California, 1972, in partial fulfillment of the requirements for the degree of Doctor of Philosophy.
4. Bergan A.T. and Monismith C.L. *Characterization of Subgrade Soils in Cold Regions for Pavement Design Purposes*. Highway Research Record 431, Highway Research Board, Washington, D.C., 1973.
5. Chamberlain E.J., Cole D.M. and Johnson T.C. *Resilient Response of Two Frozen and Thawed Soils*. Journal of the Geotechnical Division, Proceedings of the American Society of Civil Engineers, Vol. 105, No. GT2, February, 1979.
6. Cole D.M., Irwin L.H. and Johnson T.C. *Effect of Freezing and Thawing on Resilient Modulus of a Granular Soil Exhibiting Nonlinear Behavior*. Transportation Research Record 801, TRB, National Research Council, 1981, Washington, D.C., pp. 19-26.
7. Culley R.W. *Effect of Freeze-Thaw Cycling on Stress-Strain Characteristics and Volume Change of a Till Subjected to Repetitive Loading*. Technical Report 13, Saskatchewan Department of Highways, Saskatchewan, Canada, 1970.
8. Czajkowsky R.L. and Vinson T.S. *Dynamic Properties of Frozen Silt Under Cyclic Loading*. Journal of the Geotechnical Division, Proceedings of the American Society of Civil Engineers, Vol. 106, No. GT9, September, 1980.
9. Esch D.C., McHattie R.L. and Connor B. *Frost-Susceptibility Ratings and Pavement Structure Performance*. Transportation Research Record 809, TRB, National Research Council, 1981, Washington, D.C., pp. 27-34.
10. Janoo V.C. *Evaluating Pavement Performance in Cold Regions*. ISCORD 2000 proceedings, Hobart, Tasmania, Australia, February 2000.
11. Janoo V.C., Eaton R. and Barna L. *Evaluation of Airport Subsurface Materials*. The U.S. Army Cold Regions Research and Engineering Laboratory, Special Report 97-13, May 1997.

12. Janoo V.C. and Berg R.L. *Thaw Weakening of Pavement Structures in Seasonal Frost Areas*. Transportation Research Record 1286, TRB, National Research Council, 1990, Washington, D.C., pp. 217-233.
13. Jong D., Bosscher P.J. and Benson C.H. *Field Assessment of Changes in Pavement Moduli Caused by Freezing and Thawing*. Transportation Research Record 1615, TRB, National Research Council, 1998, Washington, D.C., pp. 41-48.
14. MacLeod D.R. *Some Fatigue Considerations in the Design of Thin Pavements*. Thesis presented to the University of Saskatchewan, at Saskatchewan, Canada, 1970, in partial fulfillment of the requirements for the degree of Master of Science.
15. Mickleborough B.W. *An Experimental Study of the Effects of Freezing on Clay Subgrades*. Thesis presented to the University of Saskatchewan, at Saskatchewan, Canada, 1970, in partial fulfillment of the requirements for the degree of Master of Science.
16. Robnett Q.L. and Thompson M.R. *Effect of Lime Treatment on the Resilient Behavior of Fine Grained Soils*. Transportation Research Record 560, TRB, National Research Council, 1976, Washington, D.C., pp. 11-20.
17. Vinson T.S. *Parameter Effects on Dynamic Properties of Frozen Soils*. Journal of the Geotechnical Division, Proceedings of the American Society of Civil Engineers, Vol. 104, No. GT10, October, 1978.
18. Witczak M.W. *Design of Full-Depth Asphalt Airfield Pavements*. The University of Michigan Third International Conference on the Structural Design of Asphalt Pavements, Vol. I, Proceedings, September 11 – 15, 1972, Grosvenor House, Park Lane, London, England.
19. Witczak M.W., Houston W.N., Zapata C.E., Richter C., Larson G. and Walsh K. *Improvement of the Integrated Climatic Model for Moisture Content Predictions*. Development of the 2002 Guide for the Development of New and Rehabilitated Pavement Structures, NCHRP 1-37 A, Inter Team Technical Report (Seasonal 4), June 2000.
20. Witczak M.W., Andrei D. and Houston W.N. *Resilient Modulus as Function of Soil Moisture – Summary of Predictive Models*. Development of the 2002 Guide for the Development of New and Rehabilitated Pavement Structures, NCHRP 1-37 A, Inter Team Technical Report (Seasonal 1), June 2000.
21. Witczak M.W., Houston W.N. and Andrei D. *Resilient Modulus as Function of Soil Moisture – A Study of the Expected Changes in Resilient Modulus of the Unbound Layers with Changes in Moisture for 10 LTPP Sites*. Development of the 2002 Guide

for the Development of New and Rehabilitated Pavement Structures, NCHRP 1-37 A,  
Inter Team Technical Report (Seasonal 2), June 2000.

Copy No. \_\_\_\_\_

# **Guide for Mechanistic-Empirical Design OF NEW AND REHABILITATED PAVEMENT STRUCTURES**

**FINAL DOCUMENT**

## **APPENDIX DD-4: IMPROVEMENT OF THE INTEGRATED CLIMATIC MODEL FOR MOISTURE CONTENT PREDICTIONS**

**NCHRP**

**Prepared for  
National Cooperative Highway Research Program  
Transportation Research Board  
National Research Council**

**Submitted by  
ARA, Inc., ERES Division  
505 West University Avenue  
Champaign, Illinois 61820**

**June 2000**

## **Acknowledgment of Sponsorship**

This work was sponsored by the American Association of State Highway and Transportation Officials (AASHTO) in cooperation with the Federal Highway Administration and was conducted in the National Cooperative Highway Research Program which is administered by the Transportation Research Board of the National Research Council.

## **Disclaimer**

This is the final draft as submitted by the research agency. The opinions and conclusions expressed or implied in this report are those of the research agency. They are not necessarily those of the Transportation Research Board, the National Research Council, the Federal Highway Administration, AASHTO, or the individual States participating in the National Cooperative Highway Research program.

## **Acknowledgements**

The research team for NCHRP Project 1-37A: Development of the 2002 Guide for the Design of New and Rehabilitated Pavement Structures consisted of Applied Research Associates, Inc., ERES Consultants Division (ARA-ERES) as the prime contractor with Arizona State University (ASU) as the primary subcontractor. Fugro-BRE, Inc., the University of Maryland, and Advanced Asphalt Technologies, LLC served as subcontractors to either ARA-ERES or ASU along with several independent consultants.

Research into the subject area covered in this Appendix was conducted at ASU. The authors of this Appendix are Dr. M. W. Witczak, Dr. W. N. Houston, Dr. C. E. Zapata, Mrs. Cheryl Richter, Mr. Gregg Larson, Dr. Ken Walsh. Dr. Witczak coordinated the overall research effort of the 2002 Design Guide Team, outlined the problems, monitored progress, set schedules and deadlines, and provided periodic technical review of research results as they became available. Ms. Cheryl Richter acquired the input data needed for running the EICM moisture predictions, made EICM runs in parallel with Dr. Zapata, and helped to identify relevant issues to be addressed during team meetings. Drs. Houston, Zapata and Walsh collected the data needed to develop the prediction of the SWCC based on soil properties and developed the SWCC model itself. The EICM modifications were coordinated by Dr. Houston and Zapata with important input from Mr. Gregg Larson. The model code changes were performed by Mr. Gregg Larson.

## **Foreword**

This appendix presents the derivation of reasonable values of MR for both frozen and thawed unbound materials through evaluation of published results.. The information contained in this appendix serves as a supporting reference to the resilient modulus discussions presented and PART 2, Chapter 3, and PART 3, Chapters 3, 4, 6, and 7 of the Design Guide.

This appendix is the fourth in a series of four volumes on environmental effects on pavements. The other volumes are:

- |                |  |
|----------------|--|
| Appendix DD-1: | Resilient Modulus As Function Of Soil Moisture-Summary Of Predictive Models  |
| Appendix DD-2: | Resilient Modulus As Function Of Soil Moisture – A Study Of The Expected<br>Changes In Resilient Modulus Of The Unbound Layers With Changes In Moisture<br>For 10 LTPP Sites |
| Appendix DD-3: | Selection Of Resilient Moduli For Frozen/Thawed Unbound Materials  |

---

# Abstract

The Enhanced Integrated Climatic Model (EICM), developed under contract with the Federal Highway Administration (FHWA), was designed to simulate the behavior of pavement materials and subgrade materials over several years of operation. An evaluation of the model's moisture prediction capabilities showed that its performance with regard to moisture predictions for the unbound materials was initially poor and exceeded the error typically found in field moisture measurements. Those findings pointed to the need for significant modifications and additions to the EICM moisture content prediction algorithms. The required modifications were subsequently made, creating version 2.6 of the EICM.

Modifications to the EICM include the addition of a better functional fit for the soil-water characteristic curve (SWCC); the incorporation of an algorithm capable of predicting the SWCC based on soil index properties; the addition of an algorithm for the prediction of the unsaturated hydraulic conductivity based on the SWCC; and, the development of sets of default soil parameters based on the ASSHTO Soil Classification System. Verification of the Version 2.6 showed great improvement on the prediction of the moisture content for the unbound materials.



---

# Table of Contents

<b>List of Tables.....</b>	<b>vii</b>
<b>List of Figures.....</b>	<b>viii</b>
 <b>Chapter 1</b>	
<b>Introduction</b>	
<b>The Enhanced Integrated Climatic Model .....</b>	<b>1</b>
General Features of the Model .....	1
Objectives of the Research.....	2
Organization of the Report.....	3
 <b>Chapter 2</b>	
<b>Assessment of the Performance of the EICM</b>	
<b>Version 2.1 .....</b>	<b>5</b>
Introduction .....	5
Input Requirements for the EICM version 2.1 .....	5
Collected Data .....	8
Climatic Boundary Conditions .....	9
Infiltration and Drainage.....	19
Asphalt Material Properties .....	19
Material Properties .....	19
Initial Moisture Content Profile.....	20
Initial Temperature Profile.....	20
Basis for Comparison .....	20
Results .....	21
Factors that Contributed to the Poor Predictions of the Water Contents by the EICM.....	30
Short-term Actions Recommended for the Improvement of the EICM.....	31
 <b>Chapter 3</b>	
<b>Modifications to the EICM version 2.1</b>	
<b>Moisture Content Prediction .....</b>	<b>33</b>
Proposed Modifications to the EICM – version 2.1 .....	33
The Soil-Water Characteristic Curve.....	33
Correlation Between the Fredlund and Xing Fitting Parameters and Soil Index Properties ...	37
Correlations for Soils with $PI > 0$ .....	37
Correlations for Soils with $PI = 0$ .....	38
Correlation Results .....	39
Best-Estimate SWCCs Based on AASHTO Classification.....	45
Best-Estimate SWCCs for Base Course Materials .....	45
Default Values for Saturated Hydraulic Conductivity, Specific Gravity, and Saturated Volumetric Water Content.....	45
Unsaturated Hydraulic Conductivity Function.....	47
Summary .....	48
 <b>Chapter 4</b>	
<b>Assessment of the EICM Moisture Content Prediction after Modifications</b>	
<b>EICM Version 2.6 .....</b>	<b>49</b>
Introduction .....	49
Data Collected .....	49
Results .....	50

## **Chapter 5**

### **User's Guide and Recommendations**

<b>EICM version 2.6 - Moisture Content Prediction .....</b>	<b>77</b>
Introduction .....	77
Input Parameters .....	77
Soil Classification .....	78
Thickness of the Layer .....	78
Number of Elements for this Layer .....	79
Porosity of the Layer Material .....	79
Specific Gravity .....	81
Saturated Permeability .....	81
Dry Density .....	81
Plasticity Index .....	82
Percent Passing #200 .....	82
Diameter $D_{60}$ .....	83
Initial Volumetric Water Content .....	83
Equilibrium Volumetric Water Content .....	83

## **Chapter 6**

### **Development of Procedures for Estimating Moisture Content from the Initial State to**

<b>Equilibrium Conditions for Newly Constructed Pavements .....</b>	<b>86</b>
Introduction .....	86
Correlation for $S_{opt}$ .....	87
Correlation for $w_{opt}$ .....	89
Intended Use of Correlations .....	91
Check on Internal Consistency for $S_{opt}$ , $w_{opt}$ , and $G_s$ .....	94

## **Chapter 7**

### **Conclusions .....**

Part I.	
Conclusions Relative to the Maximization of the Agreement between EICM Predicted Moisture Contents and TDR Measured Moisture Contents for Existing Pavements .....	97
Part II.	
Conclusions Relative to the Optimization of Procedures for Predicting the Moisture Content Change from the Initial to the Equilibrium Condition .....	99

## **Chapter 8**

### **Recommendations for Implementation of EICM Input for Use in the 2002 Design**

<b>Guide .....</b>	<b>101</b>
Introduction .....	101
Unbound Compacted Layers .....	102
Data Required Including Sources and Tests to be Performed .....	102
Unbound Natural (In-Situ) Layers .....	105
Data Required Including Sources and Tests to be Performed .....	105

## **APPENDICES .....**

### **APPENDIX A**

#### **VOLUMETRIC WATER CONTENT PROFILES**

##### **CONNECTICUT (91803)**

EICM – Version 2.1 .....	108
--------------------------	-----

### **APPENDIX B**

#### **VOLUMETRIC WATER CONTENT PROFILES**

##### **MINNESOTA (91803)**

EICM – Version 2.1 .....	116
--------------------------	-----

<b>APPENDIX C</b>	
VOLUMETRIC WATER CONTENT PROFILES	
MAINE (231026)	
EICM – Version 2.1 .....	123
<b>APPENDIX D</b>	
VOLUMETRIC WATER CONTENT PROFILES	
NEW HAMPSHIRE (331001)	
EICM – Version 2.1 .....	131
<b>APPENDIX E</b>	
VOLUMETRIC WATER CONTENT PROFILES	
VERMONT (501002)	
EICM – Version 2.1 .....	139
<b>APPENDIX F</b>	
VOLUMETRIC WATER CONTENT PROFILES	
MANITOBA (831801)	
EICM – Version 2.1 .....	147
<b>APPENDIX G</b>	
BEST-ESTIMATE SOIL-WATER CHARACTERISITC CURVES	
BASED ON AASHTO CLASSIFICATION .....	156
<b>APPENDIX H</b>	
BEST-ESTIMATE SOIL-WATER CHARACTERISITC CURVES	
FOR BASE COURSE MATERIALS.....	163
<b>APPENDIX I</b>	
VOLUMETRIC WATER CONTENT PROFILES	
CONNECTICUT (91803)	
EICM – Version 2.6 .....	167
<b>APPENDIX J</b>	
VOLUMETRIC WATER CONTENT PROFILES	
MINNESOTA (271018)	
EICM – Version 2.6 .....	174
<b>APPENDIX K</b>	
VOLUMETRIC WATER CONTENT PROFILES	
MAINE (231026)	
EICM – Version 2.6 .....	182
<b>APPENDIX L</b>	
VOLUMETRIC WATER CONTENT PROFILES	
NEW HAMPSHIRE (331001)	
EICM – Version 2.6 .....	190
<b>APPENDIX M</b>	
VOLUMETRIC WATER CONTENT PROFILES	
VERMONT (501002)	
EICM – Version 2.6 .....	198
<b>APPENDIX N</b>	
VOLUMETRIC WATER CONTENT PROFILES	

MANITOBA (831801)	
EICM – Version 2.6 .....	206
 <b>APPENDIX O</b>	
VOLUMETRIC WATER CONTENT PROFILES	
GEORGIA (131005)	
EICM – Version 2.6 .....	213
 <b>APPENDIX P</b>	
VOLUMETRIC WATER CONTENT PROFILES	
COLORADO (81053)	
EICM – Version 2.6 .....	221
 <b>APPENDIX Q</b>	
VOLUMETRIC WATER CONTENT PROFILES	
ARIZONA (41024)	
EICM – Version 2.6 .....	233
 <b>APPENDIX R</b>	
VOLUMETRIC WATER CONTENT PROFILES	
TEXAS (481077)	
EICM – Version 2.6 .....	238
<b>REFERENCES</b> .....	<b>247</b>

---

## List of Tables

Table 1.	Input Variables Needed by the EICM - Version 2.1 .....	7
Table 2.	Input Data and Sources for the EICM - Version 2.1 for the Connecticut (91803) and Minnesota (271018) Sites.....	10
Table 3.	Input Data and Sources for the EICM - Version 2.1 for the Maine (231026), New Hampshire (331001), Vermont (501002), and Manitoba (831801) Sites .....	14
Table 4	Equations Used to Represent the Soil-Water Characteristic Curve .....	34
Table 5.	Soil Properties Default Values vs. AASHTO Soil Classification System.....	44
Table 6.	Best Estimated $D_{60}$ for Base Course Materials.....	46
Table 7.	Summary of Input Parameters for the EICM – Version 2.6 for the Connecticut, Minnesota, Maine, New Hampshire, Vermont, and Manitoba LTPP Sections .....	51
Table 8.	Summary of Input Parameters for the EICM – Version 2.6 for the Georgia, Colorado, Arizona, and Texas LTPP Sections .....	56
Table 9.	Input Variables Needed by the EICM (version 2.6) for the Material Properties and Initial Temperature and Water Content Profiles Sections.....	78
Table 10.	Options for Determining the Porosity of the Layer, Depending on the Known Soil Properties.....	80
Table 11.	Options for Determining the Specific Gravity of the Layer, Depending on the Known Soil Properties.....	81
Table 12.	Determination of the SWCC based on Percentage Passing #200, Plasticity Index and Diameter $D_{60}$ .....	82
Table 13.	Available Options for the Initial and Equilibrium Water Contents.....	84
Table 14.	Listing of Input Parameters Required by the EICM, Including Climatic Data, Infiltration and Drainage Data, Asphalt/PCC Properties and Material Properties for Compacted and Natural In-Situ Layers.....	104

---

## List of Figures

Figure 1.	Measured versus Predicted Moisture Content – EICM version 2.1 Connecticut (91803) .....	22
Figure 2.	Measured versus Predicted Moisture Content – EICM version 2.1 Minnesota (271018) .....	23
Figure 3.	Measured versus Predicted Moisture Content – EICM version 2.1 Maine (231026).....	24
Figure 4.	Measured versus Predicted Moisture Content – EICM version 2.1 New Hampshire (331001) .....	25
Figure 5.	Measured versus Predicted Moisture Content – EICM version 2.1 Vermont (501002).....	26
Figure 6.	Measured versus Predicted Moisture Content – EICM version 2.1 Manitoba (831801) .....	27
Figure 7.	Summary of Measured versus Predicted Moisture Content for the Base Course Materials – EICM version 2.1 .....	28
Figure 8.	Summary of Measured versus Predicted Moisture Content for the Subgrade Materials – EICM version 2.1 .....	29
Figure 9.	Range of SWCCs for Soils with wPI between 0.1 and 3.....	40
Figure 10.	Range of SWCCs for Soils with wPI between 3 and 10.....	40
Figure 11.	Range of SWCCs for Soils with wPI between 10 and 30.....	41
Figure 12.	Range of SWCCs for Soils with wPI between 30 and 50.....	41
Figure 13.	Range of SWCCs for Soils with $D_{60}$ between 1 and 0.4 mm. ....	42
Figure 14.	Range of SWCCs for Soils with $D_{60}$ between 0.4 and 0.1 mm. ....	42
Figure 15.	Predicted SWCC based on $D_{60}$ and wPI.....	43
Figure 16.	Measured versus Predicted Moisture Content – EICM version 2.6 Connecticut (91803) .....	64
Figure 17.	Measured versus Predicted Moisture Content – EICM version 2.6 Minnesota (271018) .....	65
Figure 18.	Measured versus Predicted Moisture Content – EICM version 2.6 Maine (231026).....	66

Figure 19.	Measured versus Predicted Moisture Content – EICM version 2.6 New Hampshire (331001) .....	67
Figure 20.	Measured versus Predicted Moisture Content – EICM version 2.6 Vermont (501002).....	68
Figure 21.	Measured versus Predicted Moisture Content – EICM version 2.6 Manitoba (831801) .....	69
Figure 22.	Measured versus Predicted Moisture Content – EICM version 2.6 Georgia (131005) .....	70
Figure 23.	Measured versus Predicted Moisture Content – EICM version 2.6 Colorado (81053).....	71
Figure 24.	Measured versus Predicted Moisture Content – EICM version 2.6 Arizona (41024) .....	72
Figure 25.	Measured versus Predicted Moisture Content – EICM version 2.6 Texas (481077).....	73
Figure 26.	Summary of Measured versus Predicted Moisture Content for the Base Course Materials – EICM version 2.6.....	74
Figure 27.	Summary of Measured versus Predicted Moisture Content for the Subgrade Materials – EICM version 2.6 .....	75
Figure 28.	Summary of Measured versus Predicted Moisture Content for ALL sites – EICM version 2.6 .....	76
Figure 29.	Correlation between Degree of Saturation at Optimum and wPI .....	88
Figure 30.	Correlation between Gravimetric Water Content at Optimum and wPI.....	88
Figure 31.	Correlation between Gravimetric Water Content at Optimum and D <sub>60</sub> .....	90
Figure 32.	Correlation between Gravimetric Water Content at Optimum (T99) and Difference between w <sub>opt</sub> (T99) and w <sub>opt</sub> (T180) .....	90
Figure 33.	Correlation between Dry Unit Weight and wPI .....	95
Figure 34.	Correlation between Dry Unit Weight and D <sub>60</sub> .....	96
Figure 35.	Comparison of $\gamma_{dry\ max}$ from Optimum Conditions with $\gamma_{dry\ max}$ from wPI/D <sub>60</sub> Correlations.....	96

---

# Introduction

## The Enhanced Integrated Climatic Model

### General Features of the Model

The Enhanced Integrated Climatic Model (EICM) is a one-dimensional coupled heat and moisture flow program developed for the Federal Highway Administration (FHWA). The model is intended to predict or simulate the changes in the behavior and characteristics of pavement and subgrade materials in conjunction with climatic conditions over several years of operation. The EICM is comprised of three major components:

- 1) The Infiltration and Drainage Model (ID Model) developed at the Texas A&M University;
- 2) The Climatic-Materials-Structural Model (CMS Model) developed at the University of Illinois; and,
- 3) The CRREL Frost Heave and Thaw Settlement Model (CRREL Model) developed at the United States Army Cold Regions Research and Engineering Laboratory (CRREL).

The EICM computes and predicts the following information throughout the entire pavement profile: temperature, resilient modulus, pore water pressure, water content, frost and thaw depths, frost heave and drainage performance. The data is generated for a period that ranges from one day to several years. The model may be applied to either asphaltic concrete pavements or Portland cement concrete pavements.

The original version of the EICM was developed at Texas A&M University, Texas Transportation Institute in 1989 (Lytton et al. 1990). The original version was modified and released in 1997 under version 2.0 (Larson and Dempsey, 1997). Additional modifications were performed in 1999, under version 2.1. Improvements in version 2.1 included the implementation of a standard Microsoft® Windows style interface as well as user input, computational engine, and output file manipulation improvements. This report provides a list of the input parameters for the EICM and present results of the model performance on moisture content predictions. It is not intended to show the user how to operate the



model. Those wishing to investigate the details of the original programs are referred to the original papers and users guide concerning them. Lytton et al. (1990) provides an overview of each of the components of the model and Larson and Dempsey (1997) provide the user with a detailed guide in dealing with the Integrated Model.

## Objectives of the Research

The objectives of the research reported herein were to:

- 1) Evaluate the moisture predictive capabilities of EICM version 2.1;
- 2) Correct the deficiencies found in EICM version 2.1, to the extent feasible given the constraints governing the project;
- 3) Evaluate and document the moisture predictive capabilities of the improved model, EICM version 2.6.

This work was undertaken to support decisions as to the adequacy and applicability of the EICM as a component of the flexible pavement design procedures being developed for the 2002 Guide for Design of New and Rehabilitated Pavement Structures.

The objectives of this report are:

- 1) Document the evaluation of the EICM version 2.1 moisture content prediction.
- 2) Describe modifications to the EICM version 2.1 to improve its moisture content predictive capabilities.
- 3) Present the results of the validation of the new model version (2.6).

In addition, guidance on the selection of the new input parameters required for the moisture content predictions is presented.

Improvement and validation of the EICM are obviously research and development tasks. The most logical means to these ends are iterative applications of the EICM to sites for which measured moisture contents are available, such as the LTPP sites. An important characteristic of these LTPP sites is that the moisture contents had already reached mean, equilibrium values by the time direct measurements of moisture content by TDR were obtained. Thus, the TDR measurements reflect primarily the seasonal oscillations

about the equilibrium moisture contents, rather than the moisture content changes from initial to equilibrium conditions.

It was known at the outset that the TDR moisture contents were widely scattered about lab-measured moisture contents and were in most cases somewhat suspect themselves. Nevertheless, the decision was made to do the best job possible if improving the EICM with the data available. The major part of the research study was aimed at optimizing the ability of the EICM to predict the moisture contents reported for the TDR, with emphasis on the seasonal oscillations after equilibrium is reached. During the later stages of the studies, the EICM outputs were transported to resilient moduli predictive models. These computations showed that the effects of seasonal oscillations on resilient moduli were typically fairly small compared to the effects of the change from the initial condition to the equilibrium moisture content. At this late stage, a new objective emerged. Attention was focused on the problem of optimizing the computational algorithms and the EICM for prediction of the change in moisture content from the initial condition to the equilibrium condition. This corresponds to focusing on the EICM as a tool for predicting equilibrium moisture contents for new pavements not yet constructed, rather than comparing with values measured by TDR for existing pavements. Thus, the emphasis for this last objective was to develop reliable computational techniques for characterizing the initial conditions and to use the EICM to predict equilibrium moisture contents for new construction. A secondary, related objective was to devise a procedure for hand computation (or spreadsheet) of the equilibrium degrees of saturation as a check on EICM outputs, or as an alternative method of obtaining approximate equilibrium values.

## Organization of the Report

In Chapter 2, results of the evaluation of the moisture prediction capabilities of model version 2.1 are presented. Recommendations to improve the predictive capabilities of the model are also outlined in this chapter. Chapter 3 presents the modifications made to improve the EICM version 2.1. A new set of default parameters is also presented in this chapter. In Chapter 4, the assessment of the new version of the EICM (version 2.6) on the moisture content prediction is presented. Chapter 5 provides guidance on proper application of the new model inputs and capabilities, for application to research and development studies wherein the EICM is being required to predict moisture changes for existing pavement sections for which moisture content measurements are typically available (e. g., TDR values for the LTPP sites). Thus, Chapters 2 through 5 are devoted to the issues of predicting moisture content changes for existing pavement sections, the LTPP sites where measurements are available. Chapter 6 provides procedures and

recommendations for optimizing EICM and related computations to predict changes from the initial state to the equilibrium condition for new construction. Chapter 7 presents the conclusions.

---

# Assessment of the Performance of the EICM

## Version 2.1

### Introduction

The moisture prediction capabilities of the EICM Version 2.1 were evaluated by applying the model to predict subsurface moisture contents for selected Long Term Pavement Performance (LTPP) Seasonal Monitoring test sections, and then comparing the results obtained to the data collected at those test sections.<sup>1</sup>

Comparisons of predicted moisture profiles by the EICM version 2.1 with those measured in the field are presented in this Chapter.

### Input Requirements for the EICM version 2.1

The EICM version 2.1 input requirements are subdivided into seven dialog boxes:

- 1) Integrated model initialization
- 2) Climatic/boundary conditions
- 3) Thermal properties
- 4) Infiltration and drainage variables
- 5) Asphalt material properties
- 6) Unbound material properties, and
- 7) Initial temperature and water content profiles.

---

<sup>1</sup> The Long Term Pavement Performance Program (LTPP) is a 20-year investigation of pavement performance. It was initiated in 1987 as a part of the Strategic Highway Research Program, and has been managed by the Federal Highway administration since 1992. Data characterizing the pavement structure, materials, and performance are being collected for test sections on in-service highways throughout the United States and Canada. Within LTPP, the Seasonal Monitoring program involves a more intensive level of data collection targeted at advancing our understanding of temporal variations in the pavement structure.

The input variables in each group are listed in [Table 1](#).

The EICM allows for two types of climatic analysis, a default analysis for a particular climatic region or user defined climatic inputs. The Integrated Model Initialization dialog box controls which type of analysis is performed. Control parameters for length of the analysis period and output calculations are also set in the initialization screen.

In the Climatic/Boundary Conditions dialog box, the users may elect to use representative data from any of the nine climatic regions included in the program or import their own climatic data. The EICM accepts either hourly or daily climatic data sets. The required climatic data includes temperature, precipitation, wind speed, percent sunshine/cloud cover, and the depth of the water table.

Default values for the thermal properties are provided by the EICM and generally are appropriate, unless the user has information on the site to be modeled. The user needs to specify the time of the day when maximum and minimum temperatures occur when utilizing daily climatic data.

In the Infiltration and Drainage properties dialog box, the parameters required for the Infiltration and Drainage component module of the EICM are displayed. The User's Guide provides default values for most of the variable in this dialog box. However, variables such as the linear length of cracks and the composition of the base course have a significant impact on the results and should be measured, if possible.

The pavement parameters required by the model depend on the material type chosen by the user. Table 1 shows the properties required for the Asphalt Material. The asphalt materials include both asphalt concrete pavements and asphalt concrete overlays. A single asphalt layer is allowed in each model document. Those interested on the Portland Cement Concrete (PCC) properties required by the EICM, should consult the complete User's Guide.

The unbound material properties required by the model are listed in Table 1. Generally, the EICM provides the user with reasonable default values, however the accuracy of the model is sacrificed if only default material parameters are used.

Finally, the temperature and water content profiles for the first day of the analysis at every node are input in the Initial Temperature and Water Content Profiles dialog box.

Table 1. Input Variables Needed by the EICM - Version 2.1

Integrated Model Initialization	
Variable	Notes
Climatic region	Default or User-Defined
Weather station	Default or User-Defined
Year to be modeled	
First month in the analysis period	
First day of month in analysis period	
Length of analysis period	Maximum of 365 days
Time increment for output	Between 0.1 and 6 hours
Time increment for calculation	Between 0.01 and 1 hour
Latitude	Only if User-Defined weather station
Climate/Boundary Conditions	
Variable	Notes
Daily Maximum/Minimum Temperatures	For the entire analysis period. Default or User-Defined
Daily Rainfall	For the entire analysis period. Default or User-Defined
Daily Windspeed	For the entire analysis period. Default or User-Defined
Daily Percent Sunshine	For the entire analysis period. Default or User-Defined
Daily Water Table Depth	For the entire analysis period.
Thermal Properties	
Variable	Notes
Modifier of Overburden Pressure	Default value recommended
Emissivity Factor	Default available. Between 0 and 1
Surface short-wave Absorptivity	Default available. Between 0 and 1
Maximum convection coefficient	Default available
Coefficient of Variation of Unsaturated Permeability	Default or User Defined. Value of 1 recommended
Time of Day When Minimum/Maximum Temperatures Occur	EICM uses the input values for the entire analysis period
Limits Freezing Range	Default or User-Defined
Infiltration and Drainage	
Variable	Notes
Linear length of cracks/joints one side pavement	
Total length surveyed for cracks and joints	
Composition of Base Course	
Base %fines	Sieve analysis recommended
Base % gravel	Sieve analysis recommended
Base % sand	Sieve analysis recommended
Type of fines added to base course	PI analysis recommended
One side width of base	
Slope ratio/base tangent value	Default available
Internal boundary condition	Suction or flux condition
Evaluation period	Default or User-Defined. Value of 10 years recommended
Constant K for intensity-duration-recurrence equation	Default or User-Defined
Power of recurrence interval	Default recommended for eastern USA or User-Defined
Power of rainfall duration	Default recommended for eastern USA or User-Defined
Shape constant	Default recommended for eastern USA or User-Defined

Table 1. Cont'd

Asphalt Material Properties	
Variable	Notes
Thickness of layer	
Number of elements for this layer	
Coarse Aggregate Content in Asphalt	Default or User-Defined
Air content asphalt layer	Default or User-Defined
Gravimetric water content	Default or User-Defined
M <sub>r</sub> vs. T	Default or input at least 3 couple of values
Thermal conductivity of asphalt	Unfrozen/Freezing/Frozen. Default or User-Defined
Heat capacity of asphalt	Unfrozen/Freezing/Frozen. Default or User-Defined
Total unit weight of asphalt	Unfrozen/Freezing/Frozen. Default or User-Defined
Material Properties	
Variable	Notes
Classification	
Thickness	
Number of elements for this layer	
Porosity of layer material	Default or User-Defined
Dry unit weight	Default or User-Defined
Saturated permeability	Default or User-Defined
Dry thermal conductivity	Default or User-Defined
Dry heat capacity	Default or User-Defined
Coefficient of volume compressibility	Default or User-Defined
Gardner's unsaturated permeability function parameters	Default recommended
Gardner's soil-water characteristic curve parameters	Default recommended
Resilient modulus	Frozen/Unfrozen. Default or User-Defined
Poisson's ratio	Frozen/Unfrozen. Default or User-Defined
Length of Recovery Period	For fine-grained soils. Default or User-Defined
Modulus Reduction	For fine-grained soils. Default or User-Defined
Initial Temperature and Water Content Profiles	
Variable	Notes
Output nodes	
Initial temperature profile	For the first day of the analysis
Initial water content profile	For the first day of the analysis

## Collected Data

Six LTPP sections were chosen to assess the performance of the EICM version 2.1:

- 1) 91803 (Connecticut)
- 2) 271018 (Minnesota)
- 3) 231026 (Maine)

- 4) 331001 (New Hampshire)
- 5) 501002 (Vermont)
- 6) 831801 (Manitoba)

In general, the data used in the evaluation of the EICM version 2.1 were drawn from DataPave 2.0 (1999). In a few instances, data were obtained from the Seasonal Monitoring site installation reports for the test sites (Jiang and Tayabji, 1999). Data from these sources are annotated as such in the tables presenting the input data

The input data used to model these sites are summarized in [Tables 2 and 3](#). To the extent possible, the values used as input to the model site and material specific data or test results were obtained for the specific sites being modeled. However, several of the required data elements involve testing or data collection not conducted for the LTPP test sites and/or materials. Also, there are a few instances where data ordinarily collected for the LTPP test sites was missing for a particular section. In these cases, reasonable values were assumed, based on the available data, and the guidance provided in the documentation for the EICM (Lytton et al., 1990). Finally, where the variables in question were unrelated to the prediction of in situ moisture, program default values were used in the interest of expediency. Assumed values are denoted by shading in the tables. Specific comments regarding the origins or basis for selection of the values used are discussed below.

## Climatic Boundary Conditions

Daily temperature and rainfall data (including the times at which the daily maximum and minimum temperature occurred), and (nominally) monthly depth to ground water data collected at each site for the time period of the simulation were used in the models. Wind speed and percent sunshine data used were those provided with the EICM for the weather stations identified in Tables 2 and 3, as these data are not collected at the seasonal monitoring sites. The recommended default values were used for the remaining variables.



Table 2. Input Data and Sources for the EICM - Version 2.1 for the Connecticut (91803) and Minnesota (271018) Sites

Variable	Connecticut (91803)	Minnesota (271018)	Remarks/Notes
Integrated Model Initialization			
Climatic Region	I-A	II-A	
Weather Station	User-defined	User-defined	
Year	1994	1993	
First Month	6	9	
First Day	30	23	
Length of analysis period (days)	360	365	
Time increment for output (hrs)	6	6	
Time increment for calculation (hrs)	0.01	0.01	
Latitude	41°23'41.5"	46°1'32.7"	LTPP database table INV_ID
Climate/Boundary Conditions			
Daily Max/Min Temperatures			Site specific data from LTPP database table SMP_ATEMP_RAIN_DAY
Daily Rainfall			
Daily Windspeed	Boston	Average for region II-A	Default weather station data
Daily Percent Sunshine	Boston	Average for region II-A	
Daily Water Table Depth	Range: 1.33 to 3.23 m	Range: 1.28-2.27 m	Site-specific data from LTPP database table SMP_WATERTAB_DEPTH_MAX
Thermal Properties			
Modifier of Overburden Pressure	0.5	0.5	Default
Emissivity Factor	0.93	0.93	Default
Surface short-wave absorptivity	0.85	0.85	Default
Maximum convection coefficient	44.7	44.7	Default
Coefficient of Variation of Unsaturated Permeability	1	1	Default
Time of Day When Max and Min Temperatures Occur	Max: 13:29 Min: 5:43	Max: 14:09 Min: 6:25	Site averages derived from LTPP database table SMP_ATEMP_RAIN_DAY
Limits Freezing Range	0/-1 or 30/32	0/-1 or 30/32	Default
Infiltration and Drainage			
Linear length of cracks/joints one side pavement (m)	94	648	Derived from LTPP database table MON_DIS_AC_REV

Table 2. Cont.

Variable	Connecticut (91803)	Minnesota (271018)	Remarks/Notes
Total survey length (m)	152.4	152.4 m	Standard LTPP test section length
Base %fines	6	7.5	Derived from LTPP database tables TST_SS04_UG08, TST_SS01_UG01_UG02, TST_SS02_UG03, and TST_UG04_SS03. Data for sample location closest to instrumentation used where available.
Base % gravel	60	45	
Base % sand	34	47.5	
Base fines type	Silt	Silt	
One side base width (m)	4.57	5.18	Computed from data in LTPP database tables INV_GENERAL and INV_SHOULDER
Slope ratio/base tangent	1.5	1.5	Default
Internal boundary condition	Suction	Suction	Based on data in LTPP database table SMP_WATERTAB_DEPTH_MAN
Evaluation period (years)	10	10	Default
Constant K	0.3	0.3	Default
Power of recurrence interval	0.25	0.25	Default
Power of rainfall duration	0.75	0.75	Default
Shape constant	1.65	1.65	Default
Material Properties			
Layer 1 material	AC	AC	LTPP database table TST_L05A
Layer 2 material	A-1-a	A-1-b	LTPP database table TST_SS04_UG08 or derived from TST_SS01_UG01_UG_2 and TST_UG04_SS03. Data for sample location closest to instrumentation used where available.91803 LAYER 3 from Klemunes (1995).
Layer 3 material	A-2-4	A-3	
Asphalt Material Properties			
Thickness (m)	0.18	0.11	LTPP database table TST_L05A. Data for sample location closest to instrumentation.
Number of elements	6		
Coarse Aggregate Content	80% (AC = 4.3%)	80% (AC = 5.1%)	Derived from LTPP database table INV_PMA_ORIG_MIX
Air content	5.4	4.3	
Gravimetric water content	2	2	

Table 2. Cont.

Variable	Connecticut (91803)			Minnesota (271018)			Remarks/Notes
M <sub>r</sub> vs T	-4.1, 214643 11.8, 97252 23.4, 44203			-16.3, 153462 2.2, 78337 19.6, 63883			Backcalculation results
Thermal Conductivity	8.94			8.94			Default
Heat capacity	0.22/1.2/0.22			0.22/1.2/0.22			Default
Total unit weight (gm/cm³)	2.494			2.371			Derived from LTPP database table TST_AC02
Material Properties							
Thickness (m)	0.37	1.45		0.10	2.25		LTPP database table TST_L05A
Number of Elements	16	58		10	60		
AASHTO Classification	A-1-a	A-2-4		A-1-b	A-3		LTPP database table TST_SS04_UG08 or derived from TST_SS01_UG01_UG_2 and TST_UG04_SS03. Data for sample location closest to instrumentation used where available. 91803 LAYER 3 from Klemunes (1995).
Porosity	0.33	0.37		0.23	0.31		Inferred from moisture and density data
Dry unit weight (gm/cm³)	2.260	1.64		2.034	1.829		LTPP database table TST_ISD_MOIST, 91803 A-2-4 table INV_SUBGRADE
Saturated permeability (cm/hr)	6.096	6.096		6.096	1.524		Default
Dry thermal conductivity	4.47	4.023		4.47	5.066		Default
Dry heat capacity	0.17	0.17		0.17	0.2		Default
Volume compressibility	0.1	1.0		0.1	0.5		Default
Gardner's SWCC parameter AWL	0.6	0.4		0.6	0.02		Default
XWL	0.3	0.9		0.3	0.8		Default
Gardner's permeability parameter AKL	1e-2	1e-4		1e-2	4e-4		Default
XKL	2.6	3.5		2.6	2.9		Default
Resilient modulus (unfrozen)	3569	2039		4079	1530		Backcalculation Results
Resilient modulus (frozen)	3569	2039		688284	91771		
Poisson's ratio	0.4	0.42		0.4	0.42		
Length of Recovery Period							(Not pertinent to moisture prediction)
Modulus Reduction							(Not pertinent to moisture prediction)

Table 2. Cont.

Variable	Connecticut (91803)	Minnesota (271018)	Remarks/Notes
Initial Temperature and Water Content Profile			
Output nodes	All	All	
Initial temperature profile	See data file	See data file	Derived from LTPP database table SMP_MRCTEMP_AUTO_DAY_STAT (interpolation required)
Initial water content profile	See data file	See data file	LTPP database table SMP_TDR_AUTO_MOISTURE; number of elements in each layer selected such that a node is close to each TDR probe depth.

Table 3. Input Data and Sources for the EICM - Version 2.1 for the Maine (231026), New Hampshire (331001), Vermont (501002), and Manitoba (831801) Sites

Variable	Maine (231026)	New Hampshire (331001)	Vermont (501002)	Manitoba (831801)	Remarks/Notes
Integrated Model Initialization					
Climatic Region	I-A	I-A	I-A	II-A or III-A	
Weather Station	User-Defined	User-Defined	User-Defined	User-Defined	
Year	1994	1994	1994	1994	
First Month	6	6	7	2	
First Day	20	23	20	14	
Length of analysis period (days)	365	365	365	365	
Time increment for output (hrs)	6	6	6	6	
Time increment for calculation (hrs)	0.01	0.01	0.01	0.01	
Latitude	44°34'27.2"	43°13'20.1"	44°7'10.4"	49°46'9.6"	LTPP database table INV_ID
Climate/Boundary Conditions					
Daily Max/Min Temperatures	See data file	See data file	See data file	See data file	Site specific data from LTPP database table SMP_ATEMP_RAIN_DAY
Daily Rainfall	See data file	See data file	See data file	See data file	
Daily Windspeed	Boston	Boston	Boston	Fargo	Default weather station data
Daily Percent Sunshine	Boston	Boston	Boston	Fargo	
Daily Water Table Depth (m)	See data file (Range: 1.67 to 3.92)	See data file (Range: 3.80 to 4.11)	See data file (Range: 0.78 to 1.44)	See data file (Range: 1.64 to 3.30)	Site-specific data from LTPP database table SMP_WATERTAB_DEPTH_MAX
Thermal Properties					
Modifier of Overburden Pressure	0.5	0.5	0.5	0.5	Default
Emissivity Factor	0.9	0.9	0.9	0.9	Default
Surface short wave absorptivity	0.85	0.85	0.85	0.85	Default
Maximum convection coefficient	44.7	44.7	44.7	44.7	Default
Coefficient of Variation of Unsaturated Permeability	1	1	1	1	Default

Table 3. Cont.

Variable	Maine (231026)	New Hampshire (331001)	Vermont (501002)	Manitoba (831801)	Remarks/Notes
Time of Day When Max and Min Temperatures Occur	Max: 1:55 pm Min 5:12 am	Max: 2:07 pm Min: 5:49 am	Max: 1:13 pm Min: 6:12 am	Max: 2:29 pm Min: 8:48 am	Site averages derived from LTPP database table SMP_ATEMP_RAIN_DAY
Limits Freezing Range (°C)	0/-1 or 30/32	0/-1	0/-1 or 30/32	0/-1 or 30/32	Default
Infiltration and Drainage					
Linear length of cracks/joints one side of pavement (m)	12	133	125	108	Derived from LTPP database table MON_DIS_AC_REV
Total survey length (m)	152.4	152.4	152.4	152.4	Standard LTPP test section length
Base %fines	4	4.5	3.3	10.9	Derived from LTPP database tables TST_SS04_UG08, TST_SS01_UG01_UG02, TST_SS02_UG03, and TST_UG04_SS03. Data for sample location closest to instrumentation used where available.
Base % gravel	73.5	62.9	89.9	52	
Base % sand	22.5	32.6	6.8	37.1	
Base fines type	Silt	Silt	Silt	Silt	
One side base width (m)	6.71	5.79	3.35	3.66	Computed from data in LTPP database tables INV_GENERAL and INV_SHOULDER
Slope ratio/base tangent	1.5	1.5	1.5	1.5	Default
Internal boundary condition	Suction	Suction	Suction	Suction	Based on GWT data
Evaluation period	10	10	10	10	Default
Constant K	0.3	0.3	0.3	0.3	Default
Power of recurrence interval	0.25	0.25	0.25	0.25	Default
Power of rainfall duration	0.75	0.75	0.75	0.75	Default
Shape constant	1.65	1.65	1.65	1.65	Default

Table 3. Cont.

Variable	Maine (231026)			New Hampshire (331001)				Vermont (501002)			Manitoba (831801)				Remarks/Notes
Material Properties															
Layer 1 material	AC			AC				AC			AC				LTPP database table TST_L05A
Layer 2 material	A-1-a			A-1-a				A-1-a			A-1-a				LTPP database table TST_SS04_UG08 or derived from TST_SS01_UG01_UG_2 and TST_UG04_SS03. Data for sample location closest to instrumentation used where available.91803 LAYER 3 from Klemunes (1995).
Layer 3 material	A-2-4			A-1-b				A-1-a			A-1-a				
Layer 4 material				A-2-4							A-2-4				
Layer thickness (cm)	16.3	48.8	224.4	21.6	49.0	36.6	142.8	22.4	70.1	157.5	5.6	15.2	30.5	198.7	LTPP database table TST_L05A
Number of elements	1	10	58	1	20	27	28	1	24	64	1	5	16	40	Selected to “optimize” proximity to TDR probe depths
Asphalt Material Properties															
Thickness (cm)	16.3			21.6				22.4			5.6				LTPP Database Table TST_L05A
Number of elements	1			1				1			1				Use default AC material
Coarse Aggregate Content	80			80				80			80				
Air content	4			4				4			4				
Gravimetric water content	2			2				2			2				
M <sub>r</sub> vs T	-23.3, 119521 15.6, 3023.2 54.4, 105.5			-23.3, 1.17e+7 15.6, 296475 54.4, 10342.1				-23.3, 1.17e+7 15.6, 296475 54.4, 10342.1			-23.3, 1.17e+7 15.6, 296475 54.4, 10342.1				
Thermal Conductivity of Asphalt	8.94			8.94				8.94			8.94				Default
Heat capacity	0.22			0.22				0.22			0.22				Default
Total unit weight	2.37			2.37				2.37			2.37				Default

Table 3. Cont.

Variable	Maine (231026)			New Hampshire (331001)			Vermont (501002)			Manitoba (831801)			Remarks/Notes
Material Properties													
Classification	A-1-a	A-2-4		A-1-a	A-1-b	A-2-4	A-1-a	A-1-a		A-1-a	A-1-a	A-2-4	
Porosity	0.29	0.37		0.22	0.24	0.43	0.29	0.46		0.22	0.21	0.46	Inferred from maximum observed volumetric moisture for layer (LTPP database table SMP_TDR_AUTO_MOISTURE)
Dry unit weight (gm/cm³)	2.27	1.96		2.10	2.15	1.86	2.09	1.76		2.08	1.71	2.13	Sites 231026 and 501002: LTPP database table TST_ISD_MOIST; sites 331001 and 831801: SMP Installation Reports
Saturated permeability (cm/hr)	60	15.24		0.2	0.2	0.5	0.2	0.2		0.2	0.2	0.5	
Dry thermal conductivity	4.47	4.023		0.3	0.3	0.27	0.3	0.3		0.3	0.3	0.27	
Dry heat capacity	0.17	0.17		0.17	0.17	0.17	0.17	0.17		0.17	0.17	0.17	
Volume compressibility	0.10	0.3		0.10	0.10	0.3	0.10	0.10		0.10	0.10	0.3	
AWL (moisture)	0.6			0.6	0.6	0.4	0.6	0.6		0.6	0.6	0.4	Default
XWL	0.3			0.3	0.3	0.9	0.3	0.3		0.3	0.3	0.9	
AKL (permeability)	0.01			0.01	0.01	1e-4	0.01	0.01		0.01	0.01	1e-4	
XKL	2			2	2	3.5	2	2		2	2	3.5	
Resilient modulus (Unfrozen)	3000	3000		3000	3000	3000	3000	3000		3000	3000	3000	Arbitrary (kg/cm²). Not used in moisture prediction.
Resilient modulus (Frozen)	3000	3000		3000	3000	3000	3000	3000		3000	3000	3000	
Poisson's ratio	0.4	0.42		0.4	0.42	0.45	0.4	0.4		0.4	0.40	0.45	
Length of Recovery Period Modulus Reduction													Not required for coarse materials; not used in moisture prediction



Table 3. Cont.

Variable	Maine (231026)	New Hampshire (331001)	Vermont (501002)	Manitoba (831801)	Remarks/Notes
Initial Temperature and Pore Pressure Profile					
Output nodes	All	All	All	All	
Initial temperature profile	See data file	See data file	See data file	See data file	Derived from LTPP database table SMP_MRCTEMP_AUTO_DAY_STAT (interpolation required)
Initial water content profile	See data file	See data file	See data file	See data file	LTPP database table SMP_TDR_AUTO_MOISTURE; number of elements in each layer selected such that a node is close to each TDR probe depth.

## Infiltration and Drainage

The linear length of cracks and joints used in the simulation was estimated from the yearly mean<sup>1</sup> distress quantities for the year considered in the simulation.

## Asphalt Material Properties

For the most part, the program default values were used for the asphalt materials, as it was assumed that these variables would have no impact on the predicted moisture contents for the unbound layers.

## Material Properties

The number of elements used in each of the unbound layers was selected to yield nodes close to the depths at which the TDR probes, used to monitor in situ moisture contents, were installed. Early efforts to use the number of elements required to achieve exact correspondence of nodes and TDR probe depths yielded model stability problems.

The basis for the porosity values used in the simulations varied from site-to-site. For site 271018, the values used were derived from in situ density and moisture data, using an assumed specific gravity of the solids of 2.65. Use of values derived in the same fashion for site 91803 was not possible, as the computed porosity was less than the maximum observed volumetric moisture content, implying a degree of saturation in excess of 100%. It is likely that several factors contribute to this discrepancy. Possibilities include differences between the actual (unknown) and assumed values of the specific gravity of solids, and differences in density between the location at which the in situ density and moisture were measured, and the TDR probe locations.

ICM Version 2.0, and prior versions required that the user specify the Gardner's pore pressure coefficients for each unbound pavement layer, along with the lower boundary suction, and an initial pore pressure profile. The program documentation provides recommended default values (as a function of material type) for the Gardner's coefficients, and recommends that the lower boundary suction and initial pore pressure profile be estimated from the depth of the water table. With Version 2.1, entry of the Gardner's coefficients was made optional, and the initial pore pressure and lower boundary suction inputs were replaced by the initial moisture content profile, and the depth to the water table. Initial results obtained using version 2.1 without entry of the Gardner's coefficients were significantly better than those obtained using assumed values for the Gardner's

---

<sup>1</sup> Distress surveys having been conducted approximately four times per year.

coefficients with Version 2.0. For this reason, user-supplied Gardner coefficients were not used with Version 2.1.

### Initial Moisture Content Profile

The in situ moisture content of the unbound layers at each LTPP Seasonal Monitoring site is monitored to a depth of approximately 1.8 meters using Time Domain Reflectometry (TDR) technology. TDR provides an indirect measure of volumetric moisture, in that the data obtained from the TDR instrumentation is interpreted to estimate the dielectric constant of the soil, which is in turn correlated with the soil volumetric moisture content. Ten TDR probes are installed in each test site, with the precise spacing depending on the layer profile of the site.

The number of elements used to model each unbound layer in the pavement was selected to yield nodes as close as possible to the depths at which the TDR probes used to monitor moisture were placed. This being the case, the daily mean moisture contents for the first day of the simulation period were treated as being the moisture contents at the nodes closest to the actual TDR probe depths. This approximation is deemed reasonable because moisture contents derived from TDR measurements are not point measurements, but rather, reflect the moisture content of the soil mass surrounding the TDR probe.

### Initial Temperature Profile

Subsurface temperatures at the Seasonal Monitoring sites are monitored via thermistor probes installed in both the asphalt concrete surface, and the unbound layers. Unlike the TDR-based moisture data, the temperature profile data may be considered point specific, and correspondence between temperature monitoring depths and nodal depths was not considered in establishing the model geometry. Therefore, linear interpolation was used to estimate the soil temperature at each node. The temperature data used in this process were the daily average values.

### Basis for Comparison

TDR-based moisture contents obtained at each of the test sections studied were also used as the basis for evaluating the accuracy of the EICM predicted moisture contents. As with any test method, there is some uncertainty (error) in the TDR-based moisture contents. Jiang and Tayabji (1999) expressed the uncertainty in the TDR-based moisture

content data derived for the LTPP test sections in terms of a series of estimated 95% confidence intervals. The confidence interval applicable to any particular moisture observation is a function of the standard error of estimate of the regression model used in the derivation of the moisture content, and the errors in the model parameters. The applicable confidence limits are shown in the figures comparing the monitored and predicted moisture contents.

## Results

Field (TDR-based) measurements of volumetric water content along with the corresponding 95% confidence estimated error were compared with the predicted volumetric water content profile obtained by the EICM version 2.1. In making these comparisons, the EICM predicted moisture contents for the two nodes adjacent to each TDR monitoring depth were interpolated to obtain the predicted moisture content corresponding to the monitored value. Review of the predicted moisture profiles shows that this is a reasonable approach to resolving small differences in the depths used for moisture monitoring and moisture prediction.

The results of the comparison are shown in [Figures 1 through 6](#). The comparisons between the measured volumetric water content and the predicted volumetric water content correspond to the dates on the analysis period when TDR measurements were available. The moisture content profiles are shown in [Appendices A through F](#).

The summary of the results is presented in [Figures 7 and 8](#). Figure 7 shows the water content prediction for the base course material from the 6 sites previously discussed, and the results of a linear regression through the data points. Poor agreement between the monitored and predicted values is reflected in the low coefficient of determination ( $R^2$ ) of 0.05 for the regression. Figure 8 depicts the measured versus predicted volumetric water content for the subgrade materials along with a linear regression to the data. The regression of the subgrade materials shows a coefficient of determination of 0.34, better than that for the base, but still poor. Note also that a substantial number of data points in both figures fall outside the estimated confidence limits for the field data, even though these limits are very broad.

The results obtained were presented in a meeting held in Champaign, IL on September 23, 1999. The following persons participated in the meeting: Dr. Matt Witczak (ASU – led the meeting), Dr. Barry Dempsey (U of I), Dr. Waseem Mirza (ASU), Dr. Bill Houston

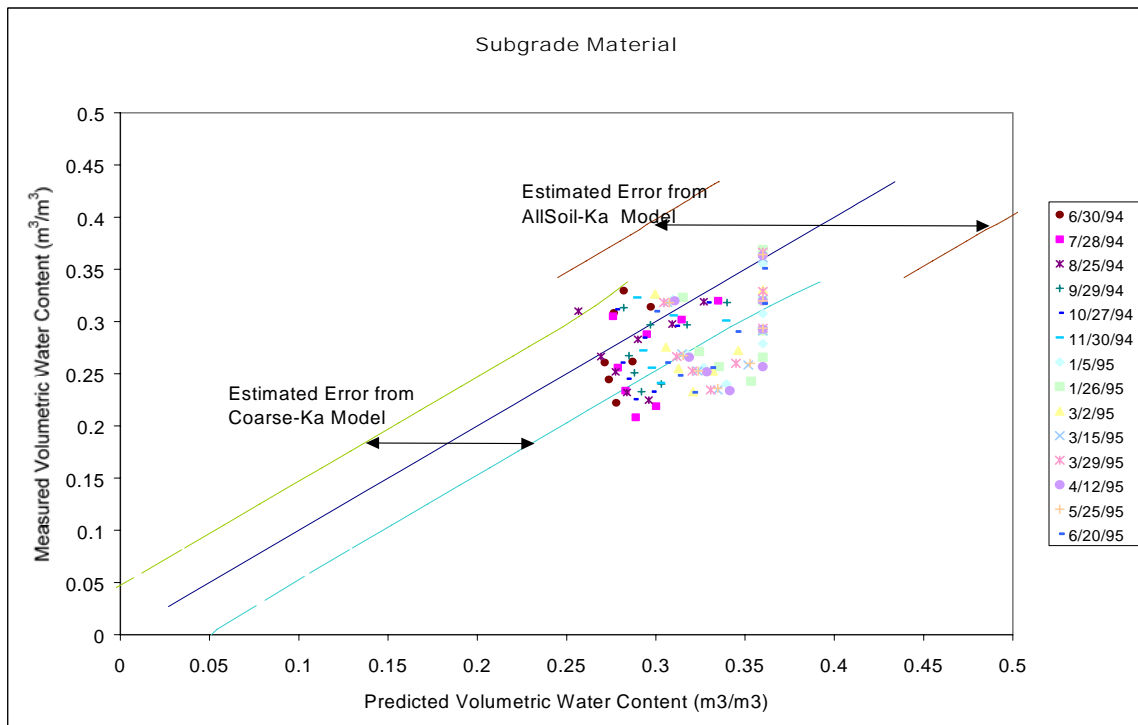
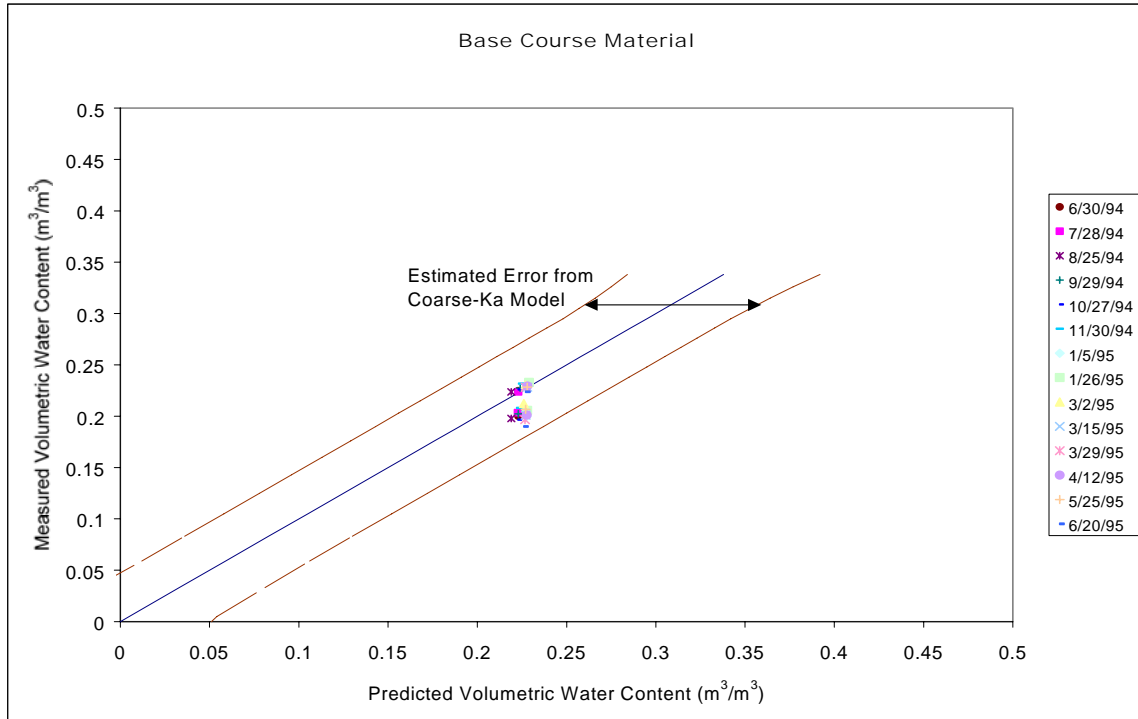


Figure 1. Measured versus Predicted Moisture Content – EICM version 2.1  
Connecticut (91803)

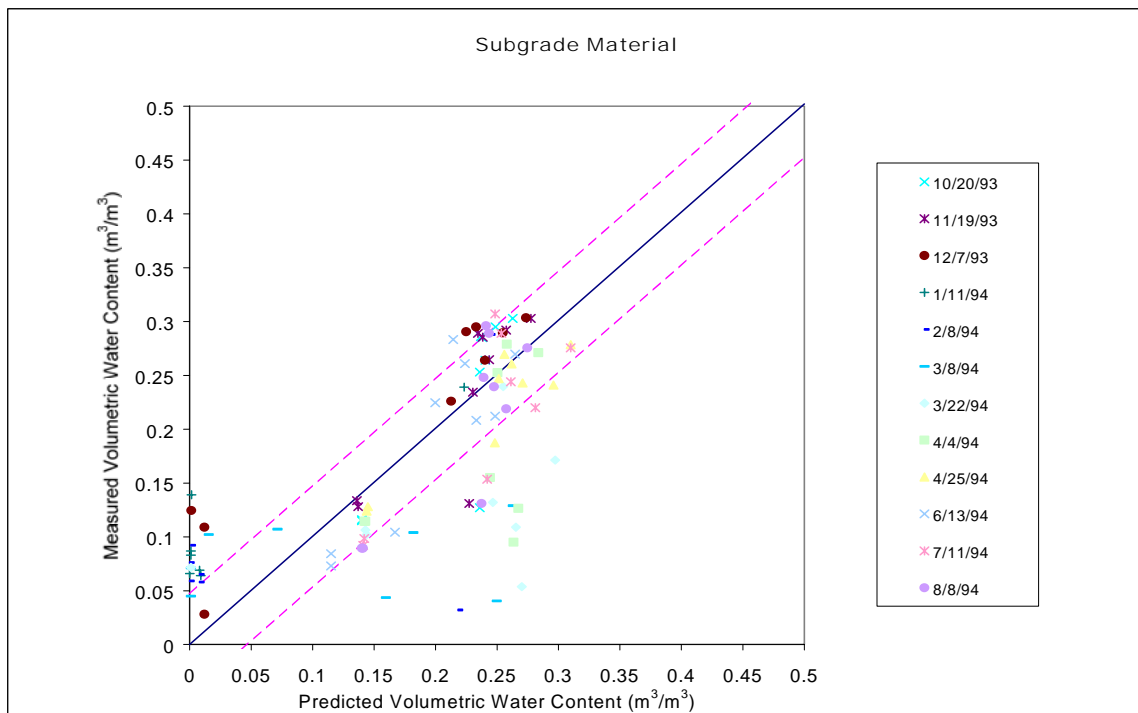
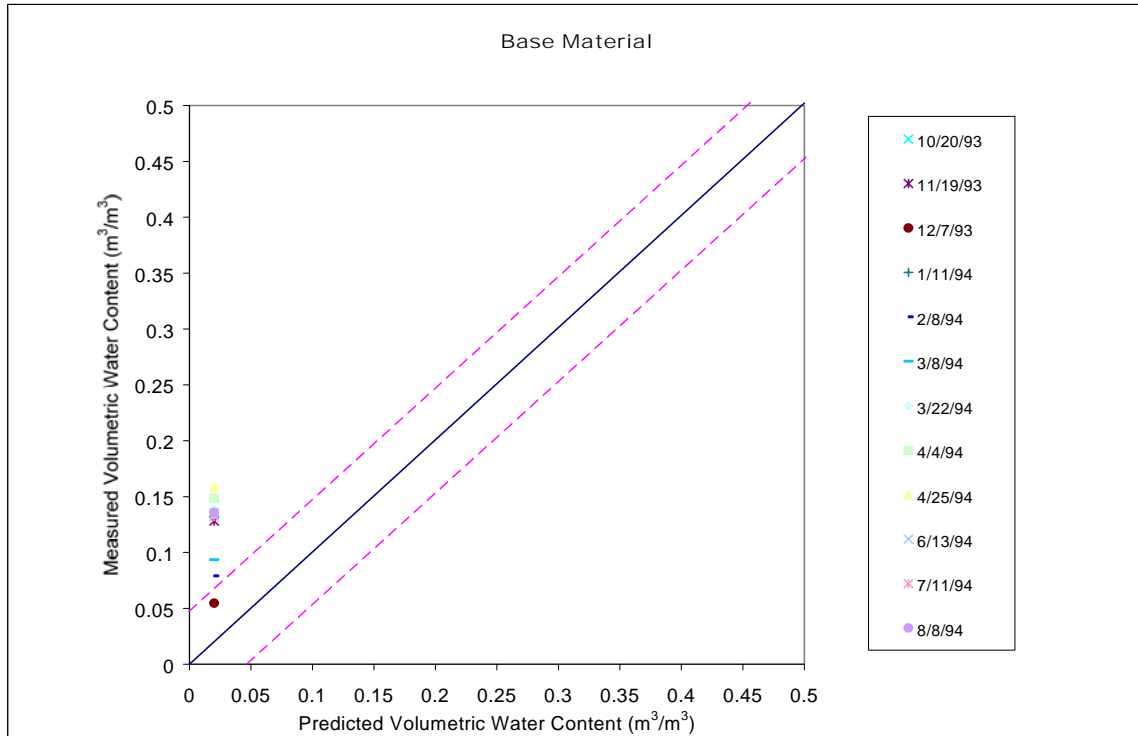


Figure 2. Measured versus Predicted Moisture Content – EICM version 2.1  
Minnesota (271018)

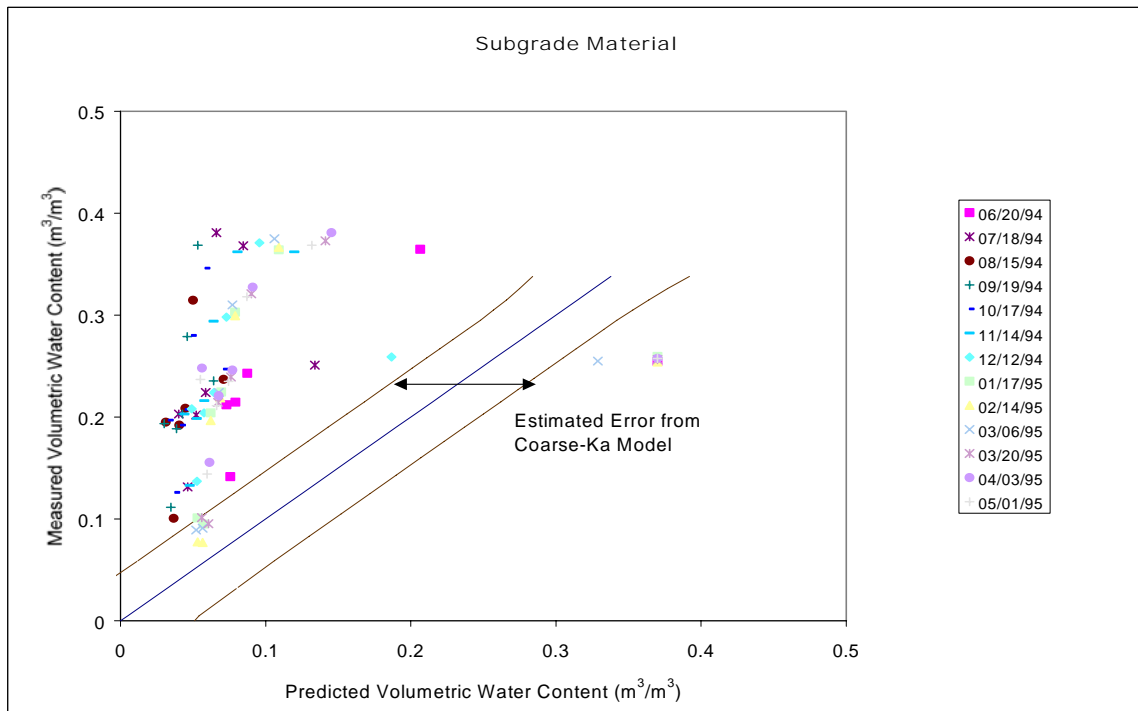
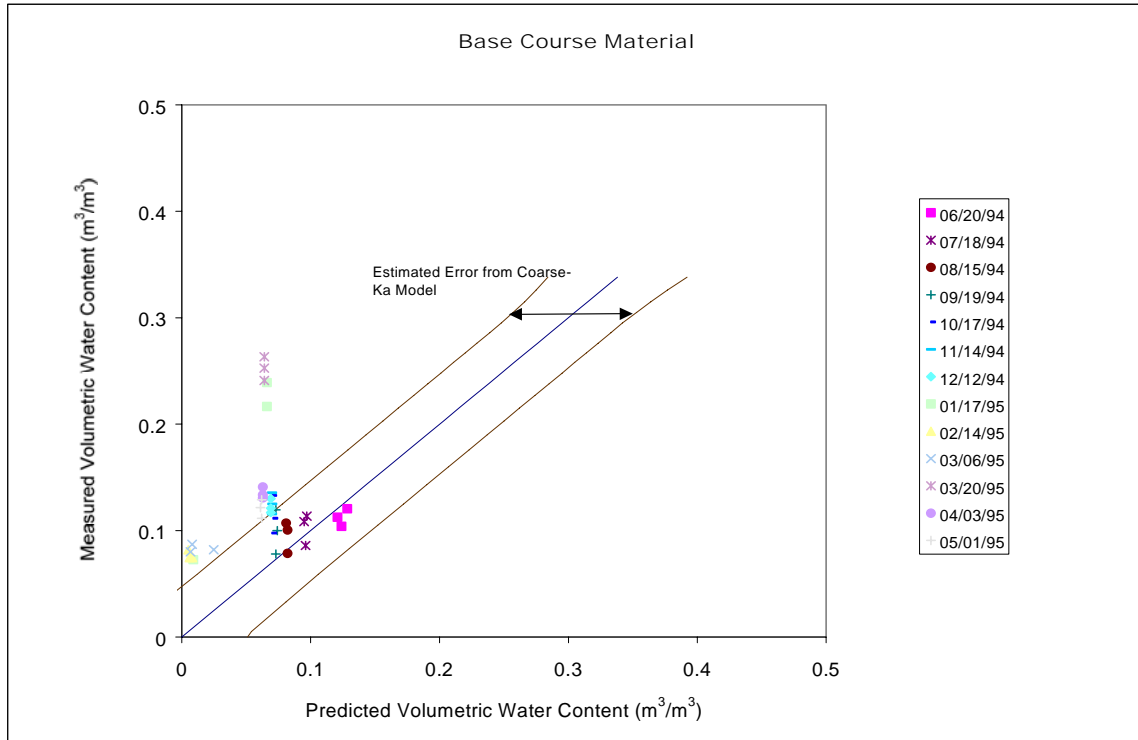


Figure 3. Measured versus Predicted Moisture Content – EICM version 2.1  
Maine (231026)

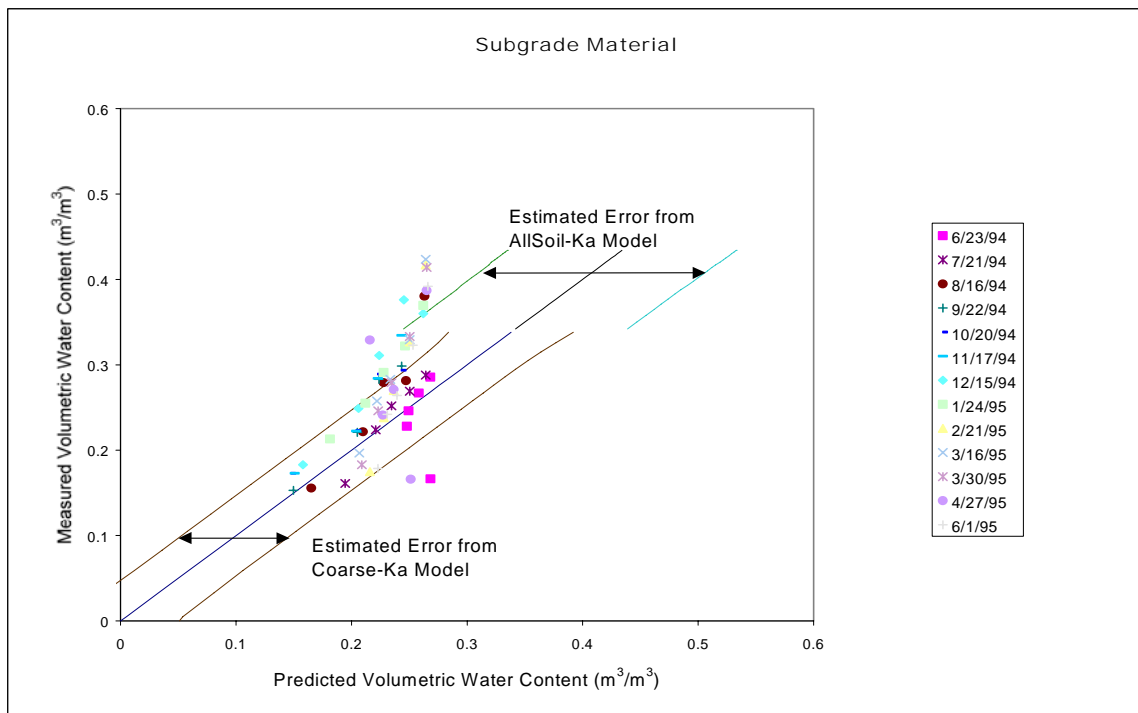
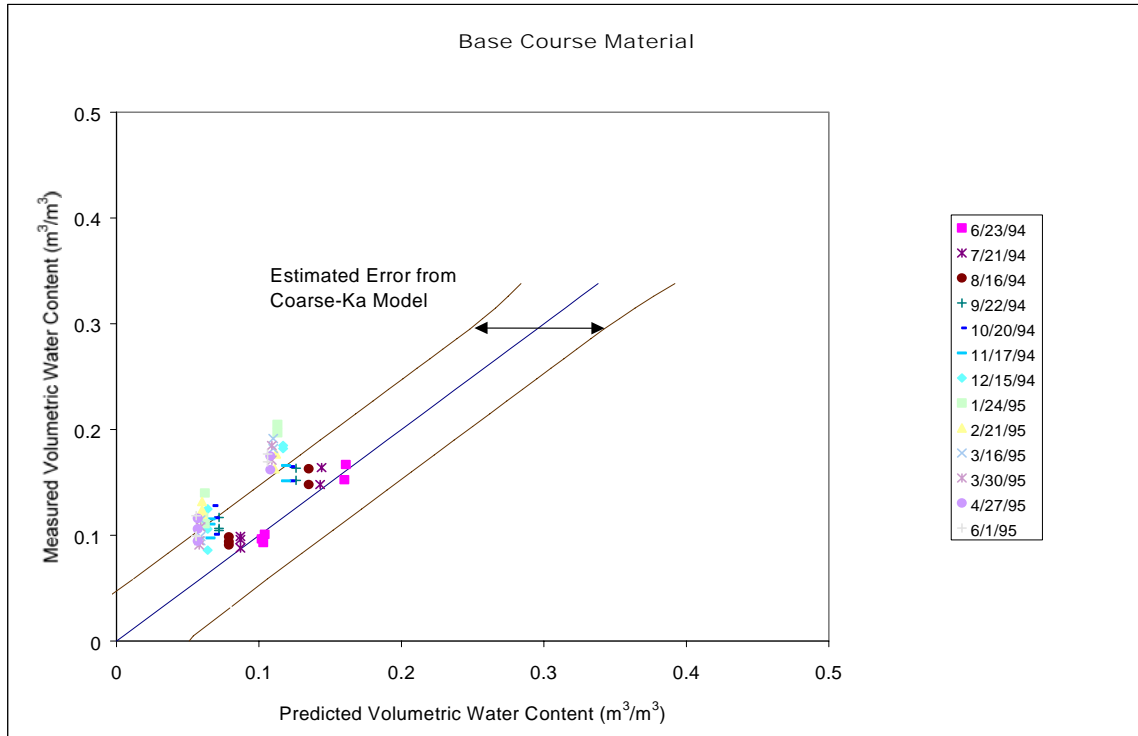


Figure 4. Measured versus Predicted Moisture Content – EICM version 2.1  
New Hampshire (331001)



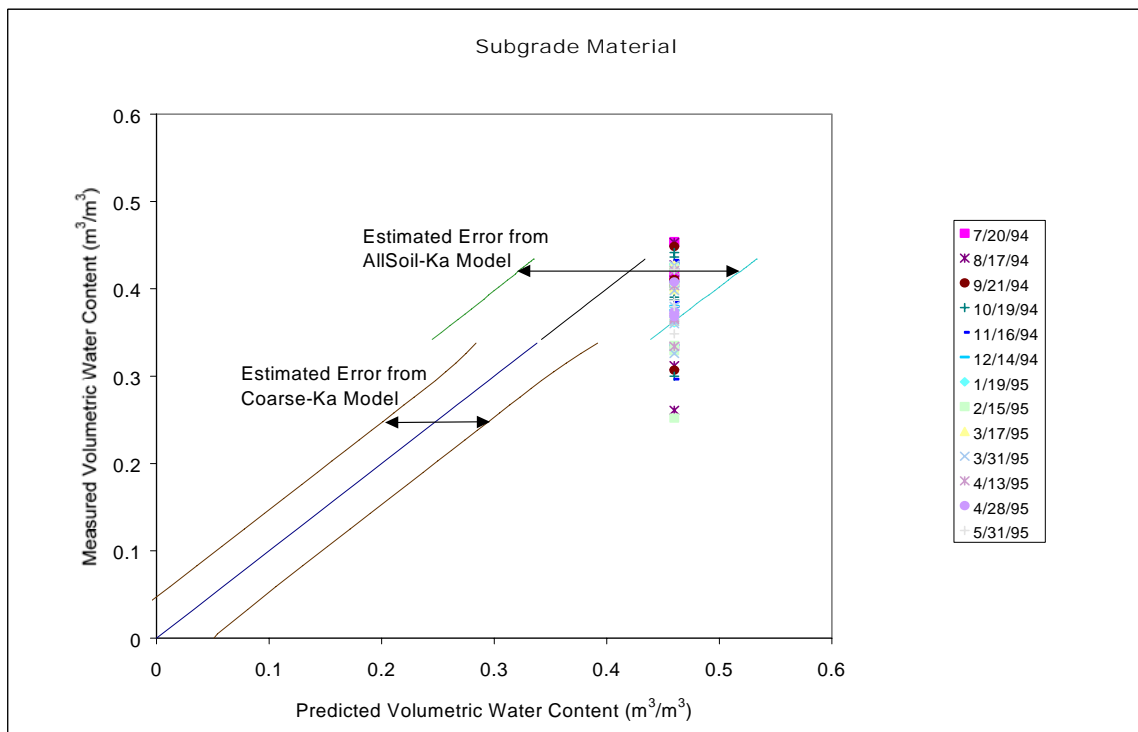
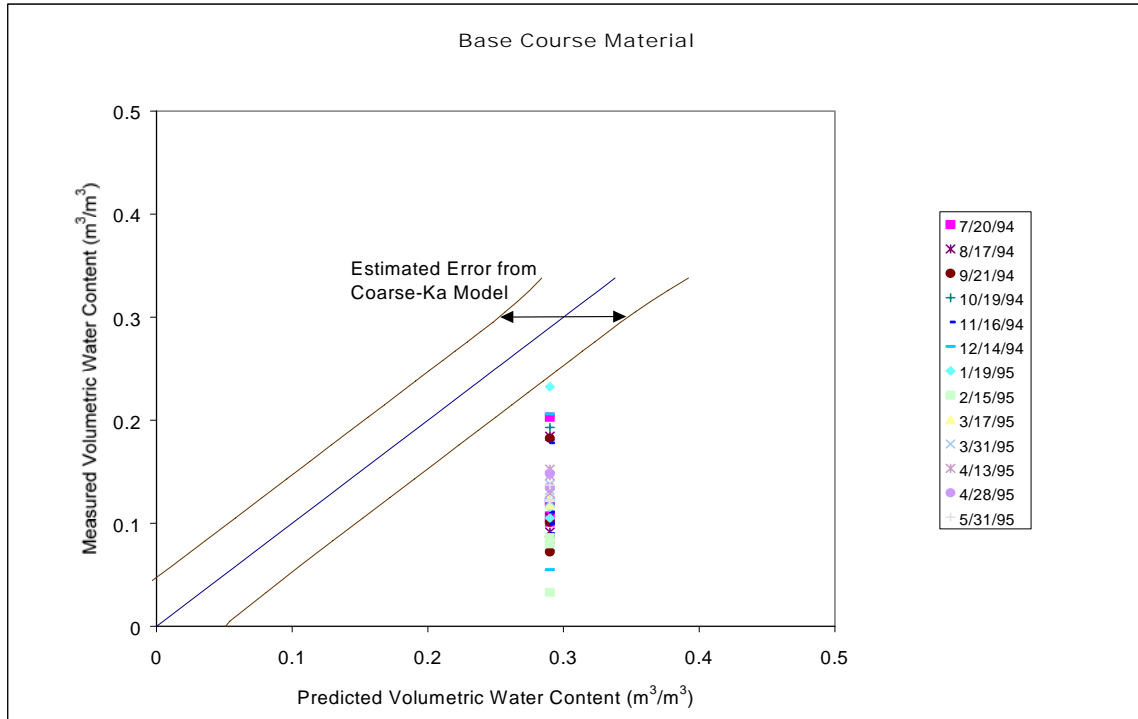


Figure 5. Measured versus Predicted Moisture Content – EICM version 2.1  
Vermont (501002)

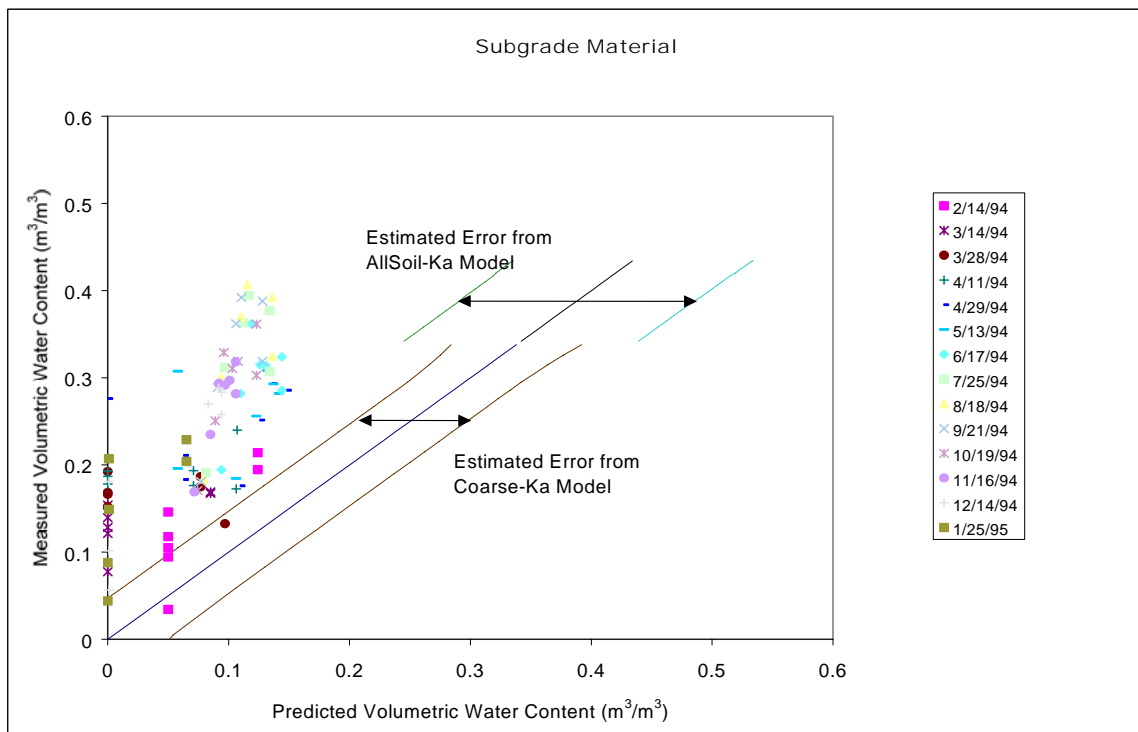
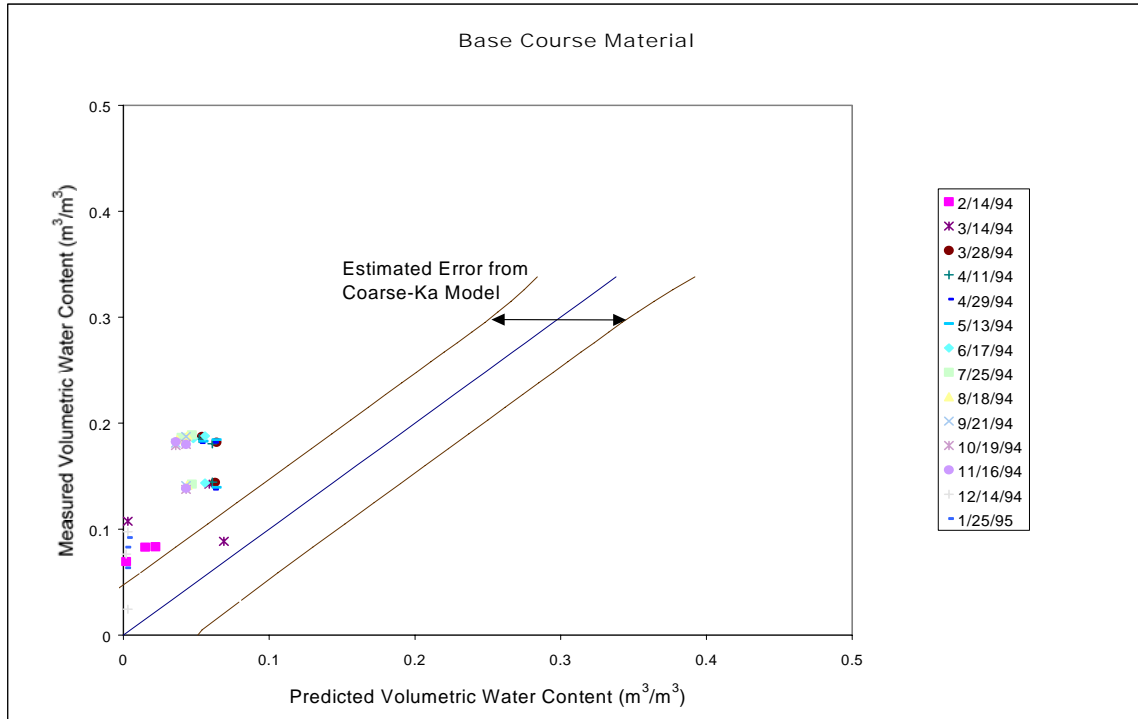


Figure 6. Measured versus Predicted Moisture Content – EICM version 2.1  
Manitoba (831801)

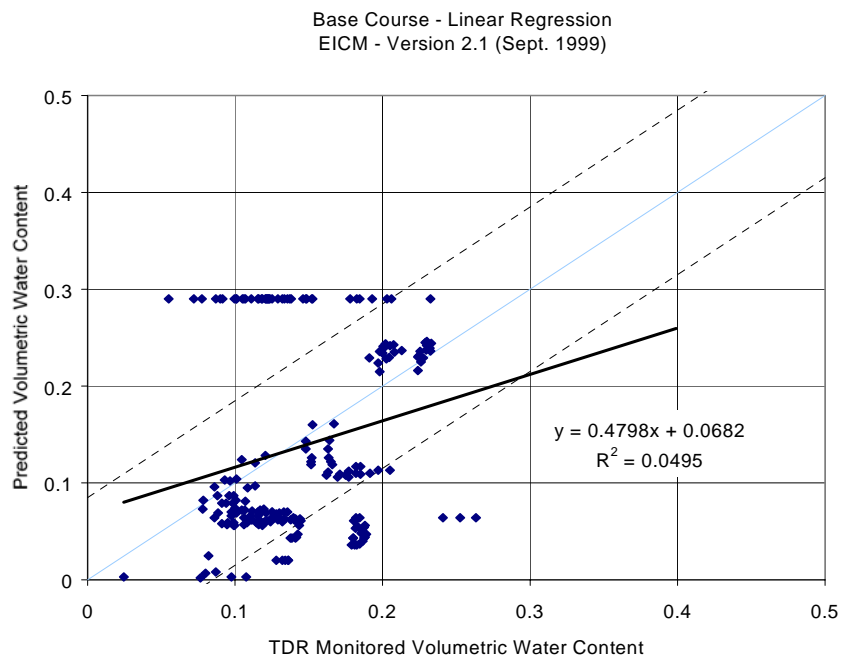
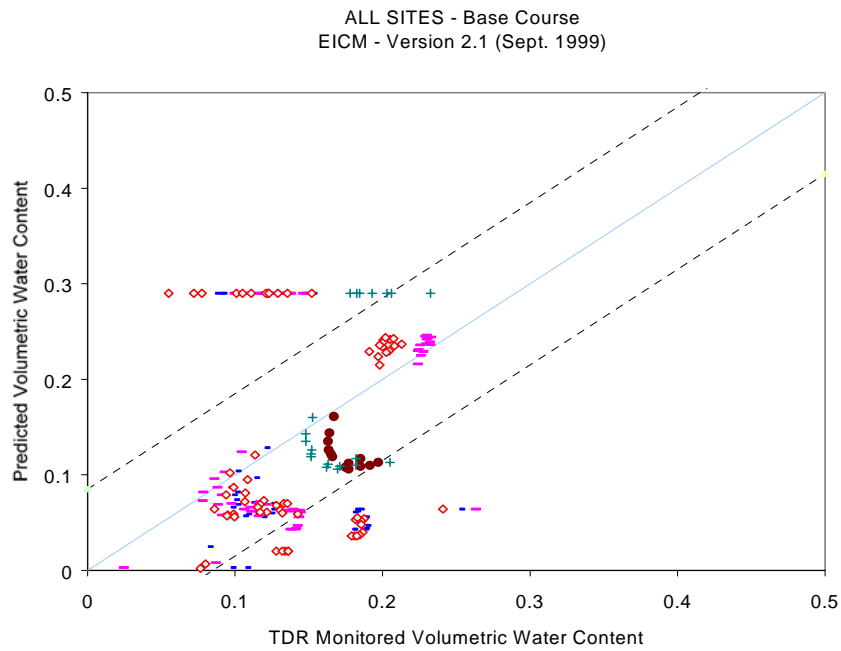


Figure 7. Summary of Measured versus Predicted Moisture Content for the Base Course Materials – EICM version 2.1

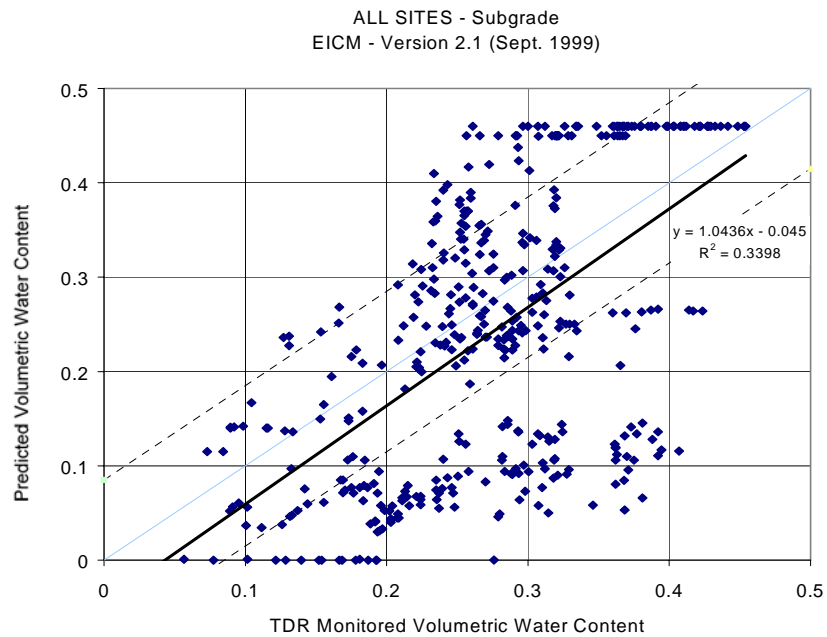
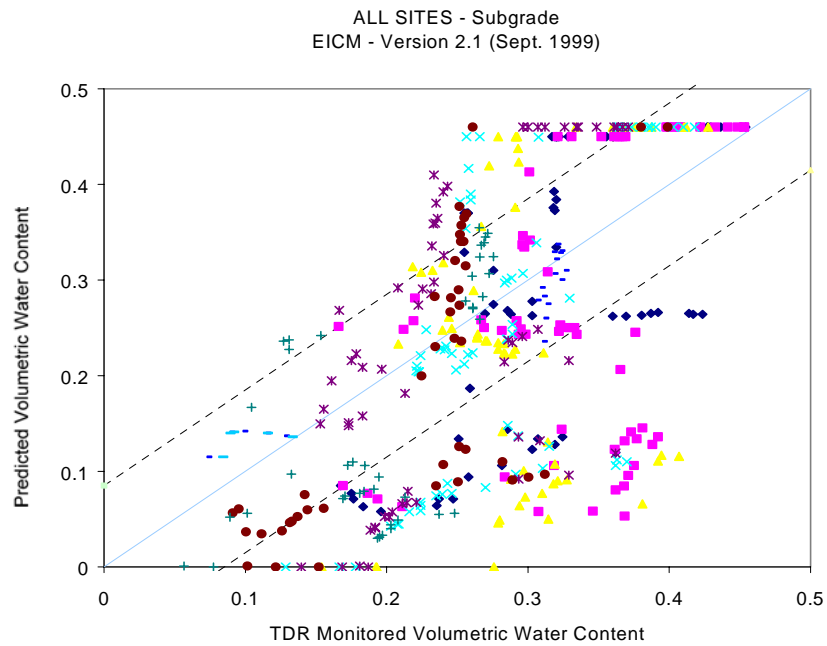


Figure 8. Summary of Measured versus Predicted Moisture Content for the Subgrade Materials – EICM version 2.1

(ASU), Cheryl Richter (FHWA), Gregg Larson (U of I), and Dr. Claudia E. Zapata (ASU). The assessment of the EICM prediction was primarily based on:

- 1) Field measurements of volumetric water content for the LTTP sites estimated by Time Domain Reflectometry (TDR)
- 2) Pattern of moisture content change with time
- 3) Magnitude of fluctuations

As shown in Figures 7 and 8, the initial comparisons were not good, with problems appearing on all three bases of comparison. Several factors that may have contributed to the poor estimation of the water contents given by the EICM were discussed. The following section presents a summary of the factors that were considered important to the prediction of the moisture content by the EICM.

#### Factors that Contributed to the Poor Predictions of the Water Contents by the EICM

- The field measurements of volumetric water content were obtained by using regression type equations that correlated with the bulk dielectric constant ( $K_a$ ) given by the TDR. The correlation was done by subdividing the entire database used in the regression analysis into two major soil groups: coarse and fine-grained soils. It was recommended that the use of predictive models developed by Klemunes (1997) for individual soil classes be explored, as a means of improving the accuracy of the TDR-based moisture data.
- The soil properties needed to input the EICM is rather extensive and usually is not included in routine soil surveys. Saturated/unsaturated hydraulic conductivity, soil-water characteristic curve parameters, and porosity are unique for a particular soil and the use of default values may lead to a poor modeling of the transient moisture conditions. It was recommended at this meeting to advocate the good practice of measuring those parameters in order to obtain better predictions.
- The main changes in the EICM version 2.1 were focussed on the Flux boundary condition and no substantial improvements were implemented for the Suction boundary condition. It was recommended to run the EICM in the Flux boundary condition mode, as a possible means of improving the predictions.

- More care should be exercised when dividing the soil profile into the different sub-layers. It is recommended to add sub-layers around the TDR experimental points in the subbase and subgrade layers to improve the prediction for the first day of the analysis period.
- The EICM makes use of seven sets of Gardner's parameters to represent the soil-water characteristic curve (SWCC) and the unsaturated hydraulic conductivity. Each set represents one of the major AASHTO classification groups. The recommendations were based on use of a hierarchical approach:
  - 1) Generate additional SWCC / unsaturated hydraulic conductivity parameters for the different soil sub-groups recognized in the AASHTO soil classification system.
  - 2) Replace the SWCC Gardner equation with an equation providing a better functional fit.
  - 3) Predict the SWCC based on grain-size distribution (GSD) and soil properties, and
  - 4) Incorporate experimentally measured SWCCs and unsaturated hydraulic conductivity functions into the EICM, when available.
- It was recommended that all frozen volumetric water content values be removed from the comparisons with the EICM results, given the fact that the meaning of TDR-based moisture contents in frozen or freezing soils is uncertain.

### Short-term Actions Recommended for the Improvement of the EICM

The short-term actions recommended for the improvement of the EICM included:

- Generate additional soil-water characteristic curves (SWCCs) as a function of soil properties and the AASHTO soil classification system.
- In place of the Gardner equation, substitute a better functional fit for the SWCC and the unsaturated hydraulic conductivity function.
- Improve estimates of saturated permeability and saturated volumetric water content (porosity) as a function of the AASHTO classification system.
- Impose sub-layers around TDR measuring points.

- Remove all frozen volumetric water content data points from the comparisons with the EICM results.
- Explore use of Klemunes class-specific moisture models for computation of TDR-based moisture contents.
- Repeat comparisons using flux boundary conditions.
- Add three or four new sites, including one or more in the southwestern climatic region.

All of the above recommendations have been implemented. However, the exploration of the use of Klemunes class-specific moisture models for computation of TDR-based moisture contents did not result in the application of those models in the analysis, for the following reasons:

- 1) All of Klemunes models use the soil specific gravity as one of the predictor variables. This parameter is available for only some of the soils considered in this investigation.
- 2) The goodness of fit statistics (coefficient of determination, and standard error of estimate) for the models currently used in the LTPP moisture computation are better than those for Klemunes A-2-4, A-6, A-7-5, and A-7-6 models. Thus, it does not appear that application of Klemunes models will improve the accuracy of the computed moisture contents for those soils. This is particularly true for the A-6 and A-7 models, which were based on data for only two soils.
- 3) Based on review of the goodness of fit statistics and number of soils used in their development, it was deemed worthwhile to pursue application of Klemunes models for: (1) A-3 soils where the required specific gravity data are available; and (2) A-1-b soils from the two sites used in the model development. However, when the models were applied on a trial basis, it was found that there was no benefit in doing so. Thus, further consideration of these models was abandoned.

Details of the improvements arising from the remaining recommendations are described in Chapter 3.

## Modifications to the EICM version 2.1

### Moisture Content Prediction

#### Proposed Modifications to the EICM – version 2.1

The proposed changes to the EICM's moisture prediction algorithm included:

- 1) Select the best functional fit for the soil-water characteristic curve (SWCC)
- 2) Given Grain Size Distribution (GSD) and Plasticity Index (PI), develop improved estimates of SWCCs, saturated permeability ( $k_{sat}$ ), and porosity ( $\theta_{sat}$ ).
- 3) Given AASHTO Classifications, develop improved estimates of SWCCs,  $k_{sat}$ , and  $\theta_{sat}$
- 4) Use the initial water content values, together with distance from the Groundwater Table (GWT) as guidance in choosing the SWCC.

#### The Soil-Water Characteristic Curve

The SWCC has been defined as the variation of water storage capacity within the macro and micro pores of a soil, with respect to suction (Fredlund et al., 1995). This relationship is generally plotted as the variation of the water content (gravimetric, volumetric or degree of saturation) with soil suction. Several mathematical equations have been proposed to represent the SWCC. Most of the equations are empirical in nature and are based on the shape of measured SWCCs. A summary of the most commonly used equations is presented in [Table 4](#).

The EICM Version 2.1 makes use of the equation proposed by Gardner (1958). Even though Gardner's equation is widely used, it does not represent a sigmoid, which is currently believed to be the most accurate shape representing the SWCC. Notice that this equation has three fitting parameters:  $\theta_r$ ,  $a$ , and  $b$  (See Table 4 for definition). Also, in the EICM version 2.1 and prior versions only two of the three Gardner equation parameters were treated as variables, with the third, the residual volumetric water content ( $\theta_r$ ) taken to



be zero. An equation with two parameters has shown, in many cases, to misrepresent the SWCC due to excessive constraints to the relationship.

Table 4. Equations Used to Represent the Soil-Water Characteristic Curve

Reference	Equation	Unknowns
Fredlund and Xing (1994)	$\theta_w = C(h) \times \frac{\theta_s}{\left[ \ln \left[ \exp(1) + \left( \frac{h}{a} \right)^b \right] \right]^c}$ $C(h) = \left[ 1 - \frac{\ln \left( 1 + \frac{h}{h_r} \right)}{\ln \left( 1 + \frac{10^6}{h_r} \right)} \right]$	$\theta_w$ = volumetric water content $h$ = soil matric suction in kPa $a$ = a soil parameter which is primarily a function of the air entry value of the soil in kPa. $b$ = a soil parameter which is primarily a function of the rate of water extraction from the soil, once the air entry value has been exceeded. $c$ = a soil parameter which is primarily a function of the residual water content. $h_r$ = a soil parameter which is primarily a function of the suction at which residual water content occurs in kPa.
van Genuchten (1980)	$\theta_w = \theta_r + \frac{\theta_s - \theta_r}{\left[ 1 + \left( \frac{h}{a} \right)^b \right]^c}$	$\theta_r$ = residual volumetric water content. $a$ = a soil parameter which is primarily a function of the air entry value of the soil in kPa. $b$ = a soil parameter which is primarily a function of the rate of water extraction from the soil, once the air entry value has been exceeded. $c$ = a soil parameter which is primarily a function of the residual water content.
McKee and Bumb (1987)	$\theta_w = \theta_r + \frac{\theta_s - \theta_r}{1 + \exp(1) \left[ \frac{(h-a)}{b} \right]}$	$\theta_r$ = residual volumetric water content. $a$ = curve-fitting parameter $b$ = curve-fitting parameter
van Genuchten and Mualem (1980)	$\theta_w = \theta_r + \frac{\theta_s - \theta_r}{\left[ 1 + \left( \frac{h}{a} \right)^{b_m} \right]^{\left( 1 - \frac{1}{b_m} \right)}}$	$\theta_r$ = residual volumetric water content. $a$ = a soil parameter which is primarily a function of the air entry value of the soil in kPa. $b_m$ = a soil parameter which controls the slope at the inflection point in the soil-water characteristic curve.
van Genuchten and Burdine (1980)	$\theta_w = \theta_r + \frac{\theta_s - \theta_r}{\left[ 1 + \left( \frac{h}{a} \right)^b \right]^{\left( 1 - \frac{2}{b} \right)}}$	$\theta_r$ = residual volumetric water content. $a$ = a soil parameter which is primarily a function of the air entry value of the soil in kPa. $b$ = a soil parameter which is primarily a function of the rate of water extraction from the soil, once the air entry value has been exceeded.

Table 4. Cont.

Reference	Equation	Unknowns
Gardner (1958)	$\theta_w = \theta_r + \frac{\theta_s - \theta_r}{1 + \left(\frac{h}{a}\right)^b}$	$\theta_r$ = residual volumetric water content. $a$ = a soil parameter which is primarily a function of the air entry value of the soil in kPa. $b$ = a soil parameter which is primarily a function of the rate of water extraction from the soil, once the air entry value has been exceeded.
Brooks and Corey (1964)	$\theta_w = \theta_r + (\theta_s - \theta_r) \left(\frac{a_b}{h}\right)^{b_b}$	$\theta_r$ = residual volumetric water content. $a_b$ = bubbling pressure in kPa. $b_b$ = pore size index.
Williams et al. (1983)	$\ln \Theta_e = A + B \ln h$	$A$ = fitting parameter $B$ = fitting parameter
Farrel and Larson (1972)	$h = (u_a - u_w)_b \exp[\alpha(\theta_s - \theta_w)]$	$\alpha$ = empirical constant $(u_a - u_w)_b$ = air-entry value
Assouline et al. (1998)	$\theta_w = \theta_L + (\theta_s - \theta_L) \left[ 1 - \exp \left[ -\xi \left( \frac{1}{\Psi} - \frac{1}{\Psi_L} \right)^\eta \right] \right]$	$\Psi$ = capillary head $\Psi_L$ = capillary head that corresponds to a very low water content, at which the hydraulic conductivity is negligible. $\theta_L$ = volumetric water content at capillary head $\Psi_L$ . $\eta$ = fitting parameter $\xi$ = fitting parameter

Several studies have been conducted on comparing the different equations outlined in Table 4 (Leong and Rahardjo, 1996; Zapata, C., 1999, among others). Those studies have generally shown that the equations with three and four parameters are more suitable to represent the SWCC. Among those equations, the one proposed by Fredlund and Xing (1994) has shown good agreement with a rather extended database. The equation reads as follows:

$$\theta = C(h) \times \frac{\theta_{sat}}{\left[ \ln \left[ \exp(1) + \left( \frac{h}{a} \right)^b \right] \right]^c} \dots \dots \dots (1)$$

$$C(h) = \left[ 1 - \frac{\ln\left(1 + \frac{h}{h_r}\right)}{\ln\left(1 + \frac{10^6}{h_r}\right)} \right] \dots\dots\dots (2)$$

Where:

$\theta$  = Volumetric water content

$\theta_{\text{sat}}$  = Saturated volumetric water content

$a$  = A soil parameter which is primarily a function of the air entry value of the soil in kPa.

$b$  = A soil parameter which is primarily a function of the rate of water extraction from the soil, once the air entry value has been exceeded.

$c$  = A soil parameter which controls the shape and position of the drier portion of the SWCC.

$h_r$  = A soil parameter which is primarily a function of the suction at which the drier portion of the SWCC tends to level out (kPa).

$C(h)$  = An adjustment factor which forces all curves through a suction of 1,000,000 kPa at zero water content.

In terms of degree of saturation, the Fredlund and Xing equation reads as follows:

$$S = C(h) \times \left[ \frac{1}{\left[ \ln \left[ \exp(1) + \left( \frac{h}{a} \right)^b \right] \right]^c} \right] \dots\dots\dots (3)$$

Where:

$S$  = Degree of saturation,  $\theta/\theta_{\text{sat}}$

## Correlation Between the Fredlund and Xing Fitting Parameters and Soil Index Properties

In recently studies conducted by William N. Houston and Claudia E. Zapata (Zapata, C., 1999), the fitting parameters of the Fredlund and Xing equation were statistically correlated with well-known soil properties. A database characterizing approximately 190 soils was assembled from research papers and a knowledge-based program developed by Soilvision Systems Ltd (Dunn and Palmer, 1994; Escario and Juca, 1989; Fredlund, 1995; Fredlund et al., 1995; Gan et al., 1988; Ghosh, 1980; Haverkamp and Parlange, 1986; Houston et al., 1999; Krahn and Fredlund, 1972; Livneh et al., 1970; Marinho and Stuermer, 1998; Oberg and Sallfors, 1997; Rahardjo et al., 1995; Rohm and Vilar, 1995; Sabbagh, 1995; Vanapalli et al., 1998). The soils were divided into two categories: soils having a Plasticity Index (PI) greater than zero and those soils having a PI equal to zero. Approximately 70 soils with PI greater than zero and 120 soils with PI equal to zero were collected.

The data assembled for the soils with PI greater than zero included the Percentage Passing #200 sieve and the Atterberg Limits, particularly the Plasticity Index. For soils with PI equal to zero or non-plastic soils, the Diameter  $D_{60}$  was gathered. Included in the collected data was a measured and well-defined SWCC.

For the soils with PI greater than zero, the product of the Percentage Passing #200 as a decimal was multiplied by the PI as a percentage to form the weighted PI. This value was designated as  $wPI$ , and used as a main soil property for correlation. The  $D_{60}$  was the main soil property for correlation for the soils with PI equal to zero.

### Correlations for Soils with $PI > 0$

The fitting parameters present in the Fredlund and Xing equation, parameters  $a$ ,  $b$ ,  $c$ , and  $h_r$ , were correlated with the new  $wPI$  parameter. The equations found are the following:

$$a = 0.00364(wPI)^{3.35} + 4(wPI) + 11 \dots\dots\dots (4)$$

$$\frac{b}{c} = -2.313(wPI)^{0.14} + 5 \dots\dots\dots (5)$$

$$c = 0.0514(wPI)^{0.465} + 0.5 \dots\dots\dots (6)$$

$$\frac{h_r}{a} = 32.44e^{0.0186(wPI)} \dots\dots\dots (7)$$

The wPI parameter in equations 4 through 7 is defined as:

$$wPI = \text{Passing \#200} \times PI \dots\dots\dots (8)$$

Where:

Passing #200 = Material passing the #200 U.S. Standard Sieve expressed as a decimal

PI = Plasticity Index (%)

In those cases where the saturated volumetric water content,  $\theta_{sat}$ , is unknown, the user can make use of the following correlation:

$$\theta_{sat} = 0.0143 (wPI)^{0.75} + 0.36 \dots\dots\dots (9)$$

However, although equation (9) produces a more or less unbiased estimate of the  $\theta_{sat}$  = porosity, the scatter is considerable and it is highly desirable to have direct measurements of density, or better yet, density and specific gravity,  $G_s$ , so that  $\theta_{sat}$  can be calculated from direct measurements. Equation (16) for estimating  $G_s$  is presented later and this equation can be used with only small to moderate error when directly measured  $G_s$  values are not available.

#### Correlations for Soils with PI = 0

For granular soils with Plasticity Index equal to zero, the parameter used to relate to the SWCC was the Diameter  $D_{60}$  from the grain-size distribution (GSD) curve. The correlations found are the following:

$$a = 0.8627(D_{60})^{-0.751} \dots\dots\dots (10)$$

$$\bar{b} = 7.5 \dots\dots\dots (11)$$

$$c = 0.1772 \ln(D_{60}) + 0.7734 \dots\dots\dots(12)$$

$$\frac{h_r}{a} = \frac{1}{D_{60} + 9.7e^{-4}} \dots\dots\dots(13)$$

Where:

$D_{60}$  = Grain diameter corresponding to 60% passing by weight or mass (mm)

$\bar{b}$  = Average value of fitting parameter b

No correlation between the 'b' parameter and  $D_{60}$  was found. Therefore, a constant average b value is suggested. In those cases where the  $\theta_{sat}$  is unknown, the following constant is recommended for soils with PI equal to zero:

$$\bar{\theta}_{sat} = 0.36 \dots\dots\dots(14)$$

## Correlation Results

Figures 9 through 15 shows the results obtained. Figures 9 through 12 show the SWCCs for the soils with wPI greater than zero. Figures 13 and 14 show the SWCCs for the soils with wPI equal to zero. In figures 9 through 14, the solid curves represent the "predicted" band corresponding to the wPI and  $D_{60}$  values indicated. The prediction is derived from the correlations obtained from the database (190 soils) described previously, using equations 4 through 14. The data points shown in figures 9 through 14 represent the actual, measured SWCCs (after some smoothing). The goodness of the fit can be judged by observing the extent to which the "predicted" band is centered on and envelops the experimental data. For each figure, the experimental data subset represents the same range in wPI (or  $D_{60}$ ), as does the predicted band given by the solid curves. Figure 15 summarizes the results obtained for both groups of soils.

The relatively large database used to correlate the soil properties with the fitting parameters of the Fredlund and Xing equation provides insight as to what would be, perhaps, more reasonable SWCCs than those defined by the Gardner equation in the version 2.1 of the EICM. Furthermore, there is now more flexibility in choosing the SWCCs for certain soils than that offered before, because instead of having only seven

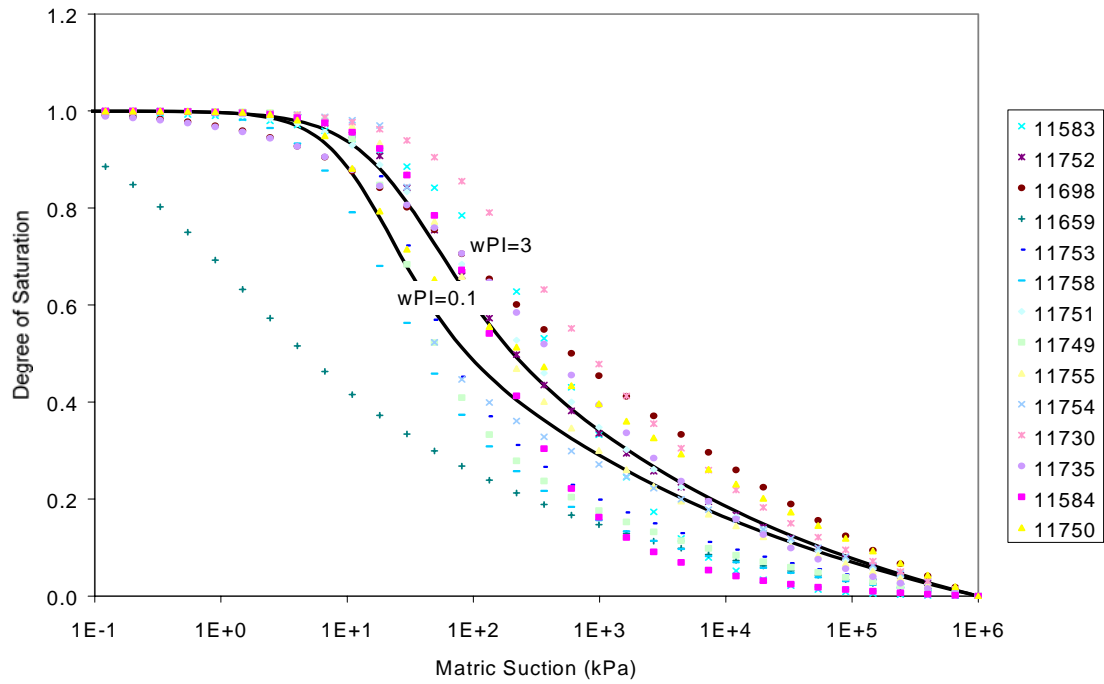


Figure 9. Range of SWCCs for Soils with wPI between 0.1 and 3

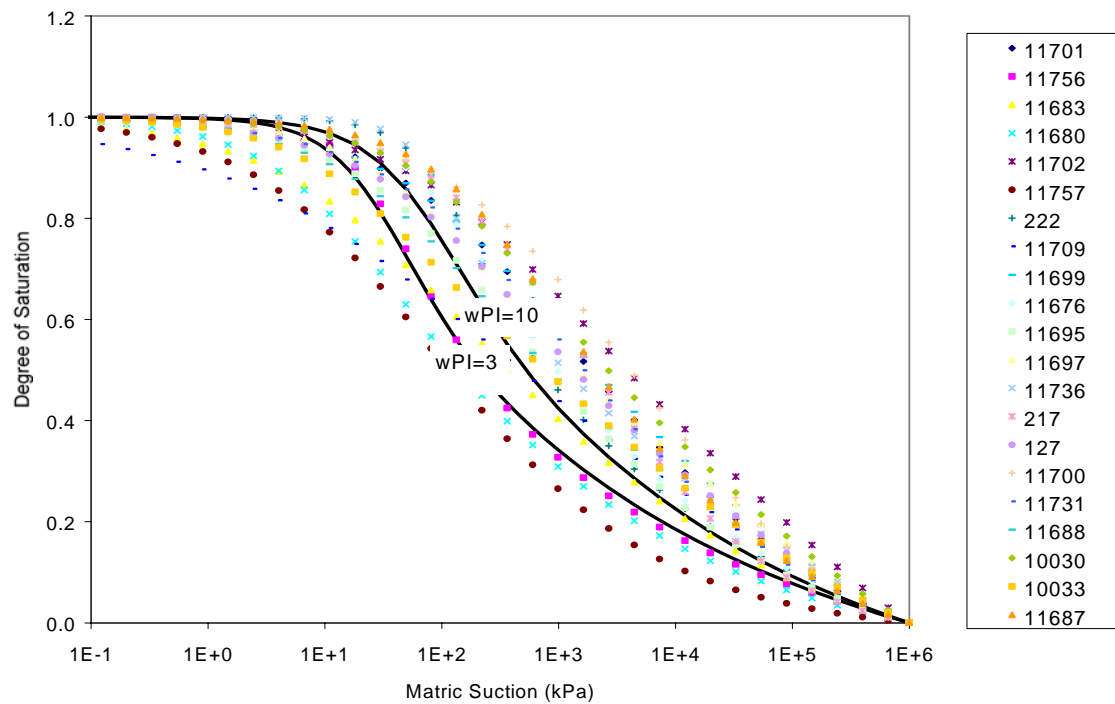


Figure 10. Range of SWCCs for Soils with wPI between 3 and 10

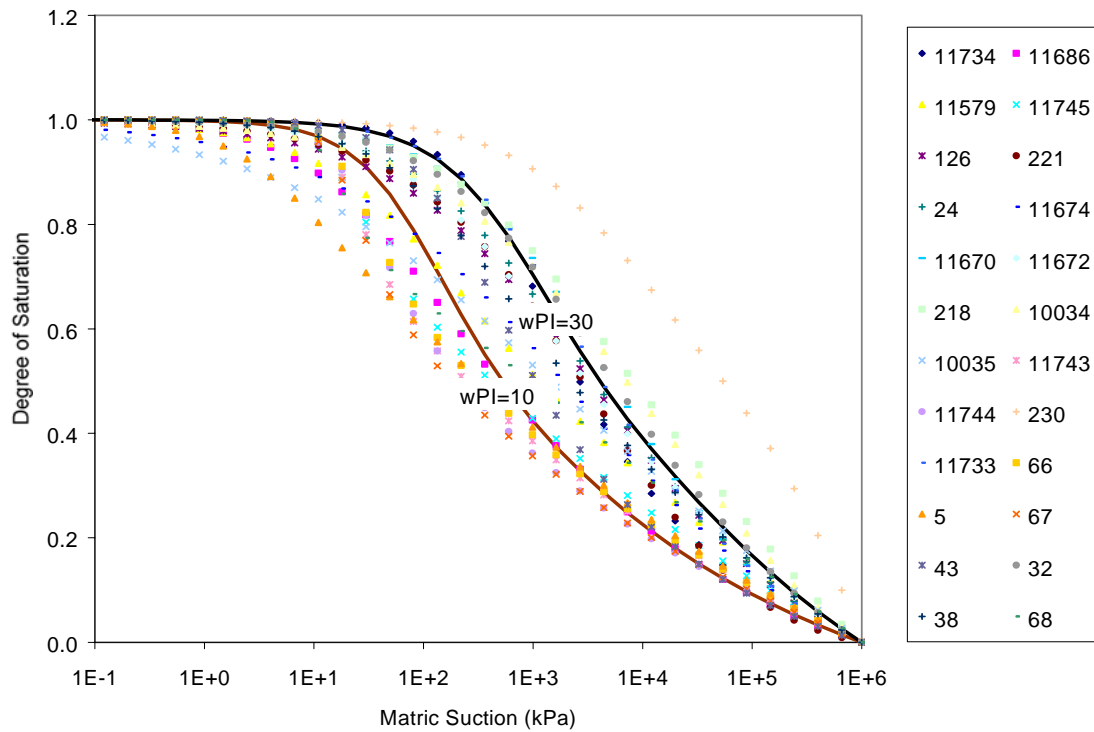


Figure 11. Range of SWCCs for Soils with wPI between 10 and 30

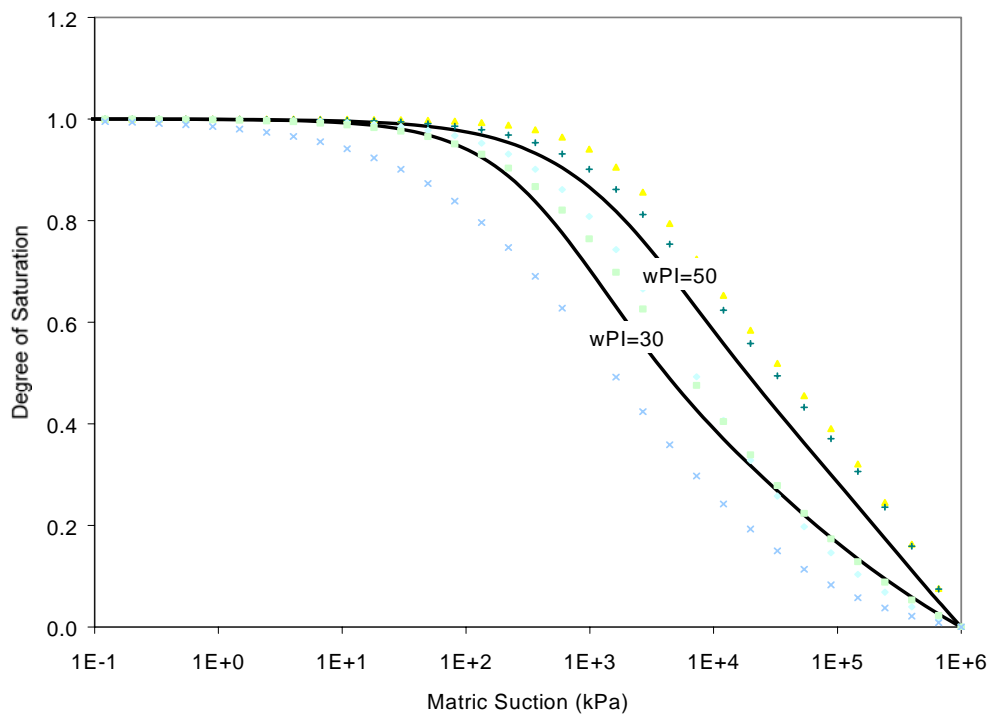


Figure 12. Range of SWCCs for Soils with wPI between 30 and 50



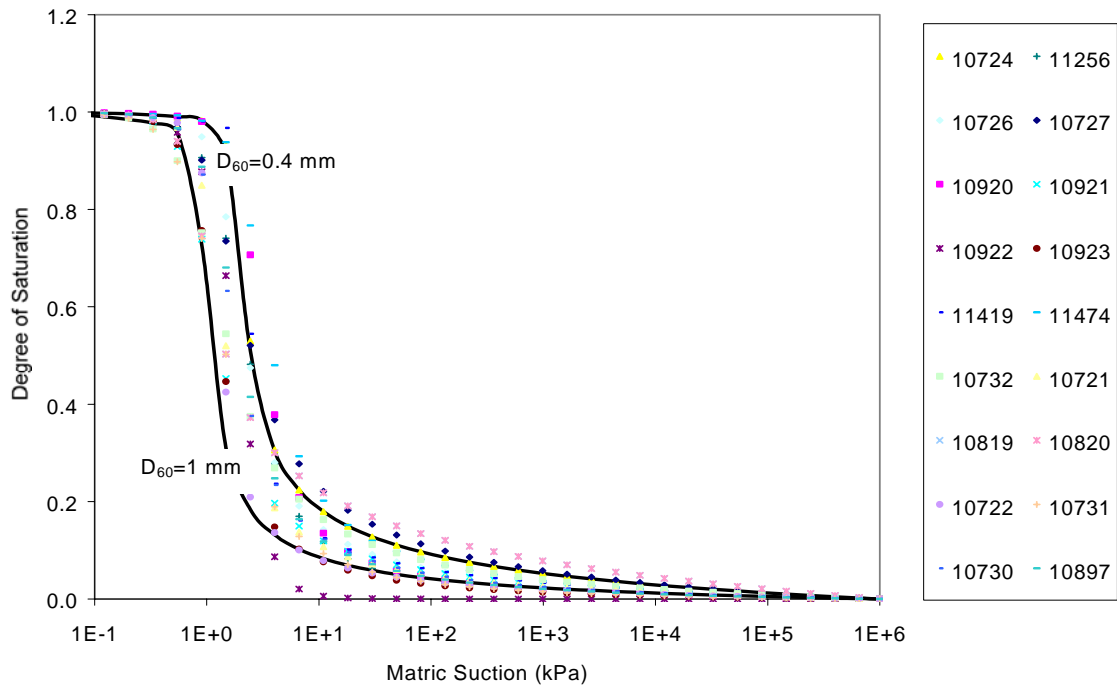


Figure 13. Range of SWCCs for Soils with  $D_{60}$  between 1 and 0.4 mm.

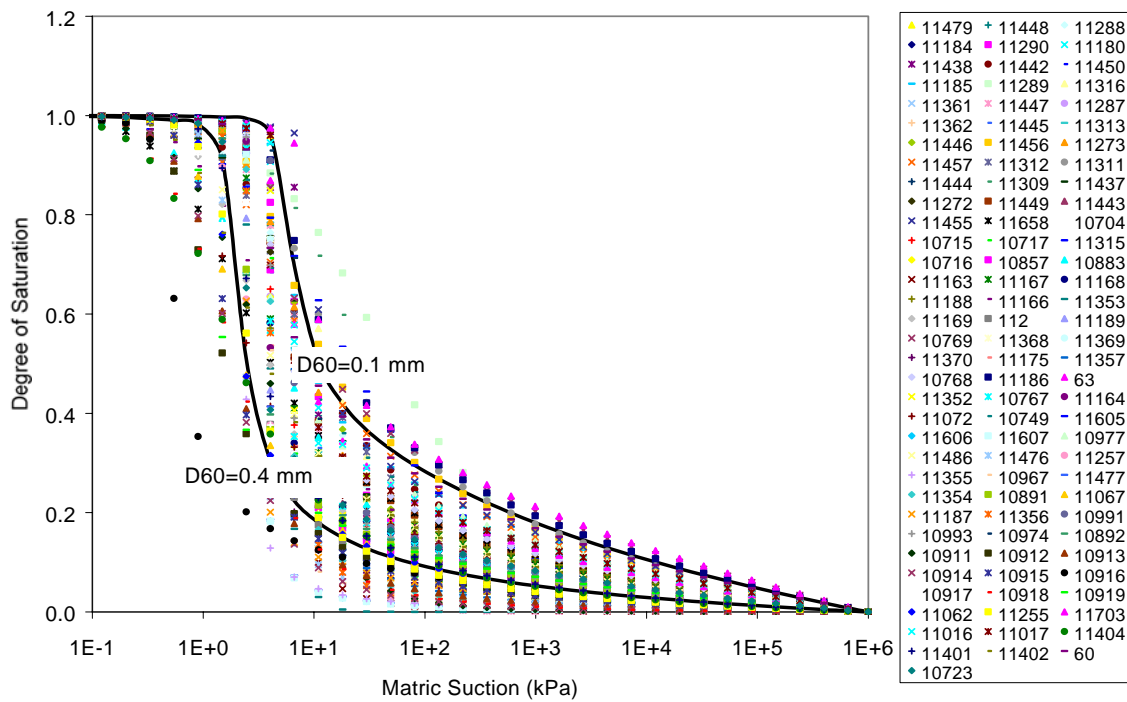


Figure 14. Range of SWCCs for Soils with  $D_{60}$  between 0.4 and 0.1 mm.

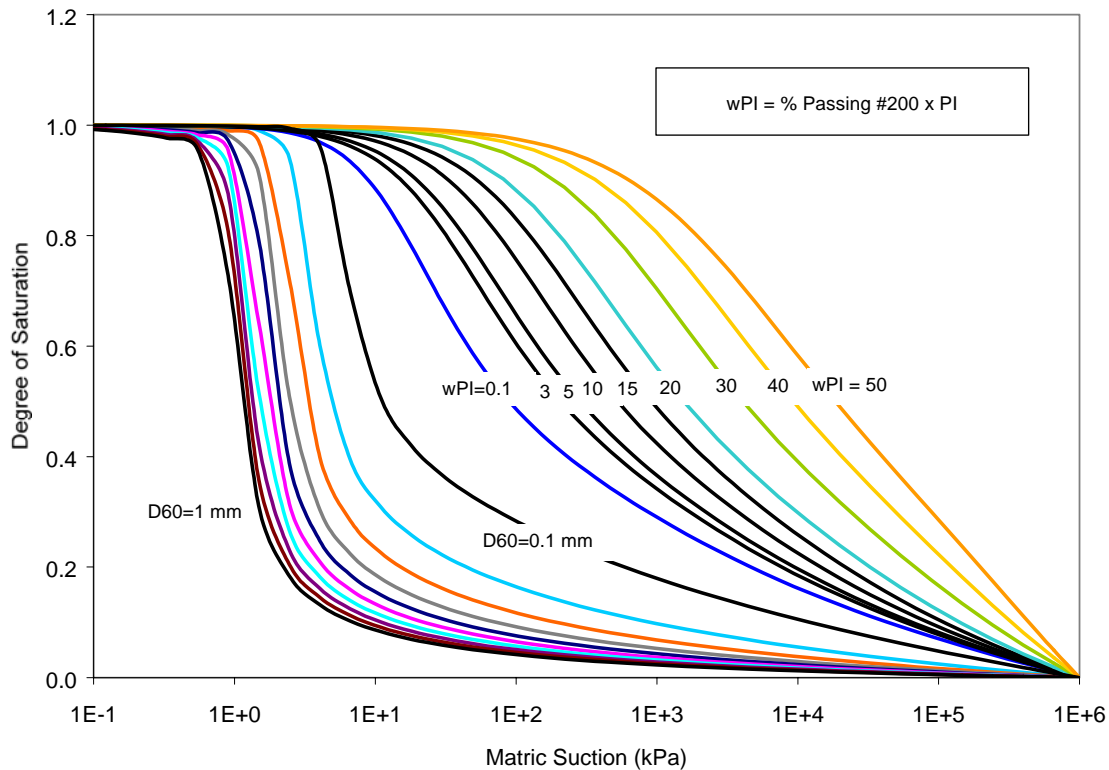


Figure 15. Predicted SWCC based on  $D_{60}$  and  $wPI$

SWCCs, there is now an infinite number of SWCCs to choose from. The Gardner parameters are still available for those who prefer to work with them or have old input files.

Data for the 190 soils used in this study and hundreds of other SWCCs examined by the authors show clearly that the SWCC moves gradually to the right with increasing plasticity. The correlations and algorithms developed for this study provide a smooth transition across the spectrum of soils with no plasticity to those with high plasticity. Although Figures 9 through 14 show that the predicted SWCC curves match the measured SWCC fairly well, and probably about as well as can be done at this time, there is nevertheless considerable scatter in the SWCCs. Data not presented in this report (Zapata, C., 1999) show that if a single soil is sent out to a dozen laboratories across the country for SWCC measurement, the results show a variability greater than that of the experimental data in Figure 11, for example. Likewise, if a single laboratory is asked to reproduce the SWCC for a single soil, the variability can typically be as greater as the difference between the  $wPI = 10$  curve and the  $wPI = 30$  curve in Figure 11. These observations have led the authors to conclude that soil suction and SWCCs simply cannot be measured with great precision at the present time. Researchers and practitioners dealing with unsaturated

soils need to recognize and acknowledge this condition. There are two corollaries to this conclusion: The first is that the SWCC can probably be estimated from  $D_{60}$  or wPI (see Figure 15) about as accurately as it can be measured, unless the laboratory or person making the measurement is highly experienced. Secondly, it is difficult to develop a predictive model for SWCCs that is consistent with all of the SWCCs reported in the literature because of the fairly high probability that any given measured SWCC has significant experimental error associated with it. It therefore follows that the agreement between predicted and measured results depicted in Figures 9 through 14 could be improved if the experimental error from the measured results could be removed. Of course, this latter conclusion is optimistic and rests on the contention that the experimental errors tend to be both positive and negative.

Table 5. Soil Properties Default Values vs. AASHTO Soil Classification System

AASHTO Classification	wPI	$D_{60}$ (mm) (Range)	$G_s$ (Range)	$\theta_{sat}$ (Range)	$\rho_{dry}$ (gm/cm <sup>3</sup> ) (Range)
A-1-a	0	3 ( $D_{60} > 2$ )	2.65	0.36	1.70
A-1-b	0	1 (0.45 - 2)	2.65	0.36	1.70
A-2-4	1.2 (0.2 - 3.5)		2.69 (2.68 - 2.71)	0.38 (0.36 - 0.40)	1.68 (1.61 - 1.72)
A-2-5	2 (0.2 - 3.5)		2.70 (2.68 - 2.71)	0.38 (0.36 - 0.40)	1.66 (1.61 - 1.72)
A-2-6	2.6 (0.55 - 5.25)		2.70 (2.68 - 2.72)	0.39 (0.37 - 0.41)	1.65 (1.58 - 1.71)
A-2-7	6 (0.75 - 15.75)		2.72 (2.69 - 2.74)	0.41 (0.37 - 0.47)	1.59 (1.42 - 1.72)
A-3	0	0.18 (0.074 - 0.45)	2.65	0.36	1.70
A-4	4.1 (1.44 - 10)		2.71 (2.70 - 2.73)	0.40 (0.38 - 0.44)	1.62 (1.51 - 1.70)
A-5	6.8 (1.44 - 10)		2.72 (2.70 - 2.73)	0.42 (0.38 - 0.44)	1.58 (1.51 - 1.70)
A-6	8.84 (3.96 - 15)		2.73 (2.71 - 2.74)	0.43 (0.40 - 0.47)	1.55 (1.44 - 1.64)
A-7-5	25.8 (10.8 - 45)		2.76 (2.73 - 2.77)	0.52 (0.45 - 0.61)	1.31 (1.07 - 1.54)
A-7-6	15 (5.4 - 29)		2.74 (2.72 - 2.76)	0.47 (0.41 - 0.54)	1.46 (1.25 - 1.63)

## Best-Estimate SWCCs Based on AASHTO Classification

In those cases where neither wPI nor  $D_{60}$  is known, but the AASHTO classification is, a best-estimate SWCC for each classification is proposed. The SWCC is based on either wPI or  $D_{60}$ . That is, for each AASHTO classification category, either the wPI or the  $D_{60}$  has been estimated. Then this estimate of either wPI or  $D_{60}$  is used together with the correlations developed to yield a best-estimate SWCC. Table 5 shows the results along with the probable range of values. This table can also be incorporated in the EICM user's manual to be used by those that prefer the prediction of the SWCC based on Fredlund and Xing parameters to the prediction using the Gardner parameters. Appendix G shows the proposed SWCCs for each AASHTO soil classification.

## Best-Estimate SWCCs for Base Course Materials

In cases where the  $D_{60}$  or the wPI for the material are not precisely known, but instead the material is identifiable as a base course material, an estimated SWCC for each grading is proposed. The estimated soil parameters to define the SWCC are presented in Table 6. The base course material classification is based on the AASHTO Designation M 147-65 (1990): *Materials for Aggregate and Soil-Aggregate Subbase, Base and Surface Courses*. If the base course material is suspected to have significant plastic fines, it is recommended that the wPI be used (bottom of Table 6) instead of the  $D_{60}$  criteria. Appendix H depicts the proposed SWCCs for base course materials.

The modified version of the EICM has not yet fully implemented this feature, but it is expected to be included in the future in the release version.

## Default Values for Saturated Hydraulic Conductivity, Specific Gravity, and Saturated Volumetric Water Content

In cases where the saturated hydraulic conductivity is not known from field or lab testing and needs to be estimated, the following equation is proposed:

$$k_{\text{sat}} = 76639(\theta_{\text{sat}} - \theta_{33\text{kPa}})^{12.9} + 10^{-12} \dots\dots\dots (15)$$

Where:

$k_{\text{sat}}$  = saturated hydraulic conductivity (m/s)

Table 6. Best Estimated D<sub>60</sub> for Base Course Materials

Base Course Material Grading <sup>1</sup>	Best Estimate D <sub>60</sub> (mm) (Range)
Grading A	11.5 (5-17.5)
Grading B	11.5 (5-17.5)
Grading C	7 (3.5-11)
Grading D	4 (1.1-7.5)
Grading E	3 (0.5-5)
Grading F	1.4 (0.3-2.5)
Base Course materials with some plasticity, used wPI = 0.5	

$\theta_{\text{sat}}$  = saturated volumetric water content = porosity

$\theta_{33\text{kPa}}$  = water content at 33 kPa of suction, from the SWCC

Equation 15 is now intrinsic to the EICM, version 2.6. When the user does not specify a value for  $k_{\text{sat}}$ , the EICM calculates it, provided the wPI, D<sub>60</sub>, or AASHTO classification is input. This information is also needed by the EICM to calculate the SWCC and the  $\theta_{33\text{kPa}}$ .

Another important soil property that is often missing from the soil exploration data is the Specific Gravity ( $G_s$ ). This important property is needed, together with the dry density, to determine the  $\theta_{\text{sat}}$  for the soil. The following equation can be used to estimate  $G_s$  when wPI is known. This equation was developed by correlation from a large database.

$$G_s = 0.041(wPI)^{0.29} + 2.65 \dots\dots\dots (16)$$

If the dry density is known but  $G_s$  and  $\theta_{\text{sat}}$  are unknown, then the best estimate of  $\theta_{\text{sat}}$  is obtained by first using Equation 16 to calculate  $G_s$ . Then the dry density and  $G_s$  are used together to calculate porosity =  $\theta_{\text{sat}}$ . This procedure for getting  $\theta_{\text{sat}}$  is superior to the use of Equation 9. Thus, Equation 9 should be used only when the dry density is not available.

---

<sup>1</sup> Based on the AASHTO Designation M 147-65 (1990): *Materials for Aggregate and Soil-Aggregate Subbase, Base and Surface Courses*

The user needs to input either the wPI for the soil (a value of zero if the soil is non-plastic) or input the AASHTO classification. The program automatically calculates the specific gravity and the saturated volumetric water content, if they are not provided. For those cases where the wPI is unknown, but the user knows the AASHTO classification, default values for  $\theta_{\text{sat}}$  have been built into the EICM. The default values for  $\theta_{\text{sat}}$  are presented in Table 5. More detailed information on issues to be considered by users applying the EICM in practice will be presented in [Chapter 5](#).

## Unsaturated Hydraulic Conductivity Function

The EICM (version 2.1) made use of the Gardner's parameters for the representation of the unsaturated hydraulic conductivity function, that is, the relationship between hydraulic conductivity and soil matric suction. As part of the modifications performed to the EICM version 2.1, the unsaturated hydraulic conductivity default parameters were replaced by an equation proposed by Fredlund, D., Xing, A., and Huang, S. in 1994. The proposed hydraulic conductivity function is an integration form of the water content versus suction relationship and makes use of the soil-water characteristic curve fitting parameters proposed by the same authors and described in Chapter 3, equations 1 and 2.

To calculate the hydraulic conductivity, the following model was integrated into the EICM:

$$k_r(h) = \frac{\int_h^{h_{\text{res}}} \frac{\theta(y) - \theta(h)}{y^2} \theta'(y) dy}{\int_{h_{\text{aev}}}^{h_{\text{res}}} \frac{\theta(y) - \theta_{\text{sat}}}{y^2} \theta'(y) dy} \dots\dots\dots (17)$$

Where:

$k_r(h)$  = relative hydraulic conductivity, which is the hydraulic conductivity at any suction  $k(h)$  referenced to the saturated hydraulic conductivity  $k_{\text{sat}}$ .

$$k_r(h) = \frac{k(h)}{k_{\text{sat}}} \dots\dots\dots (18)$$

$h_{\text{res}}$  = suction corresponding to the residual water content  $\theta_r$

$h_{\text{aev}}$  = air-entry value of the soil under consideration which is the suction where air starts to enter the largest pores in the soil

$y$  = dummy variable of integration representing suction

$\theta'$  = derivative of equation 1

Since Equation 1 is valid over the entire suction range, the integrations in Equation 17 can be performed from  $h_{aev}$  to  $10^6$  for all type of soils (Fredlund et al., 1994). Furthermore, Equation 17 assumes that the volume change of the soil structure is negligible.

## Summary

The modifications to the EICM water content prediction included:

- Representation of the Soil-Water Characteristic Curve (SWCC) by the Fredlund and Xing equation. The Gardner equation remains available to the EICM user.
- The parameters of the Fredlund and Xing equation (Fredlund and Xing, 1994) were correlated with basic soil index properties:  $D_{60}$  and  $wPI$  = Percentage Passing #200 times Plasticity Index (PI).
- Default values for the basic soil index properties needed to determine the SWCC were estimated as a function of the AASHTO Soil Classification System.
- Default values for the basic soil index properties needed to determine the SWCC were estimated for the base course materials designed under AASHTO Designation M 147-65 (1990): *Materials for Aggregate and Soil-Aggregate Subbase, Base and Surface Courses*.
- Algorithms to estimate porosity (saturated volumetric water content), specific gravity and saturated hydraulic conductivity based on  $wPI$  were developed.
- Incorporation into the EICM of unsaturated hydraulic conductivity prediction based on the SWCC proposed by Fredlund, et al. (1994). The Gardner parameters for the unsaturated hydraulic conductivity remain available for use in the EICM.

EICM Version 2.6 reflects these modifications.

# Assessment of the EICM Moisture Content Prediction after Modifications

## EICM Version 2.6

### Introduction

An evaluation of the EICM Version 2.6 was undertaken to verify that the changes made improved the moisture content predictions. Data from the six Long-Term Test Performance (LTPP) sections used to assess the EICM version 2.1, and from four additional LTPP Seasonal Monitoring Sites were used. The new sections are:

- 1) 131005 (Georgia)
- 2) 81053 (Colorado)
- 3) 41024 (Arizona)
- 4) 481077 (Texas)

### Data Collected

The data used in the evaluation of the EICM version 2.6 were drawn from DataPave 2.0 (1999), except as follows.

- Data tables SMP\_TDR\_AUTO\_MOISTURE and SMP\_FROST\_PENETRATION, SMP\_FREEZE\_STATE are from release 10.0 of the LTPP Information Management System.
- Tables TST\_... are from release 10.2 of the LTPP Information Management System.
- In a few instances, data were obtained from the Seasonal Monitoring Site installation reports for the test sites. Data from this source are annotated as such in the tables presenting the input data.



- Specific gravity data are not included in the LTPP database. However, specific gravity data for some materials are reported on laboratory data sheets associated with LTPP resilient modulus testing, and Klemunes (1995) reports values for several additional materials. Where available, these values were used.

In cases where required input data were not available, either because they were not routinely collected on the LTPP test sections, or because they were otherwise missing from the LTPP database when this work was undertaken, default values were used, as noted in the tables presenting the input data.

The data for the ten LTPP sites are presented in [Table 7](#) and [Table 8](#). In a few instances, the data used as input to Version 2.6 of the EICM differed from that used for Version 2.1. These differences arise from additional data that became available in the LTPP database, and additional information that came to the authors' attention in the intervening time period.

In the application of EICM Version 2.6, subbase and subgrade layers were subdivided, such that a mid-depth node would correspond to the depth of each TDR probe used in LTPP monitoring. The base layer was not subdivided, based on the advice of the EICM model developers. For clarity, the Material Properties information is shown for each layer and for each sub-layer, as input into the EICM, given that the water content information was often available at more than one location within a given layer. For further information on recommendations for subdividing the pavement profile, refer to the User's Guide and Recommendations Chapter.

The shading in some boxes in [Tables 7 and 8](#) indicates that a default value was used for that particular property, instead of a measured value. Also notice, that some of the information is presented as a file name (i.e., \*.txt, \*.xls). The information contained on those files is rather extensive and is not included in this report.

## Results

[Figures 16 through 25](#) show the measured versus predicted volumetric water contents by the EICM version 2.6 for the ten sites. The data for the base course material and the

Table 7. Summary of Input Parameters for the EICM – Version 2.6 for the Connecticut, Minnesota, Maine, New Hampshire, Vermont, and Manitoba LTPP Sections

	Site 91803	Site 271018	231026	331001	501002	831801	Remarks/Notes
	Connecticut	Minnesota	Maine	New Hampshire	Vermont	Manitoba	
Integrated Model Initialization							
Climatic Region	I-A	II-A	I-A	I-A	I-A	II-A	
Weather Station	User-defined	User-defined	User-defined	User-defined	User-defined	User-defined	
Year	1994	1993	1994	1994	1994	94	
First Month	6	9	6	6	7	6	
First Day	30	23	20	23	20	17	
Analysis period-day	356	365	365	365	365	365	
Time Increment for output (hours)	6	6	6	6	6	6	
Time increment for calculation (hours)	0.1	0.1	0.1	0.1	0.1	0.1	
Latitude	41°23'41.5" = 41.39	46°1'32.7" = 46.03	44°34'27.2" = 44.57	43°13'20.1" = 43.22	44°7'10.4" = 44.12	49°46'9.6" = 49.77	
Climate/Boundary Conditions							
Max/Min Temperatures	CTemp.mmt		Mainetemp.txt	Newhamptemp.txt	VERtemp.txt	MANltemp.txt	Site specific data file
Rainfall	CTraincm.rfa	MNraincm.rfa	MAINErain2.rfa	NHrain3.rfa	VERMrain4.rfa	MANlraincm.txt	Site specific data file
Windspeed	Boston	Average	Boston	Boston	Boston	Fargo	Default weather station data
Percent Sunshine	Boston	Average	Boston	Boston	Boston	Fargo	
GWT Depth (m)	CTwtd.bnd	MNwtd.txt	Mainewtd2.txt	NHwtd.txt	VERMwtd.txt	MANlwtd2.txt	Site specific data file
Thermal Properties							
Modifier of Overburden Pressure	0.5	0.5	0.5	0.5	0.5	0.5	Default
Emissivity Factor	0.93	0.93	0.93	0.93	0.93	0.93	Default
Surface short wave Absorptivity	0.85	0.85	0.85	0.85	0.85	0.85	Default
Maximum convection Coeff. (Cal/cm-sec-C°)	44.7	44.7	44.7	44.7	44.7	44.7	Default
COV of Unsaturated k	1	1	1	1	1	1	Default

Table 7. Cont.

	Site 91803	Site 271018	Site 231026	Site 331001	Site 501002	Site 831801	Remarks/Notes
Time of Day When Max and Min Temperatures Occur	Min: 5:43=5.72 Max: 13:29=13.48	Min: 6:25 = 6.42 Max: 14:09=14.15	Min: 5:12 = 5.2 Max: 13:55=13.92	Min: 5:49 = 5.82 Max: 14:07 = 14.12	Min: 6:12 = 6.2 Max: 13:13 = 13.22	Min: 8:48 = 8.8 Max: 14:29 = 14.48	
Freezing Range (°C)	0/-1	0/-1	0/-1	0/-1	0/-1	0/-1	Default
Infiltration and Drainage							
Cracks' length (m)	94	648	12	133	125	108	
Total survey length (m)	152.4	152.4	152.4	152.4	152.4	152.4	
Base fines type	Silt	Silt	Silt	Silt	Silt	Silt	Inferred from PI
Base %fines	6	7.5	4	4.5	3.5	11	
Base % gravel	60	43	74	63	90	52	
Base % sand	34	49.5	22	32.5	6.5	37	
One side base width	4.57 m	5.18 m	6.71m	5.79m	3.35m	3.66 m	
Slope ratio/base tangent	1.5	1.5	1.5	1.5	1.5	1.5	Default
Boundary condition	Flux	Flux = Suction	Flux	Flux	Flux	Flux	
Evaluation period (years)	10	10	10	10	10	10	Default
Constant K	0.3	0.3	0.3	0.3	0.3	0.3	Default
Power recurrence interv.	0.25	0.25	0.25	0.25	0.25	0.25	Default
Power rainfall duration	0.75	0.75	0.75	0.75	0.75	0.75	Default
Shape constant	1.65	1.65	1.65	1.65	1.65	1.65	Default
Asphalt Material Properties							
Thickness (cm)	18	11.2	16	21.6	21.1	11.5	
Number of elements	4	3	4	5	5	3	
Coarse Agg Content (%)	80% (AC = 4.3%)	80 (AC = 5.1%)	80	80	80	80	Default
Air content (%)	5.4	4.3	4	4	4	4	Default
Gravi. Moist Content (%)	2	2	2	2	2	2	Inventory
M <sub>r</sub> vs. T	-4.1, 214643 11.8, 97252 23.4, 44203	-16.3, 153462 2.2, 78337 19.6, 63883	-23.3, 119521 15.6, 3023.2 54.4, 105.4	-23.3, 1.17 15.6, 296475 54.4, 10342.1	-23.3, 1.17 15.6, 296475 54.4, 10342.1	-23.3, 1.17 15.6, 296475 54.4, 10342.1	
Thermal K Asphalt (cal/cm-hr-C)	8.94	8.94	8.94	8.94	8.94	8.94	Default

Table 7. Cont.

	Site 91803	Site 271018	Site 231026	Site 331001		Site 501002		Site 831801		Remarks/Notes
Heat capacity (cal/g-°C)	0.22/1.2/0.22	0.22/1.2/0.22	0.22	0.22		0.22		0.22		Default
ρ <sub>total</sub> (gm/cm <sup>3</sup> )	2.494	2.371	2.37	2.37		2.37		2.37		
Material Properties										
Layer 2	Base Course Material									
Classification	A-1-a	A-1-b	A-1-a	A-1-a		A-1-a		A-1-a		
Thickness (cm)	37	10	48	49		53.8		14.2		
Number of elements	8	3	10	10		11		3		
Porosity										
Specific Gravity	2.65	2.675	2.65	2.65		2.65		2.65		
Saturated K (cm/hr)										Default
ρ <sub>dry</sub> (gm/cm <sup>3</sup> )	2.26	2.035	2.27	2.15		2.03		2.20		
Dry thermal K (Cal/cm-hr-°C)	6	10	6	6		6		6		Default
Heat capacity (Cal/g-°C)	0.21	0.21	0.21	0.21		0.21		0.21		Default
Coeff. Vol. Compressibili.	0.10	0.10	0.10	0.10		0.10		0.10		Default
Plasticity Index (%)	0	0	0	0		0		5		
Passing #200 (%)	5.8	7.7				3.4		10.9		
Diameter D <sub>60</sub> (mm)	10	2.6	45.2	12.3		25.6				
Initial vol. w/c (%)										
Equilibrium vol. w/c (%)	22	13.4	11.2	9.7		11		18.55		
Unfrozen Mr (kPa)	3569	4079	1.4e+6	1.4e+6		1.4e+6		1.4e+6		Default
Frozen Mr (kPa)	3569	688284	2.8e+6	2.8e+6		2.8e+6		2.8e+6		Default
Length recovery per.										
Modulus reduction										
	Subbase and/or Subgrade Materials									
Sub-layers	3 to 11	3 to 12	3 to 9	3 – 4	5 to 10	3	4 to 9	3 – 4	5 to 12	
Classification	A-2-4	A-3	A-2-4	A-1-b	A-2-4	A-1-a	A-7-5	A-2-6	A-2-4	
Porosity										
Specific Gravity	2.864	2.65	2.782	2.678	2.647	2.65	2.815	2.7	2.831	
Saturated K (cm/hr)										Default

Table 7. Cont.

	Site 91803	Site 271018	Site 231026	Site 331001		Site 501002		Site 831801		Remarks/Notes
$\rho_{\text{dry}}$ (gm/cm <sup>3</sup> )	2.06	1.829	1.96	2.10	1.86	1.76	1.69	2.17	1.73	
Dry thermal K (Cal/cm-hr-°C)	5	5.066	5	10	5	6	3	5	5	Default
Heat capacity (Cal/g-°C)	0.2	0.2	0.2	0.21	0.2	0.21	0.2	0.2	0.2	Default
Coeff. Volume Compres.	0.3	0.5	0.3	0.1	0.3	0.1	1	0.3	0.3	Default
Plasticity Index (%)	0	0	0	0	0	0	13	11	0	
Passing #200 (%)	12.6	5.2	12.6			6.9	94.6	10.5	28.8	
Diameter D <sub>60</sub> (mm)	0.48	0.38	4.8	1.3	0.25	7.7			0.22	
Initial vol. w/c (%)										
Unfrozen Mr (kPa)	2039	1530	175e+3	1.4e+6	175e+3	1.4e+6	5e+4	150e+3	175e+3	Default
Frozen Mr (kPa)	2039	91771	875e+3	2.8e+6	875e+3	2.8e+6	50e+4	750e+3	875e+3	Default
Length recovery per.							60			
Modulus reduction							20			
Sub-layer 3										
Sub-layer thickness (cm)	12	19.8	20	18		34.3		16.6		
Number of elements	3	4	4	4		7		4		
Porosity	0.34									
Equilibrium vol. w/c (%)	24.8	13.5	21.2	15.3		20.3		14.35		
Sub-layer 4										
Sub-layer thickness (cm)	15	15	14	19		9.8		16.9		
Number of elements	3	3	3	4		2		4		
Porosity	0.28									
Equilibrium vol. w/c (%)	20.8	12.9	14.15	16.7		33.45		18.8		
Sub-layer 5										
Sub-layer thickness (cm)	15	20.2	16	12.4		16		14.1		
Number of elements	3	5	4	6		4		3		
Porosity	0.28									
Equilibrium vol. w/c (%)	19.4	15.1	21.45	16.7		41.8		19.45		

Table 7. Cont.

	Site 91803	Site 271018	Site 231026	Site 331001	Site 501002	Site 831801	Remarks/Notes
Sub-layer 6							
Sub-layer thickness (cm)	15	9.8	16	16	25	16	
Number of elements	3	3	4	4	5	4	
Porosity	0.28						
Equilibrium vol. w/c (%)	17.45	28.8	24.3	22.8	41.2	28.2	
Sub-layer 7							
Sub-layer thickness (cm)	16	16	37	23	30	15	
Number of elements	4	4	8	5	6	3	
Equilibrium vol. w/c (%)	26.7	29.1	36.45	24.6	45.3	36.2	
Sub-layer 8							
Sub-layer thickness (cm)	22	15	60	30	40	14	
Number of elements	5	3	12	6	8	3	
Equilibrium vol. w/c (%)	20.85	29.6	25.45	26.7	45.4	31.5	
Sub-layer 9							
Sub-layer thickness (cm)	31	23	240	31	270	22	
Number of elements	7	5	24	7	27	5	
Equilibrium vol. w/c (%)	25.3	27.9		28.6		31.4	
Sub-layer 10							
Sub-layer thickness (cm)	30	30		300		31	
Number of elements	6	6		30		7	
Equilibrium vol. w/c (%)	25.8	30.9				32.4	
Sub-layer 11							
Sub-layer thickness (cm)	189	31				29	
Number of elements	19	7				6	
Equilibrium vol. w/c (%)	25.8	30.8				28.55	
Sub-layer 12							
Sub-layer thickness (cm)		199				200	
Number of elements		20				20	
Equilibrium vol. w/c (%)							

Table 7. Cont.

	Site 91803	Site 271018	Site 231026	Site 331001	Site 501002	Site 831801	Remarks/Notes
Initial Temperature Profile							
Output nodes	All	All	All	All	All	All	
Initial temperature profile	CTinitem.inp	Mninitemp.txt	maine.inp	newhamp.inp	vermont.inp	manitoba.inp	Site specific data file

Table 8. Summary of Input Parameters for the EICM – Version 2.6 for the Georgia, Colorado, Arizona, and Texas LTPP Sections

	Site 131005	Site 81053	Site 41024	Site 481077			Remarks/Notes
	Georgia	Colorado	Arizona	Texas			
Integrated Model Initialization							
Climatic Region	I-C	II-A	III-A	III-B			
Weather Station	User-defined	User-defined	User-defined	User-defined			
Year	1995	1993	1995	1994			
First Month	8	10	11	4			
First Day	8	15	9	10			
Analysis period-day	435	571	282	439			
Time Increment for output (hours)	6	6	6	6			
Time increment for calculation (hours)	0.1	0.1	0.1	0.1			
Latitude	32°36'53.8" = 32.61	38°41'52.3" = 38.7	35°16'43" = 35.28	34°32'19.3" = 34.54			
Climate/Boundary Conditions							
Max/Min Temperatures	GAtemp.txt	COtemp.txt	AZtemp.txt	TXtemp.txt			Site specific data file
Rainfall	Garaincm.txt	COrain.txt	AZrain.txt	Txrain.txt			Site specific data file
Windspeed	Atlanta	II-A	III-A	San Angelo, TX			Default weather station data
Percent Sunshine	Atlanta	II-A	III-A	San Angelo, TX			
GWT Depth (m)	5.2 m	81053wtd.txt	90 m	TXwtd.txt			Site specific data file or assumed

Table 8. Cont.

	Site 131005	Site 81053	Site 41024	Site 481077			Remarks/Notes
Thermal Properties							
Modifier of Overburden Pressure	0.5	0.5	0.5	0.5			Default
Emissivity Factor	0.93	0.93	0.93	0.93			Default
Surface short wave Absorptivity	0.8	0.8	0.8	0.85			Default
Max convection Coeffici. (Cal/cm-sec-C°)	45	45	45	45			Default
COV of Unsaturated k	1	1	1	1			Default
Time of Day When Max and Min Temperatures Occur	Min: 7:40 = 7.67 Max: 14:59 = 14.98	Min: 8:14 = 8.23 Max: 14:00 = 14	Min: 8:08 = 8.13 Max: 14:00 = 14	Min: 8:06 = 8.1 Max: 15:00 = 15			
Freezing Range (°C)	0/-1	0/-1	0/-1	0/-1			Default
Infiltration and Drainage							
Cracks' length (m)	152	115	53	110			
Total survey length (m)	152.4	152.4 m	152.4 m	152.4 m			
Base fines type	Silt	Silt	Silt	Silt			Inferred from PI
Base %fines	9	9	9	7			
Base % gravel	59	65	77	58			
Base % sand	32	26	14	35			
One side base width	3.66 m	5.94	5.79	5.79			
Slope ratio/base tangent	1.5	1.5	1.5	1.5			Default
Boundary condition	Flux	Flux	Flux	Flux			
Evaluation period (years)	10	10	10	10			Default
Constant K	0.3	0.3	0.3	0.3			Default
Power recurrence interv.	0.25	0.25	0.25	0.25			Default
Power rainfall duration	0.75	0.75	0.75	0.75			Default
Shape constant	1.65	1.65	1.65	1.65			Default
Asphalt Material Properties							
Thickness (cm)	19.1	11.4	27.4	13.2			
Number of elements	4	3	6	3			



Table 8. Cont.

	Site 131005	Site 81053	Site 41024	Site 481077			Remarks/Notes
Coarse Agg. Content (%)	80% (AC = 4.7%)	80	80	80			Default
Air content (%)	4	4	4	4			Default
Gravi. Moist Content (%)	2	2	2	2			Inventory
M <sub>r</sub> vs. T	5.4, 161109 19.1, 89553 33.2, 52310	-20, 1.2e+7 15, 30000 55, 10000	-20, 1.2e+7 15, 30000 55, 10000	-20, 1.2e+7 15, 30000 55, 10000			
Thermal K Asphalt (cal/cm-hr-C)	10	10	10	10			Default
Heat capacity (cal/g-C)	0.22	0.22	0.22	0.22			Default
$\rho_{\text{Total}}$ (gm/cm <sup>3</sup> )	2.378	2.37	2.37	2.37			Default
Material Properties							
Layer 2	Base Course Material						
Classification	A-1-a	A-1-a	A-1-a	A-1-a			
Thickness (cm)	22.4	13.7	22.4	27.4			
Number of elements	5	3	5	6			
Porosity							
Specific Gravity	2.65	2.65	2.65	2.6			
Saturated K (cm/hr)							Default
$\rho_{\text{dry}}$ (gm/cm <sup>3</sup> )	2.23	2.17	2.28	2.14			
Dry thermal K (Cal/cm-hr-°C)	6	6	6	6			Default
Heat capacity (Cal/g-°C)	0.21	0.21	0.21	0.21			Default
Coeff. Vol. Compressibili.	0.10	0.10	0.10	0.10			Default
Plasticity Index (%)	0	0	0	0			
Passing #200 (%)	8.9	8.9	9.3	7			
Diameter D <sub>60</sub> (mm)	8.7	7.7	14.4	9			
Initial vol. w/c (%)							
Equilibrium vol. w/c (%)	16.2	16	19.9	14.9			
Unfrozen Mr (kPa)	1.4e+6	1.4e+6	1.4e+6	1.4e+6			Default
Frozen Mr (kPa)	2.8e+6	2.8e+6	2.8e+6	2.8e+6			Default

Table 8. Cont.

	Site 131005		Site 81053		Site 41024	Site 481077			Remarks/Notes
Length recovery per.									Default
Modulus reduction									Default
	Subbase and/or Subgrade Materials								
Sub-layers	3 to 6	7 to 12	3 to 6	7 to 11	3 to 12	3 to 12			
Classification	A-4	A-6	A-1-a	A-6	A-2-6	A-4			
Porosity									
Specific Gravity	2.68	2.73	2.65	2.89	2.7	2.685			
Saturated K (cm/hr)									Default
$\rho_{dry}$ (gm/cm <sup>3</sup> )	1.83	2.0	2.16	1.64	1.96	1.72			
Dry thermal K (Cal/cm-hr-°C)	4	4	6	4	5	10			Default
Heat capacity (Cal/g-°C)	0.2	0.17	0.21	0.17	0.2	0.21			Default
Coef. Vol Compressibility	0.8	1	0.1	1	0.3	0.1			Default
Plasticity Index (%)	1	20	0	22	20	0			
Passing #200 (%)	36	50	9.4	91.8	30.5	73.6			
Diameter D <sub>60</sub> (mm)			13.9			0.04			
Initial vol. w/c (%)									
Unfrozen Mr (kPa)	1e+5	1e+5	1.4e+6	1e+5	1.5e+5	1e+5			Default
Frozen Mr (kPa)	5e+5	5e+5	2.8e+6	5e+5	7.5e+5	5e+5			Default
Length recovery per.	60	60		60		60			Default
Modulus reduction	20	20		20		20			Default
Sub-layer 3									
Sub-layer thickness (cm)	10.5		15.9		8.2	12.4			
Number of elements	3		4		3	3			
Equili. water content (%)	19.55		13.0		19.9	26.7			
Sub-layer 4									
Sub-layer thickness (cm)	15		16		15	16			
Number of elements	3		4		3	4			
Equili. water content (%)	16		18.0		19.9	30.9			

Table 8. Cont.

	Site 131005	Site 81053	Site 41024	Site 481077			Remarks/Notes
Sub-layer 5							
Sub-layer thickness (cm)	16	15	15	15			
Number of elements	4	3	3	3			
Equili. water content (%)	14.85	19.0	20	29.7			
Sub-layer 6							
Sub-layer thickness (cm)	18.6	12.8	16	15			
Number of elements	4	3	4	3			
Equili. water content (%)	15.6	31.0	19.9	25.7			
Sub-layer 7							
Sub-layer thickness (cm)	11.4	16.2	15	15			
Number of elements	3	4	3	3			
Equili. water content (%)	13.5		19.9	22.1			
Sub-layer 8							
Sub-layer thickness (cm)	15	17	15	16			
Number of elements	3	4	3	4			
Equili. water content (%)	16.4		20	24.5			
Sub-layer 9							
Sub-layer thickness (cm)	23	38	23	22			
Number of elements	5	8	5	5			
Equili. water content (%)	10.45		26.4	22.4			
Sub-layer 10							
Sub-layer thickness (cm)	30	60	30	31			
Number of elements	6	12	6	7			
Equili. water content (%)	9.55		23.4	20.2			
Sub-layer 11							
Sub-layer thickness (cm)	31	184	31	30			
Number of elements	7	19	7	6			
Equili. water content (%)	9.3		19.9	20.4			

Table 8. Cont.

	Site 131005	Site 81053	Site 41024	Site 481077			Remarks/Notes
Sub-layer 12							
Sub-layer thickness (cm)	188		182	187			
Number of elements	19		19	19			
Equili. water content (%)							
Initial Temperature Profile							
Output nodes	All	All	All	All			
Initial temperature profile	GAinitemp	COinitemp.txt	Azinitemp.txt	TXinitemp.txt			site specific data file

subgrade material was sub-divided on each figure. The volumetric water content profiles comparing the results for both versions, Version 2.1 and Version 2.6, are included in [Appendices I through R](#).

The summary of the results is presented in [Figures 26 through 28](#). Figure 26 shows the water content prediction versus the measured water contents for the base course materials from the ten sites previously discussed. Note that the Coefficient of Determination ( $R^2$ ) of 0.65 is a substantial improvement over that for Version 2.1 ( $R^2 = 0.05$ , see [Figure 7](#)). Figure 27 depicts the measured versus predicted volumetric water content for the subbase and subgrade materials. Again, the  $R^2$  of 0.68 is significantly better than the  $R^2$  value obtained with the EICM version 2.1 of 0.34 (see [Figure 8](#)). The overall comparison is shown in [Figure 28](#). The  $R^2$  value obtained for the overall data was 0.73. Collectively, these results show that the moisture contents predicted with Version 2.6 of the EICM are in substantially better agreement with the field data than those from Version 2.1 of the model.

The improvements can be described and summarized as follows:

- 1) Modifications to the Computation Algorithm (ICM), which improved the match between predicted and TDR measured values:
  - a) Improvements to the SWCC ( $SWCC = f(wPI, D_{60})$ ).
  - b) Introduction of software providing an adjustment to the SWCC based on equilibrium water contents.
  - c) Introduction of correlation between  $G_s$  and  $wPI$  and the use of this relationship to obtain the best estimate of the porosity (rather than using the default values).

Based on these results, it is concluded that equilibrium and initial water contents are important, and that one or the other is needed to match TDR measured values. It is further concluded that values of porosity are fairly important and should be estimated as accurately as possible. Thus, values of density, water content, PI, and gradation for each layer are needed. Measured values of  $G_s$  would be helpful, but not essential if the other measurements are made or estimated very well.

- 2) Needed Input Parameters

As part of the site investigation and material characterization, the following should be measured to ensure the greatest possible accuracy in moisture content predictions obtained with the EICM:

- a)** Dry density
- b)** Water content
- c)** Plasticity Index
- d)** Gradation
- e)** Groundwater table depth

3) Overall Comparisons of the Performance of EICM Version 2.6 (New) with that of Version 2.1 (Old) showed:

- a)** The new version showed improved predictions in all cases and often, substantial improvement.
- b)** The available data do not permit meaningful assessment of the accuracy of EICM predicted moisture contents in and near frozen layers, because the measured (TDR) values are suspect for these layers. Thus, no judgment of the accuracy of the EICM moisture predictions for frozen and freezing materials can be made on the basis of the work reported herein.

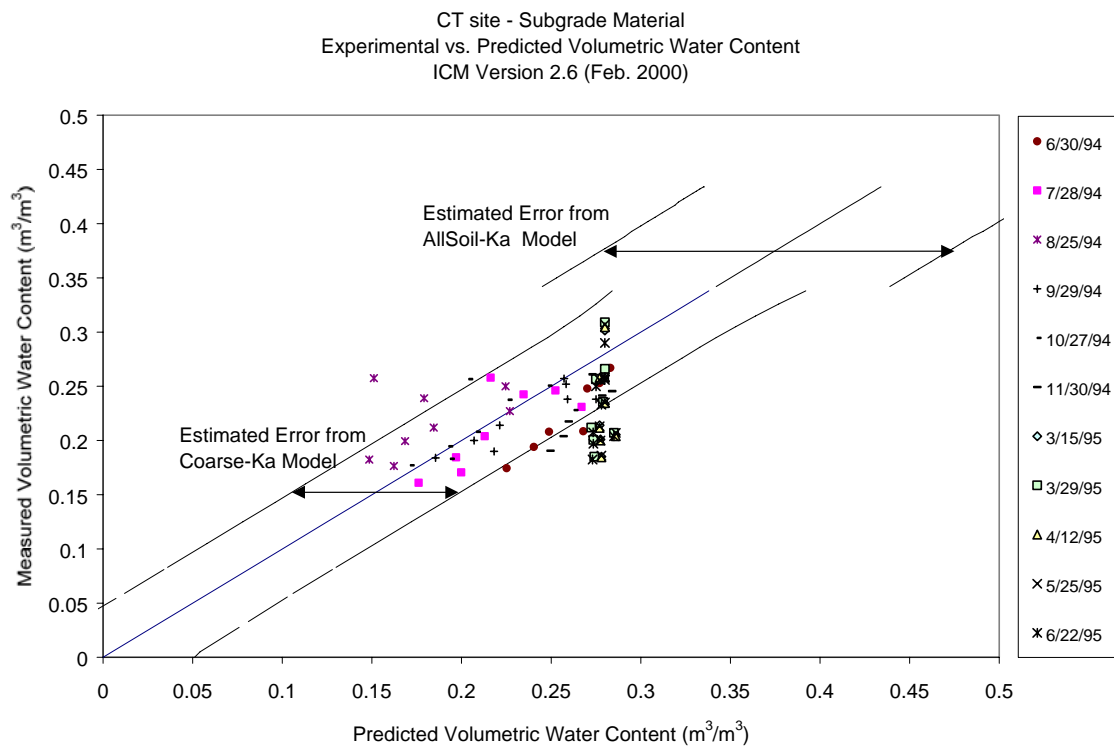
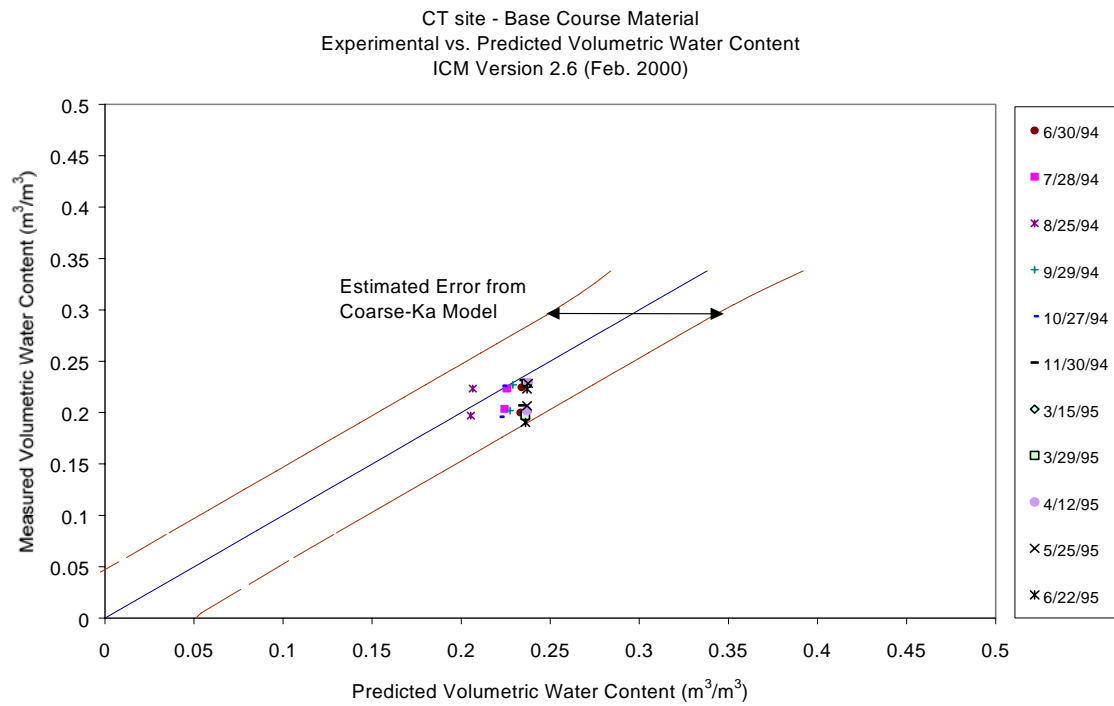


Figure 16. Measured versus Predicted Moisture Content – EICM version 2.6 Connecticut (91803)

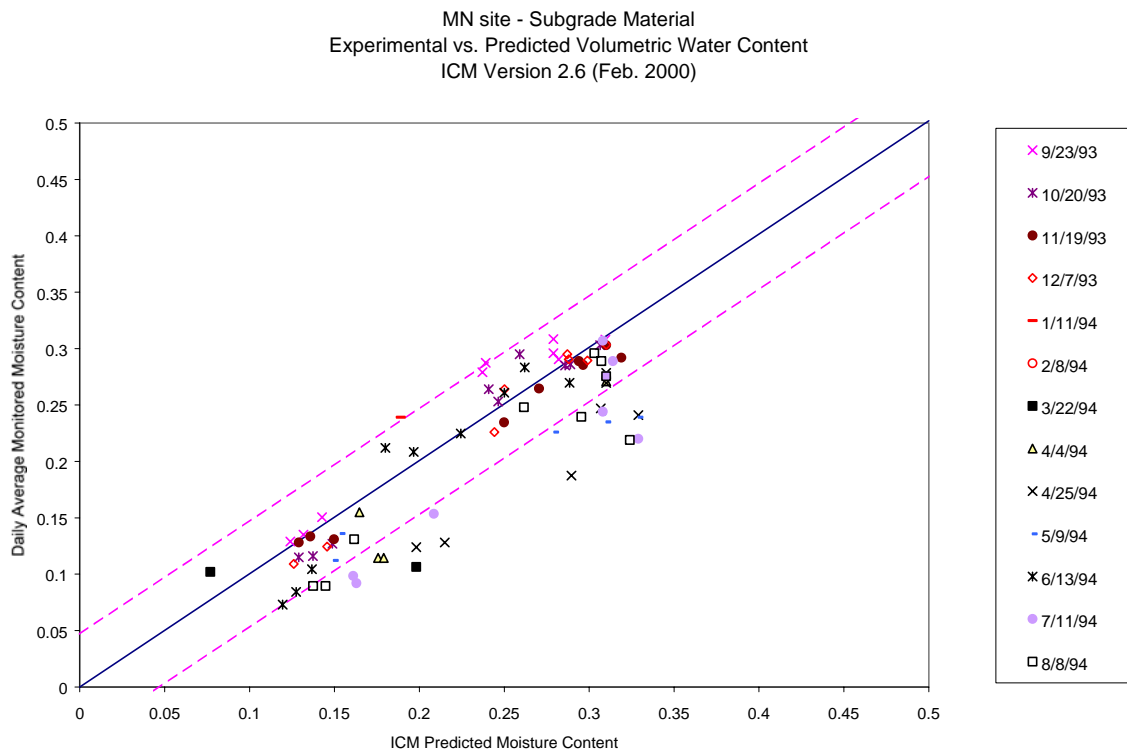
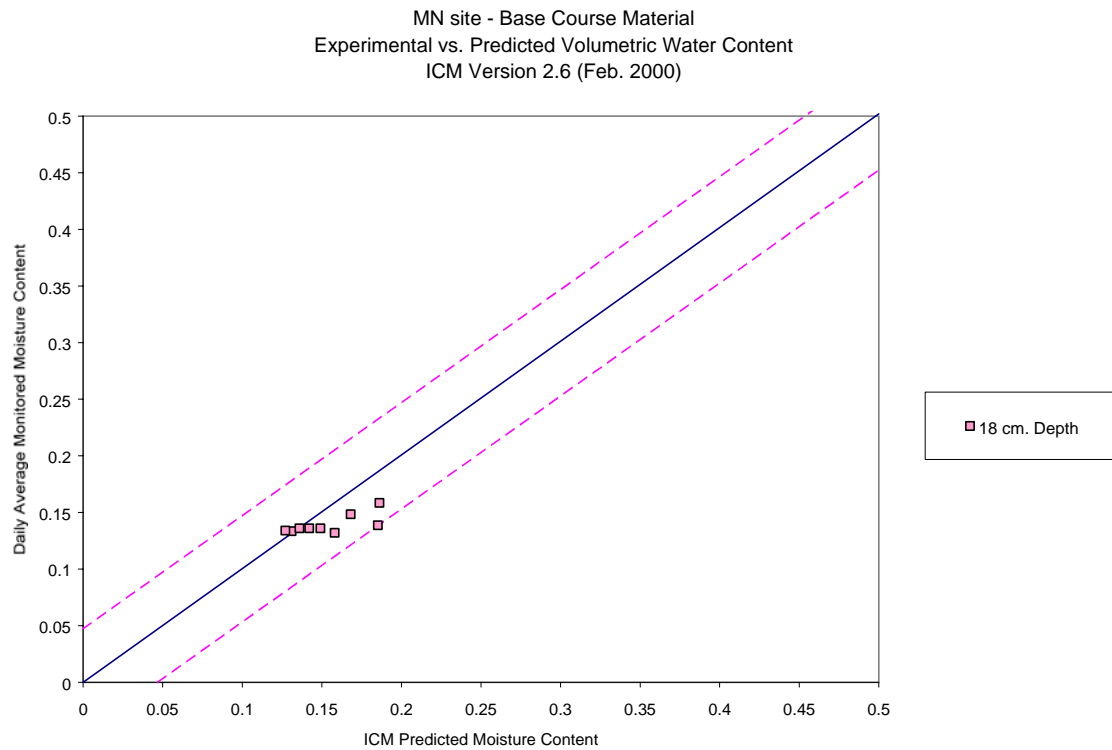
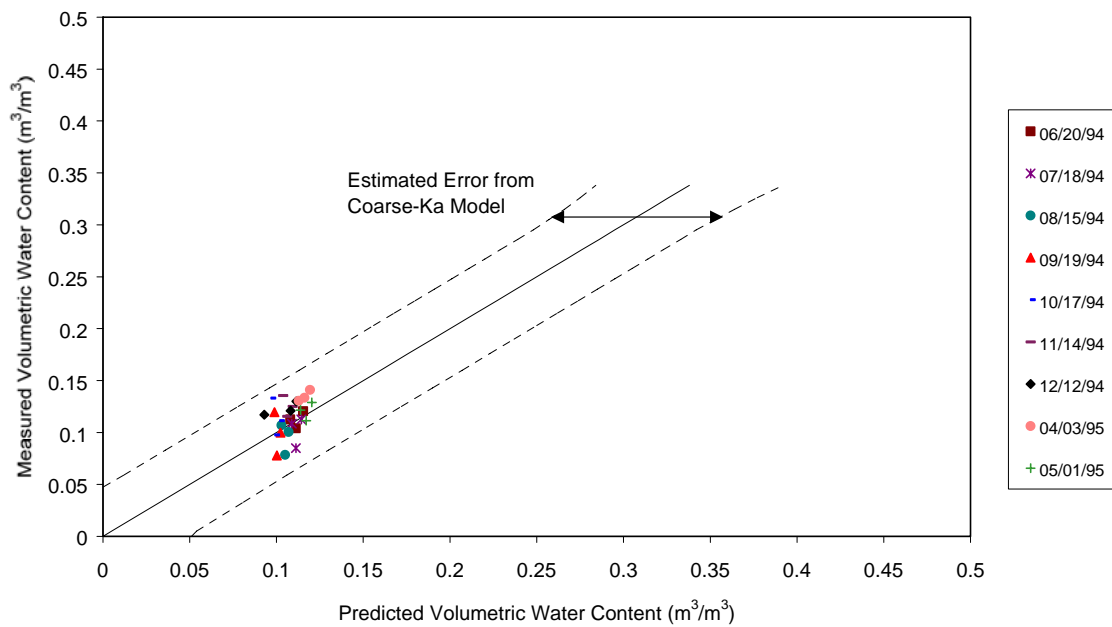


Figure 17. Measured versus Predicted Moisture Content – EICM version 2.6  
Minnesota (271018)



MAINE site - Base Course Material  
Experimental vs. Predicted Volumetric Water Content  
ICM Version 2.6 (Feb. 2000)



MAINE site - Subgrade Material  
Experimental vs. Predicted Volumetric Water Content  
ICM Version 2.6 (Feb. 2000)

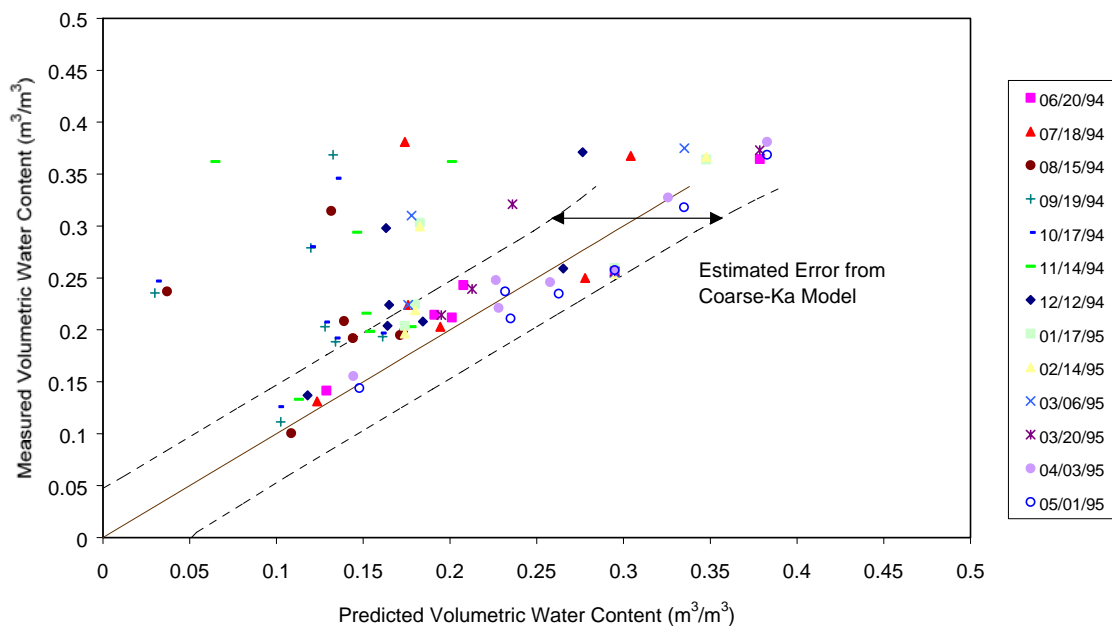


Figure 18. Measured versus Predicted Moisture Content – EICM version 2.6  
Maine (231026)

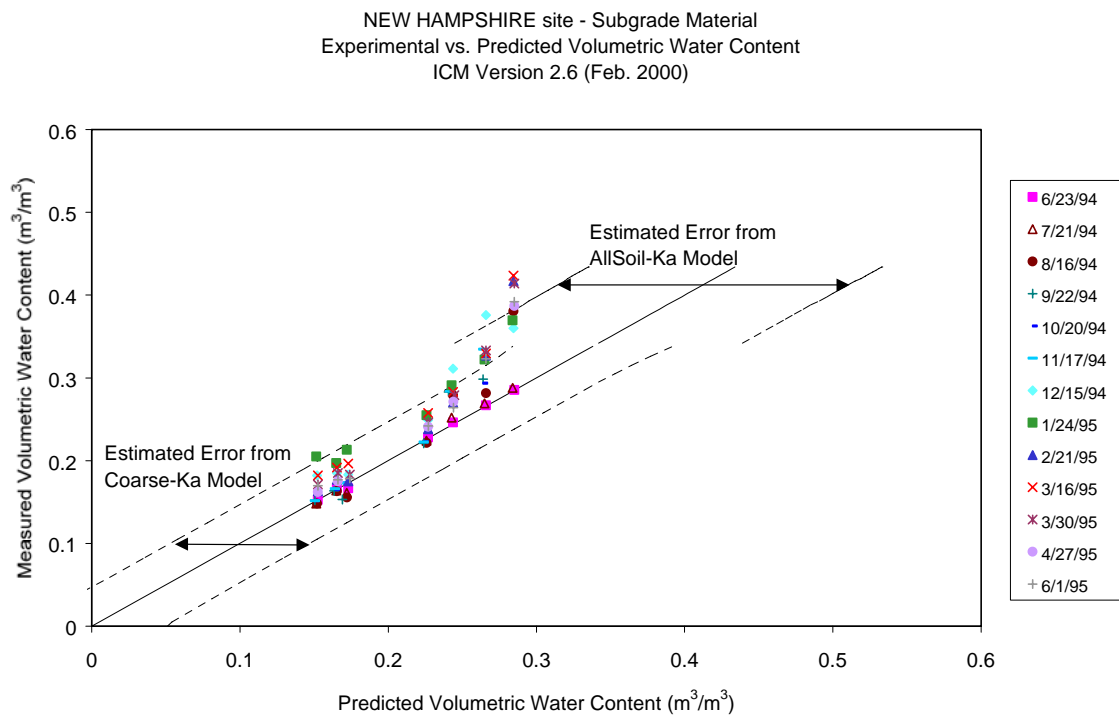
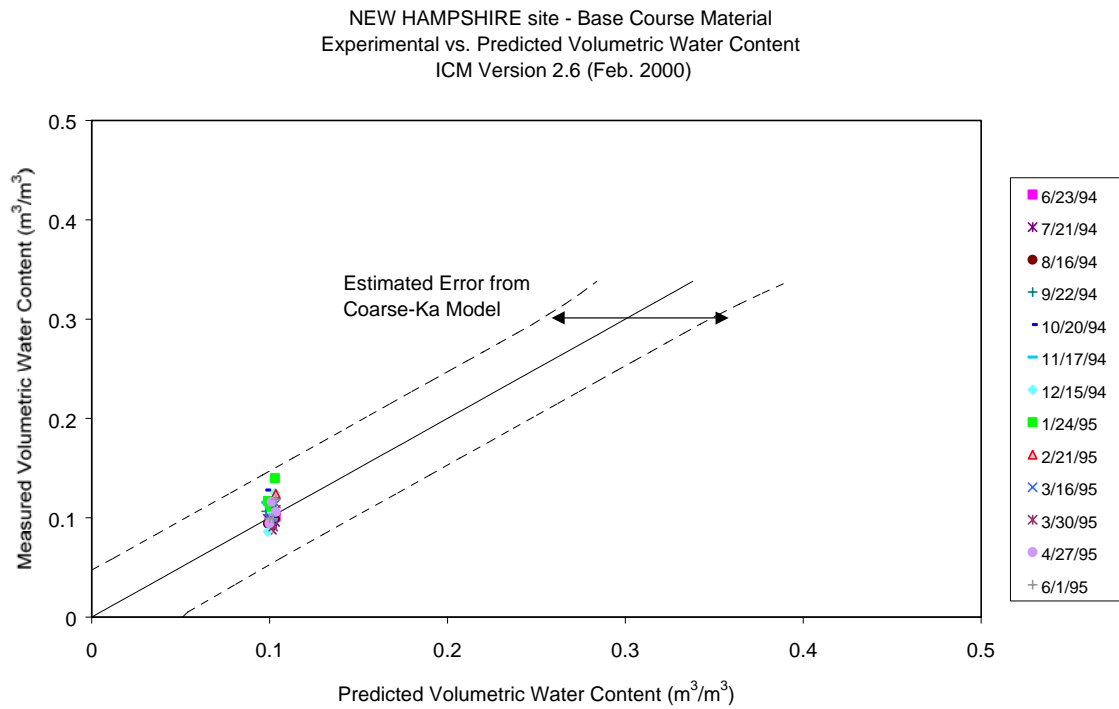
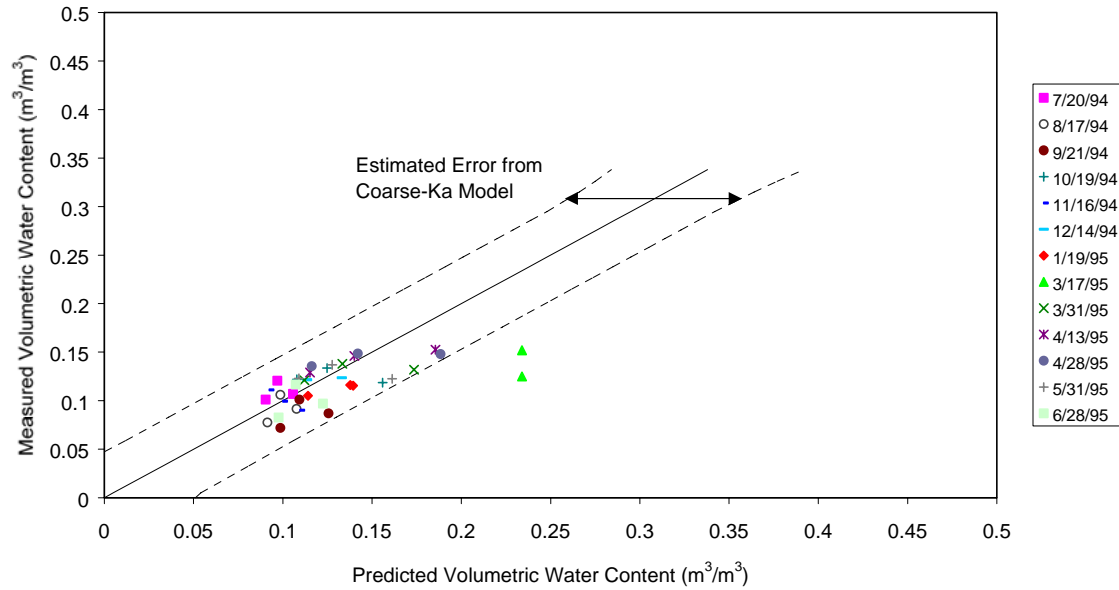


Figure 19. Measured versus Predicted Moisture Content – EICM version 2.6  
New Hampshire (331001)

VERMONT site - Base Course Material  
Experimental vs. Predicted Volumetric Water Content  
ICM Version 2.6 (Feb. 2000)



VERMONT site - Subgrade Material  
Experimental vs. Predicted Volumetric Water Content  
ICM Version 2.6 (Feb. 2000)

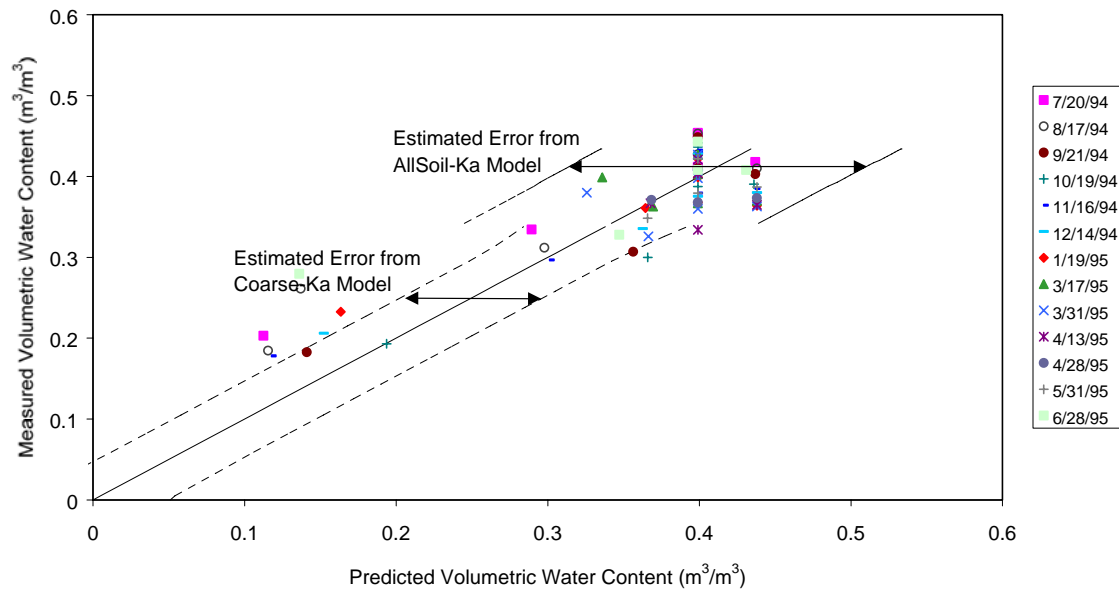
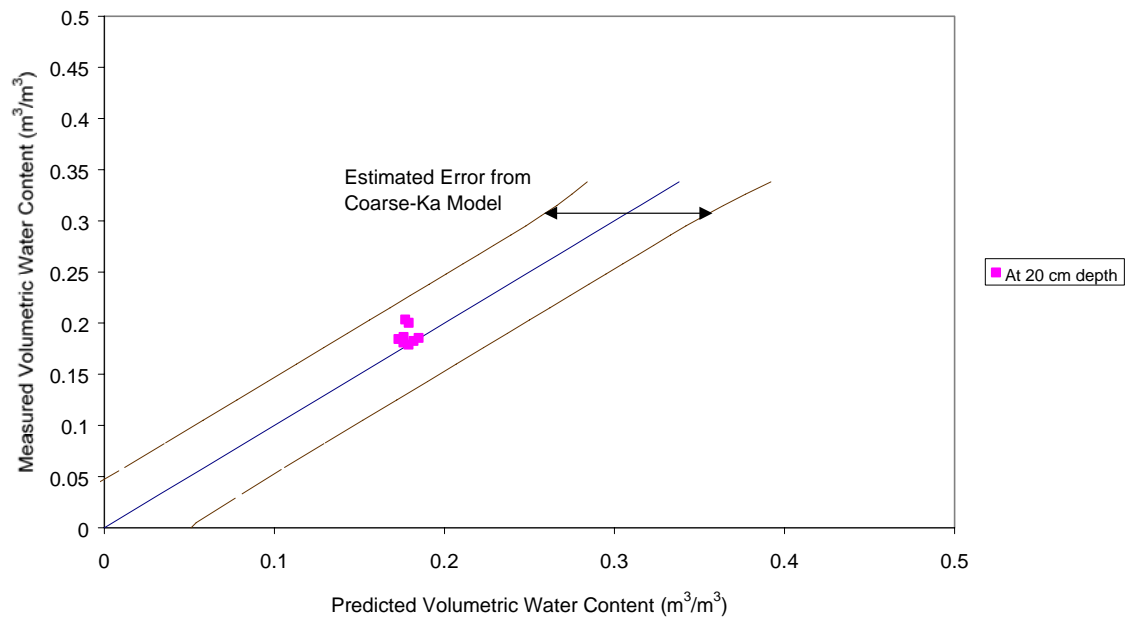


Figure 20. Measured versus Predicted Moisture Content – EICM version 2.6 Vermont (501002)

MANITOBA site - Base Course Material  
Experimental vs. Predicted Volumetric Water Content  
ICM Version 2.6 (Feb. 2000)



MANITOBA site - Subgrade Material  
Experimental vs. Predicted Volumetric Water Content  
ICM Version 2.6 (Feb. 2000)

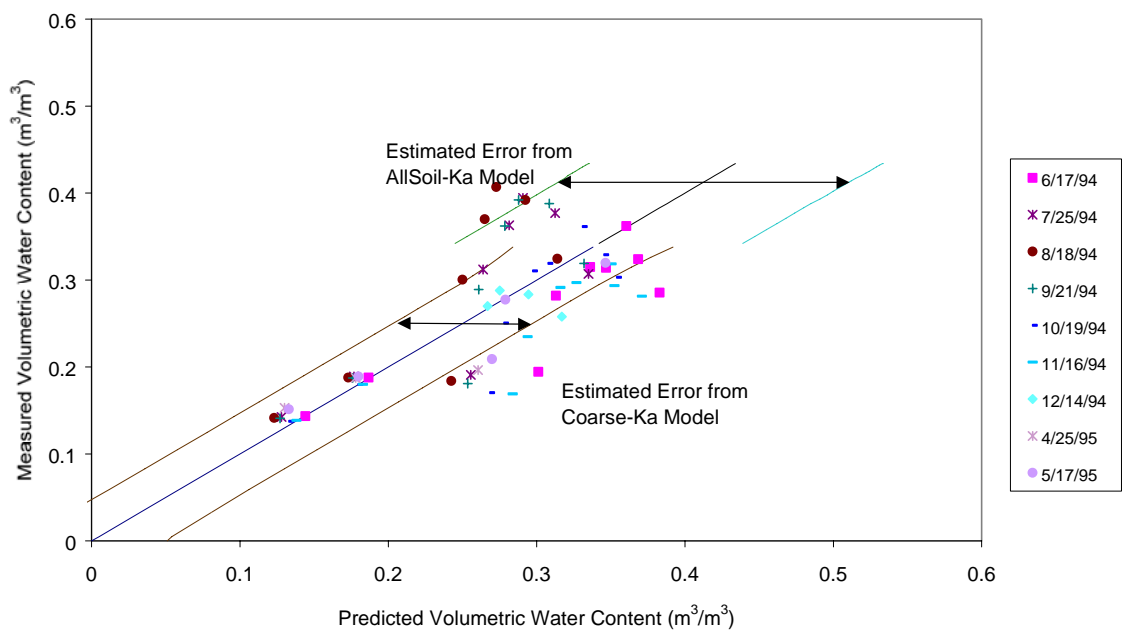


Figure 21. Measured versus Predicted Moisture Content – EICM version 2.6  
Manitoba (831801)

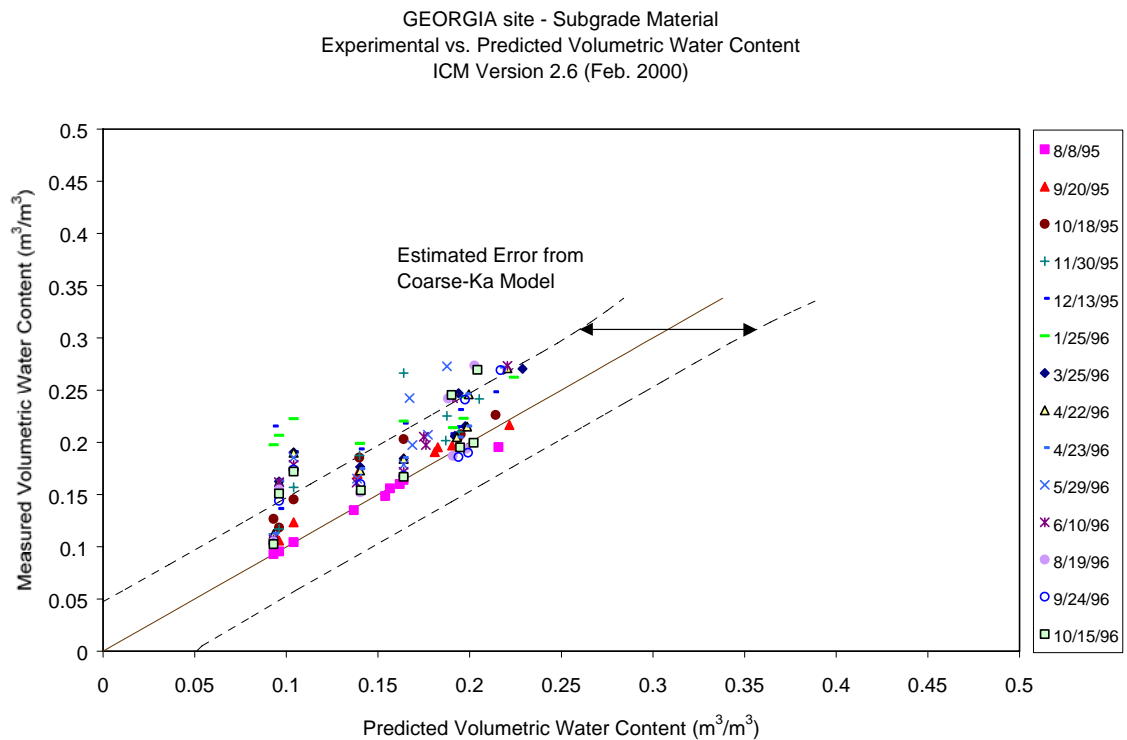
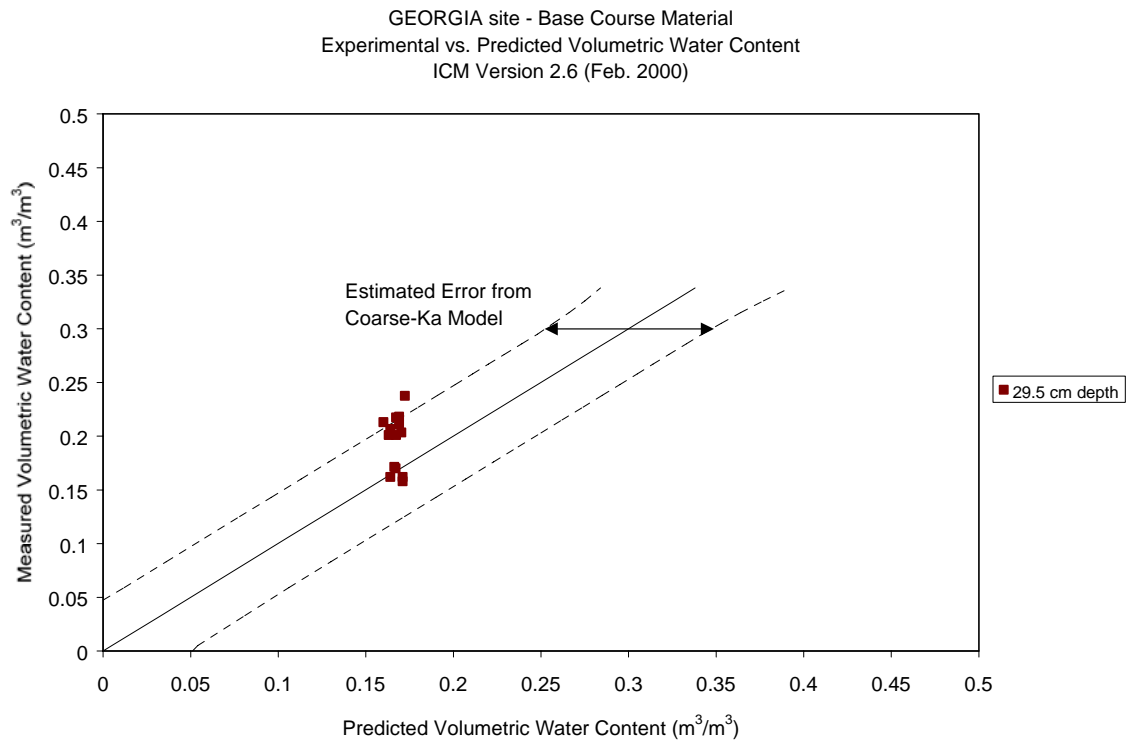
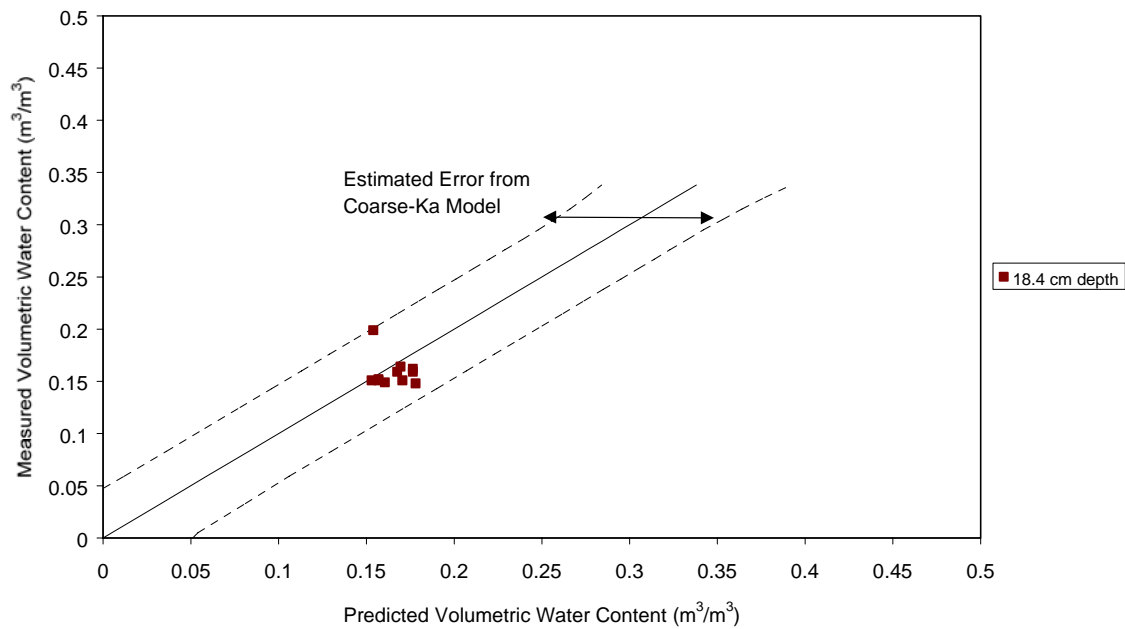


Figure 22. Measured versus Predicted Moisture Content – EICM version 2.6 Georgia (131005)

COLORADO site - Base Course Material  
Experimental vs. Predicted Volumetric Water Content  
ICM Version 2.6 (Feb. 2000)



COLORADO site - Subgrade Material  
Experimental vs. Predicted Volumetric Water Content  
ICM Version 2.6 (Feb. 2000)

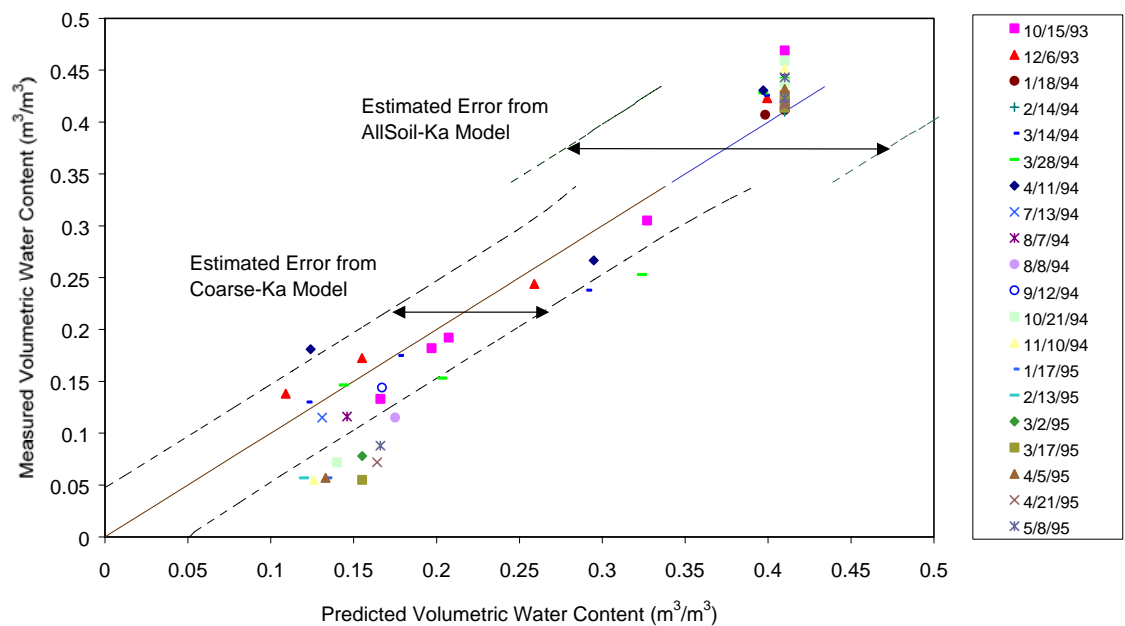
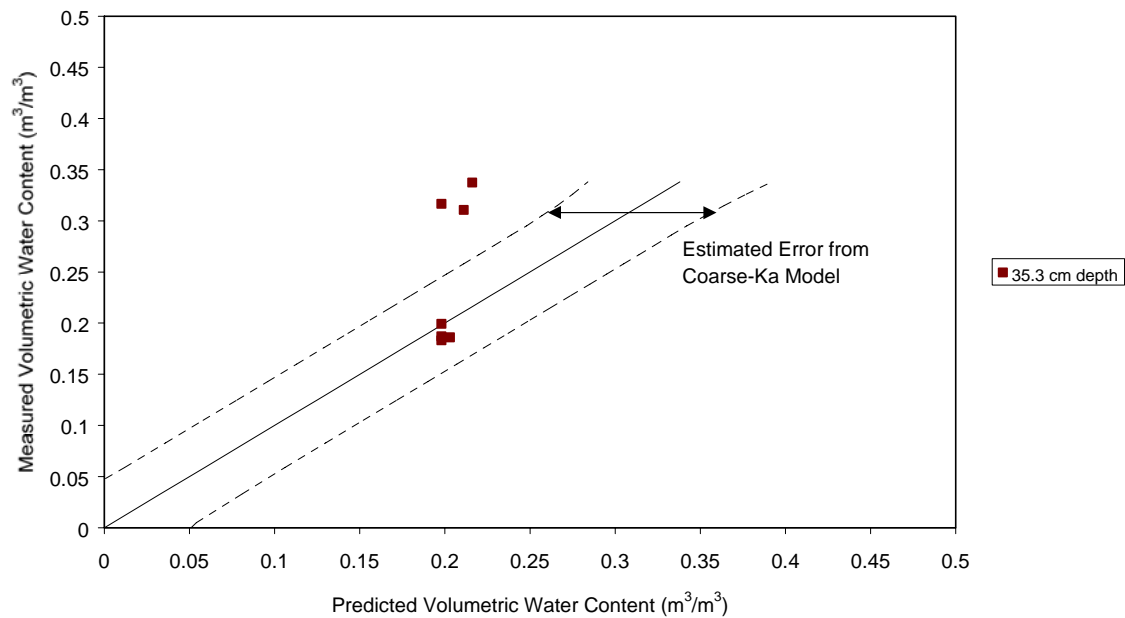


Figure 23. Measured versus Predicted Moisture Content – EICM version 2.6 Colorado (81053)

ARIZONA site - Base Course Material  
Experimental vs. Predicted Volumetric Water Content  
ICM Version 2.6 (Feb. 2000)



ARIZONA site - Subgrade Material  
Experimental vs. Predicted Volumetric Water Content  
ICM Version 2.6 (Feb. 2000)

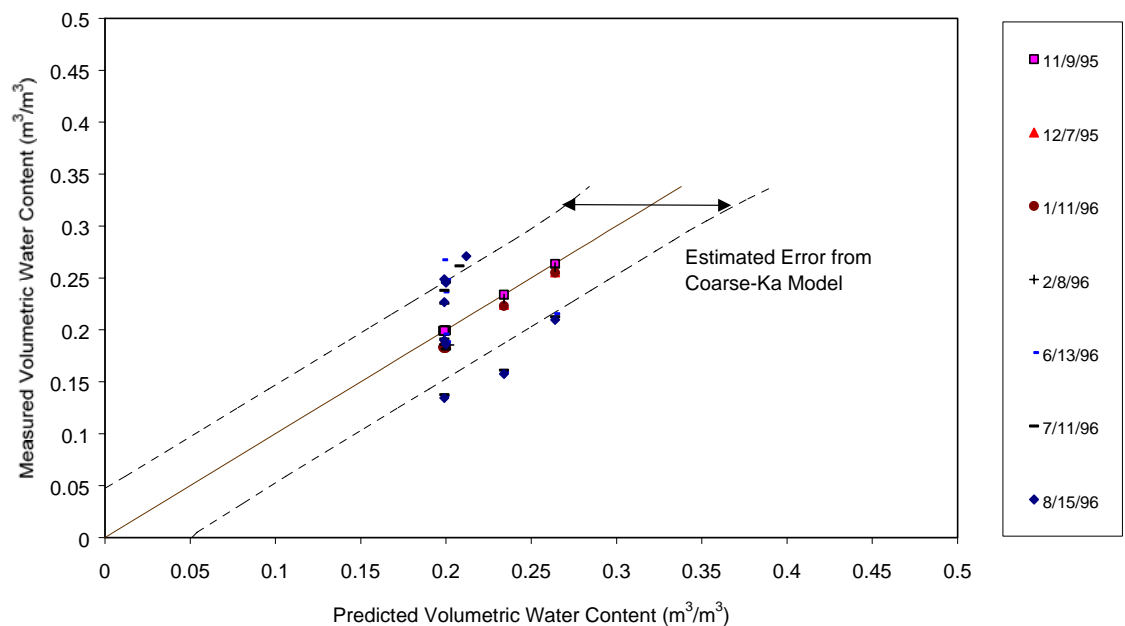
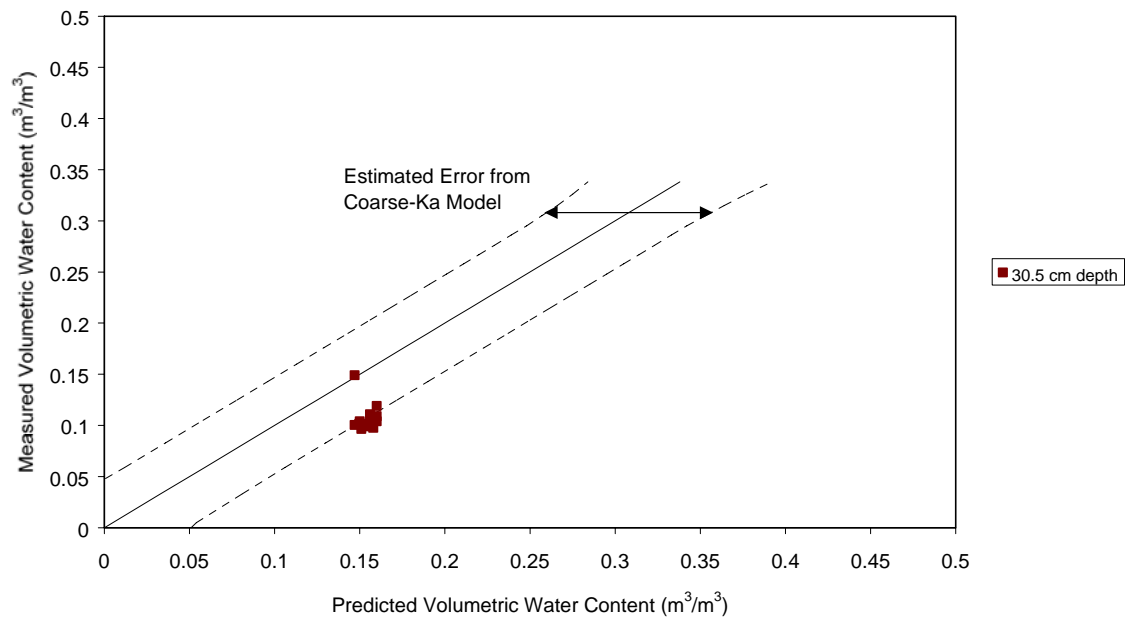


Figure 24. Measured versus Predicted Moisture Content – EICM version 2.6  
Arizona (41024)

TEXAS site - Base Course Material  
Experimental vs. Predicted Volumetric Water Content  
ICM Version 2.6 (Feb. 2000)



TEXAS site - Subgrade Material  
Experimental vs. Predicted Volumetric Water Content  
ICM Version 2.6 (Feb. 2000)

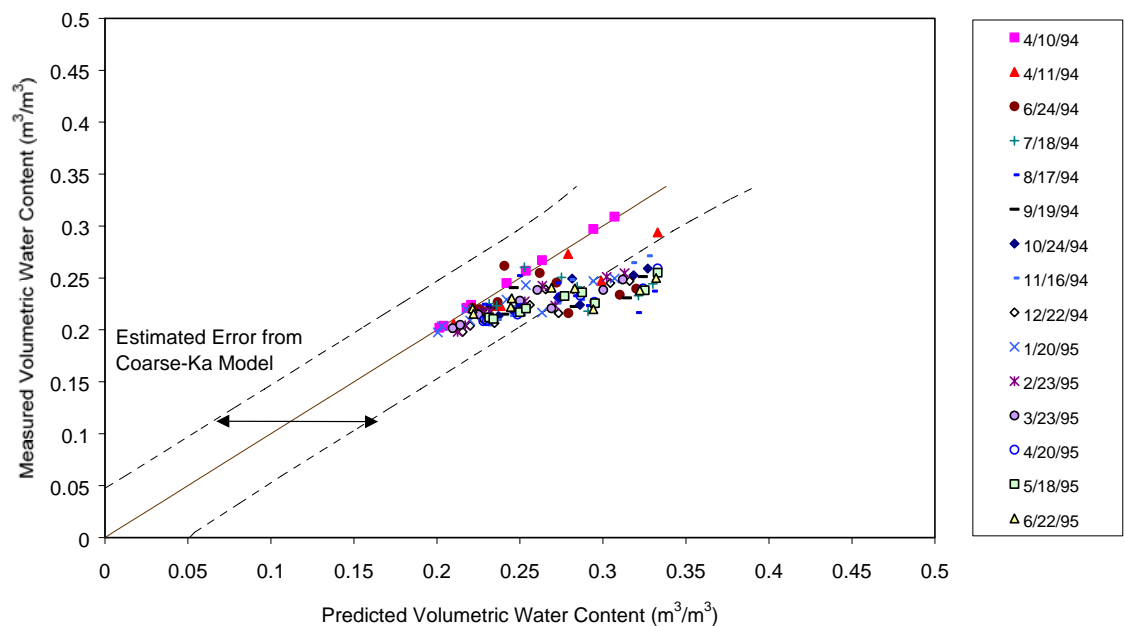


Figure 25. Measured versus Predicted Moisture Content – EICM version 2.6 Texas (481077)



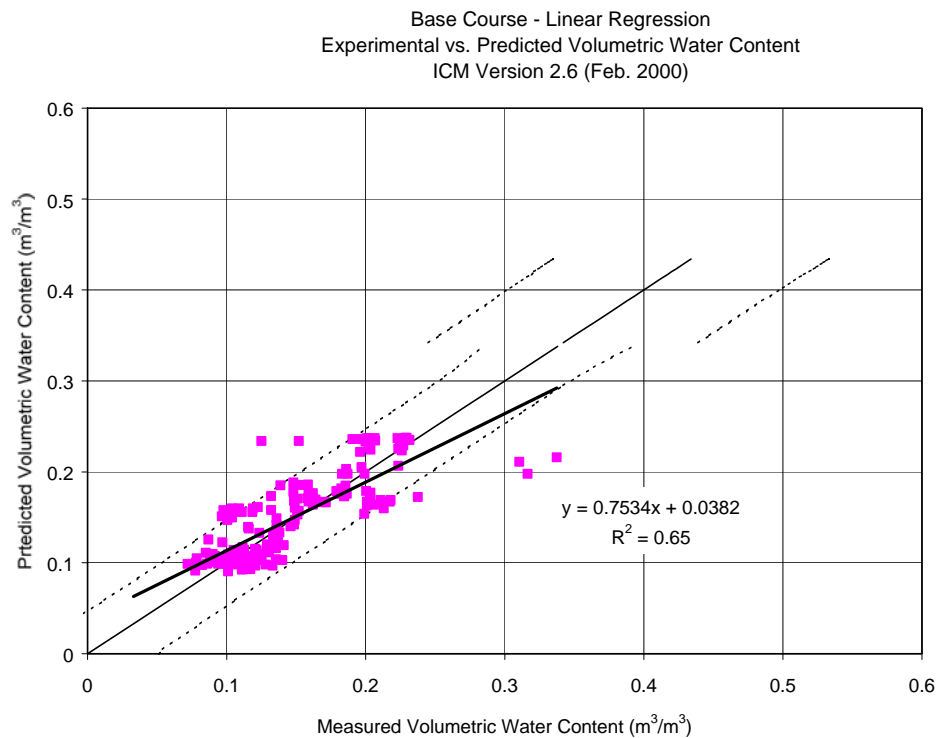
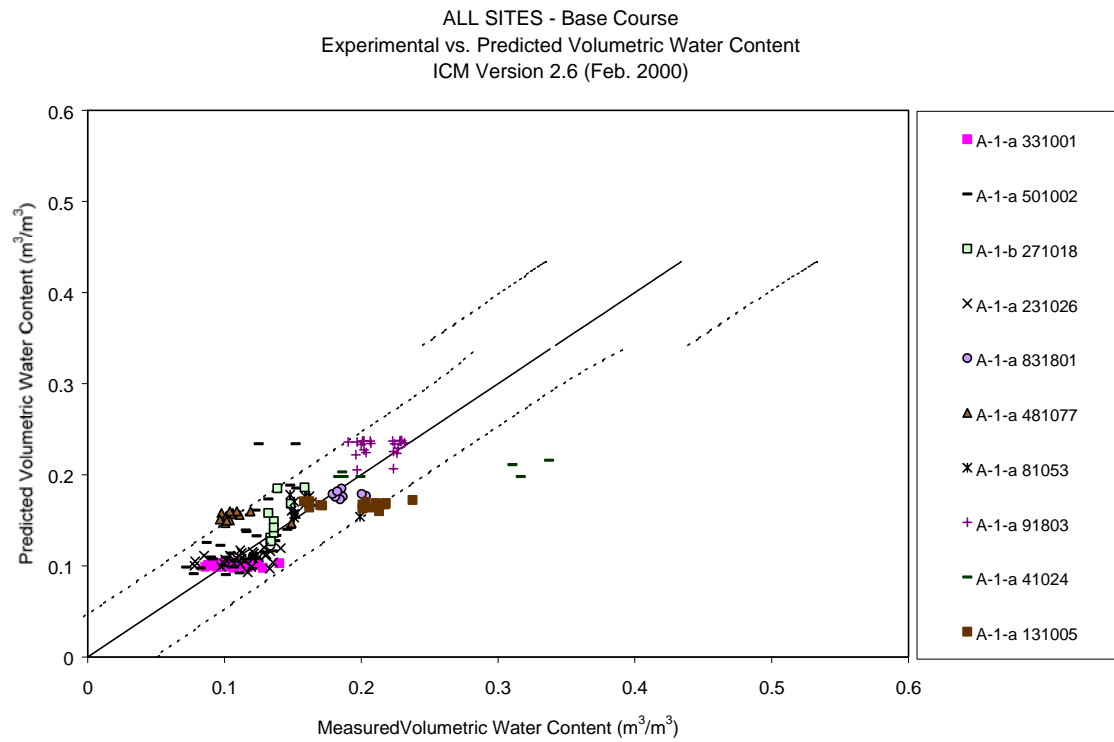


Figure 26. Summary of Measured versus Predicted Moisture Content for the Base Course Materials – EICM version 2.6

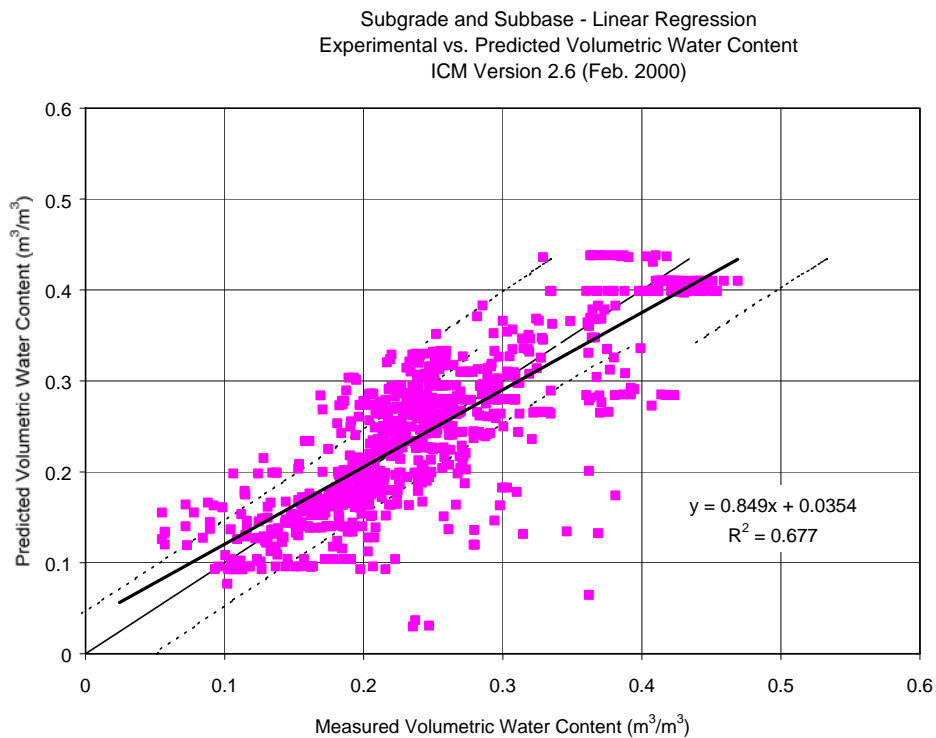
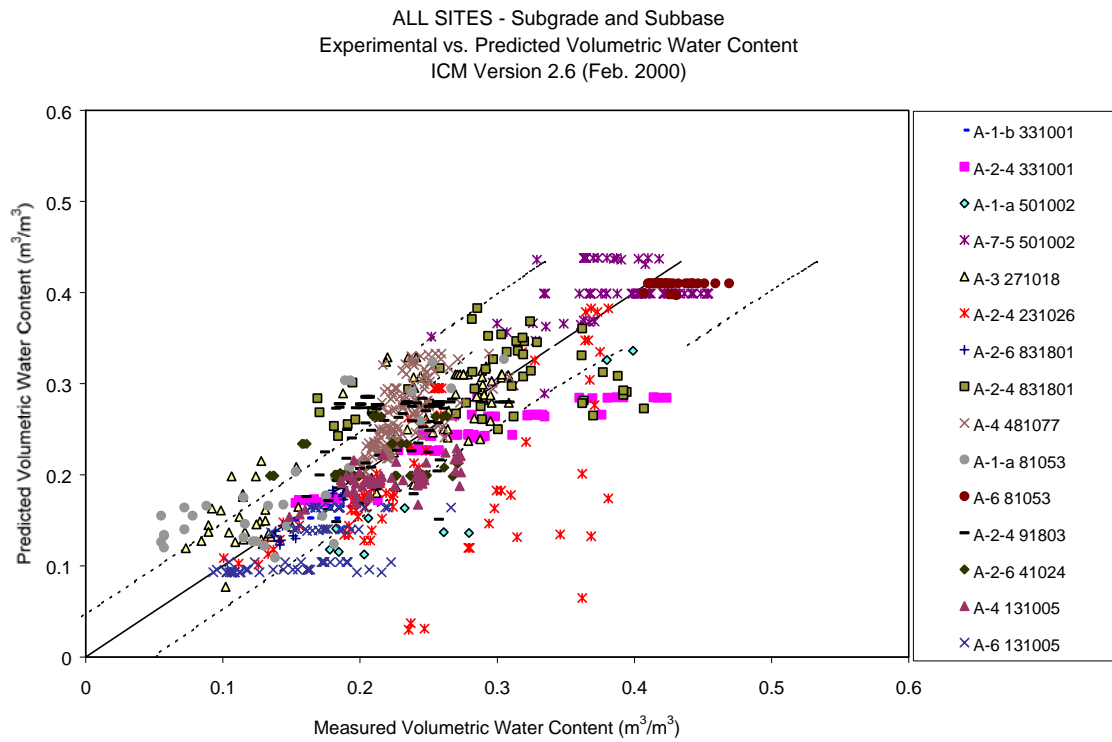


Figure 27. Summary of Measured versus Predicted Moisture Content for the Subgrade Materials – EICM version 2.6

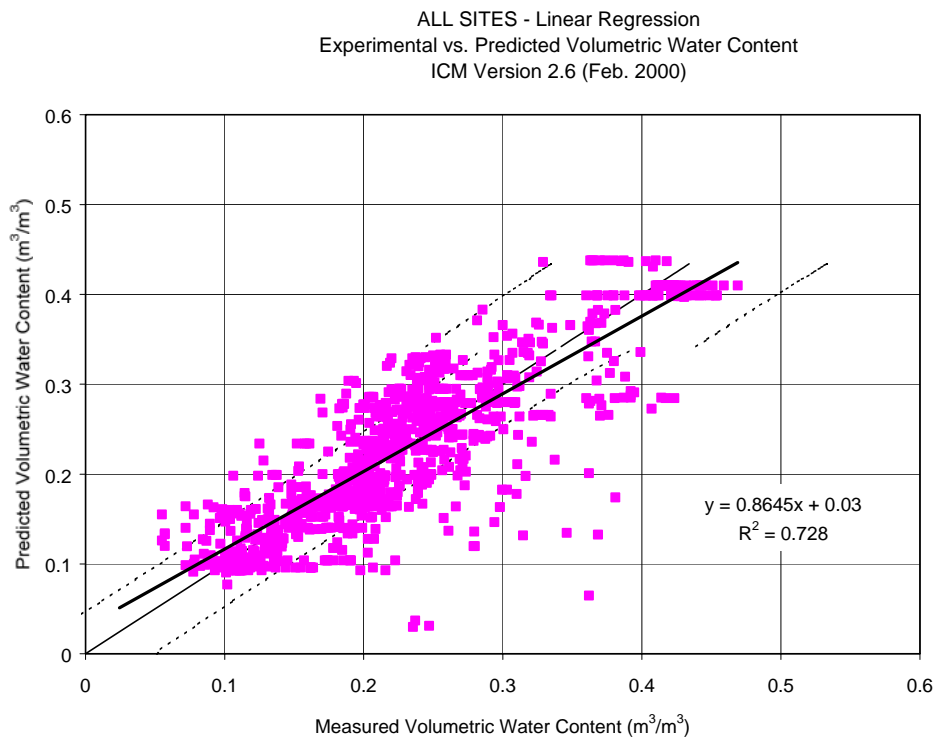
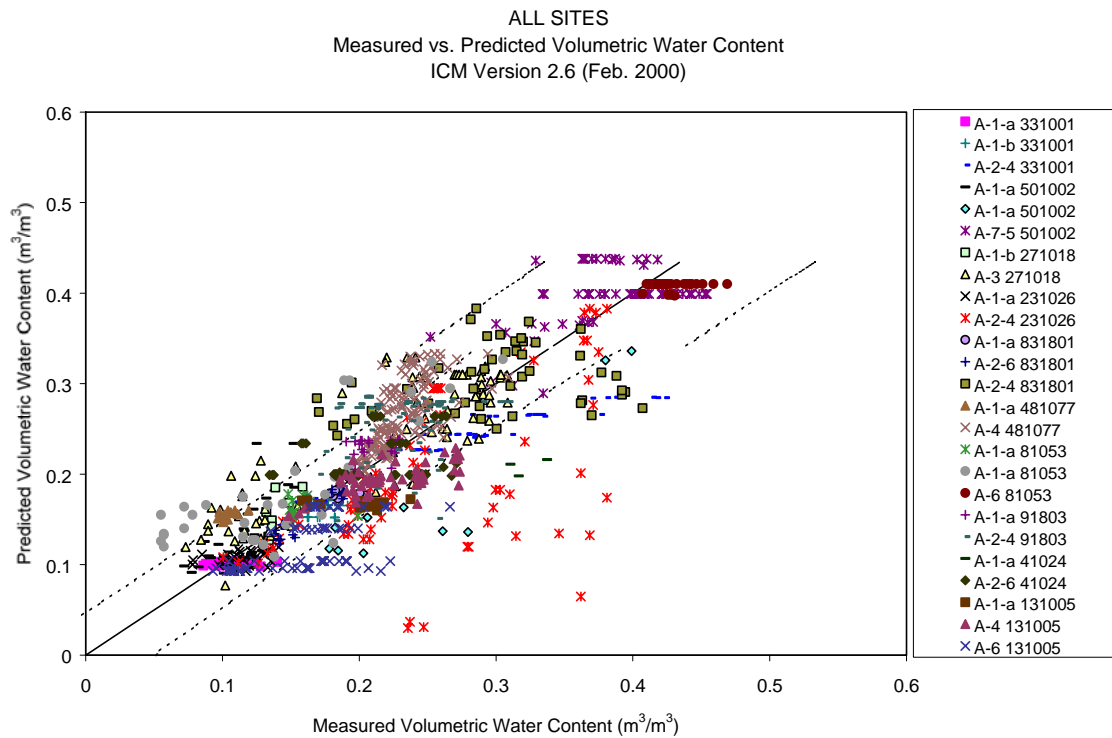


Figure 28. Summary of Measured versus Predicted Moisture Content for ALL sites – EICM version 2.6

---

## User's Guide and Recommendations

### EICM version 2.6 - Moisture Content Prediction

#### Introduction

Recommendations on how best to deal with the new features implemented to improve the model capability for moisture content predictions are presented in this Chapter. It is not the intention of the authors to provide the reader with a complete description of the EICM user's guide. For those interested in features other than the moisture content prediction, refer to the EICM User's Manual built into the program for complete information (Larson and Dempsey, 1997).

#### Input Parameters

The input parameters needed to run the EICM are essentially the same as those outlined in Chapter 2, Table 1. The main changes reside on the "Material Properties" and "Initial Temperature and Water Content Profiles" sections. [Table 9](#) shows the variables for the aforementioned sections and highlights the parameters added to the model. The input parameters for the remaining sections are unchanged from those presented in Table 1. The new parameters needed for the EICM version 2.6 will be briefly discussed in the following sections. For the rest of the parameters, please refer to the EICM's User Manual.

Several of the input variables for the soil layers have check boxes. If the box is checked, the associated input box is enabled and ready to accept input variables. If the box is unchecked, the EICM will either calculate or use a default value for the input variable in question. The accuracy of the EICM predictions are increased if material specific data is input, as opposed to the use of default values.

Table 9. Input Variables Needed by the EICM (version 2.6) for the Material Properties and Initial Temperature and Water Content Profiles Sections

Material Properties	
Variable	Notes
Classification	
Thickness	
Number of elements for this layer	
Porosity of layer material	Default or User-Defined
Specific Gravity	Default or User-Defined
Saturated permeability	Default or User-Defined
Dry density	Default or User-Defined
Dry thermal conductivity	Default or User-Defined
Dry heat capacity	Default or User-Defined
Coefficient of volume compressibility	Default or User-Defined
Plasticity index	Default or User-Defined
Percent Passing #200	Default or User-Defined
Diameter $D_{60}$	Default or User-Defined
Equilibrium volumetric water content	User Defined and Optional
Initial volumetric water content	User Defined and Optional
Resilient modulus	Frozen/Unfrozen. Default or User-Defined. Not used in moisture prediction.
Poisson's ratio	Eliminated from Version 2.6
Length of Recovery Period	For fine-grained soils. Default or User-Defined. Not used in moisture prediction.
Modulus Reduction	For fine-grained soils. Default or User-Defined. Not used in moisture prediction.
Initial Temperature and Water Content Profiles	
Variable	Notes
Output nodes	
Initial temperature profile	For the first day of the analysis. User Defined

## Soil Classification

The user may now select from the 12 categories given by the AASHTO Soil Classification System. The User's Manual provides details on how to build an Integrated Model pavement profile using the Add Layer dialog box.

## Thickness of the Layer

Input the thickness corresponding to the layer that has been added to the pavement profile. If information on initial water content is available at more than one depth within a subbase or subgrade layer, construct sub-layers around the measured points. Do not

subdivide the base course layer. More information is available under the Equilibrium Volumetric Water Content sub-section.

#### Number of Elements for this Layer

It is recommended that each layer be modeled with a minimum of two elements. In the validation of the EICM version 2.6, the elements or nodes were distributed every five cm. for layers less than 100 cm. thick. For layers thicker than 100 cm, elements every 10 cm. were used.

#### Porosity of the Layer Material

Porosity is not a property that can be measured directly in the field unless moisture measurements are made below the groundwater table. The porosity is calculated from the dry density  $\rho_{dry}$ , and the specific gravity,  $G_s$ , of the soil by the following equation:

$$\theta_{sat} = \left( 1 - \frac{\rho_{dry}}{G_s \rho_{water}} \right) \dots\dots\dots (19)$$

Where:

$\theta_{sat}$  = saturated volumetric water content = porosity of the soil

$\rho_{dry}$  = dry density

$G_s$  = specific gravity

$\rho_{water}$  = density of water (1 gm/cm<sup>3</sup>)

[Table 10](#) summarizes the possibilities for proper estimation the porosity depending on the soil properties available. If both soil properties, dry density and specific gravity, are available, the user needs to input them, and disable the porosity checkbox. The EICM will calculate the porosity automatically by using equation 19.

For those cases when the dry density is known, but the specific gravity unknown, the user inputs the dry density and the EICM automatically calculates the specific gravity by using equation 16, provided the wPI of the soil is known. Then the EICM automatically calculates the porosity by using equation 19. Again, disable the porosity checkbox. In cases where the wPI is unknown, input the dry density and disable the porosity, specific

gravity, and wPI (% Passing #200 and PI) checkboxes. EICM will use the default value for  $G_s$  from Table 5 and automatically calculate  $\theta_{sat}$  by using equation 19.

Table 10. Options for Determining the Porosity of the Layer, Depending on the Known Soil Properties

Known Parameters	Unknown Parameters	Key in		What to Do and What EICM Does
		Enable	Disable	
$\rho_{dry}$ , $G_s$		$G_s$	$\theta_{sat}$	Input $G_s$ and $\rho_{dry}$ . EICM calculates $\theta_{sat}$ automatically by using equation 19
$\rho_{dry}$ , wPI	$G_s$	%Pass #200, PI	$\theta_{sat}$ , $G_s$	Input $\rho_{dry}$ , %Pass #200, and PI. EICM automatically calculates $G_s$ by using equation 16, and $\theta_{sat}$ by using equation 19
$\rho_{dry}$	$G_s$ , wPI		$\theta_{sat}$ , $G_s$ , %Pass #200, PI	Input $\rho_{dry}$ . EICM uses the default value for $G_s$ from Table 5 and calculates $\theta_{sat}$ automatically by using equation 19
$G_s$	$\rho_{dry}$	$G_s$	$\theta_{sat}$	Input $G_s$ . EICM uses the default $\rho_{dry}$ from Table 5 and automatically calculates $\theta_{sat}$ by using equation 19
wPI	$\rho_{dry}$ , $G_s$	%Pass #200, PI	$\theta_{sat}$ , $G_s$	Input %Pass #200, and PI. EICM uses the default $\rho_{dry}$ from Table 5, calculates $G_s$ by using equation 16, and $\theta_{sat}$ by using equation 19
	$\rho_{dry}$ , $G_s$ , wPI		$\theta_{sat}$ , $G_s$ , %Pass #200, PI	EICM uses the default $\theta_{sat}$ from Table 5 which was calculated by equation 9
	$\rho_{dry}$ , $G_s$ , wPI	$\theta_{sat}$	$G_s$ , %Pass #200, PI	Input $\theta_{sat}$ if saturated volumetric water content is available from an adjacent point below the water table.

For those cases when the dry density is unknown, but the  $G_s$  is known, input  $G_s$  and disable the porosity checkbox. The EICM will use the default dry density from Table 5 and automatically calculate  $\theta_{sat}$  by using equation 19.

In cases where both the dry density and the specific gravity are unavailable, but the wPI is known, disable the porosity and specific gravity checkboxes, and input % Passing #200 and PI. The EICM will use the default dry density from Table 5, calculate  $G_s$  by using equation 16, and automatically calculate the porosity by using equation 19. If the wPI is unknown, disable the porosity, specific gravity, % Passing #200, and PI checkboxes. The EICM will use the default value for porosity from Table 5. This last option provides the least accurate estimate of  $\theta_{sat}$ , of course.

In the event that data on the volumetric moisture content below the water table are available, the saturated volumetric moisture content may provide a reasonable estimate of porosity for sublayers having the same composition, gradation, and porosity. Where these conditions exist, and no other information is available, the porosity checkbox may be

enabled, and the moisture content below the water table may be entered as the best available estimate of porosity.

## Specific Gravity

If the specific gravity of the solids is known, enable the checkbox and input the known value. In those cases where the  $G_s$  is unknown but the wPI is known, disable the  $G_s$  checkbox and the EICM will calculate  $G_s$  automatically by using equation 16.

In those cases when both, the  $G_s$  and the wPI are unknown, disable the  $G_s$ , % Passing #200 and PI checkboxes and the EICM will automatically use the default value for  $G_s$  from Table 5. The options for entering the specific gravity are summarized in [Table 11](#).

Table 11. Options for Determining the Specific Gravity of the Layer, Depending on the Known Soil Properties

Known Parameters	Unknown Parameters	Key in		What to Do and What EICM Does
		Enable	Disable	
$G_s$		$G_s$		Input $G_s$
wPI	$G_s$	%Pass #200, PI	$G_s$	Input %Pass #200 and PI. EICM automatically calculates $G_s$ by using equation 16.
	$G_s$ , wPI		$G_s$ , %Pass #200, PI	EICM automatically uses the default $G_s$ from Table 5

## Saturated Permeability

If the saturated permeability (hydraulic conductivity) is known, enable the checkbox and input the value. Otherwise, disable the  $k_{sat}$  checkbox and the EICM will calculate it by using equation 15, provided the wPI,  $D_{60}$ , or AASHTO classification is known.

## Dry Density

The EICM does not have the option for enabling/disabling the dry density checkbox given the fact that this property is used in other features of the program besides the water content predictions. If the dry density of the soil is known then enter it. Otherwise, the EICM will utilize a default value every time the user creates a layer or sub-layer. The default values, which vary with the AASHTO Soil Classification System, are presented in Table 5.



## Plasticity Index

Enable the Plasticity Index (PI) checkbox if the value is known. Otherwise, disable the checkbox and the EICM will show and use a default value every time the user creates a layer or sub-layer. The default values can be seen on [Table 5](#) and are a function of the AASHTO Soil Classification System.

If the soil is nonplastic, enable the PI checkbox and input 0.

The accuracy of the SWCC greatly depends on the Plasticity Index if the initial water content is not available as will be explained later. Particularly if the initial water content is unknown, it is recommended to perform the Atterberg Limits test to define the PI rather than approximate it by Visual Classification. Refer to [Table 12](#) for more information on how the EICM determines the SWCC based on PI information.

Table 12. Determination of the SWCC based on Percentage Passing #200, Plasticity Index and Diameter  $D_{60}$

Are any of the Following Parameters known?	If	What to Do?	What Does the EICM Do?
%Pass #200 PI $D_{60}$	Yes	Enable the appropriate checkboxes and input the known parameters	EICM assigns default values for the checkboxes that have been disabled, or calculates unknown values from known values as outlined in Tables 10 and 11. If $wPI=0$ , EICM uses eqs. 10 to 13 to define the SWCC. Otherwise, it calculates the SWCC by using eqs. 4 to 7
	No	Disable the checkboxes for the unknown parameters	

## Percent Passing #200

The fines content of the soil is another property that is important to the SWCC of the soil. Enable the Percent Passing #200 checkbox if the value is known. Otherwise, disable the checkbox and the EICM will use a default value based on the AASHTO Soil Classification System. It is recommended to perform a Sieve Analysis or the Standard Test Method for Materials Finer than #200 Sieve by Washing in order to obtain a more accurate prediction. Refer to [Table 12](#) for more information on how the EICM determines the SWCC based on Percent Passing #200 information.

## Diameter $D_{60}$

$D_{60}$  is the grain diameter (in mm) corresponding to 60% passing, by weight or mass, on the Grain Size Distribution Curve. In other words, 60% of the particles by weight are smaller than the diameter  $D_{60}$ . Having the  $D_{60}$ , the user enables the checkbox and inputs the value. Otherwise, the EICM will use a default value based on the AASHTO Soil Classification System. As is the case with the Percent Passing #200 and PI, the  $D_{60}$  is important in the determination of the SWCC. Therefore, it is recommended to perform a Sieve Analysis instead of using the default parameters. Refer to [Table 12](#) for more information on how the EICM determines the SWCC based on  $D_{60}$  information.

## Initial Volumetric Water Content

The initial water content ( $\theta_o$ ) is the water content at the start of the program or that at the first day of the analysis. If a value is specified, the entire layer will be set to that water content. [Table 13](#) presents information on how the EICM deals with the  $\theta_o$  data. If the  $\theta_o$  checkbox is enabled, then the water content will march from the given initial value toward the equilibrium water content (explained in the following sub-section) with time. On the other hand, if the  $\theta_o$  checkbox is disabled, the program sets  $\theta_o$  equal to the equilibrium water content.

## Equilibrium Volumetric Water Content

The equilibrium volumetric water content ( $\theta_{eq}$ ) is strongly tied to the SWCC of the soil. It is therefore recommended to perform measurements of water content for each layer in the pavement profile. Care should be taken to enter the equilibrium volumetric water content,  $\theta_{eq}$ , rather than the equilibrium gravimetric water content,  $\omega_{eq}$ . If  $\omega_{eq}$  is available, manually calculate the volumetric water content by the following equation, and then enter the calculated value:

$$\theta_{eq} = \frac{\omega_{eq} \rho_{dry}}{\rho_{water}} \dots\dots\dots (20)$$

Where:

$\theta_{eq}$  = equilibrium volumetric water content

$\omega_{eq}$  = equilibrium gravimetric water content

$\rho_{dry}$  = dry density

$\rho_{\text{water}}$  = density of water (1gm/cm<sup>3</sup>)

If more than one  $\theta_{\text{eq}}$  is available for a subbase or subgrade layer, subdivide the layer into sub-layers in such a way that the measured  $\theta_{\text{eq}}$  is more or less in the middle of the sub-layer. If only one value of  $\theta_{\text{eq}}$  is available per layer, there is no need to create sub-layers, provided that the layer is believed to be homogeneous with respect to composition, gradation, density, etc.

Base layers should NOT be divided into sublayers. Instead, if multiple moisture observations are available for the base layer, the mean value should be used.

Table 13 presents guidelines on how to deal with each of several possible combinations of known and unknown values of  $\theta_o$  and  $\theta_{\text{eq}}$ , for the cases when EICM calculated values are to be compared to TDR measured values. If the  $\theta_{\text{eq}}$  checkbox is enabled, the EICM will use this value to adjust the SWCC for the corresponding layer or sub-layer. On the other hand, if the  $\theta_{\text{eq}}$  checkbox is disabled, the EICM will calculate this value from a linear distribution of pore pressure above the groundwater table and no adjustment to the SWCC will occur.

Table 13. Available Options for the Initial and Equilibrium Water Contents

Known Parameters	Unknown Parameters	Key in		What to Do and What EICM Does
		Enable	Disable	
$\theta_o$ $\theta_{\text{eq}}$		$\theta_o$ $\theta_{\text{eq}}$		Input the $\theta_o$ and the $\theta_{\text{eq}}$ . EICM will use the $\theta_{\text{eq}}$ to adjust the SWCC and then the water content will march from the $\theta_o$ toward the $\theta_{\text{eq}}$ with time.
$\theta_o$	$\theta_{\text{eq}}$	$\theta_o$	$\theta_{\text{eq}}$	Input the $\theta_o$ . The $\theta_o$ will be assigned to the entire layer. EICM will calculate the $\theta_{\text{eq}}$ from a linear distribution of pore pressures above the groundwater table. No adjustment to the SWCC will occur and it will be determined solely by the wPI or $D_{60}$ . The water content will march from the $\theta_o$ toward the calculated $\theta_{\text{eq}}$ with time.
$\theta_{\text{eq}}$	$\theta_o$	$\theta_{\text{eq}}$	$\theta_o$	Input the $\theta_{\text{eq}}$ . The SWCC will be adjusted accordingly to the $\theta_{\text{eq}}$ . The EICM will assume the $\theta_o$ to be the same as the $\theta_{\text{eq}}$ .
	$\theta_o$ $\theta_{\text{eq}}$		$\theta_o$ $\theta_{\text{eq}}$	No adjustment of the SWCC will occur. . EICM will calculate the $\theta_{\text{eq}}$ from a linear distribution of pore pressures above the groundwater table and then set the $\theta_o$ equal to the $\theta_{\text{eq}}$ .

The preceding guidelines and suggestions were aimed at maximizing the accuracy with which the EICM will predict seasonal oscillations in moisture content in pavement layers. All recommendations were predicated on the following:

- 1) Predictions were to be compared with TDR measured values for existing pavements.
- 2) Seasonal oscillations were of primary interest, rather than the equilibrium value – which justifies treatment of the first-available TDR reading as  $\theta_{eq}$ , rather than using EICM to predict  $\theta_{eq}$ .

Chapter 6, which follows, is aimed at prediction of the most likely initial condition,  $\theta_o$ , but through use of the initial degree of saturation,  $S_o$ . The second objective pursued in Chapter 6 is that of predicting  $\theta_{eq}$ , but in terms of degree of saturation,  $S_{equil}$ . The tracking of seasonal oscillations in moisture content is de-emphasized. The reason for this change in emphasis in Chapter 6 is as follows:

Preliminary analyses, made after the work of Chapters 2 through 5 was completed, showed that the effects of seasonal moisture content variations on  $M_R$  were typically minor. The change from the initial condition,  $S_o$ , to the equilibrium condition,  $S_{equil}$ , typically produces the greatest change in  $M_R$ .

# Development of Procedures for Estimating Moisture Content Changes from the Initial State to Equilibrium Conditions for Newly Constructed Pavements

## Introduction

The initial conditions at which bases, subbases, and subgrades are compacted are defined by the dry unit weight, moisture content, and specific gravity of solids. These interrelationships are given by equations (21) and (22).

$$S_e = wG_s \dots\dots\dots (21)$$

$$\gamma_{\text{dry}} = \frac{G_s \gamma_w}{1 + e} \dots\dots\dots (22)$$

Where:

$S$  = degree of saturation

$e$  = void ratio

$w$  = gravimetric moisture content

$G_s$  = specific gravity of solids

$\gamma_{\text{dry}}$  = dry unit weight

$\gamma_w$  = unit weight of water

In equation (21) any three parameters determine the fourth. Thus, for example,  $e$  can be computed from equation (21) and  $e$  and  $G_s$  can be used to get  $\gamma_{dry}$  in equation (22).

The density and water content at which unbound materials are actually compacted in pavement sections are controlled by compaction specifications. It is very common practice to require that subbases and subgrades be compacted to at least 95% of and sometimes 100% of  $\gamma_{dry\ max}$  by T99 (Standard Proctor effort). Bases are commonly required to be more than 95% of the  $\gamma_{dry\ max}$  by T180 (Modified Proctor effort). Because contractors typically compact a little above the required minimum it is reasonable to assume that average initial conditions with respect to density are  $\gamma_{dry\ max}$  (T99) for subbases and subgrades and  $\gamma_{dry\ max}$  (T180) for bases. The water content is not usually controlled strictly, but contractors are encouraged to wet materials to a point near the line of optimums to facilitate compaction. Therefore, it is likewise reasonable to assume that initial compaction conditions for water content are  $w_{opt}$  by T99 for subbases and subgrades and  $w_{opt}$  by T180 for bases.

The preceding discussion relates to density and moisture content as initial conditions for compacted pavement layers in the field. On a different but related note, data from the literature on resilient modulus ( $M_R$ ) obtained from laboratory compaction has been thoroughly studied. This study shows that most lab specimens for  $M_R$  testing were compacted at  $\gamma_{dry\ max}$  and  $w_{opt}$ . Therefore, the database for  $M_R$  values has more data points at optimum conditions ( $\gamma_{dry\ max}$  and  $w_{opt}$ ) than at any other condition and is a logical choice as a reference condition for  $M_R$ . For the reasons stated above, optimum conditions have been chosen as a best estimate of initial compaction conditions in the field and as a reference state for estimating changes in  $M_R$  due to moisture content changes.

### Correlation for $S_{opt}$

Because of the importance of optimum conditions, it is desirable to be able to estimate the degree of saturation at optimum,  $S_{opt}$ , from index properties. Because  $w_{PI}$  and  $D_{60}$  were used for the SWCC parameters, they were used again for the correlations that follow.

Figure 29 shows a plot of  $S_{opt}$  versus  $w_{PI}$  for a modest-sized database available to the authors (Witczak and Yau, 1997). Most engineers with experience in compaction testing would assert that  $S_{opt}$  normally falls between 80 and 88%. These data are generally consistent with that assertion, and an average value of about 85% could easily be adopted. However, it is logical that  $S_{opt}$  should increase slightly with  $w_{PI}$ . At low values of  $S$  the soil water suction is high and tends to prevent particles from sliding past each other,

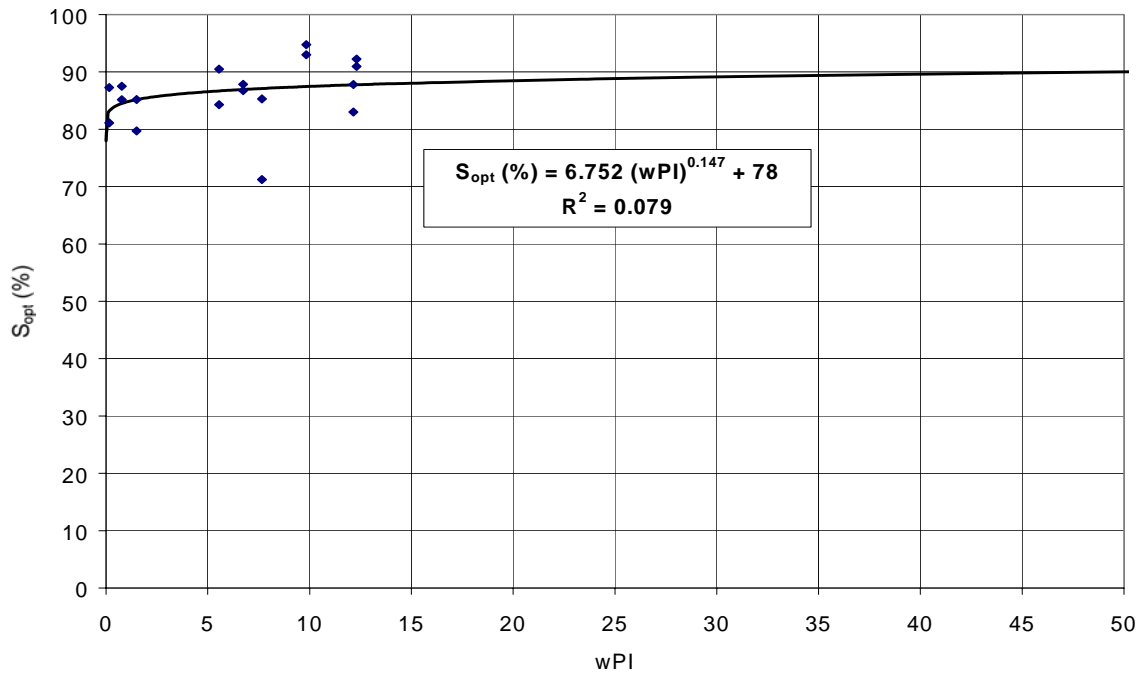


Figure 29. Correlation between Degree of Saturation at Optimum and wPI

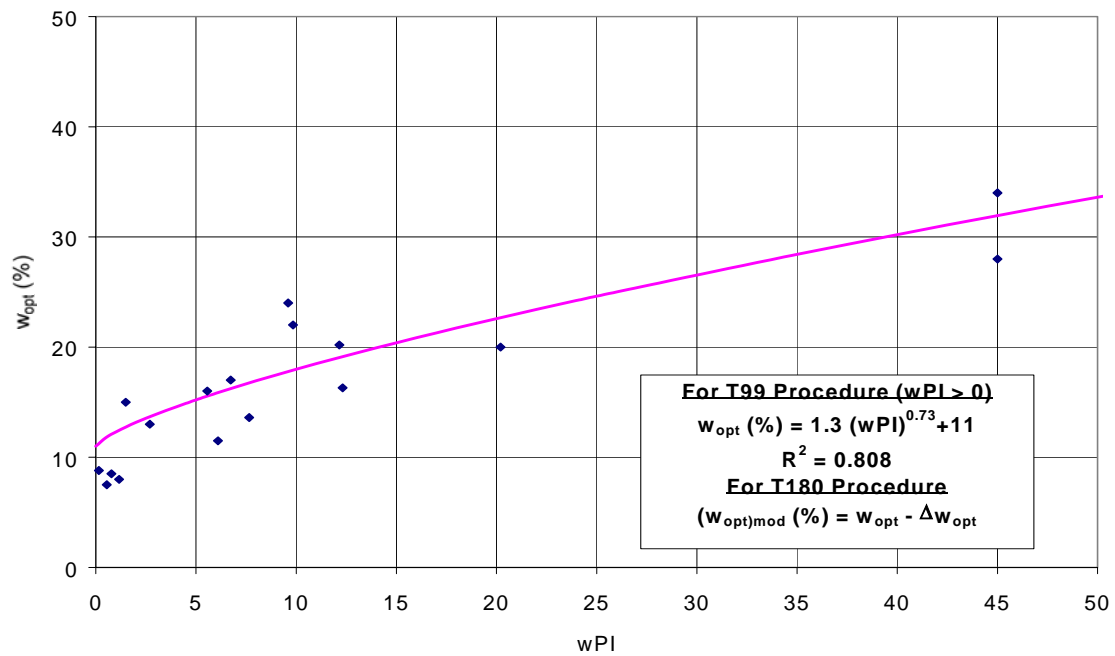


Figure 30. Correlation between Gravimetric Water Content at Optimum and wPI

into a denser packing. At higher  $S$ , suction is reduced and densification is more efficient. However, at very high  $S$ , densification is retarded by a shortage of air voids. Thus, optimum corresponds to some optimum suction value. But, for a given suction, the value of  $S$  increases with  $wPI$ , as discussed when SWCCs were developed earlier. It follows that at least a slight increase in  $S_{opt}$  with  $wPI$  should ensue. Accordingly, a function yielding this slight increase was adopted for Figure 29, more because of its logical basis than because the data required it. All soils with  $wPI = 0$  were averaged and found to have an average of about 78%, and this intercept was imposed on the function. The  $R^2$  of 0.079 is quite low for good reasons, but it is also true that a value of  $S_{opt}$  from this function is not very likely to be off more than about  $\pm 3\%$ . Thus, in spite of the low  $R^2$  value,  $S_{opt}$  can be estimated with fairly good confidence by equation (23).

$$S_{opt}(\%) = 6.752(wPI)^{0.147} + 78 \dots\dots\dots (23)$$

Correlation for  $w_{opt}$

Figure 30 shows increasing moisture content at optimum,  $w_{opt}$ , with increasing  $wPI$  as expected. The function fitted to the data is given by equation (24):

$$w_{opt}(\%) = 1.3(wPI)^{0.73} + 11 \dots\dots\dots (24)$$

Equation (24) corresponds to the T99 compactive effort for  $wPI > 0$ . For soils with  $wPI = 0$ , the  $D_{60}$  value was correlated to  $w_{opt}$  (T99) as shown in Figure 31. Although decrease in  $w_{opt}$  with increasing  $D_{60}$  was expected, the correlation is not very strong, perhaps due in part to a dearth of data for  $D_{60} > 15$  mm. The equation for the fitted curve is:

$$w_{opt}(\%) = 8.6425D_{60}^{-0.1038} \dots\dots\dots (25)$$

Equation (25) becomes irrational for  $D_{60} = 0$ , but of course  $D_{60}$  should not equal 0. At  $D_{60} = 0.1$  mm,  $w_{opt}$  is 11%, which is a good match for the lower limit of equation (24).

For base materials, the reference and initial condition is optimum for T180. The method used to estimate  $w_{opt}$  (T180) was first to estimate  $w_{opt}$  (T99) by equation (24) or (25) and then subtract  $\Delta w_{opt}$  from  $w_{opt}$  (T99), as indicated in Figures 30 and 31. The difference between  $w_{opt}$  (T99) and  $w_{opt}$  (T180) is denoted  $\Delta w_{opt}$  and is correlated with  $w_{opt}$  (T99) in Figure 32:



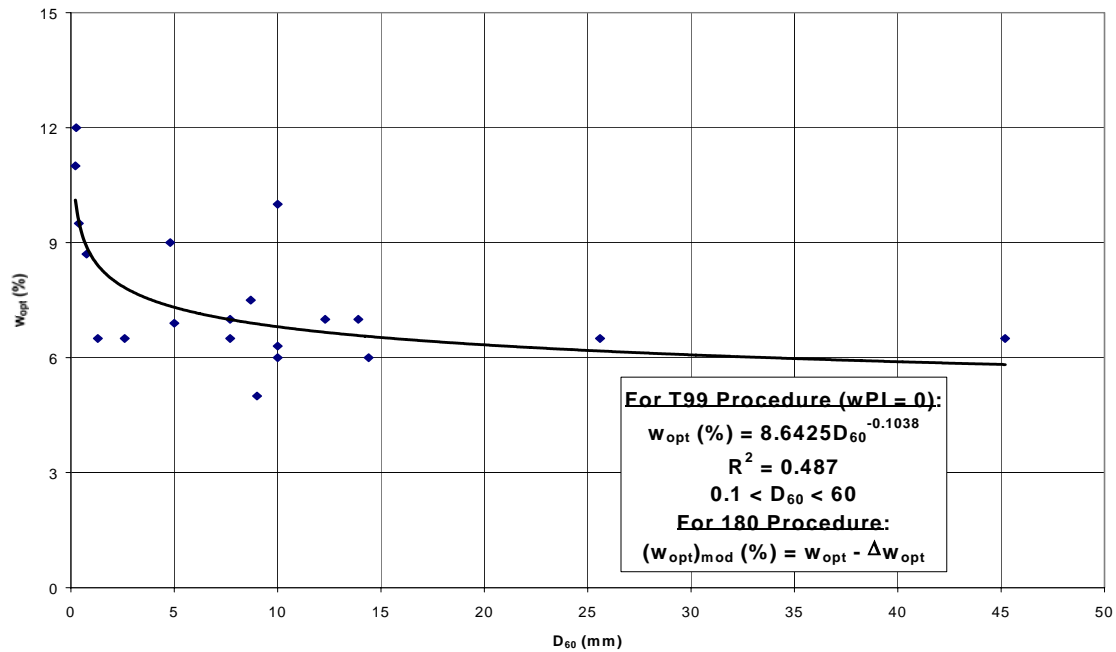


Figure 31. Correlation between Gravimetric Water Content at Optimum and  $D_{60}$

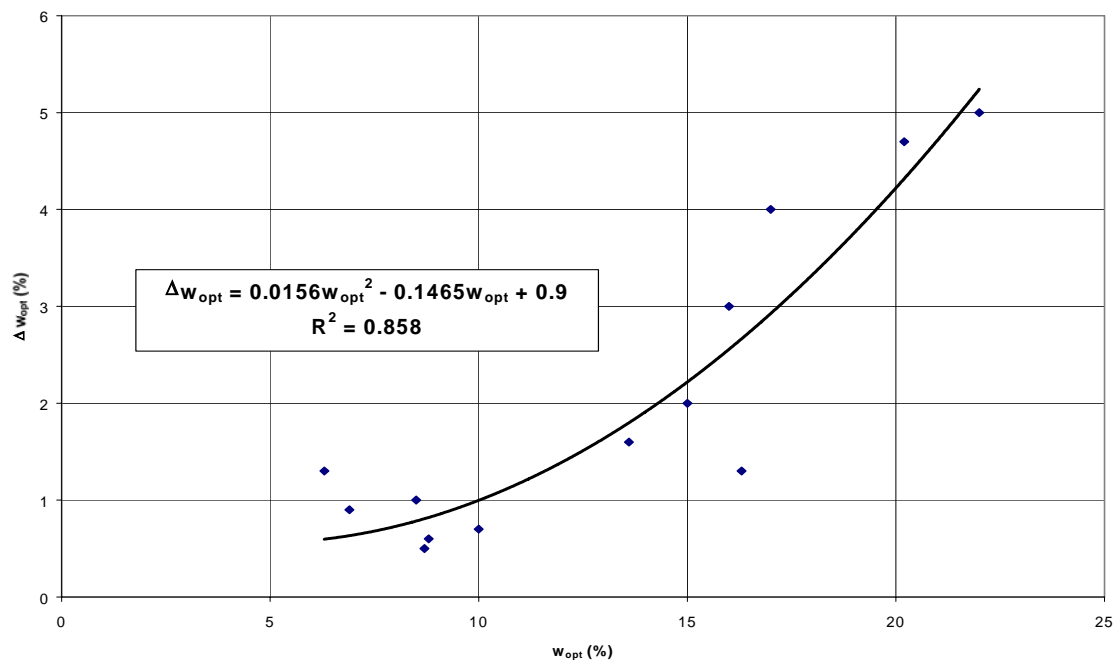


Figure 32. Correlation between Gravimetric Water Content at Optimum (T99) and Difference between  $w_{opt}$  (T99) and  $w_{opt}$  (T180)

$$\Delta w_{\text{opt}} = 0.0156w_{\text{opt}}^2 - 0.1465w_{\text{opt}} + 0.9 \dots\dots\dots (26)$$

Thus,  $w_{\text{opt}}$  (T99) is determined first, then  $\Delta w_{\text{opt}}$  is estimated from equation (26), and  $w_{\text{opt}}$  (T180) is calculated by equation (27):

$$w_{\text{opt}}(\text{T180}) = w_{\text{opt}}(\text{T99}) - \Delta w_{\text{opt}} \dots\dots\dots (27)$$

## Intended Use of Correlations

The intended use of these correlations is to support computations, both inside and outside the EICM, aimed at evaluating pavement material resilient moduli as a function of time and in consideration of moisture changes. The basic model adopted for evaluating change in  $M_R$  due to change in moisture content is given by equation (28). The development of this model is presented in Witczak et al.(2000), Volumes I and II.

$$\log\left(\frac{M_R}{M_{R\text{opt}}}\right) = a + \frac{b - a}{1 + \exp(\beta + k_s(S - S_{\text{opt}}))} \dots\dots\dots (28)$$

Where:

$M_R$  = resilient modulus at any S

$M_{R\text{opt}}$  = resilient modulus at  $\gamma_{\text{dry max}}$  and  $w = w_{\text{opt}}$  and  $S = S_{\text{opt}}$

a, b,  $\beta$ ,  $k_s$  = model parameters

$S_{\text{opt}}$  = S at optimum, in decimal

S = any degree of saturation at any time, for a layer in the pavement profile, in decimal

Note that the change in degree of saturation,  $S - S_{\text{opt}} = \Delta S$ , is an essential quantity in equation (28). The value of  $S_{\text{opt}}$  can be computed inside or outside of the EICM. In either case it is a simple application of equation (23), and requires only wPI. If wPI = 0, then  $S_{\text{opt}}$  is fixed constant at 78%. The value of S is most conveniently computed inside the EICM.

### Use of EICM

The computational algorithm, which is currently being incorporated in the EICM under Level 3 as described in Chapter 8, is as follows:

- 1) For a given pavement profile layer or point within a layer (node), wPI or  $D_{60}$  is input.
- 2)  $S_{opt}$  is computed from equation (23).
- 3)  $w_{opt}$  is computed from equation (24) or (25). For base materials, equations (26) and (27) are also employed.
- 4)  $G_s$  is computed by equation (16):  $G_s = 0.041(wPI)^{0.29} + 2.65$
- 5)  $e$  is computed from equation (21).
- 6)  $\gamma_{dry\ max}$  is computed from equation (22).
- 7) The initial degree of saturation,  $S_o$ , is set =  $S_{opt}$ , the initial moisture content,  $w_o$ , is set =  $w_{opt}$ .
- 8) The initial volumetric water content,  $\theta_o$ , is set equal to  $\theta_{opt}$  and computed by

$$\theta_o = \theta_{opt} = w_o \frac{\gamma_{dry\ max}}{\gamma_w} = w_{opt} \frac{\gamma_{dry\ max}}{\gamma_w} \dots\dots\dots (29)$$

- 9) The porosity,  $n$ , is computed by

$$n = \frac{e}{1 + e} = \theta_{sat} \dots\dots\dots (30)$$

Where:

$\theta_{sat}$  = saturated volumetric water content

*Note:* At this point, all of the initial condition material properties are established. However, the total required input data file for the EICM is voluminous and complex and includes climatic data and position of groundwater table as a function of time.

- 10) When all input data is complete and ready, the EICM can march forward through time computing values of volumetric water content,  $\theta$ . These  $\theta$  values can be converted to  $w$  and/or  $S$  values using the equations presented above.
- 11) If  $S$  is computed and plotted as a function of time its stability can be judged. Experience with the EICM has shown that  $S$  typically becomes stable, with seasonal variations due to climatic conditions and water table variations being small. Under these circumstances, the average  $S$  over a period of relative stability can be evaluated as  $S_{\text{equilibrium}}$ . This equilibrium value of  $S$  is of considerable interest because it represents a condition for which  $M_R$  is also fairly stable. Thus,  $S_{\text{equil}} - S_{\text{opt}}$  would be used in equation (28) to get  $M_{R \text{ equil}}$ .

#### *Estimation of $S_{\text{equil}}$ outside the EICM*

The algorithm outlined above represents the major steps followed by the EICM in generating initial condition data and then the computation of  $S$  in general and  $S_{\text{equil}}$  in particular. The value of  $S_{\text{equil}}$  can also be estimated outside the EICM with only modest loss in accuracy. The following steps may be used to obtain this estimate:

- 1) For the point in question, determine  $wPI$  or  $D_{60}$ . Select the corresponding SWCC from Figure 15.
- 2) Obtain the average depth to groundwater table (from the point) for a period of time for which the GWT has been fairly stable,  $D_{\text{equil}}$ .
- 3) Calculate the equilibrium soil water suction ( $u_a - u_w$ ) at the point as

$$(u_a - u_w)_{\text{equil}} = \gamma_w D_{\text{equil}} \dots\dots\dots (31)$$

- 4) Enter the appropriate SWCC from Figure 15 at  $(u_a - u_w)_{\text{equil}}$  and pick off  $S_{\text{equil}}$ .

The preceding procedure for estimating  $S_{\text{equil}}$  is based on the simplifying assumption that the effects on  $S$  of variations in GWT and rainfall are fairly minor, which has been found to be a good assumption in a great many cases. With  $S_{\text{equil}}$  in hand then  $S_{\text{opt}}$ , which can also be estimated outside the EICM, can be used to get  $S_{\text{equil}} - S_{\text{opt}}$  and evaluate the effect of the change in  $S$  from  $S_{\text{opt}}$  to  $S_{\text{equil}}$  on  $M_R$ .

## Check on Internal Consistency of Correlations for $S_{opt}$ , $w_{opt}$ , and $G_s$

Before using the correlations for  $S_{opt}$ ,  $w_{opt}$ , and  $G_s$  in the EICM and other direct computations, it was necessary to check the internal consistency of the correlations obtained. Note that Steps 1 through 6 under **Use of EICM** lead to the computation of  $\gamma_{dry\ max}$  from  $S_{opt}$ ,  $w_{opt}$ , and  $G_s$  obtained from correlations. As a check on the reasonableness of the correlations one could compare these calculated values of  $\gamma_{dry\ max}$  with measured values of  $\gamma_{dry\ max}$ . However, in order to be more consistent, it was decided to compare the calculated  $\gamma_{dry\ max}$  values with  $\gamma_{dry\ max}$  values obtained from correlations between directly measured values and  $wPI$  or  $D_{60}$ . Thus, the next task was to obtain these correlations.

### *Correlations for $\gamma_{dry\ max}$*

Figure 33 shows  $\gamma_{dry\ max}$  versus  $wPI$  for non-base materials with  $wPI > 0$  for T99 compactive effort. The equation obtained is:

$$\gamma_{dry\ max}(T99) = -6.057(wPI)^{0.461} + 127 \dots\dots\dots(32)$$

It was also found that:

$$\gamma_{dry\ max}(T180) \approx \frac{\gamma_{dry\ max}(T99)}{0.95} \dots\dots\dots(33)$$

For the base materials,  $\gamma_{dry\ max}(T99)$  was correlated with  $D_{60}$ , as shown in Figure 34. The equation obtained is:

$$\gamma_{dry\ max}(T99) = 0.1946D_{60} + 134.61 \dots\dots\dots(34)$$

Again,  $\gamma_{dry\ max}(T180)$  is estimated by equation (33). In order to broaden the database slightly and because some bases have a small  $PI$ , materials with  $PI$  up to 3 were included. Note that the  $\gamma_{dry\ max}$  values for bases are significantly higher than for non-base materials, considering T99 in both cases. This is because bases are, on average, more well-graded than non-bases. A slight increase in  $\gamma_{dry\ max}$  with  $D_{60}$  is expected because essentially all bases have some fines. Therefore, the larger is  $D_{60}$  the more well-graded the material is, as a general rule. Again, a slight increase in  $\gamma_{dry\ max}$  with  $D_{60}$  was imposed in Figure 34 because of logic, even though the data did not require it.

*Comparison of  $\gamma_{dry\ max}$  from  $S_{opt}$ ,  $w_{opt}$ , and  $G_s$  with  $\gamma_{dry\ max}$  from  $wPI$  and  $D_{60}$  Correlations*

Figure 35 shows the values of  $\gamma_{dry\ max}$  calculated from the  $S_{opt}$ ,  $w_{opt}$ , and  $G_s$  correlations (the abscissa) versus the  $\gamma_{dry\ max}$  values obtained by direct correlation with  $wPI$  or  $D_{60}$  (equations (32) or (34)). In all cases the T180 values were used for bases, both  $w_{opt}$  and  $\gamma_{dry\ max}$ . The T99 values were used for all other materials. Figure 35 shows good agreement between the  $\gamma_{dry\ max}$  values obtained by the two methods, indicating that the correlations are satisfactorily consistent internally. Accordingly, these correlations were transported to the EICM.

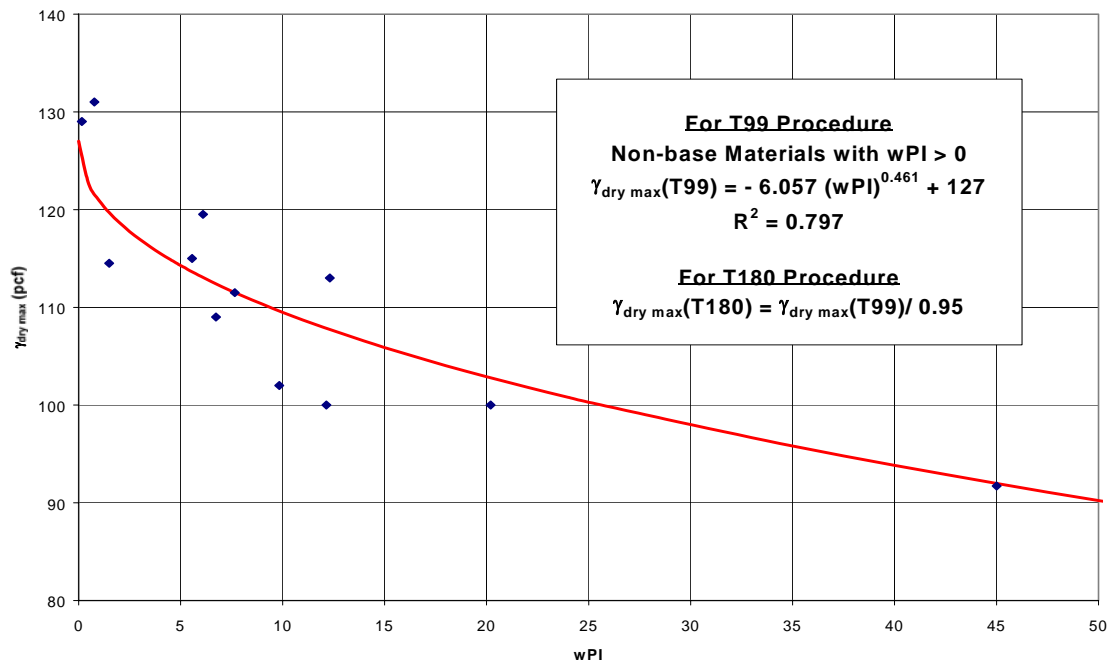


Figure 33. Correlation between Dry Unit Weight and  $wPI$

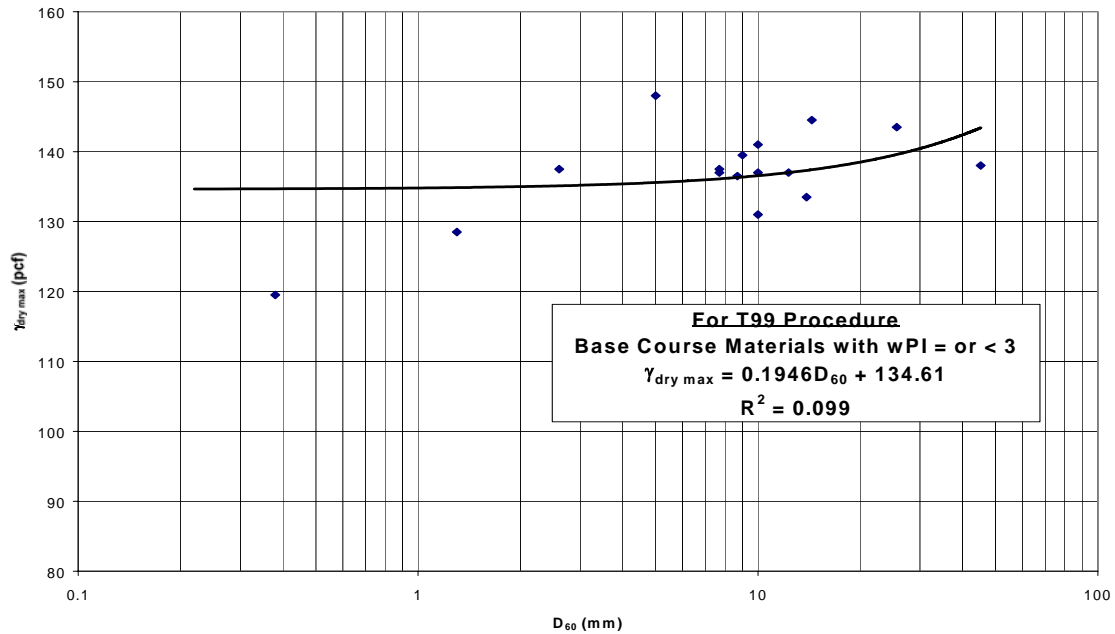


Figure 34. Correlation between Dry Unit Weight and  $D_{60}$

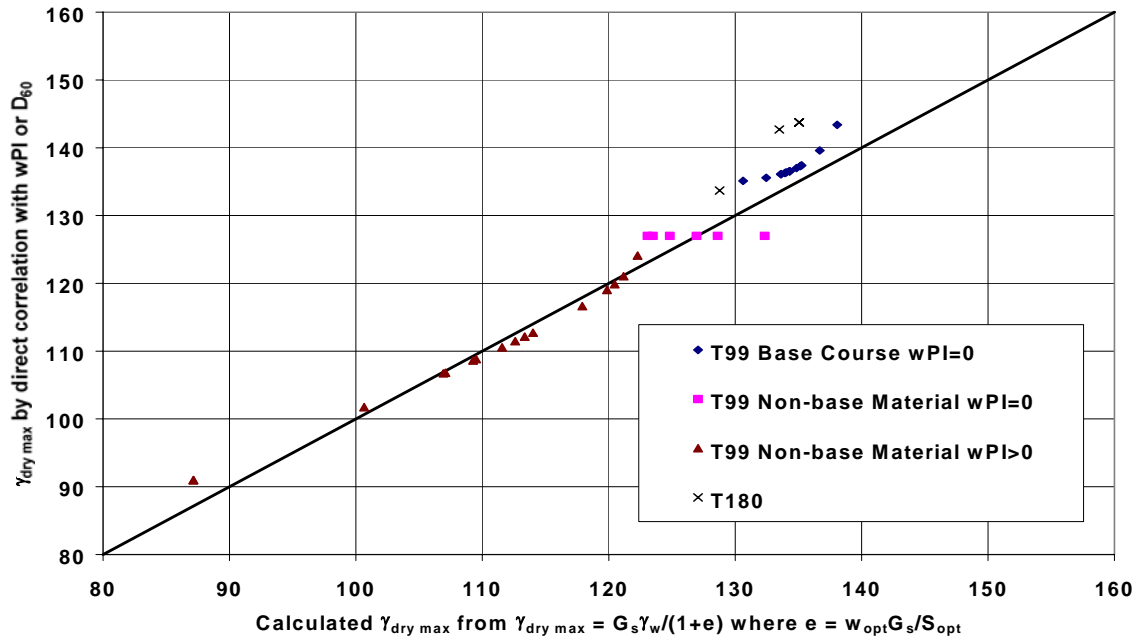


Figure 35. Comparison of  $\gamma_{dry\ max}$  from Optimum Conditions with  $\gamma_{dry\ max}$  from wPI/ $D_{60}$  Correlations

## Conclusions

The conclusions from this study are divided into two parts, because the emphases and objectives were somewhat different for Part I and Part II.

### Part I. Conclusions Relative to the Maximization of the Agreement between EICM Predicted Moisture Contents and TDR Measured Moisture Contents for Existing Pavements

- 1) There are several possible explanations for disagreement between EICM predicted and TDR measured values of moisture content as follows:
  - i) *Errors in the SWCC.* A substantial error in the position of the SWCC will produce a corresponding error in the predicted moisture content or degree of saturation,  $S$ , because the EICM simply computes the equilibrium suction as  $D\gamma_w$  – where  $D$  is the distance to the GWT – and enters the SWCC with suction to get  $\theta$  or  $S$ .
  - ii) *Error in the  $(u_a - u_w) = D\gamma_w$  assumption.* This assumption is probably fairly accurate in most cases, when the GWT is shallow. However, some research indicates that the assumption is not good, particularly when the water table is deep. If field measurements of equilibrium suctions under pavements are available, they can be used in the EICM by simply dividing the known  $u_a - u_w$  by  $\gamma_w$  and using the resultant  $D$  as the input depth to GWT.
  - iii) *Errors in the TDR values.* The known weak correlations between TDR measured moisture contents and lab measured moisture contents illustrate that the value from any particular TDR probe could be substantially in error.
- 2) Conclusions relative to these possible explanations are as follows:
  - i) As a part of this study, considerable effort was devoted to improvement of SWCCs. The Fredlund and Xing function fit that was adopted provides a better



and more complete SWCC characterization than did the Gardner equation. The SWCCs adopted (Figure 15, Chapter 3) represent a substantial database of 190 soils and agree fairly well with directly measured SWCCs. The improved match between predicted and TDR measured values cited in Chapter 3 are due in part to these new SWCCs. After much research into sources and magnitudes of errors in SWCCs, it has been concluded that the curves of Figure 15, Chapter 3, are as good as directly measured curves, unless the person / laboratory making the measurements is highly experienced and well-equipped.

- ii) It has been concluded that it is best, at least for the short term, to continue with the assumption that  $(u_a - u_w)_{equil} = D_{equil} / \gamma_w$ . If  $(u_a - u_w)_{equil}$  is known with reliability from independent sources, it should be input into the EICM, as  $D_{equil} = (u_a - u_w)_{equil} / \gamma_w$ .
  - iii) As a part of this study, attempts were made to improve correlations between TDR and lab measured moisture contents with little success. Unless or until a new set of calibrations, with less scatter and uncertainty, is obtained, the poor TDR calibration remains as a source of discrepancy between TDR measured and EICM predicted moisture contents. A partial cancellation of error due to poor TDR calibration was accomplished by dividing the prediction task into two parts: a) prediction of the  $\theta_{eq}$  and b) prediction of the seasonal oscillations over a period of a year or many years. At the outset of this study, it was assumed that the seasonal oscillations were to be the more interesting. Consequently, it was decided to use the first-measured TDR value – in a particular period of interest – as  $\theta_{eq}$ . This was accomplished by shifting the SWCC until  $u_a - u_w$ , calculated by  $u_a - u_w = D / \gamma_w$ , corresponded to  $\theta_o$ . Use of this procedure produced substantial reduction in the discrepancy between TDR measured and EICM predicted values. However, it did not cast any light on the question "How well does the EICM predict  $\theta_{eq}$  values?".
- 3) Because of the inherent nature of the SWCC, it is necessary to invoke and use mass-volume relationships in the process of making moisture content predictions. Experience shows that it is necessary to have internally consistent and reasonably accurate values of water content, density, and  $G_s$ . A significant error in as few as one of these three can produce serious problems in the predictive process.
  - 4) When the discrepancies between the TDR measured moisture contents and the EICM predicted values were compared for the (old) Version 2.1 and the (new) Version

2.6, it was found that the new version showed an improved match in all cases, and very substantial improvement in most cases.

## Part II. Conclusions Relative to the Optimization of Procedures for Predicting the Moisture Content Change from the Initial to the Equilibrium Condition

- 1) Experience has shown that, more often than not, one or more of the values needed for material mass – volume relationships is erroneous, unreasonable, or missing when these values are extracted from databases or engineering reports. When this occurs it is problematic, because the missing data is usually difficult to recover and the erroneous data is not always detectable at an early stage. Stated differently, even when a problem with the data is found, it is not usually easy to fix.
- 2) It is reasonable to assume that unbound layers are compacted at optimum moisture content,  $w_{opt}$ , and at maximum dry density,  $\gamma_{dry\ max}$ . This assumption is supported by typical compaction specifications and guidelines and by past experience. Further impetus to this assumption is added by the fact that resilient modulus,  $M_R$ , studies have led to the conclusion that optimum conditions represent the best reference state for estimation of  $M_R$  changes due to moisture changes.
- 3) It has been possible to develop internally consistent correlations between the degree of saturation at optimum,  $S_{opt}$ ,  $w_{opt}$ , and  $G_s$  with index properties  $wPI$  and  $D_{60}$ . These correlations, together with conclusions 1 and 2 above, make it possible to estimate  $S_{opt}$ ,  $w_{opt}$ , and  $G_s$  and then to calculate void ratio,  $e$ , porosity,  $n$ , and  $\gamma_{dry\ max}$  without needed reliance on typically erroneous reported values of  $\gamma_{dry}$ ,  $w$ , and  $G_s$ . By assuming the initial compaction conditions,  $S_{opt}$ , correspond to  $S_o$ , the starting point for moisture content changes is established quickly and easily, without ambiguity. The values of  $S_{opt}$  are reproducible, meaning that any user anywhere would get the same  $S_{opt}$ , given the same  $wPI$  and  $D_{60}$ .
- 4) The EICM can be required to output  $S$ , thus  $S_{equil}$  can be easily derived from the EICM output. For cases in which the effects of seasonal variations in moisture content have relatively minor effect on  $M_R$ , the  $\Delta S = S_{equil} - S_{opt}$  is available for use in the modular ratio model for  $M_R$ .

- 5) A fairly good approximation of  $S_{\text{equil}}$  can be calculated manually, using a simple procedure. This computation can be used to check the reasonableness of the EICM value, or as an independent estimate of  $S_{\text{equil}}$  when the EICM is not used.

---

# Recommendations for Implementation of EICM Input for Use in the 2002 Design Guide

## Introduction

The ICM plays a major role in the 2002 Guide computational framework aimed at quantification of pavement system response to traffic loading, as a primary step in the design process. In particular, the EICM is responsible for the provision of temperatures and temperature gradients for the surface layers as a function of time. For the unbound layers, the EICM outputs of main interest are the moisture contents and degrees of saturation as a function of time for each layer as well as the depth of freezing, including timing and duration, and parameters relating to thawing and recovery therefrom.

What follows in this chapter are recommendations relative to testing required and computational procedures to be used to obtain needed input data for the EICM for Levels 1, 2, and 3. Unbound compacted layers are treated separately from unbound natural in-situ layers lying beneath the compacted layers, because the required input typically differs. Each section contains two lists. The first list addresses the material properties most relevant to moisture content prediction (parameters defining mass-volume relationships primarily), indicates how the input data may be generated, and in some cases gives an indication as to what the EICM may do with the data internally. The second list is in the form of a table (Table 14) and is simply a listing of input data that the user is required to supply. In the second list, an attempt has been made to list all data needed to run the EICM.

---

## Unbound Compacted Layers

### Data Required Including Sources and Tests to be Performed

#### *Level I*

- 1) Plasticity Index, PI
- 2) Gradation, including  $D_{60}$
- 3) T180 compaction on bases and T99 compaction on subbases and subgrades, leading to  $\gamma_{dry\ max}$  and  $w_{opt}$ .
- 4) Specific Gravity,  $G_s$
- 5) The hydraulic conductivity under saturated conditions,  $k_{sat}$ .
- 6) The soil-water characteristic curve, SWCC. Testing may be done with pressure plate, pressure membrane, psychrometer, filter paper, or other accepted techniques. The initial density of the test specimens should be  $\gamma_{dry\ max}$ . A minimum of 4 or 5 pairs of values of soil suction and water content should be obtained. An algorithm inside the EICM will be used to fit the Fredlund and Xing equation to the data points supplied by the user.
- 7) *Note:* All three values of  $\gamma_{dry\ max}$ ,  $w_{opt}$ , and  $G_s$  should be determined by direct testing, with replications on  $G_s$  required and replications on  $\gamma_{dry\ max}$  and  $w_{opt}$  recommended. These three values should then be used to compute  $S_{opt}$  and the computed  $S_{opt}$  should be compared with the values of  $S_{opt}$  obtained by correlation with wPI described in Chapter 6. If  $S_{opt}$  is reasonable, proceed. If not, check for errors and repeat tests as needed. With reliable values of  $\gamma_{dry\ max}$ ,  $w_{opt}$ , and  $G_s$  input, the EICM can compute values of void ratio,  $e$ , and porosity,  $\theta_{sat}$ . Thus,  $\theta_{sat}$  does not need to be input for this case.
- 8) Note also that optimum conditions ( $\gamma_{dry} = \gamma_{dry\ max}$  and  $w = w_{opt}$ ) have been chosen as a best estimate of initial conditions for compacted layers. Therefore,  $w_{opt}$  will be interpreted as the initial moisture content by the EICM in the case of compacted layers. For new construction, the equilibrium moisture content will not be input (because it will not be known in advance). Rather, it will be calculated by the EICM.

### *Level 2*

- 1) PI
- 2) Gradation, including  $D_{60}$ .
- 3) T180 compaction on bases and T99 compaction on subbases and subgrades, leading to  $\gamma_{dry\ max}$  and  $w_{opt}$ .
- 4)  $G_s$  (*Note:* Reasonableness of  $S_{opt}$  should be checked as described above under Level 1).
- 5) Parameters for SWCC are determined from  $wPI$  or  $D_{60}$  internally by the EICM; i.e., no testing to get SWCC, other than  $wPI/D_{60}$ .
- 6)  $k_{sat}$  is determined from SWCC, internally by the EICM; i.e., no testing to get  $k_{sat}$ , other than  $wPI/D_{60}$ .

### *Level 3*

- 1) PI
- 2) Gradation, including  $D_{60}$ .
- 3) Internal to the EICM, correlations between  $wPI/D_{60}$  are used to get  $S_{opt}$ ,  $w_{opt}$ , and  $G_s$  from which  $\gamma_{dry\ max}$  and porosity are computed. The SWCC and  $k_{sat}$  are also derived from  $wPI/D_{60}$ . Thus, PI and gradation are the only tests, in connection with use of the EICM, to be performed for Level 3.

The list of input parameters required by the EICM, including climatic data, infiltration and drainage data, asphalt/PCC properties and material properties for compacted layers is presented in Table 14.

Table 14. Listing of Input Parameters Required by the EICM, Including Climatic Data, Infiltration and Drainage Data, Asphalt/PCC Properties and Material Properties for Compacted and Natural In-Situ Layers

EICM Variable	Level 1	Level 2	Level 3
Integrated Model Initialization			
Year to start modeling	User supplied	User supplied	User supplied
First Month	User supplied	User supplied	User supplied
Analysis period	User supplied	User supplied	User supplied
Latitude	User supplied	User supplied	User supplied
Longitude	User supplied	User supplied	User supplied
Elevation	User supplied	User supplied	User supplied
Climate/Boundary Conditions			
Groundwater table depth	User supplied	User supplied	User supplied
Infiltration and Drainage			
Cracks' length	User supplied for rehab/aging processes	User supplied for rehab/aging processes	Default or user provided for rehab/aging processes
Total survey length	User supplied for rehab/aging processes	User supplied for rehab/aging processes	Default or user provided for rehab/aging processes
Base % gravel	User supplied for drainage analysis/flux boundary	User supplied for drainage analysis/flux boundary	User supplied for drainage analysis/flux boundary
Base % sand	User supplied for drainage analysis/flux boundary	User supplied for drainage analysis/flux boundary	User supplied for drainage analysis/flux boundary
One side base width	User supplied for drainage analysis/flux boundary	User supplied for drainage analysis/flux boundary	User supplied for drainage analysis/flux boundary
Slope ratio/base tangent	User supplied for drainage analysis/flux boundary	User supplied for drainage analysis/flux boundary	User supplied for drainage analysis/flux boundary
Asphalt Material Properties			
Thickness	User supplied	User supplied	User supplied
Air content	User supplied	Default or user provided	Default or user provided
Thermal conductivity asphalt	User supplied	User supplied	Default or user provided
Heat capacity	User supplied	User supplied	Default or user provided
Total unit weight	User supplied	Default or user provided	Default or user provided
Surface short wave Absorptivity	User supplied	User supplied	Default or user provided
PCC Properties			
Layer thickness	User supplied	User supplied	User supplied
Thermal Conductivity	User supplied	User supplied	Default or user provided
Heat capacity	User supplied	User supplied	Default or user provided
Coefficient of expansion	User supplied	User supplied	Default or user provided
Compacted Material Properties			
Thickness	User supplied	User supplied	User supplied
Specific Gravity	User supplied	User supplied	Not required as input
Saturated hydraulic conductivity	User supplied	User supplied	Not required as input
Dry density	User supplied	User supplied	Not required as input
Dry thermal conductivity	User supplied	Default or user provided	Default or user provided
Heat capacity	User supplied	Default or user provided	Default or user provided
Plasticity Index	User supplied	User supplied	User supplied
Passing #200	User supplied	User supplied	User supplied

Table 14. Cont.

EICM Variable	Level 1	Level 2	Level 3
Diameter $D_{60}$	User supplied	User supplied	User supplied
Initial volumetric water content	User supplied	User supplied	Not required as input
Equilibrium volumetric water content.	User supplied for rehabilitated pavement	User supplied for rehabilitated pavement	Default or user provided for rehabilitated pavement
Soil-water characteristic curve	User supplied	Not required as input	Not required as input
Natural In-Situ Material Properties			
Thickness	User supplied	User supplied	User supplied
Specific Gravity	Not required as input	Not required as input	Not required as input
Saturated hydraulic conductivity	Not required as input	Not required as input	Not required as input
Dry density	Not required as input	Not required as input	Not required as input
Dry thermal conductivity	User supplied	Default or user provided	Default or user provided
Heat capacity	User supplied	Default or user provided	Default or user provided
Plasticity Index	User supplied	User supplied	User supplied
Passing #200	User supplied	User supplied	User supplied
Diameter $D_{60}$	User supplied	User supplied	User supplied
Initial volumetric water content	Not required as input	Not required as input	Not required as input
Equilibrium volumetric water content.	User supplied for rehabilitated pavement	User supplied for rehabilitated pavement	Default or user provided for rehabilitated pavement
Soil-water characteristic curve	Not required as input	Not required as input	Not required as input

## Unbound Natural (In-Situ) Layers

### Data Required Including Sources and Tests to be Performed

#### Level 1

- 1) PI
- 2)  $D_{60}$
- 3) The wPI or  $D_{60}$  will be used to get the SWCC and  $k_{sat}$  within the EICM. Values of wPI or  $D_{60}$  will likewise be used to get  $w_{opt}$  for T99,  $S_{opt}$ , and  $G_s$  – even though the material is not expected to be at optimum conditions. Then,  $w_{opt}$ ,  $S_{opt}$ , and  $G_s$  will be used to calculate the void ratio at optimum,  $e_{opt}$ , which is then used to compute  $\gamma_{dry\ max}$  by T99. The in-situ density,  $\gamma_{dry}$ , is approximated as  $\gamma_{dry} = 0.9\gamma_{dry\ max}$  by T99. From this value the in-situ porosity is obtained as follows:



$$\text{i) } e_{\text{in-situ}} = \frac{G_s \gamma_w}{\gamma_{\text{dry in-situ}}} - 1$$

$$\text{ii) } n_{\text{in-situ}} = \theta_{\text{sat}} = \frac{e_{\text{in-situ}}}{1 + e_{\text{in-situ}}}$$

- 4) All of the above computations are performed inside the EICM. Therefore, only the PI and  $D_{60}$  need to be measured for natural (in-situ) layers.

*Level 2*

Same as Level 1

*Level 3*

Same as Level 1

The list of input parameters required by the EICM, including climatic data, infiltration and drainage data, asphalt/PCC properties and material properties for compacted layers is presented in Table 14.

---

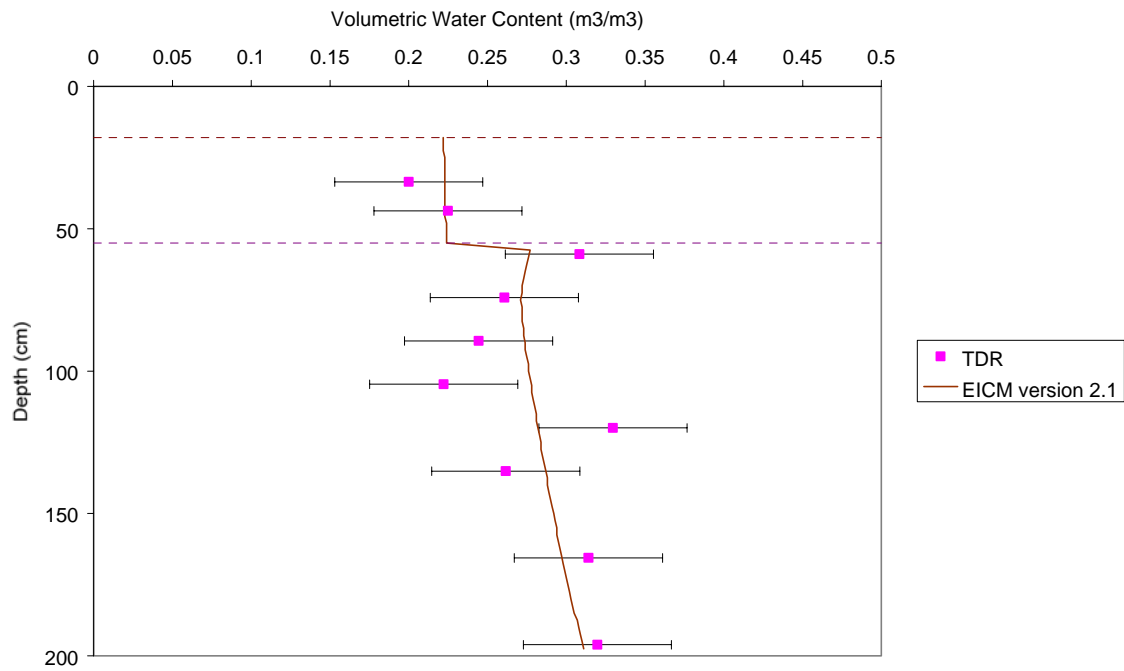
# APPENDIX A

## VOLUMETRIC WATER CONTENT PROFILES

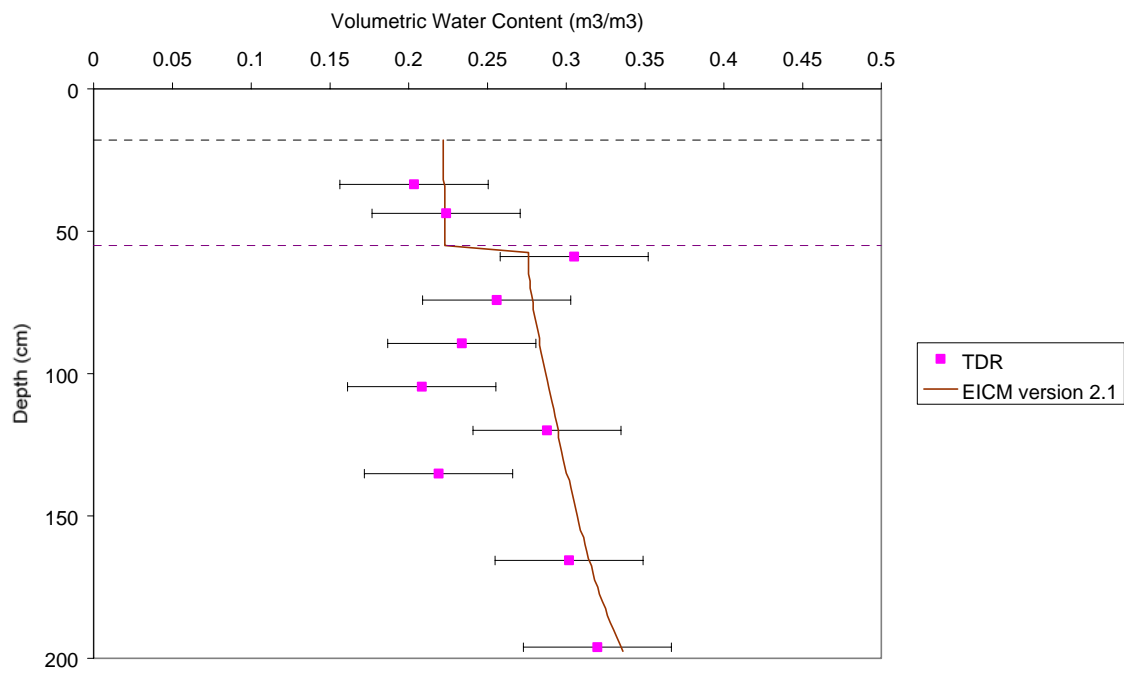
### CONNECTICUT (91803)

EICM – Version 2.1

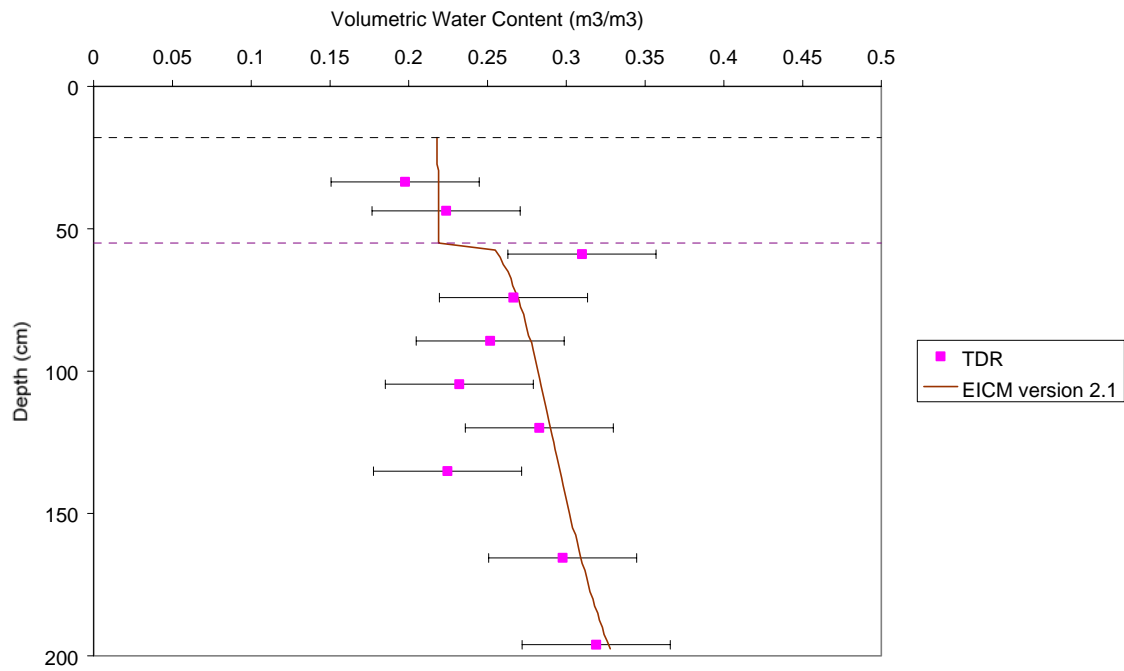
CT site - 6/30/94



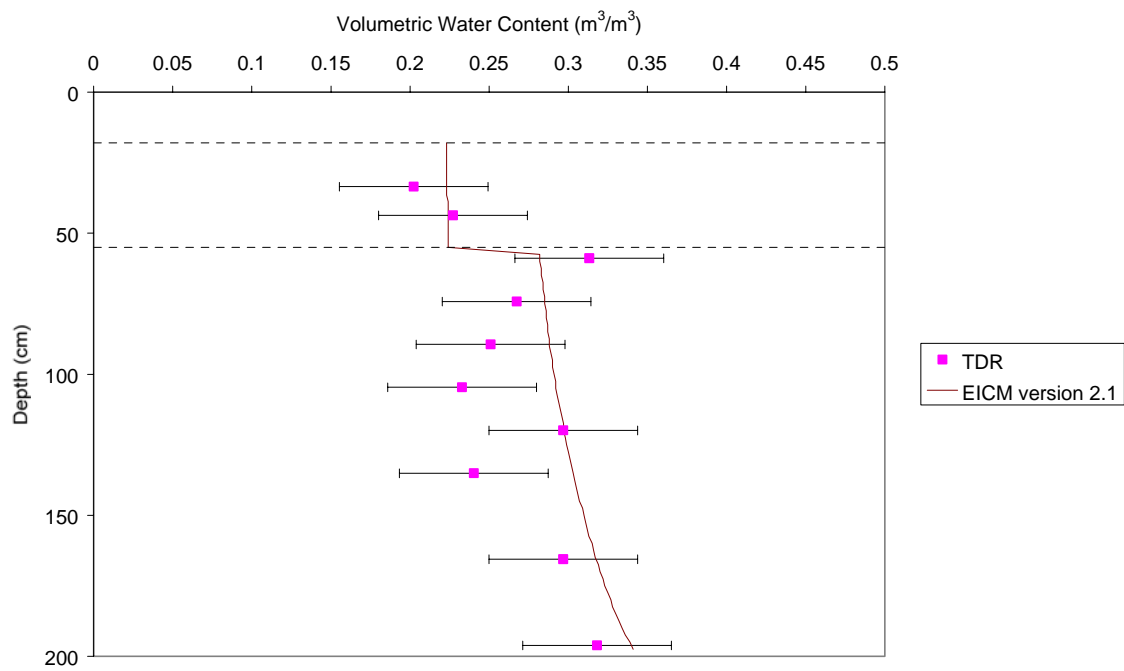
CT site - 7/28/94



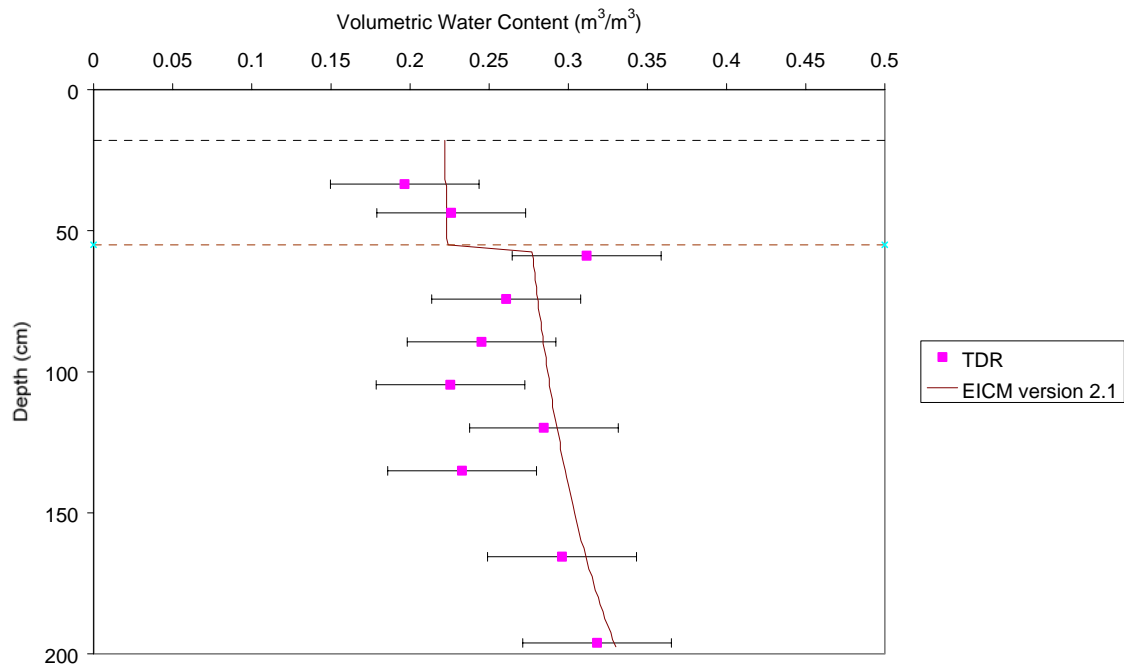
CT site -8/25/94



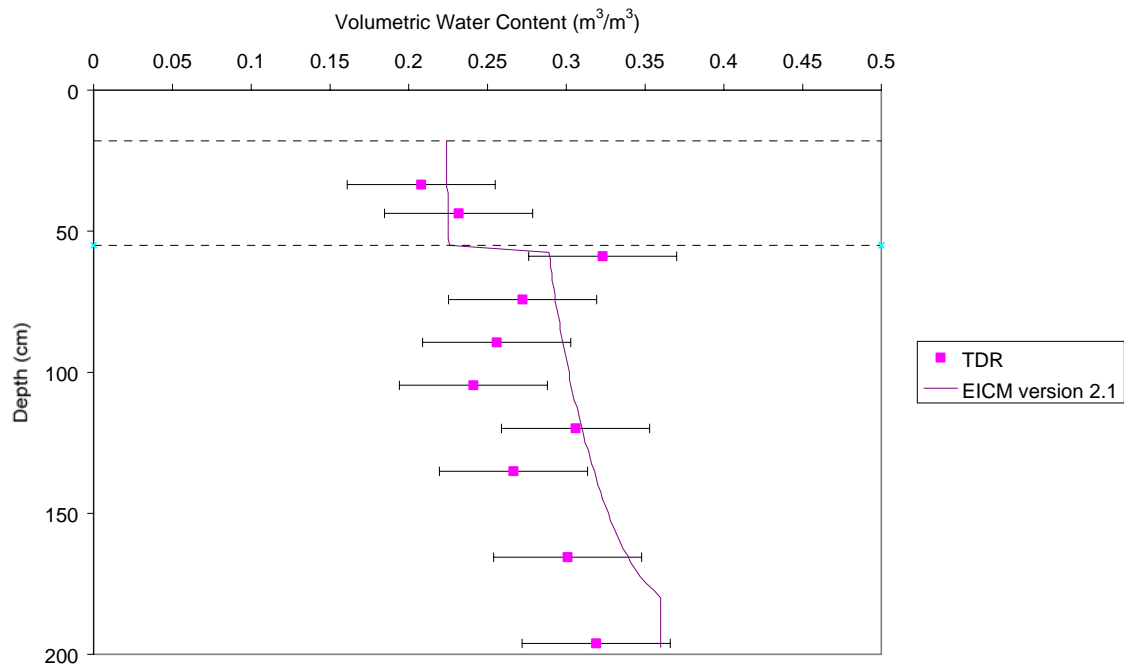
CT site - 9/29/94



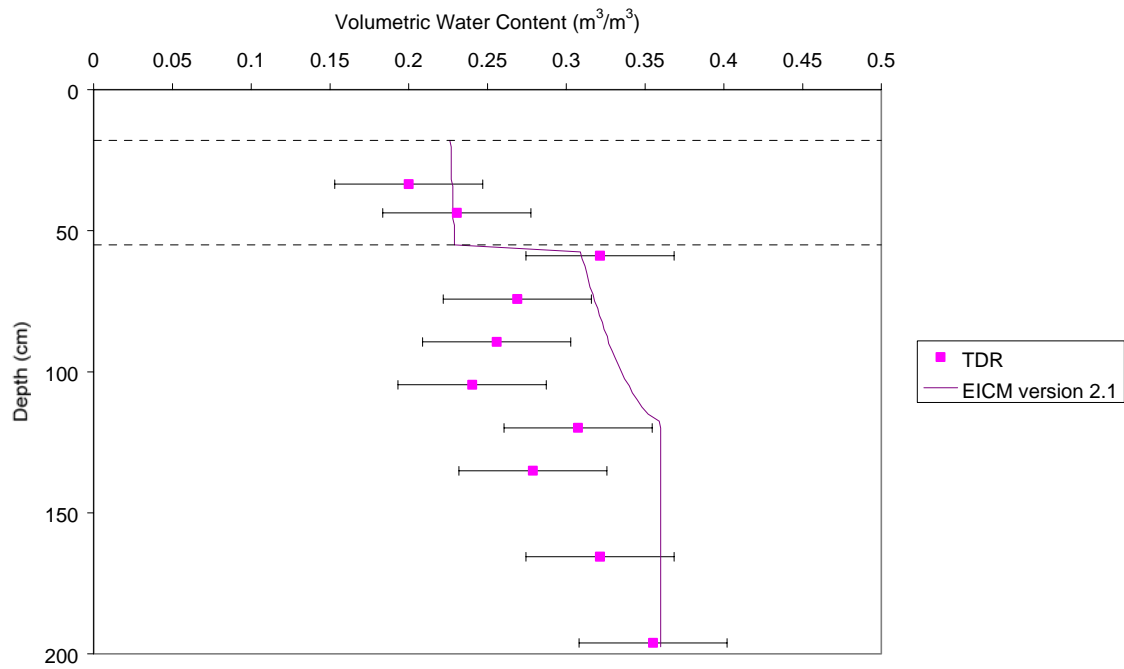
CT site - 10/27/94



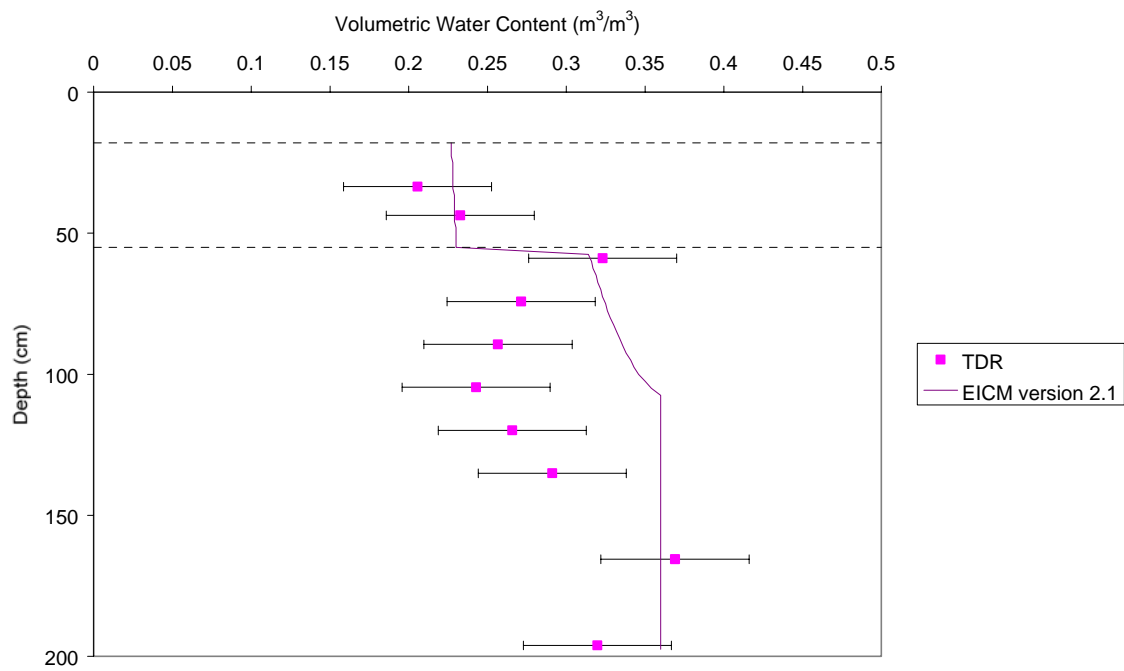
CT site - 11/30/94



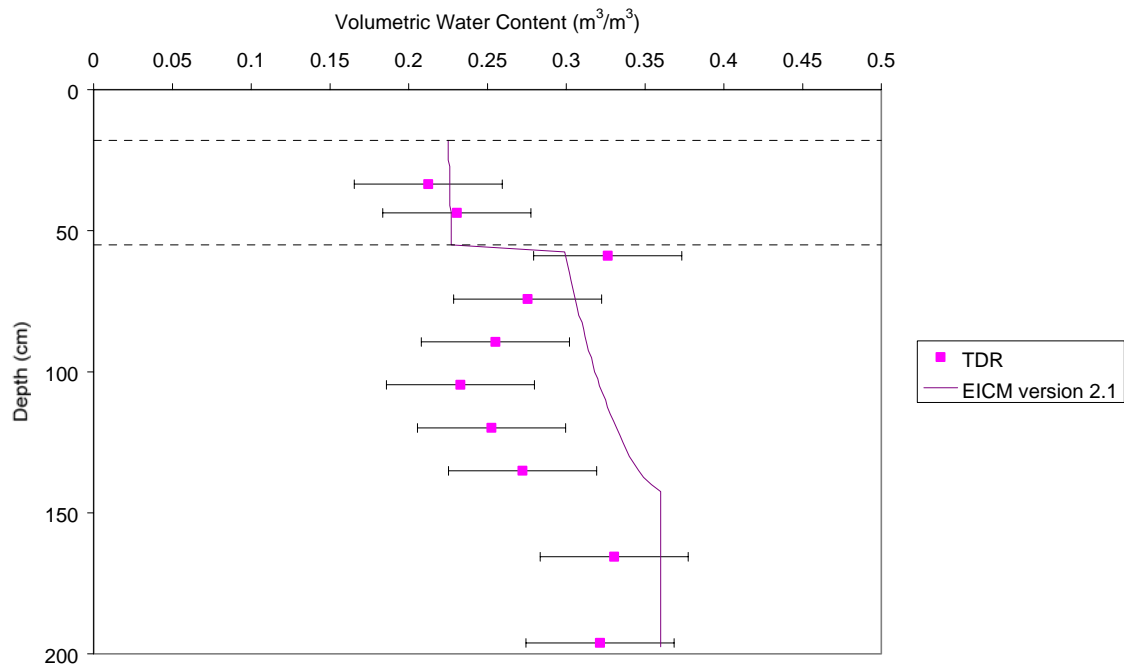
CT site - 1/5/95



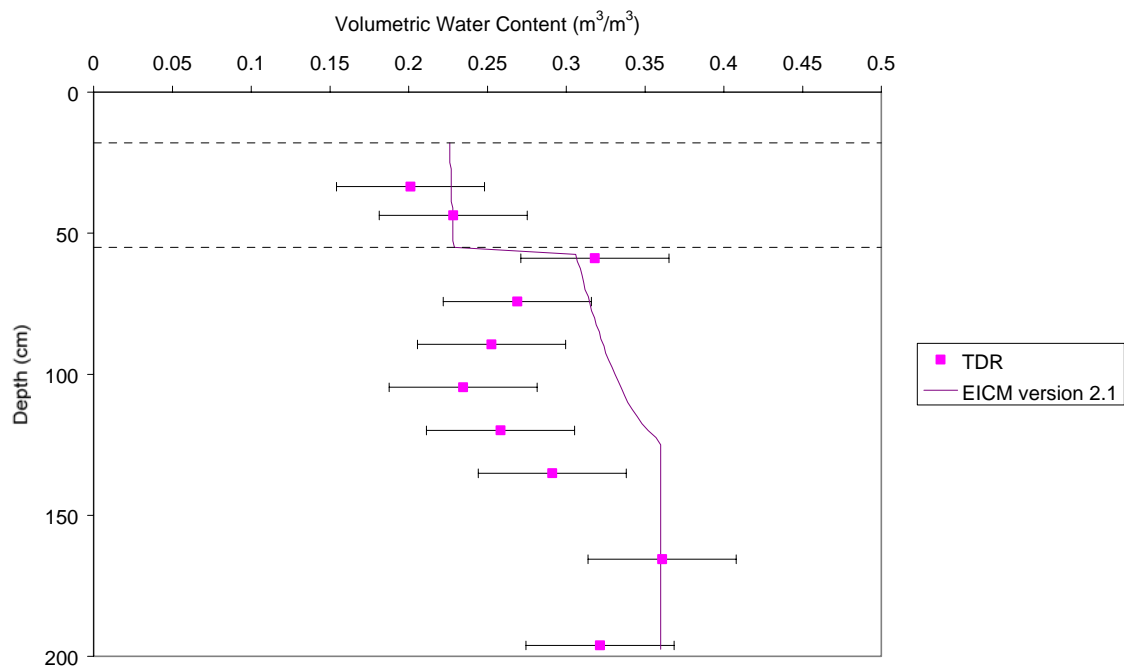
CT site - 1/26/95



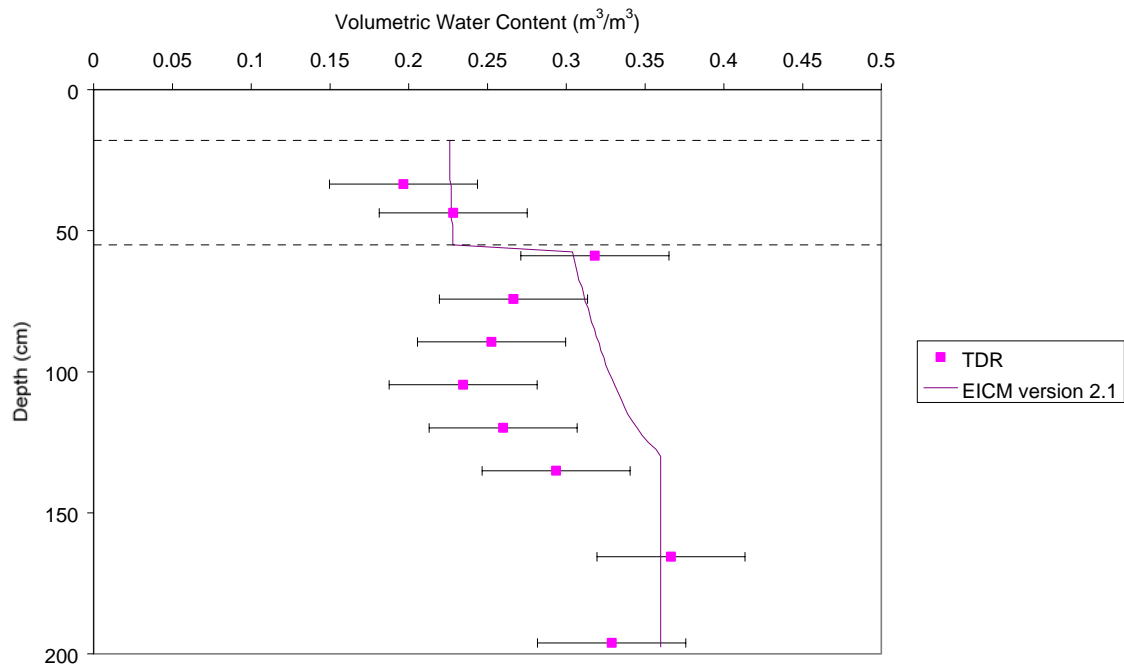
CT site - 3/2/95



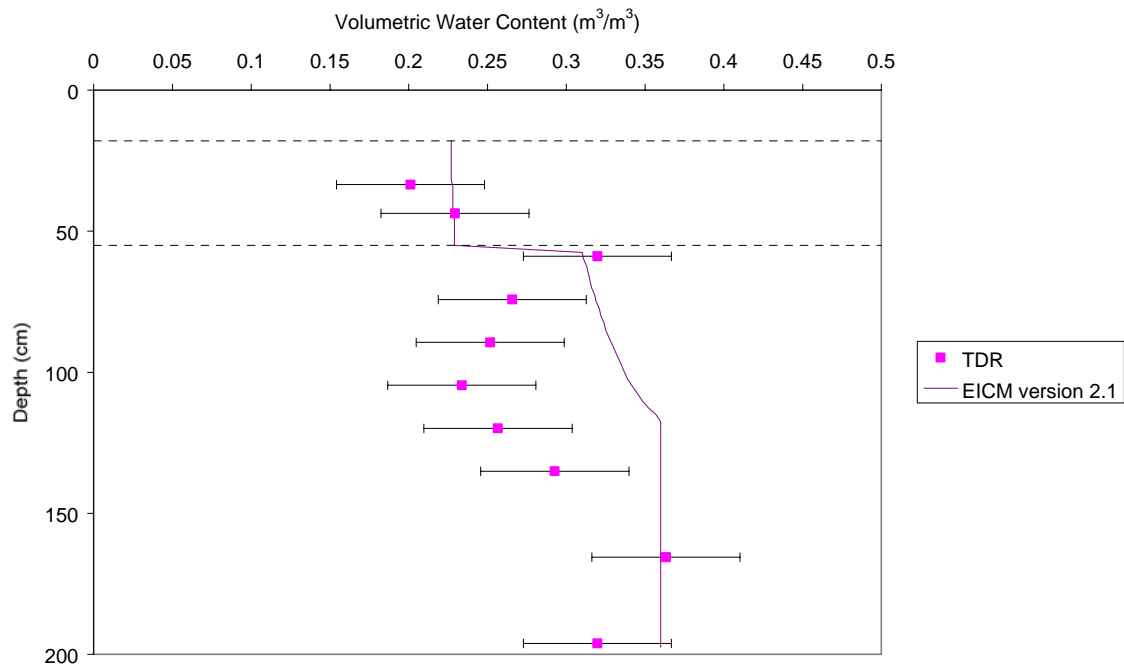
CT site - 3/15/95



CT site - 3/29/95

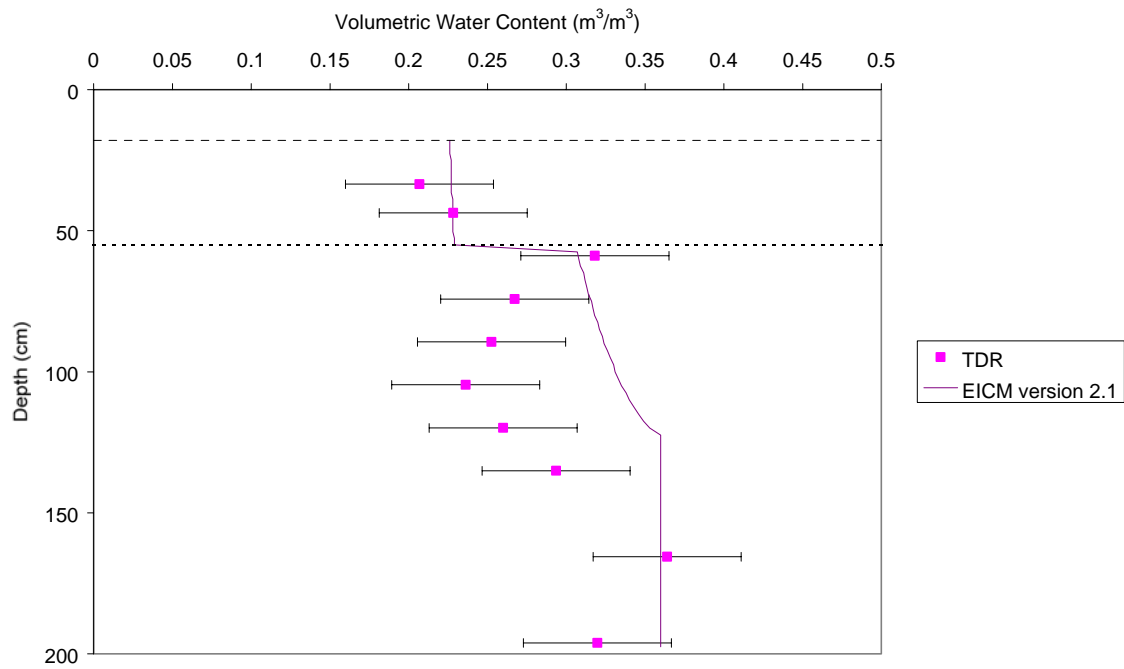


CT site - 4/12/95

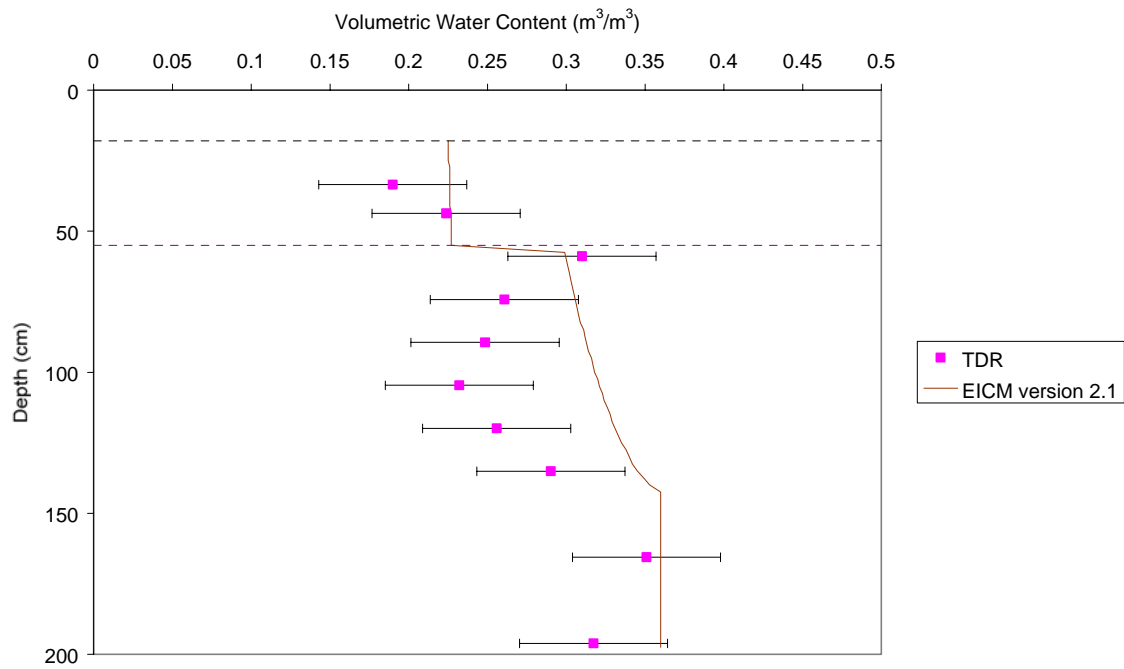




CT site - 5/25/95



CT site - 6/20/95



---

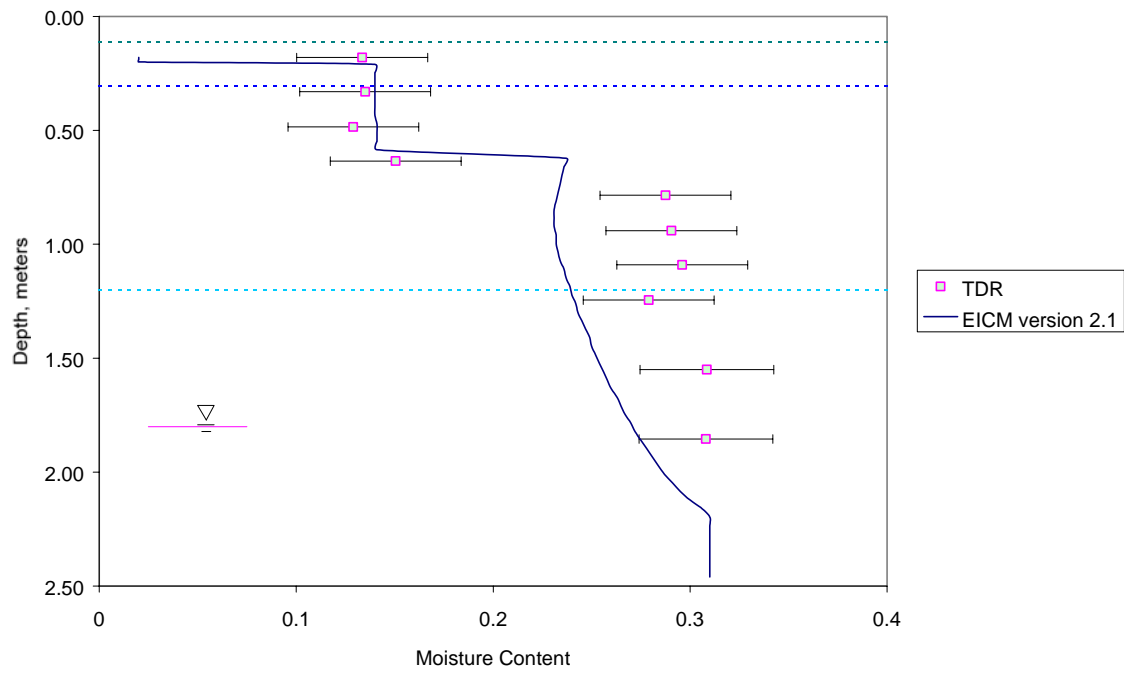
## APPENDIX B

### VOLUMETRIC WATER CONTENT PROFILES

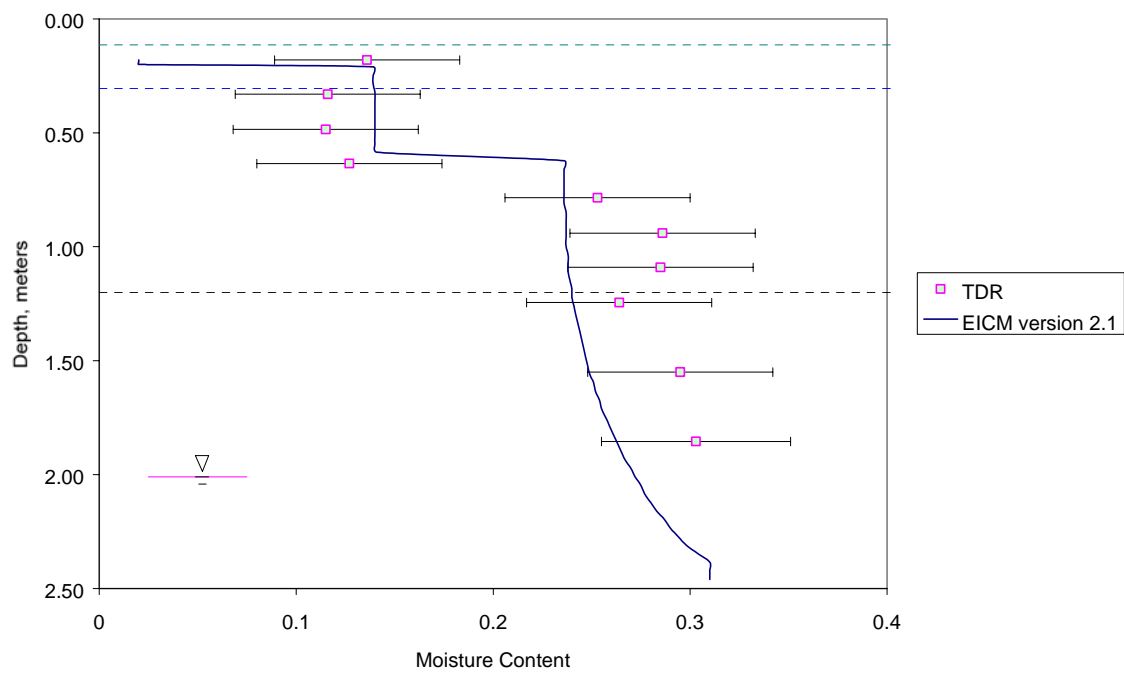
MINNESOTA (91803)

EICM – Version 2.1

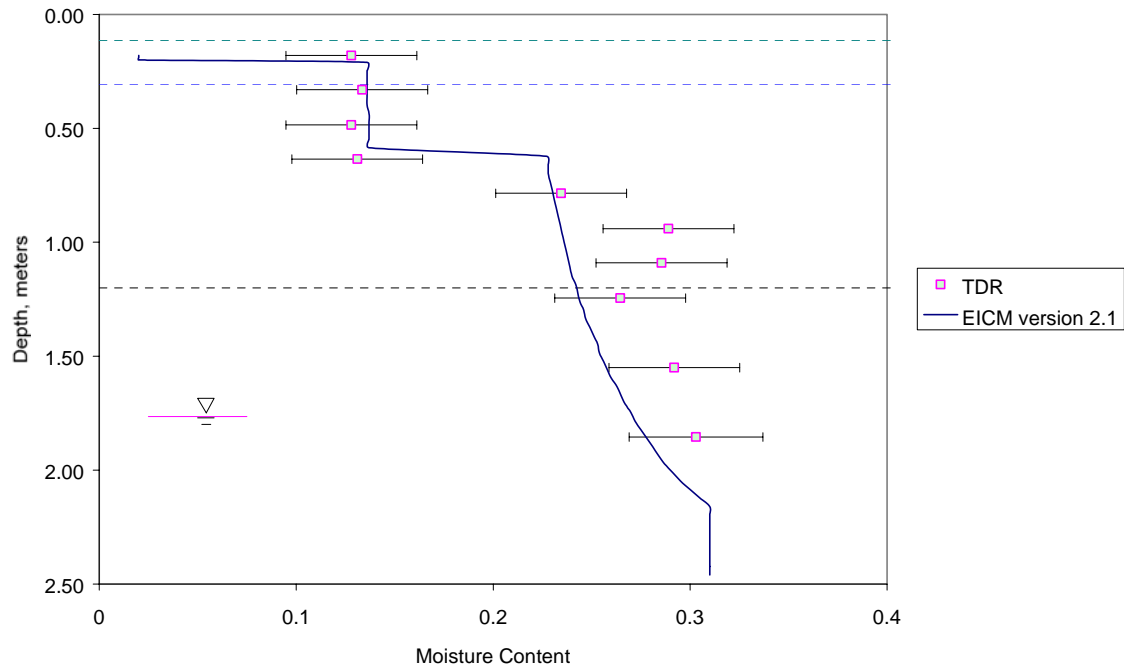
Minnesota Site - 9/23/93



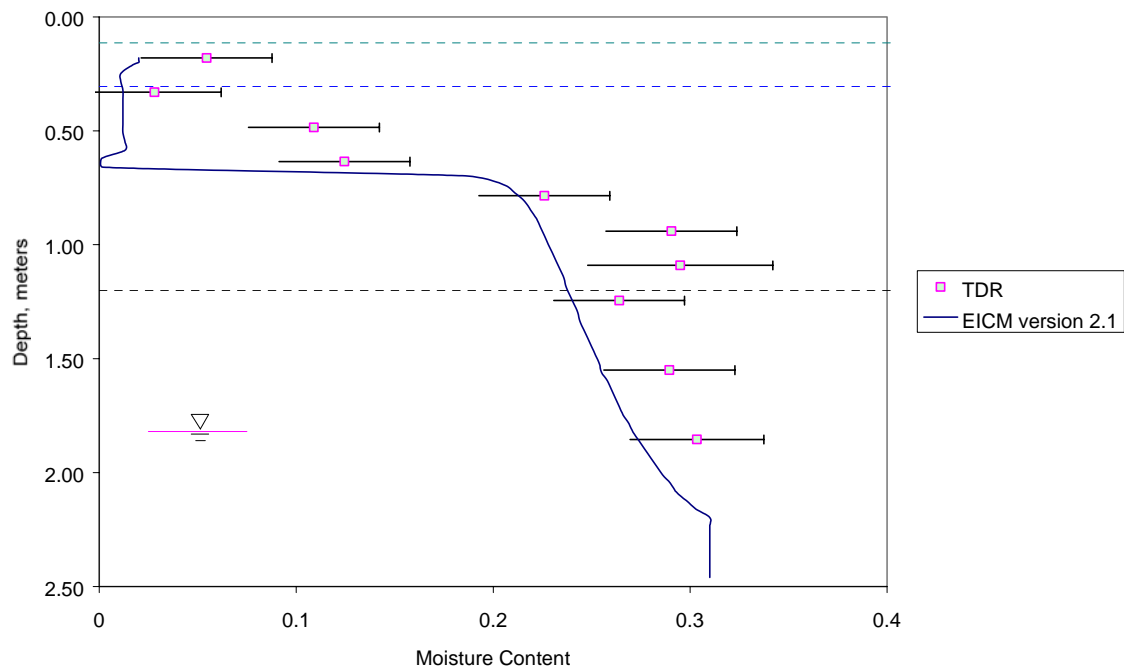
Minnesota Site - 10/20/93



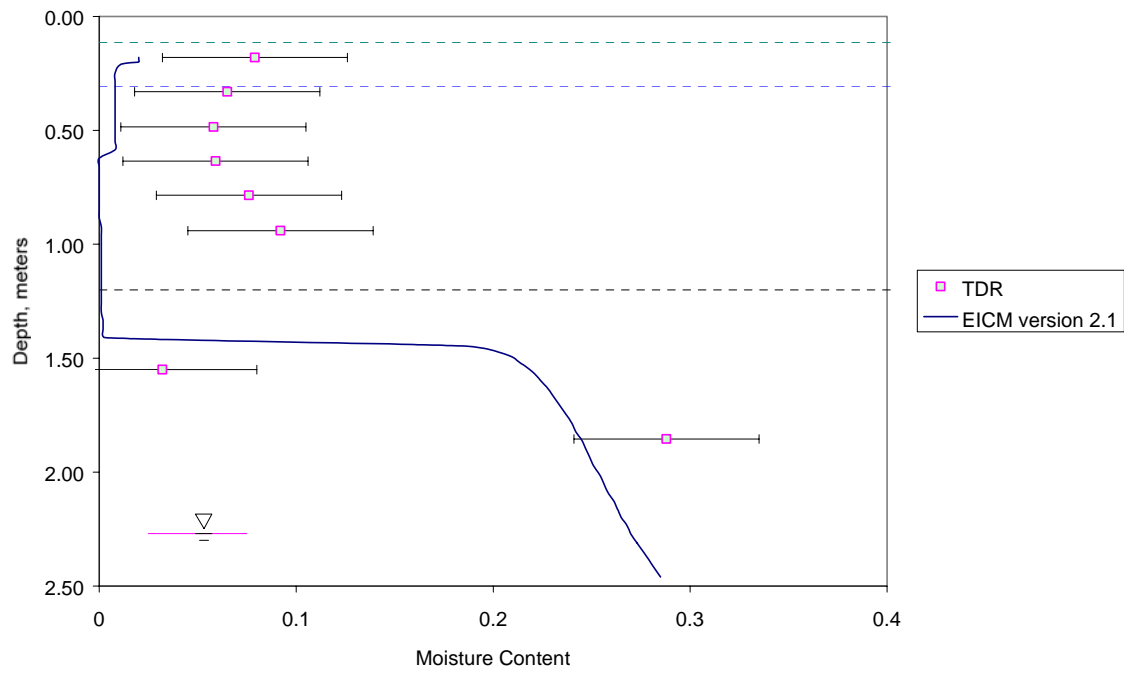
Minnesota Site - 11/19/93



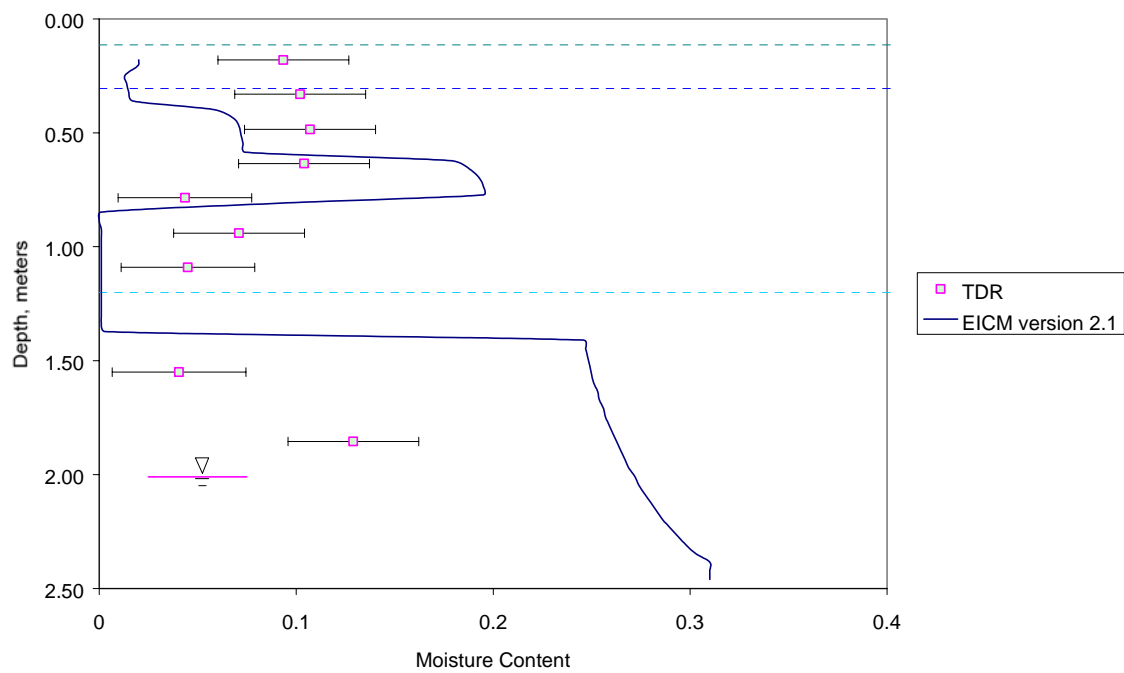
Minnesota Site - 12/07/93



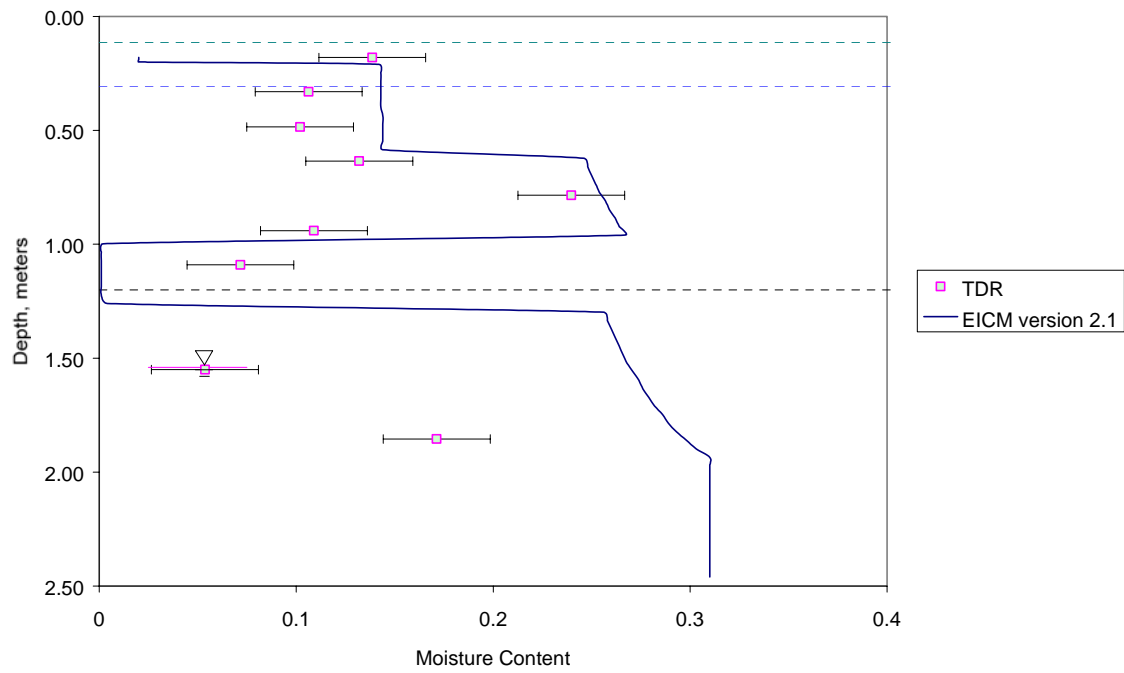
Minnesota Site - 2/08/94



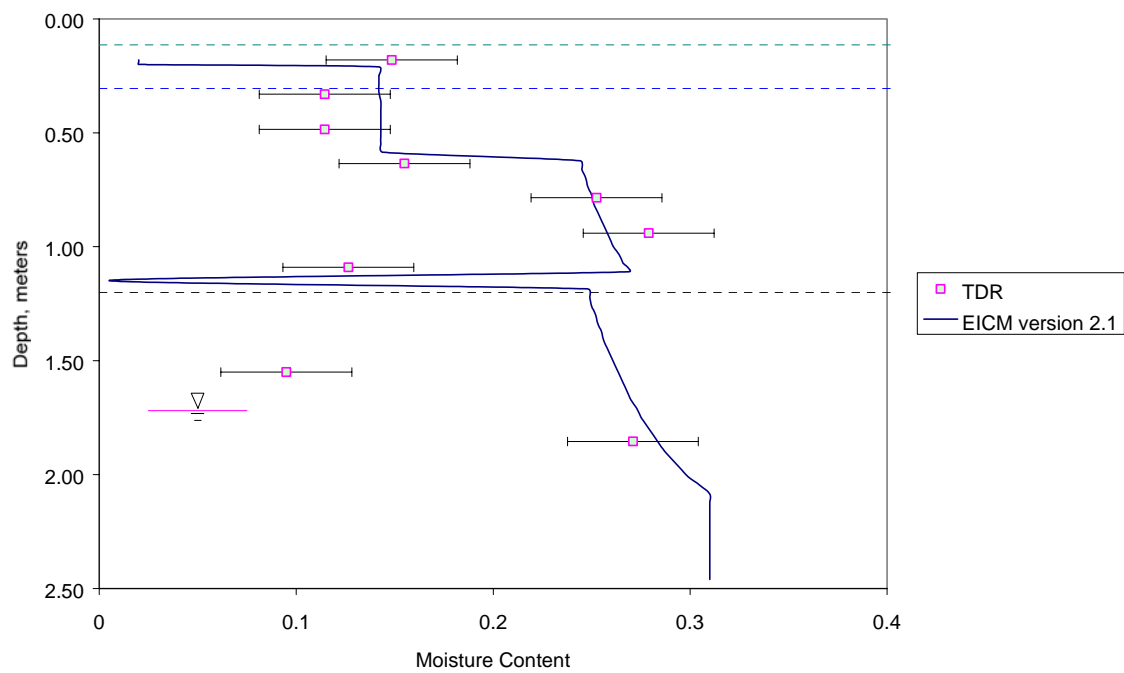
Minnesota Site - 3/08/94



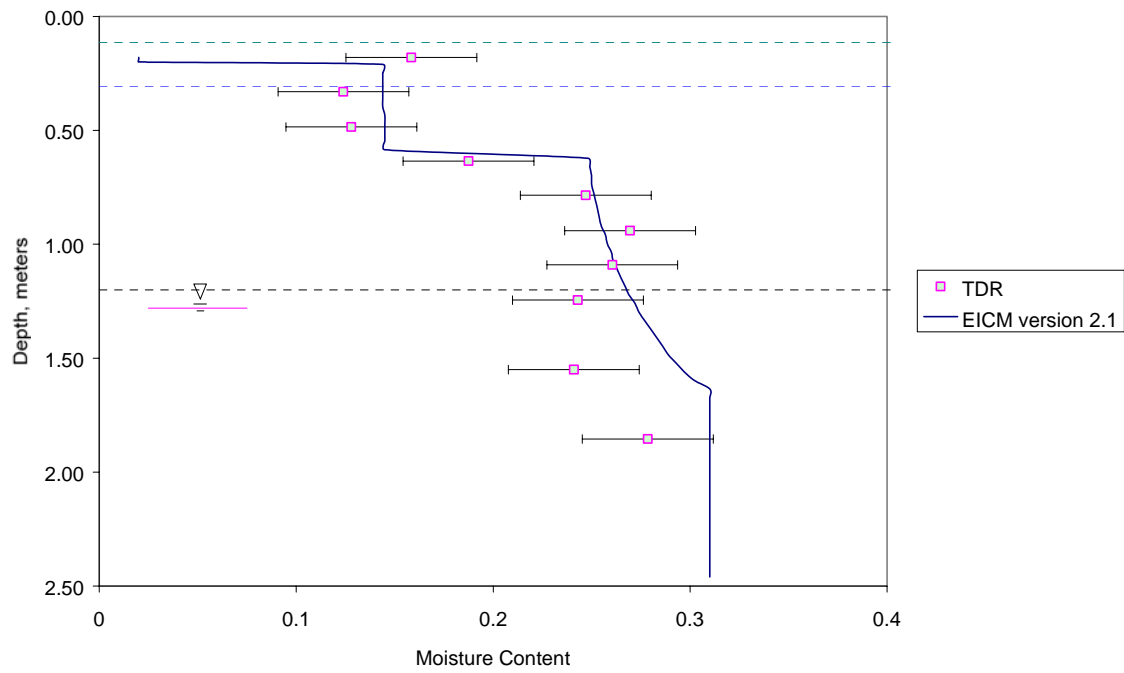
Minnesota Site - 3/22/94



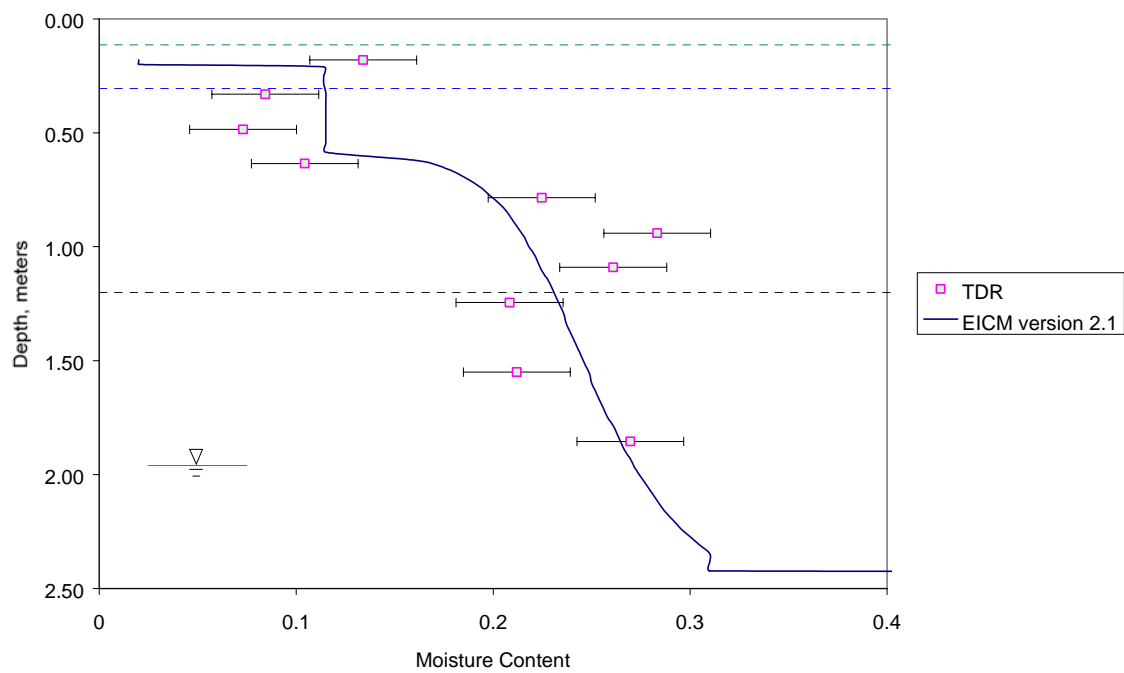
Minnesota Site - 4/04/94



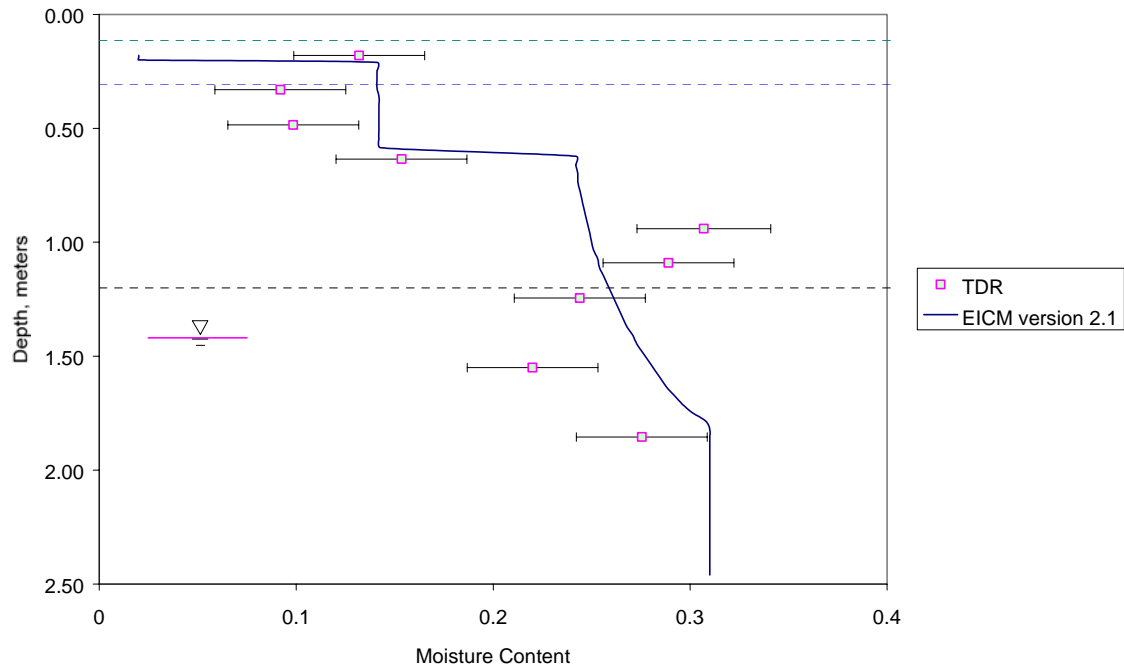
Minnesota Site - 4/25/94



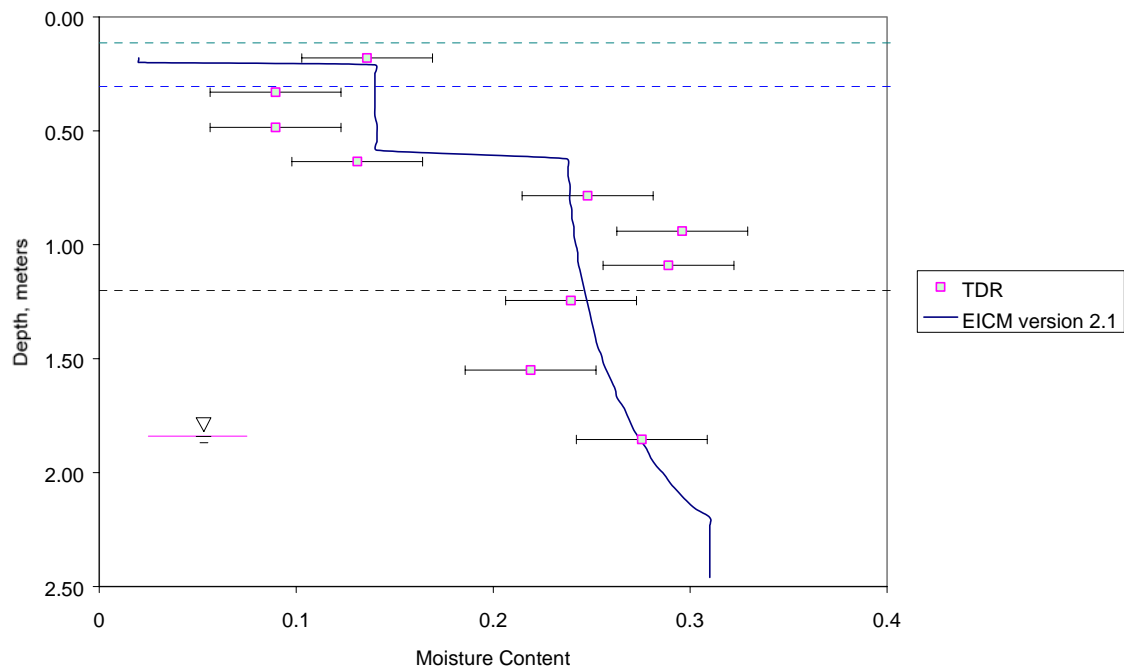
Minnesota Site - 6/13/94



Minnesota Site - 07/11/94



Minnesota Site - 8/08/94





---

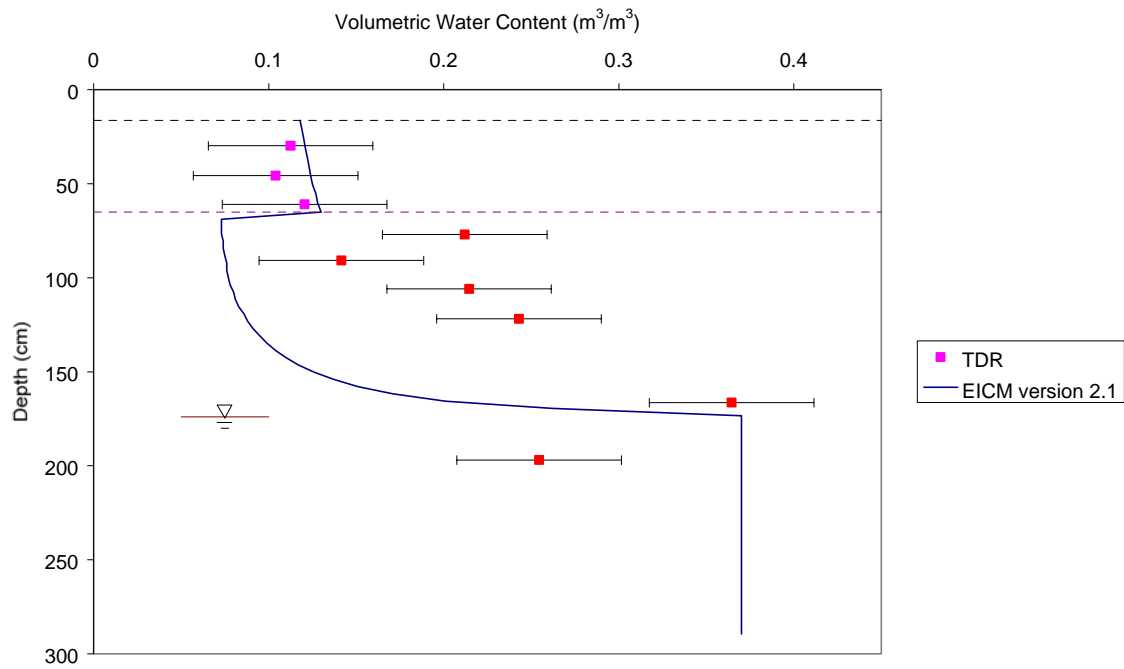
## APPENDIX C

### VOLUMETRIC WATER CONTENT PROFILES

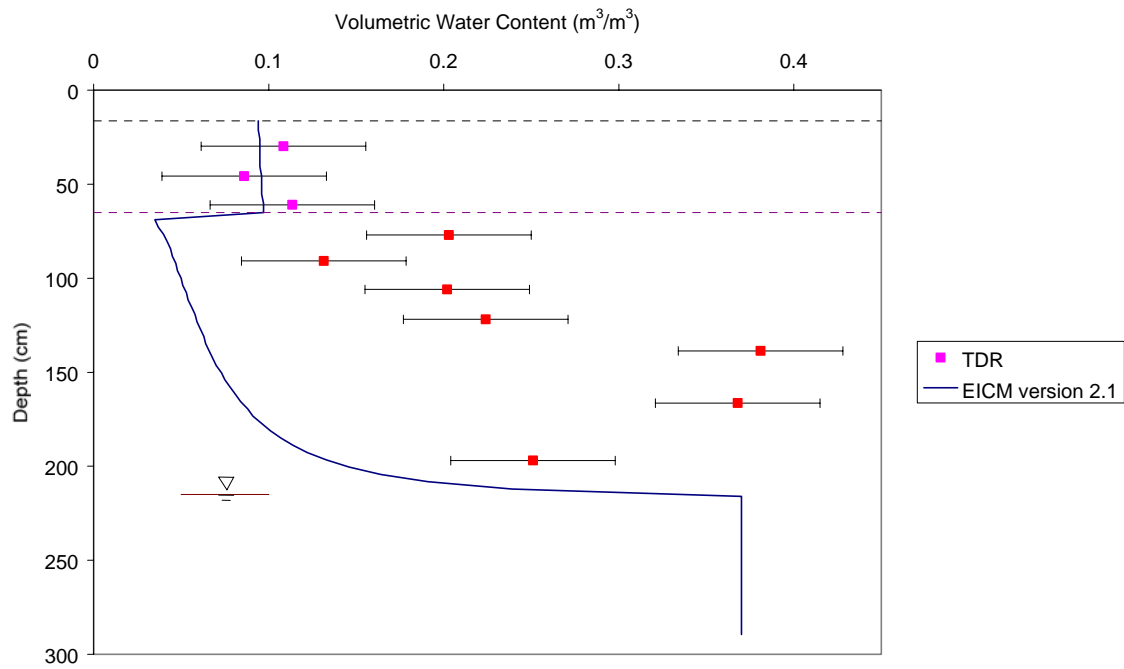
MAINE (231026)

EICM – Version 2.1

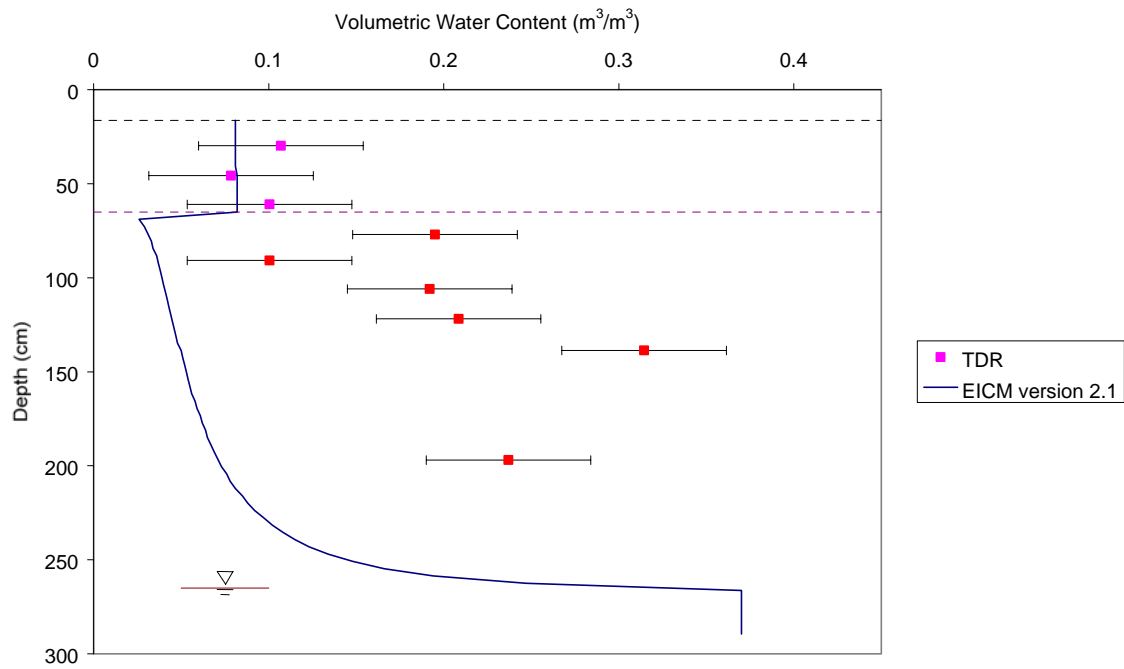
MAINE site - 6/20/94



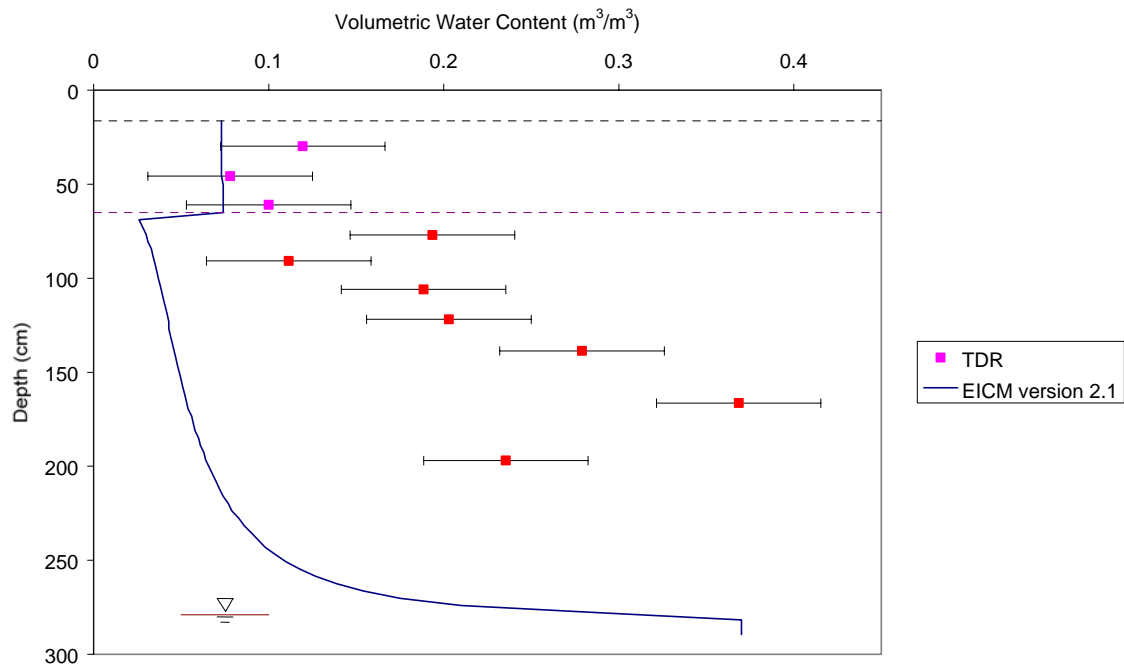
MAINE site - 7/18/94



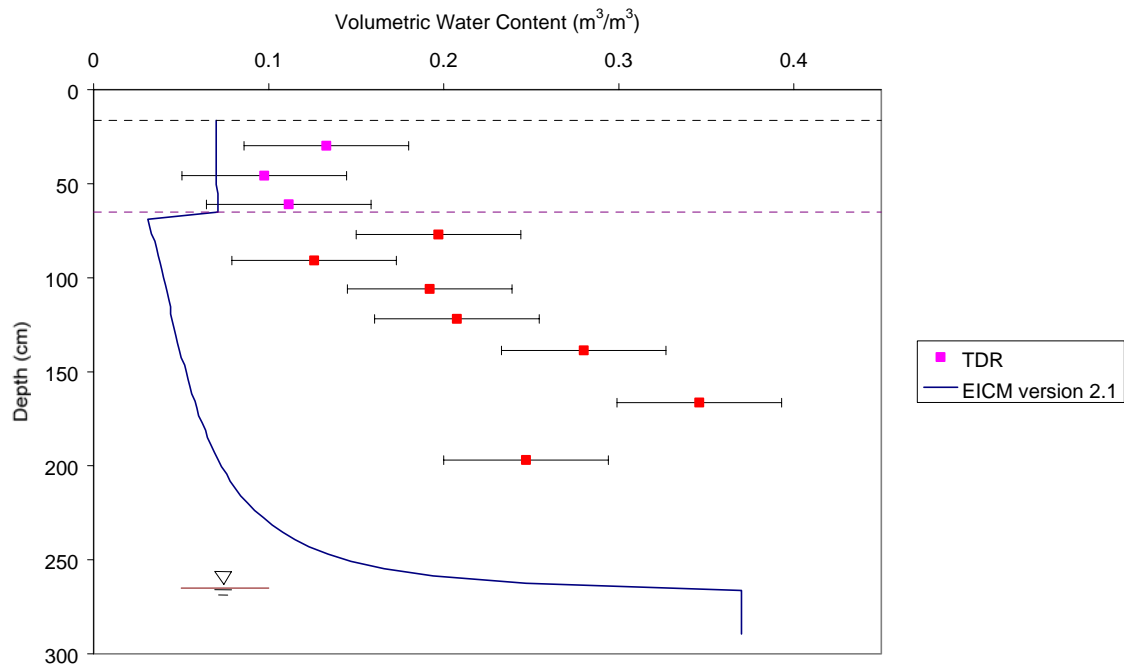
MAINE site - 8/15/94



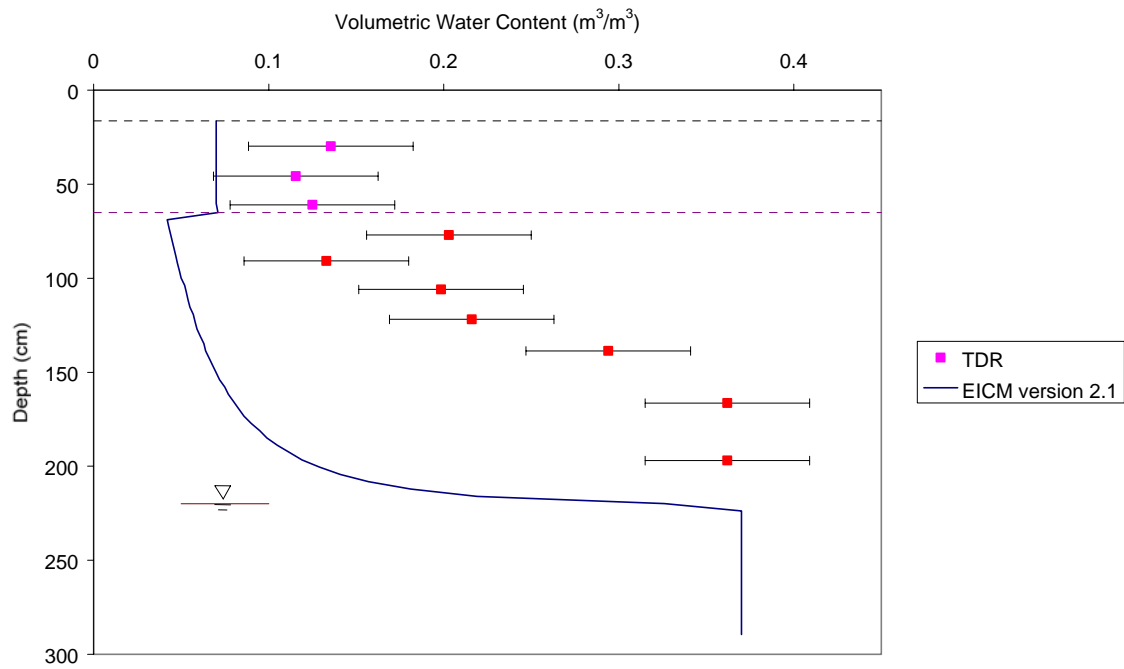
MAINE site - 9/19/94



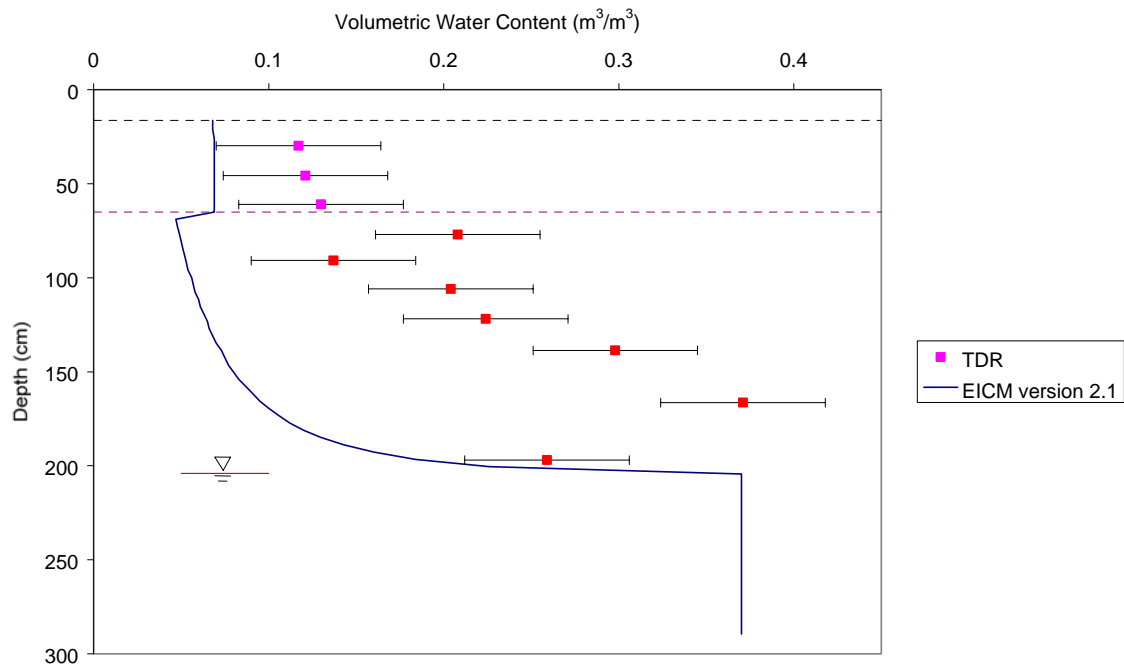
MAINE site - 10/17/94



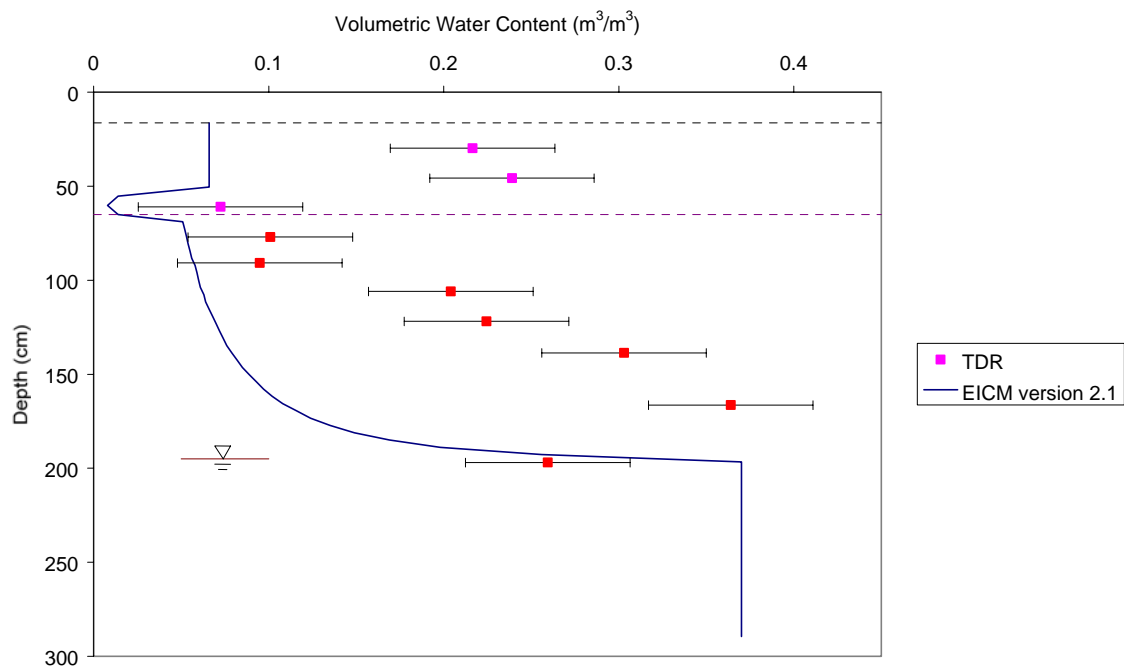
MAINE site - 11/14/94



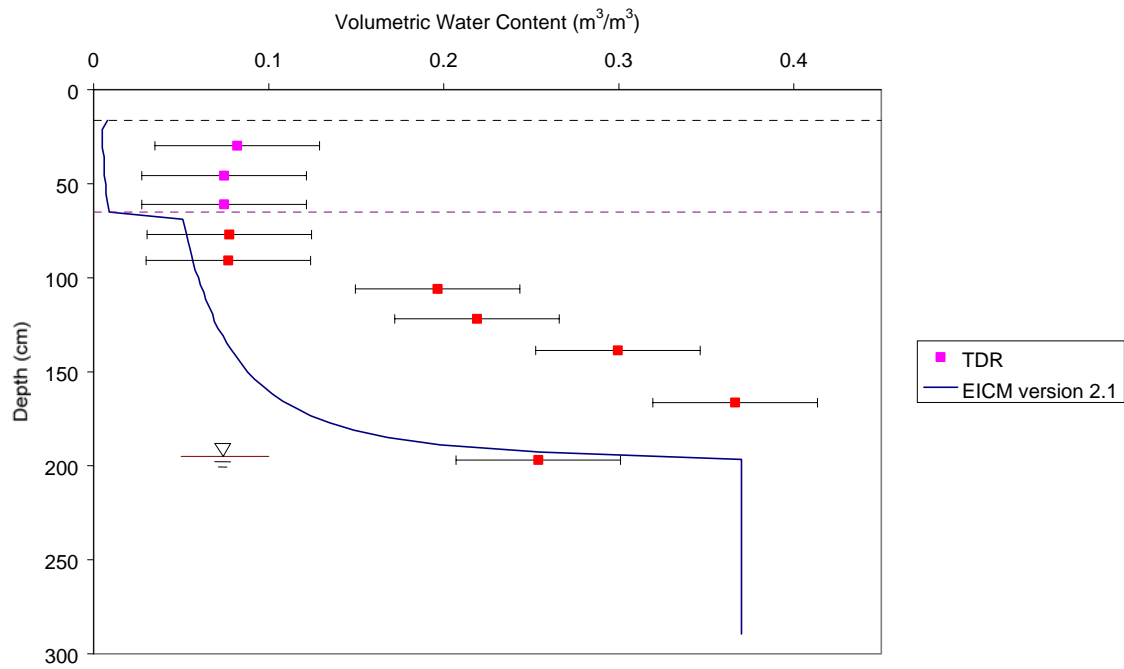
MAINE site - 12/12/94



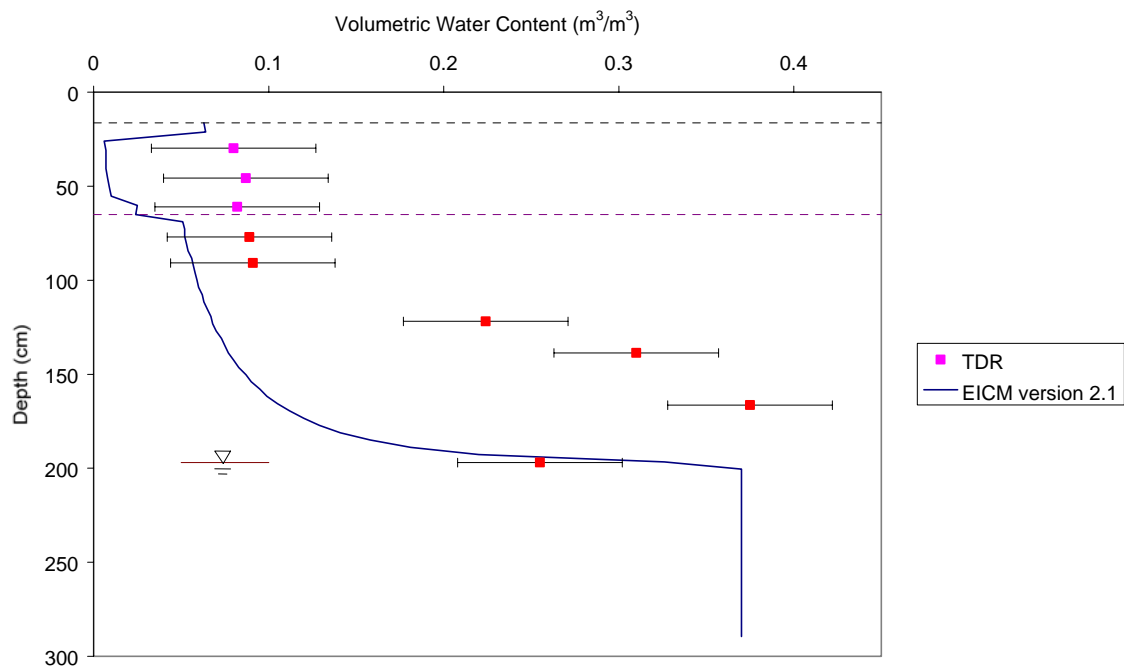
MAINE site - 1/17/95



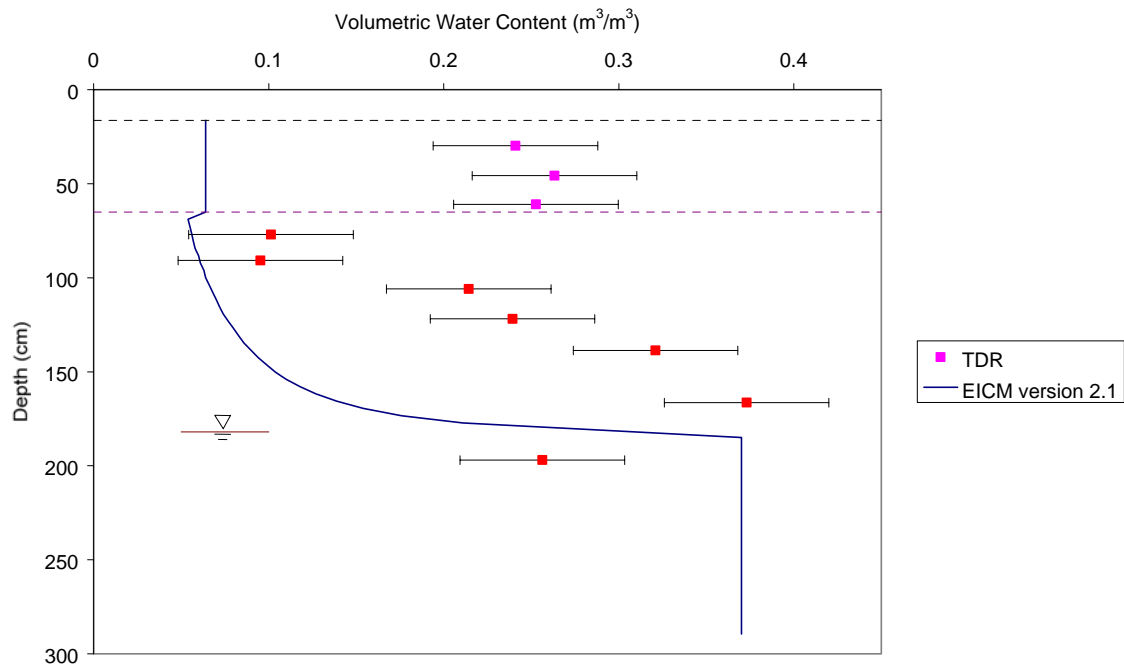
MAINE site - 2/14/95



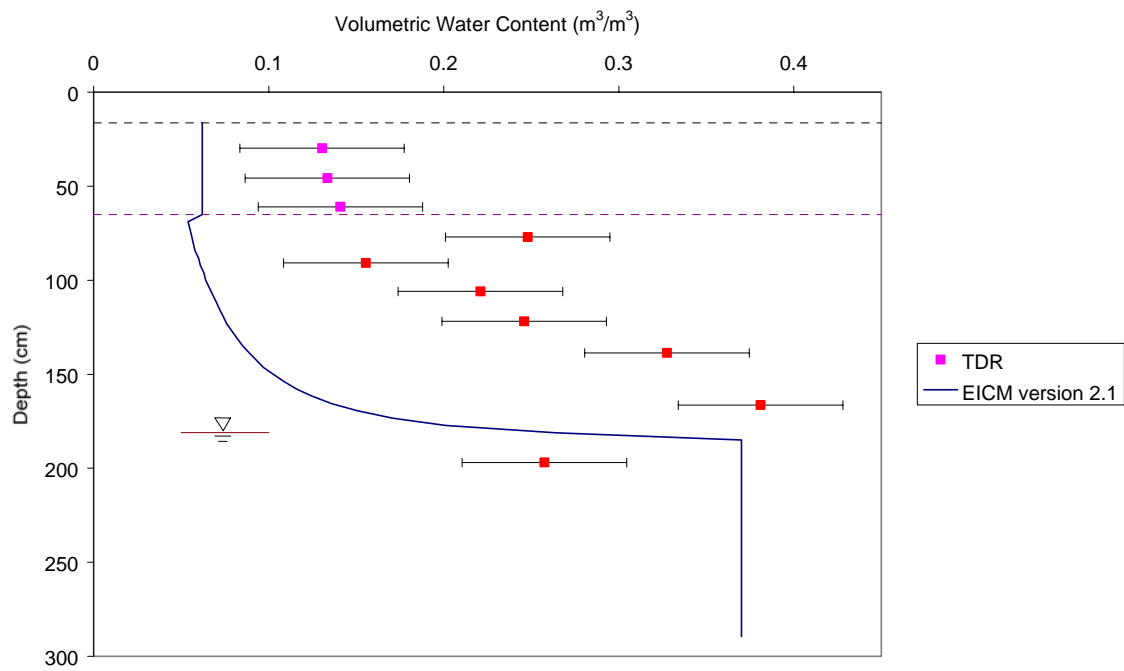
MAINE site - 3/6/95



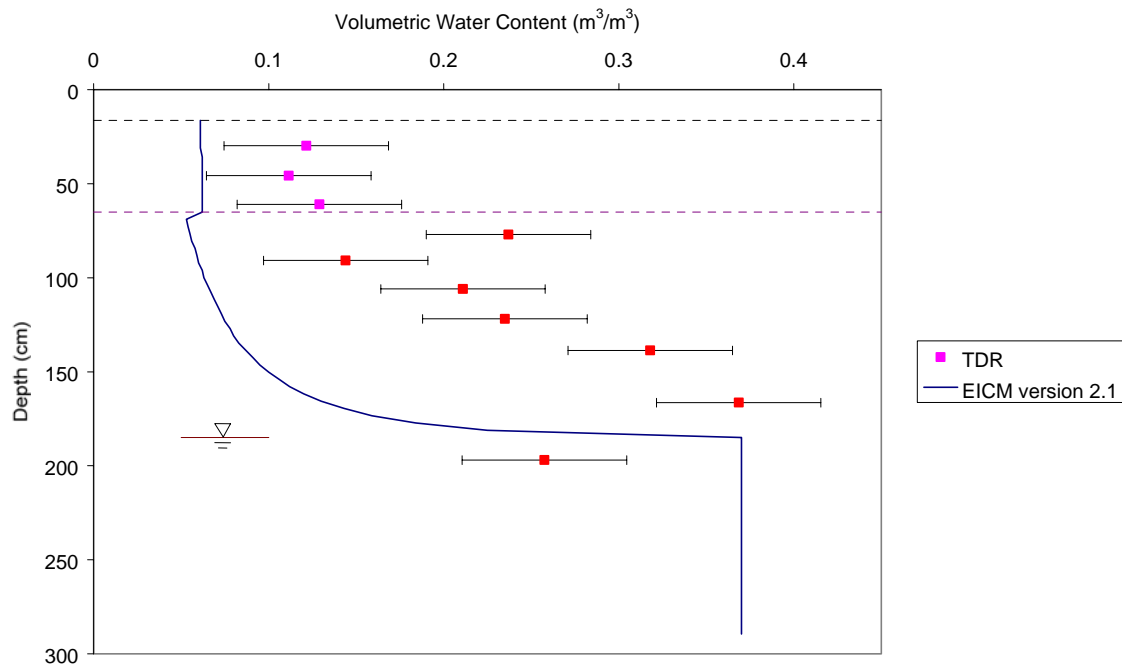
MAINE site - 3/20/95



MAINE site -4/3/95



MAINE site -5/1/95





---

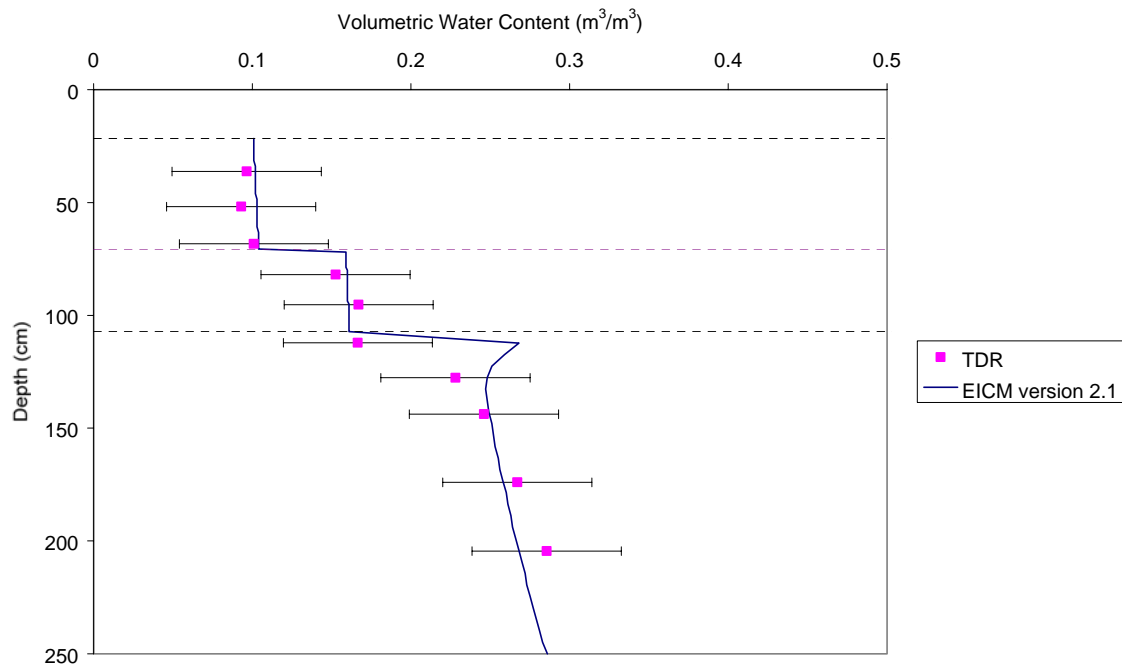
## APPENDIX D

### VOLUMETRIC WATER CONTENT PROFILES

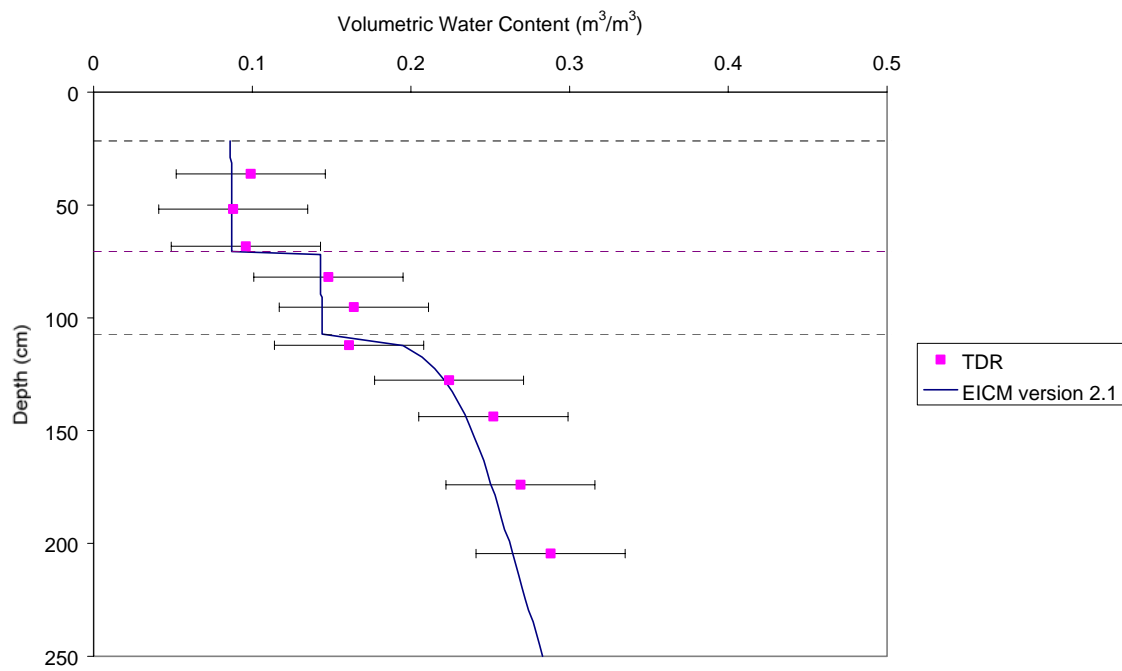
NEW HAMPSHIRE (331001)

EICM – Version 2.1

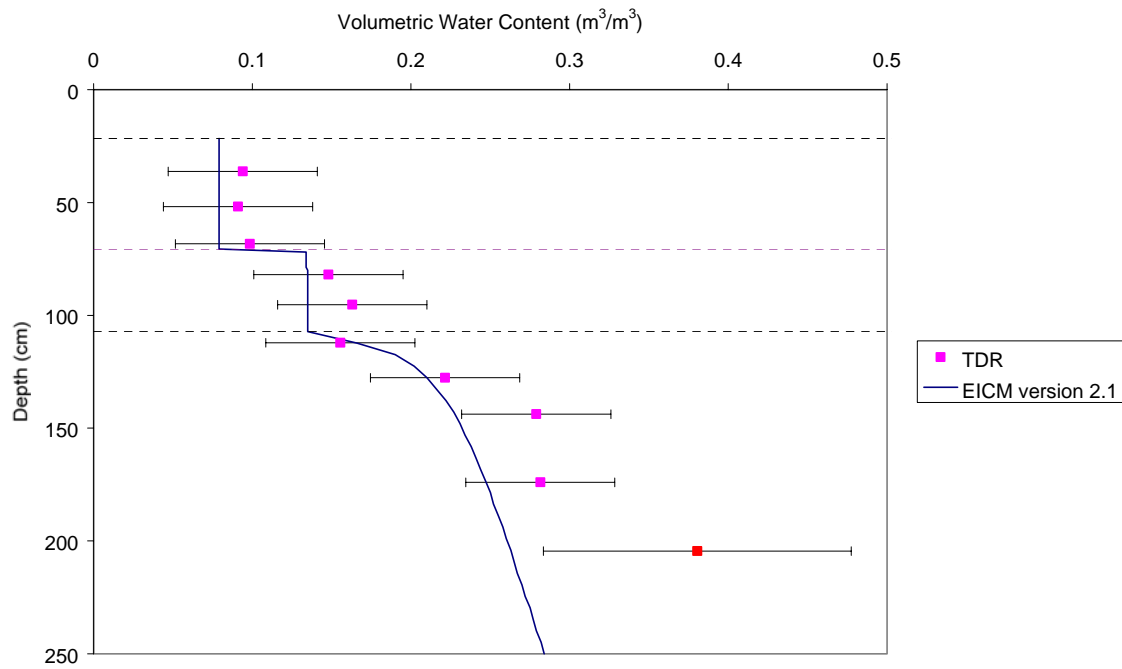
NEW HAMPSHIRE site - 6/23/94



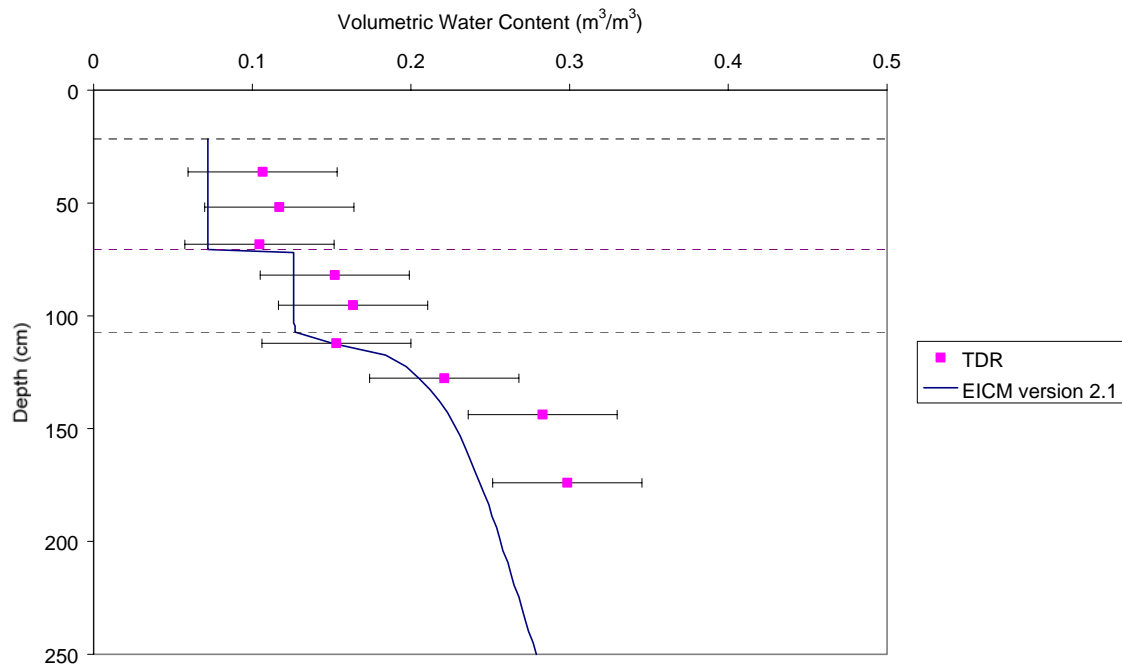
NEW HAMPSHIRE site - 7/21/94

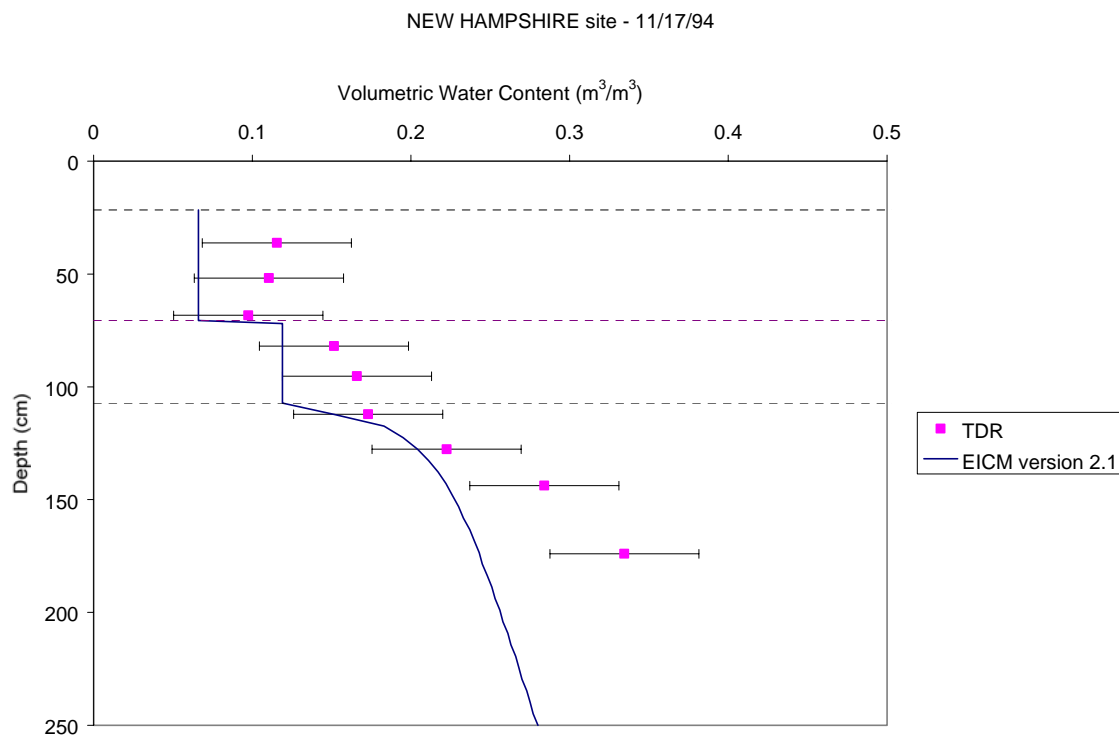
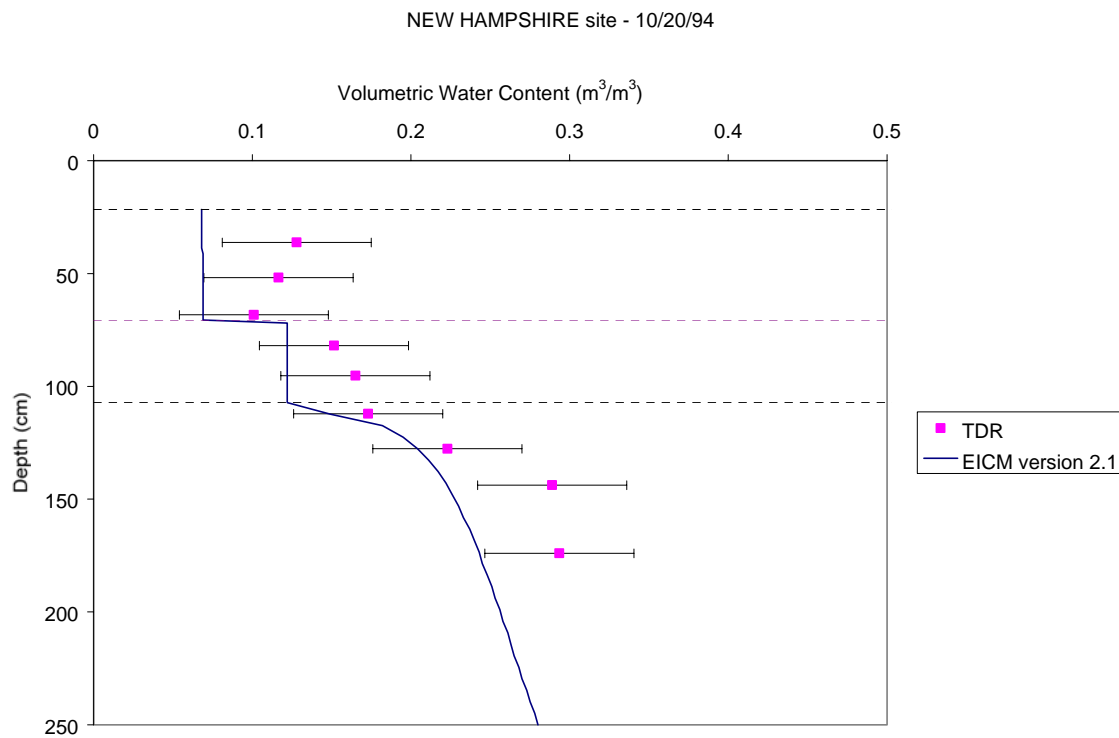


NEW HAMPSHIRE site - 8/16/94

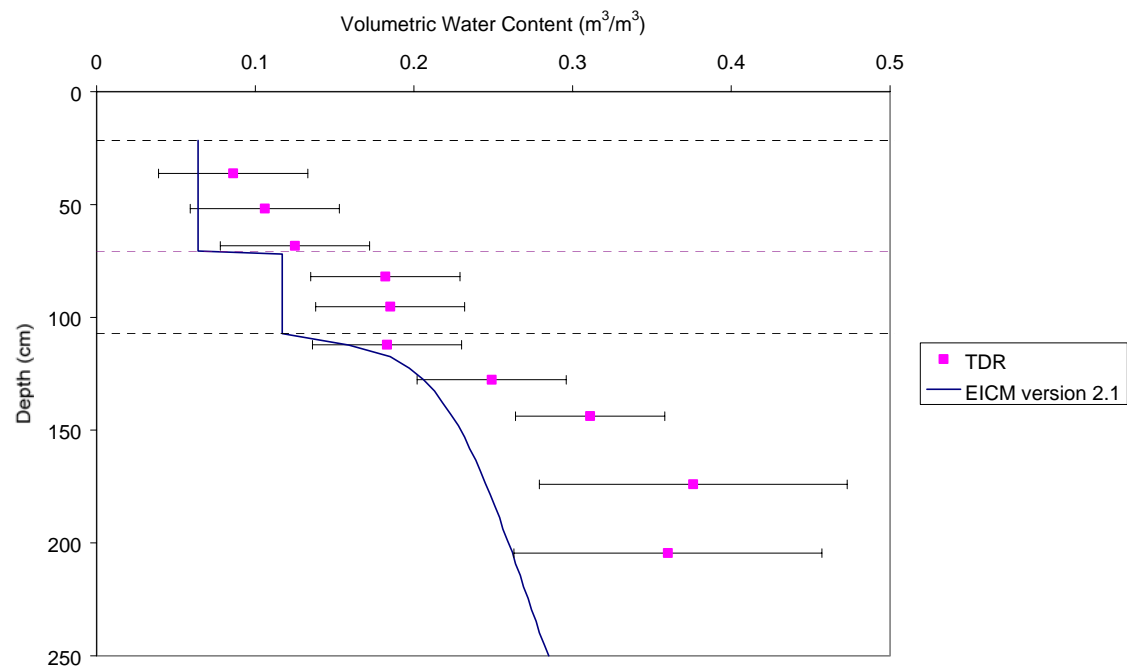


NEW HAMPSHIRE site - 9/22/94

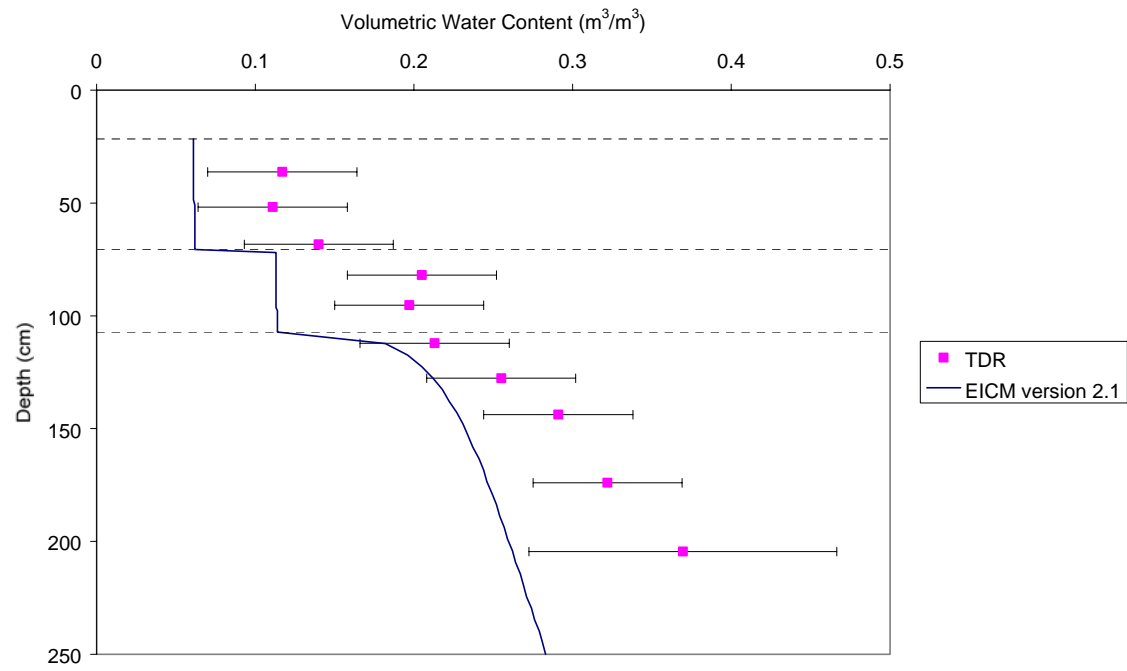




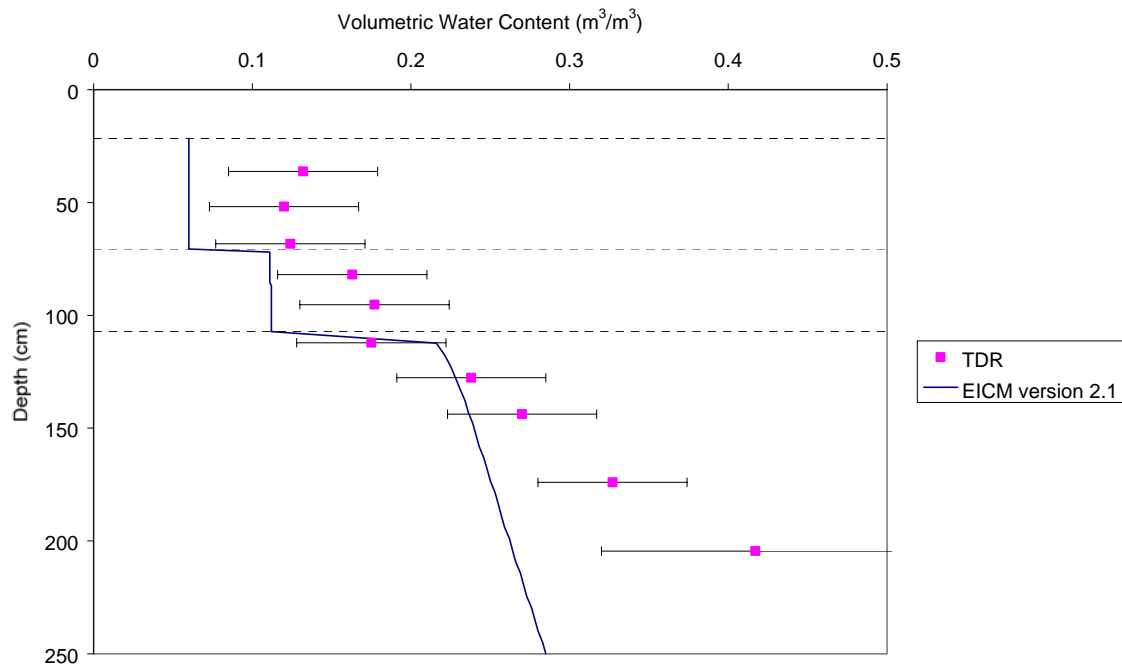
NEW HAMPSHIRE site - 12/15/94



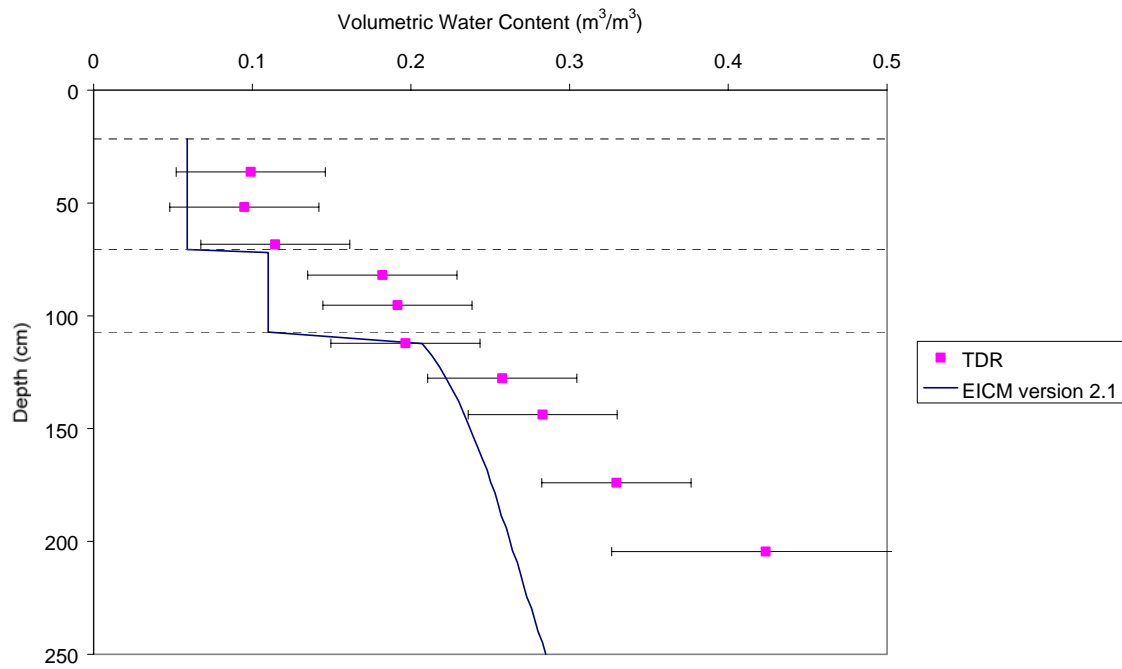
NEW HAMPSHIRE site - 1/24/95



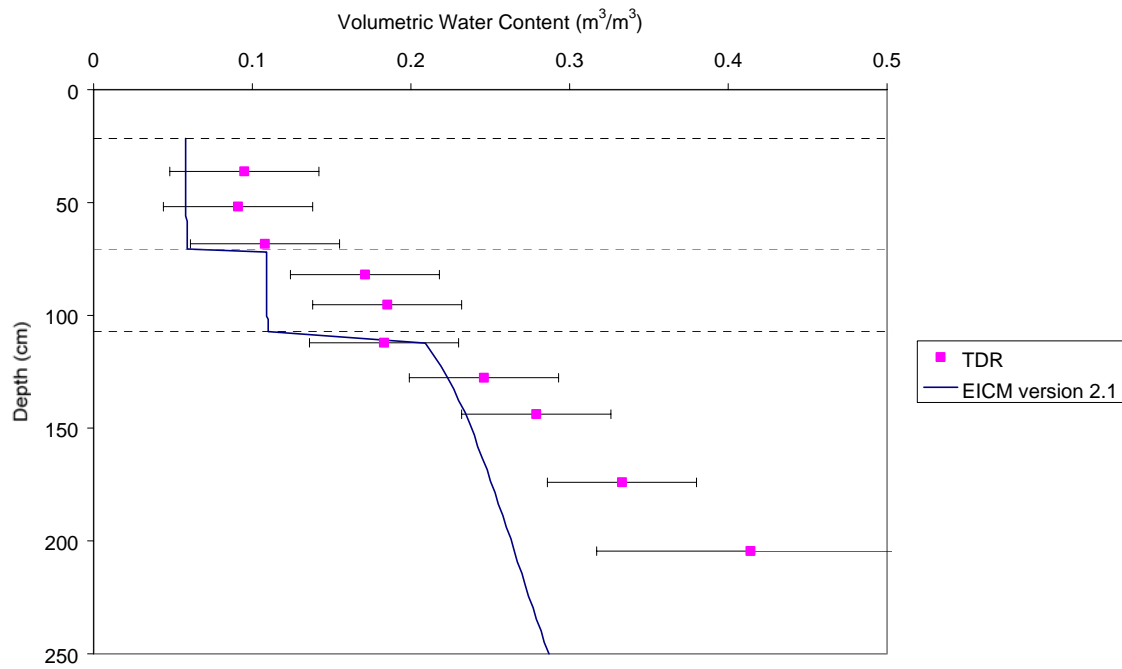
NEW HAMPSHIRE site - 2/21/95



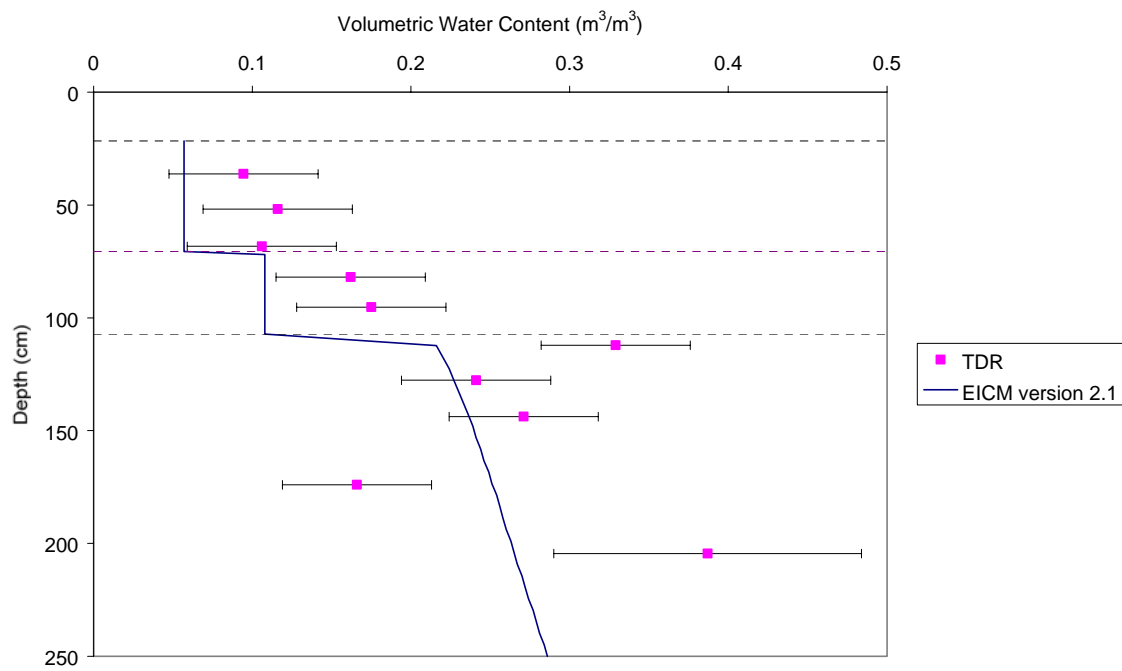
NEW HAMPSHIRE site - 3/16/95



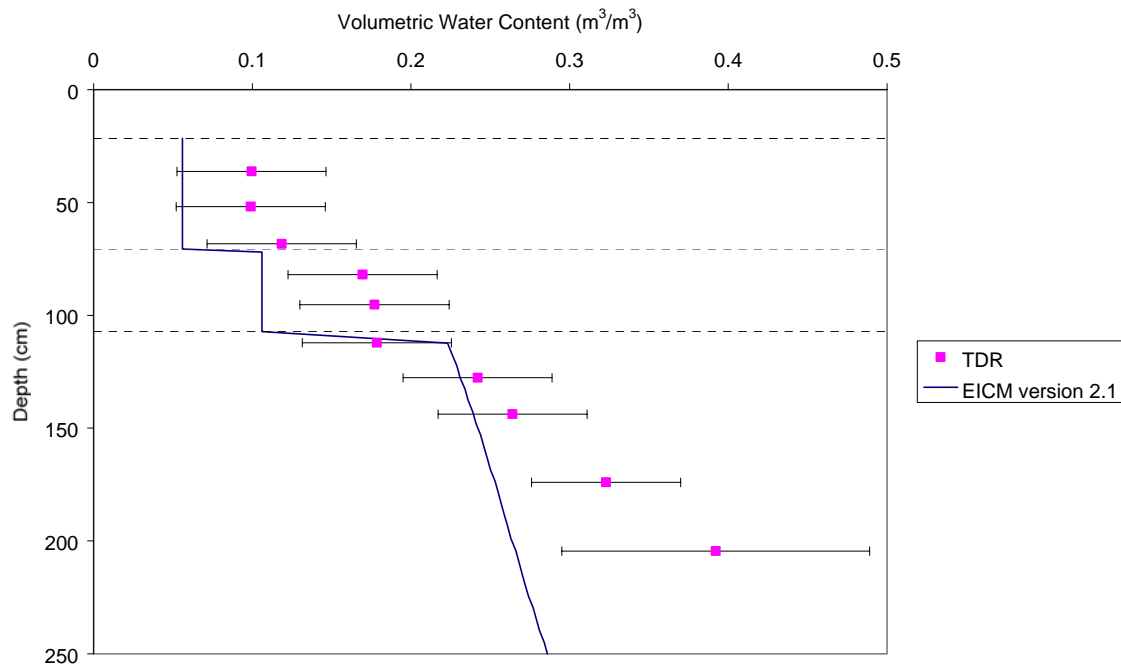
NEW HAMPSHIRE site - 3/30/95



NEW HAMPSHIRE site - 4/27/95



NEW HAMPSHIRE site - 6/1/95





---

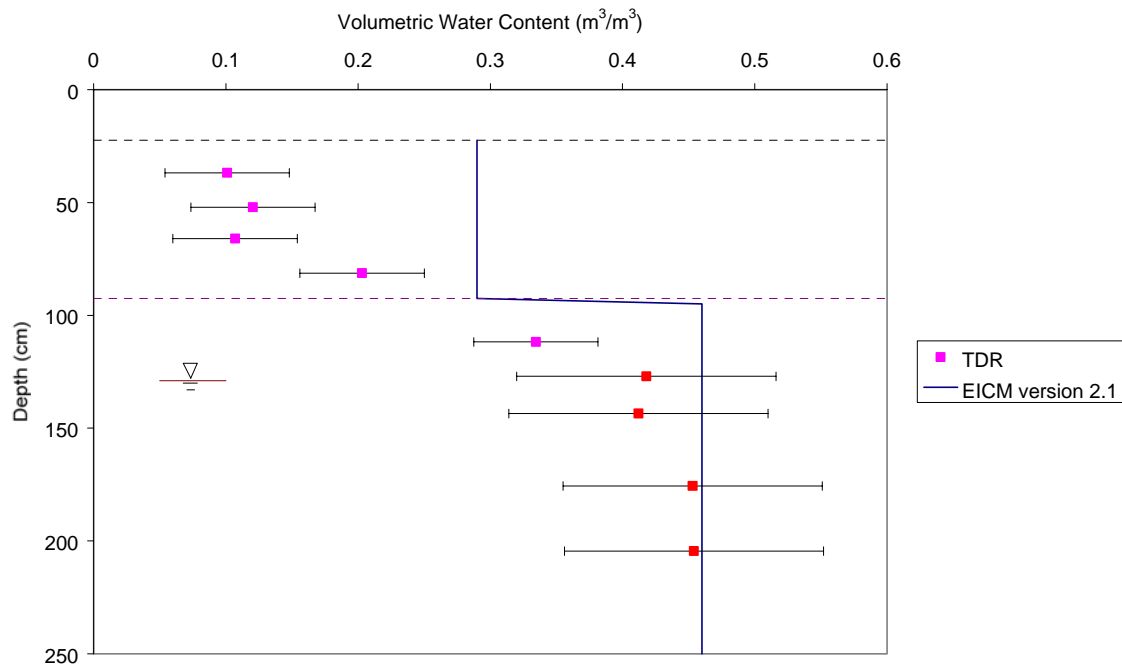
# APPENDIX E

## VOLUMETRIC WATER CONTENT PROFILES

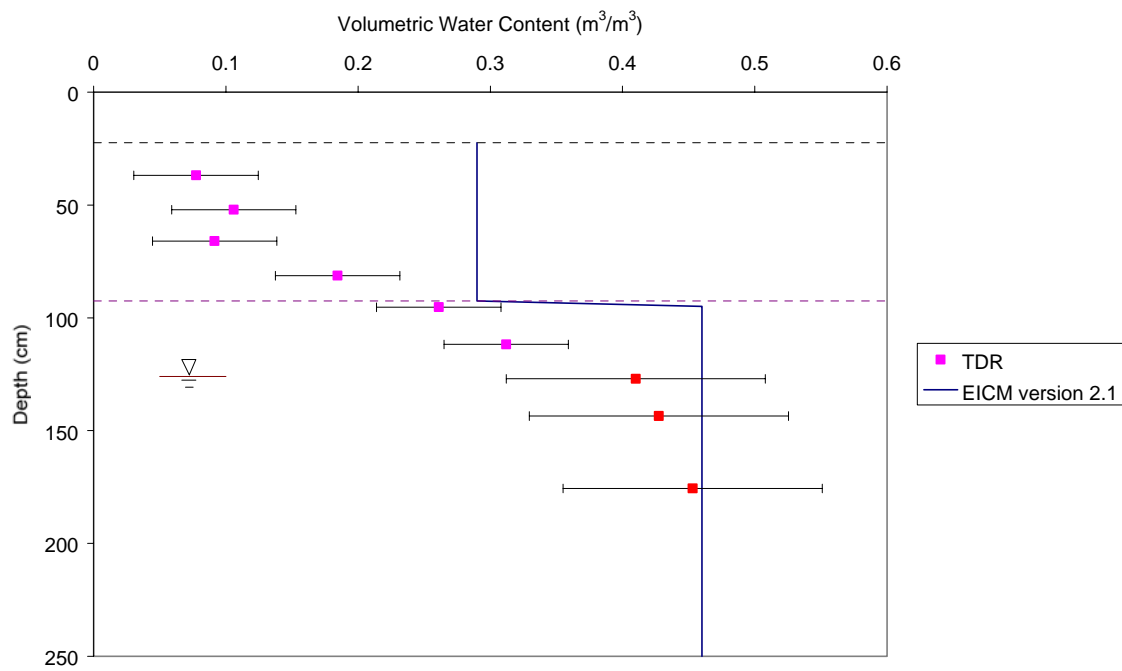
VERMONT (501002)

EICM – Version 2.1

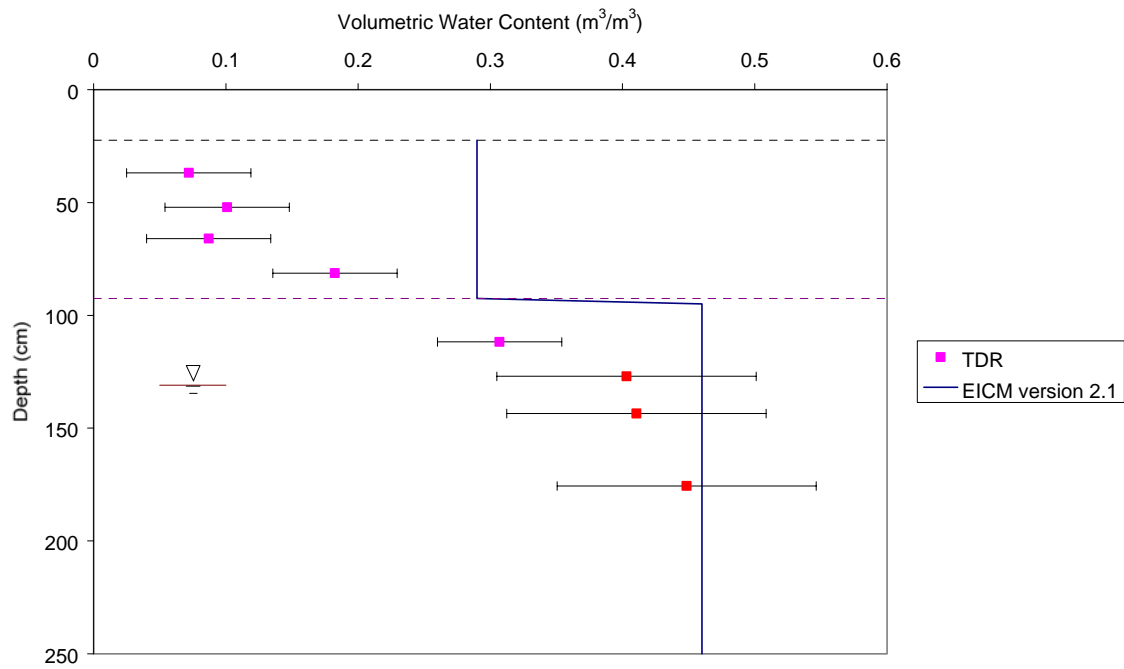
VERMONT site - 7/20/94



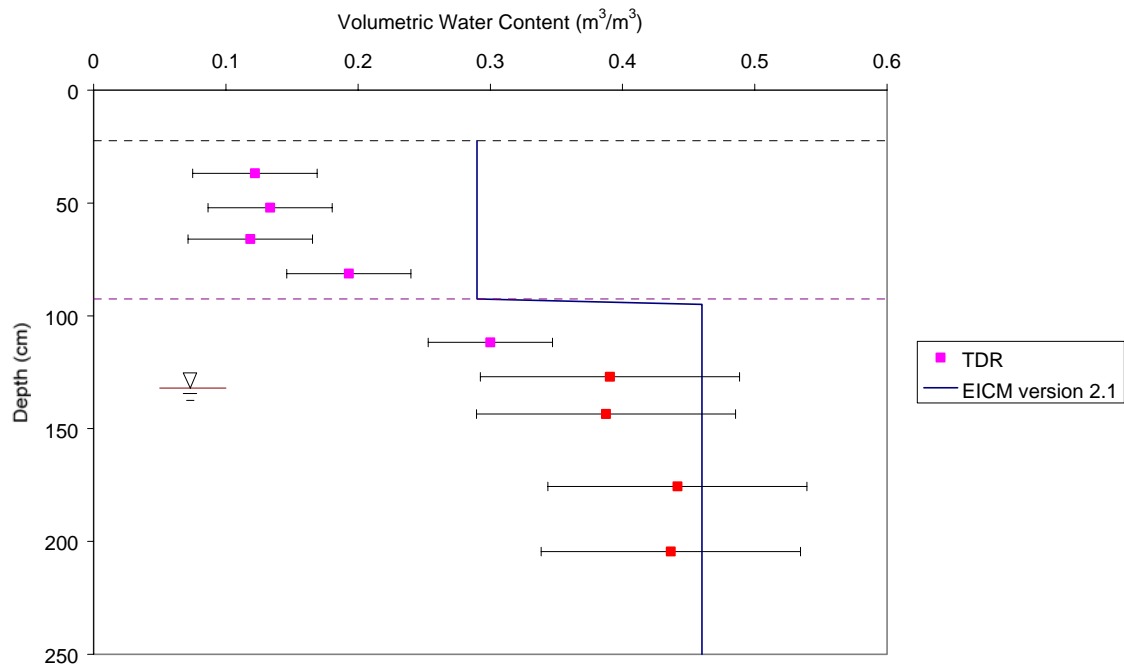
VERMONT site - 8/17/94



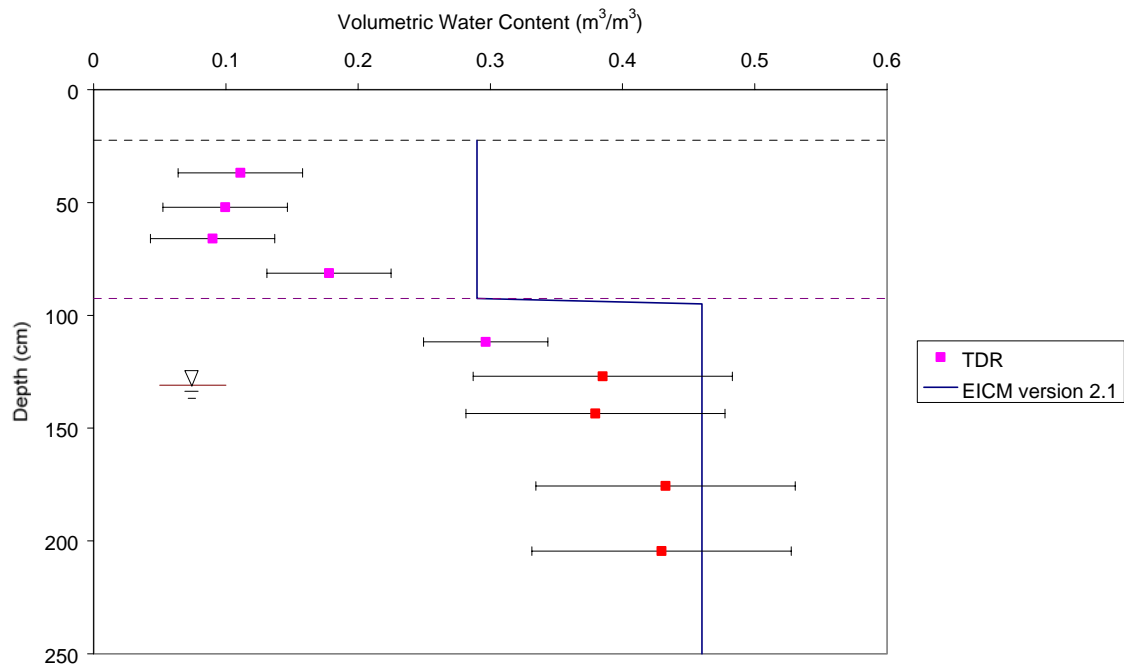
VERMONT site - 9/21/94



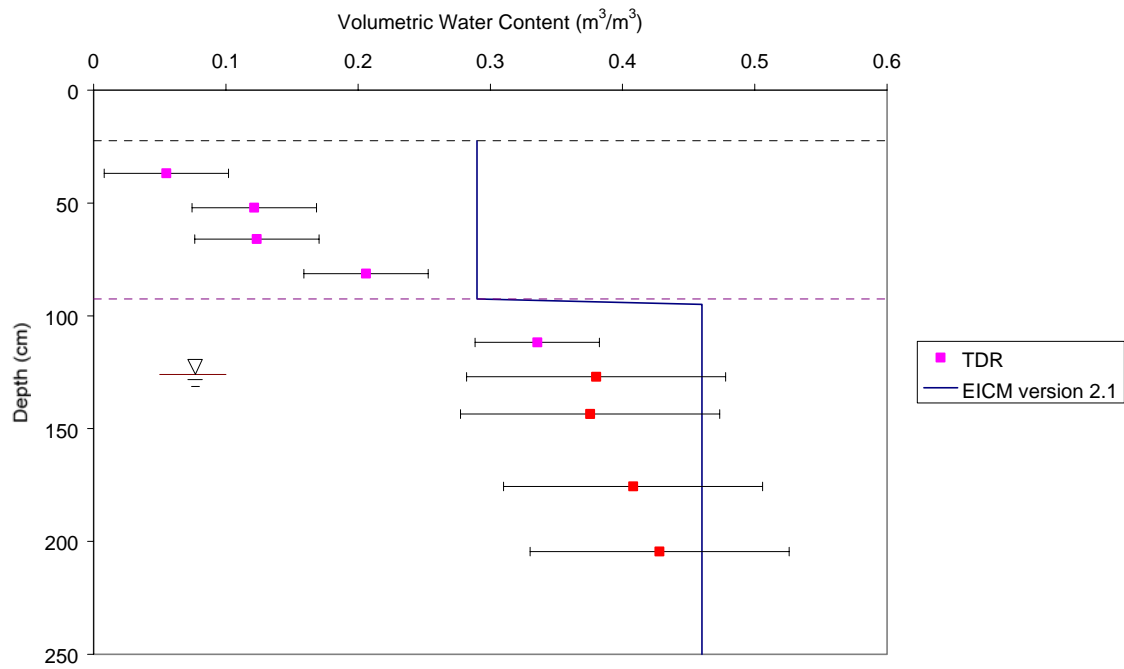
VERMONT site - 10/19/94



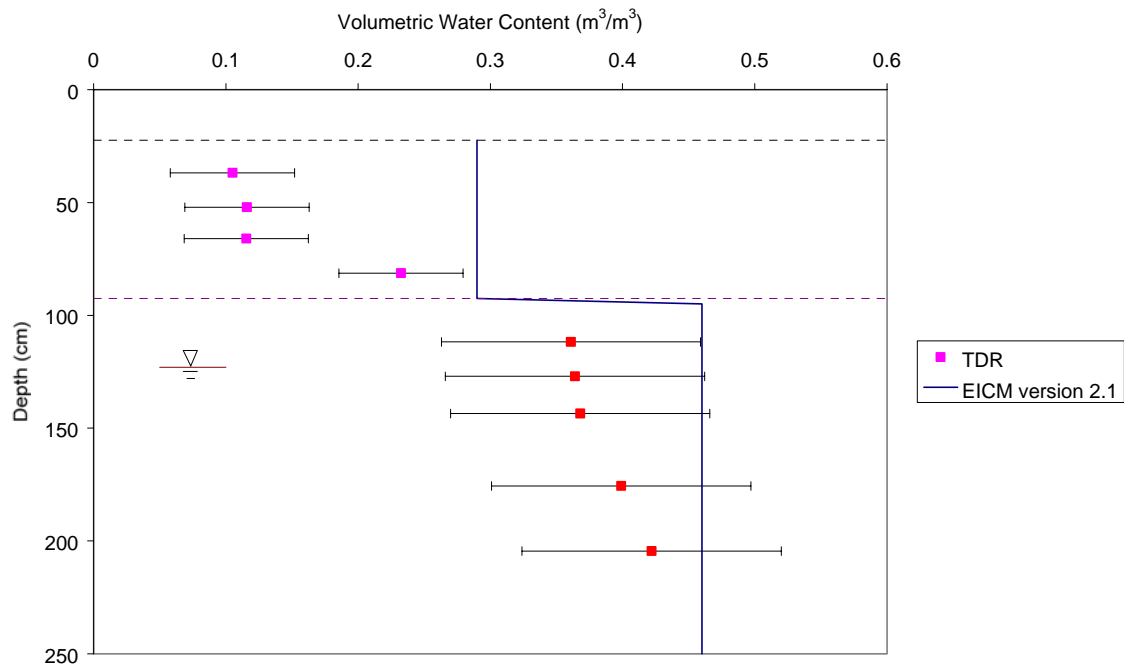
VERMONT site - 11/16/94



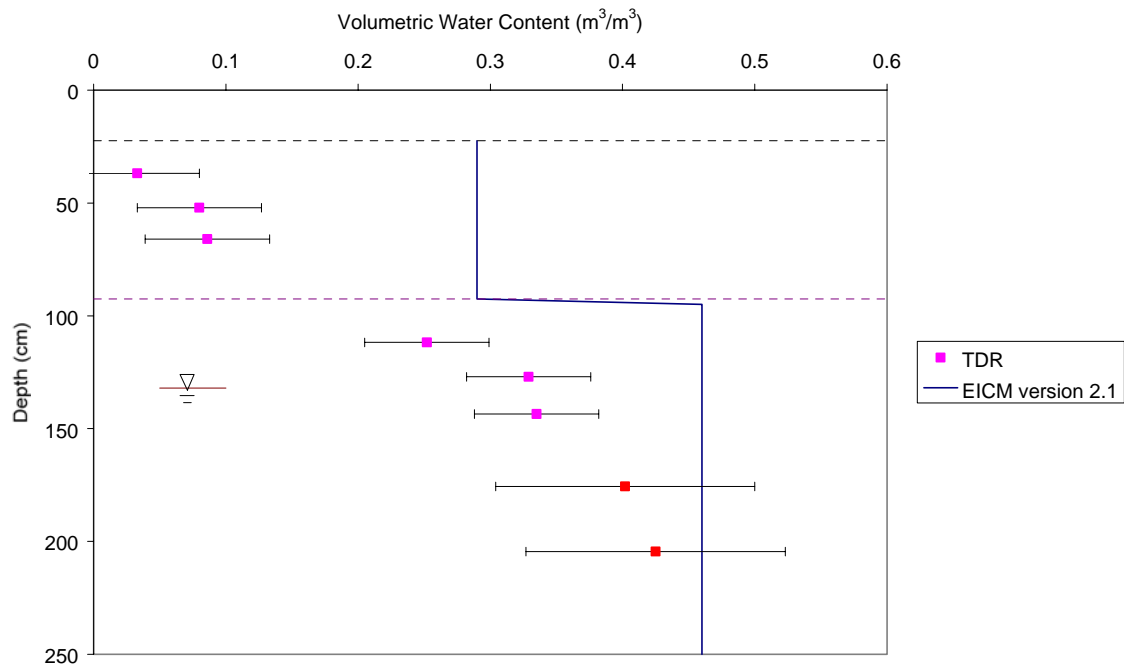
VERMONT site - 12/14/94



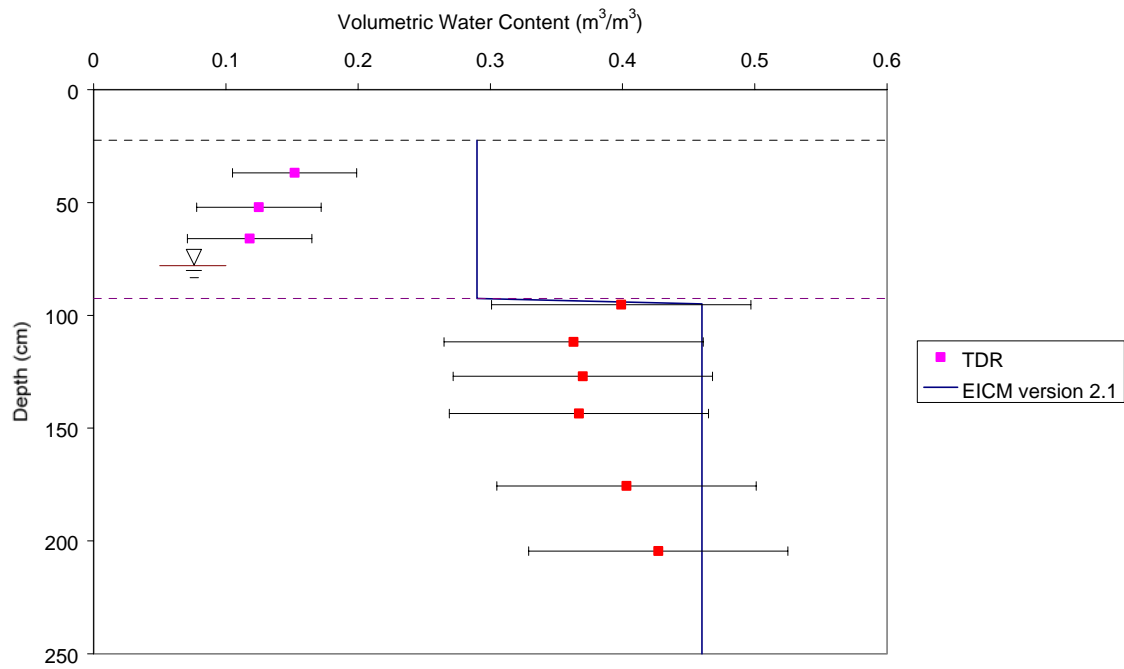
VERMONT site - 1/19/95



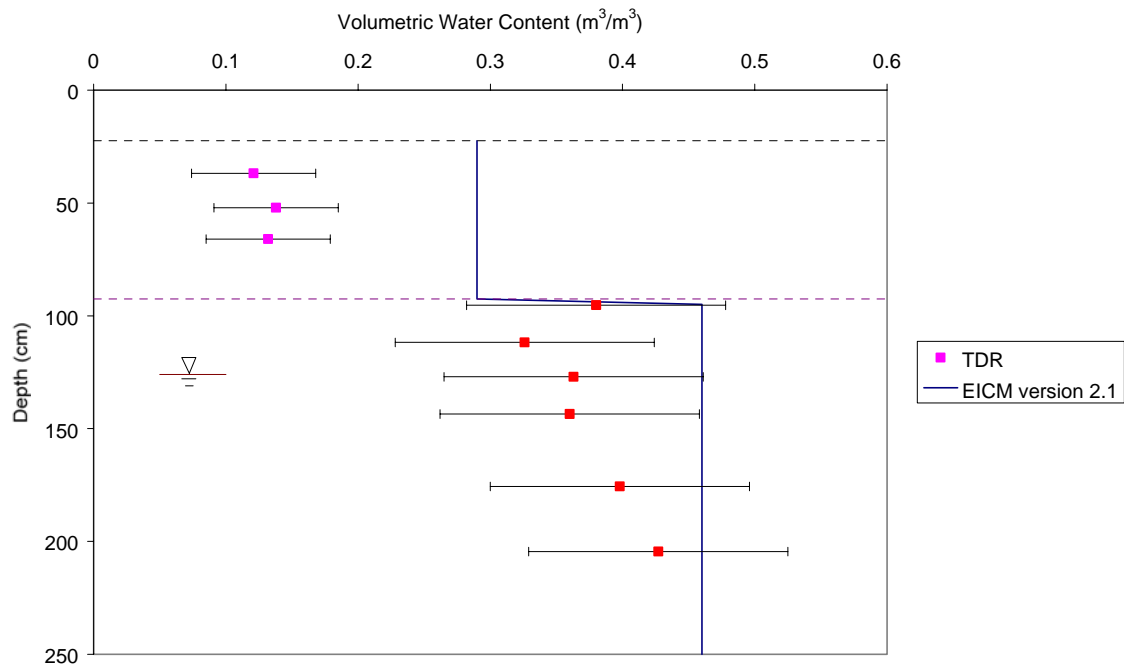
VERMONT site - 2/15/95



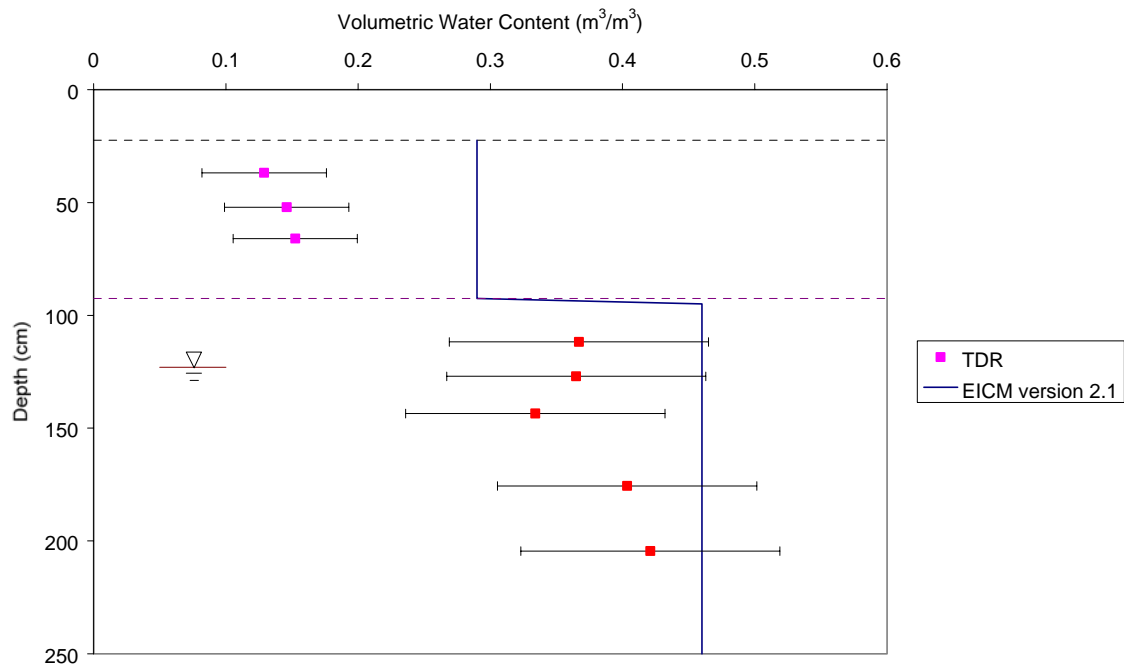
VERMONT site - 3/17/95



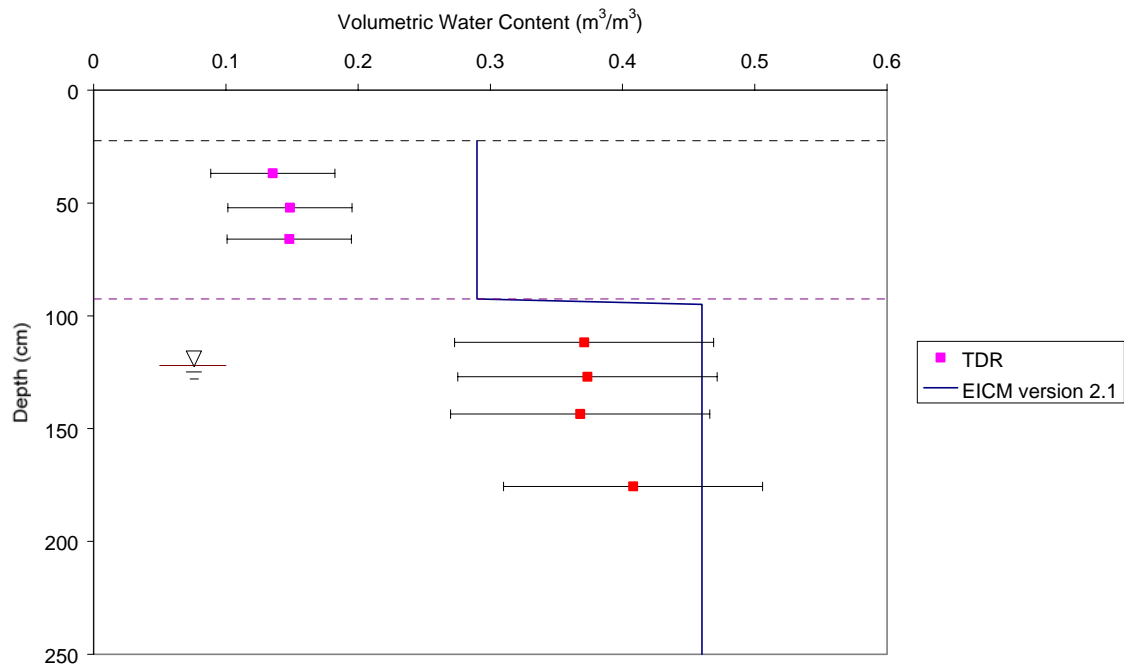
VERMONT site - 3/31/95



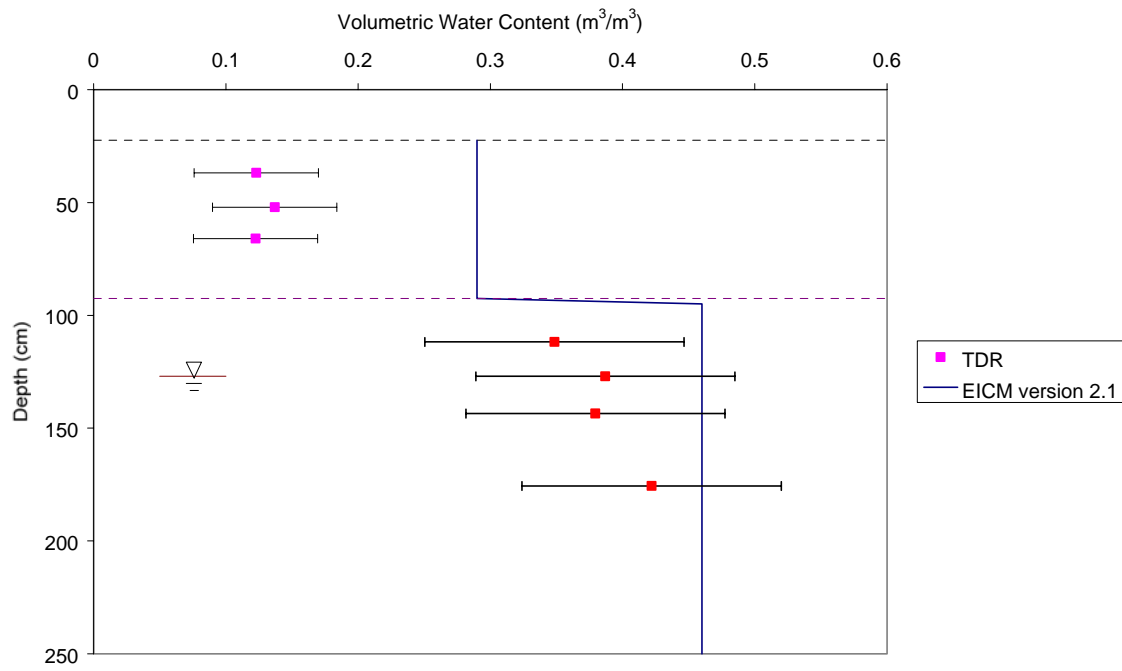
VERMONT site - 4/13/95



VERMONT site - 4/28/95



VERMONT site - 5/31/95





---

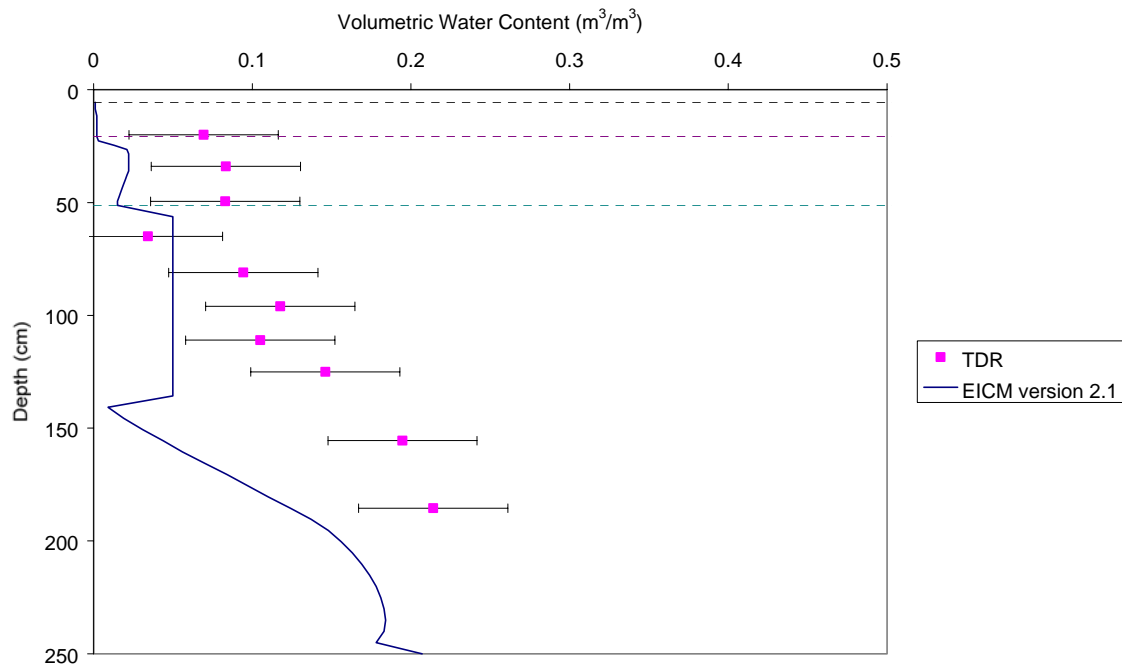
# APPENDIX F

## VOLUMETRIC WATER CONTENT PROFILES

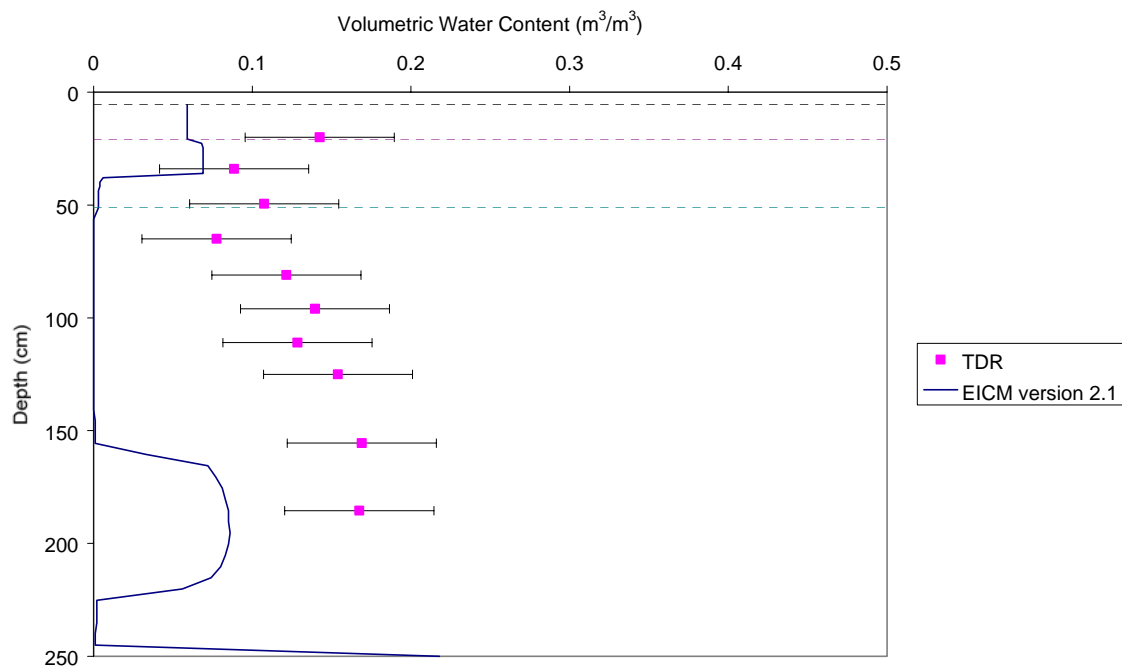
MANITOBA (831801)

EICM – Version 2.1

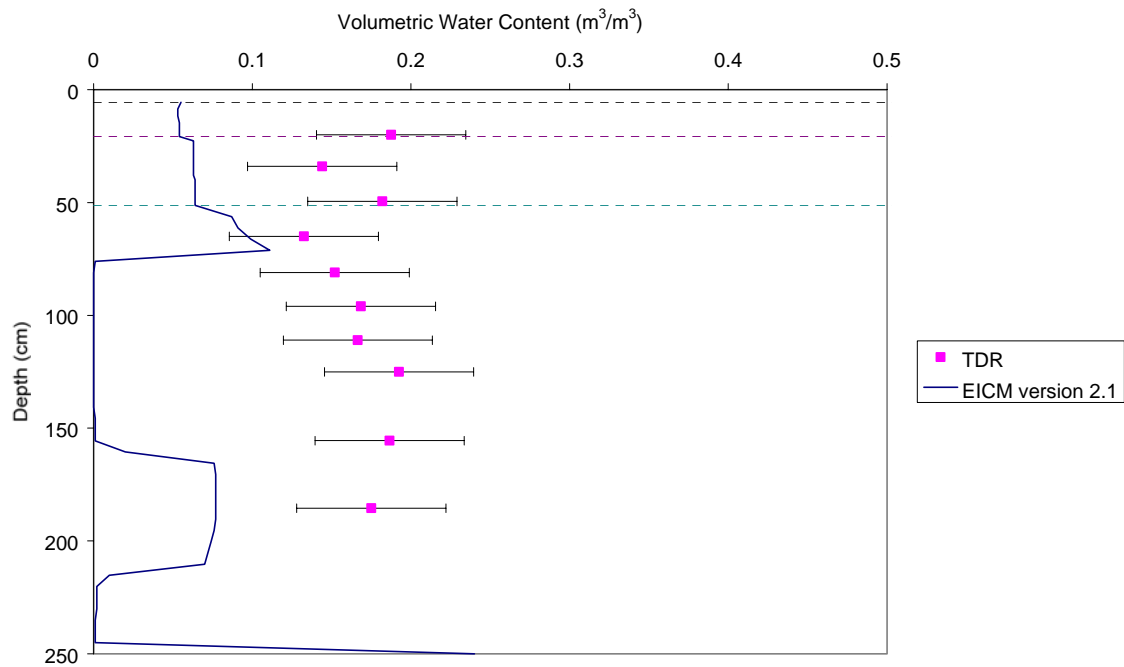
MANITOBA site - 2/14/94



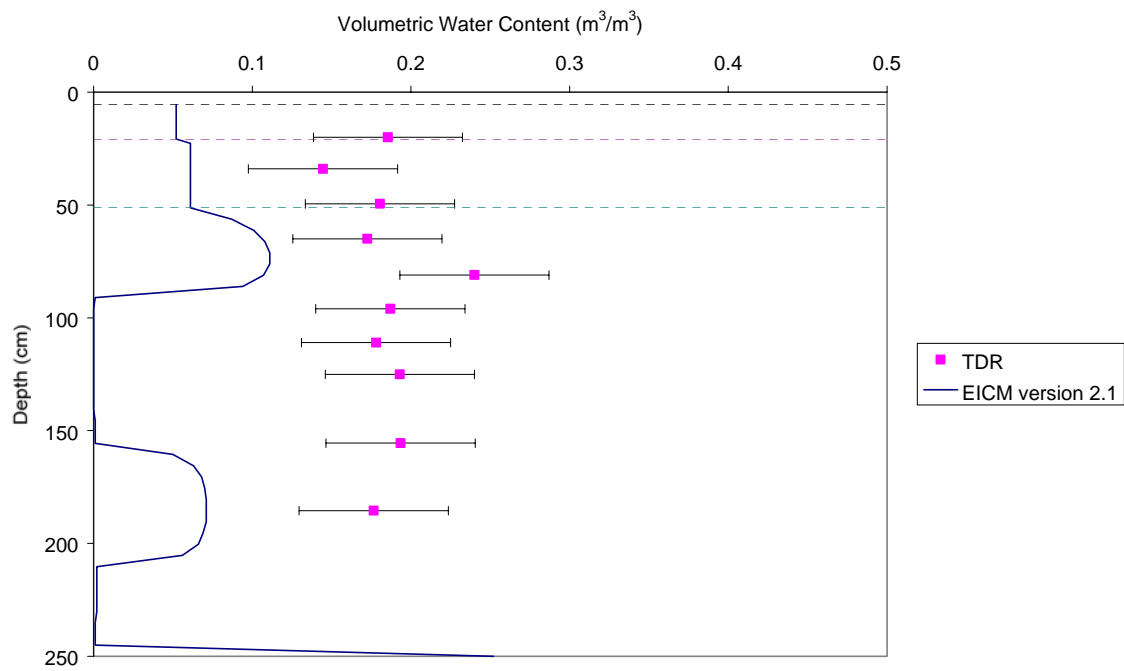
MANITOBA site - 3/14/94



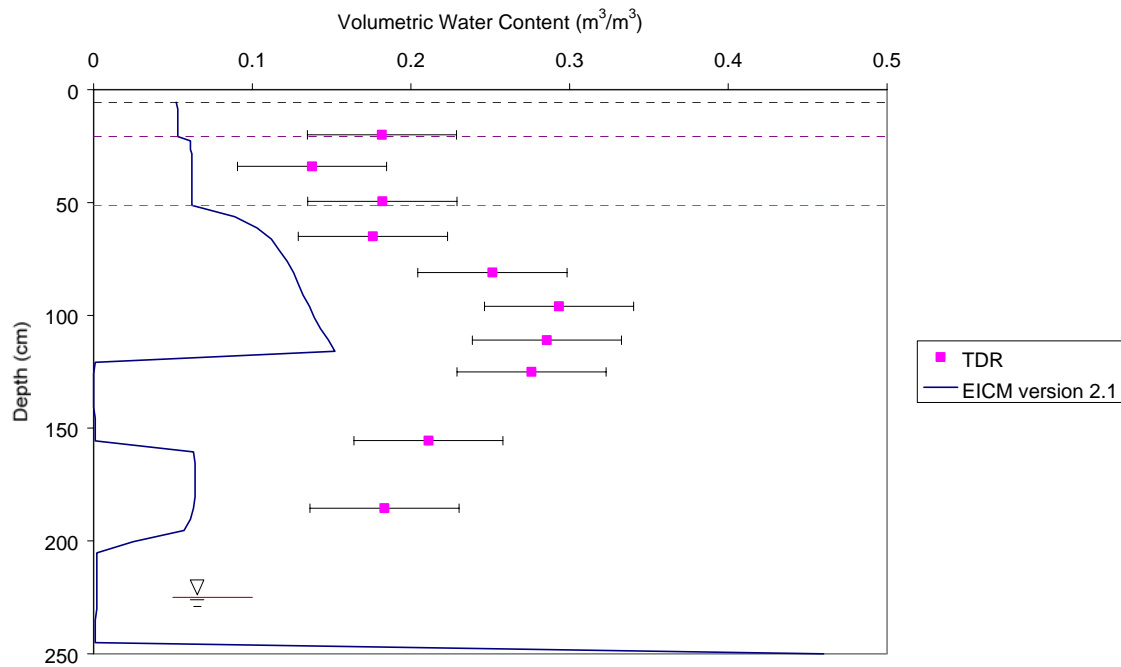
MANITOBA site - 3/28/94



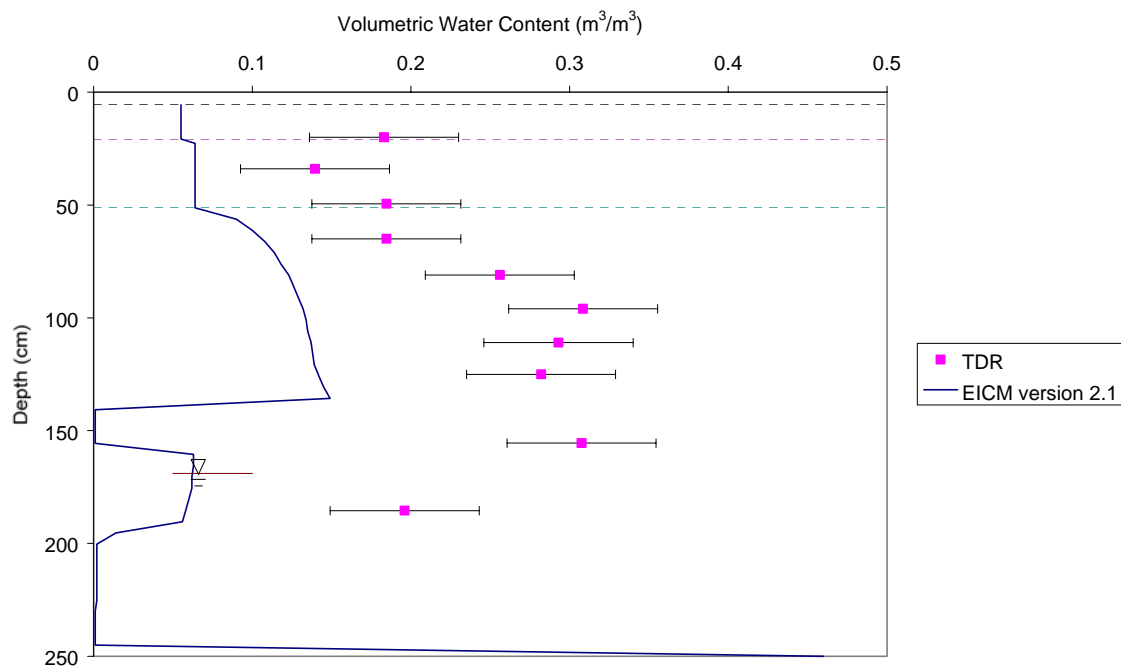
MANITOBA site - 4/11/94



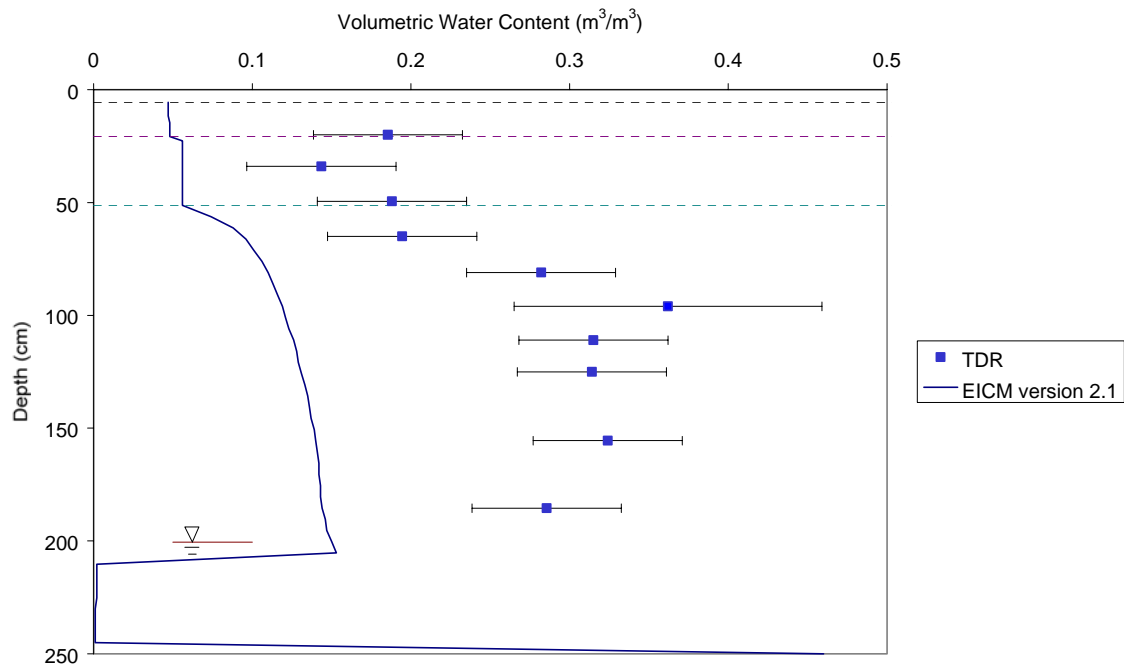
MANITOBA site - 4/29/94



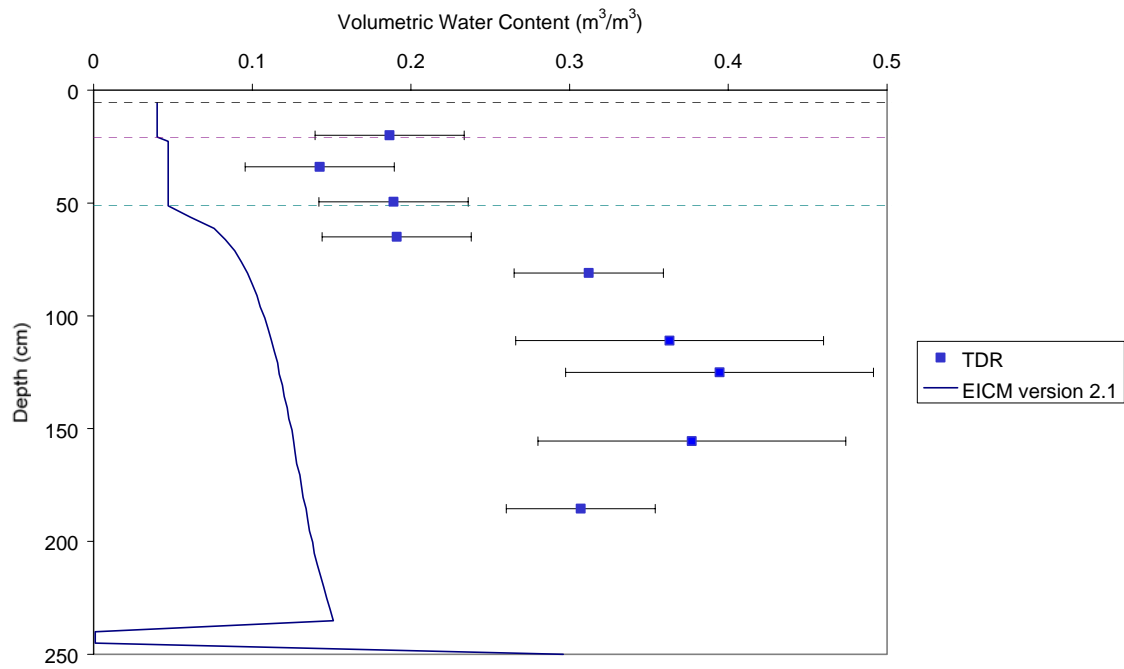
MANITOBA site - 5/13/94



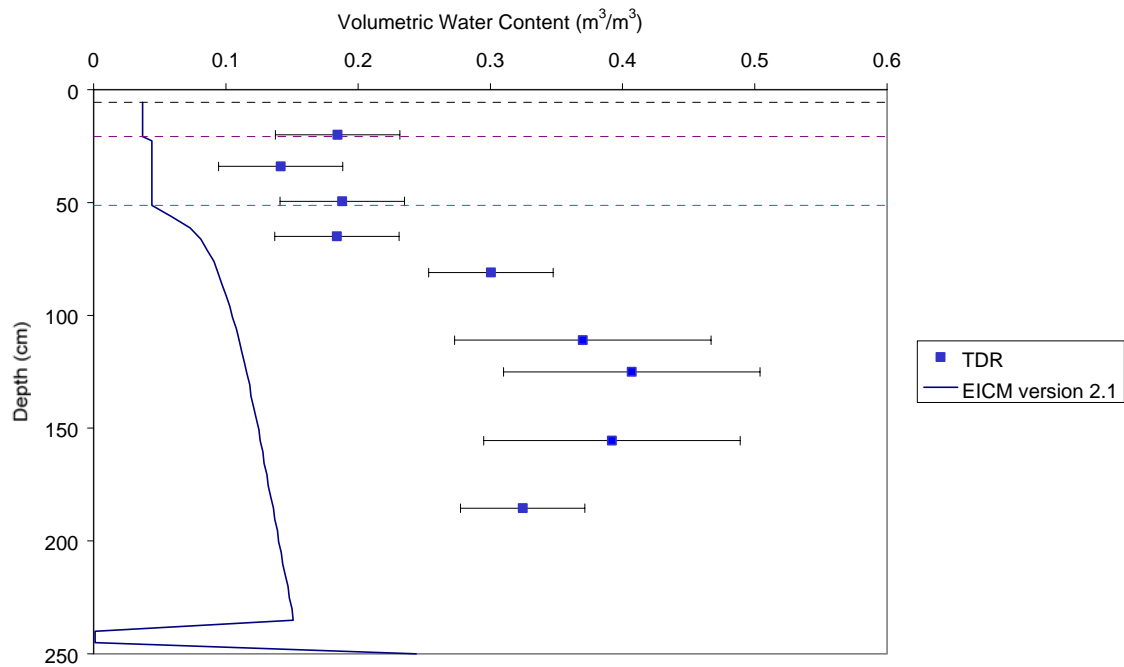
MANITOBA site - 6/17/94



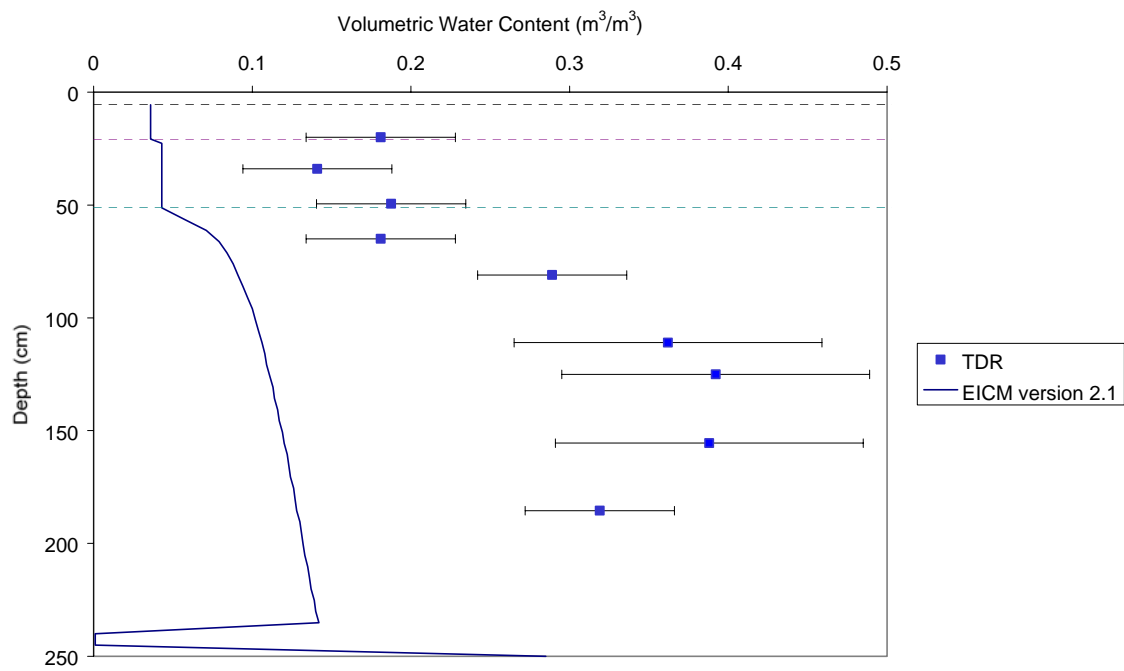
MANITOBA site - 7/25/94



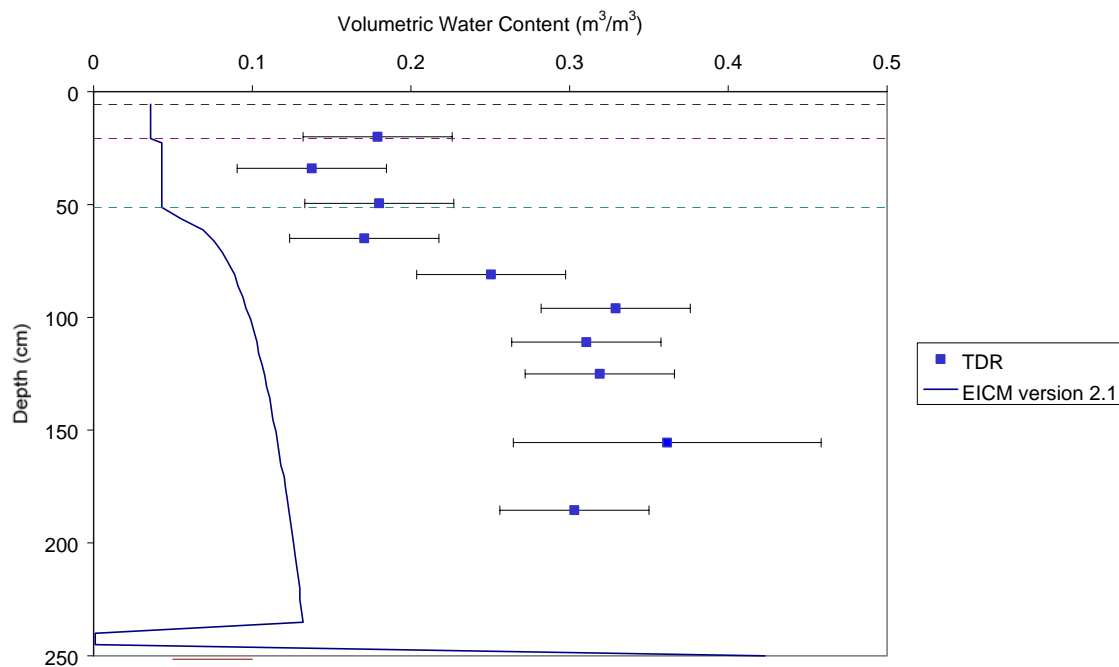
MANITOBA site - 8/18/94



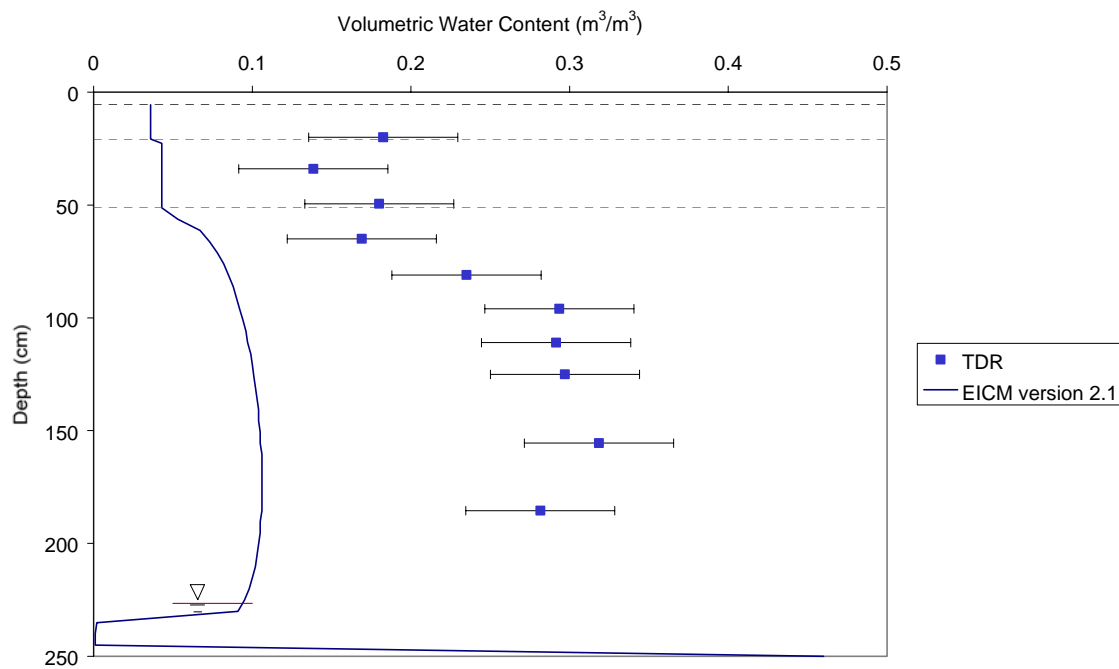
MANITOBA site - 9/21/94



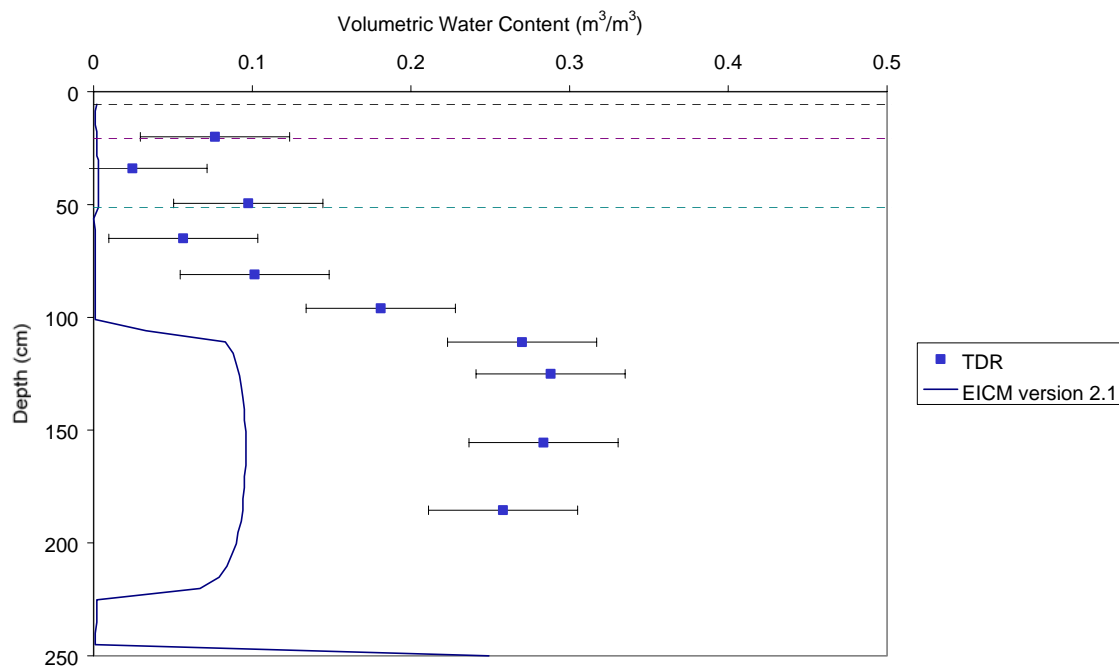
MANITOBA site - 10/19/94



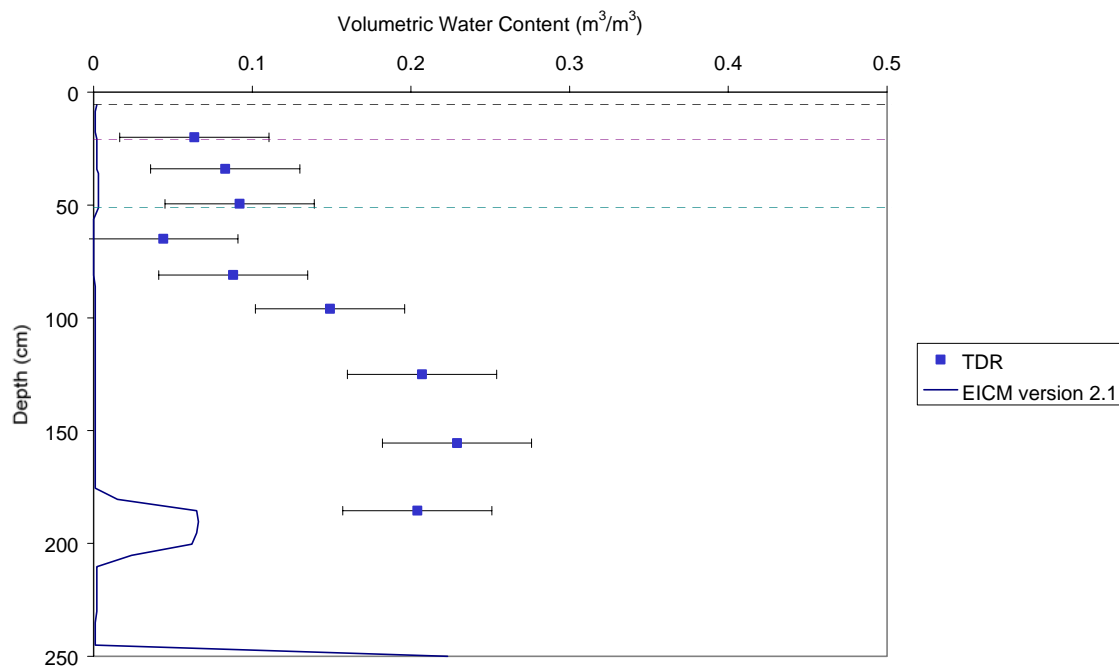
MANITOBA site - 11/16/94



MANITOBA site - 12/14/94

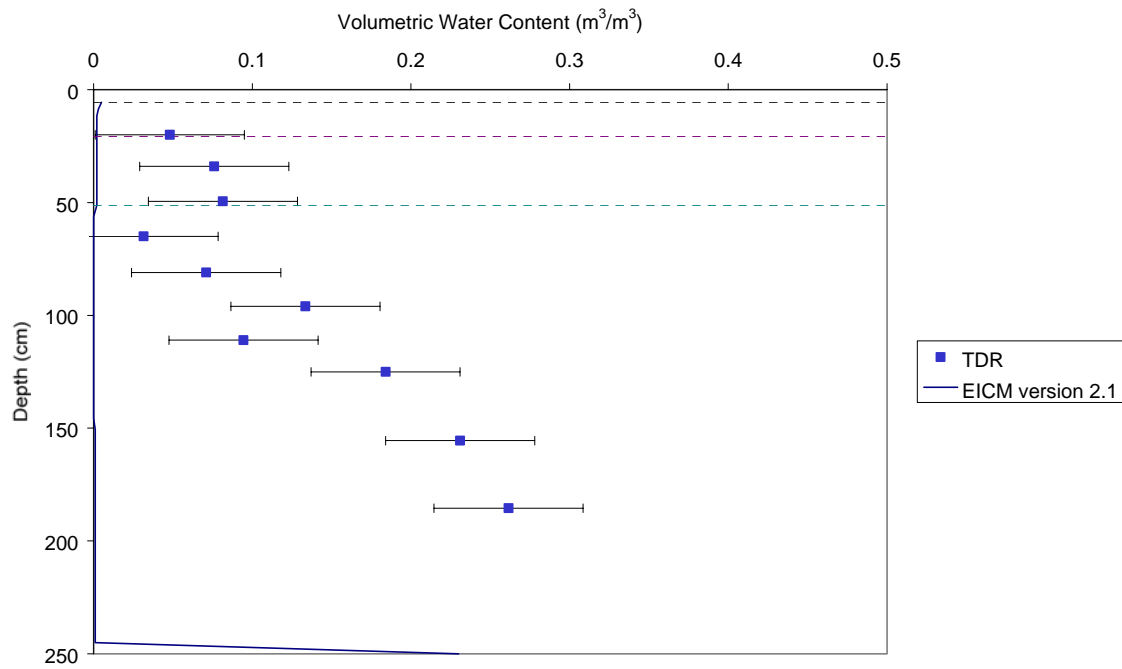


MANITOBA site - 1/25/95





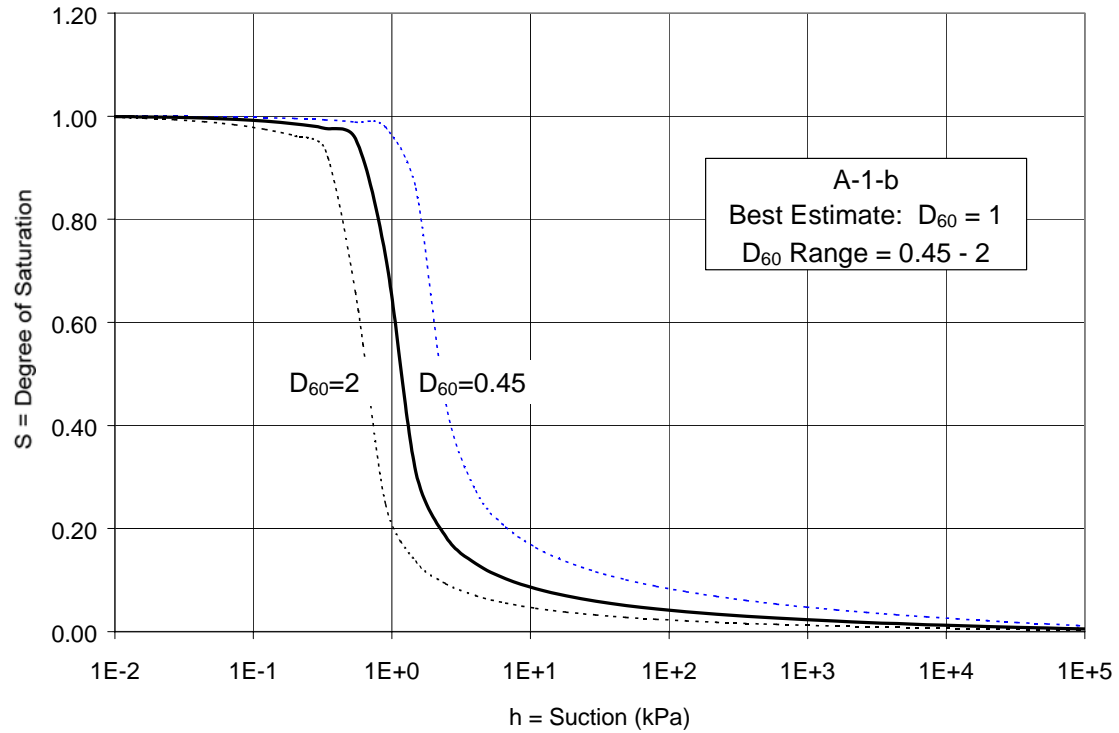
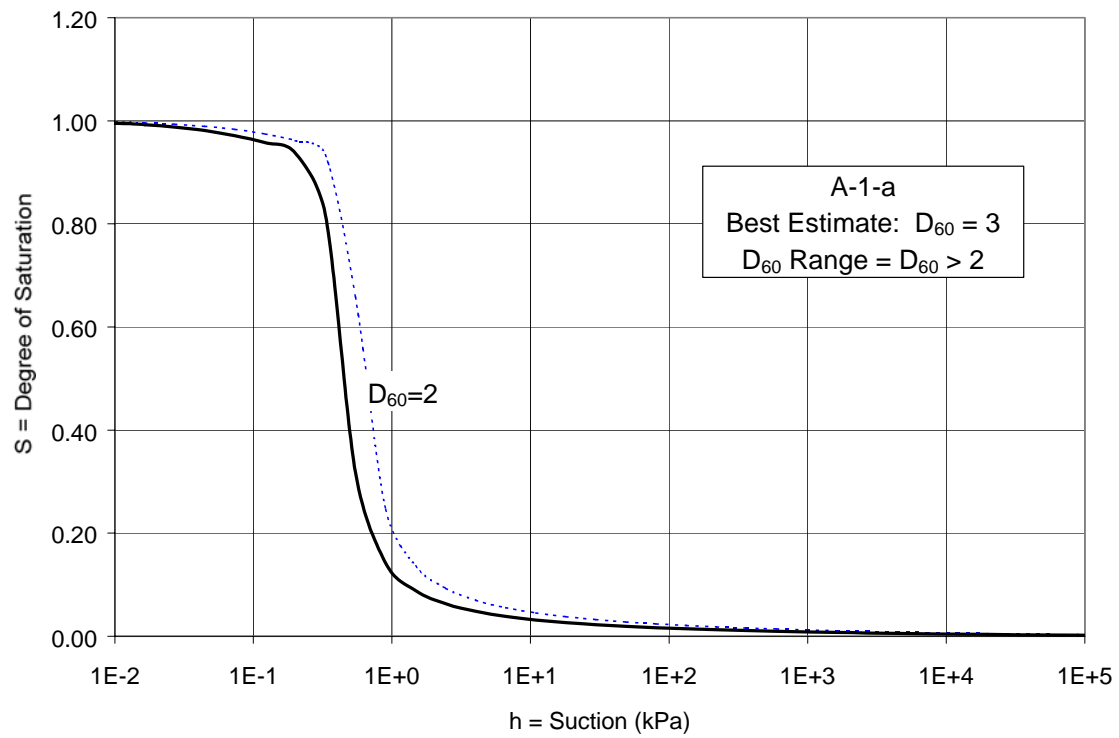
MANITOBA site - 2/15/95

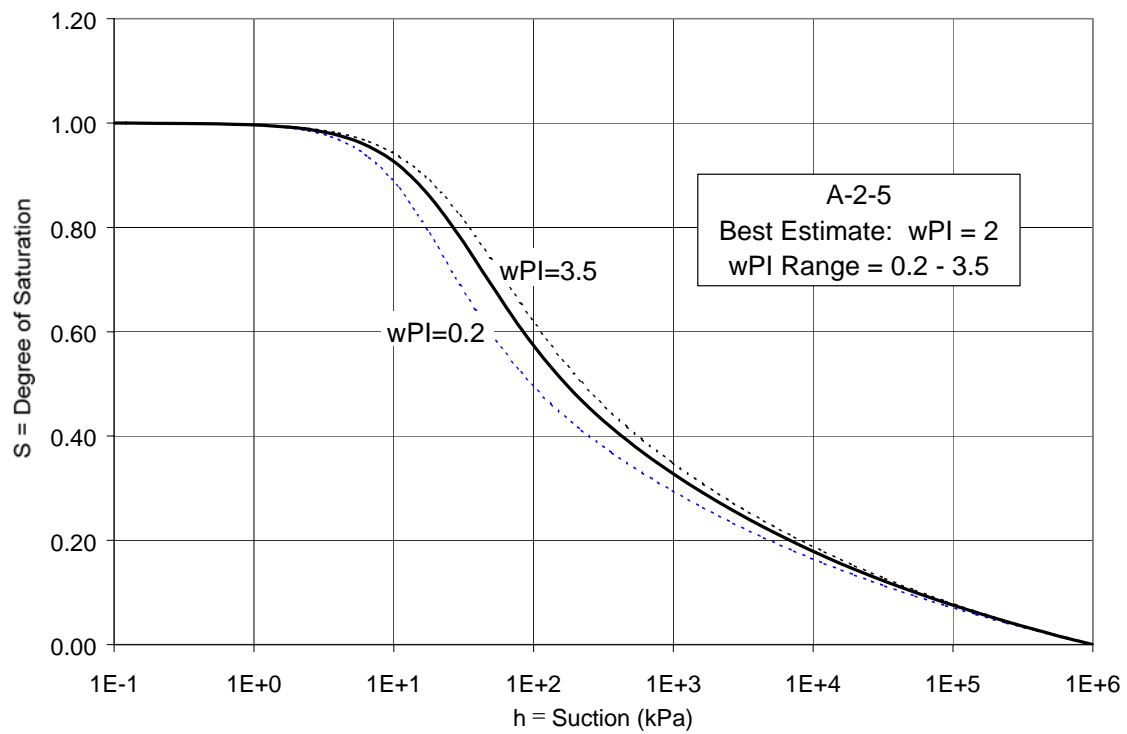
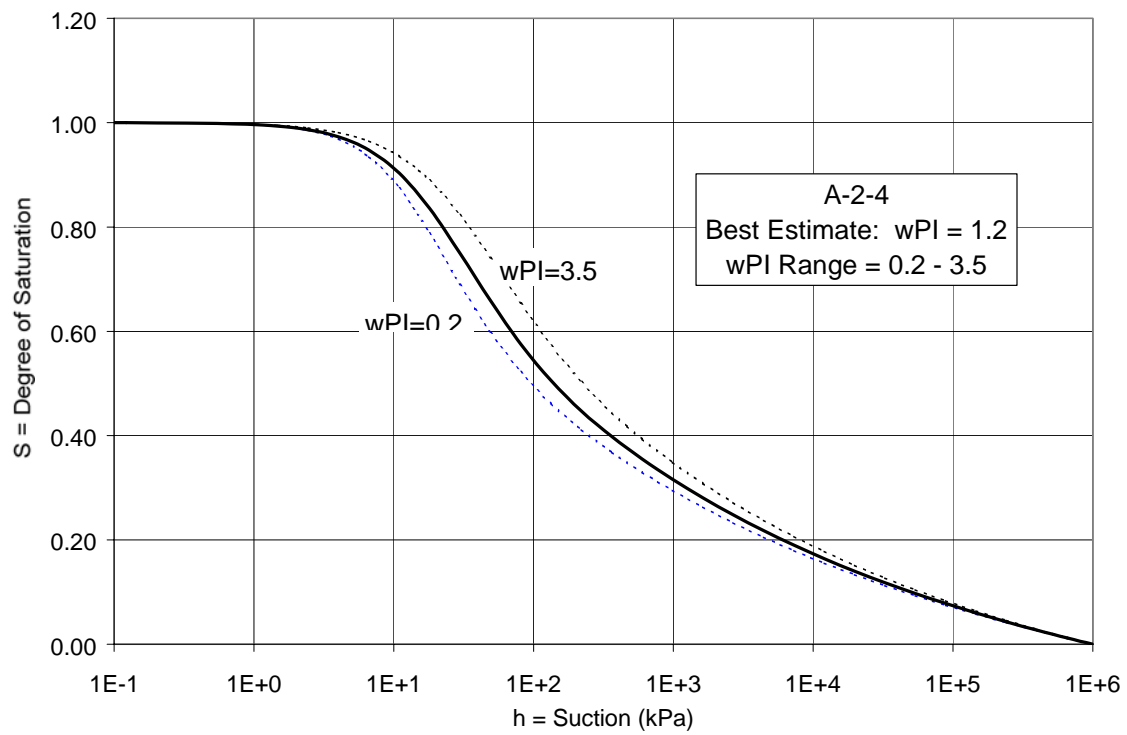


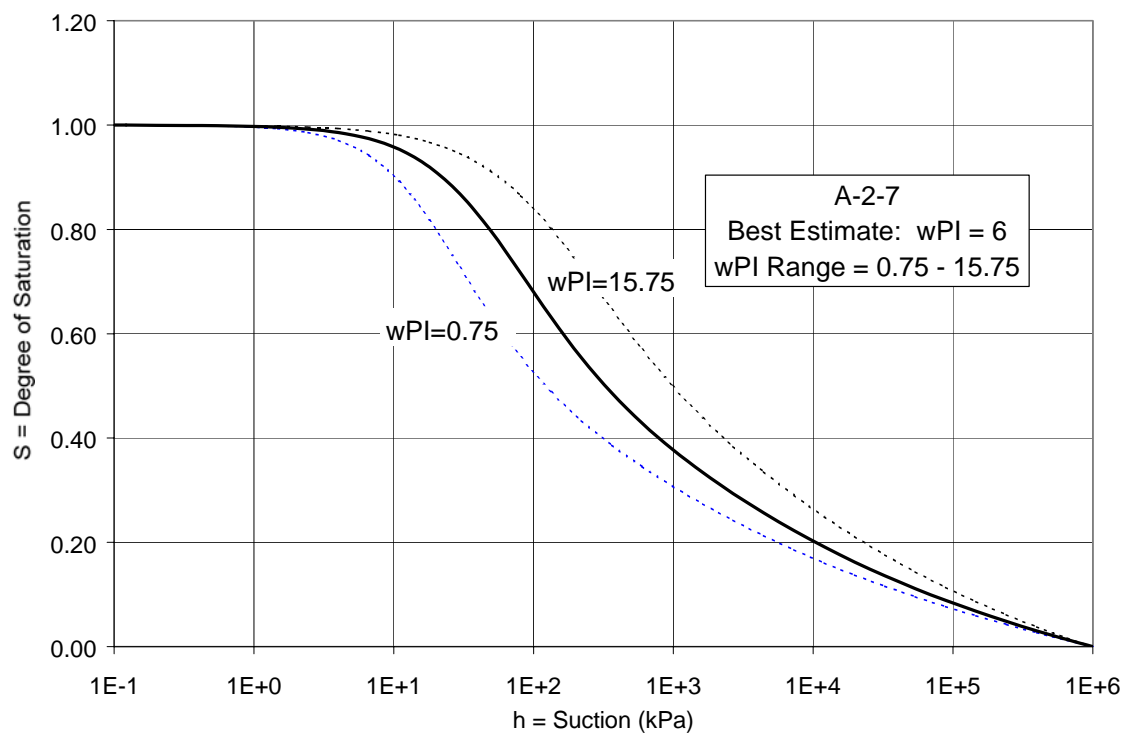
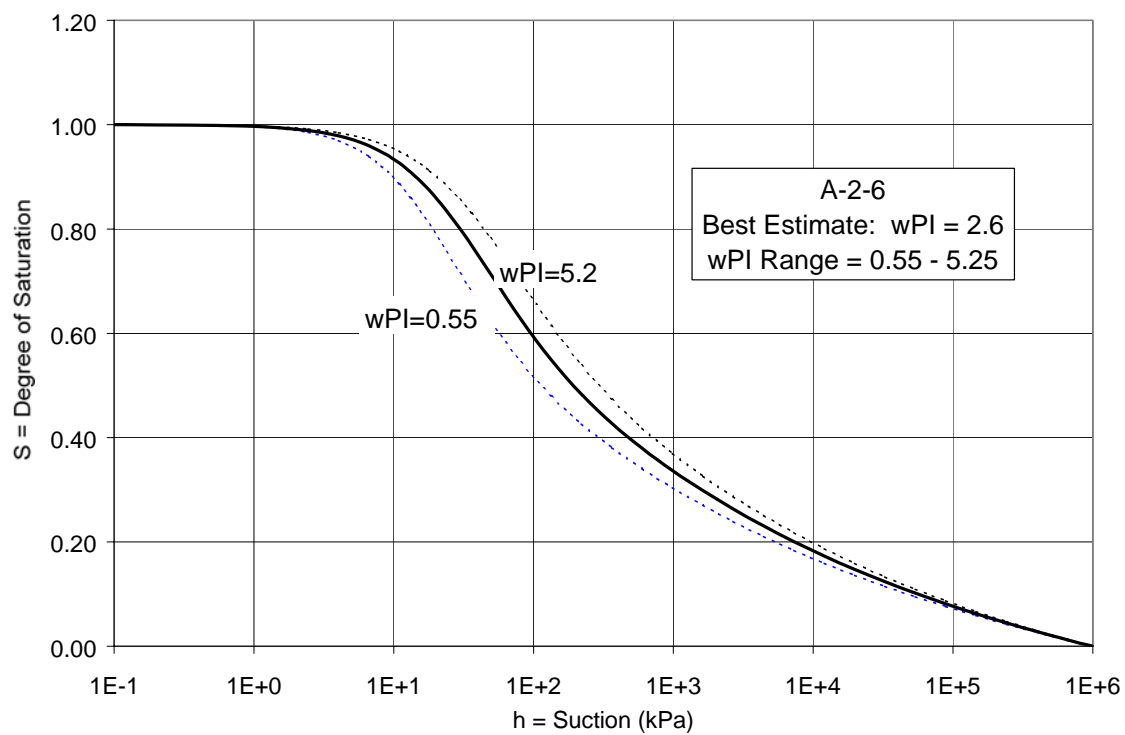
---

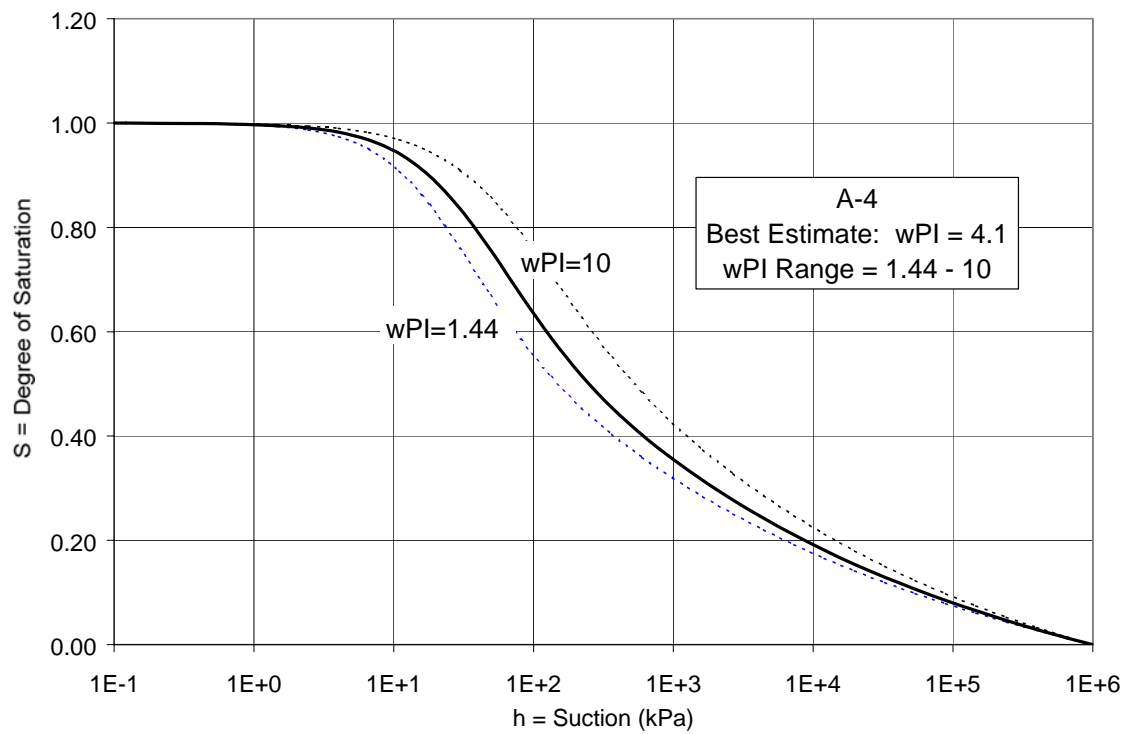
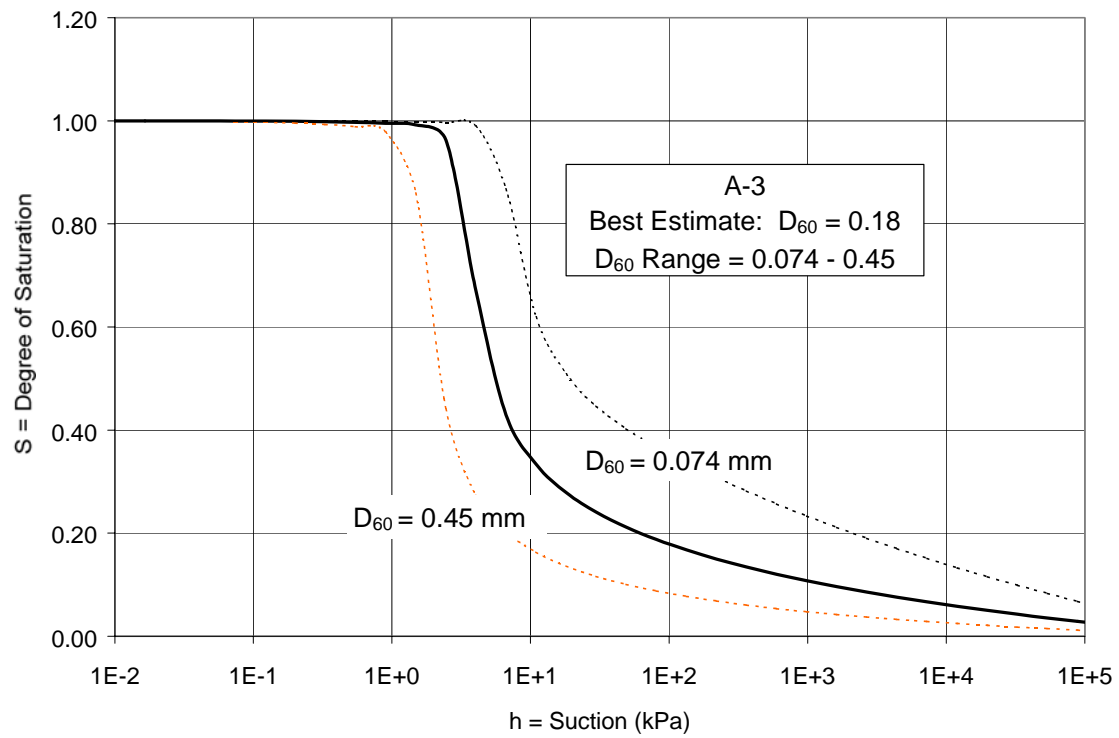
## APPENDIX G

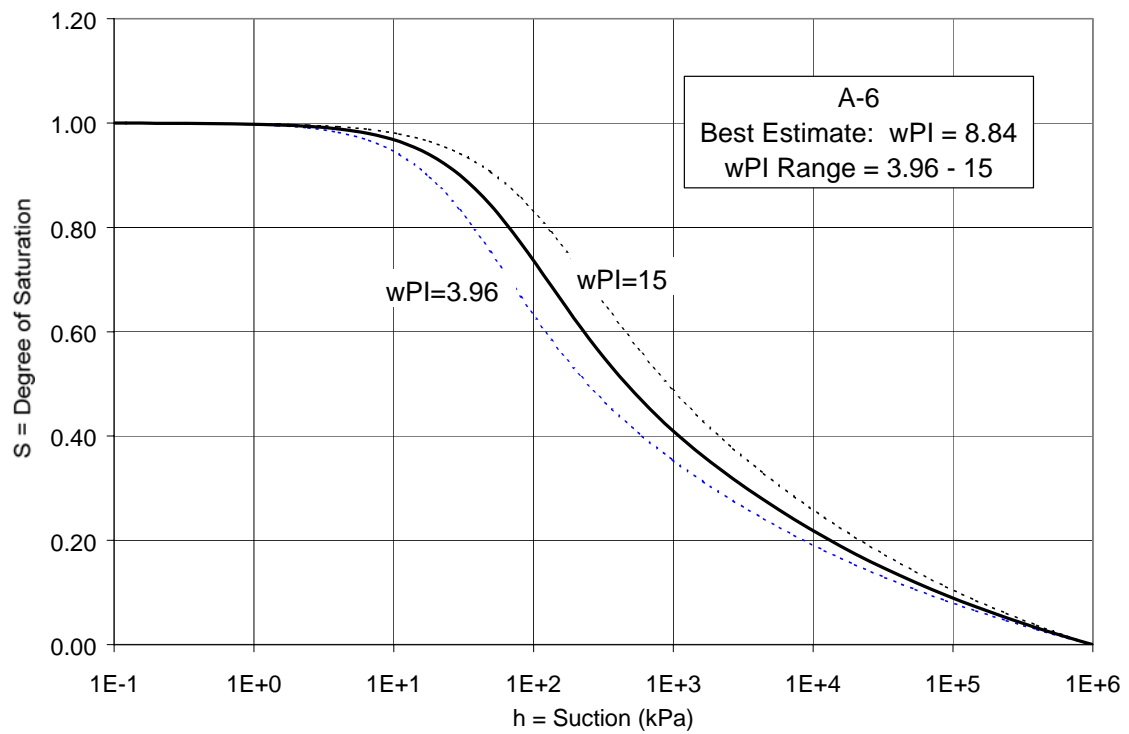
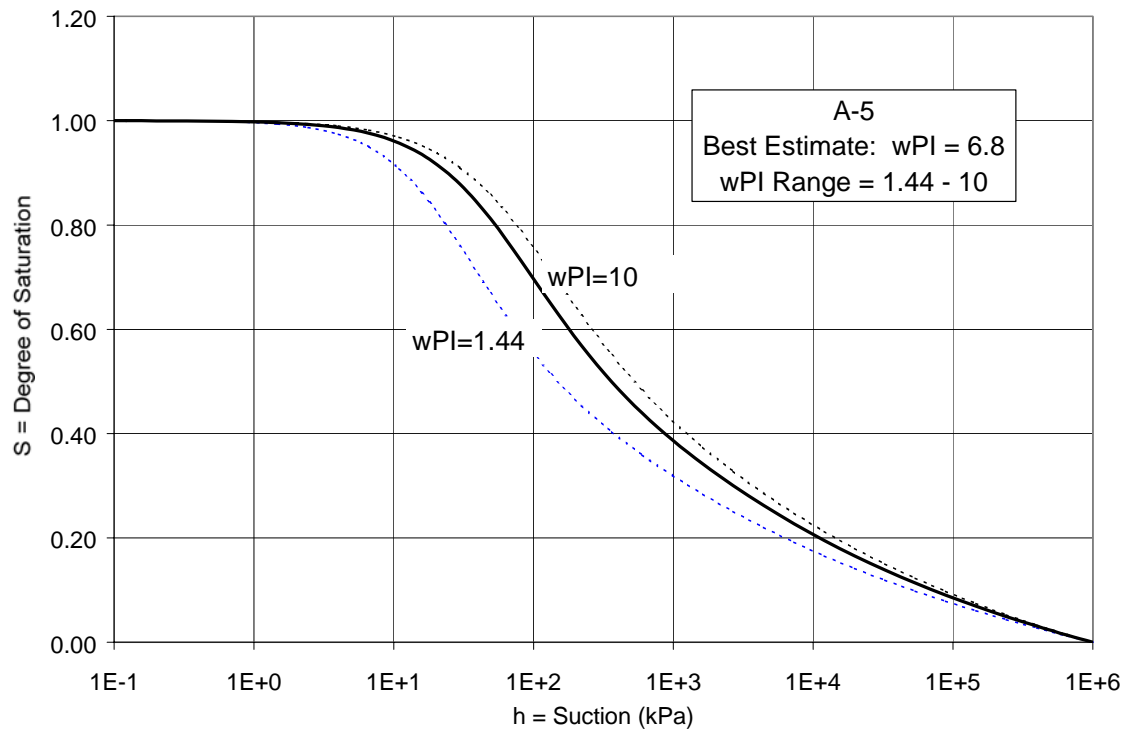
### BEST-ESTIMATE SOIL-WATER CHARACTERISTIC CURVES BASED ON AASHTO CLASSIFICATION

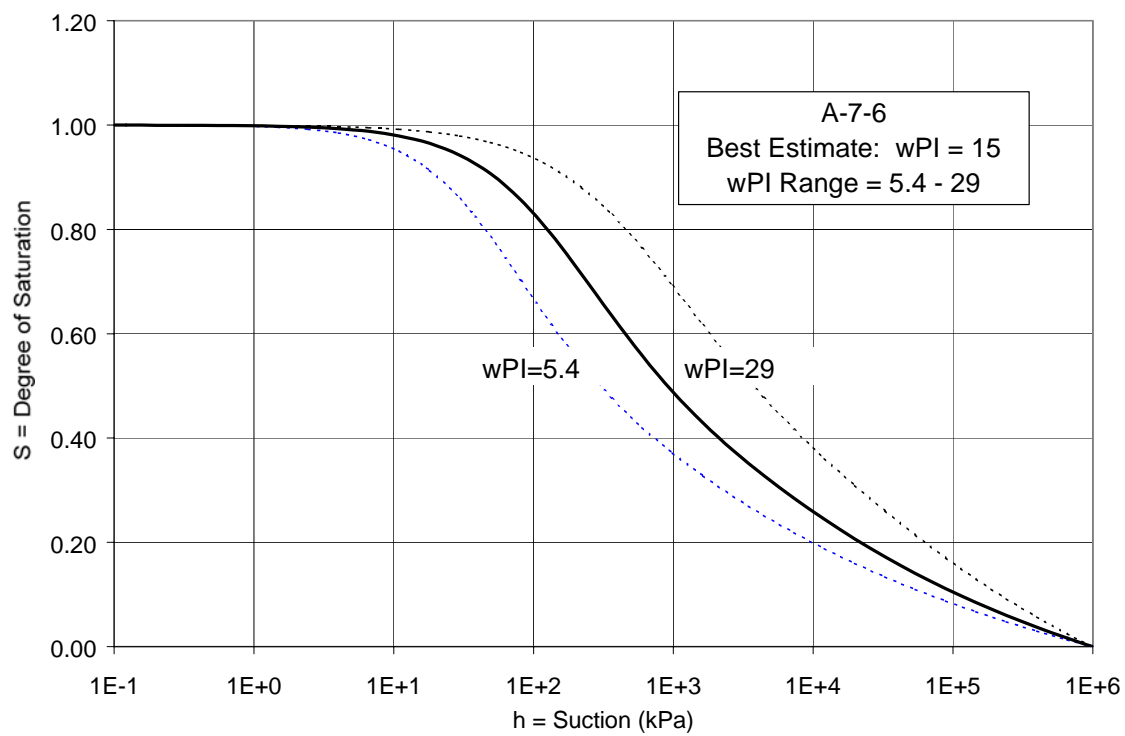
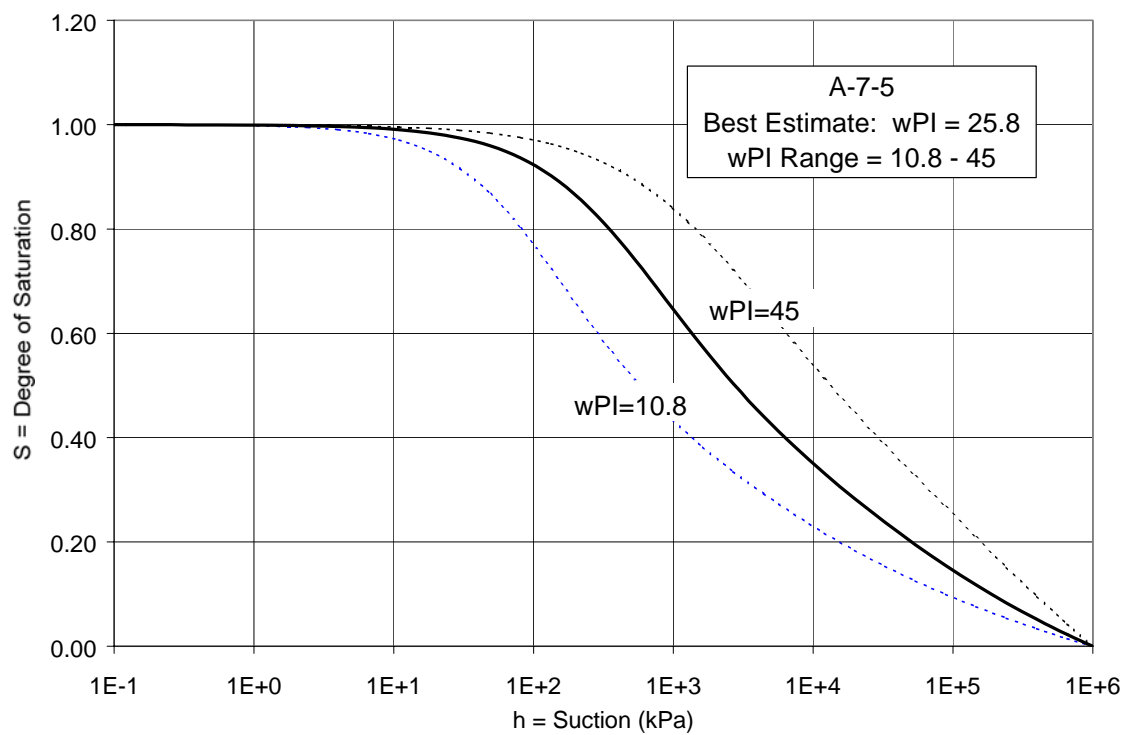










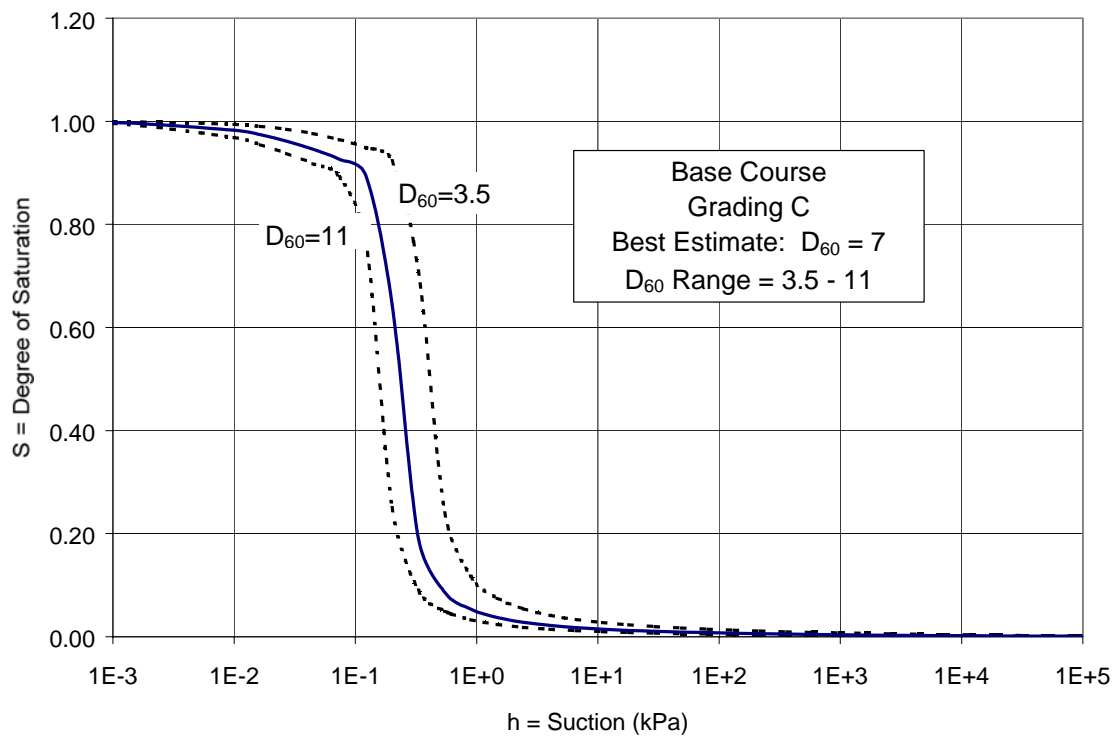
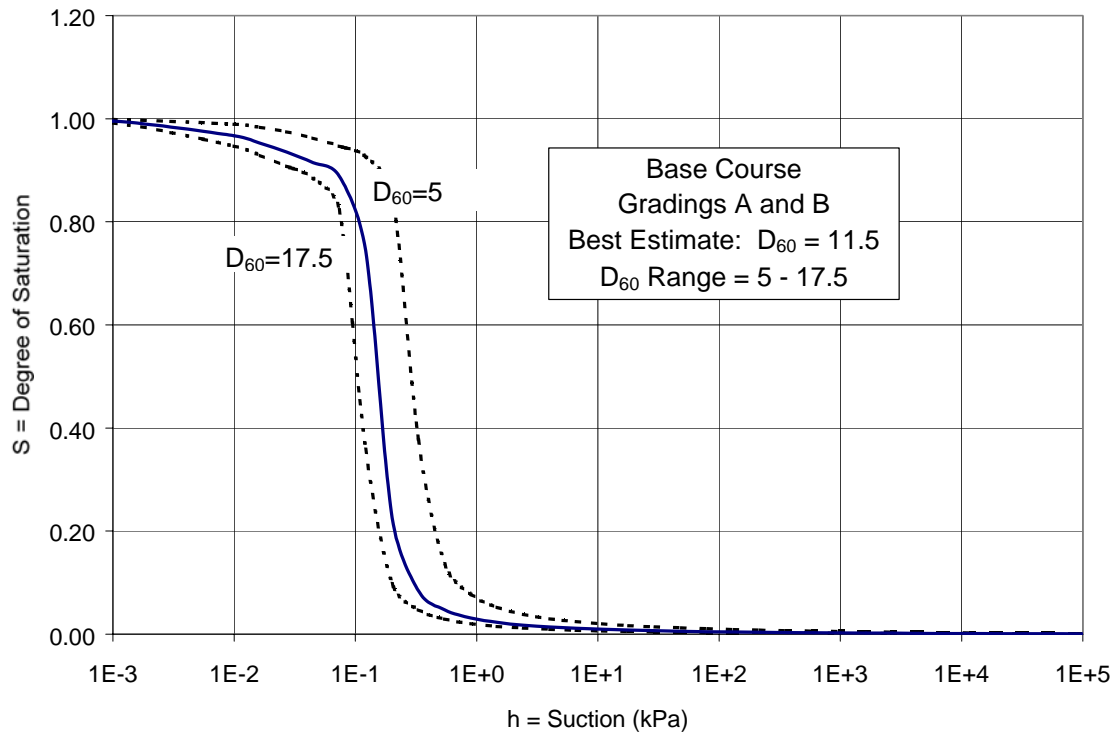


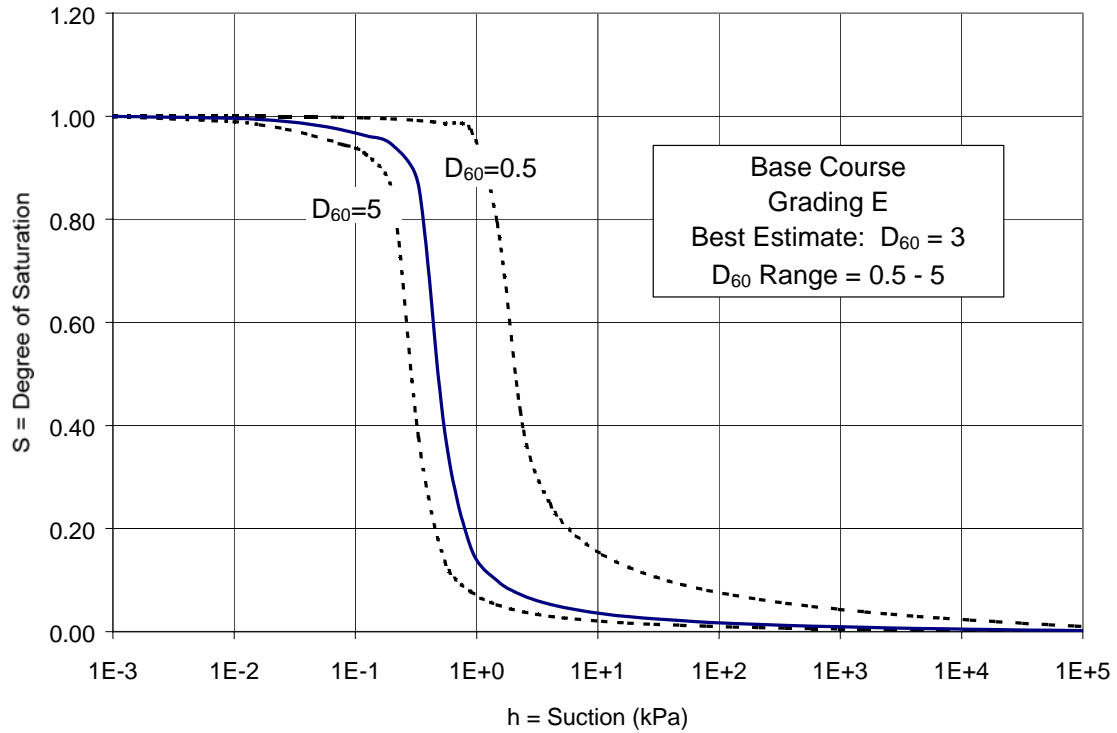
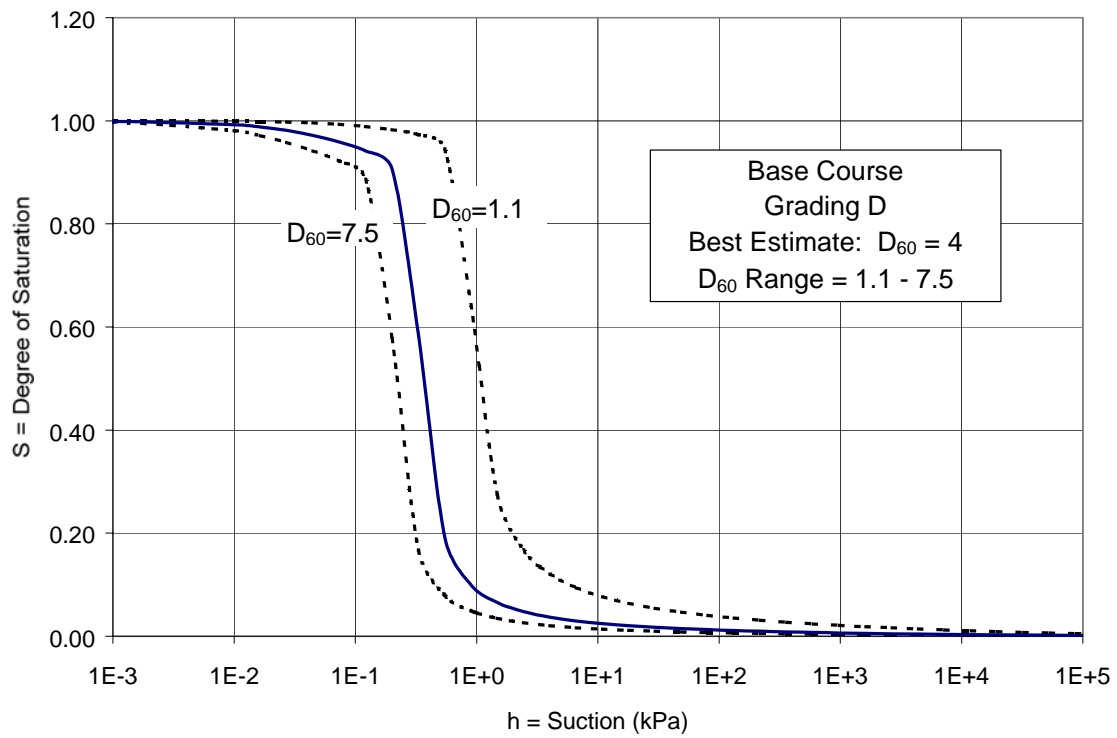


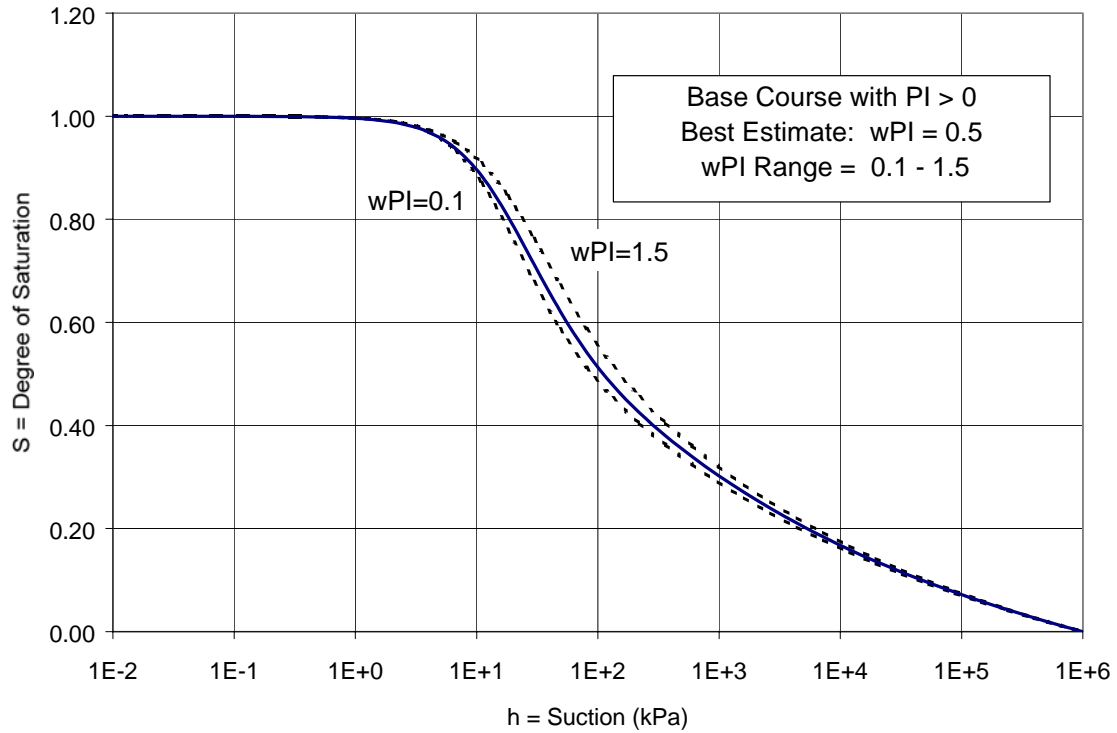
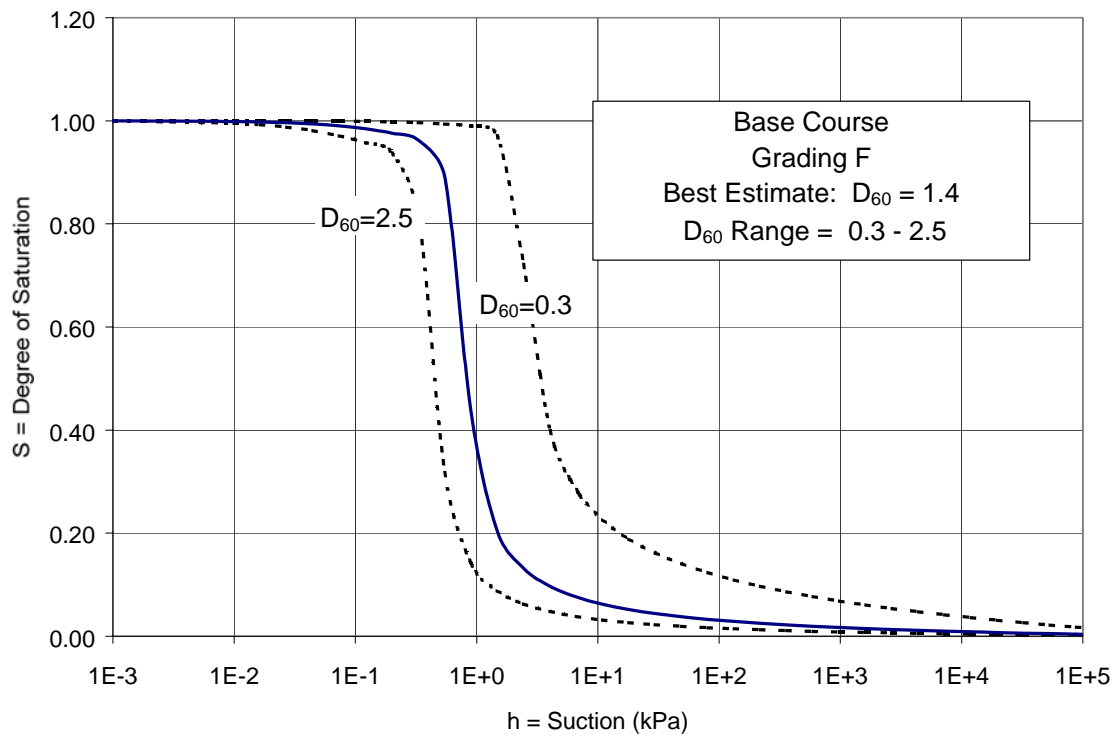
---

## APPENDIX H

### BEST-ESTIMATE SOIL-WATER CHARACTERISITC CURVES FOR BASE COURSE MATERIALS







---

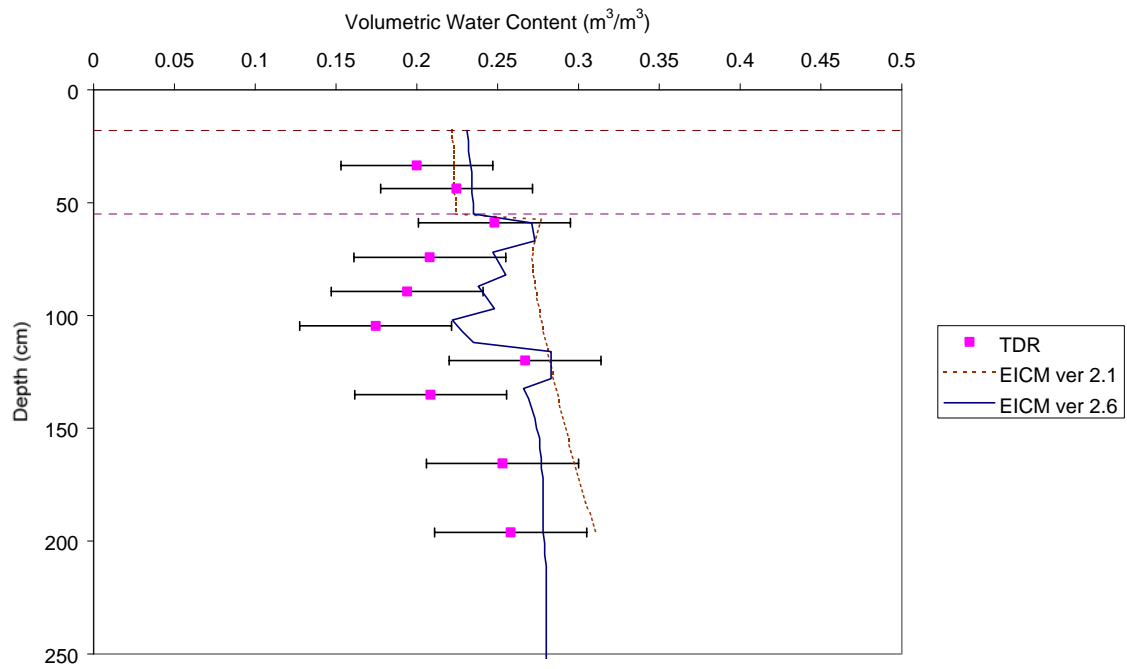
# APPENDIX I

## VOLUMETRIC WATER CONTENT PROFILES

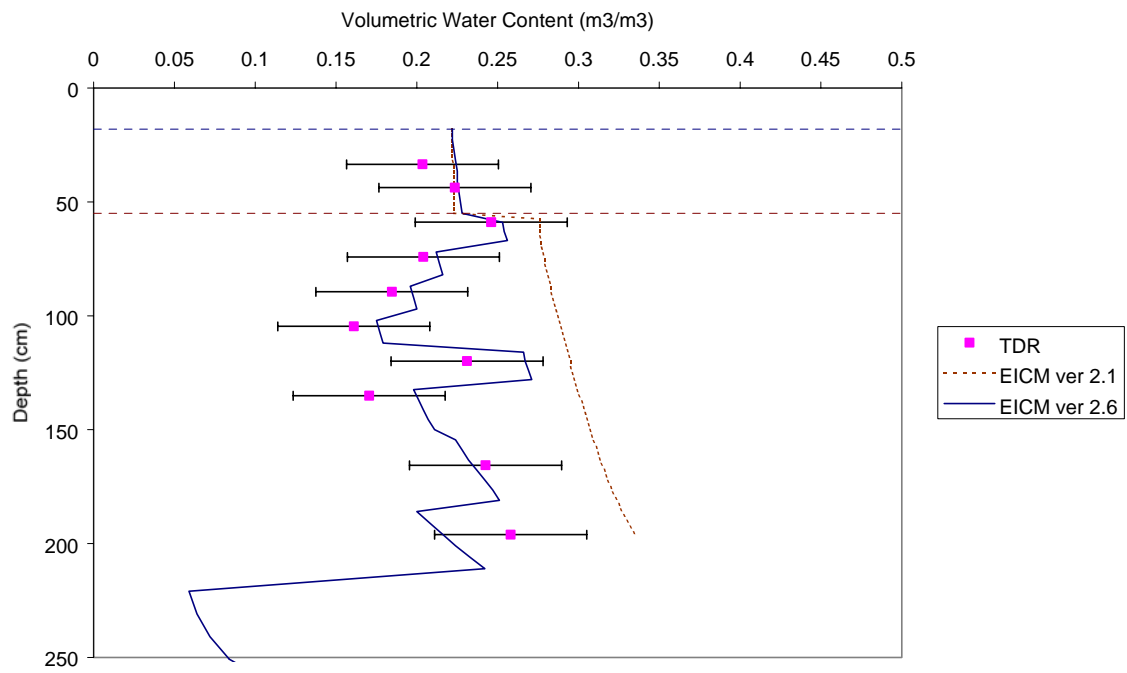
### CONNECTICUT (91803)

EICM – Version 2.6

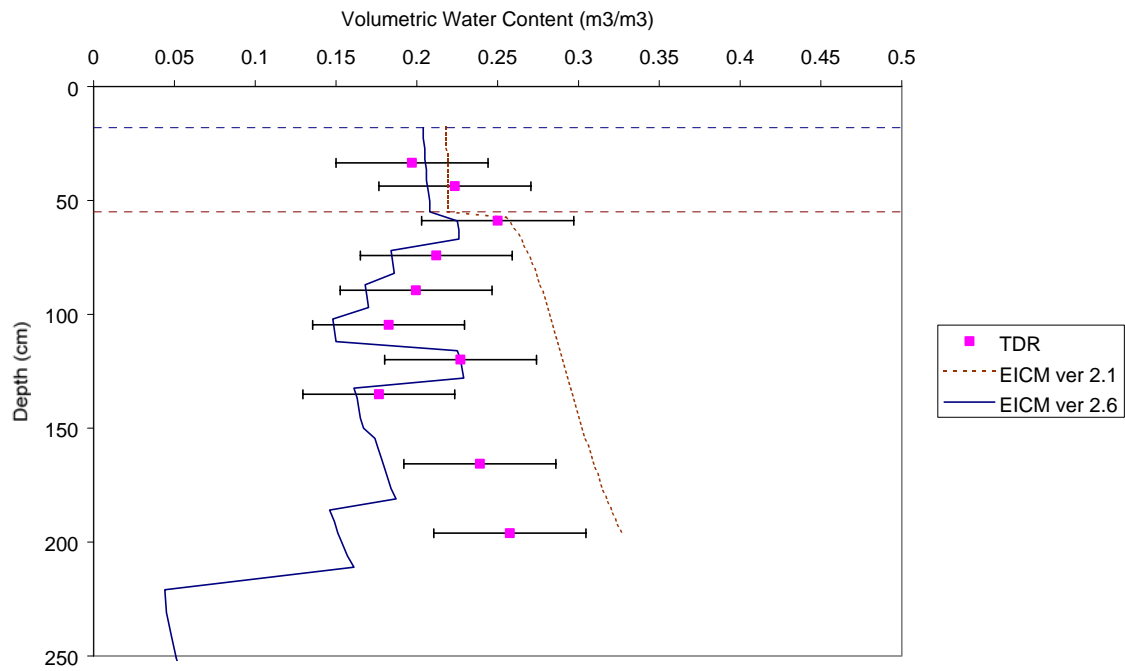
CT site - 6/30/94



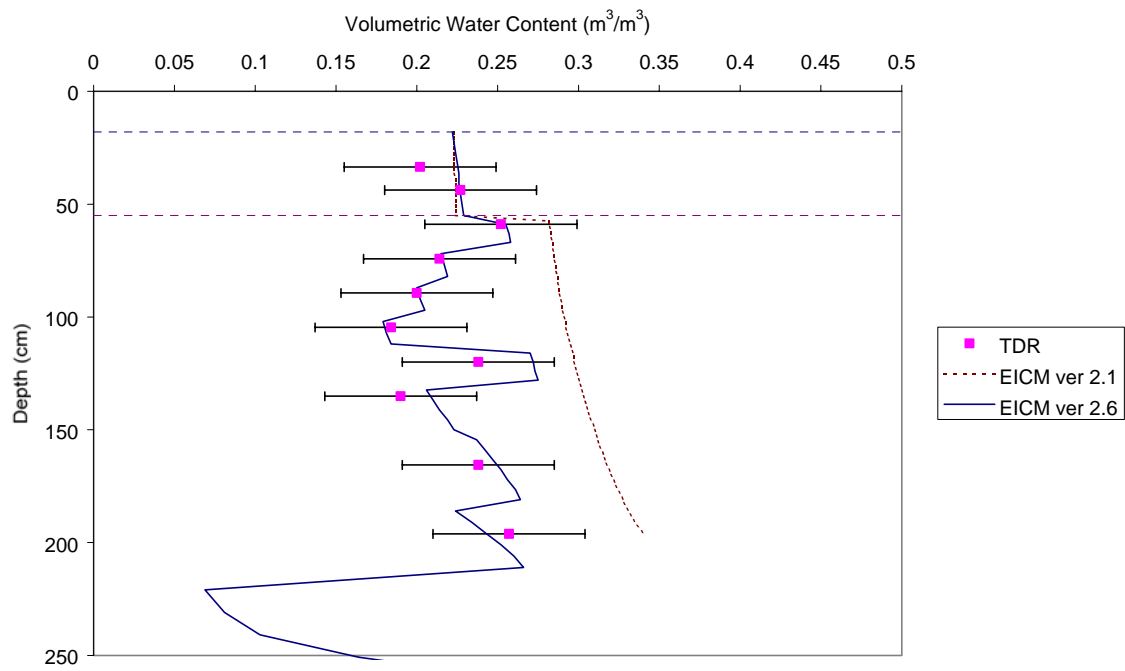
CT site - 7/28/94



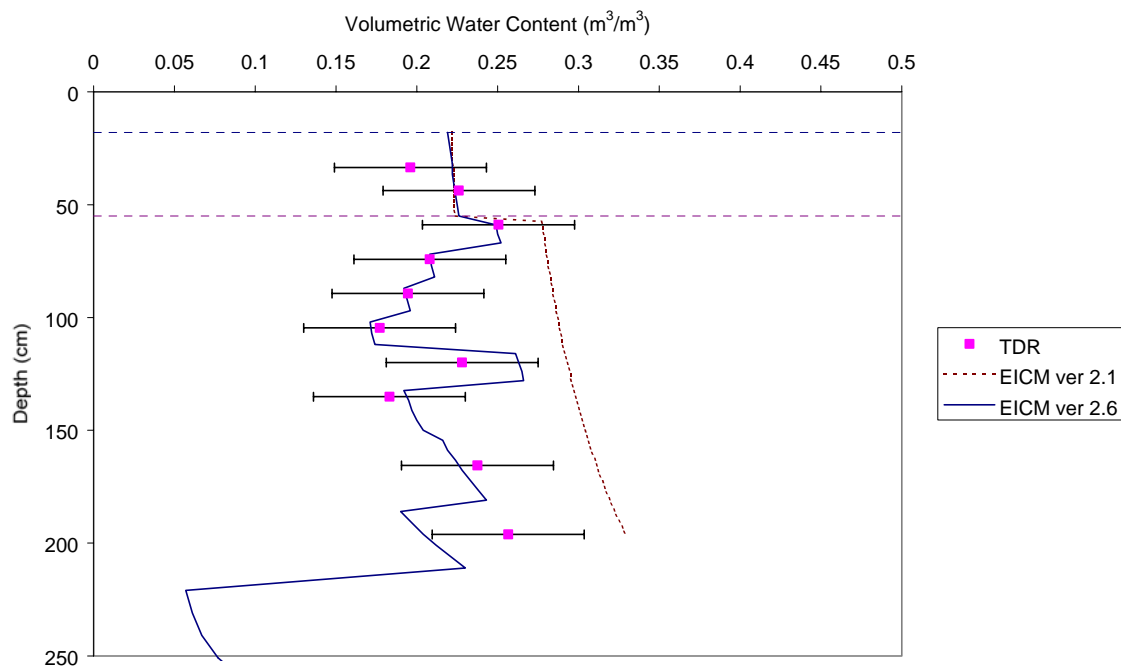
CT site -8/25/94



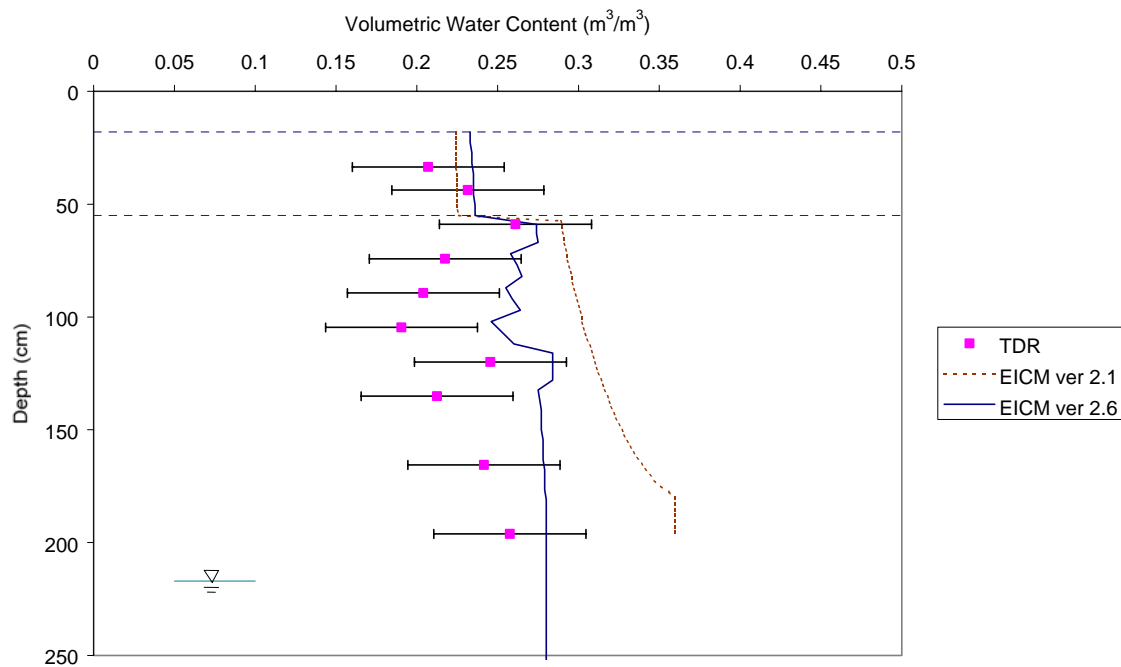
CT site - 9/29/94



CT site - 10/27/94

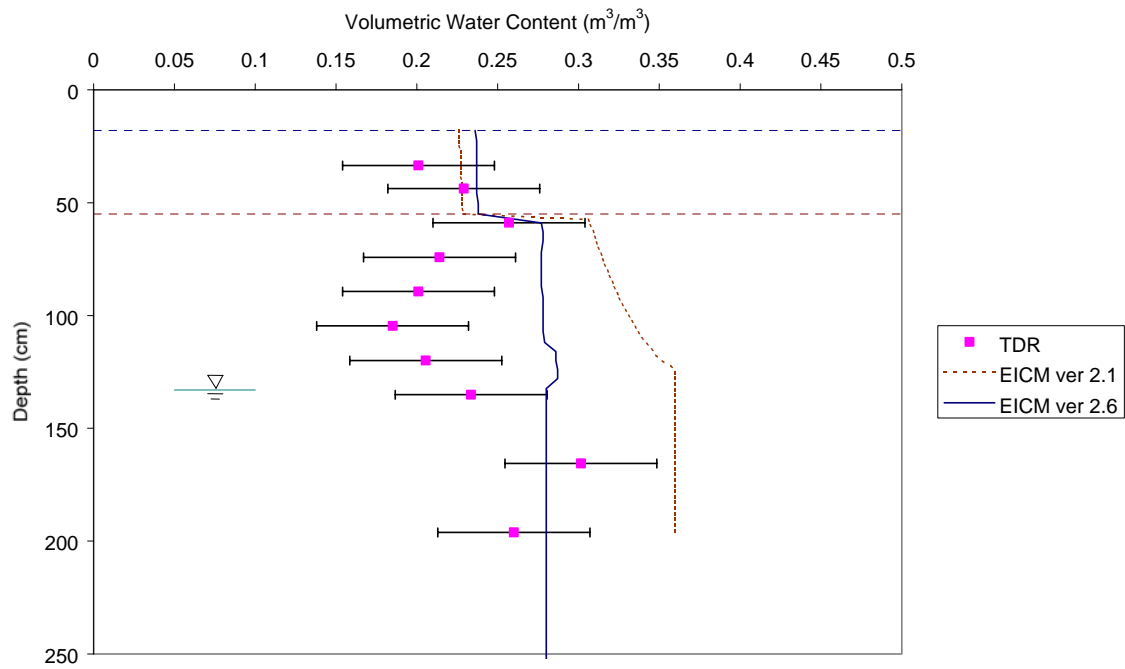


CT site - 11/30/94

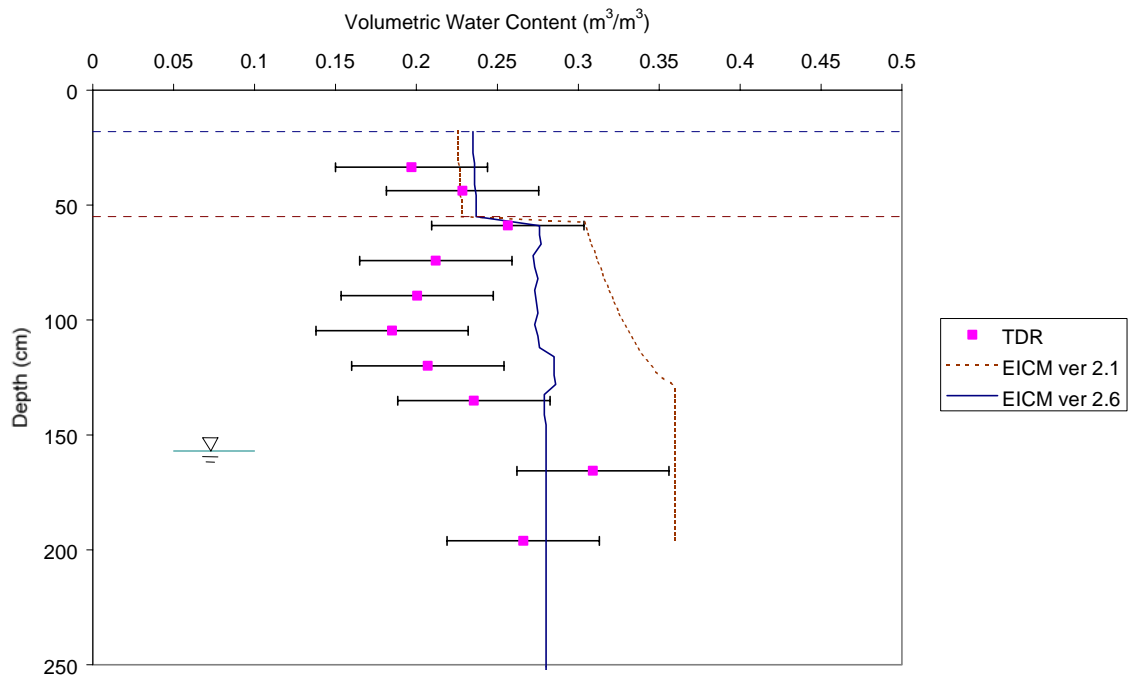




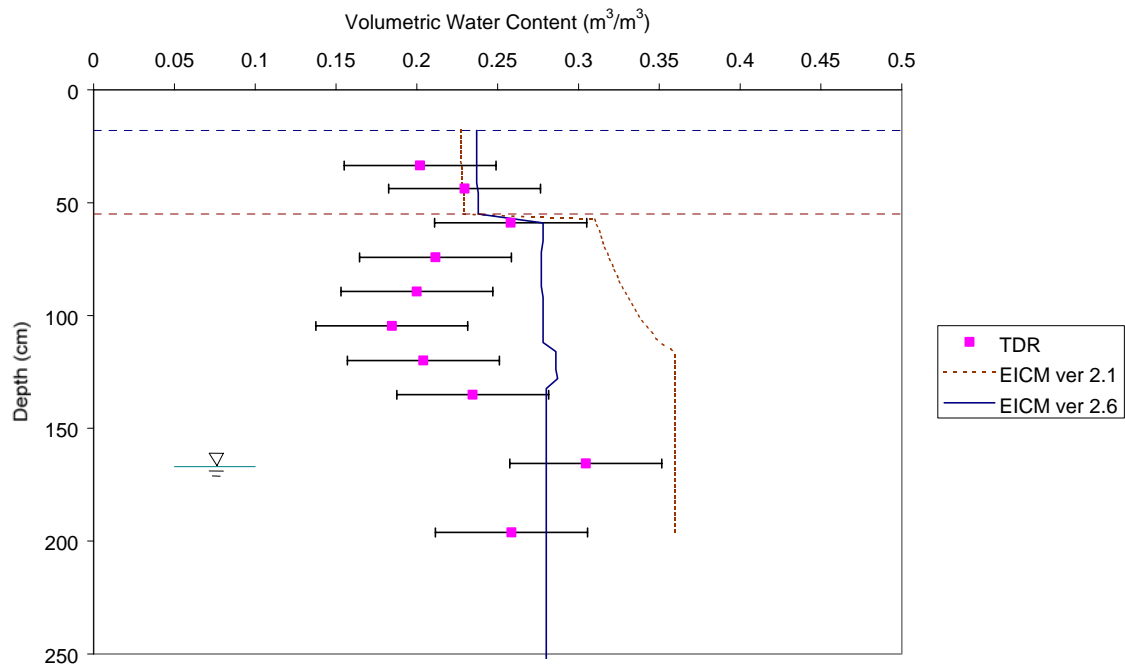
CT site - 3/15/95



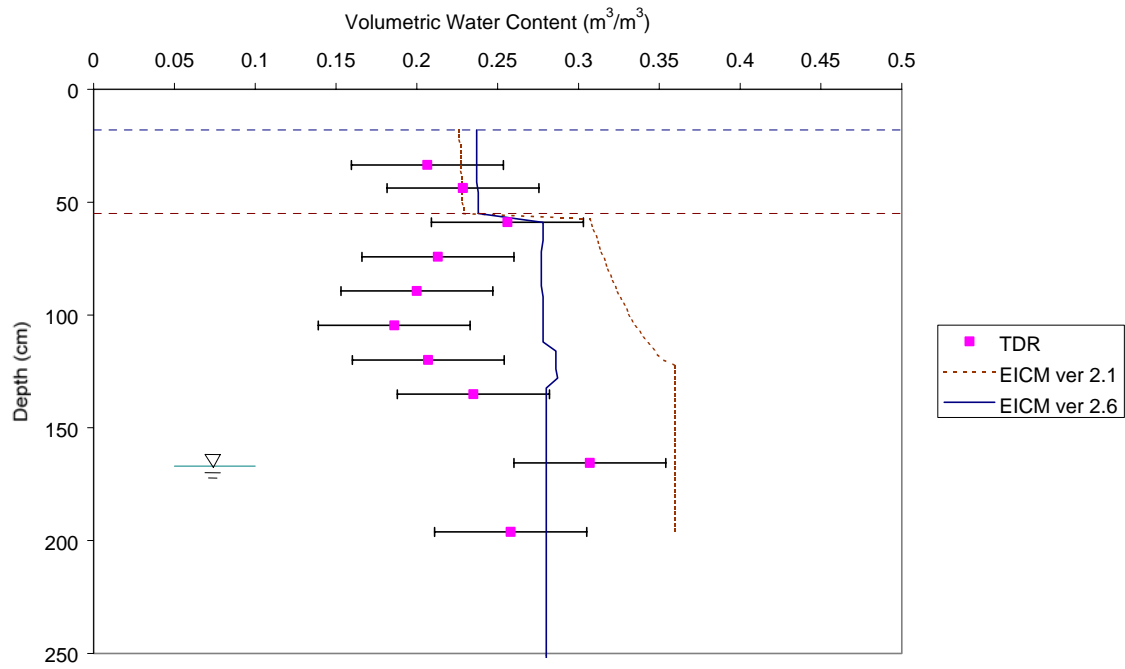
CT site - 3/29/95



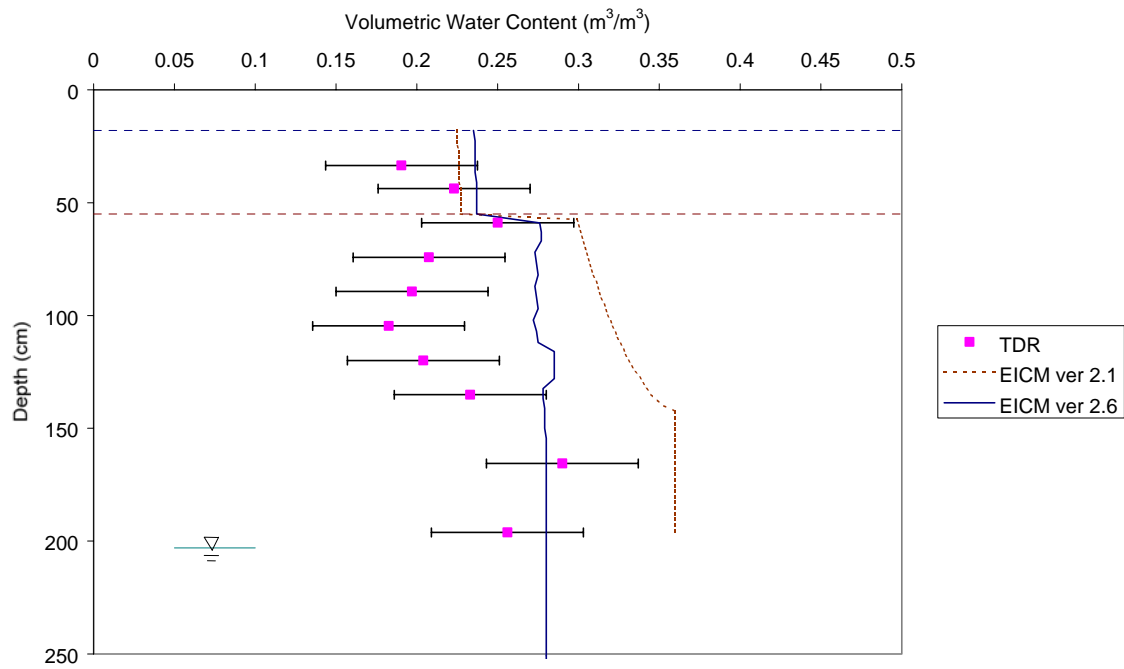
CT site - 4/12/95



CT site - 5/25/95



CT site - 6/20/95



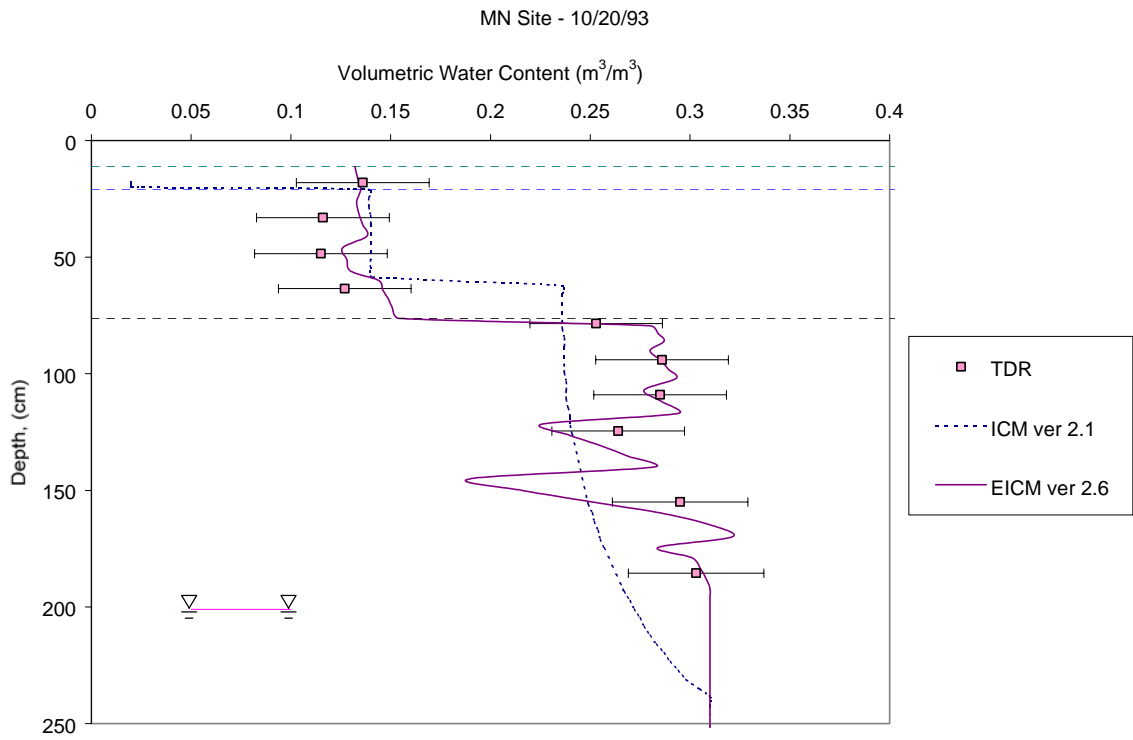
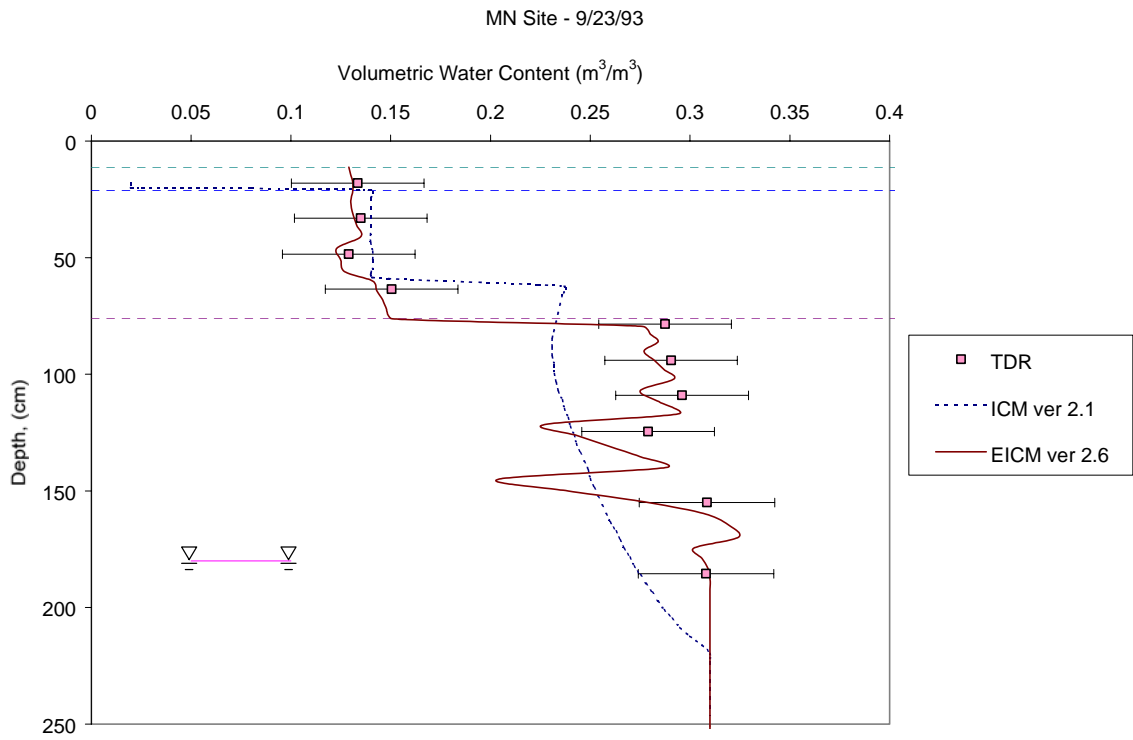
---

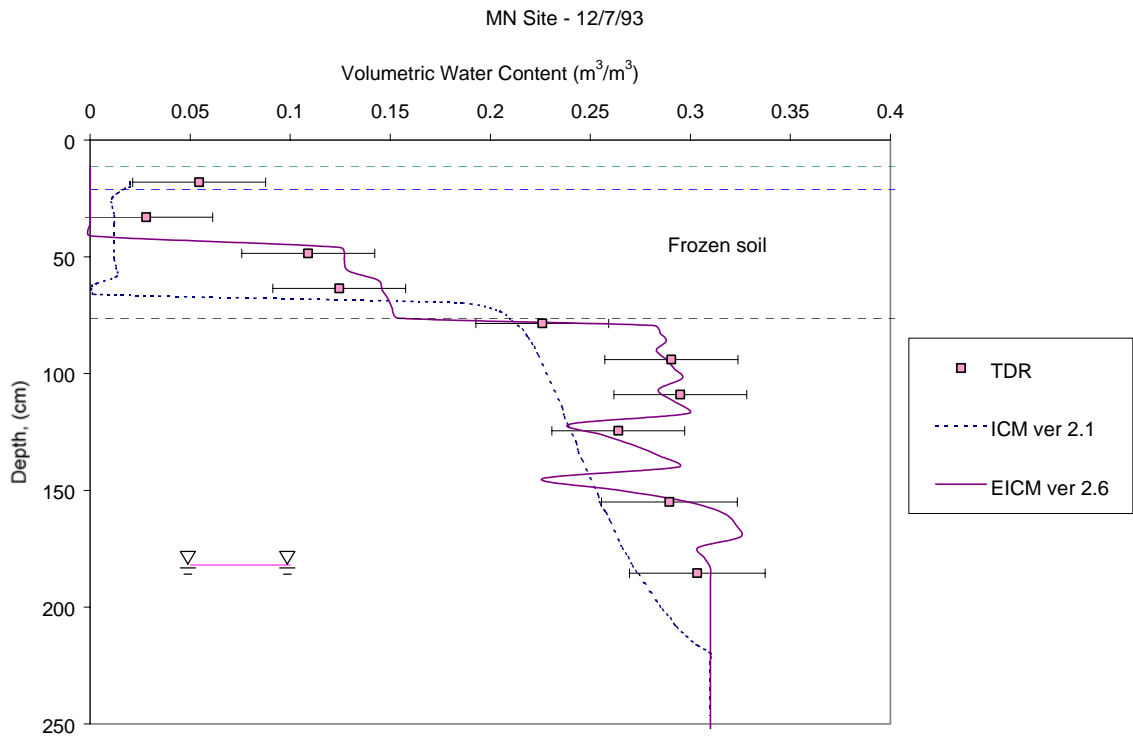
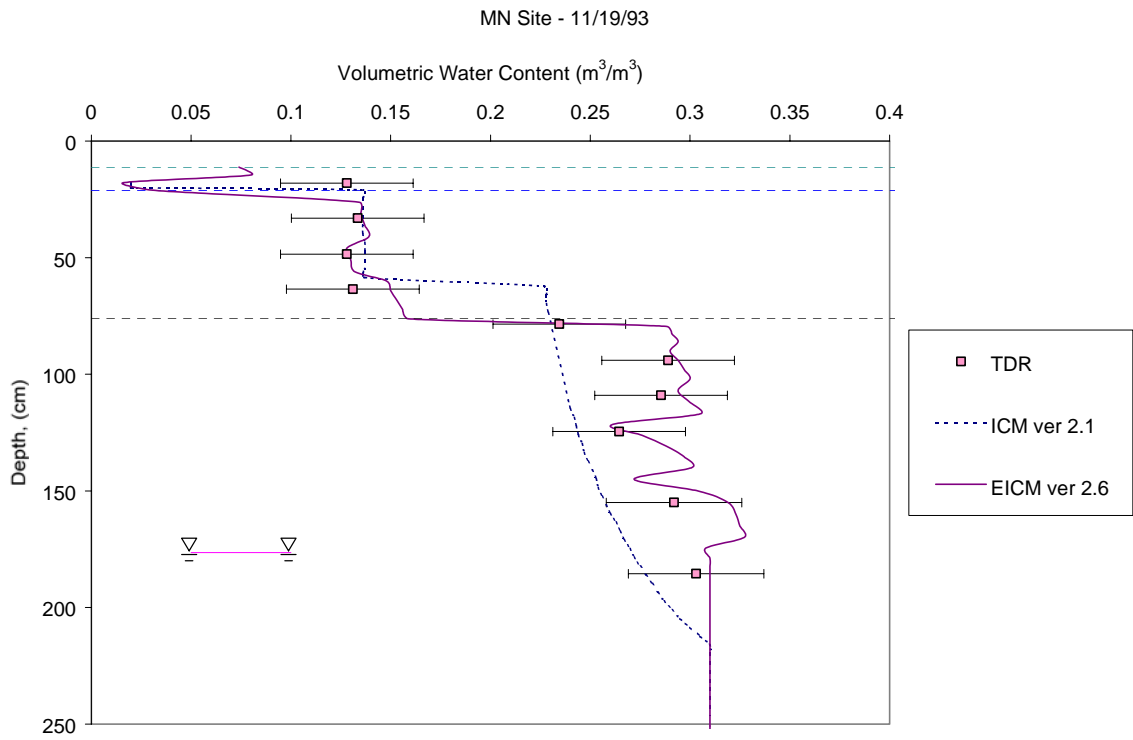
# APPENDIX J

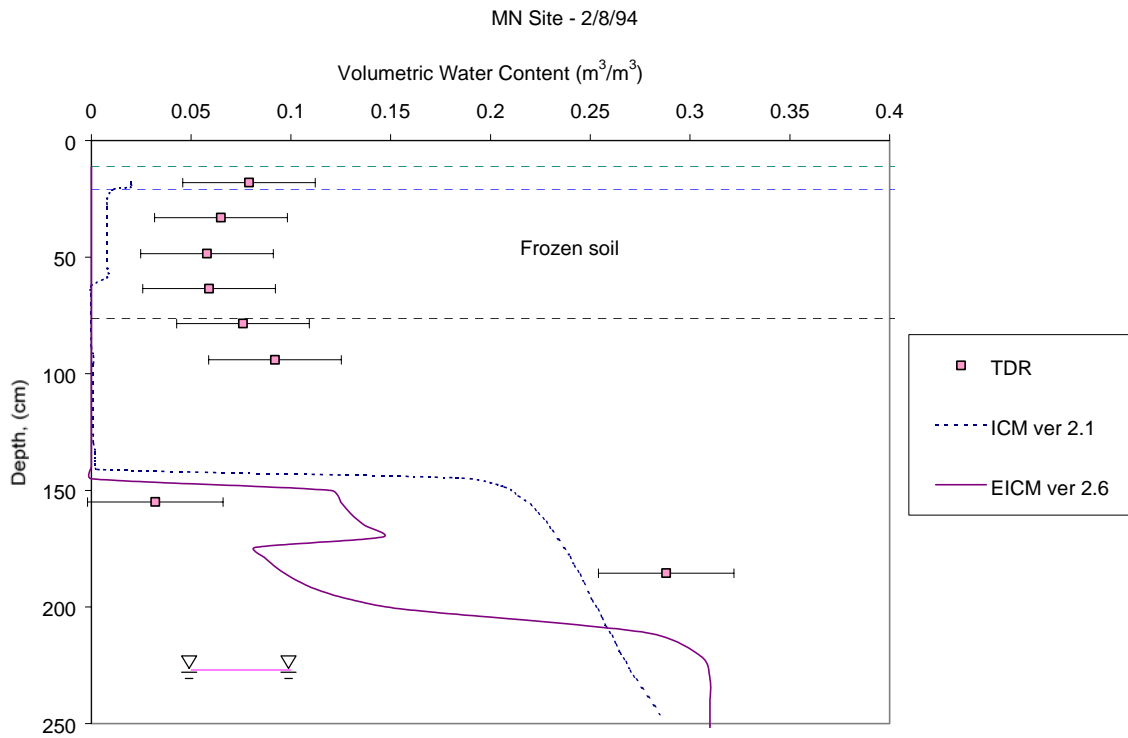
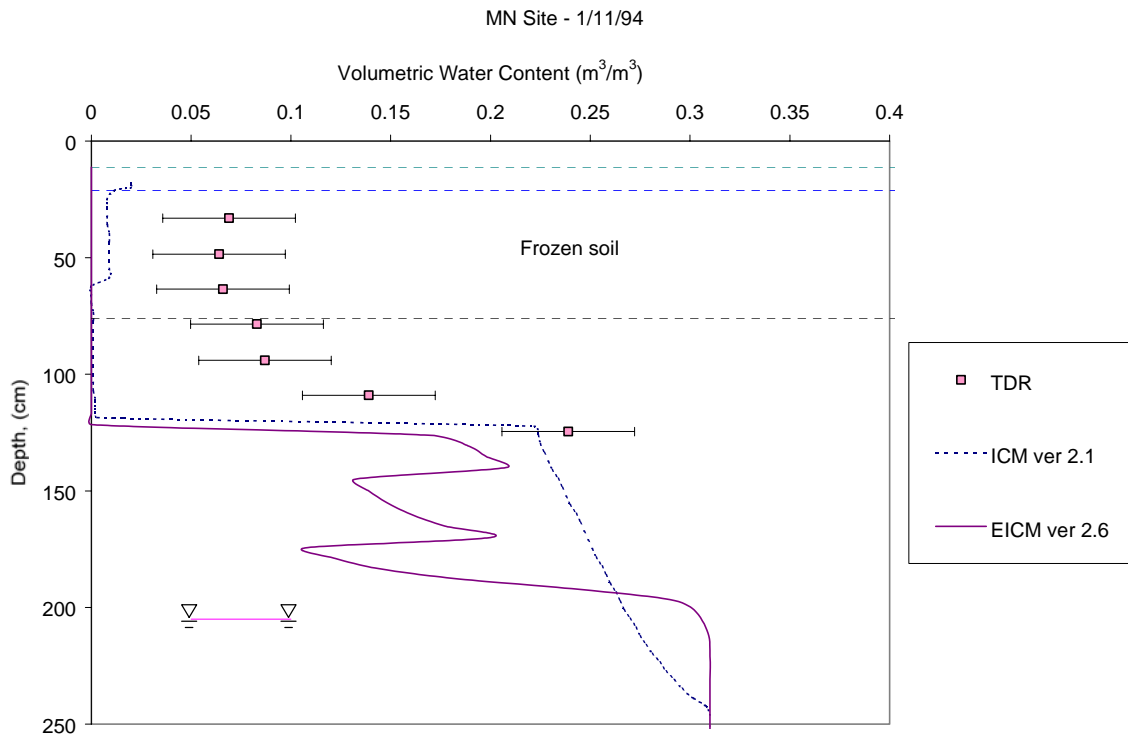
## VOLUMETRIC WATER CONTENT PROFILES

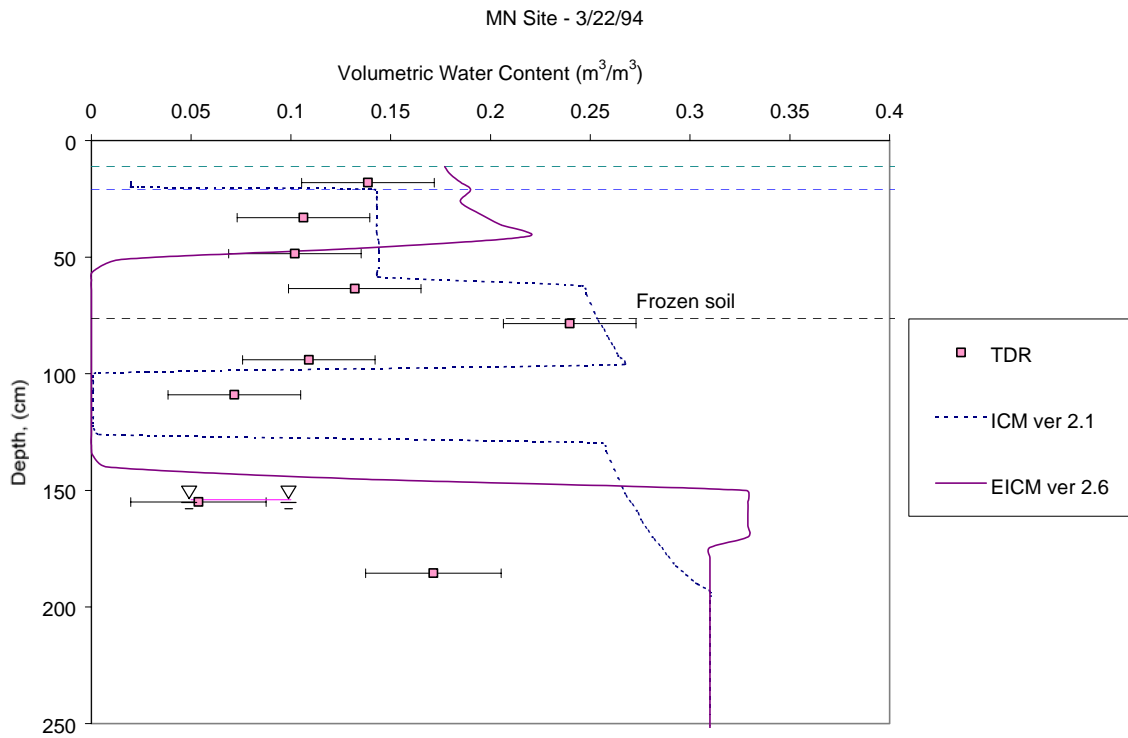
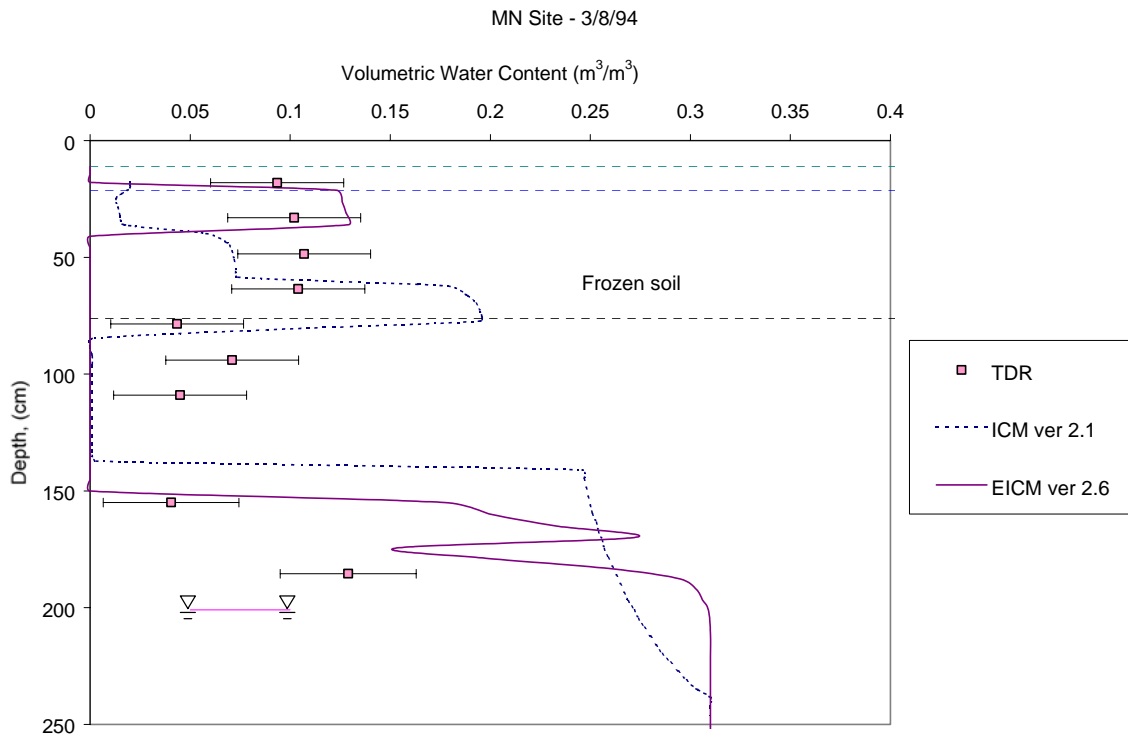
MINNESOTA (271018)

EICM – Version 2.6

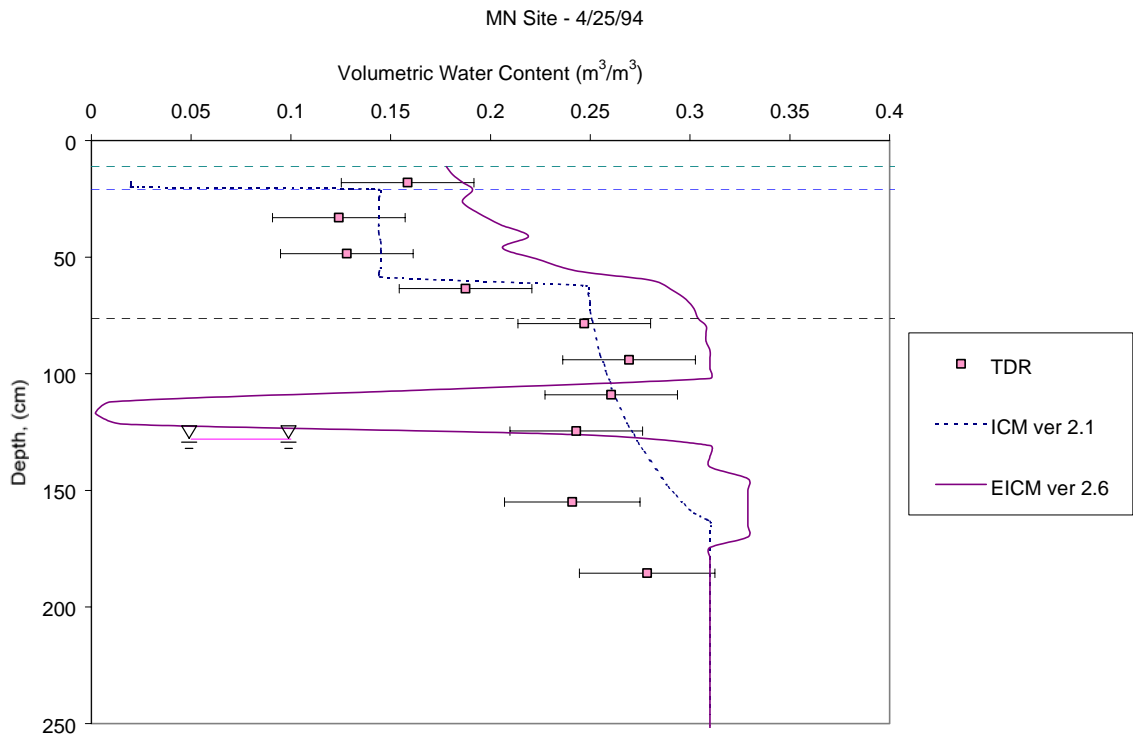
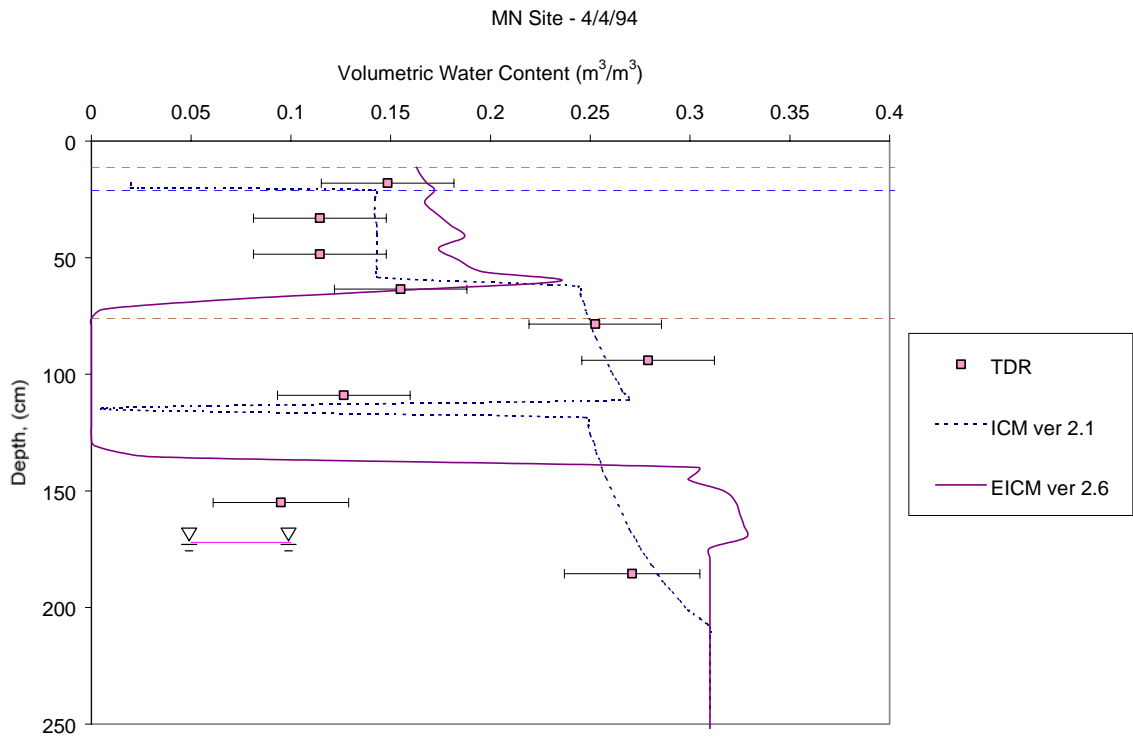


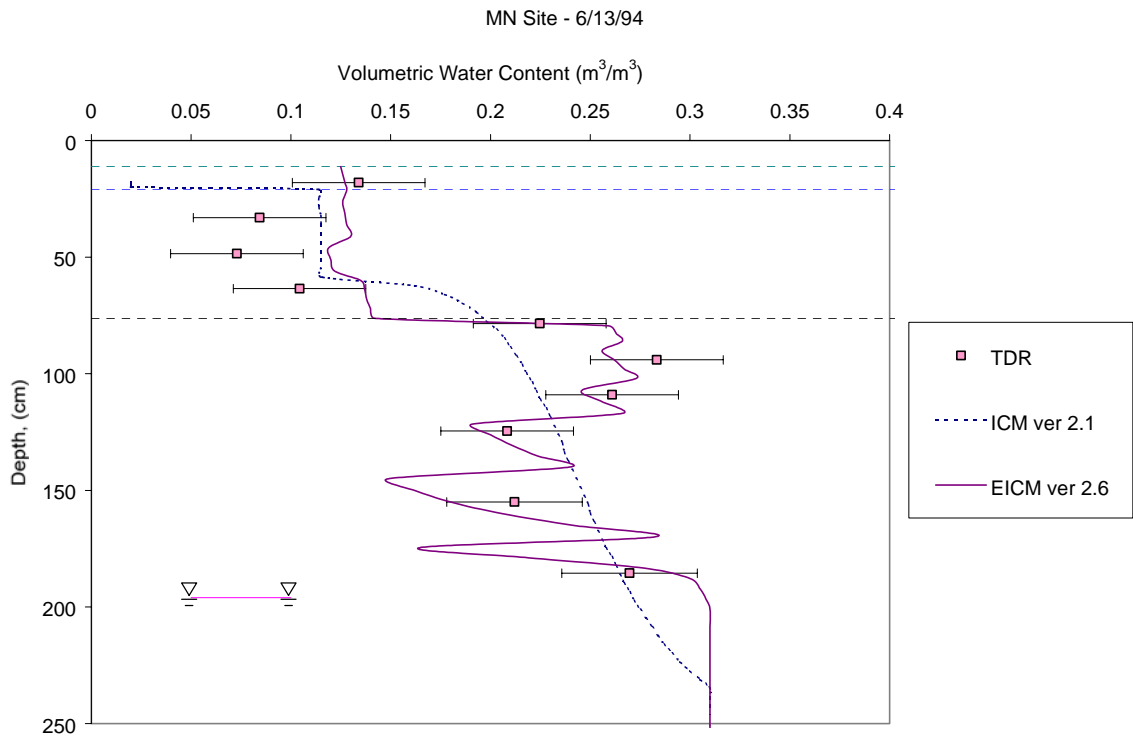
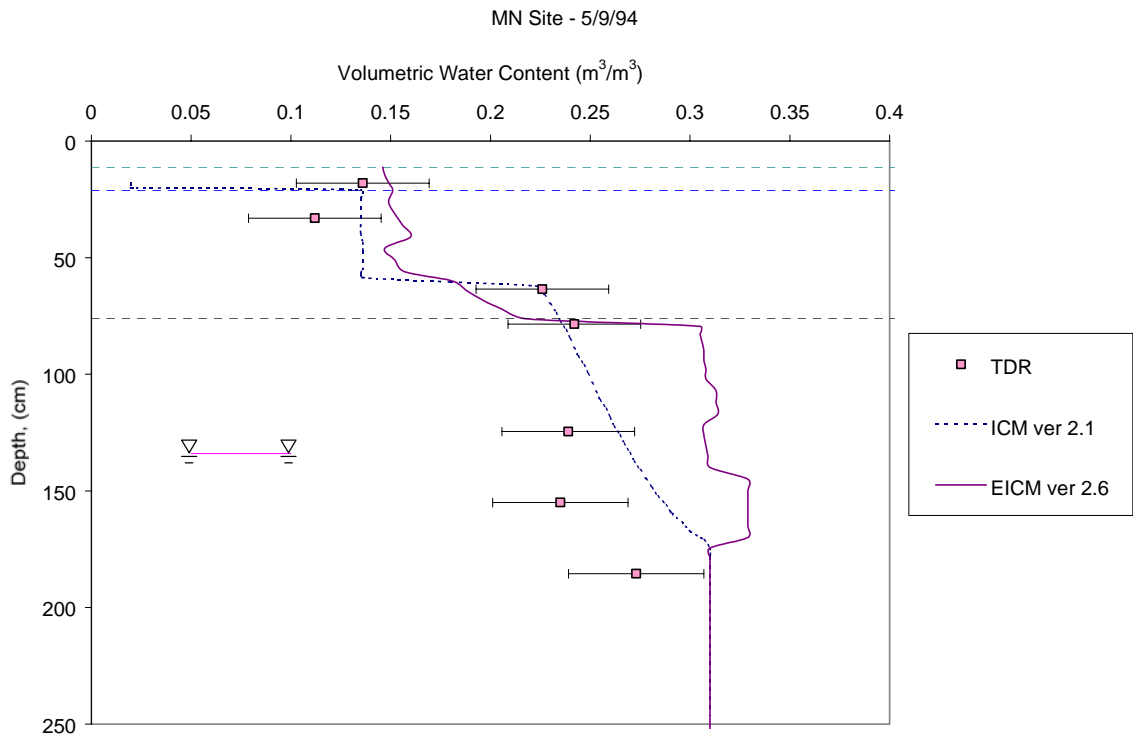


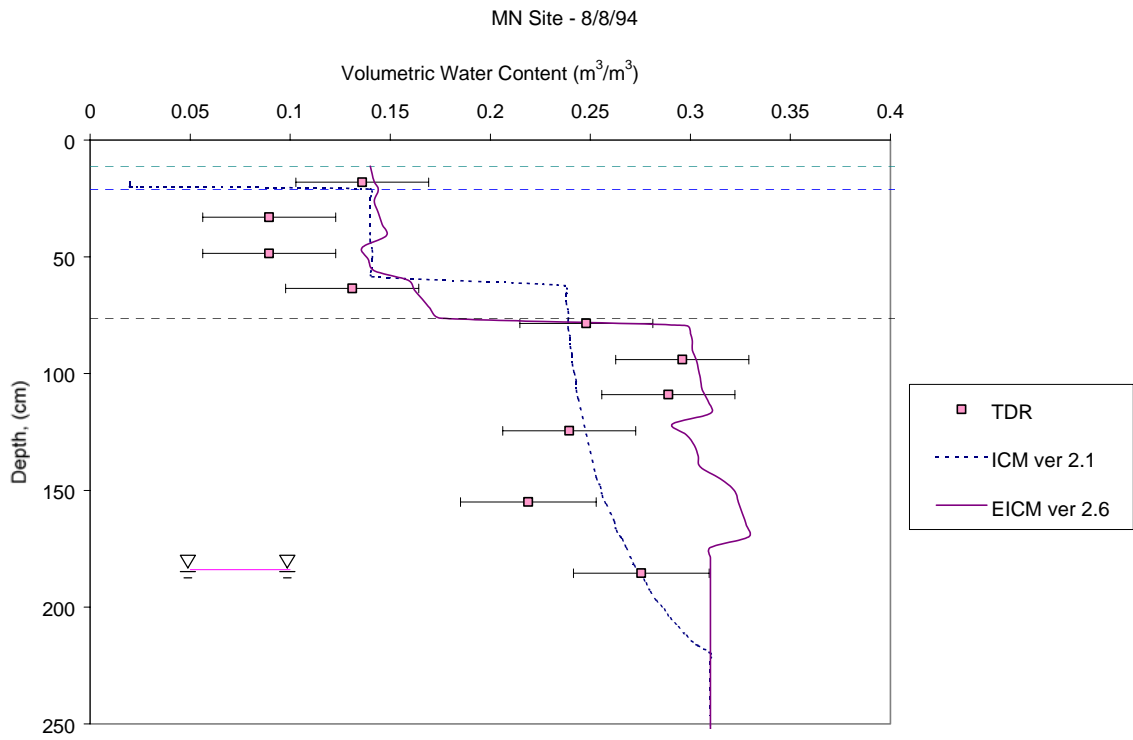
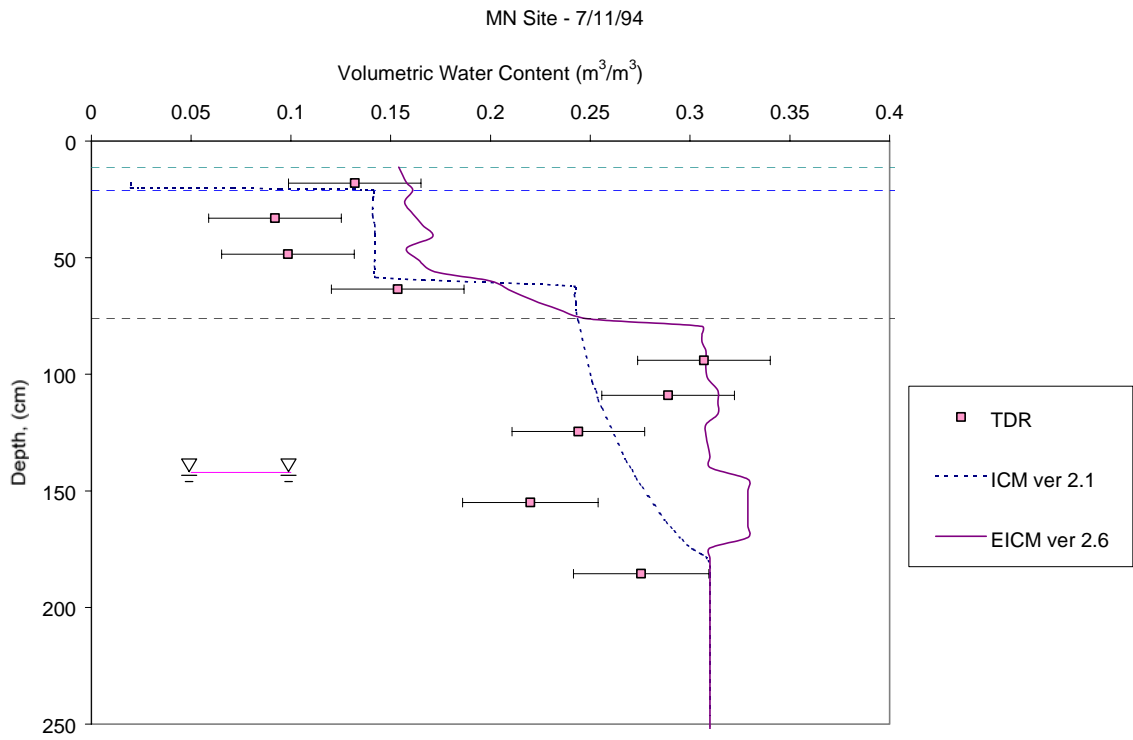












---

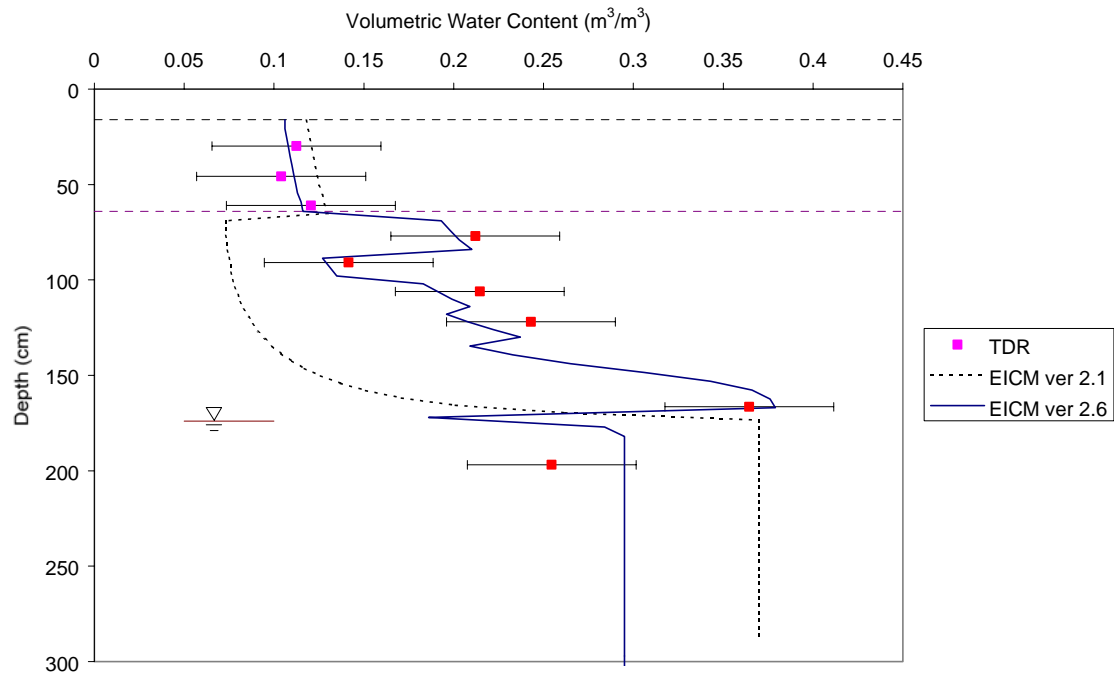
# APPENDIX K

## VOLUMETRIC WATER CONTENT PROFILES

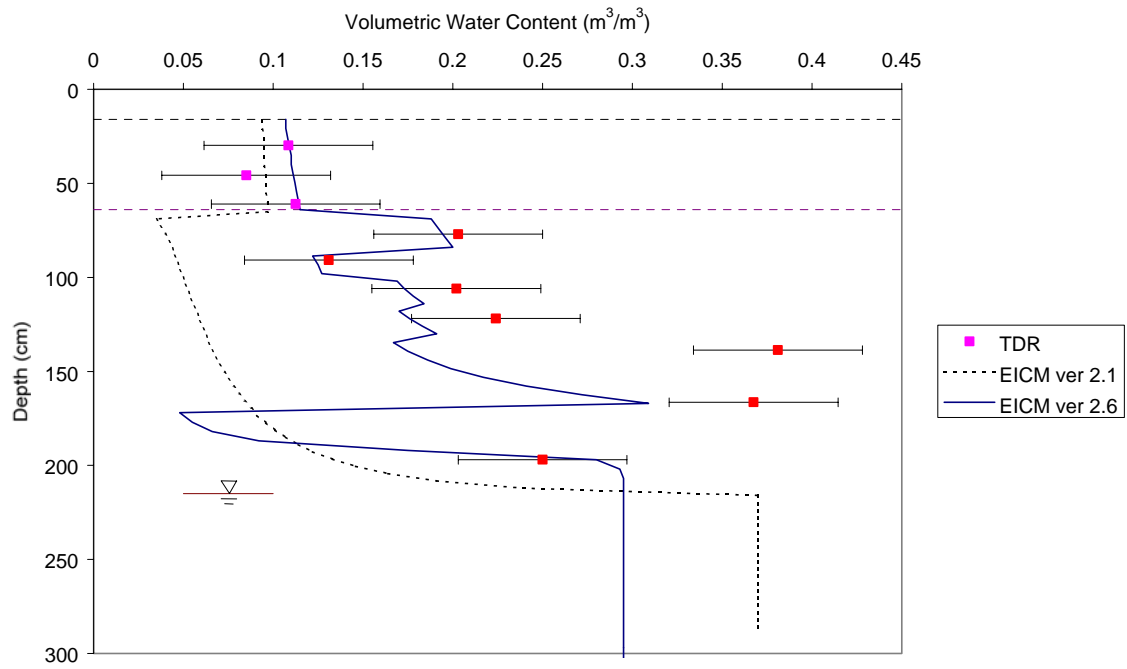
MAINE (231026)

EICM – Version 2.6

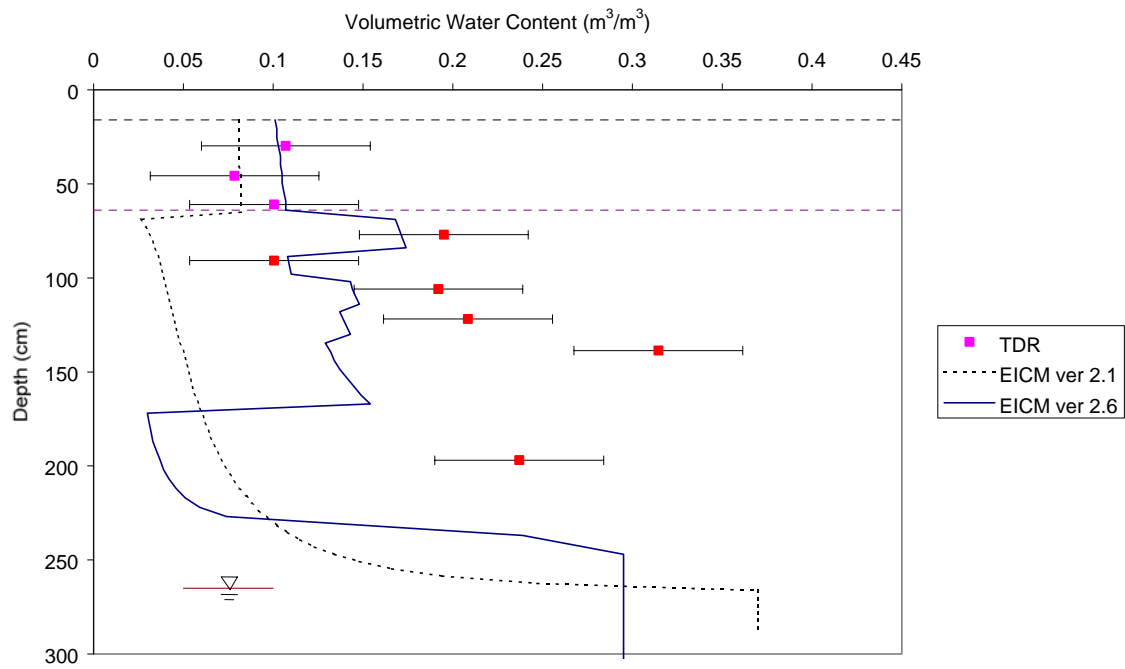
MAINE site - 6/20/94



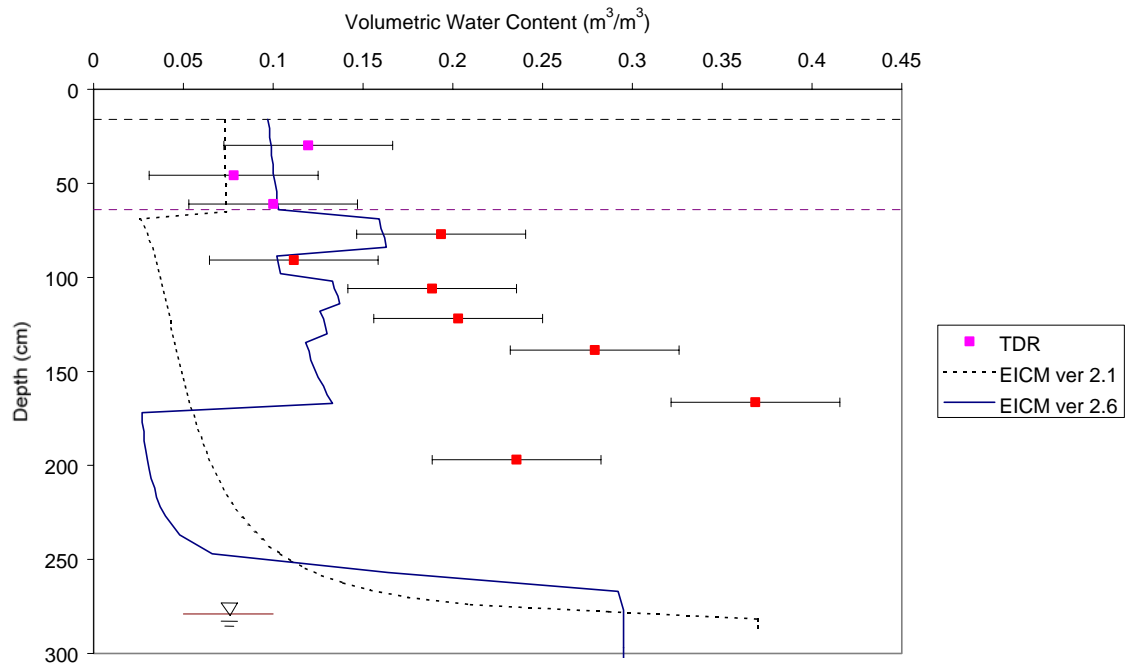
MAINE site - 7/18/94



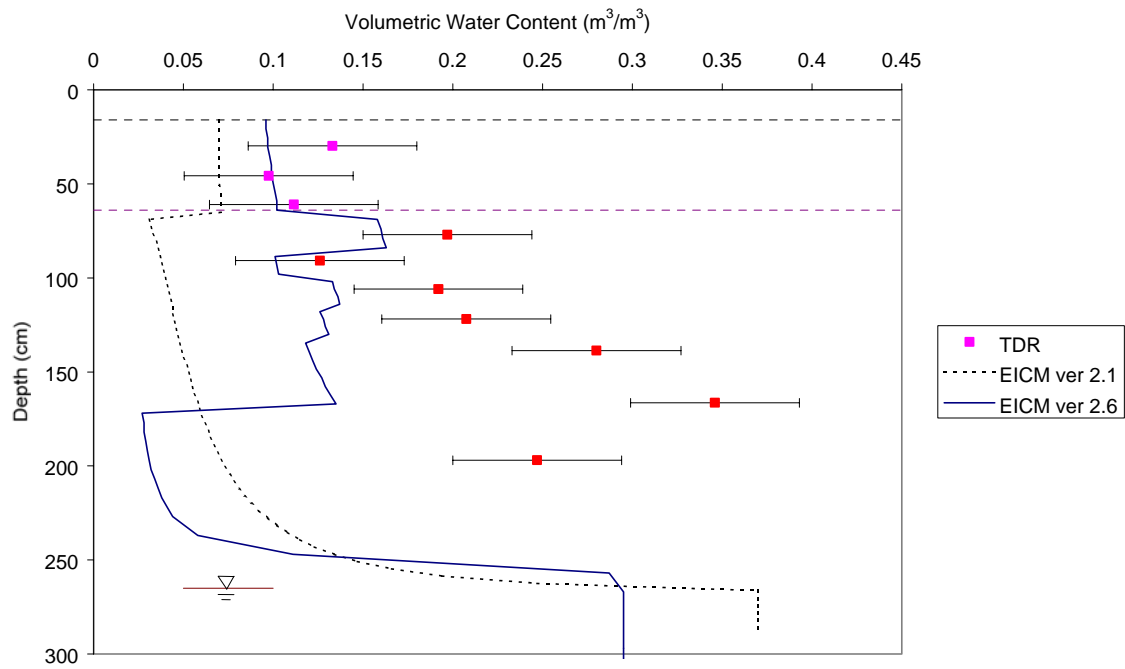
MAINE site - 8/15/94



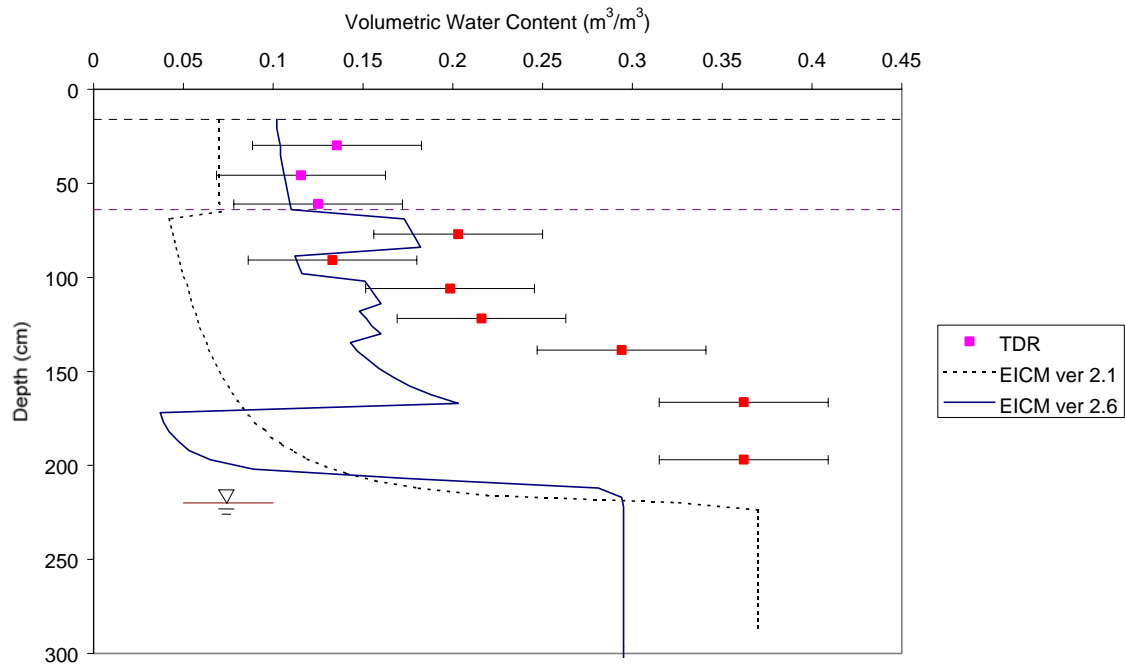
MAINE site - 9/19/94



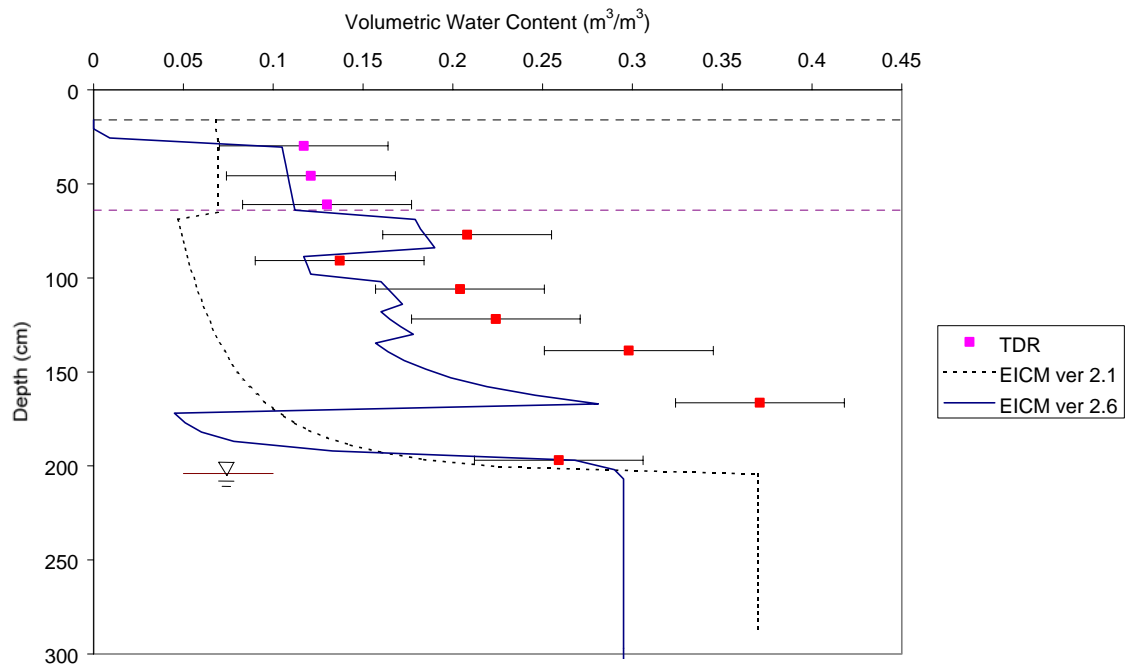
MAINE site - 10/17/94



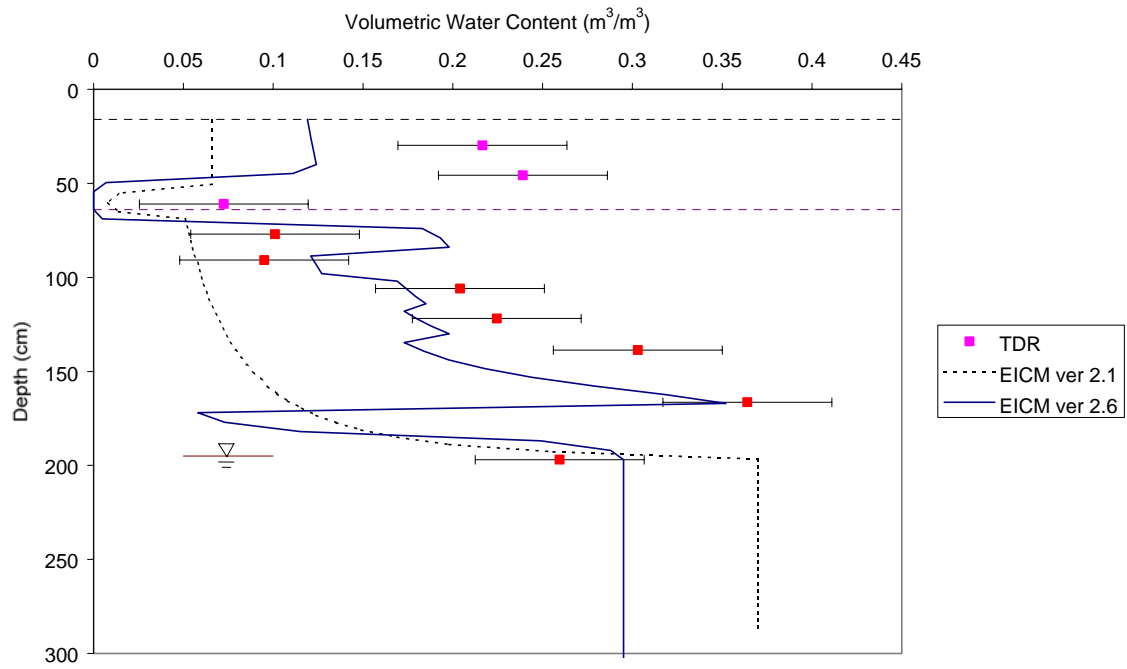
MAINE site - 11/14/94



MAINE site - 12/12/94

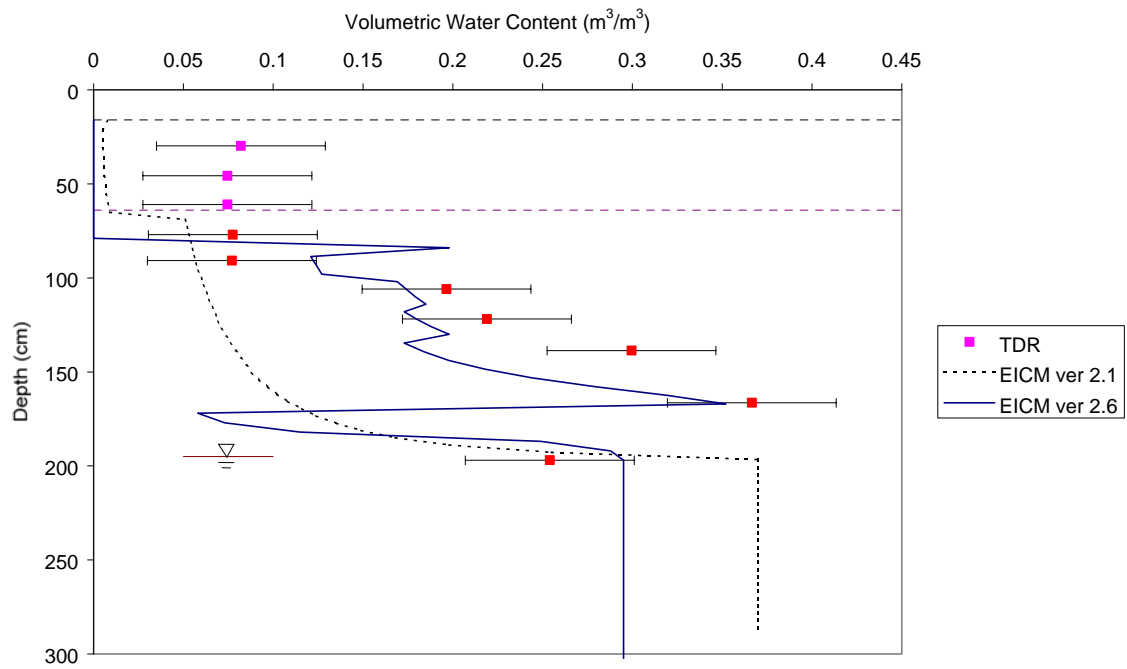


MAINE site - 1/17/95

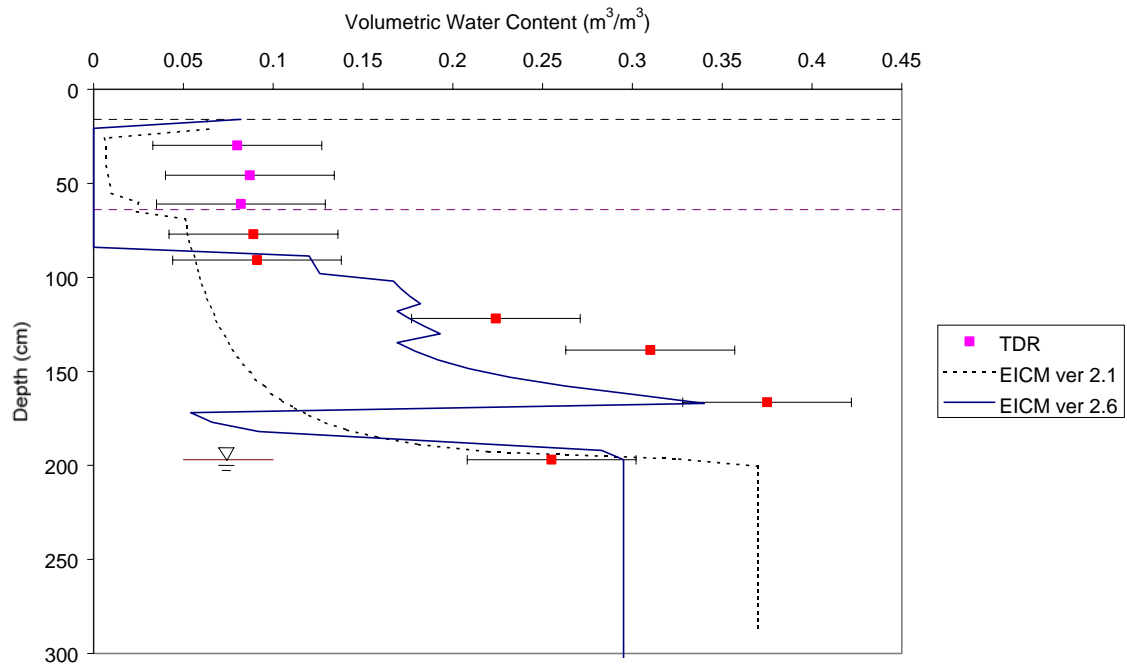




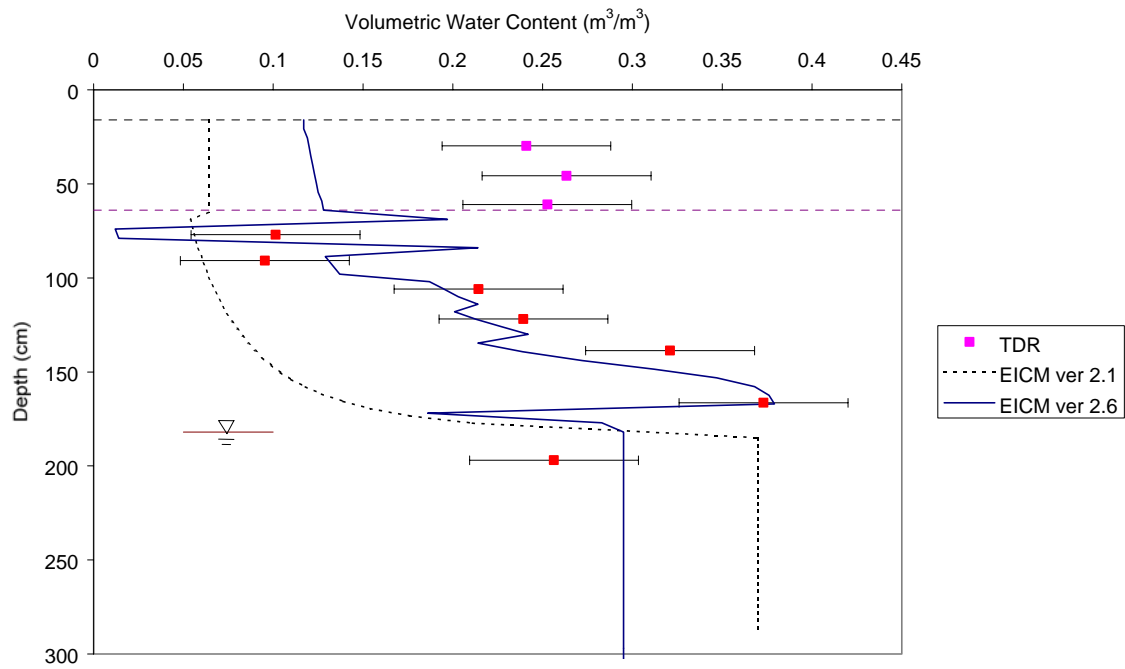
MAINE site - 2/14/95



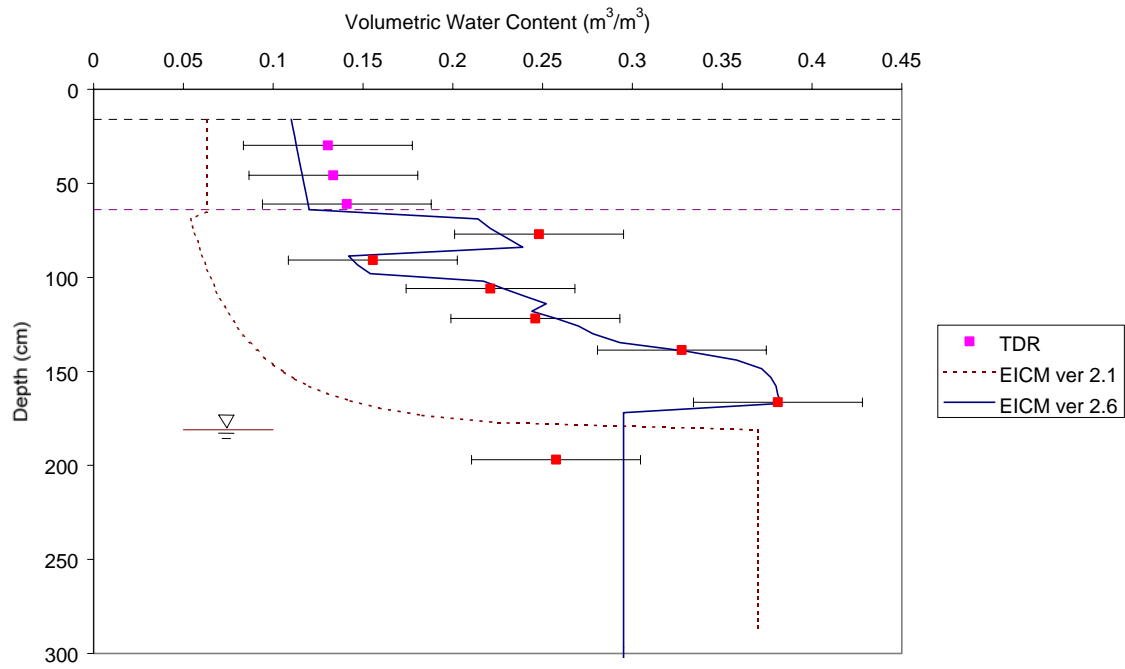
MAINE site - 3/6/95



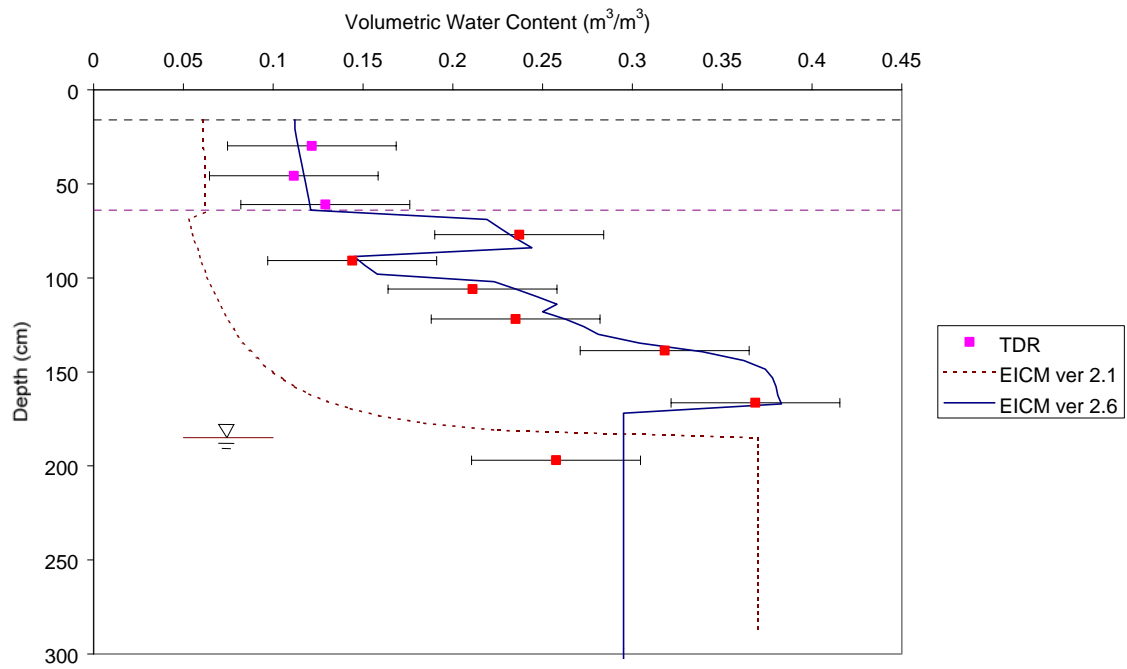
MAINE site - 3/20/95



MAINE site -4/3/95



MAINE site -5/1/95



---

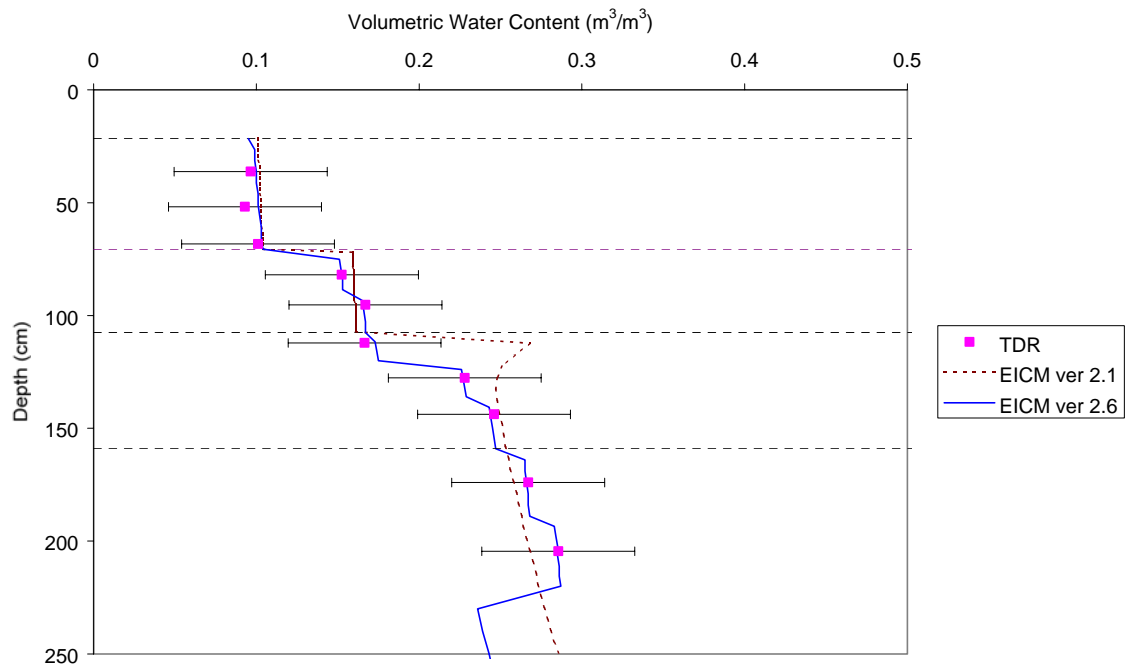
# APPENDIX L

## VOLUMETRIC WATER CONTENT PROFILES

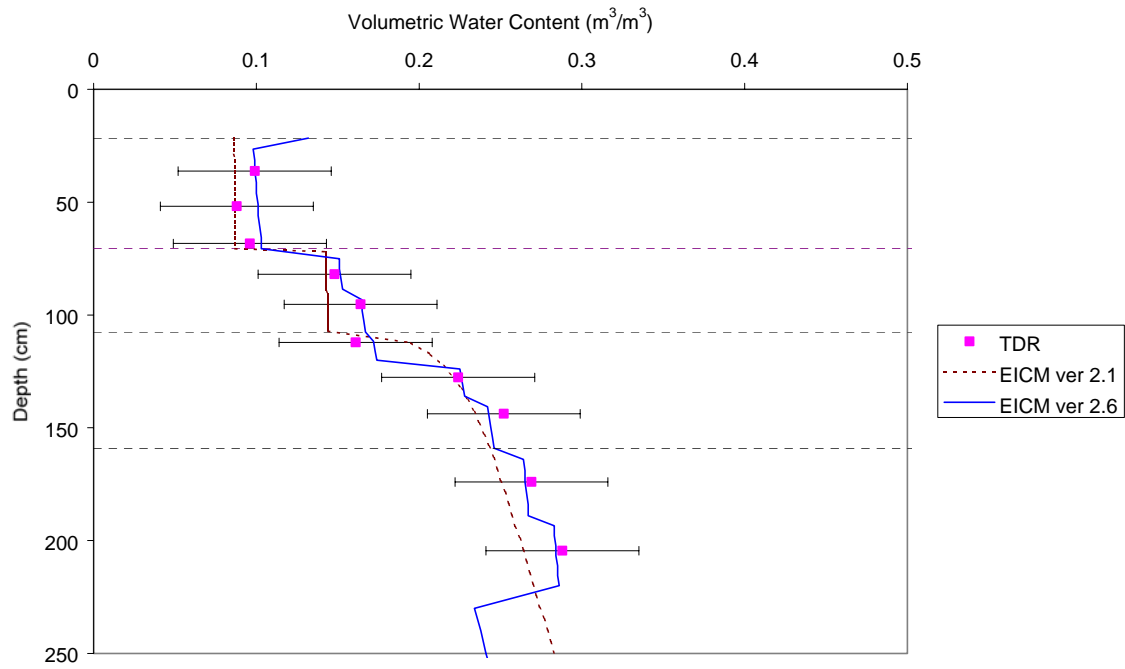
### NEW HAMPSHIRE (331001)

EICM – Version 2.6

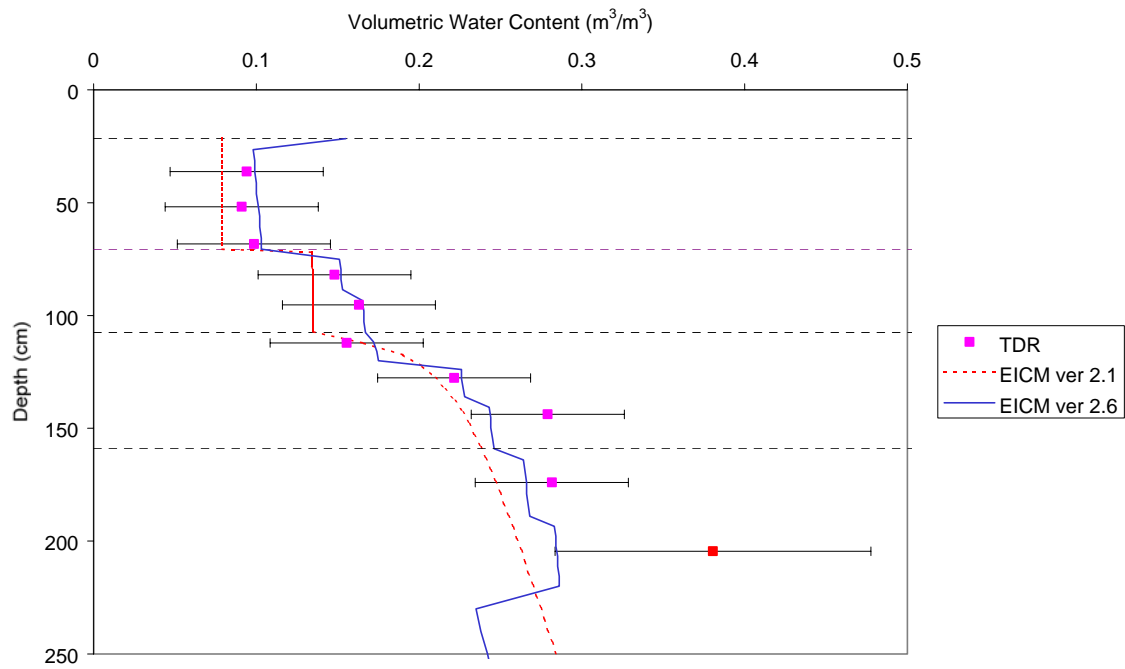
NEW HAMPSHIRE site - 6/23/94



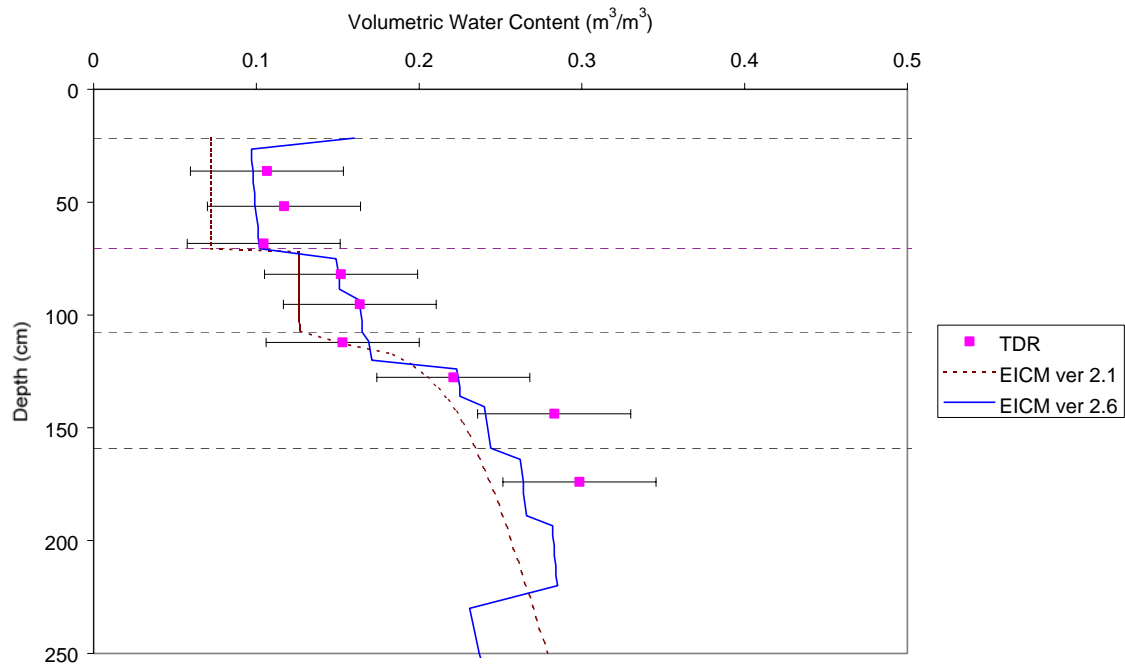
NEW HAMPSHIRE site - 7/21/94



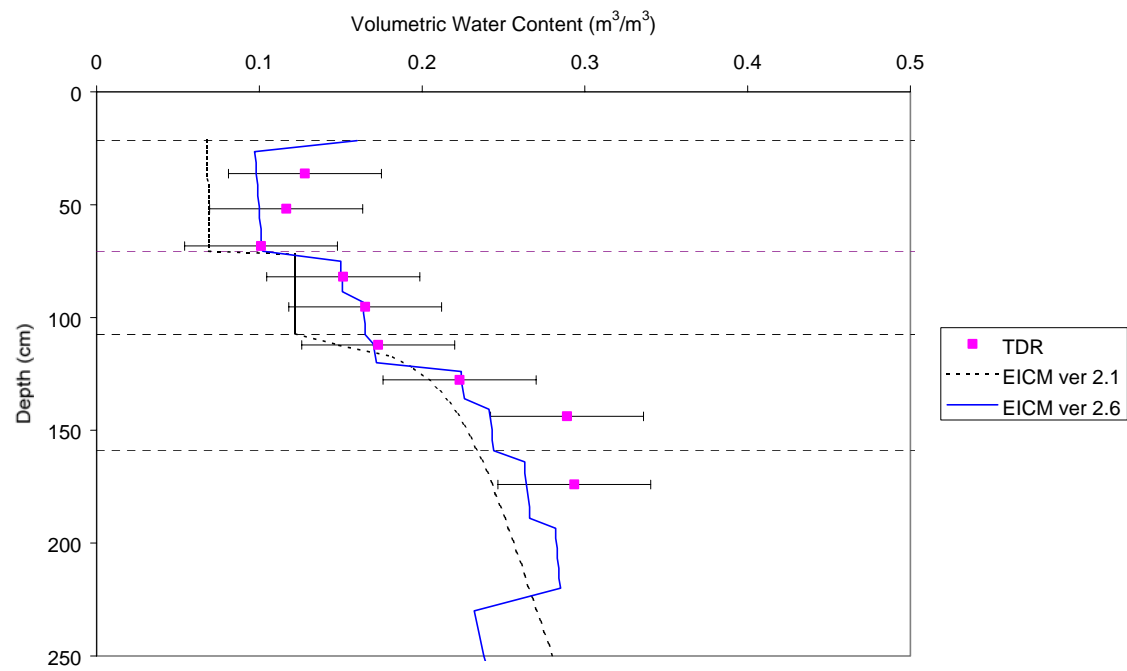
NEW HAMPSHIRE site - 8/16/94



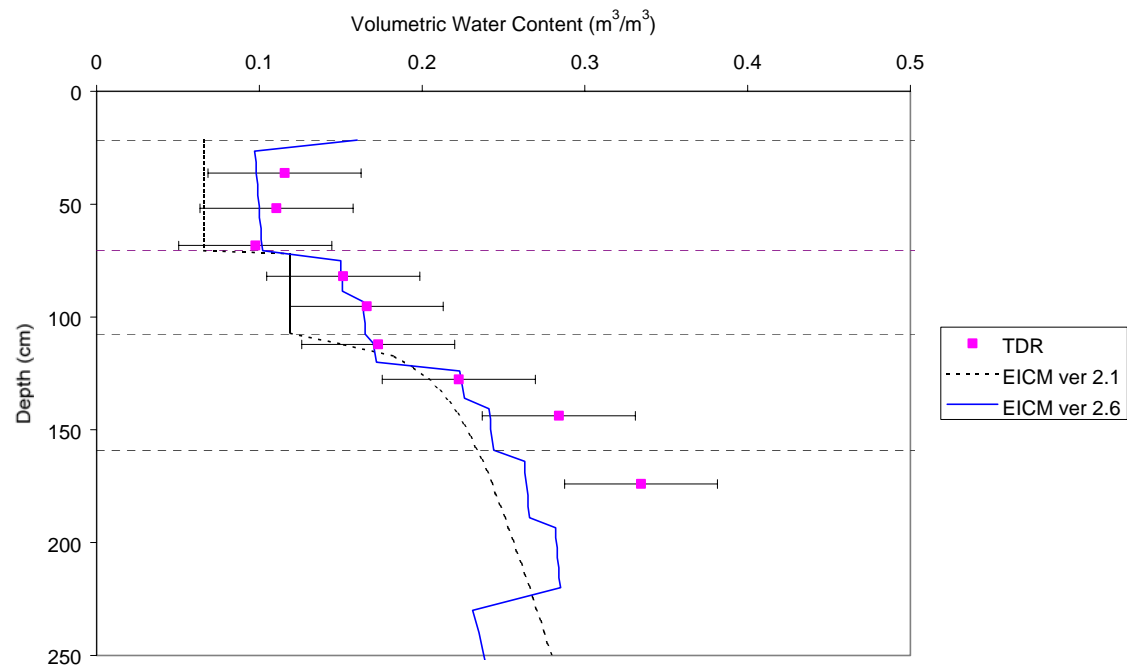
NEW HAMPSHIRE site - 9/22/94



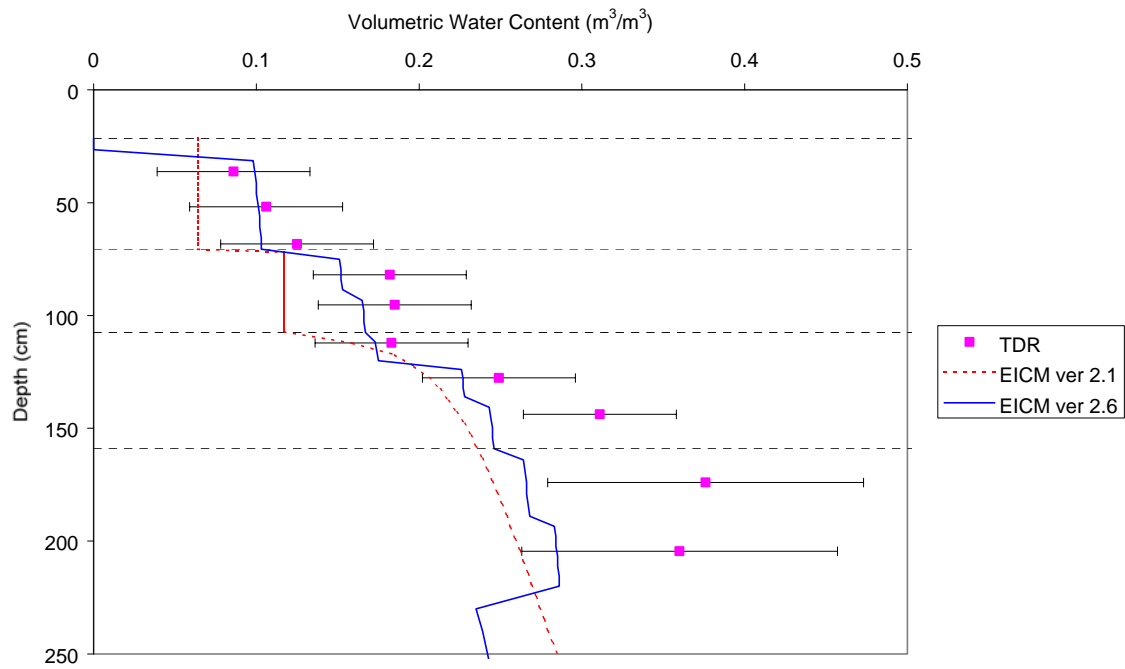
NEW HAMPSHIRE site - 10/20/94



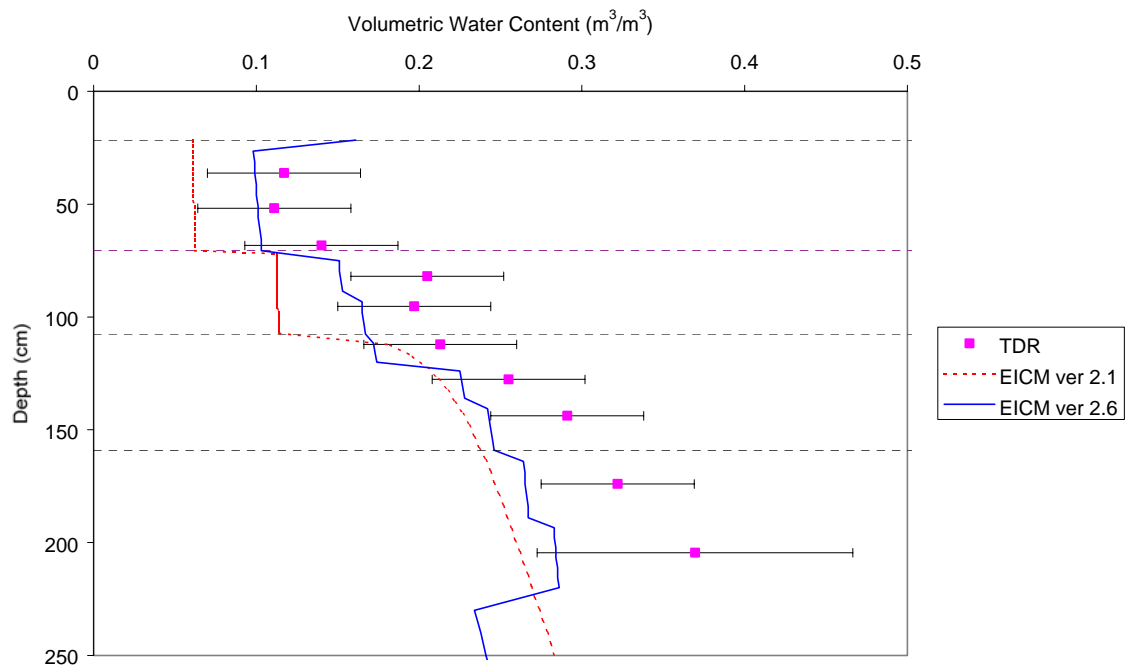
NEW HAMPSHIRE site - 11/17/94



NEW HAMPSHIRE site - 12/15/94

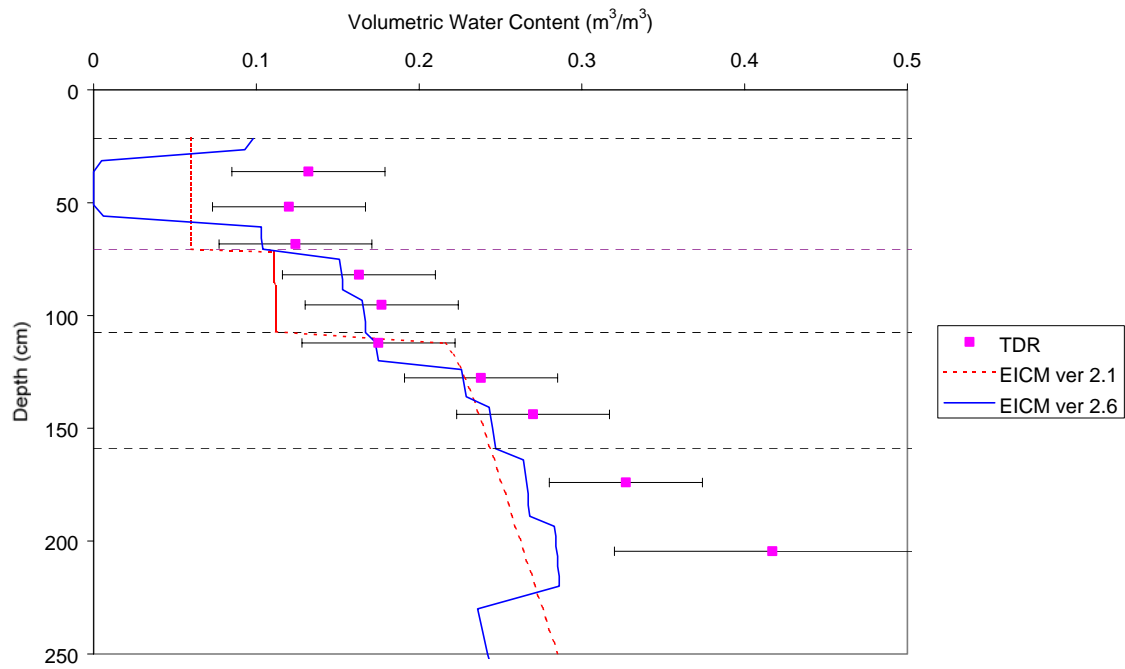


NEW HAMPSHIRE site - 1/24/95

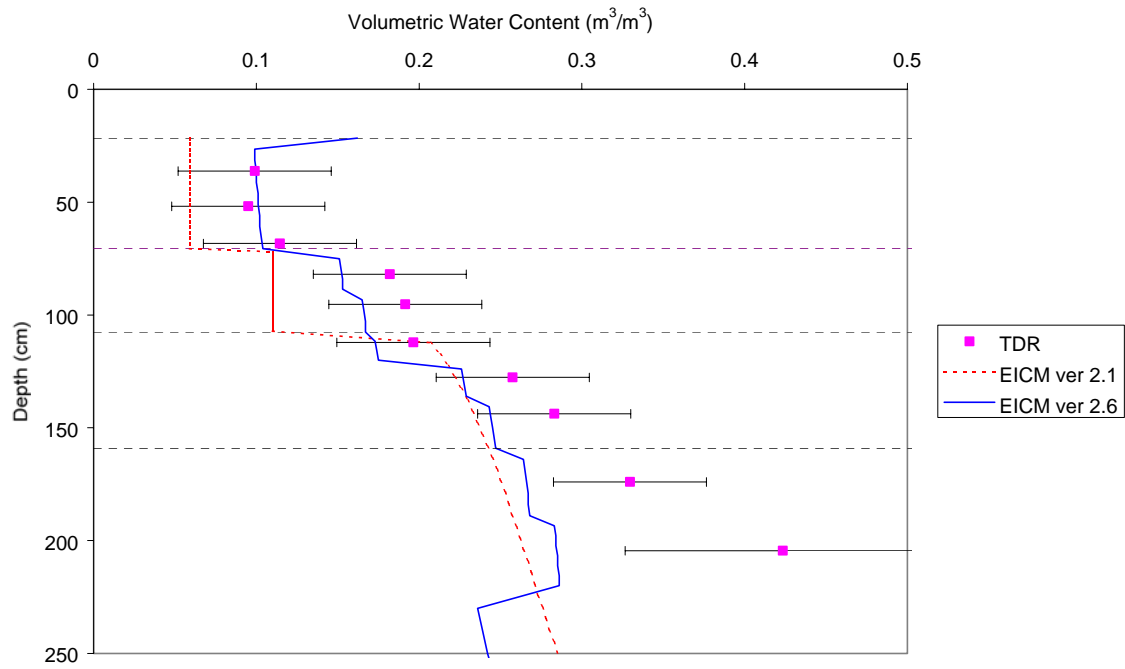




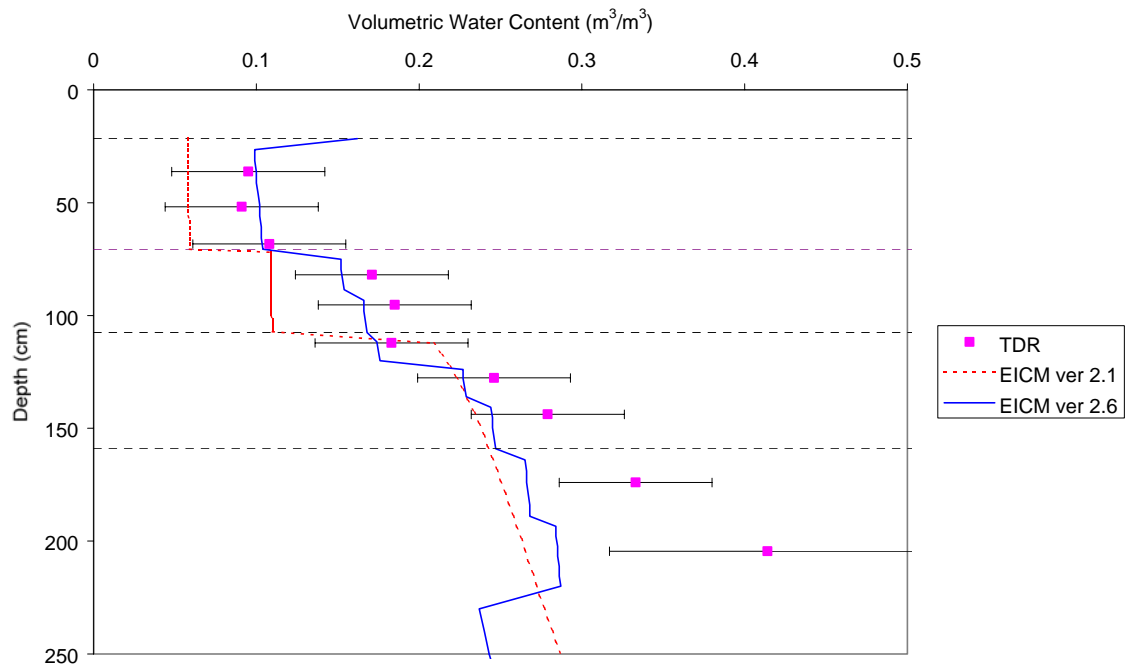
NEW HAMPSHIRE site - 2/21/95



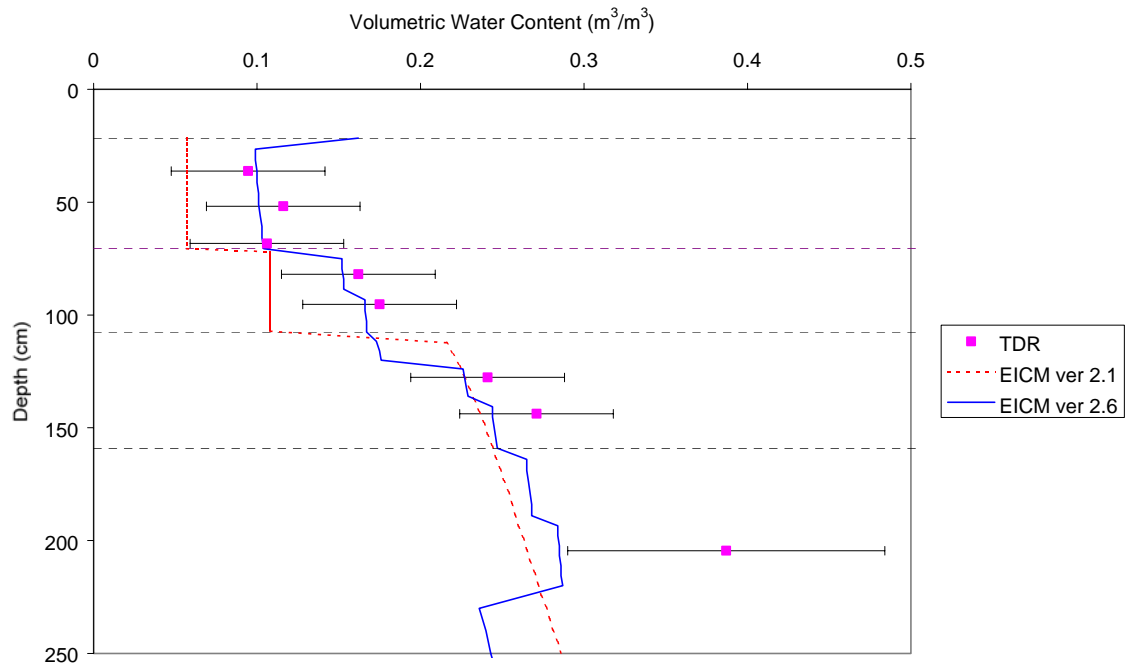
NEW HAMPSHIRE site - 3/16/95



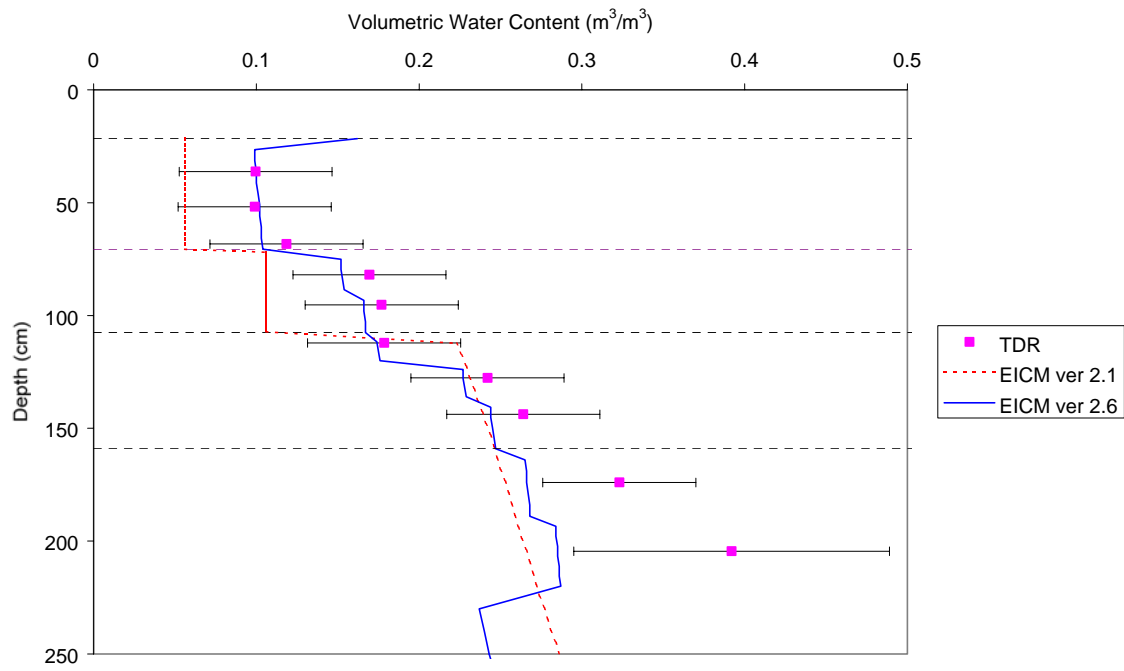
NEW HAMPSHIRE site - 3/30/95



NEW HAMPSHIRE site - 4/27/95



NEW HAMPSHIRE site - 6/1/95



---

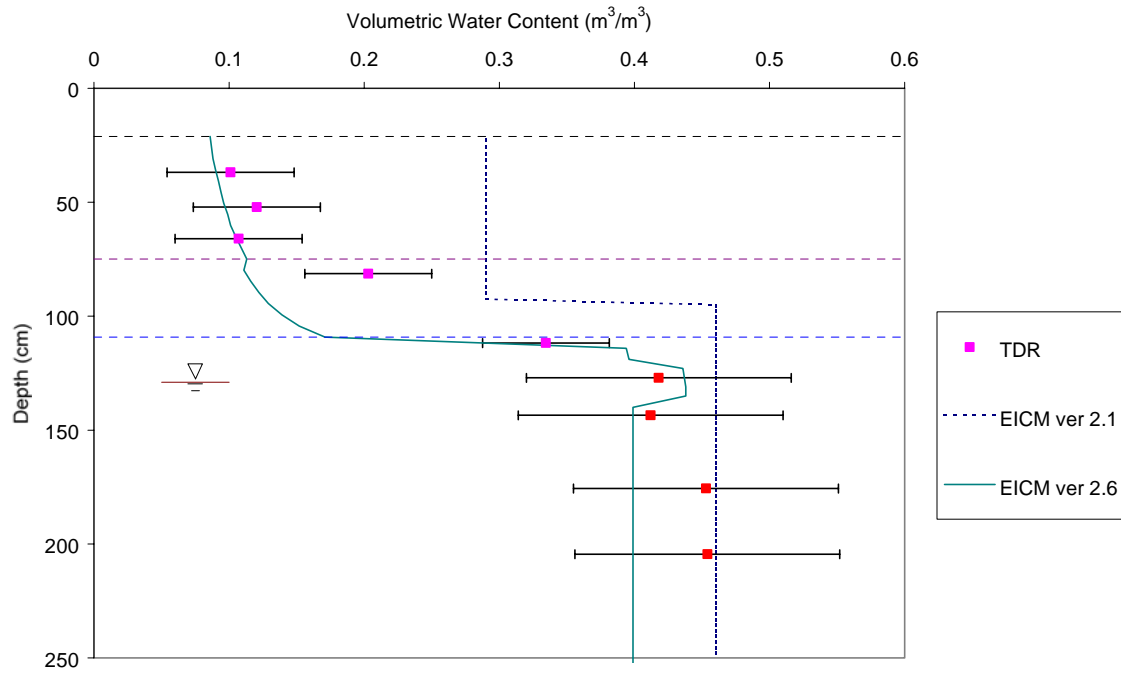
# APPENDIX M

## VOLUMETRIC WATER CONTENT PROFILES

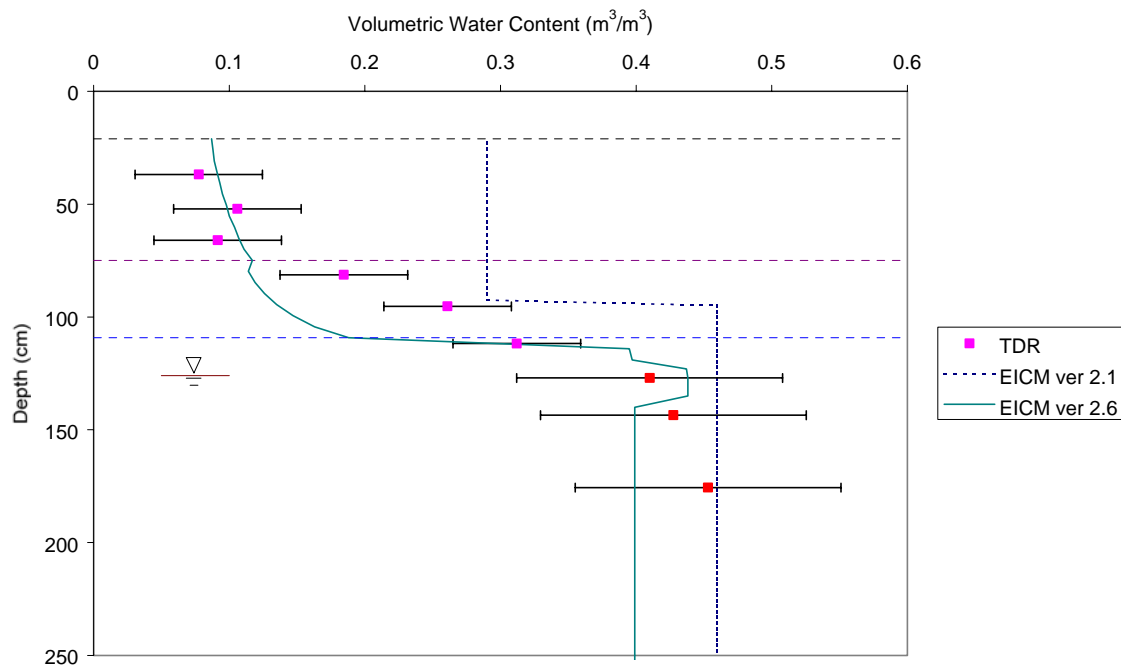
VERMONT (501002)

EICM – Version 2.6

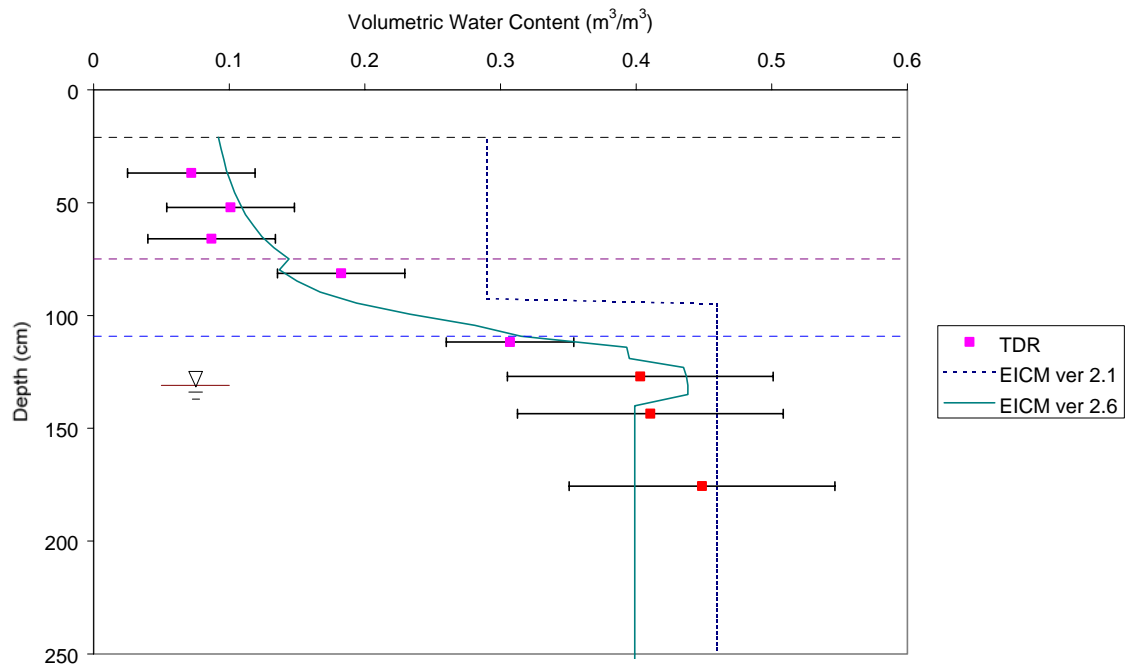
VERMONT site - 7/20/94



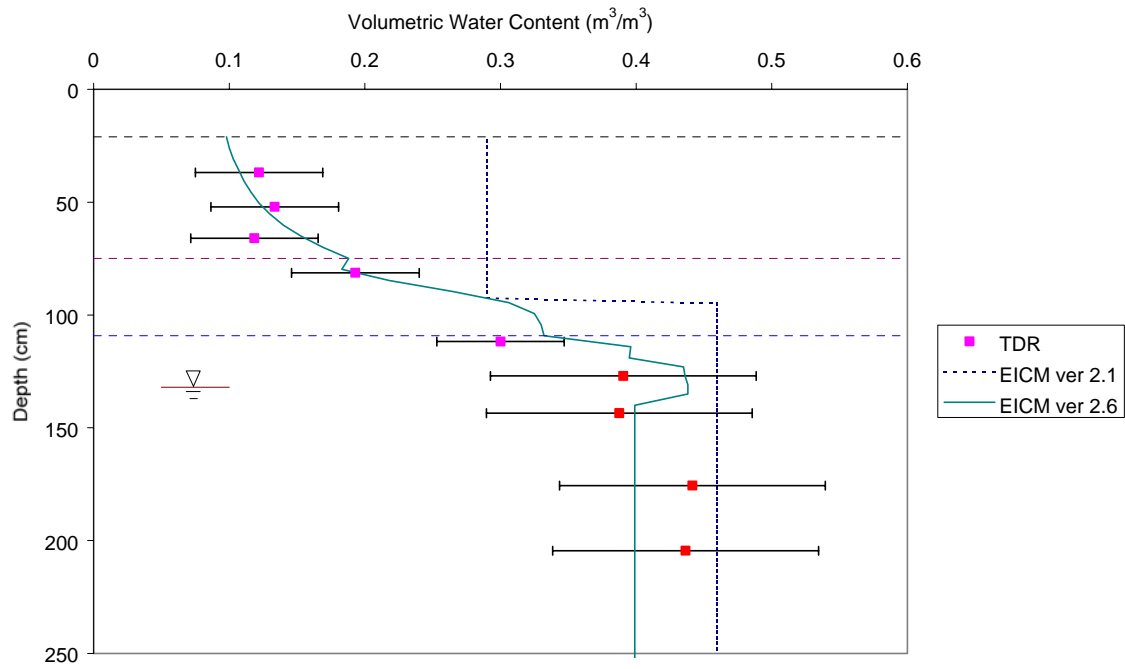
VERMONT site - 8/17/94



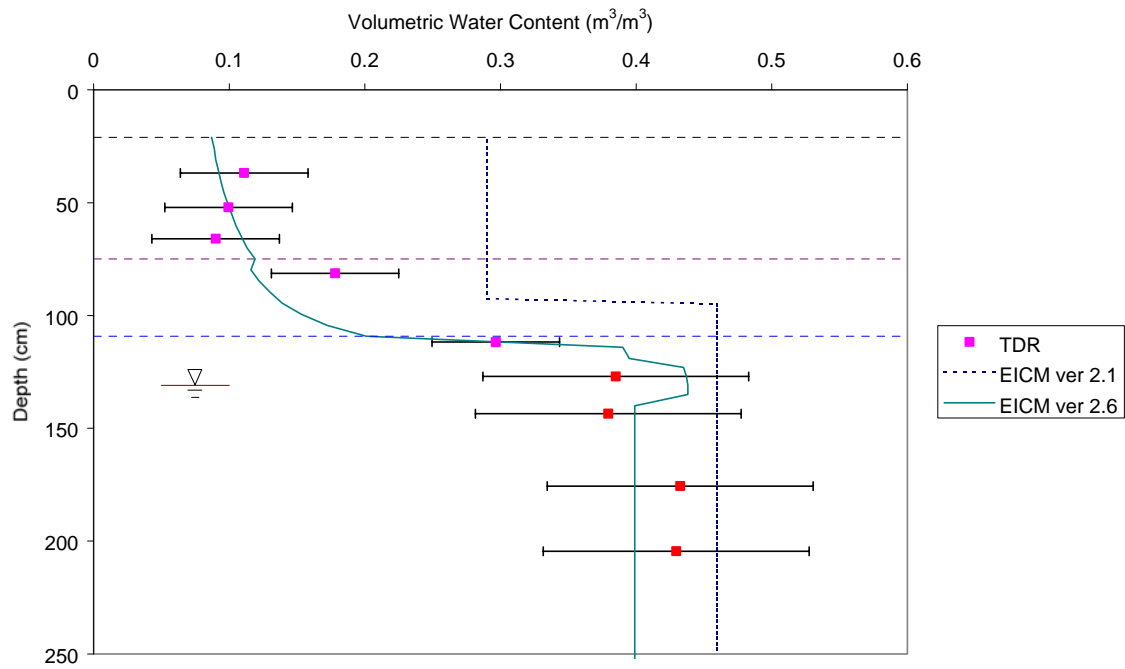
VERMONT site - 9/21/94



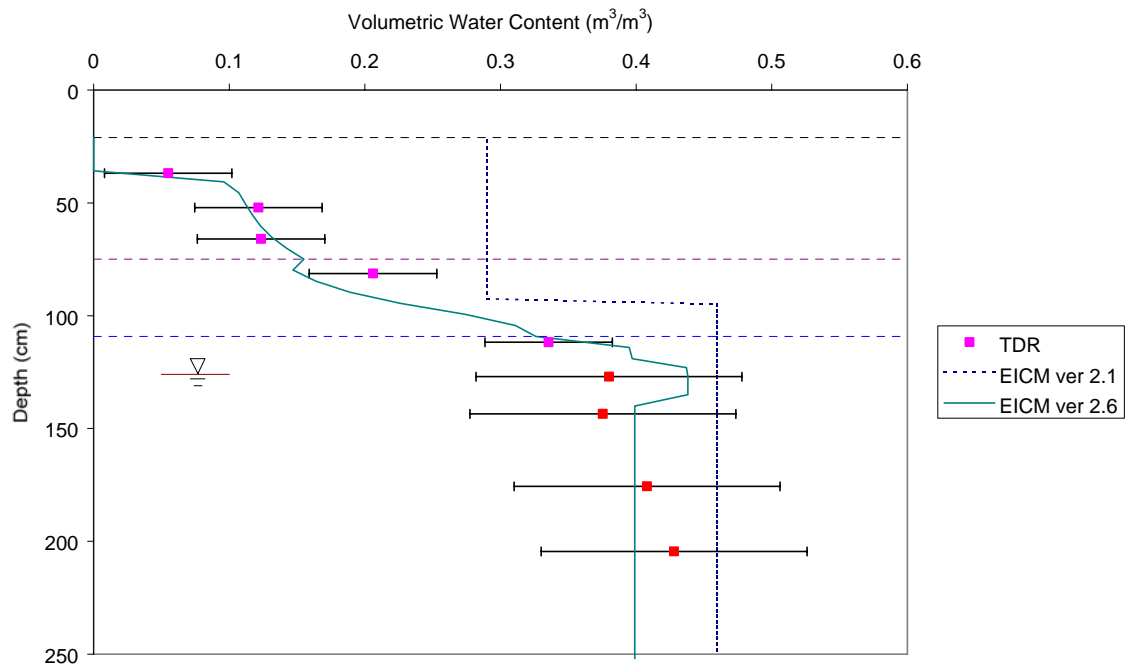
VERMONT site - 10/19/94



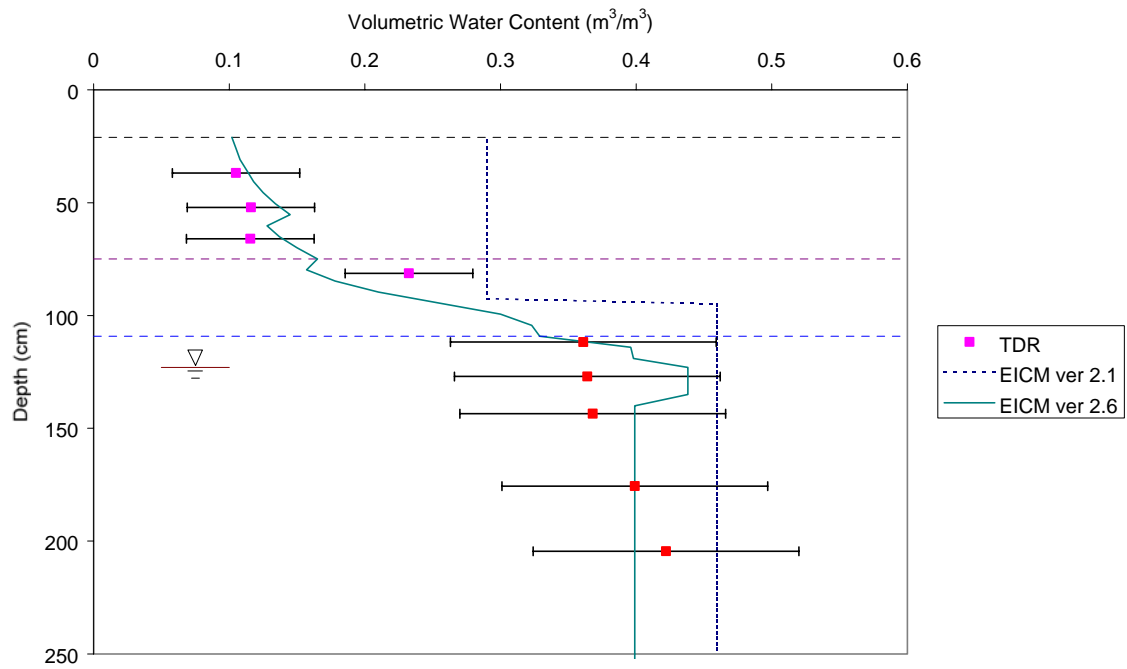
VERMONT site - 11/16/94



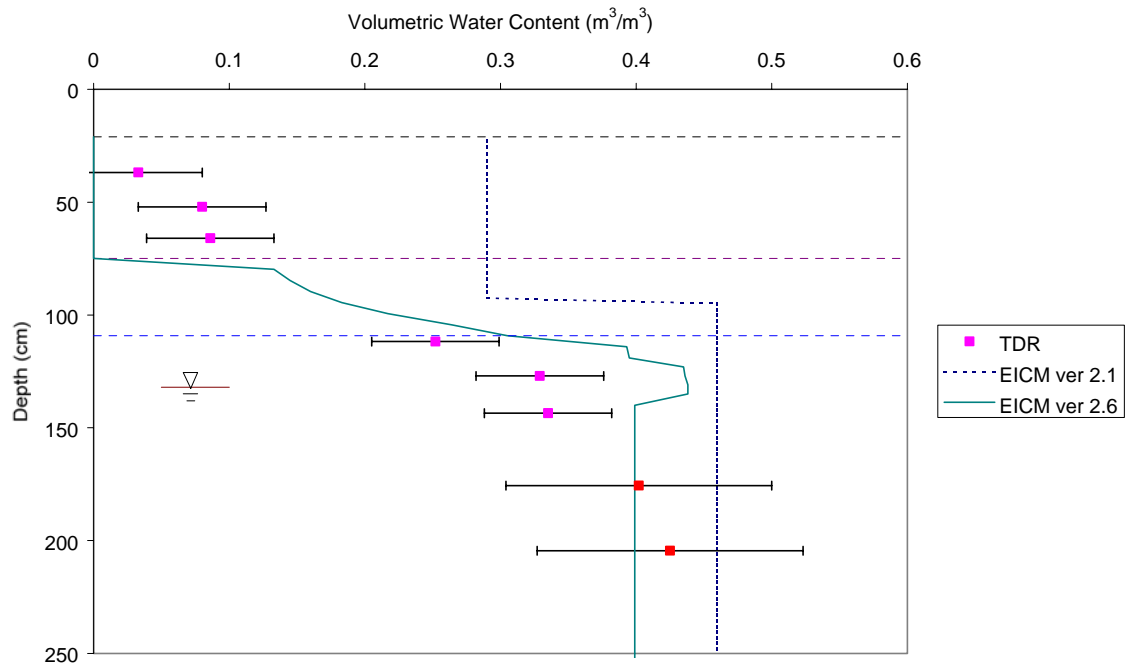
VERMONT site - 12/14/94



VERMONT site - 1/19/95

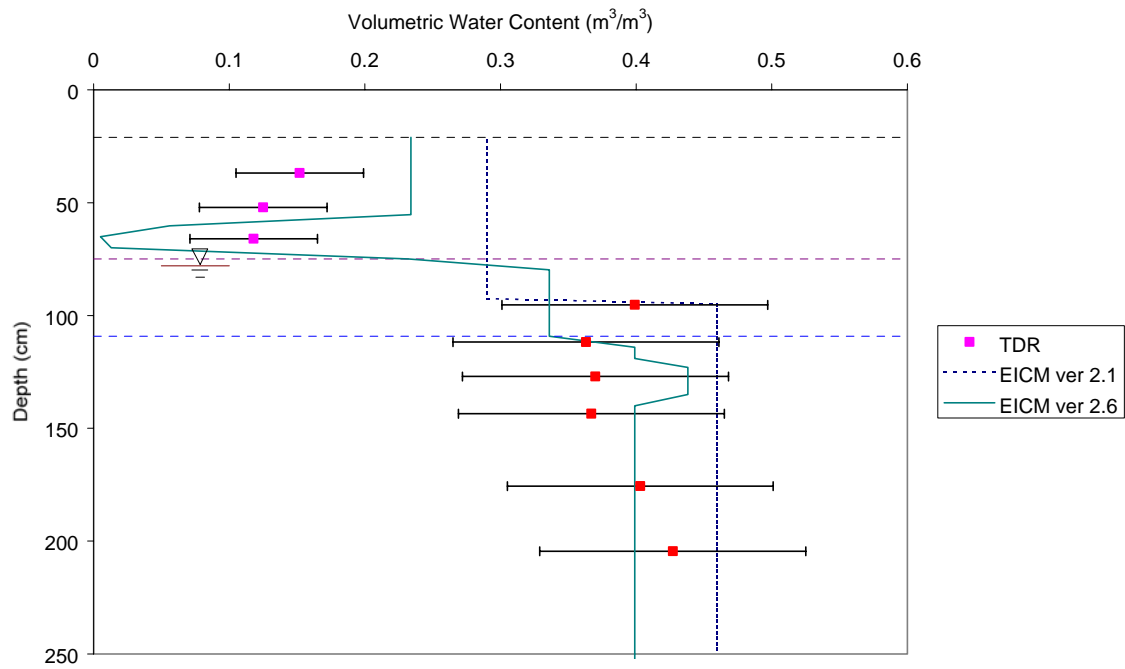


VERMONT site - 2/15/95

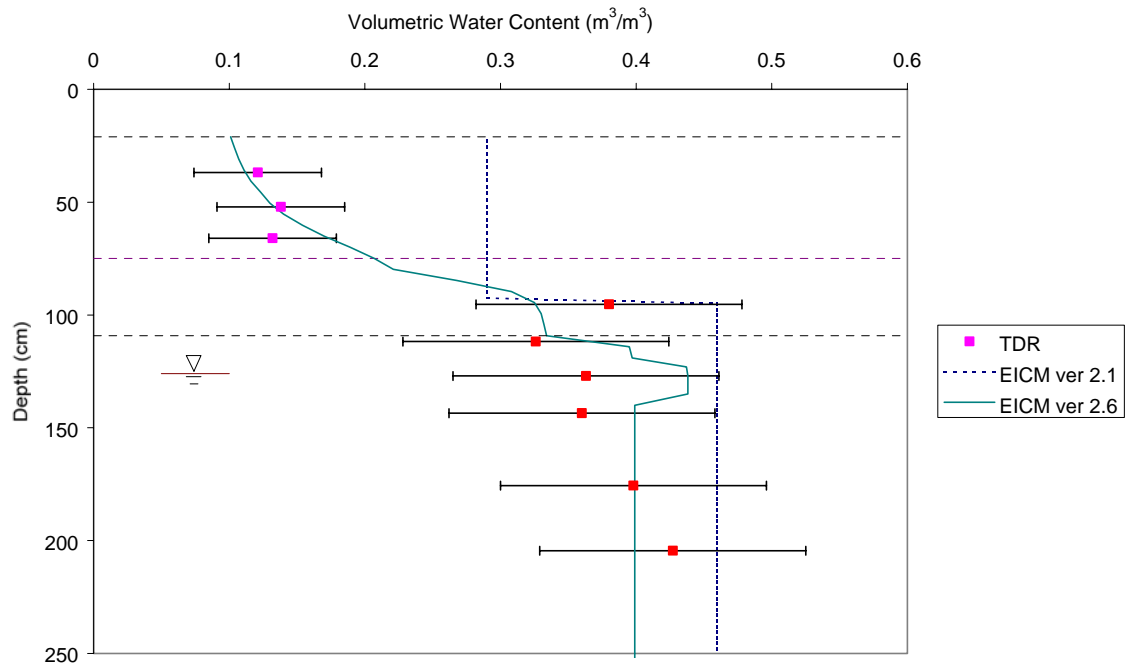




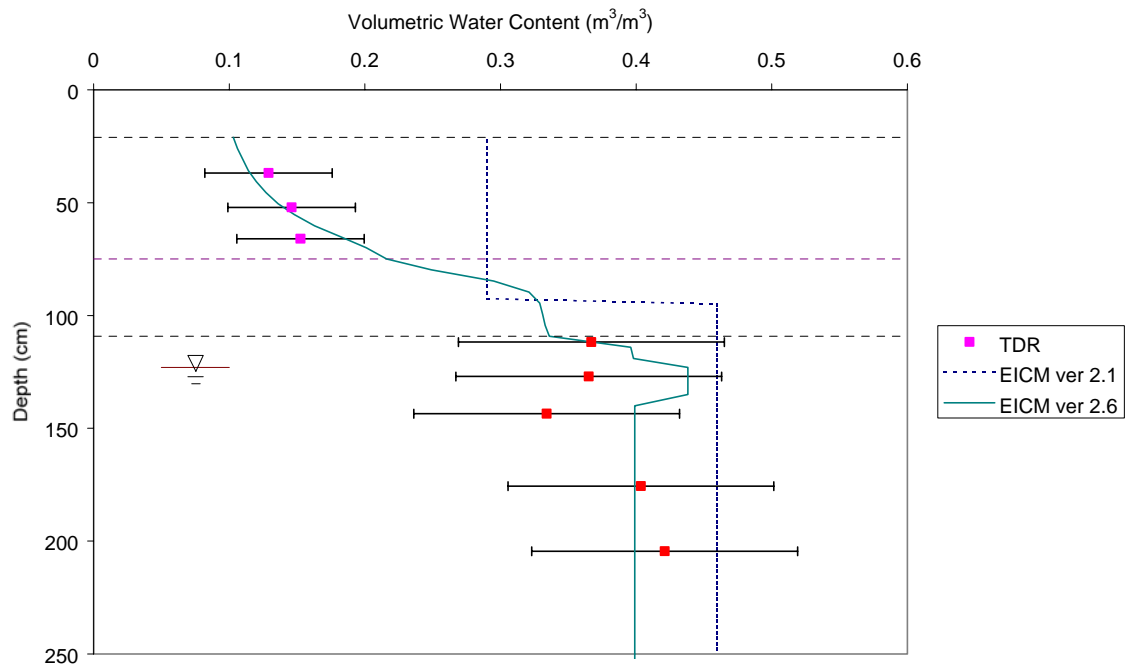
VERMONT site - 3/17/95



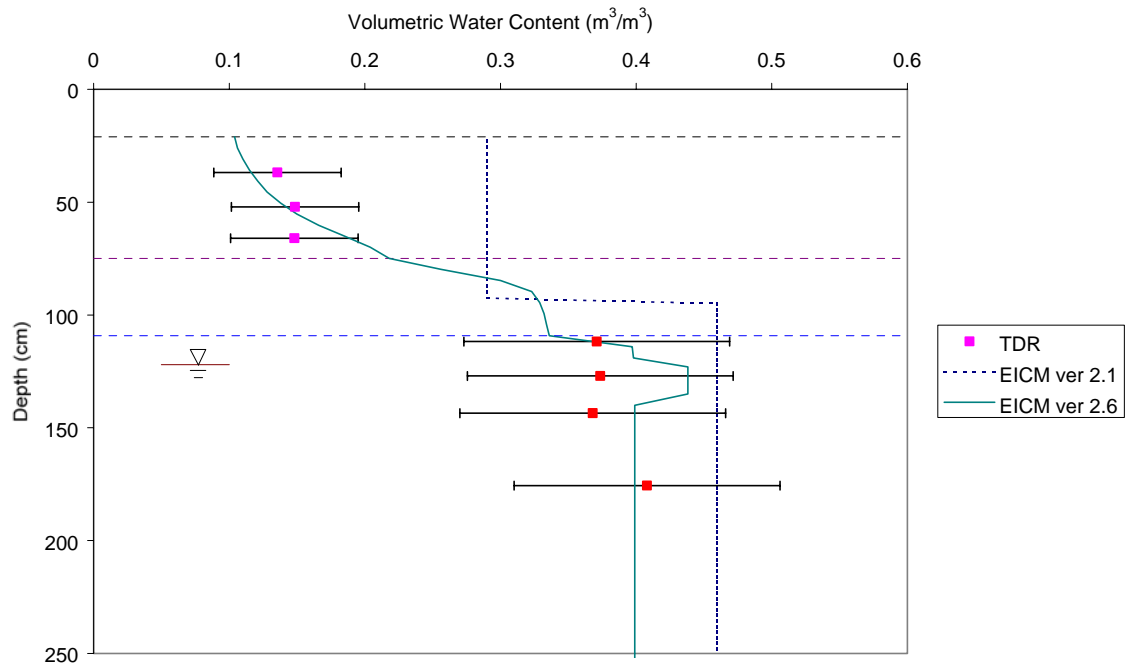
VERMONT site - 3/31/95



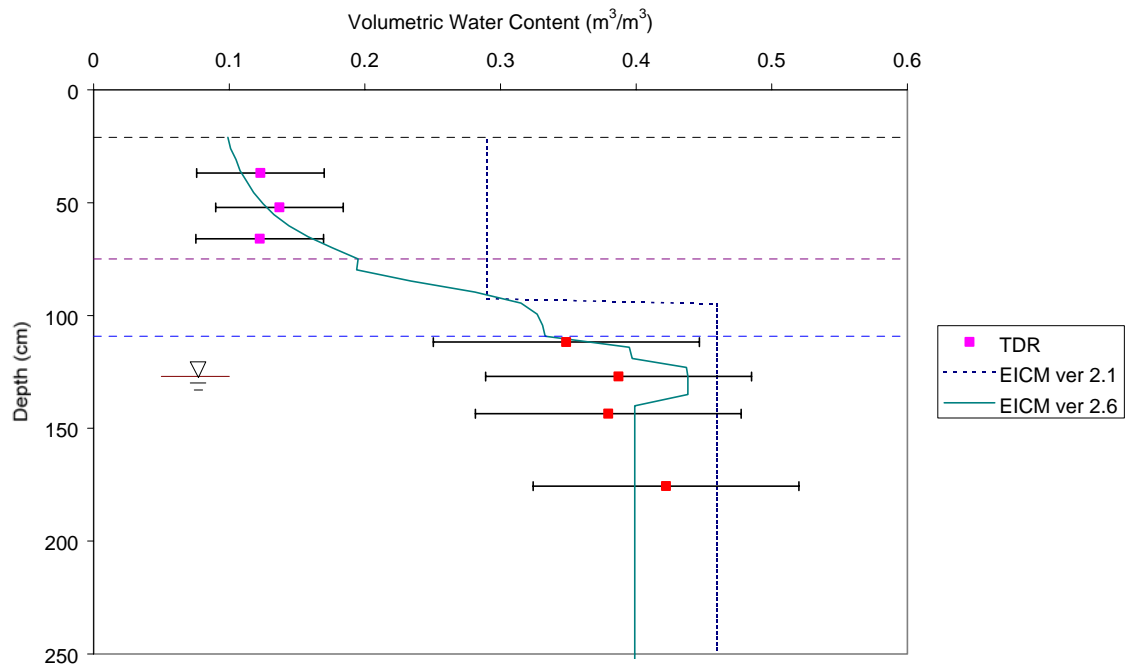
VERMONT site - 4/13/95



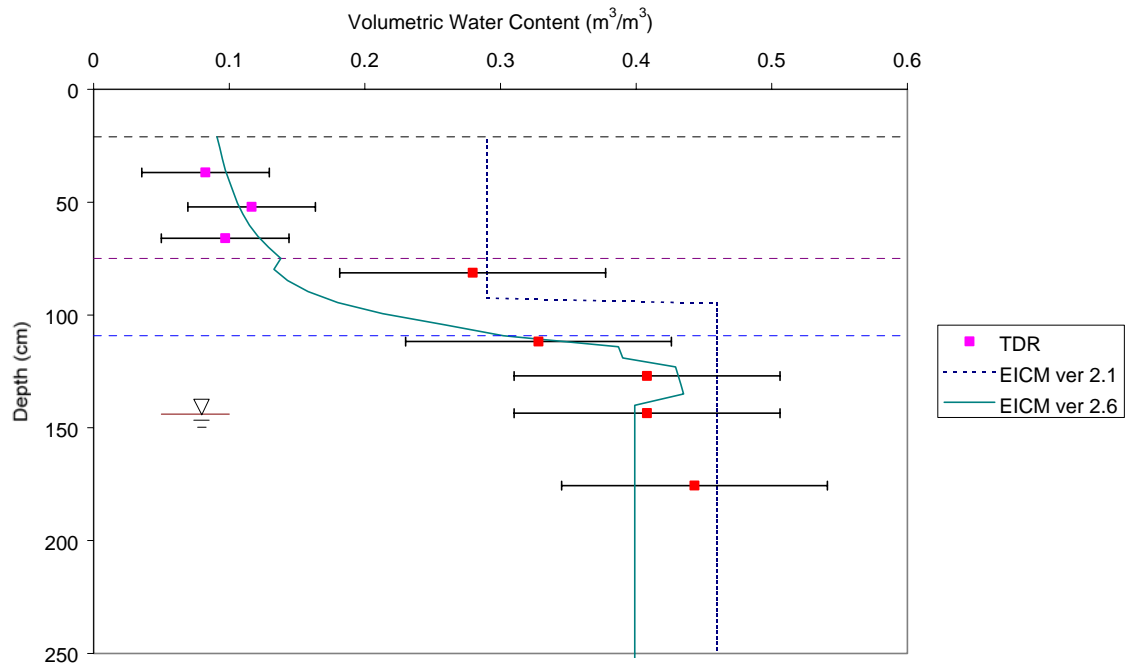
VERMONT site - 4/28/95



VERMONT site - 5/31/95



VERMONT site - 6/28/95



---

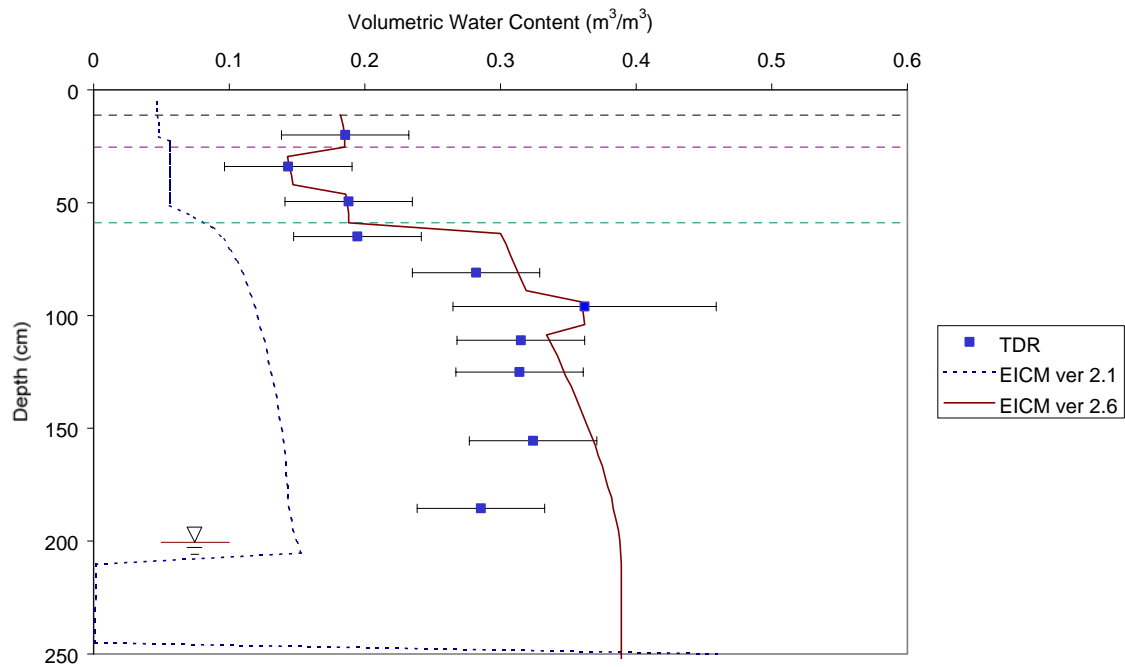
# APPENDIX N

## VOLUMETRIC WATER CONTENT PROFILES

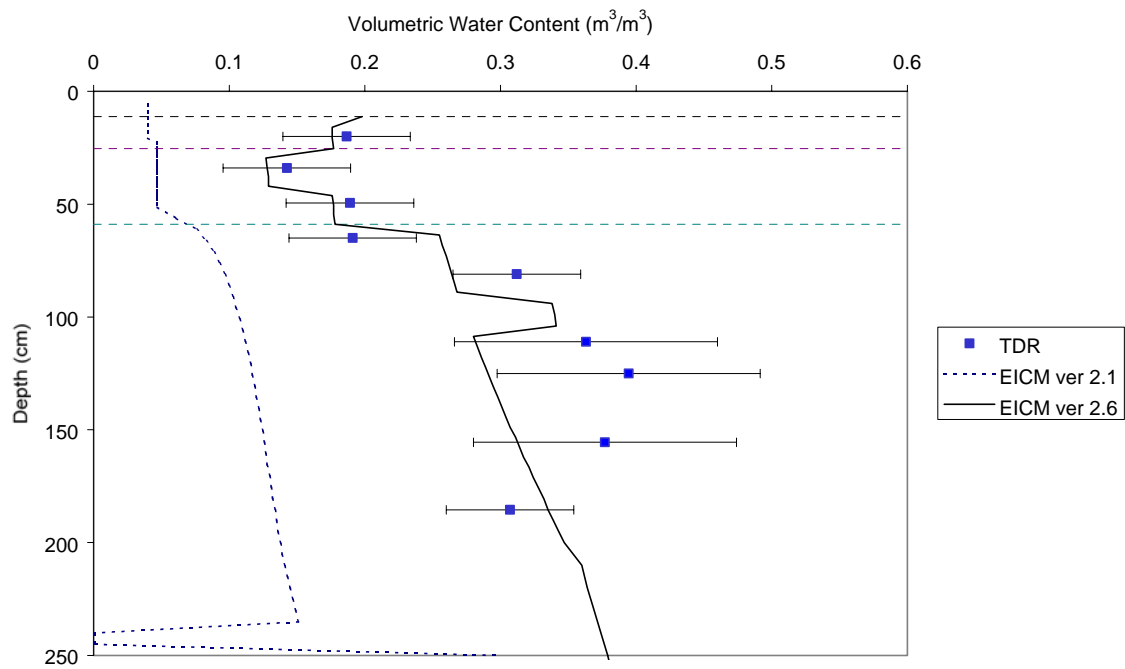
MANITOBA (831801)

EICM – Version 2.6

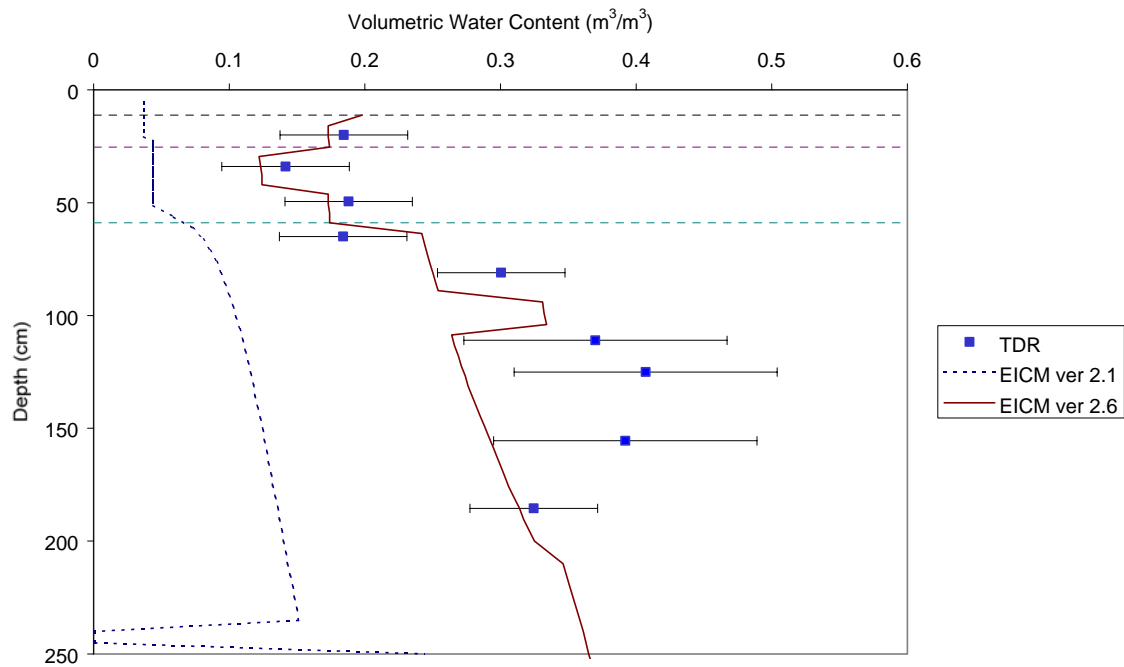
MANITOBA site - 6/17/94



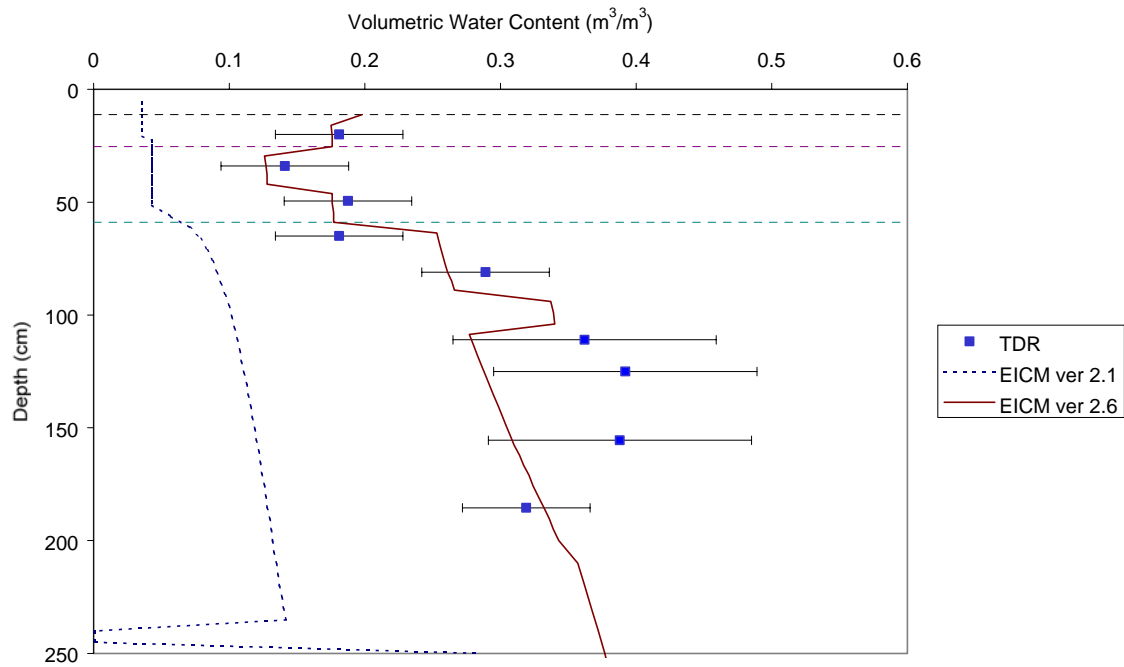
MANITOBA site - 7/25/94



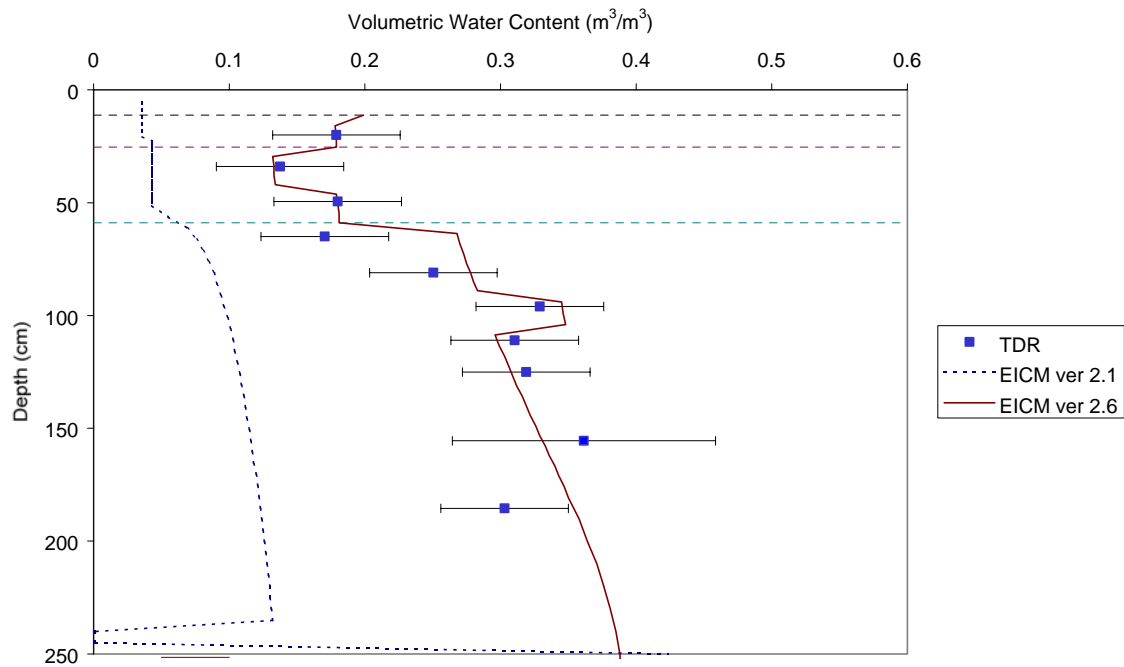
MANITOBA site - 8/18/94



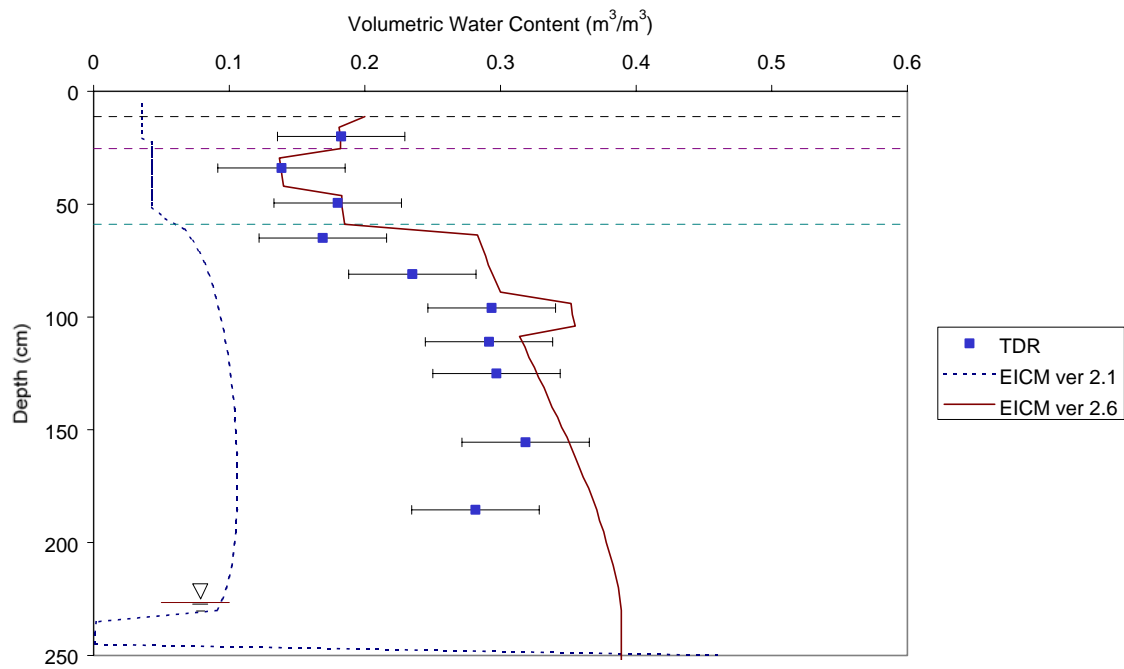
MANITOBA site - 9/21/94



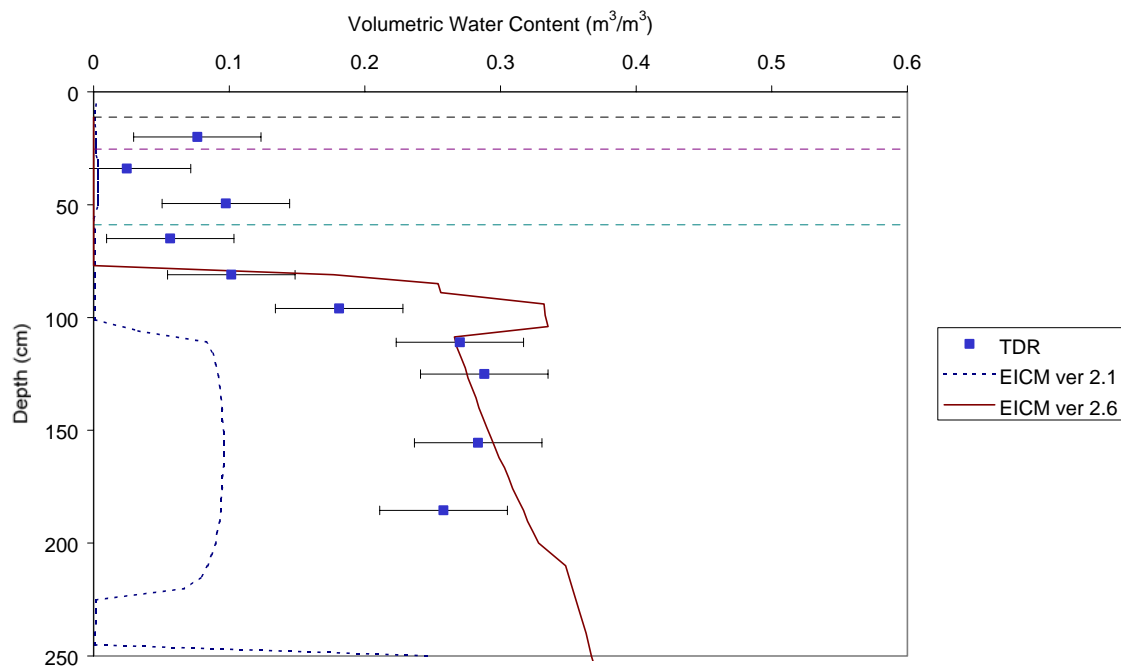
MANITOBA site - 10/19/94



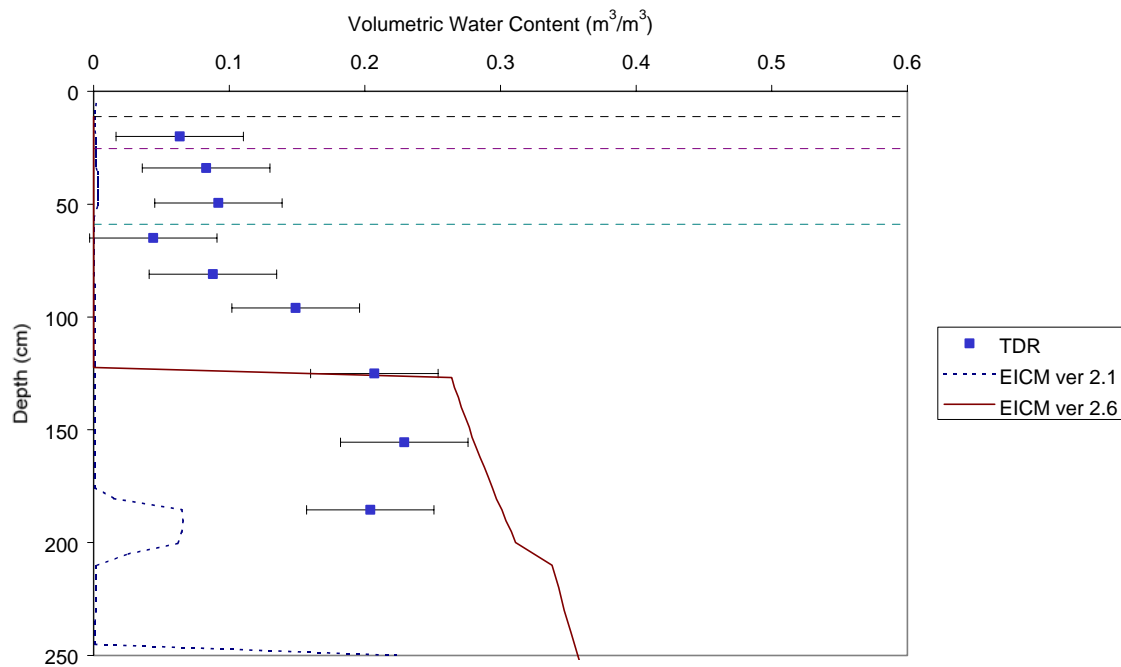
MANITOBA site - 11/16/94



MANITOBA site - 12/14/94

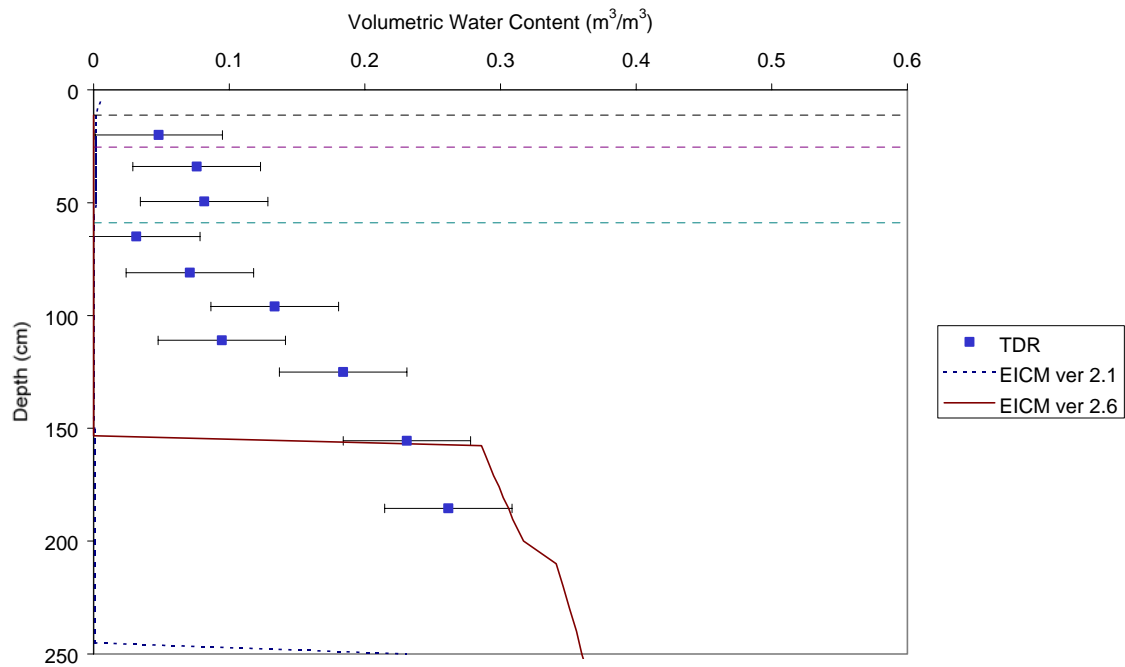


MANITOBA site - 1/25/95

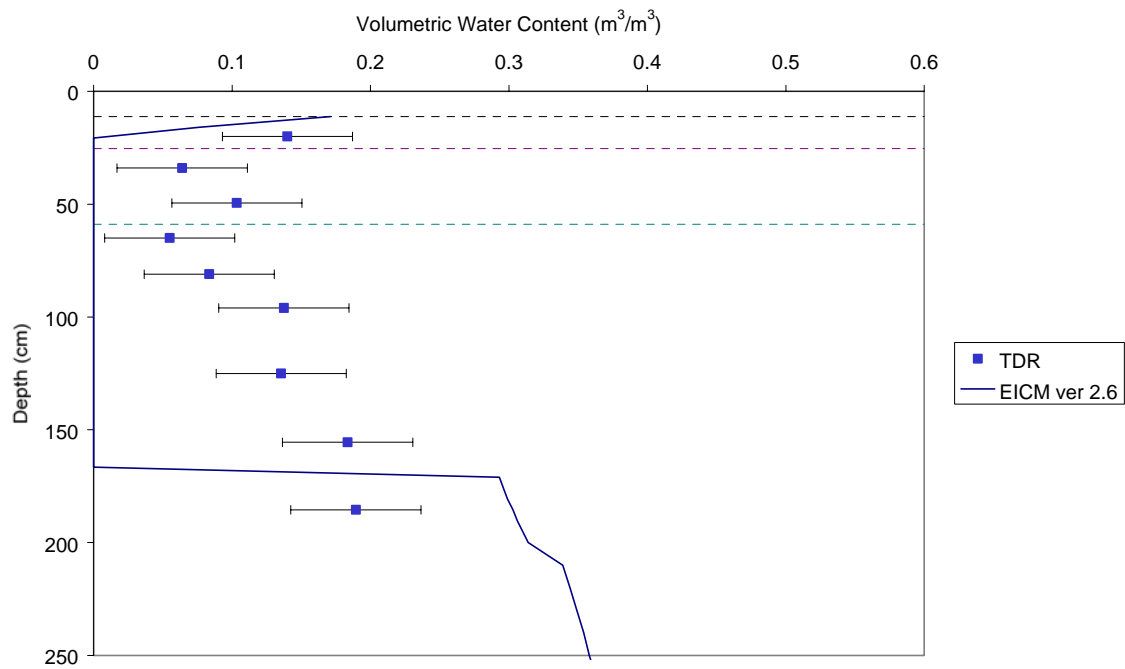




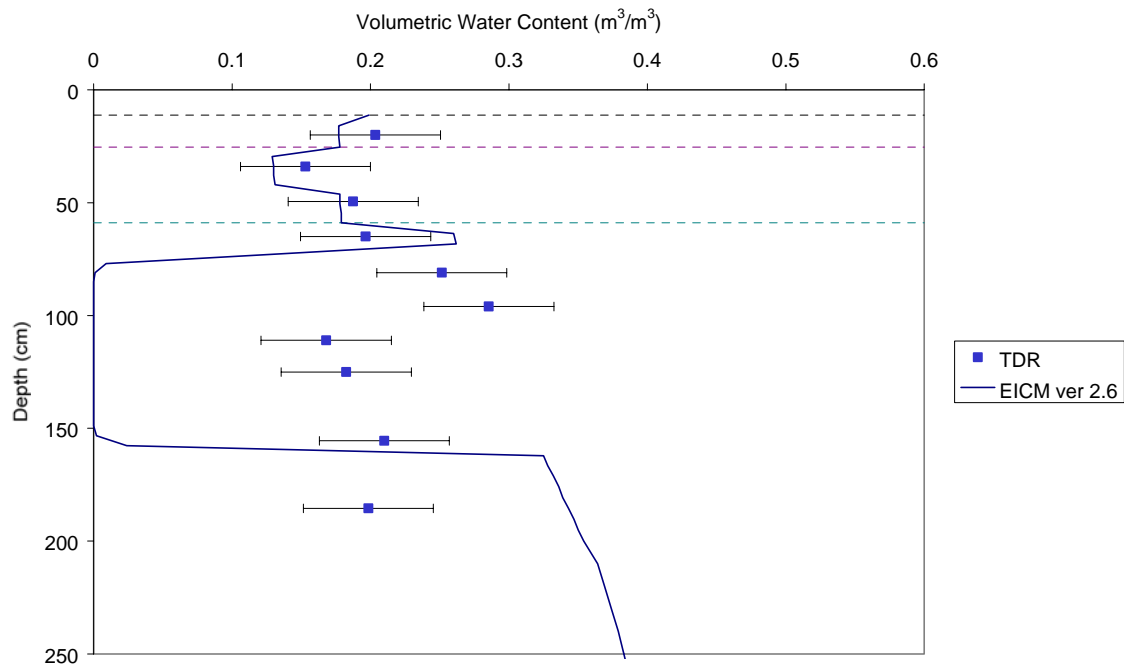
MANITOBA site - 2/15/95



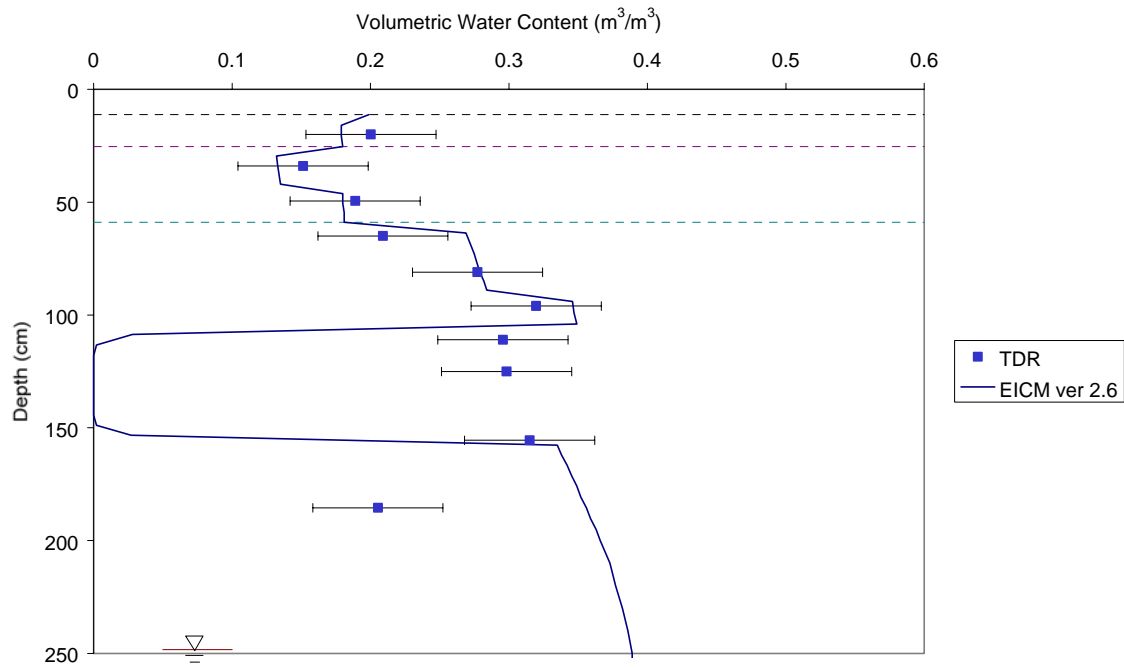
MANITOBA site - 3/14/95



MANITOBA site - 4/25/95



MANITOBA site - 5/17/95



---

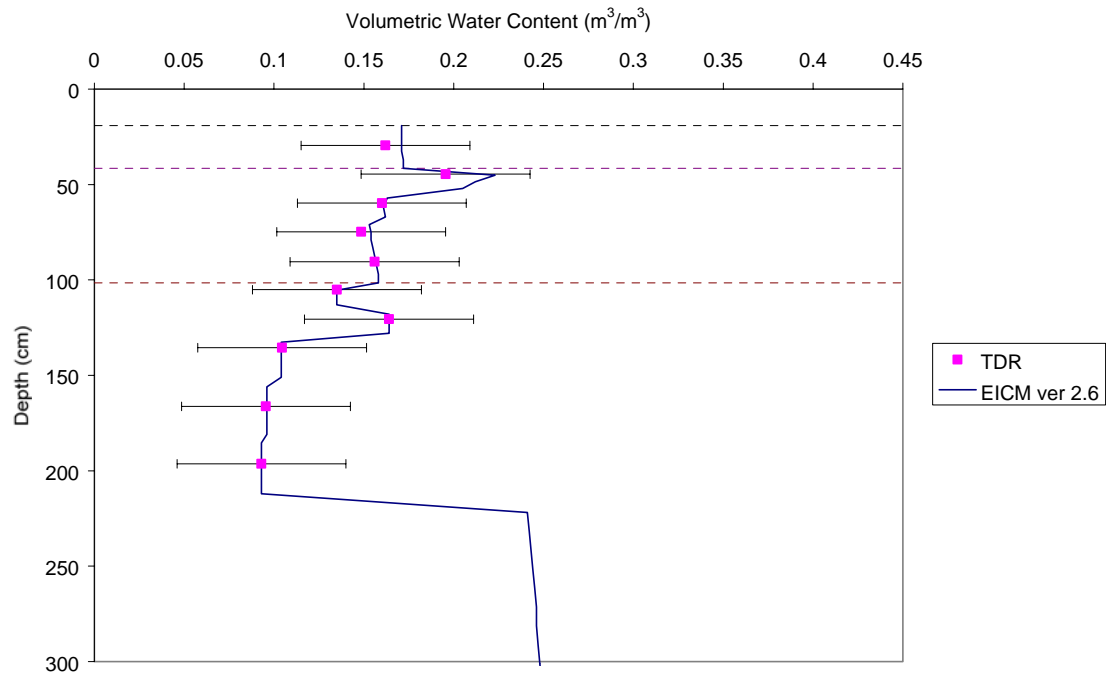
# APPENDIX O

## VOLUMETRIC WATER CONTENT PROFILES

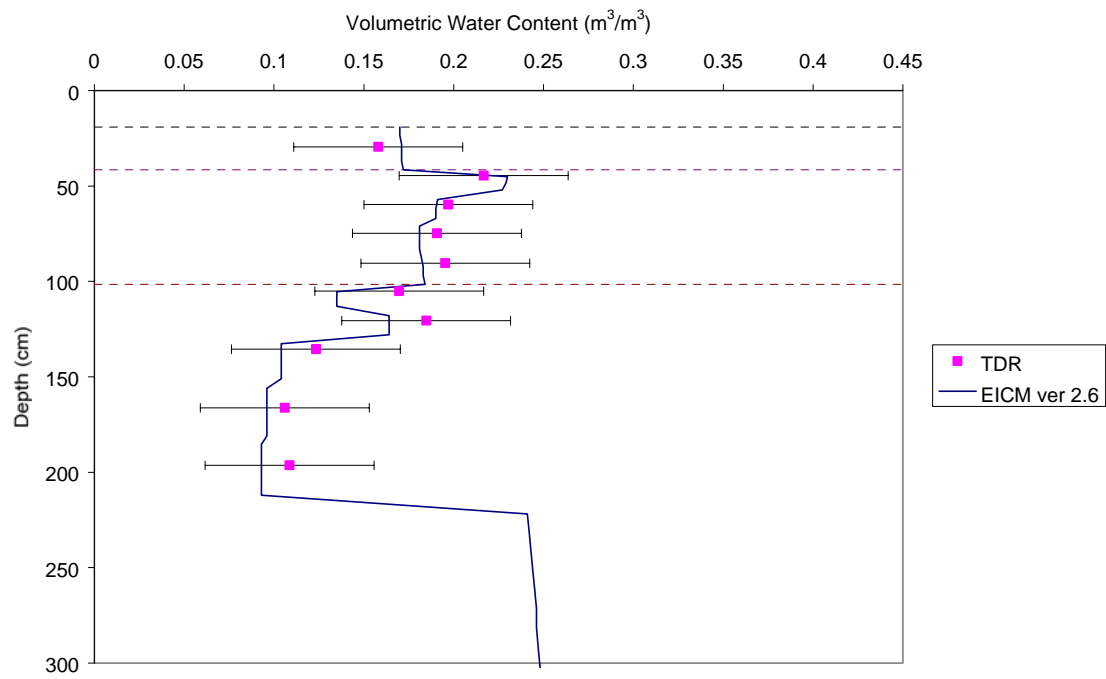
GEORGIA (131005)

EICM – Version 2.6

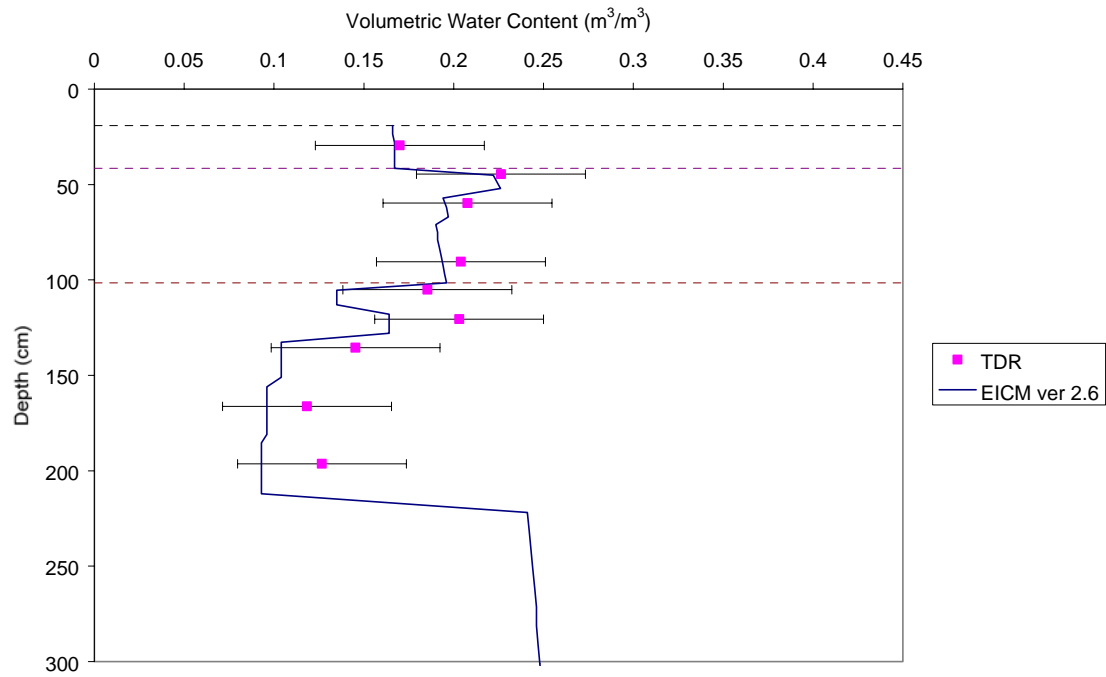
GEORGIA site - 8/8/95



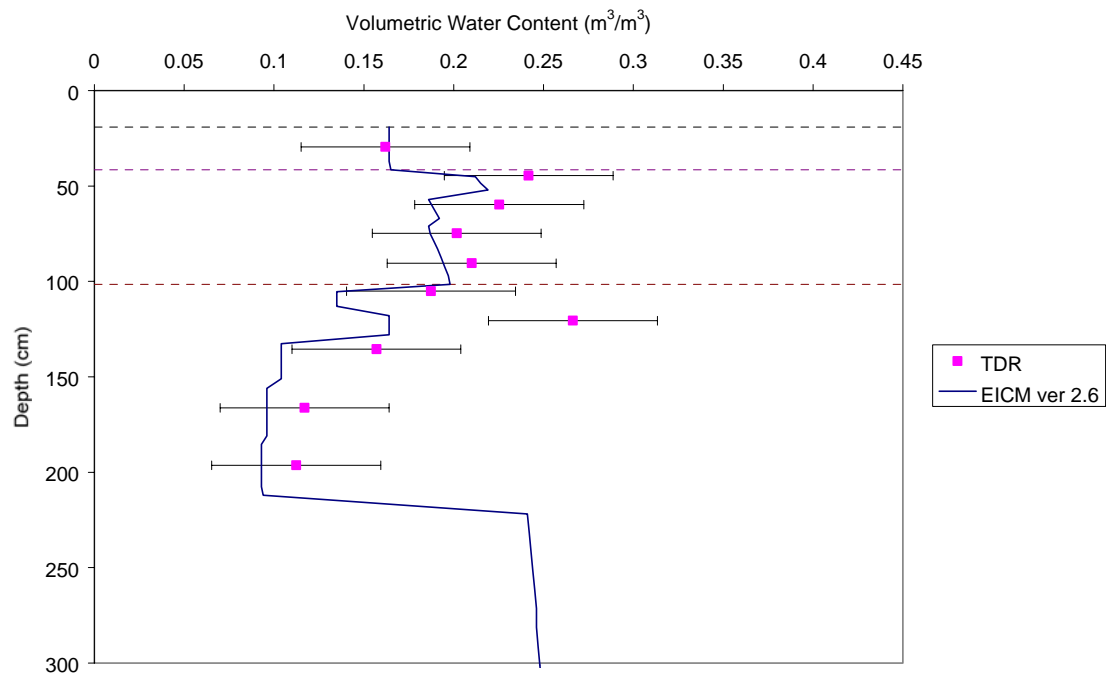
GEORGIA site - 9/20/95



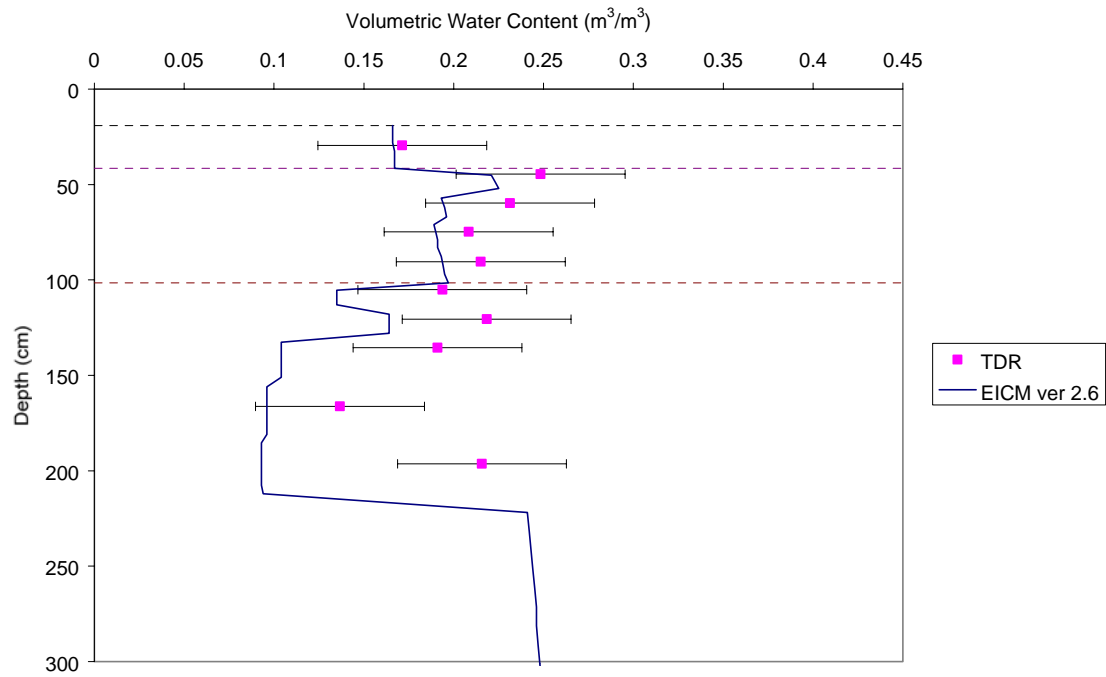
GEORGIA site - 10/18/95



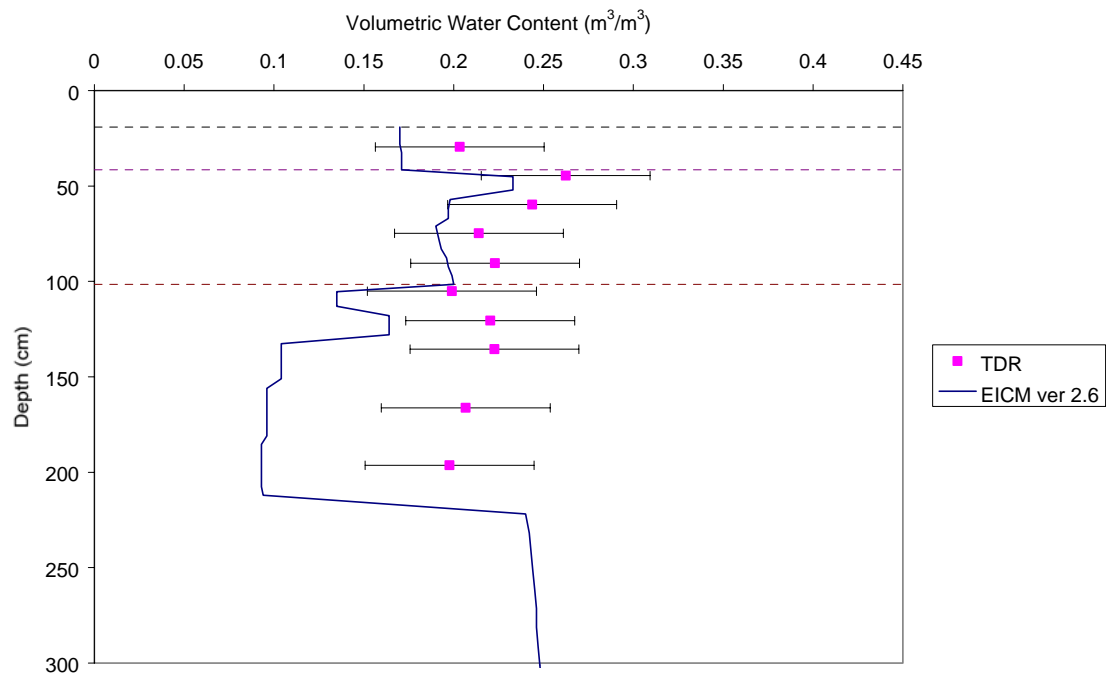
GEORGIA site - 11/30/95



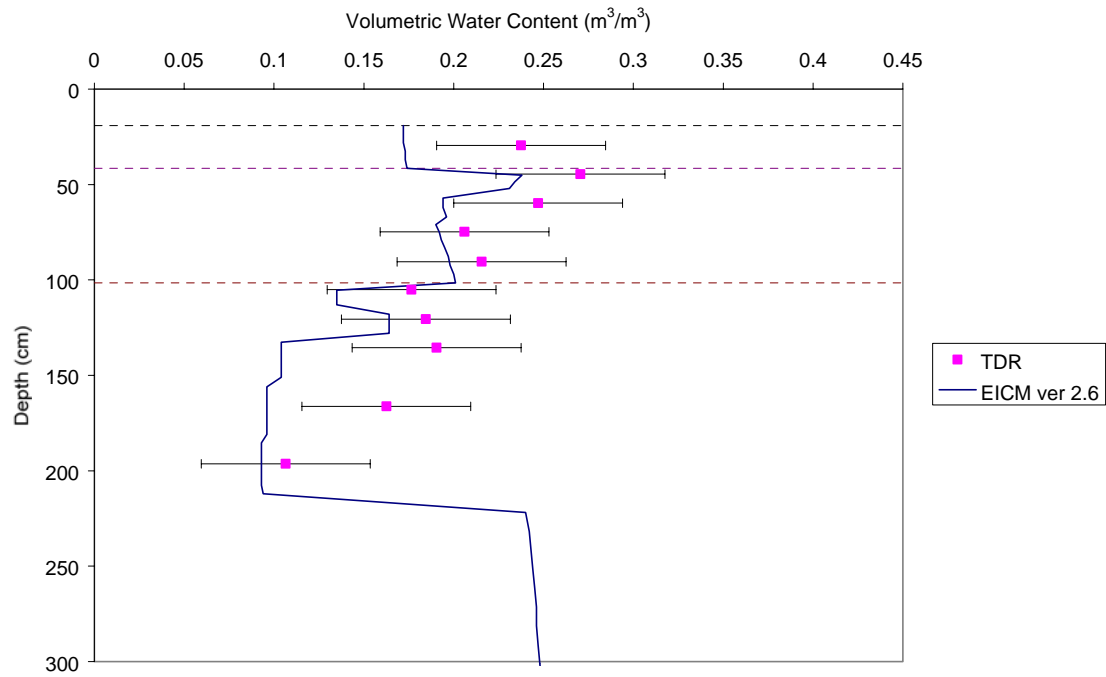
GEORGIA site - 12/13/95



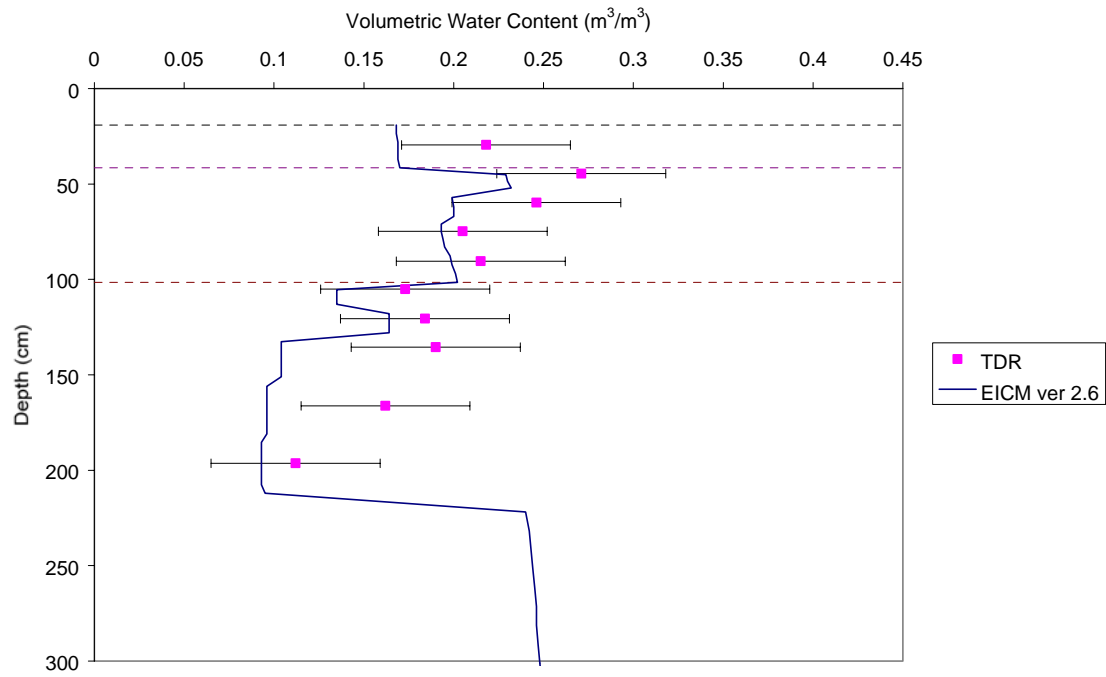
GEORGIA site - 1/25/96



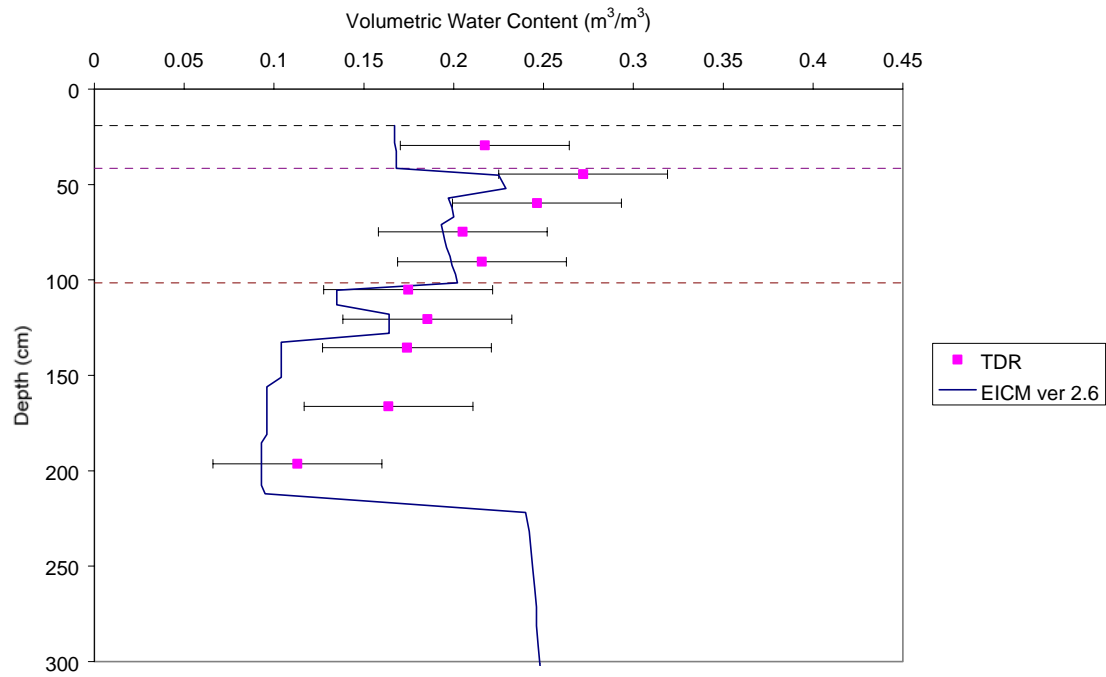
GEORGIA site - 3/25/96



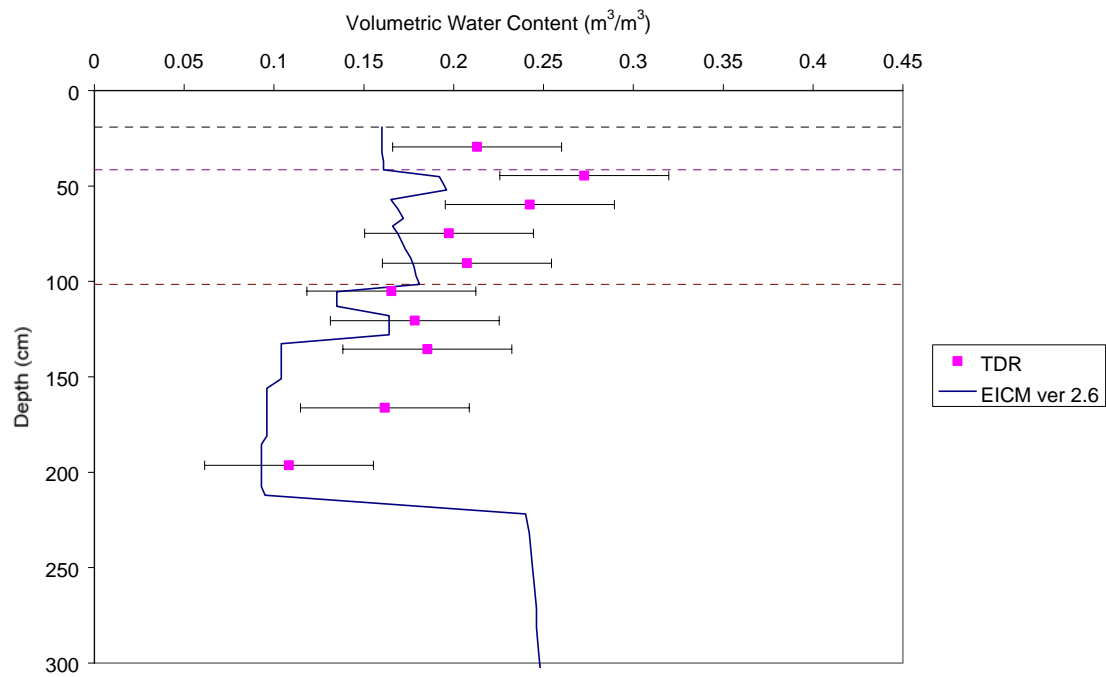
GEORGIA site - 4/22/96



GEORGIA site - 4/23/96

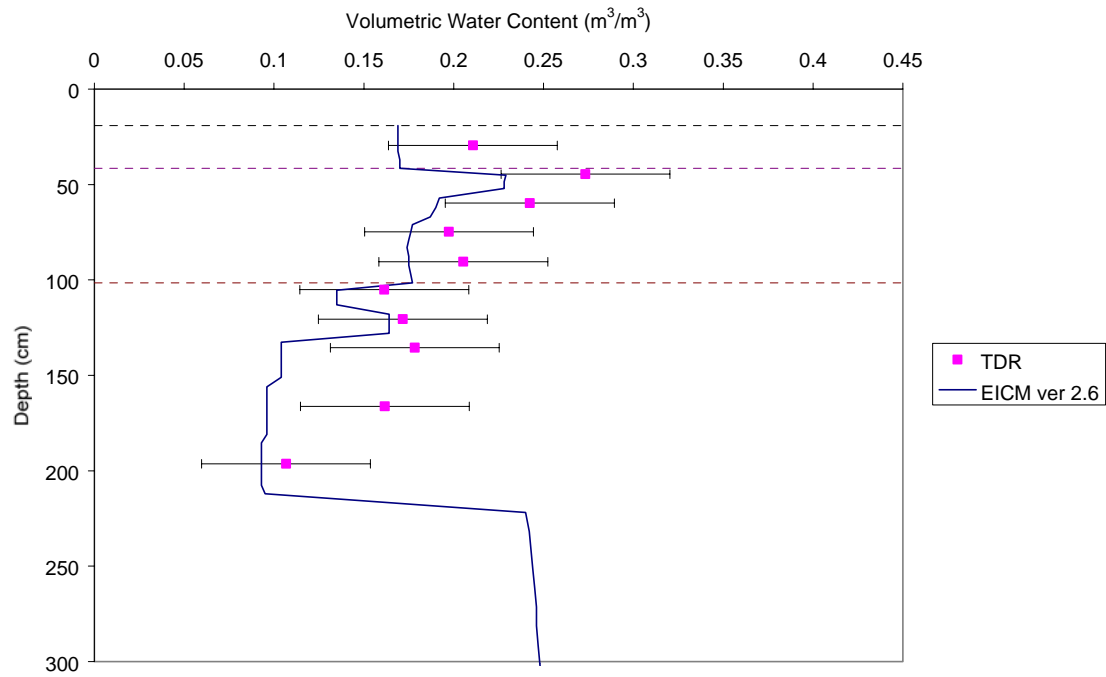


GEORGIA site -5/29/96

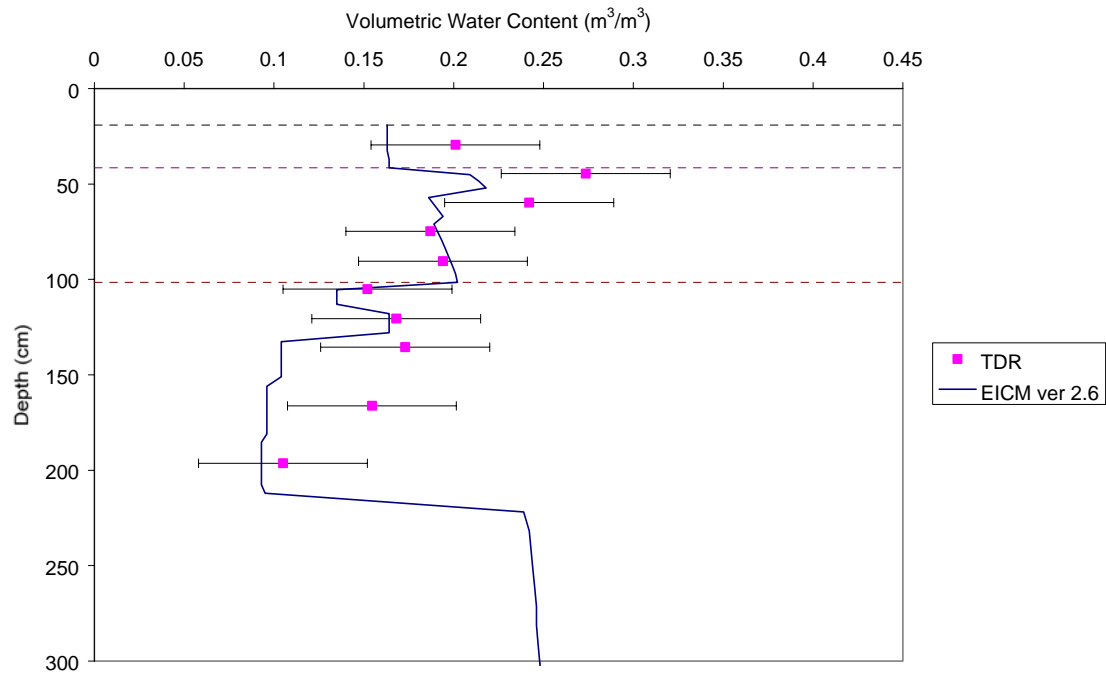




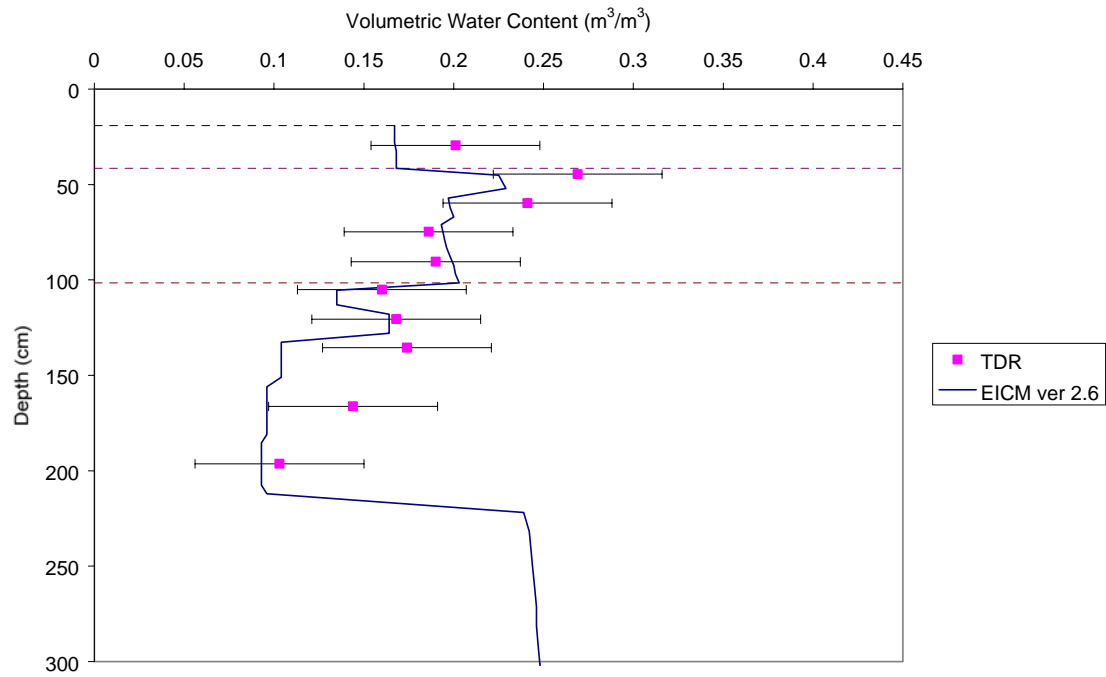
GEORGIA site -6/10/96



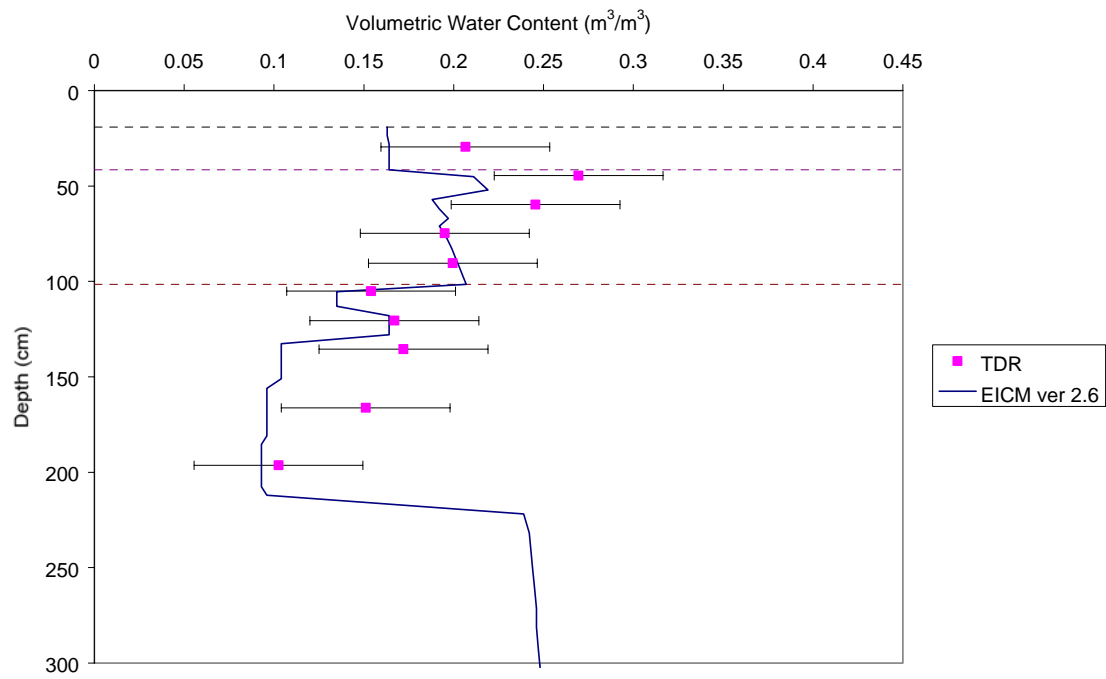
GEORGIA site -8/19/96



GEORGIA site -9/24/96



GEORGIA site -10/15/96



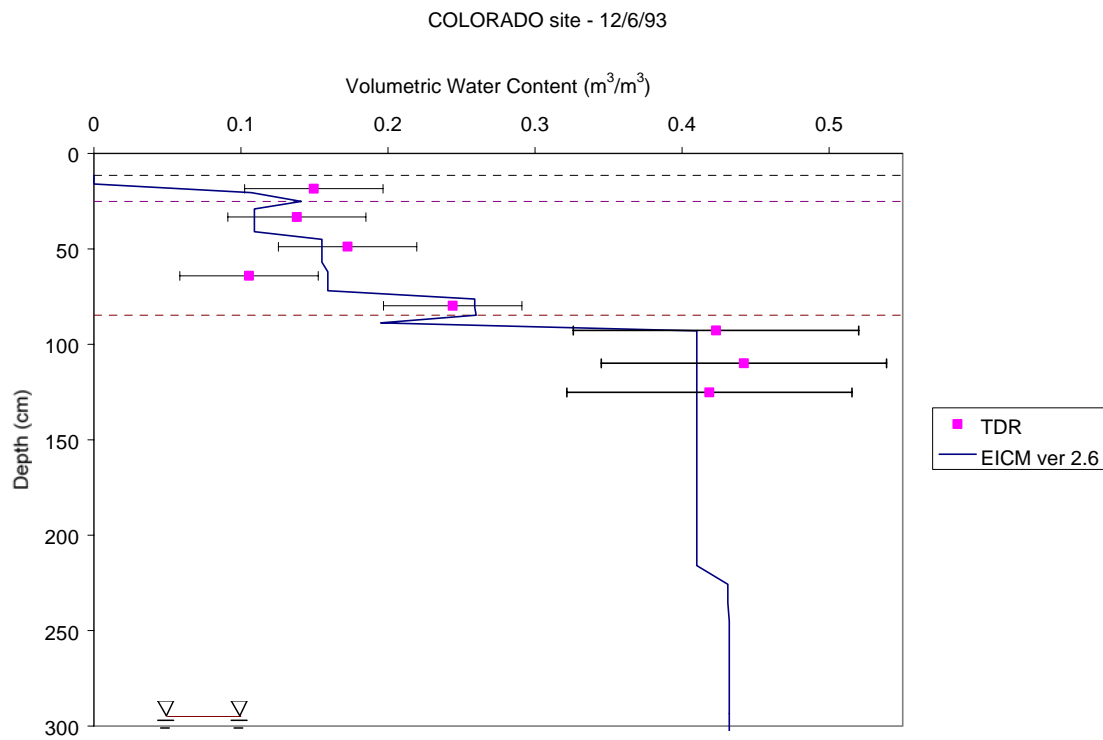
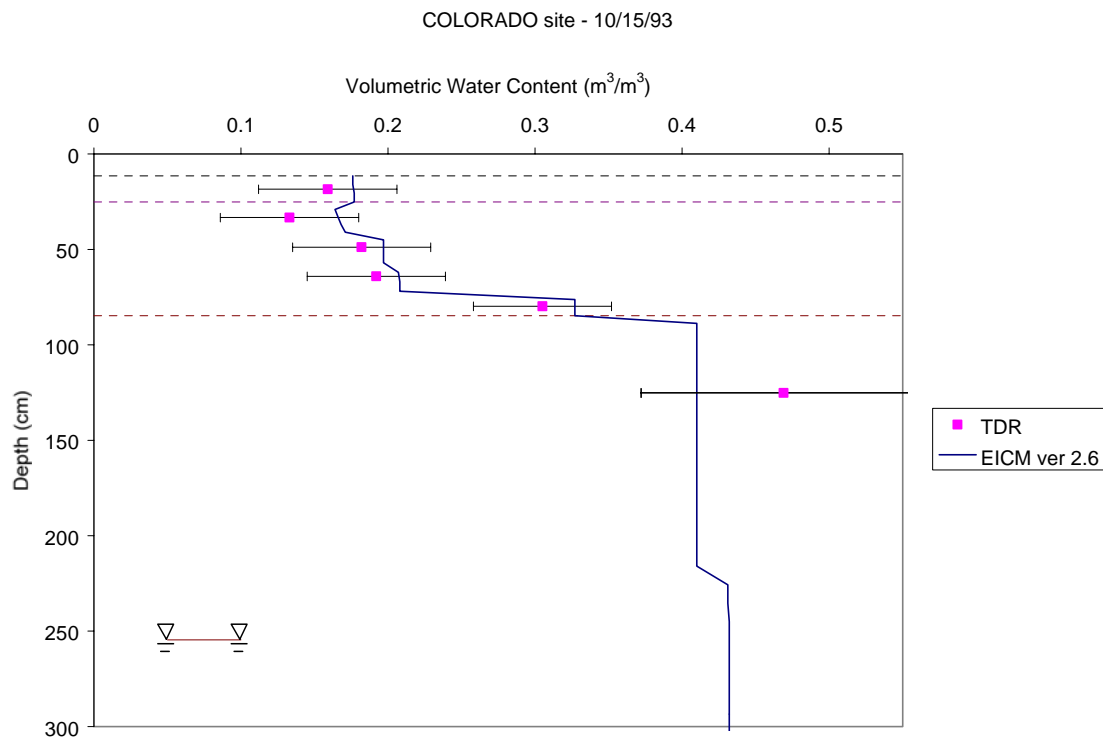
---

# APPENDIX P

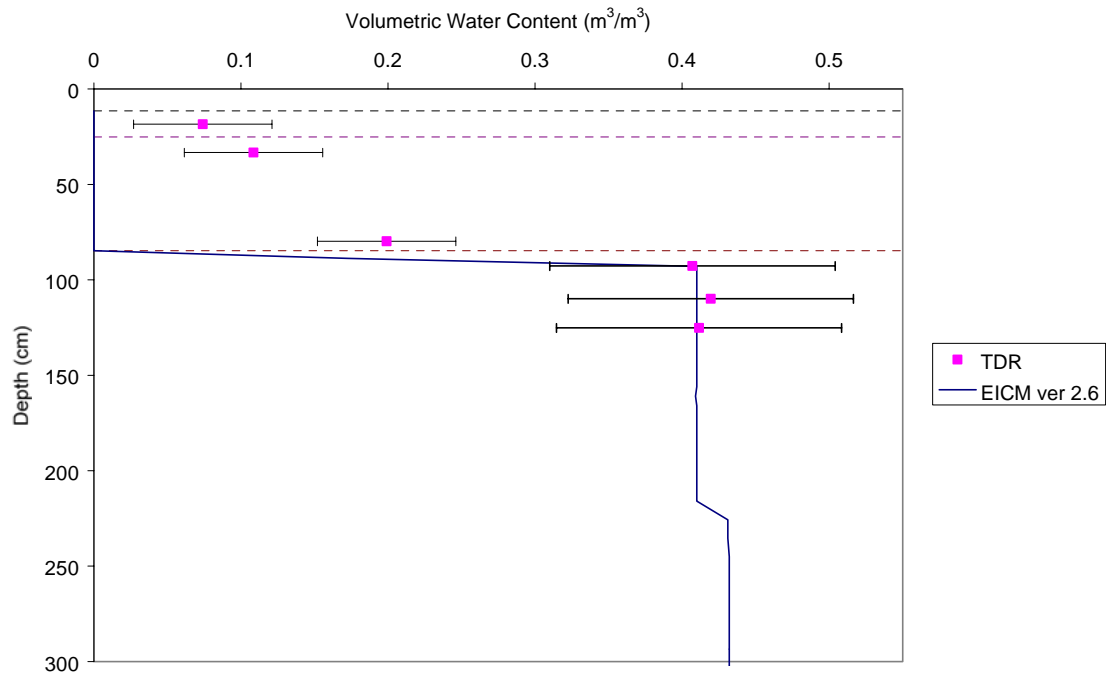
## VOLUMETRIC WATER CONTENT PROFILES

COLORADO (81053)

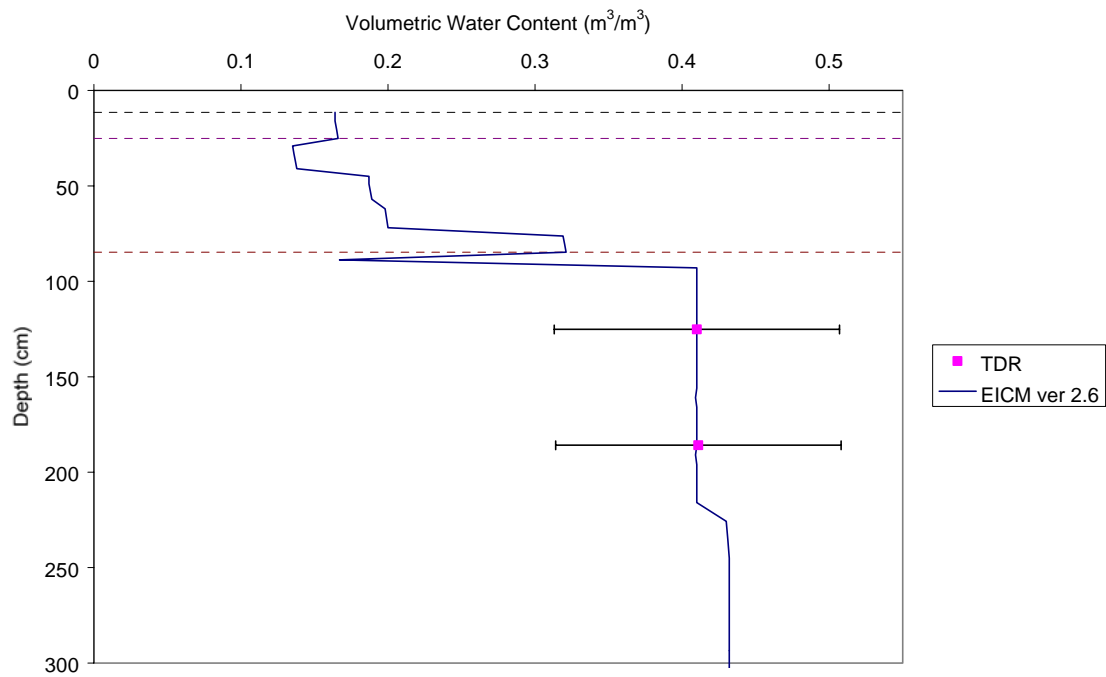
EICM – Version 2.6



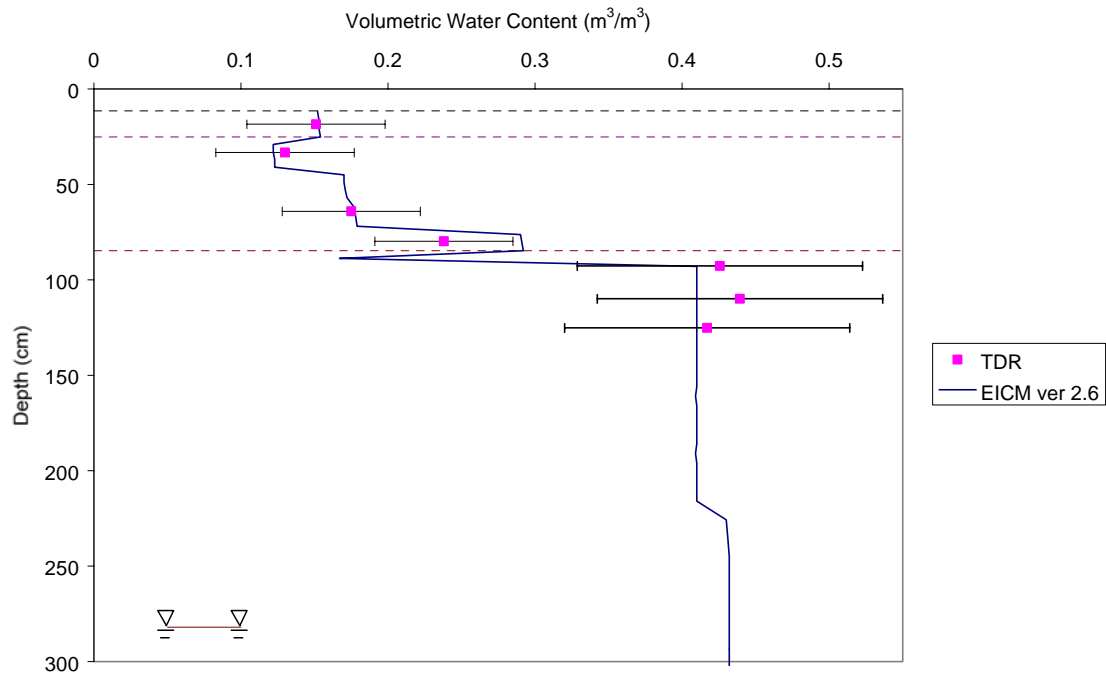
COLORADO site - 1/18/94



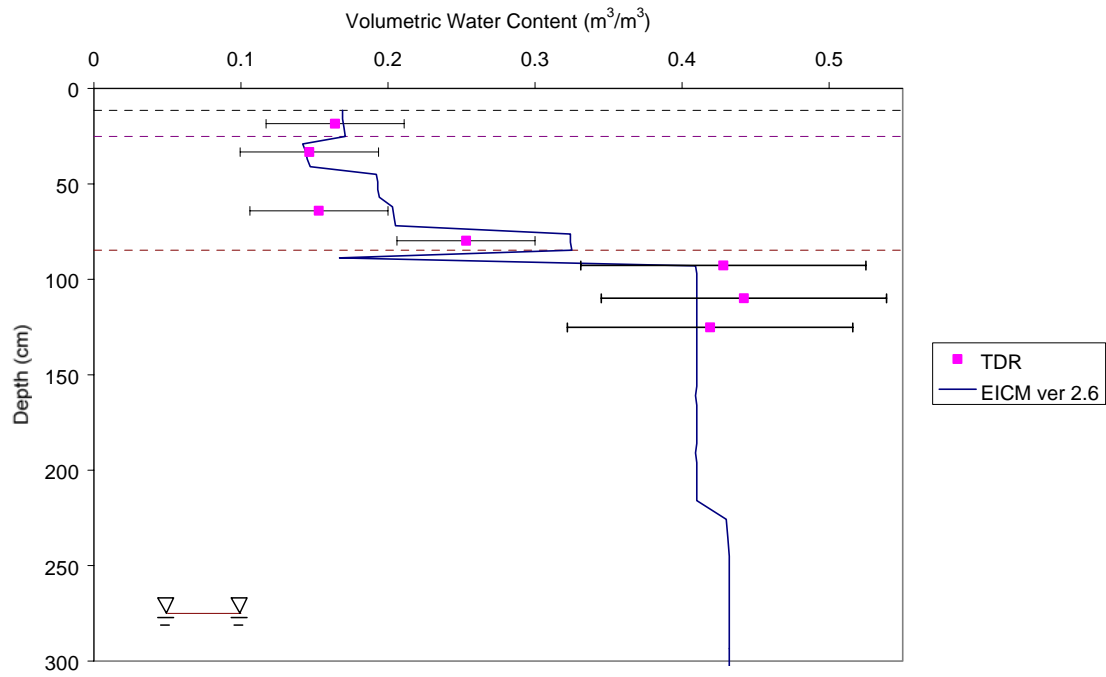
COLORADO site - 2/14/94



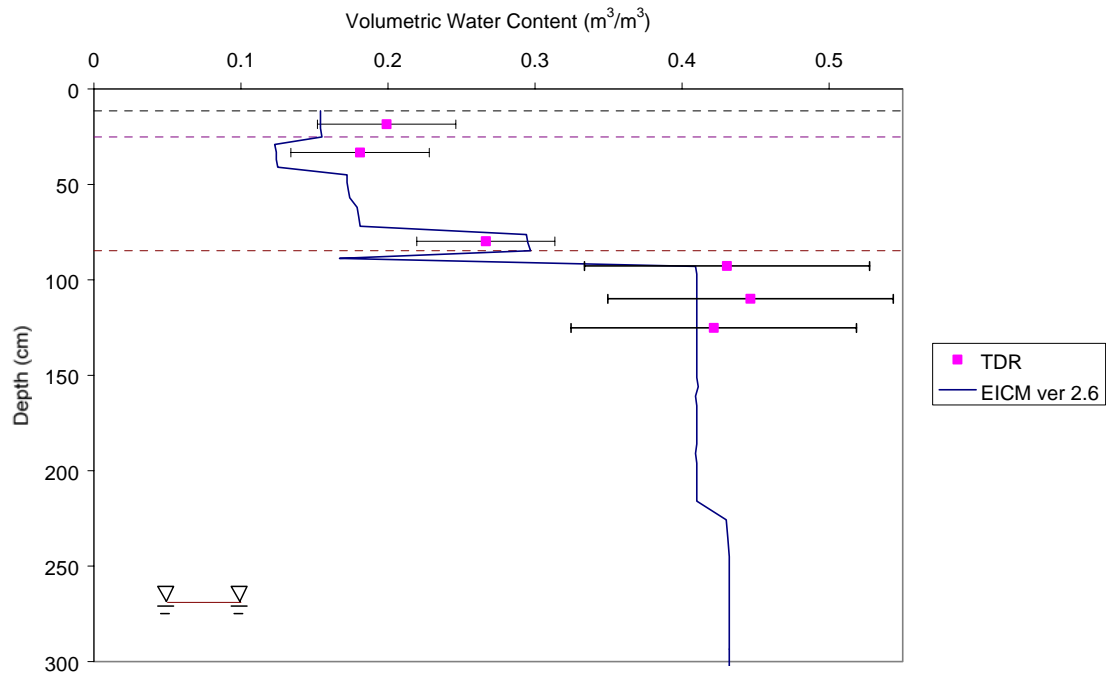
COLORADO site - 3/14/94



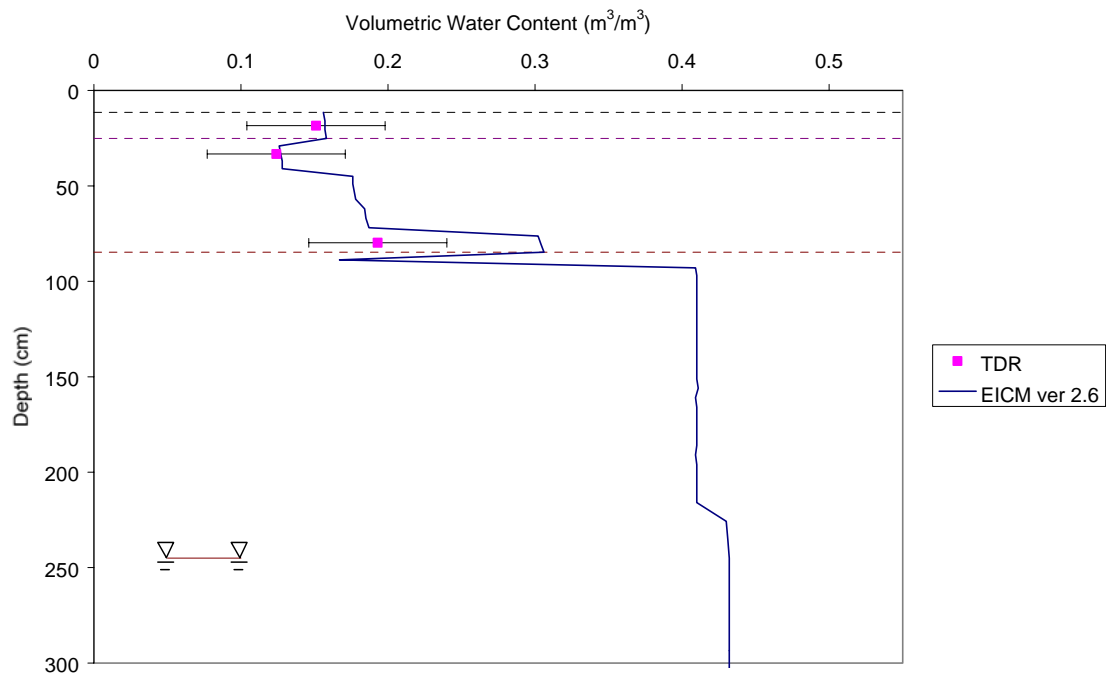
COLORADO site - 3/28/94

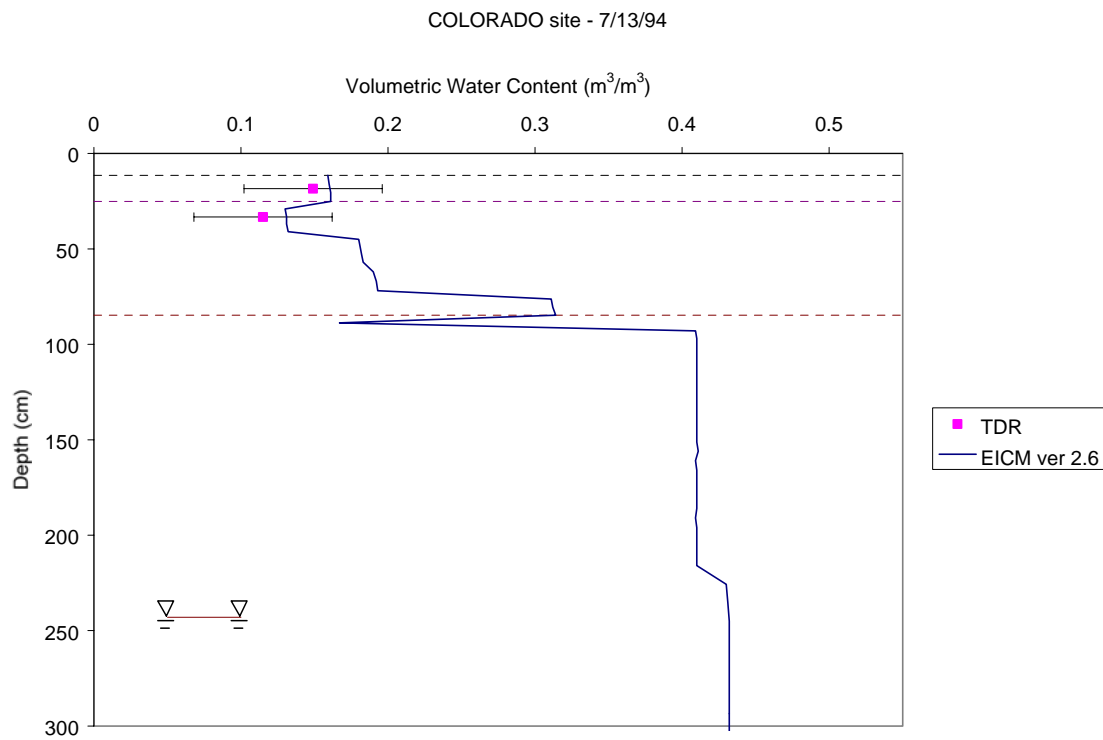
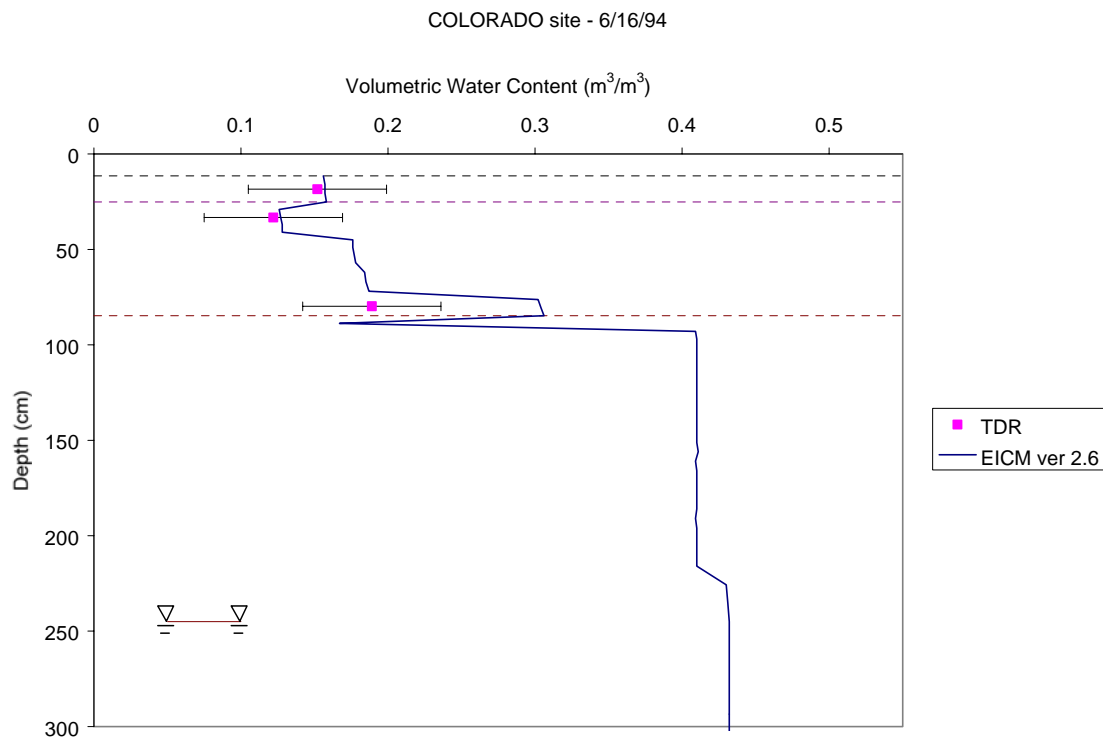


COLORADO site - 4/11/94

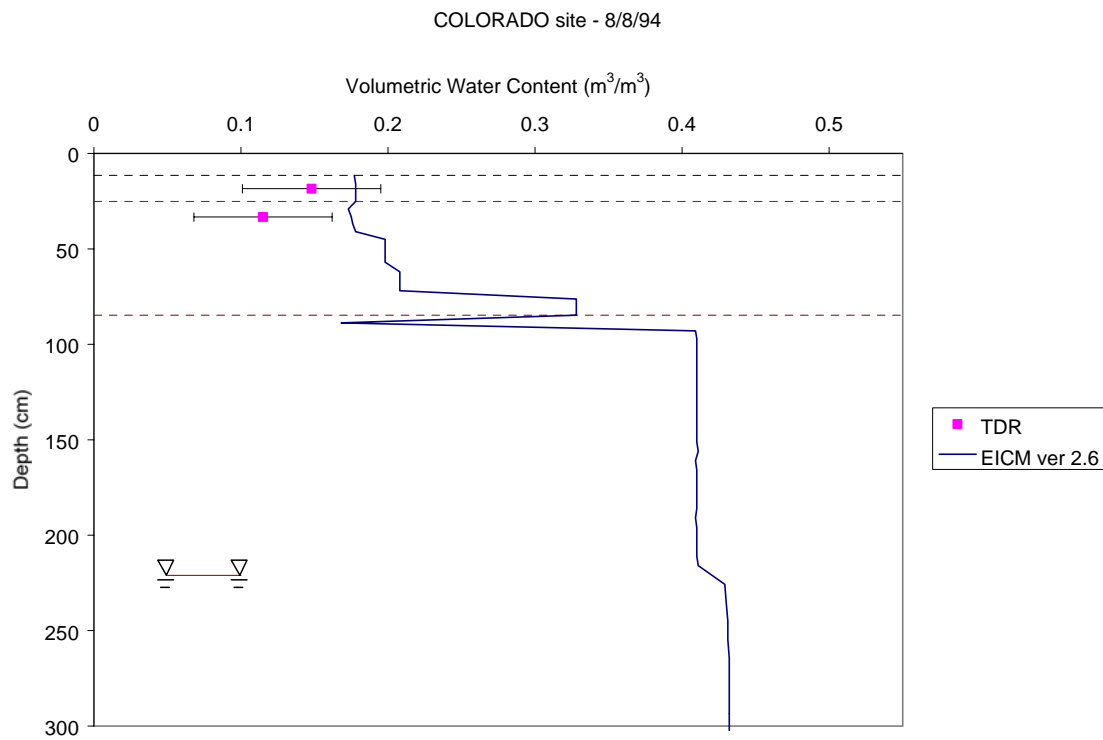
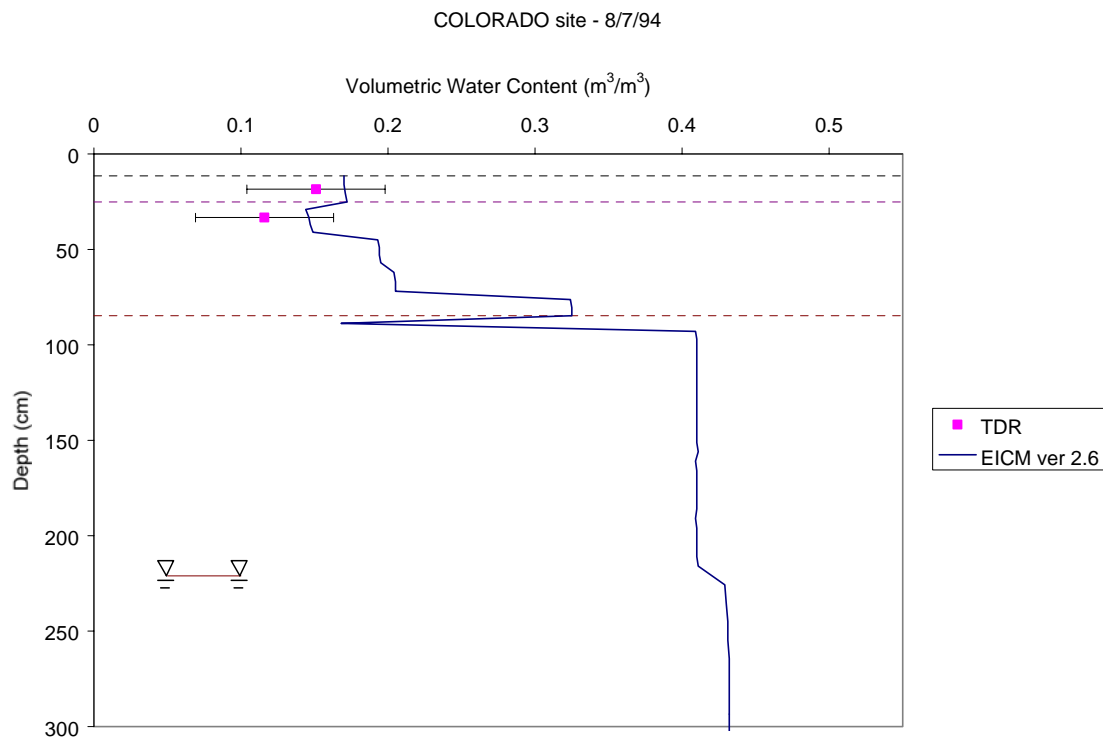


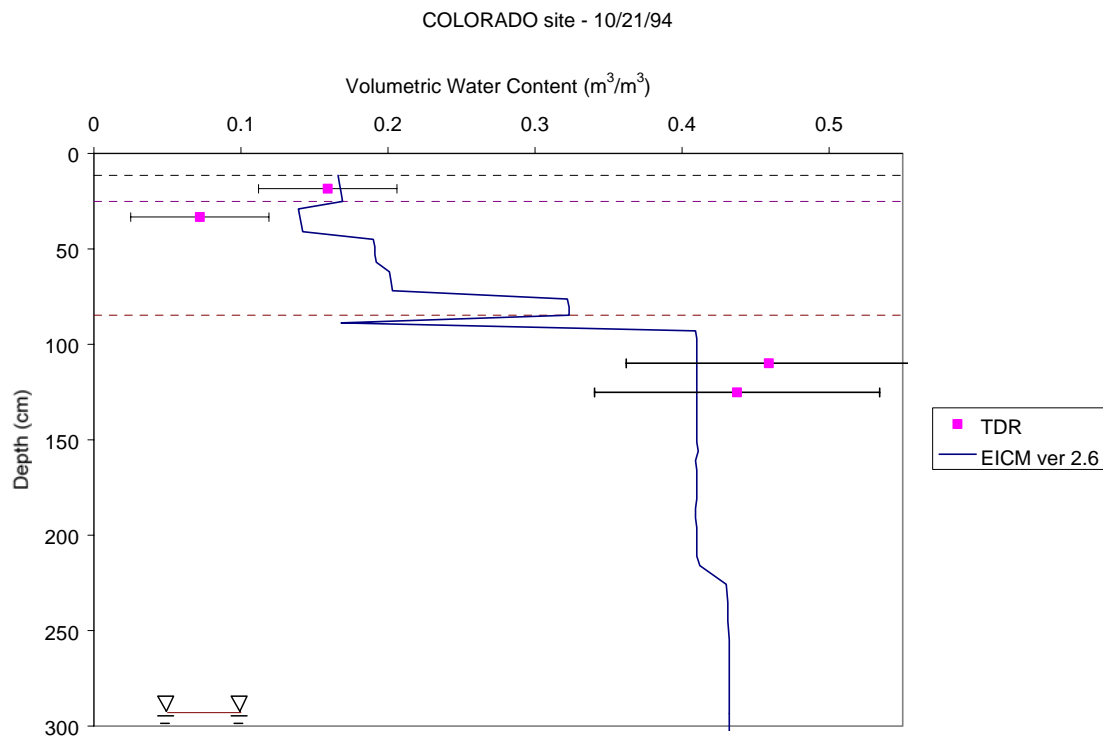
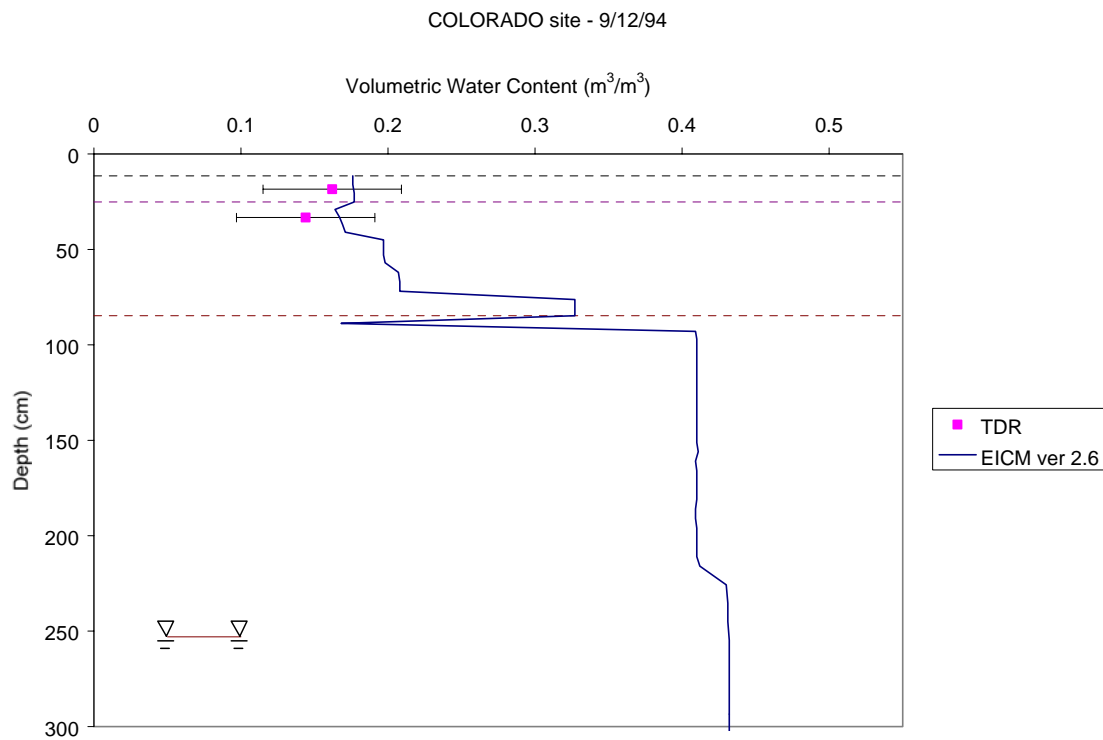
COLORADO site - 6/15/94

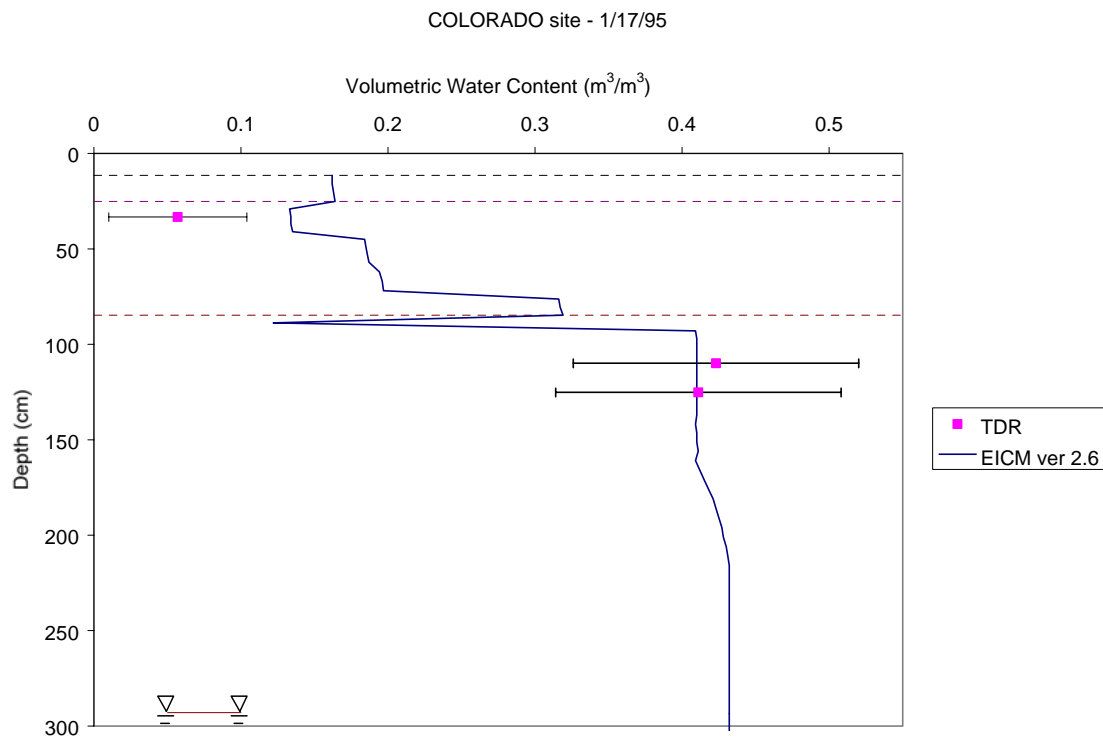
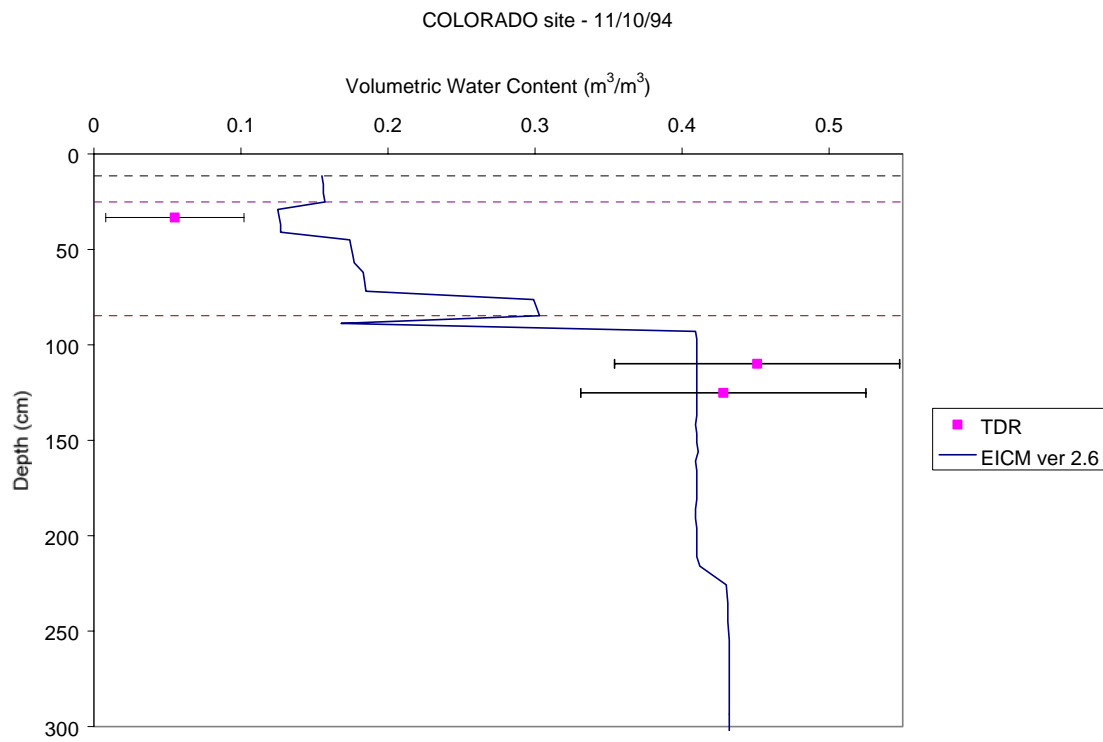




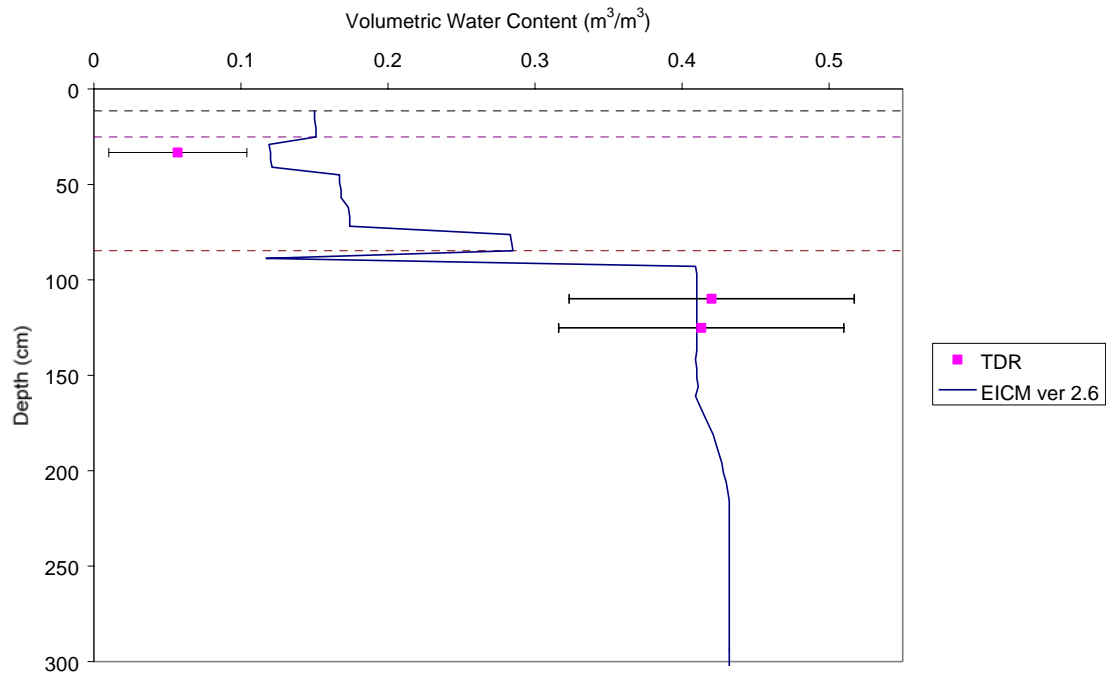




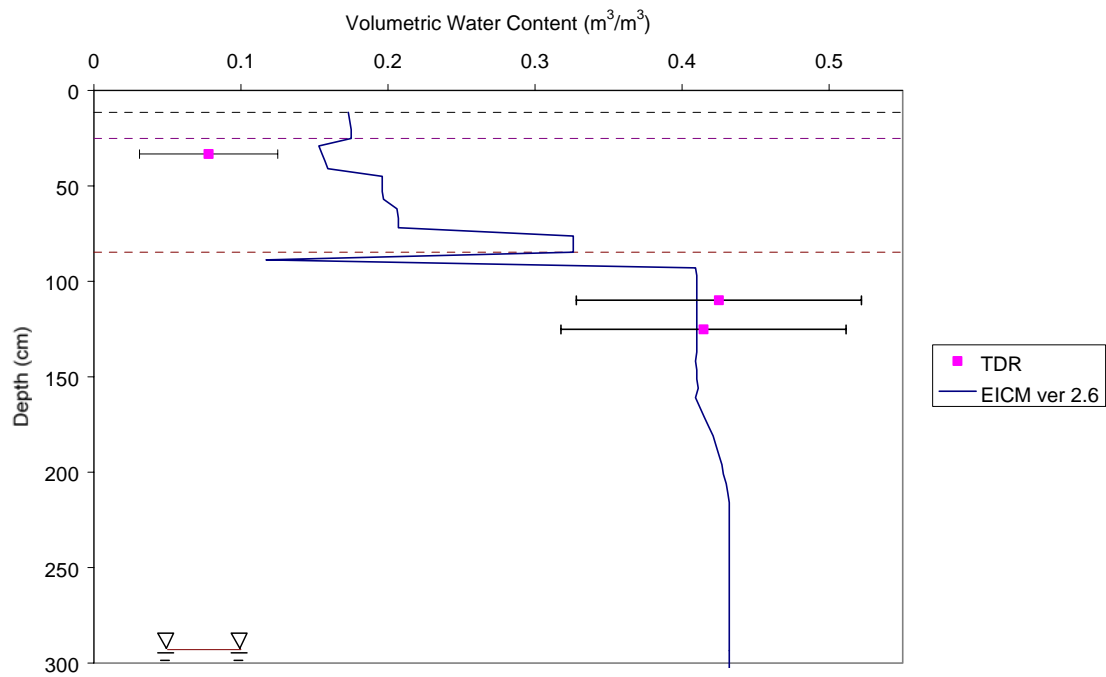




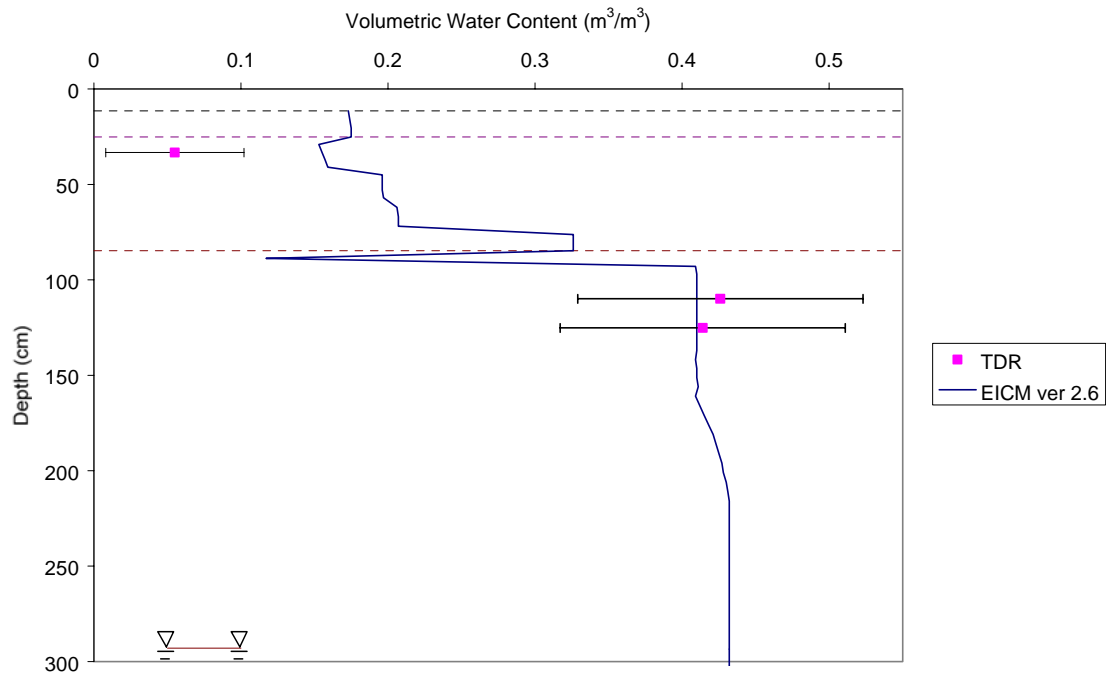
COLORADO site - 2/13/95



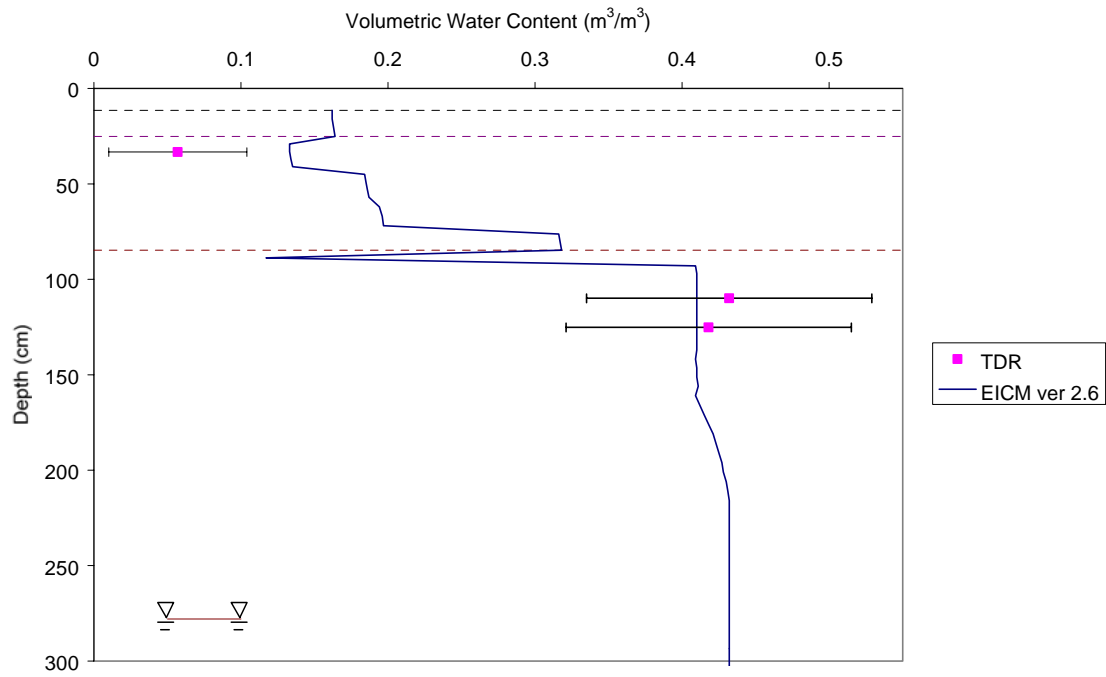
COLORADO site - 3/2/95



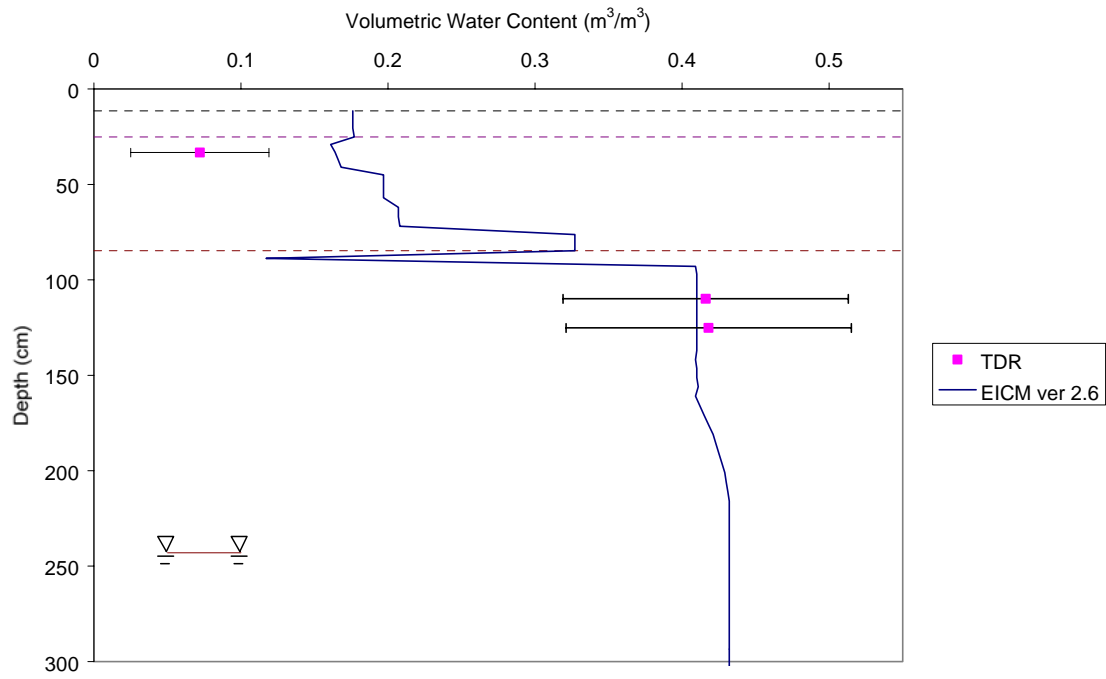
COLORADO site - 3/17/95



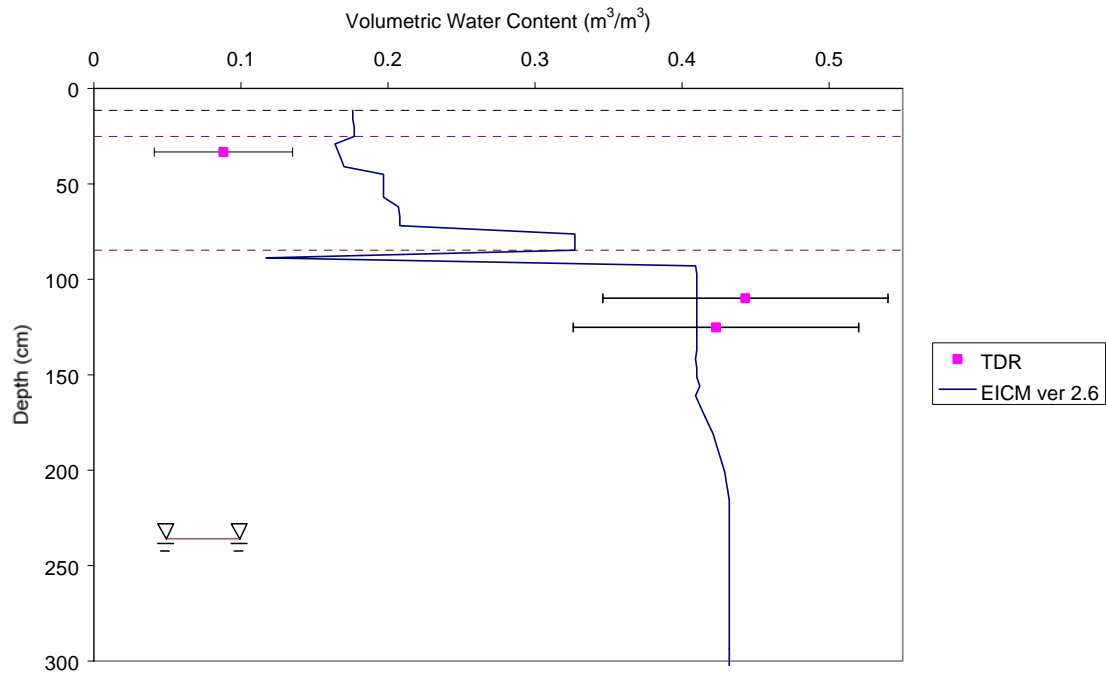
COLORADO site - 4/5/95



COLORADO site - 4/21/95



COLORADO site - 5/8/95



---

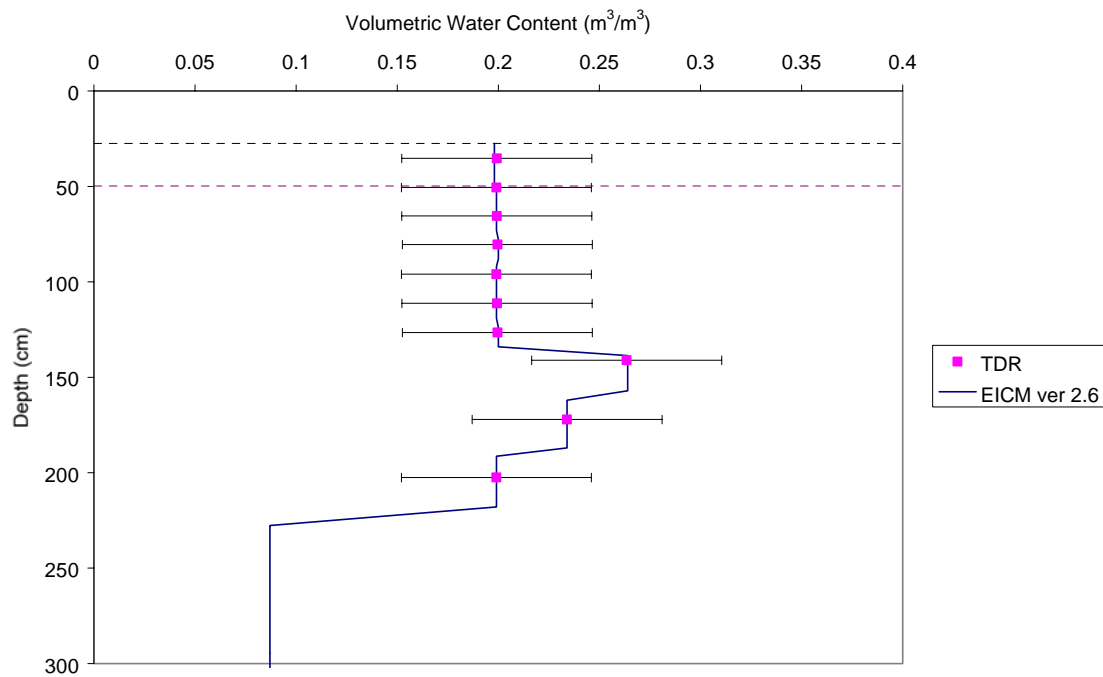
## APPENDIX Q

### VOLUMETRIC WATER CONTENT PROFILES

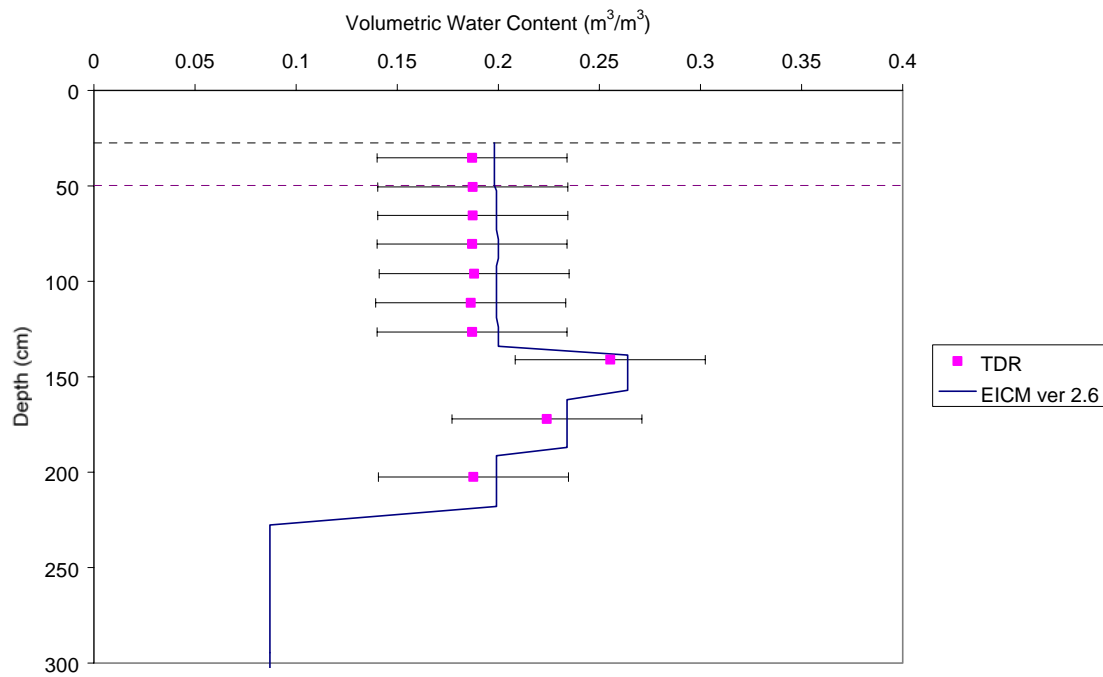
ARIZONA (41024)

EICM – Version 2.6

ARIZONA site - 11/9/95

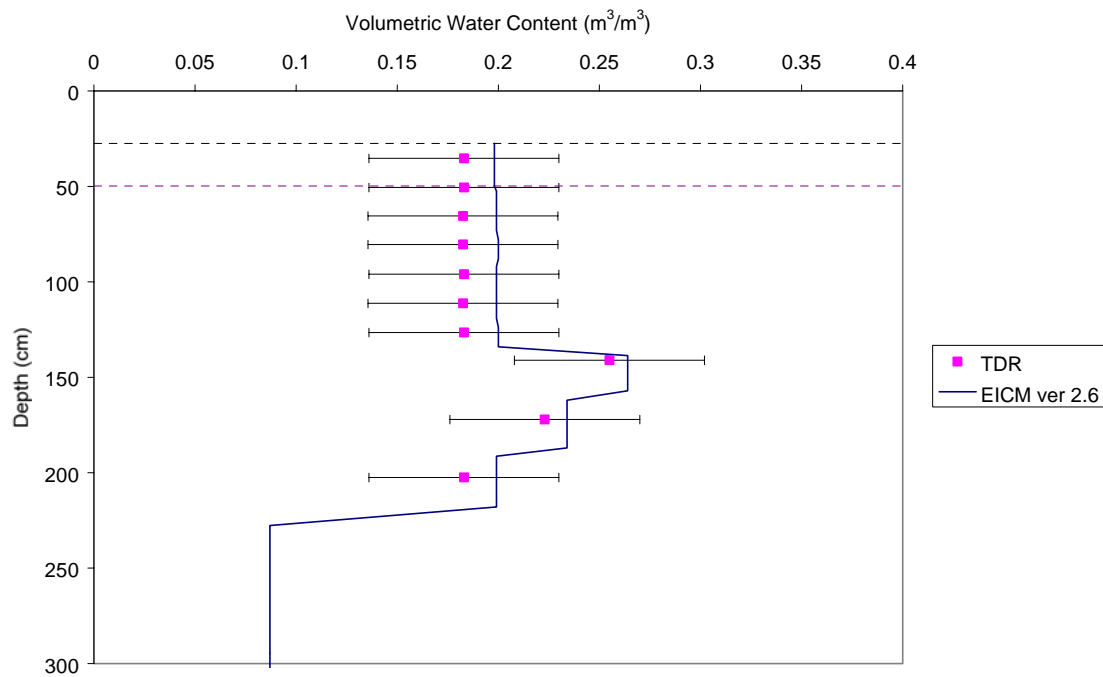


ARIZONA site - 12/7/95

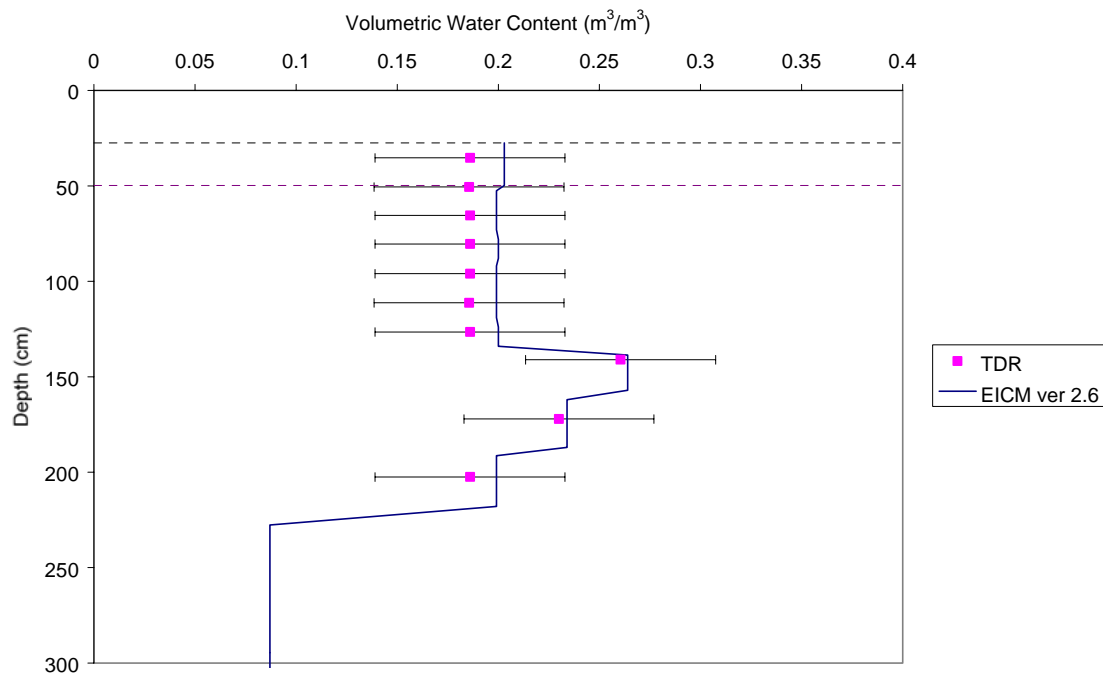




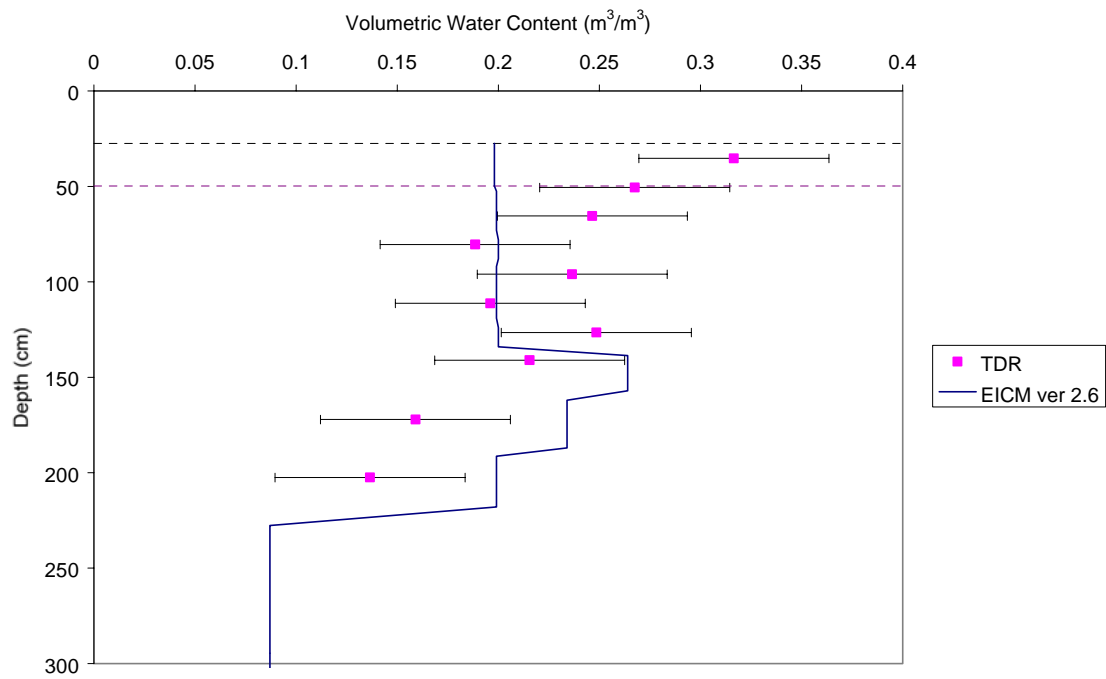
ARIZONA site - 1/11/96



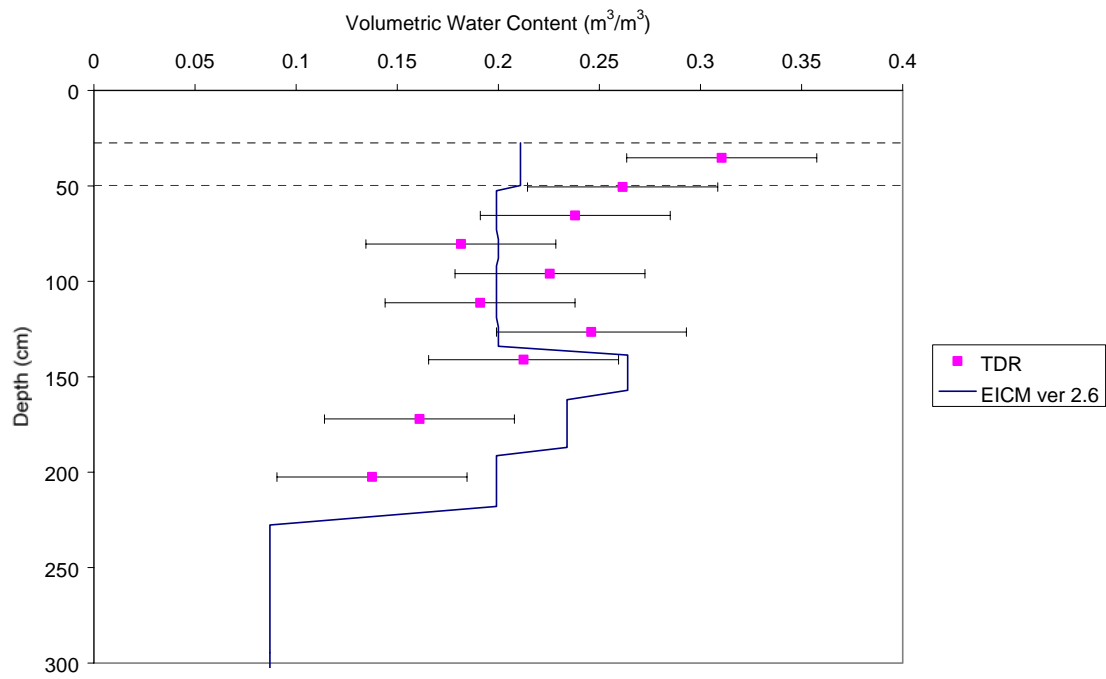
ARIZONA site - 2/8/96



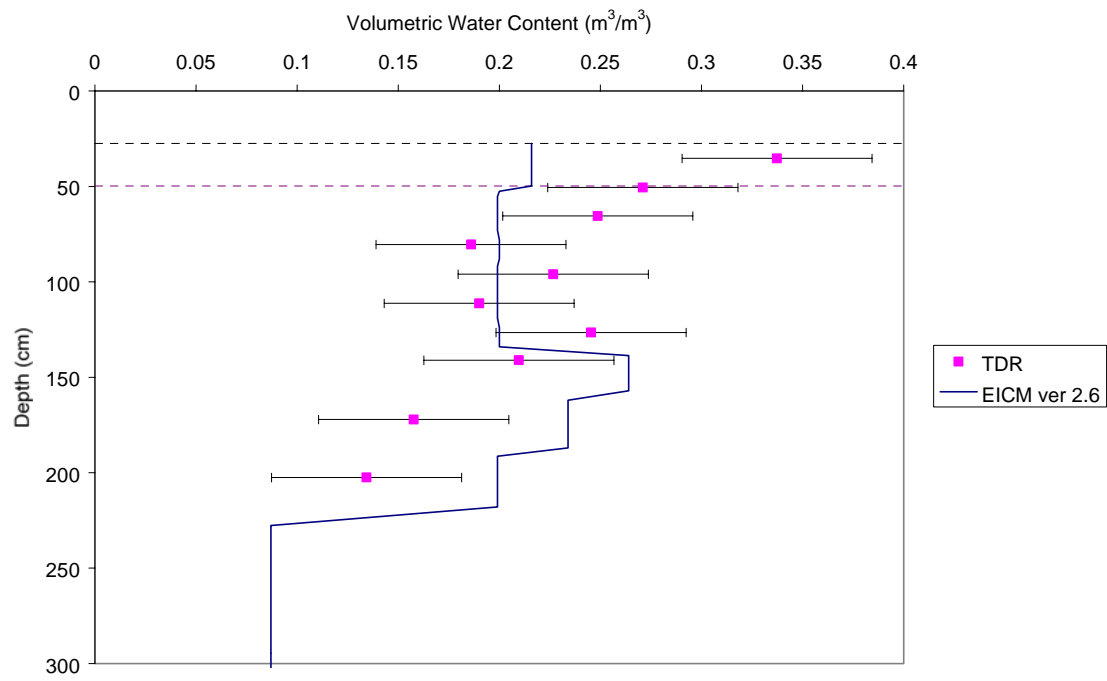
ARIZONA site - 6/13/96



ARIZONA site - 7/11/96



ARIZONA site - 8/15/96



---

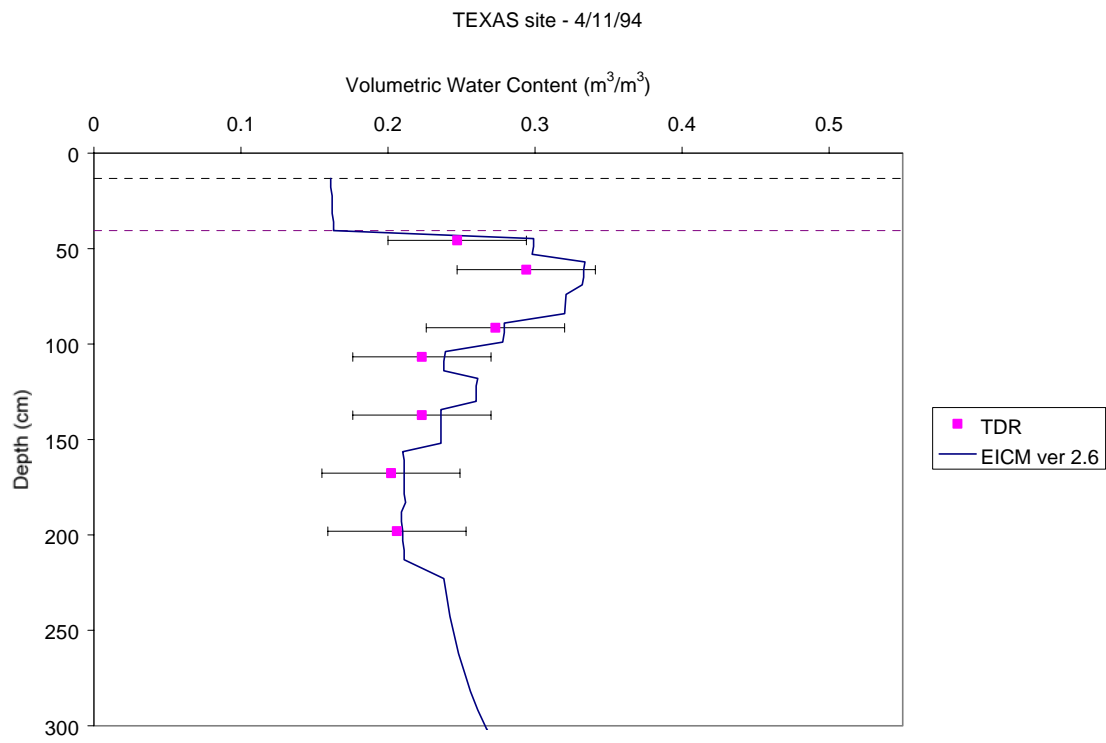
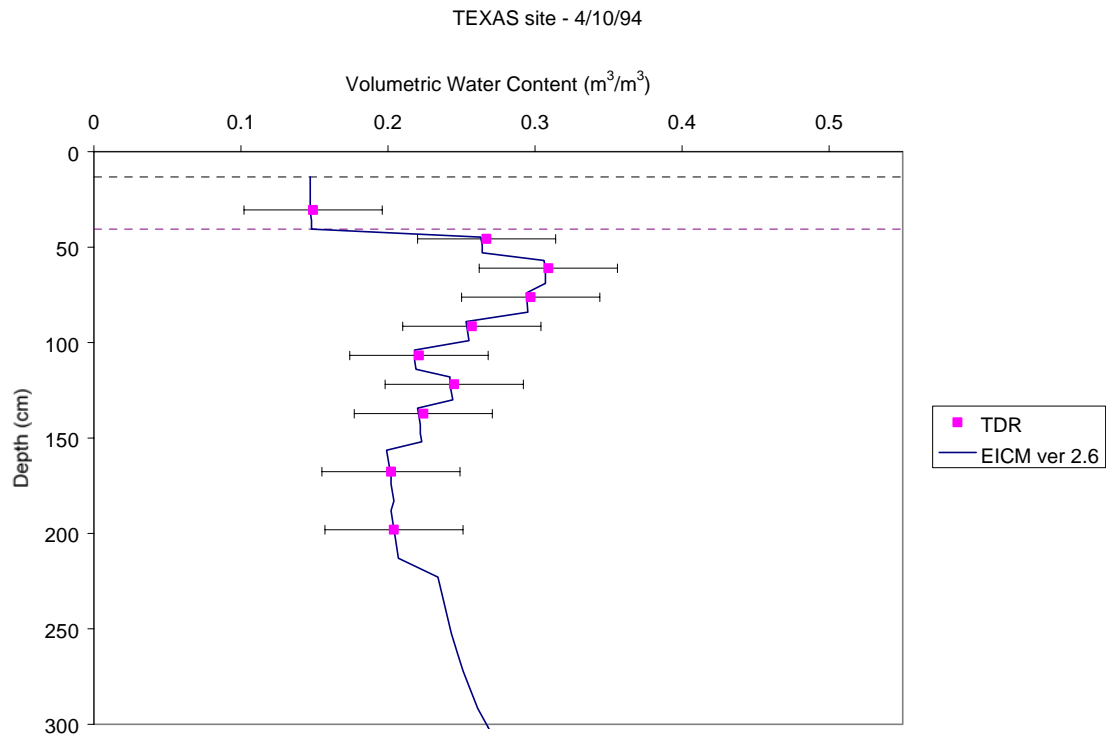
# APPENDIX R

## VOLUMETRIC WATER CONTENT PROFILES

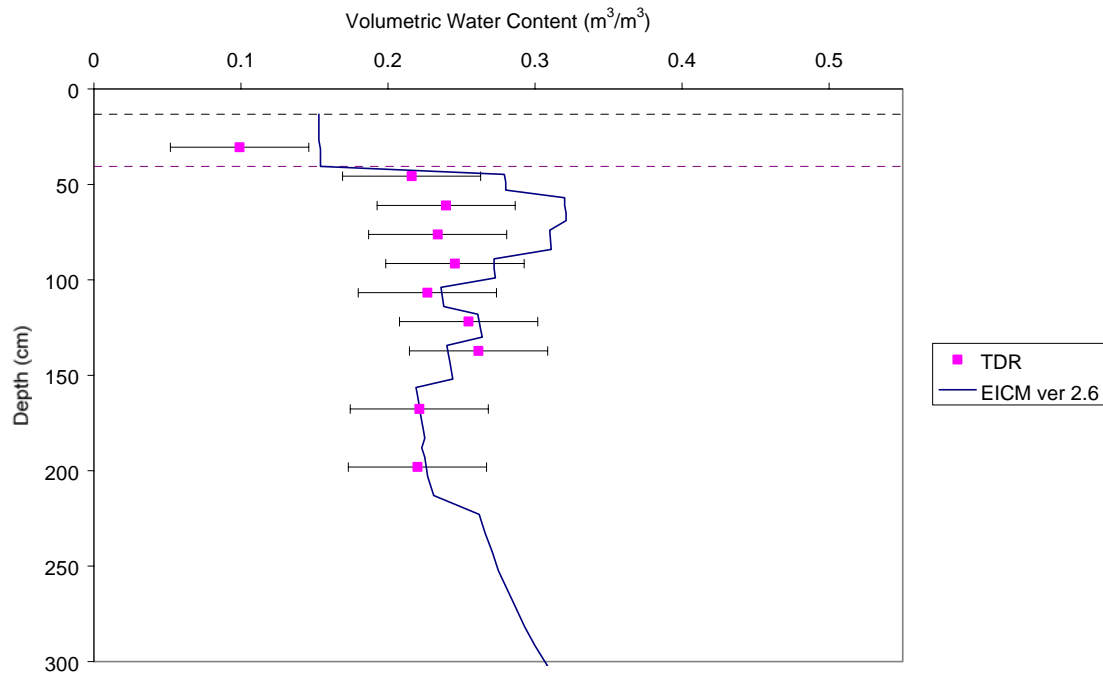
TEXAS (481077)

EICM – Version 2.6

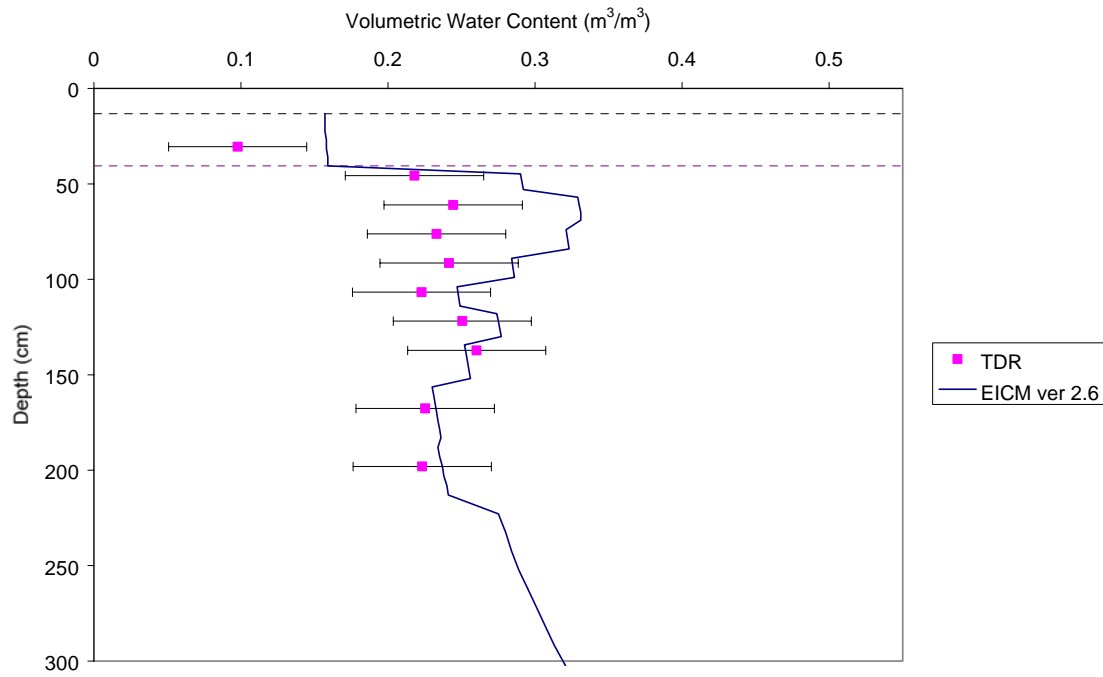
d



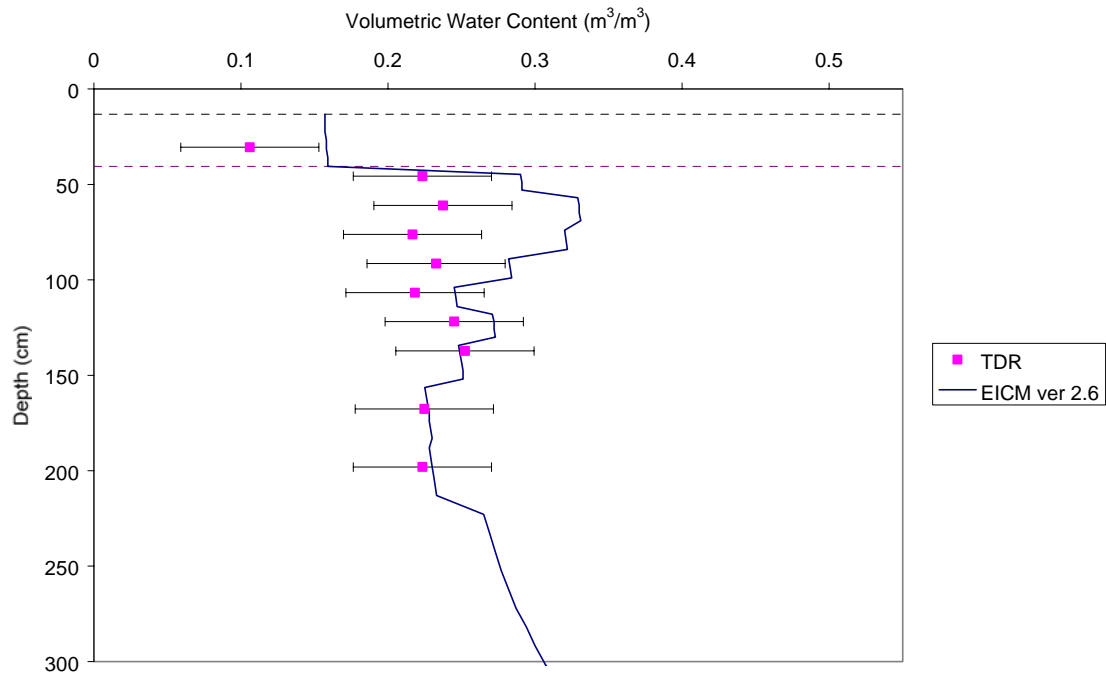
TEXAS site - 6/24/94



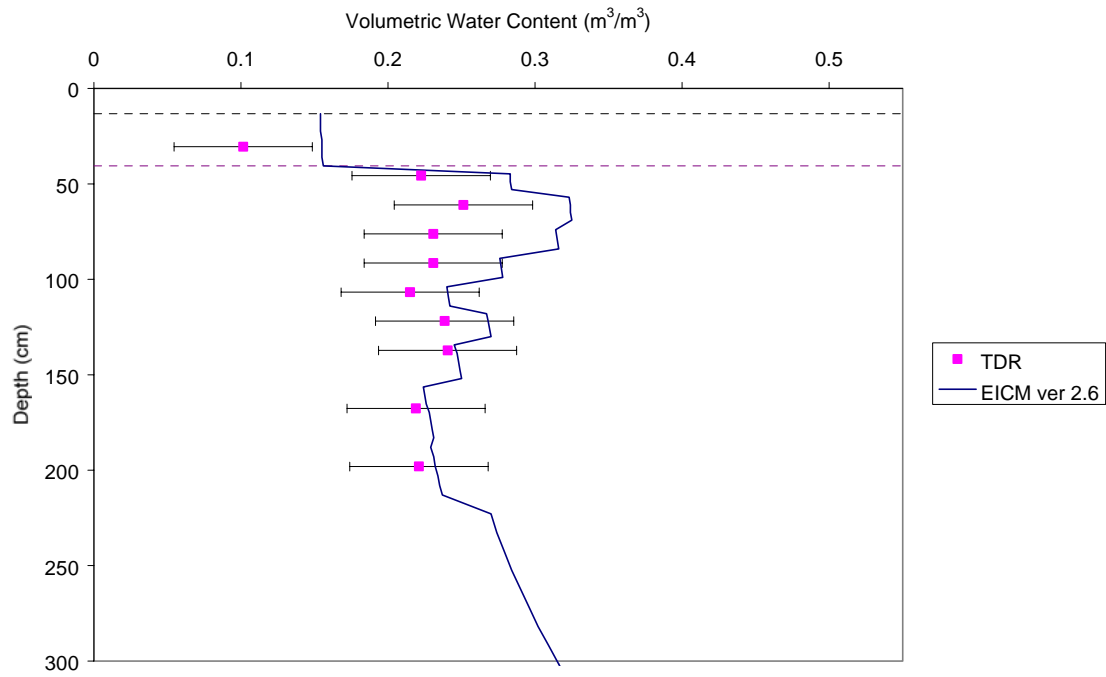
TEXAS site - 7/18/94



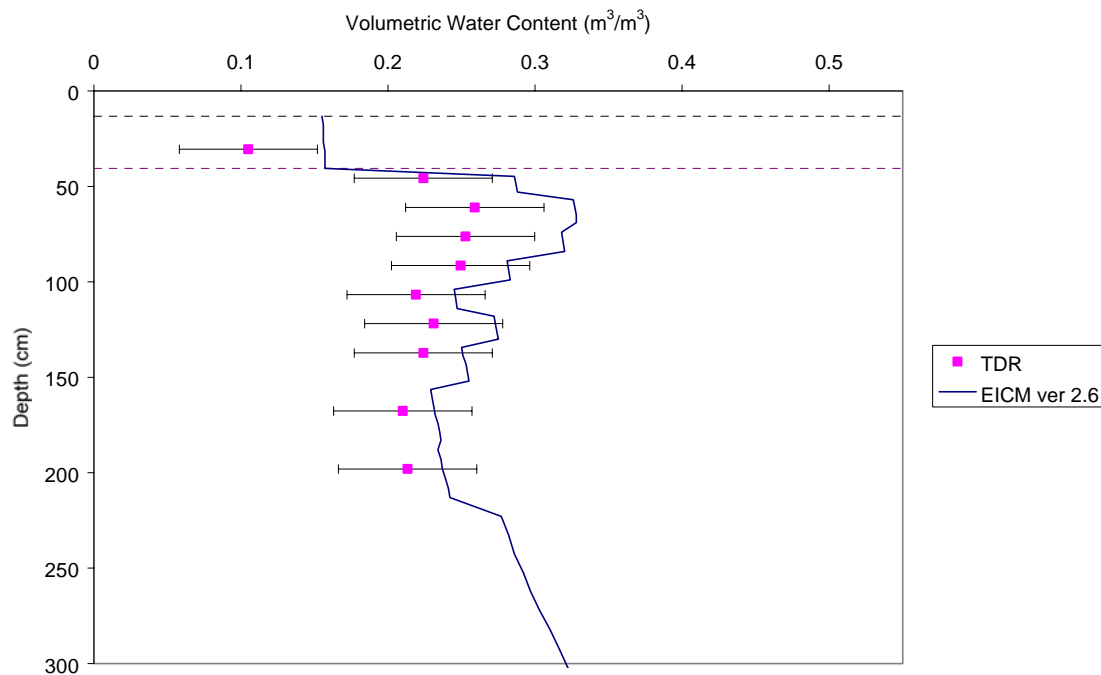
TEXAS site - 8/17/94



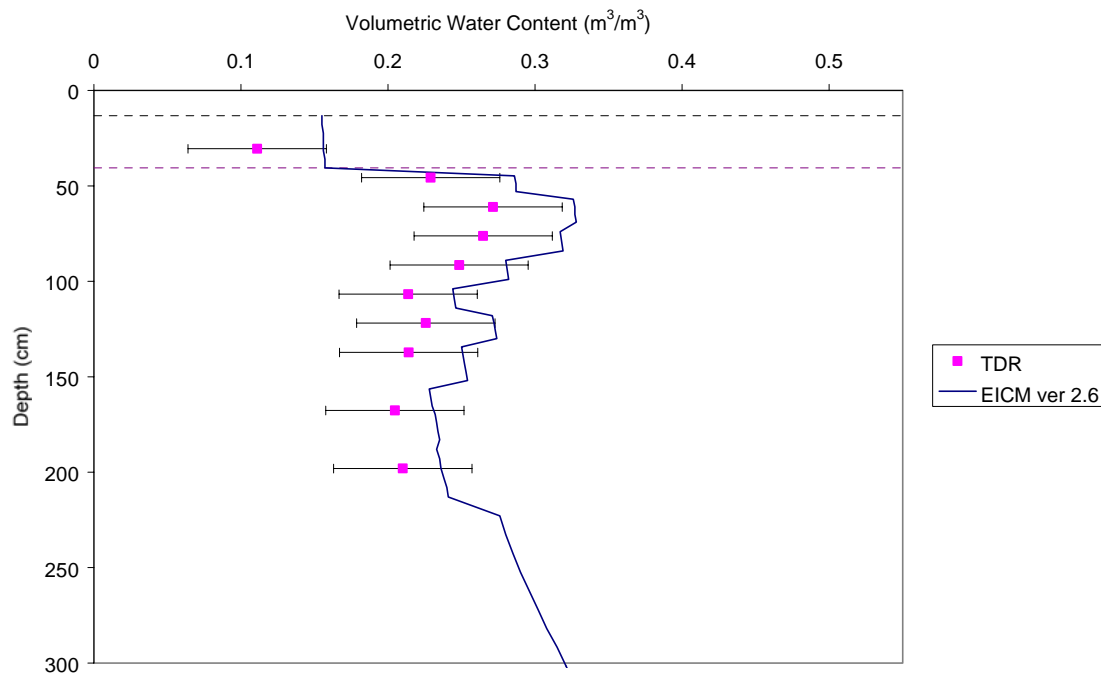
TEXAS site - 9/19/94



TEXAS site - 10/24/94

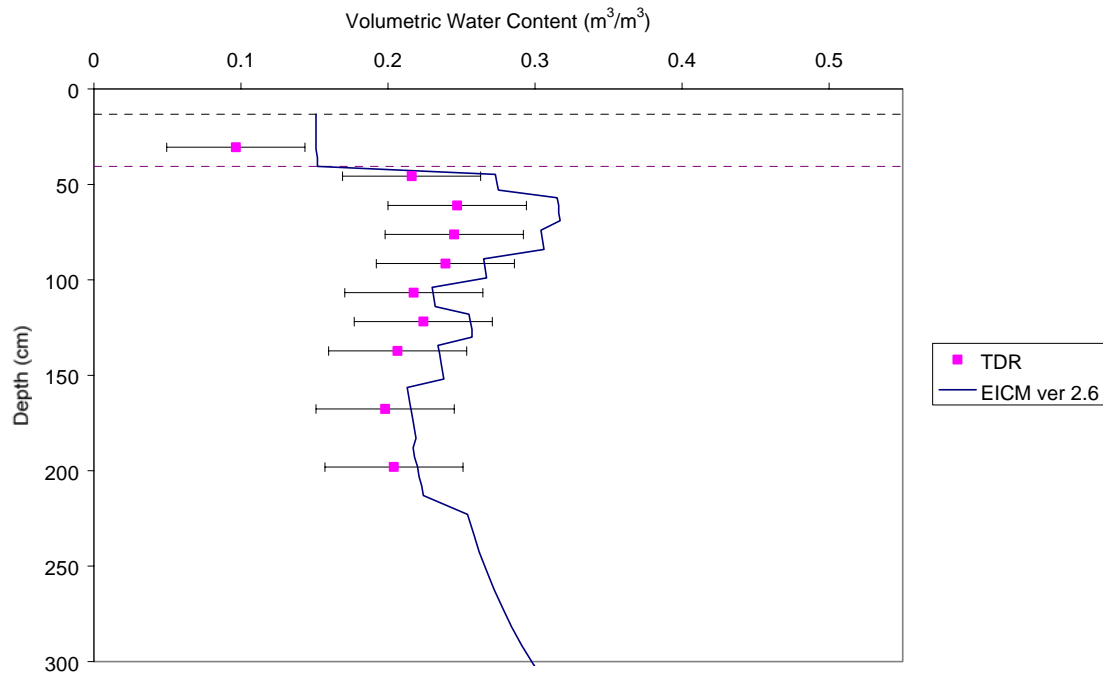


TEXAS site - 11/16/94

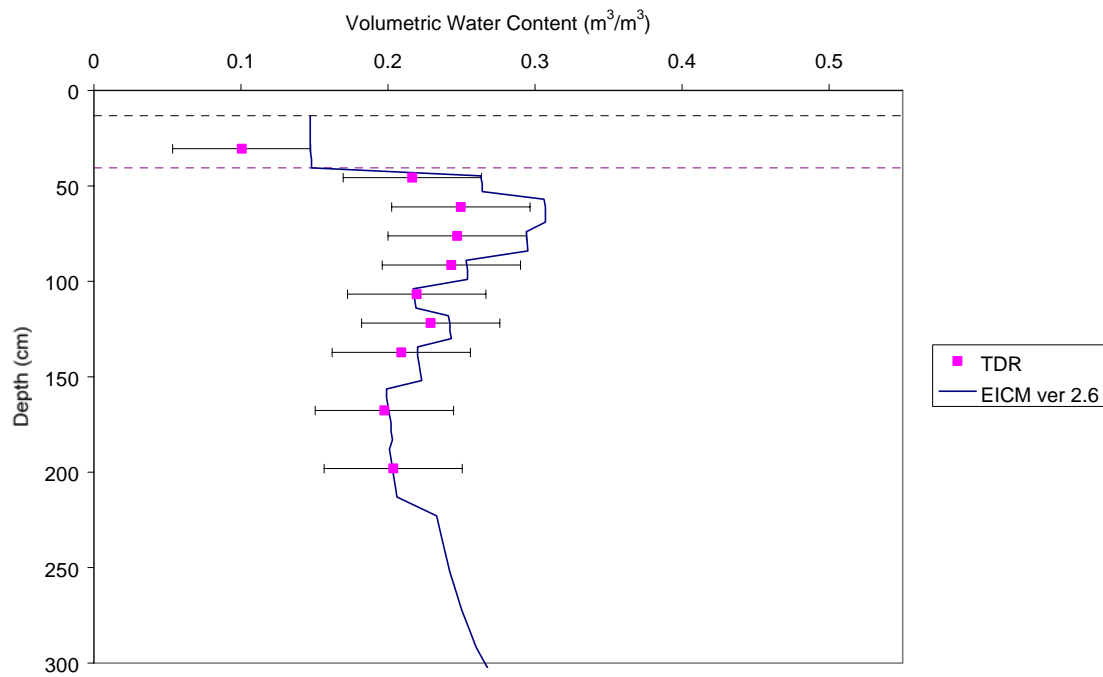




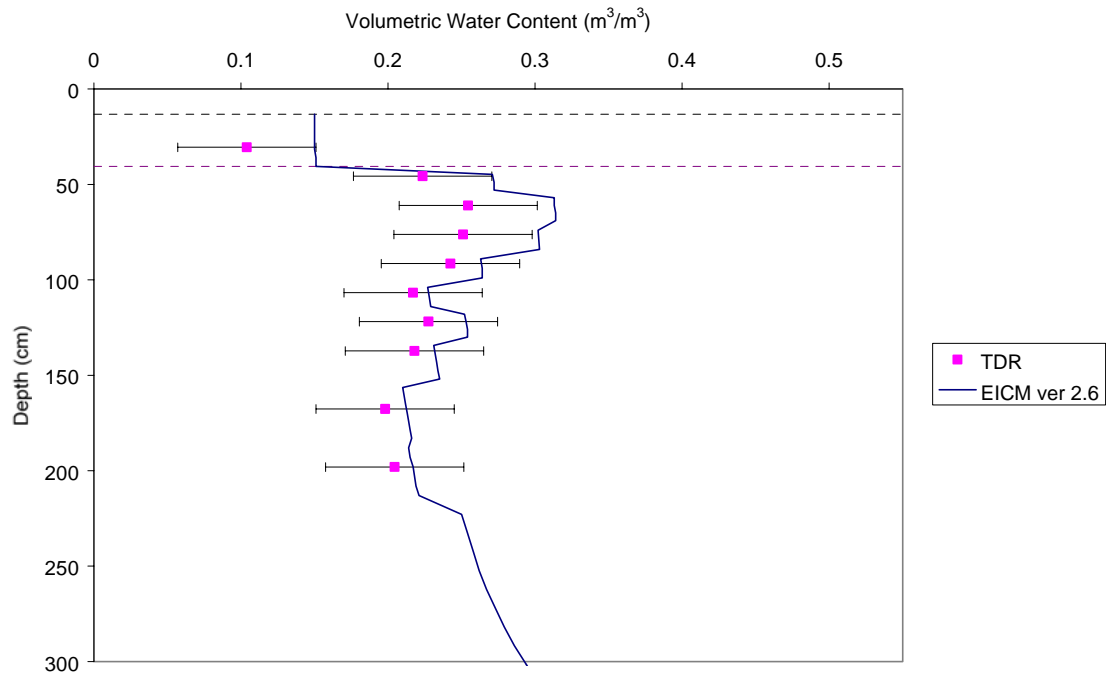
TEXAS site - 12/22/94



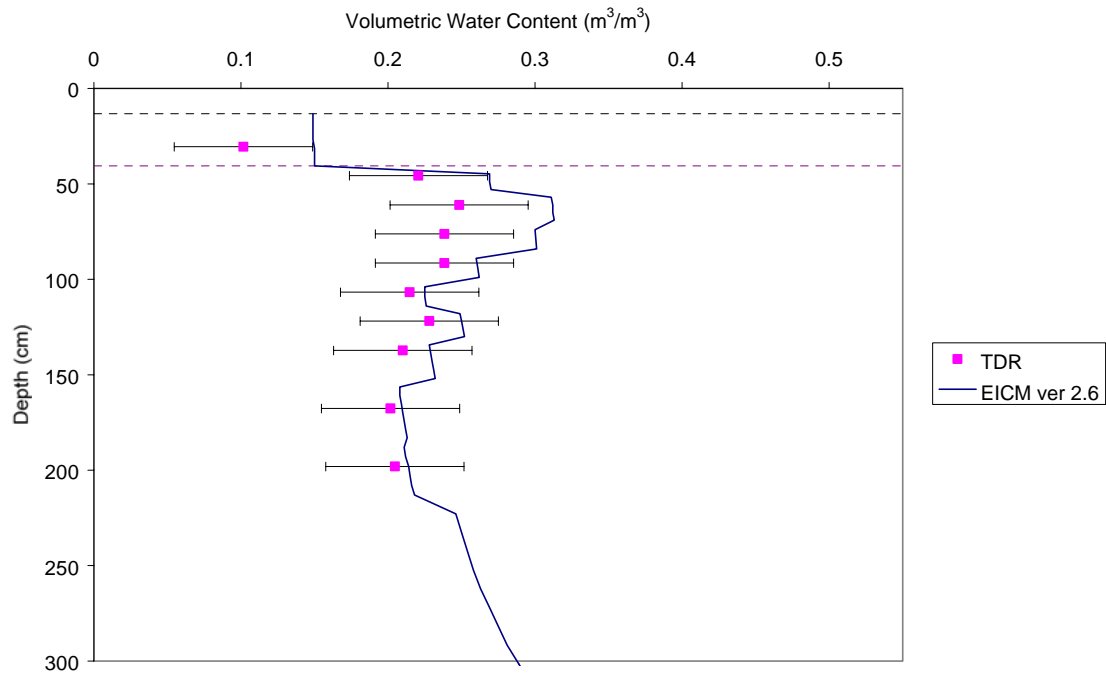
TEXAS site - 1/20/95



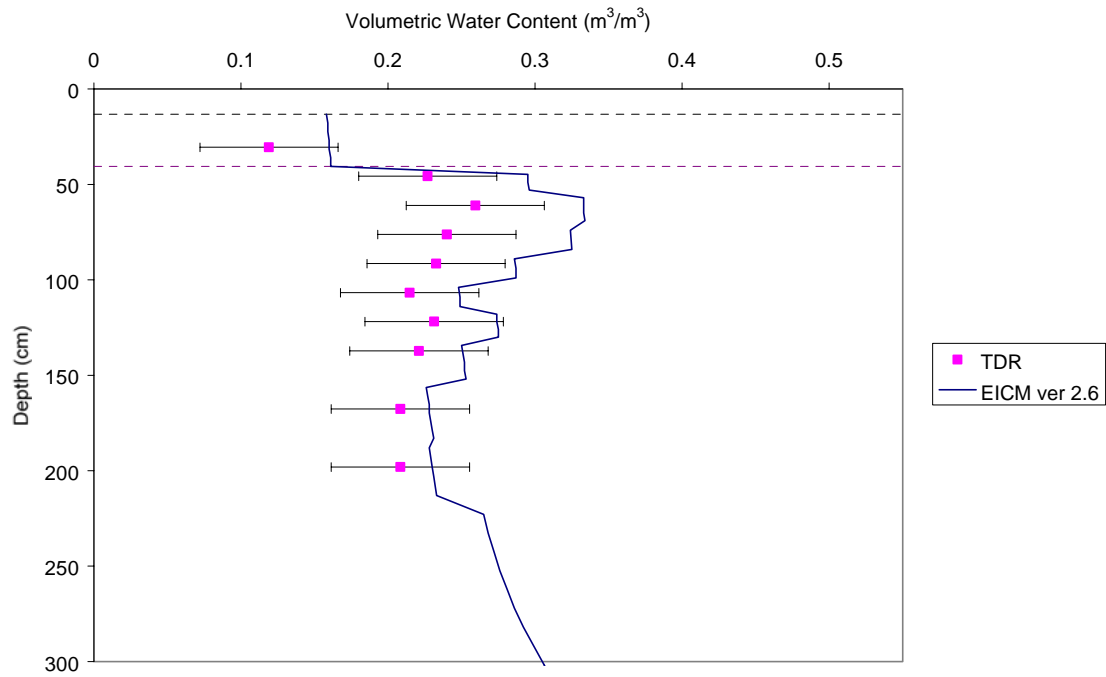
TEXAS site - 2/23/95



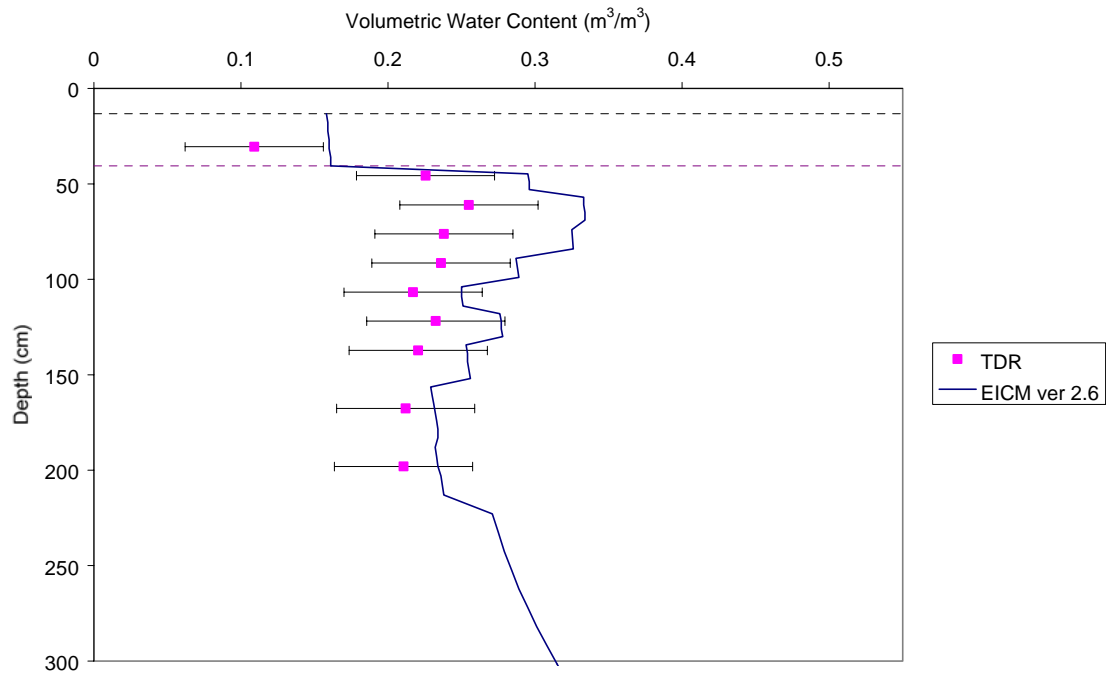
TEXAS site - 3/23/95



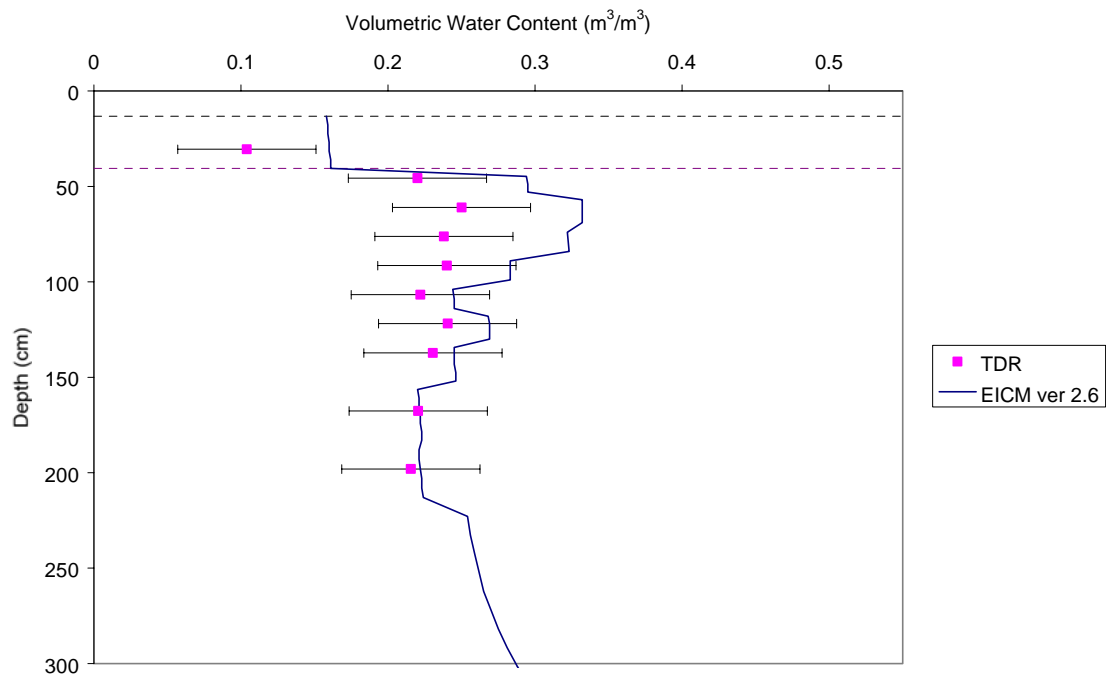
TEXAS site - 4/20/95



TEXAS site - 5/18/95



TEXAS site - 6/22/95



---

## REFERENCES

AASHTO Designation M 147-65. (1990). "Standard Specification for Materials for Aggregate and Soil-Aggregate Subbase, Base and Surface Courses". AASHTO. pp. 157-158.

DataPave 2.0. (1999). U.S. Department of Transportation, Federal Highway Administration, September 1999.

Dunn, R. J. and Palmer, B. S. (1994). "Lessons Learned from the Application of Standard Test Methods for Field and Laboratory Hydraulic Conductivity Measurement". *Hydraulic Conductivity and Waste Contaminant Transport in Soil*, ASTM STP 1142. D. E. Daniel and S. J. Trautwein, editors. American Society for Testing and Materials, Philadelphia.

Escario, V. and Juca, J. (1989). "Strength and Deformation of Partly Saturated Soils". *Proceedings of the Twelfth International Conference on Soil Mechanics and Foundation Engineering*, Rio de Janeiro, Vol. 3, pp. 43-46.

Fredlund, D. G. (1995). "Prediction of Unsaturated Soil Functions Using the Soil-Water Characteristic Curve". *Proceedings of the Bength B. Broms Symposium on Geotechnical Engineering*, Singapore, 13-15 December, pp. 113-133.

Fredlund, D. G., and Xing, A. (1994). "Equations for the Soil-Water Characteristic Curve". *Canadian Geotechnical Journal*, Vol. 31, No. 4, pp. 521 - 532.

Fredlund, D. G., Vanapalli, S. K., Xing, A., and Pufalel, D. E. (1995). "Predicting the Shear Strength Function for Unsaturated Soils Using the Soil-Water Characteristic Curve". In: *Unsaturated Soils*, Alonso and Delage, editors.

Fredlund, D. G., Xing, A., and Huang, S. (1994). "Predicting the Permeability Function for Unsaturated Soils Using the Soil-Water Characteristic Curve". *Canadian Geotechnical Journal*, Vol 3. No. 4, pp. 533 - 546.

Fredlund, D. G., Xing, A., Fredlund, M and Barbour, S. L. (1995). "The Relationship of the Unsaturated Shear Strength to the Soil-Water Characteristic Curve". *Canadian Geotechnical Journal*, Vol. 32, pp. 440-448.

Gan, J. K. M, Fredlund, D. G., and Rahardjo, H. (1988). "Determination of the Shear Strength Parameters of an Unsaturated Soil Using the Direct Shear Test". *Canadian Geotechnical Journal*. Vol. 25, pp. 500-510.

Ghosh, R. K. (1980). "Estimation of Soil-Moisture Characteristics from Mechanical Properties of Soils". *Soil Science*, Vol. 130, No. 2, pp. 60-63.

Haverkamp, R. and Parlange, J. Y. (1986). "Predicting the Water-Retention Curve from Particle-Size Distribution: 1. Sandy Soils without Organic Matter". *Soil Science*, Vol. 142, No. 6, pp. 325-339.

Holtz, R. D. and Kovacs, W. D. (1981). *An Introduction to Geotechnical Engineering*. Prentice-Hall, Inc.

Houston, W. N., Houston, S. L., Zapata, C., Manepally, C., and Lawrence, C. (1999). "Influence of Compressibility on Use and Interpretation of Soil Water Characteristic Curves". *Proceedings of the XI Panamerican Conference on Soil Mechanics and Geotechnical Engineering*. Foz do Iguassu, Brazil. pp. 947-954.

Jiang, Y. Jane and Tayabji, Shiraz D. (1999). *Analysis of Time Domain Reflectometry Data From LTPP Seasonal Monitoring Program Test Sections*. Final Report, FHWA-RD-99-115, July 1999.

Klemunes, J. A. (1995). *Determining Soil Volumetric Moisture Using Time Domain Reflectometry*. Master's Thesis. Faculty of the Graduate School, University of Maryland.

Krahn, J., and Fredlund, D. G. (1972). "On Total, Matric and Osmotic Suction". *Soil Science*, Vol. 114, No. 5, pp. 339 - 347.

Larson, G. and Dempsey, B. J. (1997). *Enhanced Integrated Climatic Model. Version 2.0*. University of Illinois at Urbana-Champaign and Newmark Civil Engineering Laboratory. Report No. DTFA MN/DOT 72114.

Leong, E. C., and Rahardjo, H., (1996). "A Review on Soil-Water Characteristic Curve Equations". *Geotechnical Research Report*, NTU/GT/96-5, Nanyang Technological University, NTU-PWD Geotechnical Research Centre, Singapore.

Livneh, M., Kinsky, J. and Zaslavsky, D. (1970). "Correlation of Suction Curves with the Plasticity Index of Soils". *Journal of Materials*, JMLSA, Vol. 5, No. 1, March 1970, pp. 209-220.

Lytton, R. L., Pufahl, D. E., Michalak, C. H., Liang, H. S., and Dempsey, B. J. (1990). *An Integrated Model of the Climatic Effects on Pavements*. Texas Transportation Institute, Texas A&M University. Report No. FHWA-RD-90-033, Federal Highway Administration, McLean, VA.

Marinho, F. A. M. and Stuermer, M. M. M. (1998). "Aspects of the Storage Capacity of a Compacted Residual Soil". *Proceedings of the Second International Conference on Unsaturated Soils*. Vol. 1. Beijing, China. August, 27-30.

Oberg AL. and Sallfors G. (1997). "Determination of Shear Strength Parameters of Unsaturated Silts and Sands Based on the Water Retention Curve". *Geotechnical Testing Journal*. Vol. 20, No. 1. pp. 40-48.

Rahardjo, H., Chang, H. M. F. and Lim, T. T. (1995). "Shear Strength and in Situ Matric Suction of a Residual Soil". In: *Unsaturated Soils*. Alonso & Delage, editors. pp. 637-643.

Rohm, S. A. and Vilar, O. M. (1995). "Shear Strength of an Unsaturated Sandy Soil". In: *Unsaturated Soils*. Alonso & Delage, editors. pp. 189-193.

Sabbagh, A. (1995). "Prediction of Volume Change in Unsaturated Clays". In: *Unsaturated Soils*. Alonso & Delage, editors. pp. 791-796.

*SoilVision User's Guide*. (1997). Version 1.2 [Computer software]. SoilVision Systems, Ltd. Saskatoon, Saskatchewan, Canada.

Vanapalli, S K., Sillers, W. S. and Fredlund, M. D. (1998). "The Meaning and Relevance of Residual State to Unsaturated Soils". *51<sup>st</sup> Canadian Geotechnical Conference*. Edmonton, Alberta, October 4-7, pp. 1-8.

Witczak, M. W., Yau, A. (1997). *Development of the Resilient and Plastic Response Parameters of Selected Unbound Base/Subbase/Subgrade Materials*, Vol. 1.

Witczak, M. W., Andrei, D., and Houston, W. N. (2000). "Resilient Modulus as Function of Soil Moisture - Summary of Predictive Models". *Development of the 2002 Guide for the Development of New and Rehabilitated Pavement Structures, NCHRP 1-37 A*, an Inter Team Technical Report. Vol. 1.

Witczak, M. W., Houston, W. N., and Andrei, D., (2000). "A Study of the Expected Changes in Resilient Modulus of the Unbound Layers with Changes in Moisture for 10 LTPP Sites". *Development of the 2002 Guide for the Development of New and*

*Rehabilitated Pavement Structures, NCHRP 1-37 A*, an Inter Team Technical Report.  
Vol. 2.

Zapata, C. E. (1999). *Uncertainty in Soil-Water Characteristic Curve and Impacts on Unsaturated Shear Strength Predictions*. Ph.D. Dissertation, Arizona State University, Tempe, United States.